Vol. 179, January 31, 1986 ISSN 0003-2670
Complete in one issue

INTERNATIONAL CONFERENCE ON FLOW ANALYSIS III, BIRMINGHAM, GREAT BRITAIN, SEPTEMBER 5–8, 1985

ANALYTICA CHIMICA ACTA

International journal devoted to all branches of analytical chemistry

ELSEVIER

ANALYTICA CHIMICA ACTA

International journal devoted to all branches of analytical chemistry
Revue internationale consacrée à tous les domaines de la chimie analytique
Internationale Zeitschrift für alle Gebiete der analytischen Chemie

PUBLICATION SCHEDULE FOR 1986

	J	F	M	A	M	J	J	A	S	O	N	D
Analytica Chimica Acta	179	180	181	182 183/1	183/2 184	185	186	187	188	189	190	191

Scope. *Analytica Chimica Acta* publishes original papers, short communications, and reviews dealing with ever aspect of modern chemical analysis both fundamental and applied.

Submission of Papers. Manuscripts (three copies) should be submitted as designated below for rapid and efficier handling:

Papers from the Americas to: Professor Harry L. Pardue, Department of Chemistry, Purdue University, West Lafayett IN 47907, U.S.A.

Papers from all other countries to: Dr. A. M. G. Macdonald, Department of Chemistry, The University, P.O. Box 36 Birmingham B15 2TT, England. Papers dealing particularly with computer techniques to: Professor J. T. Cler Universität Bern, Pharmazeutisches Institut, Baltzerstrasse 5, CH-3012 Bern, Switzerland.

Submission of an article is understood to imply that the article is original and unpublished and is not being considere for publication elsewhere. Upon acceptance of an article by the journal, authors will be asked to transfer the copyrigh of the article to the publisher. This transfer will ensure the widest possible dissemination of information.

Information for Authors. Papers in English, French and German are published. There are no page charge: Manuscripts should conform in layout and style to the papers published in this Volume. Authors should consu Vol. 170 for detailed information. Reprints of this information are available from the Editors or from: Elsevier Editori Services Ltd., Mayfield House, 256 Banbury Road, Oxford OX2 7DH (Great Britain).

Reprints. Fifty reprints will be supplied free of charge. Additional reprints (minimum 100) can be ordered. An order form containing price quotations will be sent to the authors together with the proofs of their article.

Advertisements. Advertisement rates are available from the publisher.

Subscriptions. Subscriptions should be sent to: Elsevier Science Publishers B.V., Journals Department, P.O. Box 211, 1000 AE Amsterdam, The Netherlands. Tel: 5803 911, Telex: 18582.

Publication. *Analytica Chimica Acta* appears in 13 volumes in 1986. The subscription for 1986 (Vols. 179–191) is Dfl. 2730.00 plus Dfl. 312.00 (p.p.h.) (total approx. US $1126.70). All earlier volumes (Vols. 1–178) except Vols. 23 and 28 are available at Dfl. 231.00 (US $85.56), plus Dfl. 15.00 (US $5.56) p.p.h., per volume.

Our p.p.h. (postage, packing and handling) charge includes surface delivery of all issues, except to subscribers in the U.S.A., Canada, Japan, Australia, New Zealand, P.R. China, India, Israel, South Africa, Malaysia, Thailand, Singapore, South Korea, Taiwan, Pakistan, Hong Kong, Brazil, Argentina and Mexico who receive all issues by air delivery (S.A.L. — Surface Air Lifted) at no extra cost. For the rest of the world, airmail and S.A.L. charges are available upon request. Claims for issues not received should be made within three months of publication of the issues. If not they cannot be honoured free of charge.

For further information, or a free sample copy of this or any other Elsevier Science Publishers journal, readers in the U.S.A. and Canada can contact the following address: Elsevier Science Publishing Co. Inc., Journal Information Center, 52 Vanderbilt Avenue, New York, NY 10017, U.S.A., Tel: (212) 916-1250.

0003-2670/86/$03.50

Printed in The Netherlands

P. S. ANALYTICAL LTD.

SPECIALISTS IN LABORATORY AUTOMATION

NEW PRODUCTS FOR AUTOMATED ANALYSIS

VALVE SWITCHING DATA TRANSFER INTERFACE

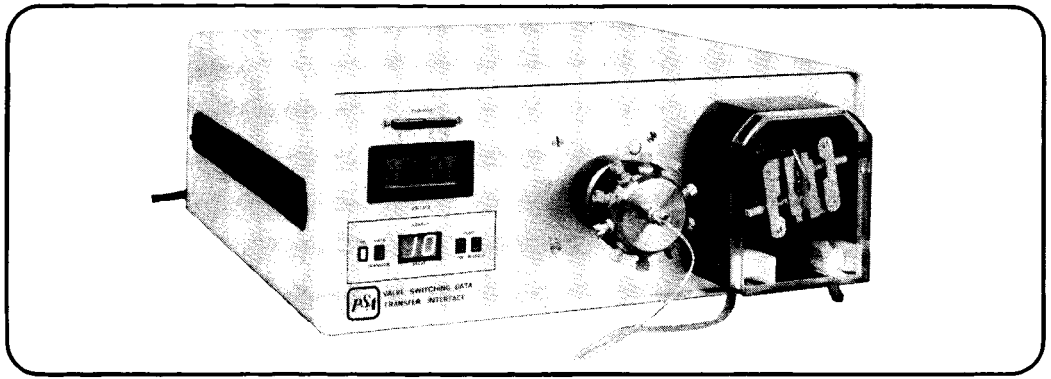

The Valve Switching and Data Transfer Interface is an intelligent building block for use in a wide range of solution handling manipulations. The heart of the unit is a multiport electronically actuated inert valve which can be randomly addressed. A unique feature of the design is that the system provides a positive indication of the valve position. Once an input is selected then it is possible to either pump from or in to this line by computer control.

The standard interface box uses 4 analogue inputs, a digital I/O port and 2 relay outputs. The unit has applications in sample preparation and liquid dispensing systems, ultraviolet and electrochemical testing, flow injection analysis, fraction collection and selection, liquid and gas chromatography and gas monitoring systems. It can be controlled using the HP85, Commodore Pet or Apple computers.

Also available **Automated Teflon Rotary Valves** and **Automated HPLC Injection Valves.**

New Range of Autosamplers

PSA has extended its range of Autosamplers by the introduction of two 80 position systems. The unit shown below is capable of stand alone operation or controlled by a computer system using simple TTL commands. The start and stop positions can be preset into analytical cycle and wash and sample times can be set up to 99 seconds. In addition the wash liquid can be varied using a series of valves on the wash inlet side.

To compliment the range an RS232 option is available which gives true random access of turntable position. Additional options include a vial septum pierce mechanism and a magnetic stirrer station.

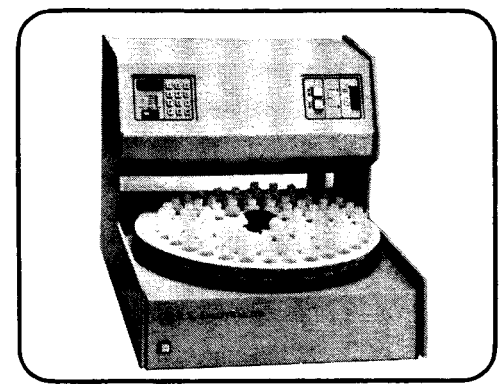

For demonstration or further details contact:

P. S. Analytical Ltd, Arthur House, Far North Building, Cray Avenue, Orpington, Kent BR5 3TR. UK. Tel No: 0689 31632/3. Telex: 8951182 Gecoms G.

Wilson and Wilson's Comprehensive Analytical Chemistry

edited by G. Svehla

Vol. XII Thermal Analysis
Part A: Simultaneous Thermoanalytical Examinations by Means of the Derivatograph

by **J. PAULIK** *and* **F. PAULIK**, *Budapest, Hungary*

Part A of this volume describes the first practical application of the simultaneous thermoanalytical technique, its further development and some results obtained with its use.
Part B comprises a list of some 1400 publications reporting results obtained by means of the derivatograph and a comprehensive subject index of 1100 compounds.

Contents: Theory and Techniques. 1. Introduction. 2. Derivate thermogravimetry. 5. Means of increasing the selectivity. 6. Thermogas titrimetry. 7. Quasi-isothermal quasi-isobaric thermogravimetry. 8. Simultaneous TG and TGT examination under quasi-isothermal quasi-isobaric conditions. 9. Quasi-isothermal thermodilatometry. Applications. 10. Inorganic compounds. 11. Complexes. 12. Catalysts. 13. Minerals. 14. Silicates. 15. Organic compounds. 16. Plastics. 17. Biological applications. 18. Miscellaneous. Basic papers. List of publications. Subject index.

1981 xviii + 278 pp. Price: US $ 71.25 / Dutch guilders 165.00. ISBN 0-444-41949-7

Vol. XII Thermal Analysis
Part B: Biochemical and Clinical Applications of Thermometric and Thermal Analysis

edited by **N.D. JESPERSEN**, *Jamaica, New York, U.S.A.*

The book is divided into an instrumental section and an application section.

". . . it has all the essential ingredients to make it relevant for many years to come. It is a well balanced review and is a must for those in clinical chemistry already using thermal techniques, as well as those contemplating its use." (The Analyst)

Contents: 1. Introduction. 2. Titration and Flow Calorimetry: Instrumentation and Data Collection (D.J. Eastough et al.). 3. Fundamentals of Differential Scanning Calorimetry (H.T. Gaud). 4. Flow Reactors (R.S. Schifreen). 5. Thermistor Probes (R.M. Ianniello and N.D. Jespersen). 6. Inorganic Ions and Small Organic Species (N.D. Jespersen). 7. Titration and Flow Calorimetry: Application to Proteins and Lipids (D.E. Eastough et al.). 8. Enzymatic Enthalpimetry (J.K. Grime). 9. Microcalorimetry in Antibiotic Bioassay (B.F. Perry). 10. Differential Scanning Calorimetry of Macromolecules and Membranes (S. Mabry-Gaud). Subject Index.

1982 xviii + 254 pp. Price: US $ 71.25 / Dutch guilders 185.00. ISBN 0-444-42062-2

Other parts of the volume include:

Part C: Emanation Thermal Analysis and Other Radiometric Emanation Methods

by **V. Balek** *and* **J. Tölgyessy**

1984 xvi + 304 pp. Price: US $ 70.25 / Dutch guilders 190.00. ISBN 0-444-99659-1

Part D: Thermophysical Properties of Solids. Their Measurements and Theoretical Thermal Analysis

by **J. Sěsták**

1984 xx + 440 pp. Price: US $ 111.00 / Dutch guilders 300.00. ISBN 0-444-99653-2

ELSEVIER SCIENCE PUBLISHERS

P.O. Box 211, 1000 AE Amsterdam, The Netherlands
P.O. Box 1663, Grand Central Station, New York, NY 10163, USA

7327

ANALYTICA CHIMICA ACTA
VOL. 179 (1986)

ANALYTICA CHIMICA ACTA

International journal devoted to all branches of analytical chemistry

ELSEVIER Amsterdam–Oxford–New York–Tokyo

Anal. Chim. Acta, Vol. 179 (1986)

0003-2670/86/$03.50

Printed in The Netherlands

SPECIAL ISSUE

FLOW ANALYSIS III

Proceedings of the International Conference held in Birmingham, Great Britain, 5–8th September, 1985

Analytica Chimica Acta, 179 (1986) 1–58
Elsevier Science Publishers B.V., Amsterdam — Printed in The Netherlands

THE FIRST DECADE OF FLOW INJECTION ANALYSIS: FROM SERIAL ASSAY TO DIAGNOSTIC TOOL

JAROMIR RŮŽIČKA* and ELO H. HANSEN

Chemistry Department A, The Technical University of Denmark, Building 207, DK-2800 Lyngby (Denmark)

(Received 15th July 1985)

SUMMARY

Some 804 papers on flow injection analysis published to the end of May 1985 are summarized. Past trends are discussed and new developments are briefly outlined.

The paper entitled "Flow Injection Analysis. Part 1. A New Concept of Fast Continuous Flow Analysis" [1], which appeared in August 1975, was the first of some 804 papers [1—804] published on flow injection analysis (f.i.a.) during the past ten years. In the present contribution, all these papers are collected to record the status quo of the general method and to reveal the present trends in applications of f.i.a. and in the geographical distribution of the research activities. Important concepts and technological innovations are reviewed and the future development of f.i.a. is briefly outlined.

STATUS QUO

The number of f.i.a. publications has increased exponentially since 1975. Depicted in a semilogarithmic diagram, showing the cumulative number of publications as a function of time (Fig. 1), the doubling time, t_d (i.e., the time span required for the literature to double in size) can be read out as the slope of the curve. Initially, this doubling time is seen to be less than one year, but of course the absolute number of f.i.a. publications was then modest. With the doubling time increasing to 1.2 years, it required six years to reach the first monograph on f.i.a. [153], while it took less than an additional four years to reach the 804 papers summarized here, the doubling time of the curve now having attained a value of 1.8 years. Compared to other analytical techniques, for which a similar type of analysis has been made, this doubling time is very short; thus the t_d values for other subsets of analytical chemistry are, for example, amperometry 8.0 years, conductometry 6.4 years, general electroanalysis 4.6 years, potentiometry 4.0 years, and voltammetry 2.8 years. Interestingly, the doubling times of the entire world chemical and analytical literature are even longer: 13.9 and 14.5 years, respectively [805].

This broad acceptance of f.i.a. is undoubtedly due to its versatility, which allows the method to be used in conjunction with a wide variety of detectors

0003-2670/86/$03.50

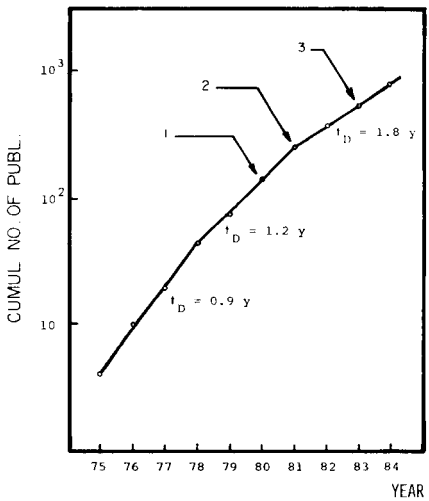

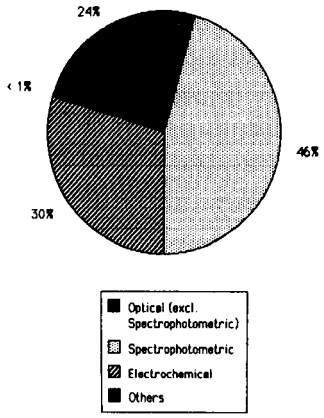

Fig. 1. Growth of publications on f.i.a. from 1975 to 1984. The arrows marked 1 and 3 refer to the previous International Conferences on Flow Analysis, reported in Anal. Chim. Acta, Vols. 114 and 145, respectively. Arrow 2 refers to the appearance of the first monograph on f.i.a. [153].

Fig. 2. Distribution of the detection principles used in conjunction with f.i.a. (cf. Table 1).

and analytical techniques (Table 1), and for the assay of a multitude of organic and inorganic substances (Table 2). A closer look at the variety of detection principles used in conjunction with f.i.a. (Fig. 2) shows that optical methods (and particularly visible spectrophotometry) predominate. This is not surprising considering that spectrophotometry generally accounts for approximately 50% of all detection principles used in analytical chemistry. Yet, a statistical scrutiny of the data for the two time periods of 1975—1980 and 1981—1984 clearly reveals that the highest relative increases in detectors used with f.i.a. actually are found in the areas of electrochemistry and optical methods (excluding spectrophotometry), and in the later time domain notably atomic absorption (a.a.s.) and inductively-coupled plasma spectrometry (i.c.p.) dominate, followed by chemiluminescence and fluorimetry. This trend is likely to continue, because flow-injection systems enhance the performance of a.a.s. and i.c.p., by increasing the sensitivity over 100 times [684, 712, 738], by allowing speciation and by removing matrix effects. For kinetic reasons, f.i.a. is an ideal vehicle for chemiluminescence [83, 330, 731].

As far as applications are concerned, several interesting trends appear when Fig. 3A and B are compared. When dedicated f.i.a. applications for the time spans 1975—1980 and 1981—1984 are considered in terms of the absolute number of publications (Fig. 3A) and in relation to the total number of f.i.a. papers (Fig. 3B) published during these two time periods, it becomes apparent that the relative number of agricultural applications in recent years

TABLE 1

Theory, methods and techniques used in flow injection analysis

Category	References
Theory	1, 10, 14, 20, 33, 39, 65, 71, 72, 73, 74, 75, 142, 146, 150, 151, 153, 155, 156, 176, 181, 183, 197, 257, 296, 339, 343, 345, 353, 363, 372, 376, 378, 422, 430, 500, 501, 526, 541, 554, 566, 608, 639, 663, 664, 665, 667, 688, 701, 702, 714, 802
Spectrometric methods	
Spectrophotometry in solution	1, 2, 3, 4, 5, 6, 7, 9, 15, 17, 18, 19, 21, 22, 25, 26, 27, 28, 30, 32, 34, 37, 38, 42, 48, 49, 51, 53, 54, 57, 59, 64, 69, 71, 78, 79, 81, 85, 89, 90, 91, 92, 93, 94, 95, 96, 97, 98, 101, 104, 106, 109, 110, 114, 116, 117, 118, 119, 120, 121, 122, 123, 124, 125, 126, 128, 129, 130, 132, 133, 135, 136, 138, 139, 145, 147, 148, 152, 154, 157, 158, 160, 161, 162, 163, 164, 166, 167, 169, 171, 174, 175, 177, 179, 180, 182, 183, 186, 189, 190, 191, 196, 197, 199, 202, 203, 207, 212, 220, 221, 224, 226, 228, 232, 233, 234, 235, 236, 237, 238, 239, 240, 241, 243, 245, 246, 252, 253, 256, 258, 259, 261, 262, 264, 266, 267, 268, 272, 273, 274, 275, 277, 279, 281, 284, 286, 293, 294, 295, 299, 303, 304, 305, 311, 312, 319, 320, 321, 325, 326, 328, 334, 339, 341, 346, 348, 349, 350, 351, 357, 361, 362, 363, 365, 369, 371, 375, 378, 379, 384, 387, 388, 390, 391, 394, 398, 400, 401, 402, 403, 408, 409, 413, 415, 420, 422, 423, 424, 425, 430, 432, 433, 442, 443, 444, 447, 454, 457, 459, 461, 462, 463, 467, 470, 474, 477, 480, 481, 485, 486, 493, 494, 495, 496, 499, 508, 511, 514, 517, 520, 522, 524, 533, 544, 546, 548, 549, 551, 555, 556, 557, 560, 564, 567, 568, 570, 573, 575, 577, 579, 581, 585, 591, 596, 597, 600, 601, 602, 603, 604, 608, 609, 610, 614, 615, 619, 623, 624, 625, 626, 627, 629, 631, 632, 633, 634, 635, 636, 637, 638, 640, 641, 643, 647, 648, 649, 650, 662, 669, 670, 671, 672, 673, 679, 681, 682, 686, 688, 691, 695, 696, 697, 699, 701, 710, 711, 721, 722, 723, 725, 727, 729, 730, 733, 734, 737, 740, 741, 742, 743, 749, 750, 751, 753, 755, 756, 757, 758, 759, 762, 766, 767, 768, 769, 771, 773, 774, 775, 782, 786, 787, 793, 796, 801, 802
Atomic absorption spectrometry	43, 62, 66, 108, 114, 127, 137, 145, 184, 195, 208, 223, 227, 263, 331, 339, 352, 353, 372, 383, 395, 396, 397, 414, 421, 428, 436, 439, 445, 458, 471, 472, 489, 497, 513, 526, 527, 535, 543, 550, 562, 576, 579, 583, 614, 617, 622, 628, 651, 683, 684, 693, 707, 715, 734, 735, 736, 738, 739, 754, 777, 780, 790, 791, 792

TABLE 1 (continued)

Category	References
Atomic emission spectrometry	43, 114, 318
Atomic fluorescence spectrometry	475
Chemi- or bio-luminescence	58, 83, 99, 140, 172, 178, 193, 265, 280, 302, 315, 327, 330, 337, 358, 374, 399, 406, 484, 488, 498, 523, 545, 553, 571, 587, 660, 674, 675, 678, 686, 705, 731, 760, 761, 783, 788, 797
Fluorimetry	31, 47, 80, 88, 185, 194, 214, 231, 260, 269, 278, 287, 310, 317, 318, 322, 329, 339, 347, 426, 444, 468, 480, 509, 529, 611, 677, 700, 724, 726, 748, 776, 781, 795, 800
Inductively-coupled plasma emission spectrometry	105, 188, 206, 354, 385, 518, 528, 565, 612, 656, 661, 712, 736, 738, 739, 763, 789, 790
Laser-based detection	317, 642, 644, 685
Molecular emission cavity analysis	538
Phosphorimetry	448, 698
Refractometry	27, 162, 164, 232, 362
Thermal lens spectrometry	642, 644, 685
Turbidimetry/nephelometry	11, 18, 37, 52, 87, 160, 254, 298, 355, 525, 530, 568, 706, 729
Electrochemical methods	16, 29, 61, 67, 82, 92, 149, 159, 165, 168, 174, 187, 192, 198, 209, 233, 285, 309, 332, 339, 360, 404, 412, 483, 504, 510, 539, 595, 618, 673, 680, 732, 744, 745, 746, 752, 779
Amperometry	61, 86, 102, 103, 115, 143, 155, 218, 219, 221, 231, 242, 247, 249, 255, 283, 290, 316, 356, 376, 377, 381, 386, 419, 452, 453, 455, 460, 465, 476, 478, 490, 491, 507, 531, 534, 546, 563, 592, 606, 609, 630, 637, 657, 658, 659, 676, 703, 704, 708, 713, 716, 719, 721, 747, 764, 765, 770, 785, 799
Conductometry	318, 362, 363, 479, 605
Coulometry	61, 113, 156, 187, 487, 507, 521, 536, 542, 594
Polarography	144, 159, 210, 289, 341, 443, 459, 506, 593
Potentiometry	1, 3, 152, 173, 196, 199, 213, 238, 262, 271, 332, 336, 416, 537, 547, 556, 572, 592, 616, 659, 717, 757, 778, 794
Chronopotentiometry/potentiometric stripping	215, 366, 521
Ion-selective electrodes/ISFETS	8, 12, 13, 20, 21, 24, 38, 50, 60, 68, 111, 112, 134, 170, 204, 229, 248, 250, 251, 268, 270, 282, 323, 359, 405, 407, 429, 446, 473, 479, 537, 552, 561, 578, 586, 608, 621, 652, 653, 666, 687, 709, 749
Voltammetry	20, 40, 67, 131, 200, 217, 225, 276, 288, 300, 324, 370, 389, 410, 449, 464, 466, 483, 492, 503, 512, 515, 558, 574, 580, 582, 613, 620, 639, 646, 668, 720, 747

TABLE 1 (continued)

Category	References
Enthalpimetry	516, 532
Radiochemistry	211
Enzymatic methods	9, 20, 46, 60, 65, 79, 154, 167, 194, 199, 226, 231, 233, 234, 247, 262, 264, 265, 278, 280, 283, 287, 322, 330, 340, 344, 345, 346, 348, 360, 369, 386, 387, 420, 422, 426, 432, 444, 460, 465, 478, 488, 493, 504, 510, 516, 530, 542, 546, 547, 557, 573, 585, 589, 592, 596, 615, 632, 660, 674, 678, 679, 680, 681, 686, 694, 703, 704, 719, 744, 746, 747, 750, 752, 758, 768, 779, 781, 786, 794
Immunoassay	80, 193, 231, 322, 348, 358, 530, 674, 681, 706, 760
Kinetic methods (nonenzymatic)	39, 45, 49, 56, 85, 96, 128, 129, 133, 150, 161, 174, 181, 191, 220, 232, 235, 252, 262, 302, 315, 349, 351, 364, 365, 371, 391, 411, 484, 501, 517, 522, 529, 533, 540, 541, 549, 553, 554, 561, 564, 566, 574, 587, 603, 604, 618, 631, 670, 695, 700, 701, 706, 713, 725, 748, 766, 770, 776
Gradient techniques	32, 42, 65, 87, 135, 140, 150, 151, 154, 162, 196, 197, 201, 220, 223, 232, 264, 301, 318, 373, 418, 435, 441, 482, 540, 598, 608, 660, 692, 791
Gradient calibration	227, 264, 338, 353, 372, 385, 441, 489, 526, 693, 707, 790
Gradient dilution	264, 275, 338, 441, 449, 707
Gradient scanning	275, 288, 338, 441, 449, 464, 492
Merging zones	23, 42, 43, 46, 48, 64, 65, 71, 79, 80, 126, 137, 166, 202, 206, 268, 286, 369, 393, 394, 530, 532, 610, 645, 681, 706
Sample splitting	3, 4, 701, 759, 776, 795
Selectivity studies	253, 338, 378, 441
Standard addition	354, 372, 385, 496, 513, 565
Stopped flow	20, 46, 64, 65, 71, 79, 80, 119, 154, 177, 191, 226, 253, 264, 266, 268, 275, 321, 338, 348, 349, 369, 393, 394, 414, 420, 422, 530, 540, 559, 611, 613, 681, 700, 706, 755
Titrations	10, 44, 59, 64, 71, 76, 82, 158, 183, 211, 213, 221, 253, 275, 288, 312, 318, 338, 373, 393, 414, 427, 559, 608, 671
Zone sampling	145, 166, 202, 415, 496, 540
Separation methods	
Liquid chromatography	89, 163, 195, 290, 304, 460, 514, 560, 574, 604, 721, 732, 751, 801
Dialysis	6, 9, 160, 199, 262, 393, 660, 686, 719, 743, 747, 758, 771

TABLE 1 (continued)

Category	References
Extraction	19, 20, 22, 31, 41, 55, 63, 64, 71, 77, 84, 90, 101, 116, 124, 136, 185, 189, 211, 214, 268, 304, 306, 307, 320, 352, 393, 437, 445, 447, 457, 462, 508, 528, 559, 584, 649, 651, 688, 697, 699, 714, 715, 729, 772, 777, 782, 791
Filtration	298, 308
Gas diffusion	57, 58, 124, 173, 196, 273, 402, 430, 451, 471, 475, 494, 500, 586, 608, 609, 629
Ion exchange	103, 110, 172, 237, 412, 428, 439, 497, 511, 576, 608, 628, 647, 683, 684, 712, 758, 766, 780
Isothermal distillation	50, 238, 268
Preconcentration	412, 428, 439, 503, 576, 583, 608, 628, 683, 684, 712, 754, 763, 773
Other techniques	
Hydrodynamic injection	338, 373, 394, 559, 608, 645
Intermittent pumping	48, 71, 132, 355
Viscosimetry	7, 162, 224, 362, 363
Microprocessor control	76, 91, 111, 118, 224, 260, 261, 286, 305, 312, 336, 346, 349, 361, 362, 365, 366, 373, 382, 418, 434, 501, 516, 530, 556, 588, 597, 635, 707, 726, 753, 756, 758
Incorporated column reactor	71, 146, 176, 199, 212, 233, 234, 280, 283, 284, 296, 340, 343, 344, 345, 348, 360, 386, 387, 422, 428, 439, 459, 460, 478, 490, 497, 501, 502, 511, 542, 546, 554, 566, 573, 576, 589, 608, 609, 638, 647, 648, 650, 678, 679, 680, 683, 684, 686, 694, 697, 703, 704, 712, 719, 747, 752, 754, 758, 759, 761, 763, 773, 774, 779, 781, 786, 789, 794, 795, 801
Microconduits	441, 608, 684
Special reactor geometry	567, 568, 608, 795

has decreased considerably (although it has stayed almost constant in terms of absolute numbers), whereas pharmaceutical and environmental applications have remained practically at the same percentage level, and there has been a marked increase in clinical and particularly industrial and biochemical (including biotechnological) uses of f.i.a. (Table 3). One of the reasons for these extensions of f.i.a. outside research laboratories may be the large number of international seminars, workshops and conferences at which f.i.a. has been the focus of attention. Another reason may be the increasing availability of commercial instrumentation for f.i.a., which is now produced in Sweden (Bifok/Tecator), U.S.A. (FIAtron, Lachat, Control Equipment), Japan (Hitachi) and Brazil (Micronal); the manufacturers are arranged in the same sequence in which they introduced their equipment.

When the publications on f.i.a. are arranged according to their country of origin (Fig. 4), the story of f.i.a. is highlighted. Overall, 28 countries are

TABLE 2

Species determined by flow injection analysis

Species	References
Acetaminophen	464, 491, 558
Acetoacetate	596
Acid/base	44, 59, 253, 414, 532, 671, 716, 717
Acidity constants	782
Acids, volatile	312
Alanine	596
Albumin	42, 47, 80, 95, 138, 262, 369, 553, 681, 713
Alcohols	131, 218, 226, 247, 387, 510, 680
Alkalinity, total	619, 749
α-Amylase	557
Aluminium	25, 48, 166, 206, 245, 259, 293, 295, 520, 656, 757, 769
Amines	255, 310, 324, 448
Aminoacylase	615
Amino acids	255, 290, 310, 480, 604, 618, 732, 783, 788
Ammonia/ammonium	1, 52, 91, 110, 173, 238, 245, 246, 266, 273, 415, 451, 494, 580, 632, 737, 741, 745, 749
Amoxillin	536
Anilide	217
Aniline	410
Antimony	458
Aromatic hydrocarbons	214, 306
Arsenic	102, 103, 225, 384, 518, 612, 617, 735
Ascorbic acid	20, 29, 61, 478, 536, 563, 764
Aspirin	410
Barium	518, 572, 656, 712
Benzoquinone	143, 316
Beryllium	241, 712
Bile acid	677
Bilirubin	623, 733
Bismuth	135, 208, 414, 421, 458, 558
Boron	38, 105, 169, 206, 245, 468, 793
Bromamine	277
Bromide	767
Bromine	129, 235
Brucine	388
Butylated hydroxyanisole	503
Cadmium	37, 90, 172, 215, 366, 370, 377, 428, 462, 464, 508, 515, 518, 521, 527, 558, 639, 683, 684, 712
Caffeic acid	464, 491, 595
Caffeine	19
Calcium	10, 21, 26, 43, 49, 54, 56, 85, 108, 112, 114, 195, 202, 206, 223, 244, 245, 248, 250, 253, 258, 270, 349, 350, 373, 383, 397, 425, 473, 497, 528, 543, 550, 570, 572, 608, 622, 634, 656, 717, 792
Carbohydrates	219, 514, 618
Carbonate (total)	451

TABLE 2 (continued)

Species	References
Carbon dioxide	57, 196, 430, 451
Catecholamine	770, 799
Cephalosporins	516, 679
Chemical oxygen demand	104, 117, 120, 123, 125, 175, 180, 261, 274, 294, 303, 305, 384
Chloramine	277
Chloranilines	448
Chlorate	755
Chloride	4, 6, 59, 91, 148, 171, 204, 207, 245, 250, 251, 253, 282, 355, 394, 398, 409, 416, 525, 616, 662, 666, 749, 756, 767
Chlorine	129, 235, 271, 272, 400, 646
8-Chlorotheophylline	447
Chlorophenols	448, 563, 490, 721
Chlorpromazine	412, 464, 558
Cholesterol (free)	386, 625
Choline	386
Cholinesterase	460, 602
Chromium	30, 69, 253, 353, 388, 391, 442, 513, 518, 555, 579, 656, 707, 711, 763
Citric acid	605
Cobalt	27, 83, 140, 191, 203, 220, 232, 252, 302, 371, 411, 423, 484, 498, 518, 527, 549, 564, 572, 712
Codeine	41
Colouring matter (food)	200, 582
Complex stability constants	522, 604
Concanavelin A	530
Copper	24, 27, 37, 62, 122, 127, 135, 140, 162, 174, 203, 206, 215, 220, 232, 282, 315, 331, 352, 354, 366, 377, 436, 442, 464, 470, 485, 515, 527, 528, 529, 535, 571, 572, 576, 583, 622, 651, 683, 684, 700, 712, 720, 722, 748, 754, 757, 780, 792, 797
Corticosteroids	78, 239
Creatinine	408, 632
Cyanide	251, 452, 455, 561, 578, 586, 611, 616, 621, 640, 669, 726
Cysteine	448, 490, 563
Cystine	490
Diffusion coefficients	142, 162, 224, 325, 363, 519
Dihydroxyphenylalanine	61, 285
Diphenylhydramine	447
Dithionite	632
Dopamine	61, 285, 464, 492, 536, 613, 764
Drugs	193, 347, 361, 488, 740
Elements (multi-)	105, 162, 188, 206, 354, 385, 518, 528, 572, 656, 661
Epinephrine	61, 536
Ethanol	131, 207, 218, 226, 247, 387, 510, 680

TABLE 2 (continued)

Species	References
Ferroxidase	768
α-Fetoproteins	674, 760
Fluoride	111, 282, 359, 652, 653, 725, 729, 749
Formaldehyde	459, 637, 650
Free fatty acids	556, 649
Fructose	514
Galactose	386, 747, 758
Gallium	88, 185, 260
Germanate	225
Glucose	9, 20, 46, 64, 71, 199, 231, 269, 280, 287, 330, 345, 348, 360, 386, 422, 493, 542, 547, 573, 626, 659, 660, 678, 686, 703, 704, 719, 743, 779
Glucose oxidase	231, 247, 287
Glutamate	680
Glutamyl transferase	394
Glycerol	7, 23
Glycine	47
Glutarate oxaloacetate transaminase	420
Glutarate pyruvate transaminase	420
Hardness (water)	524
Heterocyclic nitrogen compounds	448
Hexacyanoferrate (II/III)	459, 487, 491, 492, 536, 559, 609, 637
Hydrazine	28, 563, 574, 580, 609, 632, 637, 705
Hydrogen peroxide	58, 194, 247, 265, 356, 345, 546, 603, 643, 747, 761, 781, 795
Hydroquinone	487, 536
Hydroxyacetanilide	217
Hydroxybutyrate	596
17-α-Hydroxyprogesterone	760
Hydroxy compounds (aliph./arom.)	448
Hypohalites	580
Immuno-γ-globulin (IgG)	322, 530, 706
Indole derivatives	523
Iodate	357, 459, 609, 637
Iodide	102, 282, 376, 381, 453, 534, 561, 616, 618, 767, 796
Iodine	327, 364, 545, 670
Iodine value	556
Insulin	760
Iron	29, 86, 166, 206, 243, 245, 281, 293, 395, 423, 442, 461, 474, 508, 527, 528, 579, 581, 594, 614, 622, 627, 636, 656, 658, 682, 749, 757, 759, 773, 776
Isoniazid	410, 476
Isoprenaline	413, 443
Isosorbide	144
Ketone bodies	402

TABLE 2 (continued)

Species	References
β-Lactams	516
Lactate	278, 283, 369, 373, 426, 585, 596, 680, 694
Lactate dehydrogenase	264, 369, 785
Lead	32, 37, 90, 215, 232, 334, 352, 366, 370, 428, 457, 458, 464, 515, 518, 521, 527, 558, 572, 683, 684, 712
Lipids	624
Lithium	263, 528, 792
α-Macroglobulin	369
Magnesium	43, 45, 49, 56, 66, 85, 195, 206, 349, 383, 397, 403, 518, 526, 528, 543, 550, 570, 572, 622, 656, 707, 792
Maleic acid	459, 637
Maltose	514
Manganese	53, 162, 206, 220, 232, 245, 378, 518, 572, 622, 695, 712, 774, 776
Meptazinol	67
Mercury	165, 381, 453, 471, 475, 518, 748
Metals (traces)	20, 115, 127, 184, 188, 189, 220, 352, 354, 366, 384, 428, 439, 442, 445, 515, 527, 528, 551, 651, 683, 712
Molybdenum	22, 55, 351, 561, 610, 631, 656
Nicotinamide adenine dinucleotide	493, 589, 630
Nickel	203, 220, 232, 352, 354, 371, 527, 564, 572, 628, 683, 707, 712
Nitrate	8, 12, 34, 51, 71, 81, 91, 148, 157, 170, 245, 284, 326, 357, 373, 389, 424, 459, 480, 481, 496, 609, 637, 640, 687, 737, 749
Nitrite	15, 51, 71, 81, 132, 148, 245, 266, 284, 300, 326, 357, 424, 459, 480, 481, 499, 512, 609, 637, 640, 708, 757
Nitrogen/total nitrogen	3, 5, 13, 38, 50, 68, 109, 126, 228, 245, 258, 268, 425
o-Nitrophenol	459
Nitroprusside	765
Norepinephrine	558
Nucleotides	746
Ochratoxin A	800
Oxygen	345, 346
Ozone	575
Penicillins	516, 723, 794
Penicilloic acid	289
Perchlorate	777
pH	21, 64, 112, 244, 248, 270, 429, 608, 640, 757, 778
Phenols	249, 316, 410, 483, 558, 646
Phosphate/phosphates	1, 6, 23, 59, 64, 89, 106, 113, 133, 163, 182, 225, 237, 266, 276, 279, 320, 375, 401, 466, 480, 495, 512, 567, 568, 601, 606, 616, 632, 737, 749, 751

TABLE 2 (continued)

Species	References
Phospholipids	465
Phosphonate	601, 751
Phosporus	2, 5, 13, 38, 94, 109, 126, 190, 206, 245, 258, 267, 268, 425, 433, 544, 548, 560, 696, 789
Polynuclear aromatic hydrocarbons	214, 306
Potassium	8, 13, 31, 38, 43, 112, 114, 145, 206, 245, 248, 250, 323, 446, 472, 528, 622, 656
Procyclidine	304
Propantheline bromide	635
Protein	17, 118, 406, 425, 587, 591, 674, 706, 713
Pyridoxal	724
Pyrophosphatase	432
Pyruvate	596
Reaction rate constants	517, 541
Refractive index	27, 98, 442
Salicylamide	635
Selenium	518, 617, 734
Silicate	177, 225, 319, 466, 477, 480, 565, 656, 697, 710
Silver	381, 419, 453, 458, 508
Sodium	8, 114, 250, 472, 528, 622, 656
Strontium	45, 85, 518
Sugars	219, 514, 704, 747, 758
Sulphamethizole	635
Sulphanilamide	618, 740
Sulphate	11, 87, 160, 162, 171, 186, 245, 254, 256, 298, 355, 508, 511, 533, 538, 647, 672, 729, 730
Sulphide	83, 134, 179, 381, 453, 454, 467, 538, 640, 672, 676, 709
Sulphite	16, 321, 374, 407, 451, 538, 616, 672
Sulphonyl haloamines (aromatic)	277
Sulphur dioxide	71, 147, 212, 266
Sulphur organics	448, 618
Surfactants	63, 101, 136, 437, 531, 762
Terbium	329, 545
Terbutaline sulphate	361
Tetracycline	675
Theophylline	681
Thiamine	77, 509
Thiocyanate	616, 618
Thiols	134
Thiourea	618
Thorium	135
Thyroxine	358
Titanium	311, 656
Triethylamine	99
Triglycerides	119, 231, 681
Trypsin	167, 379
Tungsten	561, 656

TABLE 2 (continued)

Species	References
Uranium	390, 459, 577, 637, 775
Urea	60, 64, 71, 79, 199, 360, 744
Uric acid	633, 678, 752
Valinomycin	539
Vanadium	32, 128, 161, 232, 459, 637, 656, 766
Viscosity	7, 162, 224, 362, 363
Water	82, 221, 414, 537, 638
Zinc	62, 172, 203, 206, 245, 331, 352, 354, 377, 428, 436, 445, 515, 521, 527, 528, 558, 562, 572, 622, 684, 715, 720, 771, 792.
Zirconium	656

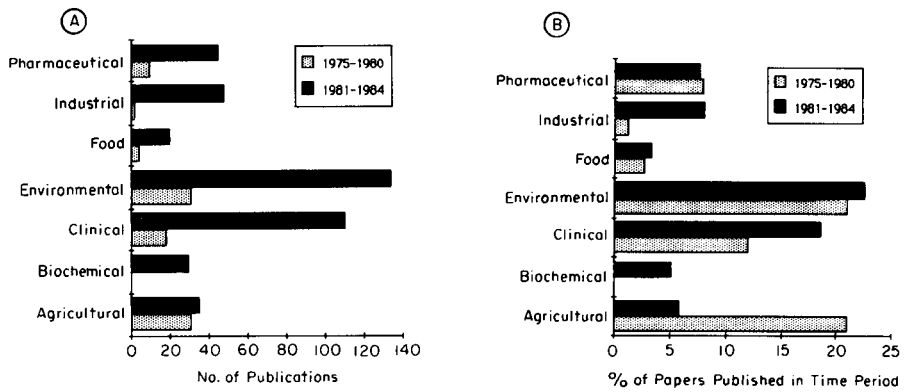

Fig. 3. Dedicated f.i.a. publications in the time spans 1975—1980 and 1981—1984 depicted as: (A) absolute values; (B) relative values.

represented; the U.S.A. and Japan clearly dominate the field at present (each accounting for 20—30% of all the papers published annually over the past four years), closely followed by Great Britain. Obviously, in these countries, there are various groups working independently on f.i.a. [according to N. Ishibashi (private communication) over 60 groups are conducting f.i.a. research in Japan]. In contrast, no paper originating in the U.S.S.R. could be traced in the accessible literature.

It is interesting to note that the overall increase in the volume of publications of f.i.a. gained momentum in 1979, and it is therefore relevant to ask what triggered the interest in this new technique. It takes one to two years from the time when a research project is conceived to the time when a paper is published, thus 1978 seems to be the year in or before which the "trigger" papers on f.i.a. were published. Until then, 60% of all published f.i.a. papers

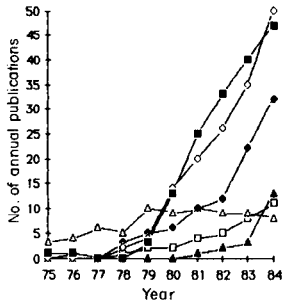

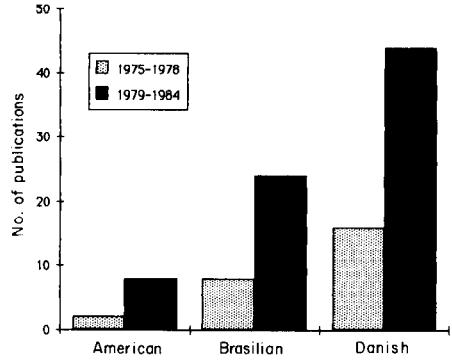

Fig. 4. Growth of publications on f.i.a. published annually in 6 different countries; Japan (◇), USA (▪) and England (◆) represent the most prolific development, while China (□) and Germany (▲) are examples of nations where the number of publications, after an initial delay time, is now increasing significantly. The annual output from Denmark (△) has varied little for some years.

Fig. 5. Distribution of f.i.a. publications amongst the three original research teams in 1978 and in 1984.

originated from three research teams: one in the U.S.A. (headed by K. K. Stewart), one in Brazil, and the Danish group, the latter two working in close cooperation and publishing a number of joint papers [2—5, 13, 14] (Fig. 5). By 1979, the versatility of f.i.a. had been proven by the development of a number of multiline and two-channel systems [1—23], and the feasibility of separations like dialysis [6], liquid-liquid extraction [19] and gas diffusion [57] had been demonstrated. Importantly, f.i.a. was shown to be based on the combination of sample injection, controlled dispersion and reproducible timing, and the concept of limited, medium and large dispersion was thus established in Part X of the series of papers originating from the Danish group [20], thereby allowing the rational design of any f.i.a. manifold. Since at that time the Stewart team used only a single-line system and was only to adopt the f.i.a. term a year later (a.m.f.i.a. [62]), it was mainly the experimental evidence published outside the U.S.A., summarized in an excellent review by Betteridge in 1978 [33], which was the triggering factor for future proliferation.

Since then, numerous significant advances have been made in the concepts and technology of f.i.a. The concept of controlled dispersion led to the development of gradient techniques [264, 338]. Reversed f.i.a., in which the sample rather than the reagent serves as carrier stream, was suggested by Johnson and Petty [279]. The reagent-saving merging zones approach (Mindegaard [42] and Bergamin et al. [23]) became the first step towards truly economical flow-injection systems, and various ingenious intermittent sampling modes, based on the original design of the Brazilian sampling device, were reported. The group at CENA in Piracicaba (Brazil) further

TABLE 3

Areas of application of flow injection analysis and general references

Area of application	References
Agricultural	93, 268, 673
Feed	26, 258, 425
Fertilizers	12, 13, 38, 190
Plant material	2, 3, 5, 11, 17, 22, 23, 25, 43, 48, 50, 53, 55, 92, 109, 126, 145, 166, 169, 202, 206, 238, 245, 281, 310, 355, 457, 496, 612, 617, 622, 631
Soil	8, 12, 30, 48, 52, 68, 69, 81, 92, 94, 170, 202, 204, 228, 267, 424, 429, 520, 621, 622, 627, 710, 769, 778, 793
Biochemical	167, 219, 255, 301, 309, 345, 347, 348, 379, 402, 404, 406, 436, 478, 488, 516, 539, 587, 591, 597, 615, 630, 632, 633, 770, 787, 799
Biotechnology	679, 680, 723, 743, 750, 771
Clinical	58, 95, 108, 118, 138, 154, 178, 193, 194, 195, 231, 250, 262, 269, 270, 301, 323, 358, 369, 387, 394, 396, 436, 474, 488, 530, 588, 645, 674, 692, 694, 706, 734
Blood	42, 57, 173, 226, 244, 273, 348, 426, 460, 623, 629, 675, 686, 719, 744, 745, 800
Blood serum	6, 8, 9, 21, 47, 60, 71, 80, 95, 112, 131, 174, 199, 248, 251, 263, 278, 280, 287, 322, 330, 331, 347, 360, 369, 383, 386, 394, 395, 397, 408, 420, 446, 465, 470, 472, 485, 493, 528, 543, 550, 553, 562, 570, 573, 596, 602, 623, 624, 625, 626, 629, 633, 656, 660, 677, 678, 681, 682, 700, 703, 704, 713, 719, 733, 740, 741, 744, 745, 758, 760, 768, 777, 785, 792
Urine	160, 359, 408, 412, 462, 606, 629, 633, 703, 752, 777
Environmental	90, 384, 471, 646, 673
Air	147, 212, 235, 374, 409, 560, 745
Water	4, 7, 11, 12, 15, 21, 24, 25, 28, 34, 52, 53, 63, 69, 81, 87, 89, 91, 101, 104, 106, 110, 113, 114, 117, 120, 123, 125, 132, 136, 157, 170, 171, 175, 180, 182, 186, 202, 210, 215, 236, 237, 245, 246, 254, 256, 261, 265, 272, 274, 279, 281, 284, 294, 295, 298, 303, 305, 310, 319, 320, 326, 327, 349, 350, 351, 355, 359, 366, 375, 388, 391, 398, 400, 401, 403, 407, 409, 411, 415, 416, 419, 424, 428, 432, 433, 437, 439, 451, 452, 454, 455, 457, 461, 467, 468, 473, 475, 477, 480, 481, 483, 494, 495, 499, 508, 511, 515, 520, 524, 525, 527, 531, 570, 575, 576, 579, 586, 612, 617, 619, 621, 628, 634, 640, 641, 643, 647, 650, 652, 666, 669, 676, 683, 684, 696, 709, 711, 729, 730, 735, 737, 741, 745, 754, 757, 762, 766
Speciation	474, 555, 579, 581, 594, 614, 636, 711, 759, 763, 780
Food	16, 47, 54, 62, 200, 556, 582, 605, 617, 680, 700, 701, 708, 746, 747
Beer	312, 510
Beverages	226, 402, 451, 488, 503, 653, 704

TABLE 3 (continued)

Area of application	References
Industrial	207, 214, 243, 356, 385, 393, 409, 466, 508, 557, 580, 649, 682, 717, 723, 747
Geological/mineralogical	86, 223, 293, 311, 329, 390, 533, 548, 578, 579, 581, 670, 775
Metallurgical	122, 203, 241, 259, 353, 354, 458, 513, 544, 586, 610, 722, 789
Process control	261, 338, 393, 546, 556, 578, 598, 680, 718, 743
Pharmaceutical	19, 29, 37, 41, 56, 57, 61, 67, 77, 78, 144, 193, 221, 239, 247, 249, 264, 276, 277, 283, 285, 289, 304, 307, 316, 325, 328, 341, 349, 361, 364, 399, 409, 410, 413, 447, 448, 464, 476, 490, 491, 492, 503, 509, 514, 516, 523, 536, 563, 569, 589, 635, 638, 740, 767, 783, 788, 794, 798
General	1, 10, 20, 44, 45, 49, 51, 66, 79, 82, 83, 92, 98, 102, 105, 111, 116, 124, 127, 128, 140, 148, 152, 156, 158, 159, 161, 163, 164, 165, 168, 172, 177, 179, 185, 191, 208, 209, 210, 211, 213, 220, 223, 224, 225, 242, 252, 257, 265, 282, 285, 286, 288, 291, 300, 302, 306, 308, 313, 314, 315, 317, 318, 321, 324, 329, 332, 334, 339, 340, 342, 346, 352, 357, 362, 363, 365, 367, 368, 370, 371, 372, 373, 376, 377, 378, 379, 381, 389, 392, 396, 405, 414, 422, 423, 430, 434, 435, 440, 442, 443, 444, 449, 453, 459, 463, 469, 479, 482, 486, 487, 495, 497, 498, 500, 502, 504, 506, 507, 512, 517, 518, 519, 521, 522, 526, 529, 532, 534, 535, 537, 538, 541, 542, 547, 549, 551, 552, 554, 558, 562, 565, 566, 567, 568, 571, 572, 574, 577, 583, 584, 593, 594, 595, 599, 600, 601, 603, 604, 607, 709, 611, 613, 614, 616, 618, 620, 637, 639, 642, 644, 648, 651, 657, 658, 659, 661, 662, 667, 671, 672, 682, 685, 687, 688, 689, 690, 691, 693, 695, 697, 698, 702, 705, 707, 712, 714, 715, 716, 720, 721, 724, 725, 726, 732, 736, 738, 739, 748, 751, 753, 755, 756, 761, 764, 765, 773, 774, 776, 779, 781, 782, 791, 795, 796, 797, 801, 802, 803, 804
Educational	59, 139, 253, 299, 333, 446, 727
Review articles	20, 33, 35, 36, 64, 65, 71, 93, 96, 97, 100, 107, 121, 124, 130, 137, 139, 141, 152, 162, 178, 184, 188, 196, 197, 198, 201, 205, 216, 222, 227, 229, 230, 232, 233, 234, 240, 262, 266, 268, 275, 292, 296, 297, 301, 328, 335, 337, 338, 373, 382, 384, 393, 418, 427, 431, 438, 440, 441, 450, 456, 480, 488, 489, 501, 505, 540, 545, 559, 569, 588, 590, 592, 598, 608, 645, 654, 655, 673, 692, 699, 718, 731, 742, 749, 784, 790, 798
Books	153, 663, 664, 665

demonstrated the practicability of the f.i.a. approach by routinely analysing in 1982 over 300 000 samples of agricultural and environmental origin in their laboratory [440]. New research groups discovered special ways of exploiting f.i.a. Thus, for example, biochemical and biotechnological applications using immobilized reagents and enzymes [344, 758], formation of active reagents in situ [637], kinetic advantages of f.i.a. [755], f.i.a./a.a.s. using hydride generation and Karl Fischer methods [208, 638], and comprehensive studies of liquid-liquid extraction mechanisms in flow-injection systems [688] have been reported by different groups. Clinical applications have been actively pursued in England [645, 689] and Japan [623—626]. Advanced electrochemical applications have recently appeared from two American groups [618, 639]. A very active spanish group has contributed to both theoretical and practical aspects of f.i.a. [665, 784, 802].

FUTURE DEVELOPMENTS

While the first decade of development of f.i.a. has fulfilled the initial promise of "a new concept of fast continuous flow analysis", a new, more general rôle of f.i.a. is becoming increasingly apparent, being best illustrated by the following examples.

Within the last two years, f.i.a. has started to become a novel tool for on-line process control. The arrangement for this application is depicted in Fig. 6. The flow-injection system, comprising a detector, recording device, carrier and reagent lines, and a pump, is connected via a sampling device to a reactor. At the start, the response of the detector is calibrated by repeated injections of standards or by means of a solution of a final or intermediate product, depending on the nature of the process to be monitored. Once a desired level has thus been established (cf. the three injections shown on the

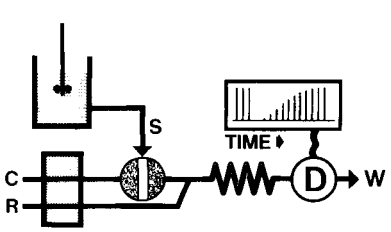

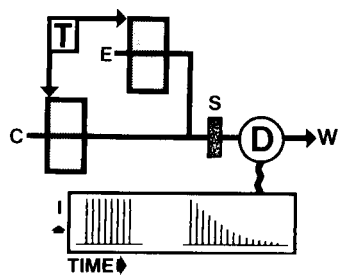

Fig. 6. Flow-injection system for on-line process control comprising carrier (C) and reagent (R) lines, a detector (D) connected to a recording device, and a sampling unit (S) communicating with a reactor vessel, the content of which is monitored intermittently.

Fig. 7. Impulse-response system comprising a line with carrier stream (C), test liquid (E), timer (T) for control of two separate pumps, target material (S), and a recording obtained via the detector (D).

left of Fig. 6), the sampling valve is connected to the reactor and the formation of the desired species is monitored by intermittent injections. By repeatedly monitoring the baseline (carrier stream) and the product formation (sample injection), the function of the sensor (detector) used is checked regularly and any drift in the baseline or deterioration of the detector function can easily be diagnosed and accounted for. In this way, it is possible to eliminate discrepancies between actual changes of the process to be monitored and variations of the observed signal, which may be due to sensor deterioration. By now, well over 100 f.i.a.-based process control analysers are used on line at Shell, Dow Chemicals, Kodak, Conoco and Ciba-Geigy. So far all these instruments have been custom-made; as the need for this type of instrumentation has become recognized, the first f.i.a. process control monitor will soon be marketed by FIAtron. Recently, the ingenious combination of hydrodynamic injection and exploitation of exponential concentration gradients for process monitoring was discussed by Gisin [806].

The capability of performing highly reproducible, fast, repetitive measurements is the hallmark of f.i.a., allowing the economical data collection so frequently needed in research and applied areas. Therefore the impulse-response technique (Fig. 7) is perhaps the most important future embodiment of this new technology. This technique is based on the repetitive action of a well-defined concentration zone of a selected chemical species (E) on a target (S), situated in an unsegmented carrier stream consisting of an inert solvent. By continuously monitoring the behaviour of the target material, the response of the target can be recorded automatically over prolonged testing periods, using a variety of test solutions (E). Thus, the rate of corrosion of metals from surfaces, the efficiency of corrosion inhibitors, etc., may be studied by injecting corrosive species and by monitoring the material released into the carrier stream, by means of a.a.s. or i.c.p. Pioneering work of Wightman et al. [807] on the measurement of the rate of release of DOPA from superfused brain tissue is an example of such an approach in the biochemical field. Another example is the study of receptor stimulant interaction on thin membranes [404], which according to M. Thompson (private communication) is a widely applicable approach for the study of biological systems because it employs dynamic conditions. Additionally, the technique has very promising potential in pharmacological research for the study of drug extraction and transport in membranes. Obviously, the applications of the impulse-response flow-injection technique may range from scientific to industrial ones while the target may vary from inorganic to biological materials. The target may, of course, even be a detector in itself, so that its lifetime, speed and slope of response may be scrutinized and compared with the performance of other devices. A recently developed f.i.a. conversion technique, which will be reported at a later date, and the flow-injection ellipsometry method described by Jönsson et al. [787] are yet other variations on the theme of a chemically controlled release from a solid phase.

In addition to the exploitation of f.i.a. as a tool for repetitive measurements on other systems, the general technique is well suited to perform such

measurements on itself under computer control. Selectivity studied [378] and simplex optimization [413] are the first steps towards this goal. Chemometrics and f.i.a. will benefit from mutual interaction, f.i.a. yielding highly reproducible data and the methods of chemometrics providing their rational interpretation. A multiarray detector/f.i.a. combination should be ideal for such purposes.

Inherently, f.i.a. allows microvolumes to be handled in a protected environment. This capability of the method is particularly advantageous in the following four areas: (a) when the samples and/or the reagents used are toxic; (b) when the samples to be assayed contain concentrations of analyte at trace levels, in which case individual samples can be protected effectively against cross-contamination and blank values can continuously be monitored via the baseline signal; (c) when sensitive reagents are used, like those which are easily oxidized or reduced [637], or decomposed by light; and (d) when volatile solvents are used to dissolve the material under study. In the latter category, the most inspiring example is the work of Olesik et al. [808] on the use of supercritical carbon dioxide for the study of the decomposition of organic compounds by Fourier-transform infrared spectroscopy. Olesik et al. use a flow-injection system operated at 115 atm. and an injected volume of 0.2 μl; the research shows the technical feasibility of such of an approach (with standard h.p.l.c. components to construct the system). The idea could be taken to a further level by simultaneously injecting two zones (i.e., sample and reagent) and exploiting the concentration profiles at the interface between these two merging zones [378]. Further, derivatization of the parent compound might be possible so that spectra of the pure compound and its derivatives could be obtained in a single experimental run, with the aim of facilitating structural studies and identification of compounds; spectral libraries can, via the derivatization, be divided into more readily accessible sections. As in the case of the previously mentioned combination of f.i.a. with a.a.s. or i.c.p., this could substantially enhance the performance of expensive detectors with negligible investment in terms of equipment and labour.

Thus, after ten years, f.i.a. is emerging as a diagnostic tool, capable of sophisticated solution handling, being fully compatible with the present status of detector and computer technology. Since it was established how flow-injection channels can be scaled down [608], the other components of flow-injection systems have been miniaturized and integrated, yielding more robust devices with improved sample and reagent economy. These integrated microconduits benefit from yet another recent innovation: optosensing at active surfaces [809]. This mode of detection, in its simplest form, uses reflectance spectrophotometry of a reagent immobilized on a suitable support in the flow channel in the manner shown in Fig. 8. Besides being well suited for miniaturization, this novel sensor allows integration of reagents (and enzymes) into the detection area of any flow-injection system, in prepacked, easily replaceable form. It is of interest that some of the immobilization

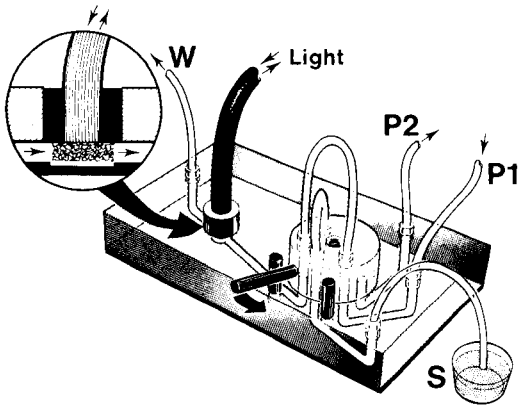

Fig. 8. Integrated microconduit (the size of a credit card) comprising an injection valve, a flow-through channel, and an optosensor furnished with a reagent, immobilized on a cellulose pad, situated in the channel within the observation field of an optical fibre (insert). S, sample; P1 and P2, connections to pumps; and W, waste.

techniques developed for solid reagents [810] are well suited for preparing optosensitive surfaces. Flow injection analysis, however, is not limited to the use of reversible reagents which can be immobilized. By using a more intricate microconduit, optosensing has been achieved successfully at the surface of a gas diffusion membrane, where reagents were renewed for each successive cycle, for the purpose of measuring traces of ammonia and/or clinically relevant levels of urea in serum. In that work, microlitre volumes of sample and reagents were used per sampling cycle, but further downscaling of such systems is presently in progress. The construction of submicrolitre devices, based on the microconduit technology and designed to operate at low pressure and pumping rates, using micropumps, valveless hydrodynamic injection and optosensing at active surfaces, has already begun. A compromise between what is feasible and what is practical to use, will be the decisive factor governing the choice between micro and submicro flow-injection systems, the parameters of which are outlined in Table 4. For industrial and environmental applications, there is not much incentive to miniaturize the flow-injection systems further, but the ability to analyse submicrolitre sample volumes could open quite new possibilities for clinical and biochemical assays.

FLOW-INJECTION SYSTEMS AS RESEARCH TOOLS

To become a general tool for chemical research, the capability of f.i.a. will have to be extended from relative measurements (based on calibration with standards) to absolute values, which are required when diffusion coefficients (Table 2), reaction rates [811] or two-phase dissociation constants [782] are to be measured. As the above references indicate, such developments with modified system designs are already in progress.

TABLE 4

Scaling of flow-injection systems[a]

System	Cross-sectional channel area (mm^2)	Channel diameter (mm)	S_v (μl)	V_r (μl)	L cm	Q ($\mu l\ min^{-1}$)
Coiled tubing 1974	1.8	1.5	500	7000	400	18000
1980	0.2	0.5	30	300	150	2500[b]
Microconduits 1983	0.8	(1.0)[c]	15	150	19	1250[b]
	0.5	(0.8)	9	94	19	780
	0.2	(0.5)	4	38	19	313
	0.1	(0.36)	2	20	19	156
	0.05	(0.25)	1	9	19	78
	0.02	(0.16)	0.4	3.8	19	31
	0.01	(0.11)	0.2	2.0	19	16

[a]The underlined numbers refer to previously and/or currently typical systems. [b]These two systems have identical dispersion factors ($S_{1/2}/V_r$ = 0.34). [c]As the flow channels of the microconduits are U-shaped, this dimension denotes the "effective diameter".

The state of the theory of f.i.a., unfortunately, is still at a rather lamentable level compared with the sophisticated level of many of the practical developments. The concept of controlled dispersion, based on the dispersion coefficient, the time and the dispersion factor [608], is a useful tool for the rational design of a flow system and for comparison and scaling of channels in f.i.a., yet it does not describe the response in a comprehensive fashion. While the models of physical dispersion in a single-line channel under laminar flow conditions are relatively straightforward, the description of a real flow-injection system, with merging streams and chemical reactions, still has to be worked out. Despite a number of papers on the theory of f.i.a. (Table 1), no comprehensive mathematical solution is available at the moment, and the recent zealous controversy over previous attempts to describe the physical dispersion in a flow-injection channel [802—804] illustrates how difficult it is to describe even a one-line system comprehensively. With the ever-increasing number of systems into which the concepts of f.i.a. are incorporated, this task becomes progressively more difficult. Therefore attempts to put the function of individual devices, such as dialysers [771] or gas-diffusion units [500], on a rational basis seems to be more rewarding; the authors of these papers took into account the peculiarities of each design and then subjected their conclusions to rigorous experimental tests.

Conclusion

Throughout the past decade, the flow-injection method has grown in scope, both conceptually and in the number of applications. Replacement of the established practice of homogeneous mixing by the exploitation of concentration gradients, well defined in time and space, has provided a new approach to solution handling and information gathering on chemical systems.

Flow injection analysis was initially described as "a method based on injection of a liquid sample into a moving unsegmented continuous carrier stream of a suitable liquid. The injected sample forms a zone, which is then transported towards a detector which continuously records the absorbance, electrode potential, or any other physical parameter as it continuously changes as a result of the passage of sample material through the flow cell" [153]. As the method developed further, merging zones and zone penetration techniques introduced additional components into the concentration gradient, which thus became more complex and more informative. The reversed f.i.a. technique [477] interchanged the original roles of the carrier and the sample. Also the concept of what a sample may be has evolved from the traditional view of "a sample to be analysed", to a flowing stream intermittently sampled (process control) and most recently to a target to be treated periodically by a zone of a reagent. What has remained unchanged, however, is the idea of information gathering from a concentration gradient formed while a well-defined zone of a fluid disperses into a continuous unsegmented stream of carrier. Some will object that such a description is too loose to become a definition of Flow Injection Analysis. It is, however, the remarkable versatility of the method which defies the attempt to formulate a rigid definition capable of describing not only what has been achieved but also what will be achieved by applying the basic concepts in the future.

The authors wish to express their appreciation to the Danish Council for Scientific and Industrial Research for financial assistance.

REFERENCES

1 J. Růžička and E. H. Hansen, Flow Injection Analysis. Part I. A New Concept of Fast Continuous Flow Analysis, Anal. Chim. Acta, 78 (1975) 145; Dan. Pat. Appl. No. 4846/74; U.S. Pat. No. 4.022.5.75.

2 J. Růžička and J. W. B. Stewart, Flow Injection Analysis. Part II. Ultrafast Determination of Phosphorus in Plant Material by Continuous Flow Spectrophotometry, Anal. Chim. Acta, 79 (1975) 79.

3 J. W. B. Stewart, J. Růžička, H. Bergamin F° and E. A. G. Zagatto, Flow Injection Analysis. Part III. Comparison of Continuous Flow Spectrophotometry and Potentiometry for the Rapid Determination of the Total Nitrogen Content in Plant Digests, Anal. Chim. Acta, 81 (1976) 371.

4 J. Růžička, J. W. B. Stewart and E. A. G. Zagatto, Flow Injection Analysis. Part IV. Stream Sample Splitting and Its Application to the Continuous Spectrophotometric Determination of Chloride in Brackish Waters, Anal. Chim. Acta, 81 (1976) 387.

5 J. W. B. Stewart and J. Růžička, Flow Injection Analysis. Part V. Simultaneous Determination of Nitrogen and Phosphorus in Acid Digests of Plant Material with a Single Spectrophotometer, Anal. Chim. Acta, 82 (1976) 137.

6 J. Růžička and E. H. Hansen, Flow Injection Analysis. Part VI. The Determination of Phosphate and Chloride in Blood Serum by Dialysis and Sample Dilution, Anal. Chim. Acta, 87 (1976) 353.

7 D. Betteridge and J. Růžička, The Determination of Glycerol in Water by Flow Injection Analysis — A Novel Way of Measuring Viscosity, Talanta, 23 (1976) 409.

8 J. Růžička, E. H. Hansen and E. A. G. Zagatto, Flow Injection Analysis. Part VII. Use of Ion-Selective Electrodes for Rapid Analysis of Soil Extracts and Blood Serum. Determination of Potassium, Sodium and Nitrate, Anal. Chim. Acta, 88 (1977) 1.

9 E. H. Hansen, J. Růžička and B. Rietz, Flow Injection Analysis. Part VIII. Determination of Glucose in Blood Serum with Glucose Dehydrogenase, Anal. Chim. Acta, 89 (1977) 241.
10 J. Růžička, E. H. Hansen and H. Mosbæk, Flow Injection Analysis. Part IX. A New Approach to Continuous Flow Titrations, Anal. Chim. Acta, 92 (1977) 235.
11 F. J. Krug, H. Bergamin F°, E. A. G. Zagatto and S. S. Jørgensen, Rapid Determination of Sulphate in Natural Waters and Plant Digests by Continuous Flow Injection Turbidimetry, Analyst (London), 102 (1977) 503.
12 E. H. Hansen, A. K. Ghose and J. Růžička, Flow Injection Analysis of Environmental Samples for Nitrate Using an Ion-Selective Electrode, Analyst (London), 102 (1977) 705.
13 E. H. Hansen, F. J. Krug, A. K. Ghose and J. Růžička, Rapid Determination of Nitrogen, Phosphorus and Potassium in Fertilisers by Flow Injection Analysis, Analyst (London), 102 (1977) 714.
14 J. Růžička, E. H. Hansen, H. Mosbæk and F. J. Krug, Pumping Pressure and Reagent Consumption in Flow Injection Analysis, Anal. Chem., 49 (1977) 1858.
15 S. S. Jørgensen, H. Bergamin F°, E. A. G. Zagatto, F. J. Krug and S. R. B. Bringel, Determinacao de Nitrito em Aguas Naturais Atraves do Sistema de Injecao em Fluxo Continuo. Bolet. Cientif. (CENA/ESALQ/USP), 047 (1977) 1.
16 H. Bergamin F°, F. J, Krug, E. A. G. Zagatto, H. Fonseca, M. Graner, J. N. Nogueira and A. V. K. O. Annicchino, Determinacao de Sulfito em Passa de Banana com Emprego do Electrodo com Separacao de Ar em Sistema de Fluxo Continuo. Bolet. Cientif. (CENA/ESALQ/USP), 049 (1977) 1.
17 L. Sodek, J. Růžička and J. W. B. Stewart, Rapid Determination of Proteins in Plant Material by Flow Injection Spectrophotometry with Trinitrobenzenesulfonic Acid, Anal. Chim. Acta, 97 (1978) 327.
18 H. Bergamin F°, B. F. Reis and E. A. G. Zagatto, A New Device for Improving Sensitivity and Stabilization in Flow Injection Analysis, Anal. Chim. Acta, 97 (1978) 427.
19 B. Karlberg and S. Thelander, Extraction Based on the Flow Injection Principle. Part 1. Description of the Extraction System, Anal. Chim. Acta, 98 (1978) 1.
20 J. Růžička and E. H. Hansen, Flow Injection Analysis. Part X. Theory, Techniques and Trends, Anal. Chim. Acta, 99 (1978) 37.
21 E. H. Hansen, J. Růžička and A. K. Ghose, Flow Injection Analysis for Calcium in Serum, Water and Waste Waters by Spectrophotometry and by Ion-Selective Electrode, Anal. Chim. Acta, 100 (1978) 151.
22 H. Bergamin F°, J. X. Medeiros, B. F. Reis and E. A. G. Zagatto, Solvent Extraction in Continuous Flow Injection Analysis. Determination of Molybdenum in Plant Material, Anal. Chim. Acta, 101 (1978) 9.
23 H. Bergamin F°, E. A. G. Zagatto, F. J. Krug and B. F. Reis, Merging Zones in Flow Injection Analysis. Part 1. Double Proportional Injector and Reagent Consumption, Anal. Chim. Acta, 101 (1978) 17.
24 W. E. van der Linden and R. Oostervink, Construction and Behaviour of a Micro Flow-Through Copper(II)-Selective Electrode, Anal. Chim. Acta, 101 (1978) 419.
25 B. F. Reis, M.Sc. Thesis, Determinacao Colorimetrica de Aluminio em Aguas Naturais, Plantas e Solos por Injecao em Fluxo Continuo, ESALQ/USP, Brazil, 1978.
26 W. D. Basson and J. F. van Staden, Use of Non-Segmented High-Speed Continuous Flow Analysis for the Determination of Calcium in Animal Feeds, Analyst (London), 103 (1978) 296.
27 D. Betteridge, E. L. Dagless, B. Fields and N. F. Graves, A Highly Sensitive Flow-through Phototransducer for Unsegmented Continuous Flow Analysis Demonstrating High-Speed Spectrophotometry at the Parts per Billion Level and a New Method of Refractometric Determinations, Analyst (London), 103 (1978) 897.
28 W. D. Basson and J. F. van Staden, Low Level Determination of Hydrazine in Boiler Feed Water with an Unsegmented High-Speed Continuous Flow System, Analyst (London), 103 (1978) 998.

29 B. Karlberg and S. Thelander, Determination of Readily Oxidized Compounds by Flow Injection Analysis and Redox Potential Detection, Analyst (London), 103 (1978) 1154.
30 M. A. B. Regitano, B.Sc. Thesis, Chromium in the Environment with Special Emphasis on Its Behaviour in Soils, Royal Vet. Agr. Univ., Denmark, 1978.
31 K. Kina, K. Shirashi and N. Ishibashi, Ultramicro Solvent Extraction and Fluorimetry Based on the Flow Injection Method, Talanta, 25 (1978) 295.
32 D. Betteridge and B. Fields, Construction of pH Gradients in Flow Injection Analysis and Their Potential Use for Multielement Analysis in a Single Sample Bolus, Anal. Chem., 50 (1978) 654.
33 D. Betteridge, Flow Injection Analysis, Anal. Chem., 50 (1978) 832A.
34 J. Slanina, F. Bakker, A. G. M. Bruijn-Hes and J. J. Möls, Fast Determination of Nitrate in Small Samples of Rain and Surface Waters by Means of UV Spectrophotometry and Flow Injection Analysis, Z. Anal. Chem., 189 (1978) 38.
35 B. Karlberg, Flow Injection Analysis — Teknik på Frammarsch, Sven. Kem. Tidskr., 90 (1978) 26.
36 K. Kina and N. Ishibashi, Flow Injection Analysis — A Review (in Japanese), Dojin, 10 (1978) 1.
37 E. Bylund, R. Andersson and J. Å. Carlsson, Determination of Heavy Metals by Flow Injection Analysis (in Swedish), Pharmacia, Uppsala, Sweden, 1978.
38 M. Koshino, Determination of Major Nutrients in Fertilizers (in Japanese), Bunseki, 11 (1978) 803.
39 J. H. Dahl, Ph.D. Thesis, Differentialkinetisk Analyse af Jordalkalimetallernes (CDTA-Komplexer under Anvendelse af Flow Injection Analysis Systemet, Royal Dan. School Pharm., Denmark, 1978.
40 A. U. Ramsing, M.Sc. Thesis, Udvikling og Anvendelser af Voltammetrisk Måleudstyr i Flow Injection Analysis, Tech. Univ. Den., Denmark, 1978.
41 B. Karlberg, P. A. Johansson and S. Thelander, Extraction Based on the Flow Injection Principle. Part II. Determination of Codeine as the Picrate Ion-pair in Acetylsalicylic Acid Tablets, Anal. Chim. Acta, 104 (1979) 21.
42 J. Mindegaard, Flow Multi-injection Analysis — A System for the Analysis of Highly Concentrated Samples Without Prior Dilution, Anal. Chim. Acta, 104 (1979) 185.
43 E. A. G. Zagatto, F. J. Krug, H. Bergamin F°, S. S. Jørgensen and B. F. Reis, Merging Zones in Flow Injection Analysis. Part 2. Determination of Calcium, Magnesium and Potassium in Plant Material by Continuous Flow Injection Atomic Absorption and Flame Emission Spectrometry, Anal. Chim. Acta, 104 (1979) 279.
44 O. Åström, Single-Point Titrations. Part 4. Determination of Acids and Bases with Flow Injection Analysis, Anal. Chim. Acta, 105 (1979) 67.
45 J. H. Dahl, D. Espersen and A. Jensen, Differential Kinetic Analysis and Flow Injection Analysis. Part 1. The *trans*-1,2-Diaminocyclohexanetetraacetate Complexes of Magnesium and Strontium, Anal. Chim. Acta, 105 (1979) 327.
46 J. Růžička and E. H. Hansen, Stopped-Flow and Merging Zones — A New Approach to Enzymatic Assay by Flow Injection Analysis, Anal. Chim. Acta, 106 (1979) 207.
47 J. I. Braithwaite and J. N. Miller, Flow Injection Analysis with a Fluorimetric Detector for Determination of Glycine and Albumin, Anal. Chim. Acta, 106 (1979) 395.
48 B. F. Reis, H. Bergamin F°, E. A. G. Zagatto and F. J. Krug, Merging Zones in Flow Injection Analysis. Part 3. Spectrophotometric Determination of Aluminium in Plant and Soil Materials with Sequential Addition of Pumped Reagents, Anal. Chim. Acta, 107 (1979) 309.
49 D. Espersen and A. Jensen, Differential Kinetic Analysis and Flow Injection Analysis. Part II. The (2.2.1.)Cryptates of Magnesium and Calcium, Anal. Chim. Acta, 108 (1979) 241.
50 E. A. G. Zagatto, B. F. Reis, H. Bergamin F° and F. J. Krug, Isothermal Distillation in Flow Injection Analysis. Determination of Total Nitrogen in Plant Material, Anal. Chim. Acta, 109 (1979) 45.

51 L. Andersson, Simultaneous Spectrophotometric Determination of Nitrite and Nitrate by Flow Injection Analysis, Anal. Chim. Acta, 110 (1979) 123.
52 F. J. Krug, J. Růžička and E. H. Hansen, Determination of Ammonia in Low Concentrations with Nessler's Reagent by Flow Injection Analysis, Analyst (London), 104 (1979) 47.
53 M. F. Giné, E. A. G. Zagatto and H. Bergamin F°, Semiautomatic Determination of Manganese in Natural Waters and Plant Digests by Flow Injection Analysis, Analyst (London), 104 (1979) 371.
54 W. D. Basson and J. F. van Staden, Direct Determination of Calcium in Milk on a Non-Segmented Continuous Flow System, Analyst (London), 104 (1979) 419.
55 J. X. Medeiros, M.Sc. Thesis, Determinacao de Molibdenio em Material de Plantas por Extracao com Solventes em Fluxo Continuo. CENA/ESALQ/USP, Brazil, 1979.
56 D. Espersen, Ph.D. Thesis, Differentialkinetisk Analyse under Anvendelse af Flow Injection Analysis Systemet. Samtidig Bestemmelse af Magnesium og Calcium ved hjælp af (2.2.1.)Cryptaterne, Royal Dan. School Pharm., Denmark, 1979.
57 H. Baadenhuijsen and H. E. H. Seuren-Jacobs, Determination of Total CO_2 in Plasma by Automated Flow Injection Analysis, Clin. Chem., 25 (1979) 443.
58 G. Rule and W. R. Seitz, Flow Injection Analysis with Chemiluminescence Detection, Clin. Chem., 25 (1979) 1635.
59 E. H. Hansen and J. Růžička, The Principles of Flow Injection Analysis as Demonstrated by Three Lab Exercises, J. Chem. Educ., 56 (1979) 677.
60 J. Růžička, E. H. Hansen, A. K. Ghose and H. A. Mottola, Enzymatic Determination of Urea in Serum Based on pH Measurement with the Flow Injection Method, Anal. Chem., 51 (1979) 199.
61 A. N. Strohl and D. J. Curran, Flow Injection Analysis with Reticulated Vitreous Carbon Flow-through Electrodes, Anal. Chem., 51 (1979) 1045.
62 W. R. Wolf and K. K. Stewart, Automated Multiple Flow Injection Analysis for Flame Atomic Absorption Spectrometry, Anal. Chem., 51 (1979) 1201.
63 J. Kawase, A. Nakae and M. Yamenaka, Determination of Anionic Surfactants by Flow Injection Analysis Based on Ion-pair Extraction, Anal. Chem., 51 (1979) 1640.
64 J. Růžička and E. H. Hansen, Flow Injection Analysis, Chem. Tech., 9 (1979) 756.
65 J. Růžička and E. H. Hansen, Flow Injection Analysis — A New Approach to Quantitative Measurements, in NBS Spec. Publ., 519 (1979) 501.
66 N. Yoza, Y. Aoyagi, S. Ohashi and A. Tateda, Flow Injection System for Atomic Absorption Spectrometry, Anal. Chim. Acta, 111 (1979) 163.
67 H. K. Chan and A. G. Fogg, Flow Injection Determination of Meptazinol with Electrochemical Detection, Anal. Chim. Acta, 111 (1979) 281.
68 E. H. Hansen, J. Růžička and A. K. Ghose, Rapid Determination of Nitrogen-containing Compounds by Flow Injection Potentiometry, STI/PUB/535 (IAEA) (1980) 77.
69 S. S. Jørgensen and M. A. B. Regitano, Rapid Determination of Chromium(VI) by Flow Injection Analysis, Analyst (London), 105 (1980) 292.
70 L. R. Snyder, Continuous Flow Analysis: Present and Future, Anal. Chim. Acta, 114 (1980) 3.
71 J. Růžička and E. H. Hansen, Flow Injection Analysis. Principles, Applications and Trends, Anal. Chim. Acta, 114 (1980) 19.
72 H. Poppe, Characterization and Design of Liquid Phase Flow-through Detector Systems, Anal. Chim. Acta, 114 (1980) 59.
73 R. Tijssen, Axial Dispersion and Flow Phenomena in Helically Coiled Tubular Reactors for Flow Analysis and Chromatography, Anal. Chim. Acta, 114 (1980) 71.
74 J. H. M. van den Berg, R. S. Deelder and H. G. M. Egberink, Dispersion Phenomena in Reactors for Flow Analysis, Anal. Chim. Acta, 114 (1980) 91.
75 J. M. Reijn, W. E. van der Linden and H. Poppe, Some Theoretical Aspects of Flow Injection Analysis, Anal. Chim. Acta, 114 (1980) 105.
76 K. K. Stewart, J. F. Brown and B. M. Golden, A Microprocessor Control System for Automated Multiple Flow Injection Analysis, Anal. Chim. Acta, 114 (1980) 119.

77 B. Karlberg and S. Thelander, Extraction based on the Flow Injection Principle. Part 3. Fluorimetric Determination of Vitamin B1 (Thiamine) by the Thiochrome Method, Anal. Chim. Acta, 114 (1980) 129.
78 J. B. Landis, Rapid Determination of Corticosteroids in Pharmaceuticals by Flow Injection Analysis, Anal. Chim. Acta, 114 (1980) 155.
79 A. Ramsing, J. Růžička and E. H. Hansen, A New Approach to Enzymatic Assay Based on Flow Injection Spectrophotometry with Acid-Base Indicators, Anal. Chim. Acta, 114 (1980) 165.
80 C. S. Lim, J. N. Miller and J. W. Bridges, Automation of an Energy-transfer Immunoassay by using Stopped-Flow Injection Analysis with Merging Zones, Anal. Chim. Acta, 114 (1980) 183.
81 M. F. Giné, H. Bergamin F°, E. A. G. Zagatto and B. F. Reis, Simultaneous Determination of Nitrate and Nitrite by Flow Injection Analysis, Anal. Chim. Acta, 114 (1980) 191.
82 I. Kågevall, O. Åström and A. Cedergren, Determination of Water by Flow Injection Analysis with the Karl Fischer Reagent, Anal. Chim. Acta, 114 (1980) 199.
83 J. L. Burguera, A. Townshend and S. Greenfield, Flow Injection Analysis for Monitoring Chemiluminescent Reactions, Anal. Chim. Acta, 114 (1980) 209.
84 P. A. Johansson, B. Karlberg and S. Thelander, Extractions based on the Flow Injection Principle. Part 4. Determination of Extraction Constants, Anal. Chim. Acta, 114 (1980) 215.
85 H. Kagenow and A. Jensen, Differential Kinetic Analysis and Flow Injection Analysis. Part 3. The (2.2.2.)Cryptates of Magnesium, Calcium and Strontium, Anal. Chim. Acta, 114 (1980) 227.
86 J. W. Dieker and W. E. van der Linden, Determination of Iron(II) and Iron(III) by Flow Injection and Amperometric Detection with a Glassy Carbon Electrode, Anal. Chim. Acta, 114 (1980) 267.
87 S. Baban, D. Beetlestone, D. Betteridge and P. Sweet, The Determination of Sulphate by Flow Injection Analysis with Exploitation of pH Gradients and EDTA, Anal. Chim. Acta, 114 (1980) 319.
88 N. Ishibashi, K. Kina and Y. Goto, Selective Determination of Gallium by Flow Injection Fluorimetry, Anal. Chim. Acta, 114 (1980) 325.
89 Y. Hirai, N. Yoza and S. Ohashi, Flow Injection Analysis of Inorganic Polyphosphates, Anal. Chim. Acta, 115 (1980) 269.
90 O. Klinghoffer, J. Růžička and E. H. Hansen, Flow Injection Analysis of Traces of Lead and Cadmium by Solvent Extraction with Dithizone, Talanta, 27 (1980) 169.
91 J. Slanina, F. Bakker, A. Bruyn-Hes and J. J. Möls, A. Computer-controlled Multichannel Continuous Flow Analysis System Applied to the Measurement of Nitrate, Chloride and Ammonium Ions in Small Samples of Rain Water, Anal. Chim. Acta, 113 (1980) 331.
92 Z. Fang, On the Modernization of Soil and Plant Analysis (in Chinese), Torang Tongbao, 2 (1979) 34.
93 Z. Fang, Flow Injection Analysis. A Review (in Chinese), Fenxi Huaxue, 9 (1981) 369.
94 L. Sun, Z. Gao, L. Li, X. Yu and Z. Fang, The Flow Injection Analysis of Available Phosphorus in Soils (in Chinese), Fenxi Huaxue, 9 (1981) 586.
95 B. W. Renoe, K. K. Stewart, G. R. Beecher, M. R. Wills and J. Savory, Automated Multiple Flow Injection Analysis in Clinical Chemistry: Determination of Albumin with Bromocresol Green, Clin. Chem., 26 (1980) 331.
96 D. Espersen, H. Kagenow and A. Jensen, Flow Injection Analysis and Differential Kinetic Analysis, Arch. Pharm. Chem. Sci. Educ., 8 (1980) 53.
97 K. Kina and N. Ishibashi, Rapid Automated Analysis by Flow Injection Analysis (in Japanese), Kagaku (Kyoto), 33 (1978) 1001.
98 B. Fields, Studies in Flow Injection Analysis, Anal. Proc., 16 (1979) 4.
99 J. L. Burguera and A. Townshend, Monitoring Chemiluminescent Reactions by Flow Injection Analysis, Anal. Proc., 16 (1979) 263.

100 K. Kina and N. Ishibashi, Flow Injection Analysis. Its Principles and Uses (in Japanese), A & R, 17 (1979) 1.
101 K. Kina, Determination of Anionic Surfactants by Flow Injection Analysis Based on Ion-Pair Extraction (in Japanese), Dojin, 14 (1979) 9.
102 J. A. Lown, R. Koile and D. C. Johnson, Amperometric Flow-through Wire Detector: A Practical Design with High Sensitivity, Anal. Chim. Acta, 116 (1980) 33.
103 J. A. Lown and D. C. Johnson, Anodic Detection of Arsenic(III) in a Flow-through Platinum Electrode for Flow Injection Analysis, Anal. Chim. Acta, 116 (1980) 41.
104 T. Korenaga, Apparatus for Measuring Chemical Oxygen Demand Based on Flow Injection Analysis (in Japanese), Bunseki Kagaku, 29 (1980) 222.
105 T. Ito, H. Kawaguch and A. Mizuike, Inductively-coupled Plasma Emission Spectrometry of Microlitre Samples by a Flow Injection Technique (in Japanese), Bunseki Kagaku, 29 (1980) 332.
106 Y. Hirai, N. Yoza and S. Ohashi, Flow Injection Analysis of Inorganic Ortho- and Polyphosphates using Ascorbic Acid as Reductant of Molybdophosphate, Chem. Lett., 5 (1980) 499.
107 J. Růžička and E. H. Hansen, Write On: Flow Injection Analysis, Chem. Technol., 10 (1980) 202.
108 B. W. Renoe and A. Obrien, Calcium by Flow Injection Atomic Absorption. Clin. Chem., 26 (1980) 1021.
109 N. W. Holt, Flow Injection Analysis — Adaptation to a Small Laboratory, Can. J. Plant. Sci., 60 (1980) 767.
110 H. Bergamin F°, B. F. Reis, A. O. Jacintho and E. A. G. Zagatto, Ion Exchange in Flow Injection Analysis. Determination of Ammonium Ions at the Microgram per Litre Level in Natural Waters with Pulsed Nessler Reagent, Anal. Chim. Acta, 117 (1980) 81.
111 J. Slanina, W. A. Lingerak and F. Bakker, The Use of Ion-selective Electrodes in Manual and Computer-controlled Flow Injection Systems, Anal. Chim. Acta, 117 (1980) 91.
112 A. U. Ramsing, J. Janata, J. Růžička and M. Levy, Miniaturization in Analytical Chemistry — A Combination of Flow Injection Analysis and Ion-Sensitive Field-Effect Transistors for Determination of pH, and Potassium and Calcium Ions, Anal. Chim. Acta, 118 (1980) 45.
113 T. Fujinaga, S. Okazaki and T. Hori, A Flow-coulometric Method for the Rapid Determination of Orthophosphate Ion (in Japanese), Bunseki Kagaku, 29 (1980) 367.
114 W. D. Basson and J. F. van Staden, Simultaneous Determination of Sodium, Potassium, Magnesium and Calcium in Surface, Ground and Domestic Water by Flow Injection Analysis, Fresenius Z. Anal. Chem., 302 (1980) 370.
115 P. Maitoza and D. C. Johnson, Detection of Metal Ions without Interference from Dissolved Oxygen by Reverse Pulse Amperometry in Flow Injection Systems and Liquid Chromatography, Anal. Chim. Acta, 118 (1980) 233.
116 L. Nord and B. Karlberg, Extraction based on the Flow Injection Principle. Part 5. Assessment with a Membrane Phase Separator for Different Organic Solvents, Anal. Chim. Acta, 118 (1980) 285.
117 T. Korenaga, A Flow Injection Analyzer for Chemical Oxygen-Demand using Potassium Permanganate, Chem. Biomed. Environ. Instrum., 10 (1980) 273.
118 C. E. Shideler, B. W. Renoe, J. Crump, M. R. Wills, J. Savory and K. K. Stewart, Automated Multiple Flow-Injection Analysis in Clinical Chemistry: Determination of Total Protein with Biuret Reagent, Clin. Chem., 26 (1980) 1454.
119 B. J. Compton, J. R. Weber and W. C. Purdy, Stop-Flow Analysis: An Aid in the Diagnosis and Optimization of Continuous-flow Systems, Anal. Lett., B13 (1980) 861.
120 T. Korenaga, Flow Injection Analysis using Potassium Permanganate: An Approach for Measuring Chemical Oxygen Demand in Organic Wastes and Waters, Anal. Lett., A13 (1980) 1001.

121 N. Yoza, Flow Injection Analysis (in Japanese), Bunseki, 8 (1980) 555.
122 R. Kuroda, T. Mochizuki and K. Oguma, Rapid Determination of Copper in Various Copper Based Alloys by Flow Injection Analysis (in Japanese), Bunseki Kagaku, 29 (1980) T73.
123 T. Korenaga and H. Ikatsu, Flow Injection Analysis of Chemical Oxygen Demand in Waste Waters from Laboratories (in Japanese), Bunseki Kagaku, 29 (1980) 497.
124 K. Kina and K. Ueno, Flow Injection Analysis Opens New Aspects in Analytical Chemistry (in Japanese), Kagaku (Kyoto), 36 (1980) 662.
125 T. Korenaga, H. Ikatsu, T. Moriwake and T. Takahashi, Semiautomated Determination of COD in Wastewater Samples (in Japanese), Mem. Sch. Eng., Okayama Univ., 14 (1980) 119.
126 B. F. Reis, E. A. G. Zagatto, A. O. Jacintho, F. J. Krug and H. Bergamin F°, Merging Zones in Flow Injection Analysis. Part 4. Simultaneous Spectrophotometric Determination of Total Nitrogen and Phosphorus in Plant Material, Anal. Chim. Acta, 119 (1980) 305.
127 F. Fukamachi and N. Ishibashi, Flow Injection Atomic Absorption Spectrometry with Organic Solvents, Anal. Chim. Acta, 119 (1980) 383.
128 T. Yamane and T. Fukasawa, Flow Injection Determination of Trace Vanadium with Catalytic Photometric Detection, Anal. Chim. Acta, 119 (1980) 389.
129 S. M. Ramasamy, M. S. A. Jabbar and H. A. Mottola, Flow Injection Analysis based on Two Consecutive Reactions at a Gas—Solid Interface for Determination of Bromine and Chlorine, Anal. Chem., 52 (1980) 2062.
130 D. Betteridge, Analytical Chemistry — The Numbers Game, Chem. Brit., 16 (1980) 646.
131 T. N. Morrison, K. G. Schick and C. O. Huber, Determination of Ethanol by Airstream Separation with Flow Injection and Electrochemical Detection at a Nickel Oxide Electrode, Anal. Chim. Acta, 120 (1980) 75.
132 E. A. G. Zagatto, A. O. Jacintho, J. Mortatti and H. Bergamin F°, An Improved Flow Injection Determination of Nitrite in Waters by using Intermittent Flows, Anal. Chim. Acta, 120 (1980) 399.
133 N. Yoza, Y. Kurokawa, Y. Hirai and S. Ohashi, Flow Injection Determinations of Polyphosphates Based on Coloured Metal Complexes of Xylenol Orange and Methylthymol Blue, Anal. Chim. Acta, 121 (1980) 281.
134 E. J. Duffield, G. J. Moody and J. D. R. Thomas, Development of Ion-Selective Electrodes and Flow Injection Analysis for Sulphides and Thiols, Anal. Proc., 17 (1980) 533.
135 S. Baban, Recent Developments in Flow Injection Analysis: Determination of Bismuth, Thorium and Copper with Pyrocatechol Violet by Exploitation of pH, Anal. Proc., 17 (1980) 535.
136 J. Kawase, Automated Determination of Cationic Surfactants by Flow Injection Analysis based on Ion-pair Extraction, Anal. Chem., 52 (1980) 2124.
137 K. Kina, Flow Injection Analysis (in Japanese), Dojin, 15 (1980) 8.
138 K. Kina, Automated Multiple Flow-Injection Analysis in Clinical Chemistry: Determination of Albumin with Bromocresol Green (in Japanese), Dojin, 16 (1980) 6.
139 K. Kina, Introduction to Flow Injection Analysis Systems (in Japanese), Dojin, 16 (1980) 8.
140 J. L. Burguera, M. Burguera, F. Millan and A. Townshend, Flow Injection Analysis using Chemiluminescent Reactions (in Spanish), Acta Cient. Venez., 31 (1980) 221.
141 C. B. Ranger, Flow Injection Analysis. Principles, Techniques, Applications and Design, Anal. Chem., 53 (1981) 20A.
142 J. T. Vanderslice, K. K. Stewart, A. G. Rosenfeld and D. Higgs, Laminar Dispersion in Flow-injection Analysis, Talanta, 28 (1981) 11.
143 U. Baltensperger and R. Eggli, Characterization of an Amperometric Flow-through Detector with a Renewable Stationary Mercury Electrode, Anal. Chim. Acta, 123 (1981) 107.

144 B. Persson and L. Rosén, Flow Injection Determination of Isosorbide Dinitrate with Polarographic Detection, Anal. Chim. Acta, 123 (1981) 115.
145 B. F. Reis, A. O. Jacintho, J. Mortatti, F. J. Krug, E. A. G. Zagatto, H. Bergamin F° and L. C. R. Pessenda, Zone-sampling Processes in Flow Injection Analysis, Anal. Chim. Acta, 123 (1981) 221.
146 J. M. Reijn, W. E. van der Linden and H. Poppe, Dispersion in Open Tubes and Tubes Packed with Large Glass Beads. The Single Bead String Reactor, Anal. Chim. Acta, 123 (1981) 229.
147 T. R. Williams, S. W. McElvany and E. C. Ighodalo, Determination of Sulfur Dioxide in Solutions by Pyridinium Bromide Perbromide and Titrimetric and Flow Injection Procedures, Anal. Chim. Acta, 123 (1981) 351.
148 J.-H. B. Hansen, M.Sc. Thesis, Flow Injection Analysis. Spektrofotometrisk Bestemmelse af Chlorid, Nitrit og Nitrat, Dan. Eng. Acad., Denmark, 1981.
149 W. J. Blaedel and J. Wang, Symmetrical Two-electrode Pulsed-flow Detector for Liquid Chromatography, Anal. Chem., 53 (1981) 78.
150 H. L. Pardue and B. Fields, Kinetic Treatment of Unsegmented Flow Systems. Part 1. Subjective and Semiquantitative Evaluations of Flow Injection Systems with Gradient Chamber, Anal. Chim. Acta, 124 (1981) 39.
151 H. L. Pardue and B. Fields, Kinetic Treatment of Unsegmented Flow Systems. Part 2. Detailed Treatment of Flow Injection Systems with Gradient Chamber, Anal. Chim. Acta, 124 (1981) 65.
152 A. U. Ramsing, Ph.D. Thesis, Automatisering af Kemiske Analyser Baseret på Flow Injection Analysis Princippet under Anvendelse af Spektrofotometrisk og Potentiometrisk Detektion, Tech. Univ., Denmark, 1981.
153 J. Růžička and E. H. Hansen, Flow Injection Analysis, Wiley, New York, 1981.
154 S. S. Olsen, M.Sc. Thesis, Enzymkinetiske Målinger ved hjælp af Flow Injection Analysis med Specielt Henblik på Klinisk Kemiske Anvendelser, Tech. Univ., Denmark, 1981.
155 P. L. Meschi and D. C. Johnson, The Amperometric Response of Tubular Electrodes Applied to Flow Injection Determinations, Anal. Chim. Acta, 124 (1981) 303.
156 P. L. Meschi, D. C. Johnson and G. R. Luecke, The Coulometric Response of Tubular Electrodes Applied to Flow Injection Determinations, Anal. Chim. Acta, 124 (1981) 315.
157 B. C. Madsen, Utilization of Flow Injection with Hydrazine Reduction and Photometric Detection for the Determination of Nitrate in Rain Water, Anal. Chim. Acta, 124 (1981) 437.
158 K. K. Stewart and A. G. Rosenfeld, Automated Titrations: The Use of Automated Multiple Flow Injection Analysis for the Titration of Discrete Samples, J. Autom. Chem., 3 (1981) 30.
159 S. J. Lyle and M. I. Saleh, Observations on a Dropping-mercury Electrochemical Detector for Flow Injection Analysis and HPLC, Talanta, 28 (1981) 251.
160 J. F. van Staden and W. D. Basson, Automated Flow-injection Analysis of Urinary Inorganic Sulphates, Lab. Pract., 29 (1980) 1279.
161 K. Hirayama and N. Unohara, Studies on Spectrophotometric-Catalytic Determination of Trace Amounts of Metals. Part 5. Spectrophotometric Determinations of Trace Vanadium by Means of FIA Based on the Catalytic Oxidation of Bindschedler's Green Leuco Base by Potassium Bromate (in Japanese), Nippon Kagaku Kaishi, 1 (1981) 98.
162 D. Betteridge, E. L. Dagless, B. Fields, P. Sweet and D. R. Deans, Analytical Chemistry at the Interface, Anal. Proc., 18 (1981) 26.
163 Y. Hirai, N. Yoza and S. Ohashi, Flow Injection System as a Post-Column Reaction Detector for High-Performance Liquid Chromatography of Phosphinate, Phosphonate and Orthophosphate, J. Chromatogr., 206 (1981) 501.
164 G. Ham, Refractive Index Effect in Flow Injection Analysis, Anal. Proc., 18 (1981) 69.

165 T. R. Lindstrom, The Determination of Mercury of Trace Levels by Flow Injection Analysis with Electrochemical Detection, Diss. Abstr. Int. B: 41 (1981) 3021.
166 E. A. G. Zagatto, A. O. Jacintho, L. C. R. Pessenda, F. J. Krug, B. F. Reis and H. Bergamin F°, Merging Zones in Flow Injection Analysis. Part 5. Simultaneous Determination of Aluminium and Iron in Plant Digests by a Zone-sampling Approach, Anal. Chim. Acta, 125 (1981) 37.
167 K. K. Stewart, G. R. Beecher and P. E. Hare, Rapid Analysis of Discrete Samples: The Use of Nonsegmented Continuous Flow, Anal. Biochem., 70 (1976) 167.
168 R. E. Shoup, C. S. Brunlett, P. T. Kissinger and A. W. Jacobs, Thin Transducer as Detector for Trace Organics, Ind. Res. Dev., 23 (1981) 148.
169 F. J. Krug, J. Mortatti, L. C. R. Pessenda, E. A. G. Zagatto and H. Bergamin F°, Flow Injection Spectrophotometric Determination of Boron in Plant Material with Azomethine-H, Anal. Chim. Acta, 125 (1981) 29.
170 E. B. Schalscha, T. Schirado and I. Vergara, Flow Injection Analysis of Nitrate in Soil Extracts — Evaluation of a Nitrate-selective Flow Electrode Method, J. Soil. Sci. Soc. Am., 45 (1981) 446.
171 W. D. Basson and J. F. van Staden, Simultaneous Determination of Chloride and Sulphate in Natural Waters by Flow-Injection Analysis, Water Res., 15 (1981) 333.
172 J. L. Burguera, M. Burguera and A. Townshend, Determination of Zinc and Cadmium by Flow Injection Analysis and Chemiluminescence, Anal. Chim. Acta, 127 (1981) 199.
173 M. E. Meyerhoff and Y. M. Fraticelli, Flow Injection Determination of Ammonia-N using a Polymer Membrane Electrode-based Gas Sensing System, Anal. Lett., 14 (1981) 415.
174 S. M. Ramasamy and H. A. Mottola, Flow Injection (Closed-loop Configuration) Catalytic Determination of Copper in Human Serum, Anal. Chim. Acta, 127 (1981) 39.
175 T. Korenaga and H. Ikatsu, Effect of Silver Salt on the Determination of Chemical Oxygen Demand by Flow Injection Analysis (in Japanese), Nippon Kagaku Kaishi, 4 (1981) 618.
176 J. M. Reijn, W. E. van der Linden and H. Poppe, Transport Phenomena in Flow Injection Analysis Without Chemical Reaction, Anal. Chim. Acta, 126 (1981) 1.
177 Y. Hirai, T. Yokoyama, N. Yoza, T. Tarutani and S. Ohashi, Flow Injection Analysis of Silicic Acid (in Japanese), Bunseki Kagaku, 30 (1981) 350.
178 M. L. Grayeski, J. Mullin, W. R. Seitz and E. Zygowicz, Flow Injection Analysis with Chemiluminescence Detection: Recent Advances and Clinical Applications, Biolumin. Chemilumin. (2nd Int. Symp. Anal. Appl. Biolumin. Chemilumin.), (1981) 623.
179 D. J. Leggett, N. H. Chen and D. S. Mahadevappa, Flow Injection Method for Sulfide Determination by the Methylene Blue Method, Anal. Chim. Acta, 128 (1981) 163.
180 T. Korenaga and H. Ikatsu, Continuous Flow Injection Analysis of Aqueous Environmental Samples for Chemical Oxygen Demand, Analyst (London), 106 (1981) 653.
181 C. C. Painton and H. A. Mottola, Chemical Kinetic Contributions to Practical Dispersion in Unsegmented Continuous-Flow Determinations, Anal. Chem., 53 (1981) 1713.
182 Y. Hirai, N. Yoza and S. Ohashi, Flow Injection Analysis of Phosphates in Environmental Waters (in Japanese), Bunseki Kagaku, 30 (1981) 465.
183 A. U. Ramsing, J. Růžička and E. H. Hansen, The Principles and Theory of High-speed Titrations by Flow Injection Analysis, Anal. Chim. Acta, 129 (1981) 1.
184 B. D. Mindel and B. Karlberg, A Sample Pretreatment System for Atomic Absorption Using Flow Injection Analysis, Lab. Pract., 30 (1981) 719.
185 T. Imasaka, T. Harada and N. Ishibashi, Fluorimetric Determination of Gallium with Lumogallion by Flow Injection Analysis Based on Solvent Extraction, Anal. Chim. Acta, 129 (1981) 195.
186 B. C. Madsen and J. R. Murphy, Flow Injection and Photometric Determination of Sulfate in Rainwater with Methylthymol Blue, Anal. Chem., 53 (1981) 1924.

187 R. T. Lindstrom and D. C. Johnson, Evaluations of n_{app} for the Underpotential Deposition of Mercury on Gold by Flow Injection Coulometry, Anal. Chem., 53 (1981) 1855.
188 S. Greenfield, FIA Weds ICP — A Marriage of Convenience, Ind. Res. Dev., 23 (1981) 140.
189 A. Deratani and B. Sebille, Metal Ion Extraction with a Thiol Hydrophilic Resin, Anal. Chem., 53 (1981) 1742.
190 A. D. Basson, J. F. van Staden and P. M. Cattin, Determination of Phosphorus as Molybdovanadophosphoric Acid in Phosphate Rock with a Flow-Injection Procedure, Fresenius Z. Anal. Chem., 307 (1981) 373.
191 T. Yamane, Flow Injection Determination of Traces of Cobalt by Catalysis of the SPADNS-Hydrogen Peroxide Reaction with Spectrophotometric Detection, Anal. Chim. Acta, 130 (1981) 65.
192 H. W. van Rooijen and H. Poppe, An Electrochemical Reactivation Method for Solid Electrodes Used in Electrochemical Detectors for High-Performance Liquid Chromatography and Flow Injection Analysis, Anal. Chim. Acta, 130 (1981) 9.
193 J. N. Miller, Luminescence Detection in Flow Injection Analysis, Anal. Proc., 18 (1981) 264.
194 T. A. Kelly and G. D. Christian, Fluorimeter for Flow Injection Analysis with Application to Oxidase Dependent Reactions, Anal. Chem., 53 (1981) 2110.
195 B. W. Renoe, C. E. Shideler and J. Savory, Use of a Flow-Injection Sample Manipulator as an Interface Between a "High-Performance" Liquid Chromatograph and an Atomic Absorption Spectrophotometer, Clin. Chem., 27 (1981) 1546.
196 E. H. Hansen, Flow Injection Analysis: New Analytical Methods Based on the Use of Potentiometric and Spectrophotometric Flow-through Detectors, Anal. Proc., 18 (1981) 261.
197 J. Růžička, Theory and Principles of Flow Injection Analysis, Anal. Proc., 18 (1981) 267.
198 Y. Kato, Liquid-Flow Electroanalytical Techniques (in Japanese), Bunseki, 8 (1981) 573.
199 L. Gorton and L. Ögren, Flow Injection Analysis for Glucose and Urea with Enzyme Reactors and On-line Dialysis, Anal. Chim. Acta, 130 (1981) 45.
200 A. G. Fogg and D. Bhanot, Further Voltammetric Studies of Synthetic Food Colouring Matters at Glassy Carbon and Carbon Paste Electrodes Using Static and Flowing Systems, Analyst (London), 106 (1981) 883.
201 J. Růžička, Flow Injection Analysis and Its Future Development, Proc. Int. Microchem. Symp., 8 (1981) 288.
202 A. O. Jacintho, E. A. G. Zagatto, B. F. Reis, L. C. R. Pessenda and F. J. Krug, Merging Zones in Flow Injection Analysis. Part 6. Determination of Calcium in Natural Waters, Soil and Plant Materials with Glyoxalbis(2-hydroxylanil), Anal. Chim. Acta, 130 (1981) 361.
203 R. Kuroda and T. Mochizuki, Continuous Spectrophotometric Determination of Copper, Nickel and Zinc in Copper-Base Alloys by Flow Injection Analysis, Talanta, 28 (1981) 389.
204 Z. Gao and M. Lu, Flow Injection Analysis by Ion-Selective Electrodes. Use of a Solid Membrane Chloride Ion-Selective Electrode for Determination of Chloride in Soil-Water Extracts (in Chinese), Huanjing Kexue, 2 (1981) 376.
205 Z. Fang, Flow Injection Analysis (in Chinese), Fenxi Huaxue, 3 (1981) 369.
206 A. O. Jacintho, E. A. G. Zagatto, F. Bergamin F°, F. J. Krug, B. F. Reis, R. E. Bruns and B. R. Kowalski, Flow Injection Systems with Inductively-coupled Argon Plasma Atomic Emission Spectrometry. Part 1. Fundamental Considerations, Anal. Chim. Acta, 130 (1981) 243.
207 F. J. Krug, L. C. R. Pessenda, E. A. G. Zagatto, A. O. Jacintho and B. F. Reis, Spectrophotometric Flow Injection Determination of Chloride in Ethanol, Anal. Chim. Acta, 130 (1981) 409.

208 O. Åström, Flow Injection Analysis for the Determination of Bismuth by Atomic Absorption Spectrometry with Hydride Generation, Anal. Chem., 54 (1982) 190.
209 P. L. Meschi, Tubular Electrodes in Flow Injection Analysis, Diss. Abstr. Int. B: 42 (1981) 1444.
210 H. B. Hanekamp, P. Bos and O. Vittori, The Applicability of Phase-Sensitive Alternating Current Measurements in Flow-Through Detection, Anal. Chim. Acta, 131 (1981) 149.
211 P. C. A. Ooms, G. P. Leendertse, H. A. Das and U. A. Th. Brinkman, Multielement Isotope Dilution Analysis by Means of Radiometric Titration, J. Radioanal. Chem., 67 (1981) 5.
212 S. M. Ramasamy and H. A. Mottola, Repetitive Determinations of Sulfur Dioxide Gas in Air Samples by Flow Injection and Chemical Reaction at a Gas—Liquid Interface, Anal. Chem., 54 (1982) 283.
213 S. F. Simpson and F. J. Holler, Design and Evaluation of a Potentiometric Detection System for Flow Injection Titrimetry, Anal. Chem., 54 (1982) 43.
214 D. C. Shelly, T. M. Rossi and I. M. Warner, Multiple Solvent Extraction System with Flow Injection Technology, Anal. Chem., 54 (1982) 87.
215 T. E. Hu, Potentiometric Stripping as a Detector for Flow Injection Analysis of Metal Ions, Diss. Abstr. Int. B: 42 (1981) 1874.
216 H. A. Mottola, Continuous Flow Analysis Revisited, Anal. Chem., 53 (1981) 1312A.
217 A. Ivaska and T. H. Ryan, Application of a Voltammetric Flow-through Cell to Flow Injection Analysis, Coll. Czech. Chem. Commun., 46 (1981) 2865.
218 S. Hughes, P. L. Meschi and D. C. Johnson, Amperometric Detection of Simple Alcohols in Aqueous Solutions by Application of a Triple-pulse Potential Waveform at Platinum Electrodes, Anal. Chim. Acta, 132 (1981) 1.
219 S. Hughes and D. C. Johnson, Amperometric Detection of Simple Carbohydrates of Platinum Electrodes in Alkaline Solutions by Application of a Triple-pulse Potential Waveform, Anal. Chim. Acta, 132 (1981) 11.
220 D. Betteridge and B. Fields, The Application of pH Gradients in Flow Injection Analysis. A Method for Simultaneous Determination of Binary Mixtures of Metal Ions in Solution, Anal. Chim. Acta, 132 (1981) 139.
221 I. Kågevall, O. Åström and A. Cedergren, Minimization of Interference Effects from Iodine-consuming Samples in the Determination of Water with the Karl Fischer Reagent in a Flow Injection System, Anal. Chim. Acta, 132 (1981) 215.
222 K. K. Stewart, Flow Injection Analysis. A Review of Its Early History, Talanta, 28 (1981) 789.
223 J. F. Tyson and A. B. Idris, Flow Injection Sample Introduction for Atomic-Absorption Spectrometry. Applications of a Simplified Model for Dispersion, Analyst (London), 106 (1981) 1125.
224 T. B. Goad, Ph.D. Thesis, Microprocessor-controlled Flow Injection Analysis. Univ. Coll. Swansea, U.K., 1982.
225 A. G. Fogg and N. K. Bsebsu, Differential-pulse Voltammetric Determination of Phosphate as Molybdovanadophosphate at a Glassy Carbon Electrode and Assessment of Eluents for the Flow Injection Voltammetric Determination of Phosphate, Silicate, Arsenate and Germanate, Analyst (London), 106 (1981) 1288.
226 P. J. Worsfold, J. Růžička and E. H. Hansen, Rapid Automated Enzymatic Method for the Determination of Alcohol in Blood and Beverages Using Flow Injection Analysis, Analyst (London), 106 (1981) 1309.
227 J. F. Tyson, Low-cost Continuous Flow Analysis. Flow Injection Techniques in Atomic Absorption Spectrometry, Anal. Proc., 18 (1981) 542.
228 L. J. Sun, Z. Gao, L. Li and Z. L. Fang, The Determination of Total Nitrogen in Soil Digests by Flow Injection Analysis (in Chinese), Turang Tongbao, 5 (1981) 38.
229 Z. Gao and Z. L. Fang, Ion Selective Electrodes in Flow Injection Analysis. A Review (in Chinese), Lizi Xuanze Dianji Tongxun, 1 (1981) 44.

230 W. Coakley, Handbook of Automated Analysis. Continuous Flow Techniques, M. Dekker, New York, 1981.
231 T. A. Kelly, Electrochemical, Fluorimetric and Flow Injection Analysis of Enzyme and Immunochemical Systems, Diss. Abstr. Int. B: 42 (1981) 2356.
232 B. Fields, Ph.D. Thesis, Studies in Flow Injection Analysis. Univ. Coll. Swansea, U.K., 1981.
233 L. Gorton, Ph.D. Thesis, A Study of Modified Electrodes and Enzyme Reactors. Univ. of Lund, Sweden, 1981.
234 L. Ögren, Ph.D. Thesis, Enzyme Reactors in Analytical Detection Systems. Theory and Applications. Univ. of Lund, Sweden, 1981.
235 S. M. Ramasamy, Studies in Unsegmented Continuous Flow Analysis. Part 1. Repetitive Determinations of Copper(II) Catalyst. Part II. Repetitive Determinations of Bromine and Chlorine in Gaseous Samples at a Gas—Solid Interface, Diss. Abstr. Int. B: 42 (1981) 1875.
236 H. Salvesen, M.Sc. Thesis, Flow Injection Analyse. Bestemmelse av Summen av Kationer og Anioner i Vann med FIA Sammenliknet med Ionekromatografi, Univ. of Oslo, Norway, 1981.
237 L. C. R. Pessenda, M.Sc. Thesis, Determinacao de Baixas Concentracoes de Ortofosfato em Aguas Naturais com Emprego de Resina de Troca Ionica em Sistema de Injecao em Fluxo, CENA/ESALQ/USP, Brazil, 1981.
238 K. Kina, Flow Injection Analysis of Ammonia by Isothermal Distillation (in Japanese), Dojin, 19 (1981) 7.
239 K. Kina, Rapid Determination of Corticosteroids in Medicines by Means of the Flow Injection Method (in Japanese), Dojin, 20 (1981) 13.
240 K. Kina, Introduction to the Principles of Flow Injection Analysis. VI. Experiments and Practical Applications (in Japanese), Dojin, 21 (1981) 10.
241 T. Mochizuki and R. Kuroda, Determination of Beryllium in Copper Beryllium Alloys by Flow Injection Spectrophotometry, Fresenius Z. Anal. Chem., 309 (1981) 363.
242 E. Zminkowska-Halliop, E. Soczewinski and J. Matysik, Amperometric Flow-through Detector of Very Small Detection Volume, Chem. Anal. (Warsaw), 26 (1981) 161.
243 D. J. Leggett, N. H. Chen and D. S. Mahadevappa, Flow Injection Methods for Determination of Iron(III), Ind. J. Chem., 20A (1981) 1051.
244 A. U. Ramsing and J. Růžička, Simultaneous Detection of Ca^{2+} and pH in Flow Injection Analysis with Ion-sensitive Field Effect Transistors. A Model System for In Vivo Measurements, Proc. Int. Conf. Nijmegen (Holland), (1981) 134.
245 E. A. G. Zagatto, A. O. Jacintho, B. F. Reis, F. J. Krug, H. Bergamin F°, L. C. R. Pessenda, J. Mortatti and M. F. Giné, Manual de Analises de Plantas e Aguas Empregando Sistemas de Injecao em Fluxo, Univ. de Sao Paulo, CENA, Brazil, 1981.
246 F. Oshima, Flow Injection Analysis of Ammonium Nitrogen in Environmental Waters (in Japanese), Fukuoka Kyoiku Daigaku Kiyo, 31 (1981) 57.
247 E. L. Guldberg, A. S. Attiyat and G. D. Christian, Amperometric Systems for the Determination of Oxidase Enzyme-dependent Reactions by Continuous Flow and Flow Injection Analysis, J. Autom. Chem., 2 (1980) 189.
248 J. Harrow, J. Janata, R. L. Stephen and W. J. Kolff, Portable System for Simultaneous Measurements of Blood Electrolytes, Proc. EDTA, 17 (1980) 179.
249 J. Matysik, E. Soczewinski, E. Zminkowska-Halliop and M. Przegalinski, Determination of *o*-Diphenols by Flow Injection Analysis with an Amperometric Detector, Chem. Anal. (Warsaw), 26 (1981) 463.
250 R. Virtanen, A Flow Injection Analyzer with Multiple ISE-Detector, Anal. Chem. Symp. Ser., 8 (1981) 375.
251 H. Müller, Chloride and Cyanide Determination by Use of the Flow Injection Method Using Ion-Selective Flow-type Electrodes, Anal. Chem. Symp. Ser., 8 (1981) 279.
252 T. Yamane, Flow Injection Determination of Trace Cobalt(II) (in Japanese), Nippon Kagaku Kaishi, 1 (1982) 93.

253 J. Růžička, E. H. Hansen and A. U. Ramsing, Flow Injection Analyzer for Students, Teaching and Research. Spectrophotometric Methods, Anal. Chim. Acta, 134 (1982) 55.
254 J. F. van Staden, Automated Turbidimetric Determination of Sulphate in Surface, Ground and Domestic Water by Flow Injection Analysis, Fresenius Z. Anal. Chem., 310 (1982) 239.
255 B. S. Hui and C. O. Huber, Amperometric Detection of Amines and Amino Acids in Flow Injection Systems with a Nickel Oxide Electrode, Anal. Chim. Acta, 134 (1982) 211.
256 O. Kondo, H. Miyata and K. Toei, Determination of Sulfate in River Water by Flow Injection Analysis, Anal. Chim. Acta, 134 (1982) 353.
257 J. Růžička and E. H. Hansen, Flow Injection Analysis and Its Early History (Letter to the Editor), Talanta, 29 (1982) 157.
258 W. D. Basson, Consecutive Determination of Nitrogen, Phosphorus and Calcium, in Animal Feeds on a Single-channel Flow Injection Analyzer with a Common Analytical Manifold, Fresenius Z. Anal. Chem., 311 (1982) 23.
259 T. Mochizuki and R. Kuroda, Rapid Continuous Determination of Aluminium in Copper-base Alloys by Flow Injection Spectrophotometry, Fresenius Z. Anal. Chem., 311 (1982) 11.
260 K. Mori, T. Imasaka, N. Ishibashi and C. Jin, Application of Microcomputer for Data Processing in Flow Injection Analysis (in Japanese), Bunseki Kagaku, 31 (1982) 103.
261 T. Korenaga and H. Ikatsu, Fully Automated System for Continuous Monitoring of Chemical Oxygen Demand by Flow Injection Analysis (in Japanese), Bunseki Kagaku, 31 (1982) 135.
262 B. F. Rocks and C. Riley, Flow Injection Analysis. A New Approach to Quantitative Measurements in Clinical Chemistry, Clin. Chem., 28 (1982) 409.
263 B. F. Rocks, R. A. Sherwood and C. Riley, Direct Determination of Therapeutic Concentrations of Lithium in Serum by Flow Injection Analysis with Atomic Absorption Spectroscopy Detection, Clin. Chem., 28 (1982) 440.
264 S. Olsen, J. Růžička and E. H. Hansen, Gradient Techniques in Flow Injection Analysis. Stopped-Flow Measurements of the Activity of Lactate Dehydrogenase with Electronic Dilution, Anal. Chim. Acta, 136 (1982) 101.
265 B. Olsson, Determination of Hydrogen Peroxide in a Flow System with Microperoxidase as Catalyst for the Luminol Chemiluminescence Reaction, Anal. Chim. Acta, 136 (1982) 113.
266 J. Möller, FIA — A New Analytical Method (in German), Labor Praxis, 6 (1982) 278.
267 Z. Fang, L. Sun, Z. Gao, Y. Zhu, X. Wang and L. Li, Determination of Total Phosphorus in Soil Digests by Flow Injection Analysis (in Chinese), Turang Tongbao, 4 (1982) 40.
268 Z. Fang, Development of Flow Injection Analysis. A Review (in Chinese), Turangzue Jinzhan, 10 (1982) 48.
269 K. Kina, Flow Injection Analysis. Determination of Glucose (in Japanese), Dojin, 22 (1982) 8.
270 J. Růžička and A. U. Ramsing, Flow Injection Analysis Using Ion-sensitive Field Effect Transistors. A Model System for Discrete Assays and Continuous in vitro Monitoring of pH and pCa, Scand. J. Clin. Lab. Invest., 42 (1982) 35.
271 M. Trojanowicz, W. Matuszewski and A. Hulanicki, Flow Injection Potentiometric Determination of Residual Chlorine in Water, Anal. Chim. Acta, 136 (1982) 85.
272 D. J. Leggett, N. H. Chen and D. S. Mahadevappa, Rapid Determination of Residual Chlorine by Flow Injection Analysis, Analyst (London), 107 (1982) 433.
273 G. Svensson and T. Anfält, Rapid Determination of Ammonia in Whole Blood and Plasma using Flow Injection Analysis, Clin. Chim. Acta, 119 (1982) 7.
274 T. Korenaga, The Continuous Determination of Filtered Chemical Oxygen Demand with Potassium Dichromate by Means of Flow Injection Analysis, Bull. Chem. Soc. Jpn., 55 (1982) 1033.

275 J. Růžička, Flow Injection Methods. A New Tool for Instrumental Analysis, Phil. Trans. R. Soc. London, A305 (1982) 645.
276 A. G. Fogg and N. K. Bsebsu, Flow Injection Voltammetric Determination of Phosphate. Direct Injection of Phosphate into Molybdate Reagent, Analyst (London), 107 (1982) 566.
277 D. J. Leggett, N. H. Chen and D. S. Mahadevappa, Flow Injection Analysis of Aromatic Sulphonyl Haloamines, Fresenius Z. Anal. Chem., 311 (1982) 687.
278 U. Rydevik, L. Nord and F. Ingman, Automatic Lactate Determination by Reagent Injection Analysis, Int. J. Sports Med., 3 (1982) 47.
279 K. S. Johnson and R. L. Petty, Determination of Phosphate in Seawater by Flow Injection Analysis with Injection of Reagent, Anal. Chem., 54 (1982) 1185.
280 T. Hara, M. Toriyama and M. Imaki, The Flow Injection Analysis of D-Glucose Using a Flow Cell with Immobilized Peroxidase and Its Application to Serum, Bull. Chem. Soc. Jpn., 55 (1982) 1854.
281 J. Mortatti, F. J. Krug, L. C. R. Pessenda, E. A. G. Zagatto and S. S. Jørgensen, Determination of Iron in Natural Waters and Plant Material with 1,10-Phenanthroline by Flow Injection Analysis, Analyst (London), 107 (1982) 659.
282 M. Trojanowicz and W. Matuszewski, Limitation of Linear Response in Flow Injection Systems with Ion-Selective Electrodes, Anal. Chim. Acta, 138 (1982) 71.
283 T. Yao, Y. Kobayashi and S. Musha, Flow Injection Analysis for L-Lactate with Immobilized Lactate Dehydrogenase, Anal. Chim. Acta, 138 (1982) 81.
284 J. F. van Staden, Automated Simultaneous Determination of Nitrate and Nitrite by Pre-valve Reduction of Nitrate in a Flow Injection System, Anal. Chim. Acta, 138 (1982) 403.
285 J. Wang and H. Dewald, A Porous-jet Flow-through electrode, Talanta, 29 (1982) 453.
286 C. B. Ranger, Rapid Sample Pretreatment and Analysis using Automated FIA, Am. Lab., 14 (1982) 56.
287 T. A. Kelly and G. D. Christian, Capillary Flow Injection Analysis for Enzyme Assay with Fluorescence Detection, Anal. Chem., 54 (1982) 1444.
288 J. Janata and J. Růžička, Combination of Flow Injection Analysis and Voltammetry, Anal. Chim. Acta, 139 (1982) 105.
289 U. Formsan and A. Karlsson, Polarographic Determination of Penicilloic Acid in Penicillin Preparations with a Flow Injection System, Anal. Chim. Acta, 139 (1982) 133.
290 J. B. Kafil and C. O. Huber, Flow Injection Sample Processing with Nickel Oxide Electrode Amperometric Detection of Amino Acids Separated by Ion-Exchange Chromatography, Anal. Chim. Acta, 139 (1982) 347.
291 C. W. Holy, Commentary: Flow Injection Analysis — An Idea Incomplete?, J. Autom. Chem., 4 (1982) 111.
292 B. Karlberg, Flow Injection Analysis, Chem. Deriv. Anal. Chem., 2 (1982) 1.
293 T. Mochizuki, Y. Toda and R. Kuroda, Flow Injection Analysis of Silicate Rocks for Total Iron and Aluminium, Talanta, 29 (1982) 659.
294 T. Korenaga, H. Ikatsu and T. Moriwake, The Oxidation Behaviour of Various Organic Compounds on the Determination of Chemical Oxygen Demand by Means of Flow Injection Analysis with Acidic Permanganate, Bull. Chem. Soc. Jpn., 55 (1982) 2622.
295 C. Wyganowski, S. Motomizu and K. Toei, Spectrophotometric Determination of Aluminium in River Water with Bromopyrogallol Red and n-Tetradecyltrimethylammonium Bromide by Flow Injection Analysis, Anal. Chim. Acta, 140 (1982) 313.
296 W. E. van den Linden, Flow Injection Analysis: The Manipulation of Dispersion, Trends Anal. Chem., 1 (1982) 188.
297 J. Růžička, The Flow Injection Method — A New Tool for Instrumental Analysis. Rec. Adv. Anal. Spectrosc. (Pergamon Press), (1982) 285.
298 J. F. van Staden, Automated Prevalve Sample Filtration in Flow Injection Analysis. Determination of Sulphate in Water removing Suspended Solids and Colour before Sampling, Fresenius Z. Anal. Chem., 312 (1982) 438.

299 D. Betteridge, Flow Injection Analysis in the Teaching Laboratory, Fresenius Z. Anal. Chem., 312 (1982) 441.
300 A. G. Fogg, N. K. Bsebsu and M. A. Abdalla, Flow Injection Voltammetric Determination of Nitrite by Reduction at a Glassy Carbon Electrode in Acidic Bromide or Chloride Media, Analyst (London), 107 (1982) 1040.
301 B. F. Rocks and C. Riley, Flow Injection Analysis, TIBS, 7 (1982) 315.
302 S. Nakahara, M. Yamada and S. Suzuki, Chemiluminescence for the Determination of Traces of Cobalt(II) by Continuous and Flow Injection Methods, Anal. Chim. Acta, 141 (1982) 255.
303 T. Korenaga and H. Ikatsu, The Determination of Chemical Oxygen Demand in Waste Waters with Dichromate by Flow Injection Analysis, Anal. Chim. Acta, 141 (1982) 301.
304 L. Fossey and F. F. Cantwell, Characterization of Solvent Extraction/Flow Injection Analysis with Constant Pressure pumping and Determination of Procyclidine Hydrochloride in Tablets, Anal. Chem., 54 (1982) 1693.
305 T. Korenaga and H. Ikatsu, Flow Injection Analysis System with Personal Computer Application to a Fully Automated Method for the Measurement of Dissolved Chemical Oxygen Demand in River Waters (in Japanese), Bunseki Kagaku, 31 (1982) 517.
306 T. M. Rossi, D. C. Shelly and I. M. Warner, Optimization of a Flow Injection Analysis System for Multiple Solvent Extraction, Anal. Chem., 54 (1982) 2056.
307 K. Ogata, K. Taguchi and T. Imanari, Phase Separator for Flow Injection Analysis, Anal. Chem., 54 (1982) 2127.
308 W. S. Gardner and H. A. Vanderploeg, Microsample-filtering Device for Liquid Chromatography or Flow Injection Analysis, Anal. Chem., 54 (1982) 2129.
309 M. Thompson and U. J. Krull, Bilayer Lipid Membrane Electrochemistry in a Flow Injection System, Anal. Chim. Acta, 142 (1982) 207.
310 R. L. Petty, W. C. Michel, J. P. Snow and K. S. Johnson, Determination of Total Primary Amines in Seawater and Plant Nectar with Flow Injection Sample Processing and Fluorescence Detection, Anal. Chim. Acta, 142 (1982) 299.
311 T. Mochizuki and R. Kuroda, Flow Injection Analysis of Silicate Rocks for Titanium, Analyst (London), 107 (1982) 1255.
312 J. G. Williams, M. Holmes and D. G. Porter, Titration of Spoilt Beer Samples by Flow Injection Analysis, J. Autom. Chem., 4 (1982) 176.
313 E. H. Hansen and J. Růžička, Correspondence. Flow Injection Analysis: An Idea Complete — But Yet Far from Fully Exploited, J. Autom. Chem., 4 (1982) 193.
314 K. K. Stewart, Correspondence. A Reply to H. W. Holy, J. Autom. Chem., 4 (1982) 193.
315 M. Yamada and S. Suzuki, Chemiluminescent Determination of Traces of Copper(II) by the Flow Injection Method, Chem. Lett., 11 (1982) 1747.
316 J. Wang and H. D. Dewald, Flow Injection Analysis of Oxidizable Species with Reverse-pulse Amperometric Detection, Talanta, 29 (1982) 901.
317 J. M. Harris, Flow Injection of Ultratrace Level Samples into Laser-based Detectors, Anal. Chem., 54 (1982) 2337.
318 K. K. Stewart and A. G. Rosenfeld, Exponential Dilution Chambers for Scale Expansion in Flow Injection Analysis, Anal. Chem., 54 (1982) 2368.
319 T. Yokoyama, Y. Hirai, N. Yoza, T. Tarutani and S. Ohashi, Spectrophotometric Determination of Silicic Acid by Flow Injection Analysis, Bull. Chem. Soc. Jpn., 55 (1982) 3477.
320 K. Ogata, K. Taguchi and T. Imanari, Determination of Orthophosphate by Flow Injection Analysis based on Solvent Extraction (in Japanese), Bunseki Kagaku, 31 (1982) 641.
321 Y. Hirai, N. Yoza and S. Ohashi, Flow Injection Determination of Sulfite based on the Oxidation of Phosphonic Acid with Sulfite (in Japanese), Bunseki Kagaku, 31 (1982) 681.

322 T. A. Kelly and G. D. Christian, Homogeneous Enzymatic Fluorescence Immunoassay of Serum IgG by Continuous Flow Injection Analysis, Talanta, 29 (1982) 1109.
323 A. Haemmerli and J. Janata, A Flow Injection System for Measurement of Chemical Response Time of Microelectrodes, Anal. Chim. Acta, 144 (1982) 115.
324 A. G. Fogg, N. K. Bsebsu and M. A. Abdalla, Indirect Flow Injection Voltammetric Determination of Aromatic Amines by Monitoring at a Glassy Carbon Electrode the Excess of Nitrite Remaining after Their Diazotization, Analyst (London), 107 (1982) 1462.
325 G. Gerhardt and R. N. Adams, Determination of Diffusion Coefficients by Flow Injection Analysis, Anal. Chem., 54 (1982) 2618.
326 S. Nakashima, M. Yasi, M. Zenki, A. Takahashi and K. Toel, Determination of Trace Amounts of Nitrite by Flow Injection Spectrophotometry (in Japanese), Bunseki Kagaku, 31 (1982) 732.
327 J. L. Burguera and M. Burguera, Determination of Iodine by a Chemiluminescent Reaction Using Flow Injection Analysis, An. Quim., 78B (1982) 307.
328 R. Karlicek, Flow Injection Analysis and its Use in Drug Analysis (in Czech), Cesk. Farm., 31 (1982) 190.
329 J. L. Burguera, M. Burguera and M. Gallignani, Determination of Terbium by Flow Injection Analysis and Fluorescence, Acta Cient. Venez., 33 (1982) 99.
330 C. Ridder, E. H. Hansen and J. Růžička, Flow Injection Analysis of Glucose in Human Serum by Chemiluminescence, Anal. Lett., 15 (1982) 1751.
331 B. F. Rocks, R. A. Sherwood, L. M. Bayford and C. Riley, Zinc and Copper Determination in Microsamples of Serum by Flow Injection and Atomic Absorption Spectroscopy, Ann. Clin. Biochem., 19 (1982) 338.
332 K. Kina, Potentiometric Determinations by Means of Flow Injection Analysis (in Japanese), Dojin, 25 (1982) 7.
333 K. Kina, Flow Injection Analysis for Students, Teaching and Research (in Japanese), Dojin, 23 (1982) 9.
334 T. J. Sly, D. Betteridge, D. Wibberley and D. G. Porter, An Improved Flow-through Phototransducer, J. Autom. Chem., 4 (1982) 186.
335 F. Orak, Flow Injection Techniques in Automated Analysis (in Turkish), Doga Ser. C, 6 (1982) 109.
336 S. A. McClintock and W. C. Purdy, A Microprocessor-controlled Potentiometric Detection System, Anal. Lett., 15 (1982) 1001.
337 J. L. Burguera, M. Burguera and A. Townshend, The Principles, Applications and Trends of Flow Injection Analysis for Monitoring Chemiluminescent Reactions, Rev. Roum. Chim., 27 (1982) 879.
338 J. Růžička and E. H. Hansen, Recent Developments in Flow Injection Analysis. Gradient Techniques and Hydrodynamic Injection, Anal. Chim. Acta, 145 (1983) 1.
339 H. Poppe, The Performance of Some Liquid Phase Flow-through Detectors, Anal. Chim. Acta, 145 (1983) 17.
340 H. A. Mottola, Enzymatic Preparations in Analytical Continuous-Flow Systems, Anal. Chim. Acta, 145 (1983) 27.
341 Z. Feher, G. Horvai, G. Nagy, Z. Niegreisz, K. Toth and E. Pungor, A Polarographic and Spectrophotometric Routine Analyzer for Assaying Content Uniformity in Pharmaceutical Quality Control, Anal. Chim. Acta, 145 (1983) 41.
342 S. Angelova, Optimal Speed as a Function of System Performance for Continuous Flow Analyzers, Anal. Chim. Acta, 145 (1983) 51.
343 J. M. Reijn, H. Poppe and W. E. van der Linden, A Possible Approach to the Optimization of Flow Injection Analysis, Anal. Chim. Acta, 145 (1983) 59.
344 G. Johansson, L. Ögren and B. Olsson, Enzyme Reactors in Unsegmented Flow Injection Analysis, Anal. Chim. Acta, 145 (1983) 71.
345 B. Olsson and L. Ögren, Optimization of Peroxidase Immobilization and of the Design of Packed-bed Enzyme Reactors for Flow Injection Analysis, Anal. Chim. Acta, 145 (1983) 87.

346 B. Olsson, L. Ögren and G. Johansson, An Enzymatic Flow Injection Method for the Determination of Oxygen, Anal. Chim. Acta, 145 (1983) 101.
347 G. L. Abdullahi, J. N. Miller, H. N. Sturley and J. W. Bridges, Studies of Drug—Protein Binding Interactions by Flow Injection Analysis with Fluorimetric Detection, Anal. Chim. Acta, 145 (1983) 109.
348 P. J. Worsfold, The Bioanalytical Potential of Flow Injection Analysis, Anal. Chim. Acta, 145 (1983) 117.
349 H. Kagenow and A. Jensen, Kinetic Determination of Magnesium and Calcium by Stopped-flow Injection Analysis. Anal. Chim. Acta, 145 (1982) 125.
350 G. Nakagawa, H. Wada and C. Wei, Spectrophotometric Determination of Calcium with a Flow Injection System, Anal. Chim. Acta, 145 (1982) 135.
351 Z. Fang and S. Xu, Determination of Molybdenum at Microgram per Litre Levels by Catalytic Spectrophotometric Flow Injection Analysis, Anal. Chim. Acta, 145 (1983) 143.
352 L. Nord and B. Karlberg, Sample Preconcentration by Continuous Flow Extraction with a Flow Injection Atomic Absorption Detection System, Anal. Chim. Acta, 145 (1983) 151.
353 J. F. Tyson, J. M. H. Appleton and A. B. Idris, Flow Injection Calibration Methods for Atomic Absorption Spectrometry, Anal. Chim. Acta, 145 (1983) 159.
354 E. A. G. Zagatto, A. O. Jacintho, F. J. Krug, B. F. Reis, R. E. Bruns and M. C. U. Araujo, Flow Injection Systems with Inductively-coupled Argon Plasma Atomic Emission Spectrometry. Part 2. The Generalized Standard Addition Method, Anal. Chim. Acta, 145 (1983) 169.
355 F. J. Krug, E. A. G. Zagatto, B. F. Reis, O. Bahia Filho, A. O. Jacintho and S. S. Jørgensen, Turbidimetric Determination of Sulphate in Plant Digests and Natural Waters by Flow Injection Analysis with Alternating Streams, Anal. Chim. Acta, 145 (1983) 179.
356 H. Lundbäck, Amperometric Determination of Hydrogen Peroxide in Pickling Baths for Copper and Copper Alloys by Flow Injection Analysis, Anal. Chim. Acta, 145 (1983) 189.
357 R. C. Schothorst, J. M. Reijn, H. Poppe and G. den Boef, The Application of Strongly Reducing Agents in Flow Injection Analysis. Part 1. Chromium(II) and Vanadium(II), Anal. Chim. Acta, 145 (1983) 197.
358 V. K. Mahant, J. N. Miller and H. Thakrar, Flow Injection Analysis with Chemiluminescence Detection in the Determination of Fluorescein- and Fluorescamine-labelled Species, Anal. Chim. Acta, 145 (1983) 203.
359 P. van den Winkel, G. de Backer, M. Vandeputte, N. Mertens, L. Dryon and D. L. Massart, Performance and Characteristics of the Fluoride-selective electrode in a Flow Injection System, Anal. Chim. Acta, 145 (1983) 207.
360 M. Mascini and G. Palleschi, A Flow-through Detector for Simultaneous Determinations of Glucose and Urea in Serum Samples, Anal. Chim. Acta, 145 (1983) 213.
361 M. Strandberg and S. Thelander, A Microprocessor-controlled Flow Injection Analyser for the Determination of Terbutaline Sulphate, Anal. Chim. Acta, 145 (1983) 219.
362 D. Betteridge, W. C. Cheng, E. L. Dagless, P. David, T. B. Goad, D. R. Deans, D. A. Newton and T. B. Pierce, An Automated Viscometer based on High-precision Flow Injection Analysis. Part I. Apparatus, Analyst (London), 108 (1983) 1.
363 D. Betteridge, W. C. Cheng, E. L. Dagless, P. David, T. B. Goad, D. R. Deans, D. A. Newton and T. B. Pierce, An Automated Viscometer based on High-Precision Flow Injection Analysis. Part II. Measurement of Viscosity and Diffusion Coefficients, Analyst (London), 108 (1983) 17.
364 T. Deguchi, A. Tanaka, I. Sanemasa, H. Nagai, M. Nishimura and Y. Hirama, Flow Injection Analysis of Trace Amounts of Iodine using a Catalytic Method (in Japanese), Bunseki Kagaku, 32 (1983) 23.
365 D. J. Hooley and R. E. Dessy, Continuous Flow Kinetic Techniques in Flow Injection Analysis, Anal. Chem., 55 (1983) 313.

366 A. Hu, R. E. Dessy and A. Graneli, Potentiometric Stripping with Matrix Exchange Techniques in Flow Injection Analysis of Heavy Metals in Groundwaters, Anal. Chem., 55 (1983) 320.
367 C. Riley and B. F. Rocks, Comments: Flow Injection Analysis — The end of the Beginning? Segmented-Flow Analysis — The Beginning of the End?, J. Autom. Chem., 5 (1983) 1.
368 H. I. Tarlin, Comments on Flow Injection Analysis — An Idea Incomplete, J. Autom. Chem., 5 (1983) 2.
369 C. Riley, B. F. Rocks, R. A. Sherwood, L. H. Aslett and P. R. Oldfield, A Stopped-flow/Flow Injection System for Automation of Alpha-2 Macroglobulin Kinetic Studies, J. Autom. Chem., 5 (1983) 32.
370 J. Wang, H. D. Dewald and B. Greene, Anodic Stripping Voltammetry of Heavy Metals with a Flow Injection System, Anal. Chim. Acta, 146 (1983) 45.
371 D. Betteridge and B. Fields, Two-Point Kinetic Simultaneous Determination of Cobalt(II) and Nickel(II) in Aqueous Solution using Flow Injection Analysis (FIA), Fresenius Z. Anal. Chem., 314 (1983) 386.
372 J. F. Tyson, J. M. H. Appleton and A. B. Idris, Flow Injection Sample Introduction Methods for Atomic-Absorption Spectrometry, Analyst (London), 108 (1983) 153.
373 J. Möller, FIA — New Techniques and Applications (in German), Labor Praxis, 7 (1983) 162.
374 M. Yamada, T. Nakada and S. Suzuki, The Determination of Sulfite in a Flow Injection System with Chemiluminescence Detection, Anal. Chim. Acta, 147 (1983) 401.
375 S. Motomizu, T. Wakimoto and K. Toei, Determination of Trace Amounts of Phosphate in River Water by Flow Injection Analysis, Talanta, 30 (1983) 333.
376 K. W. Pratt and D. C. Johnson, The Vibrating Wire Electrode as an Amperometric Detector for Flow Injection Systems, Anal. Chim. Acta, 148 (1983) 87.
377 P. W. Alexander and U. Akapongkul, Amperometric Determination of Metal Ions in a Flow Injection System with a Copper-amalgam Electrode, Anal. Chim. Acta, 148 (1983) 103.
378 E. H. Hansen, J. Růžička, F. J. Krug and E. A. G. Zagatto, Selectivity in Flow Injection Analysis, Anal. Chim. Acta, 148 (1983) 111.
379 G. R. Beecher, K. K. Stewart and P. E. Hare, in M. Friedman (Ed.), Protein Nutritional Quality of Foods and Feeds. Automated High-Speed Analysis of Discrete Samples. The Use of Nonsegmented, Continuous Flow, M. Dekker, New York, 1985, Part I, p. 411.
380 C. B. Ranger, Flow Injection Analysis is a Modern Technique for using Unsegmented Flowing Streams to Perform Multiparameter Analysis, Ind. Res. Dev., 21 (1979) 134.
381 H. Ma and H. Yan, The Development of an Amperometric Detector for Flow Injection Analysis (in Chinese), Kexue Tongbao, 27 (1982) 959.
382 K. Toei and T. Korenaga, Analytical Chemistry and Microcomputers. III. Uses: Flow Injection Analysis (in Japanese), Bunseki, 10 (1982) 746.
383 T. Uchida, C. S. Wei, C. Iida and H. Wada, Simultaneous Determination of Calcium and Magnesium in Serum with a Flow Injection/Atomic Absorption System (in Japanese), Nagoya Kogya Daisako Gakuho, 33 (1982) 97.
384 H. Ma and H. Yan, Application of Flow Injection Analysis to Environmental Monitoring (in Chinese), Huanjing Kexue, 4 (1983) 59.
385 S. Greenfield, Inductively Coupled Plasma-Atomic Emission Spectroscopy with Flow Injection Analysis, Spectrochim. Acta, 38B (1983) 93.
386 T. Yao and Y. Kobayashi, Amperometric Determination of Glucose, Galactose, Free Cholesterol and Choline in Sera by Flow Injection Analysis with Immobilized Enzyme Reactors (in Japanese), Bunseki Kagaku, 32 (1983) 253.
387 T. Kojima, Y. Hara and F. Morishita, Flow Injection Analysis using Immobilized Enzyme Reagent, Bunseki Kagaku, 32 (1983) E101.

388 T. Yamane and H. A. Mottola, The Transient Oxidation of Brucine in Solution as a Tool for the Determination of Chromium(VI) and Brucine, Anal. Chim. Acta, 146 (1983) 181.
389 A. G. Fogg, A. Y. Chamsi and M. A. Abdalla, Flow Injection Voltammetric Determination of Nitrate after Reduction to Nitrite, Analyst (London), 108 (1983) 464.
390 T. P. Lynch, A. F. Taylor and J. N. Wilson, Fully Automatic Flow Injection System for the Determination of Uranium at Trace Levels in Ore Leachates, Analyst (London), 108 (1983) 470.
391 J. C. de Andrade, J. C. Rocha, C. Pasquini and N. Baccan, Effect on On-line Complex Formation Kinetics on the Flow Injection Analysis Signal. The Spectrophotometric Determination of Chromium(VI), Analyst (London), 108 (1983) 621.
392 C. Pasquini, W. A. de Oliveira and C. Pasquini, Direct Reading of Signals obtained in Flow Injection Analysis, Quim. Nova, 5 (1982) 51.
393 C. B. Ranger, Flow Injection Analysis. A New Approach to Near-Real-Time Process Monitoring, Autom. Stream Anal. Proc. Control, 1 (1982) 39.
394 C. Riley, L. H. Aslett, B. F. Rocks, R. A. Sherwood, J. D. M. Watson and J. Morgon, Controlled Dispersion Analysis: Flow Injection Analysis Without Injection, Clin. Chem., 29 (1983) 332.
395 B. F. Rocks, R. A. Sherwood, Z. J. Turner and C. Riley, Serum Iron and Total Iron-binding Capacity Determination by Flow Injection Analysis with Atomic Absorption Detection, Ann. Clin. Biochem., 20 (1983) 72.
396 B. F. Rocks, R. A. Sherwood and C. Riley, Comment: More on Flow Injection/Atomic Absorption Analysis for Electrolytes, Clin. Chem., 29 (1983) 569.
397 J. L. Burguera, M. Burguera, M. Gallignani and O. M. Alarcon, More on Flow Injection/Atomic Absorption Analysis for Electrolytes, Clin. Chem., 29 (1983) 568.
398 P. Karlicek, Device for Flow Injection Analysis (in Czech), Chem. Listy, 77 (1983) 100.
399 K. Honda, J. Sekino and K. Imai, Bis(2,4-Dinitrophenyl) oxalate as a Chemiluminescence Reagent in Determination of Fluorescent Compounds by Flow Injection Analysis, Anal. Chem., 55 (1983) 940.
400 D. J. Leggett, N. H. Chen and D. S. Mahadevappa, A Flow Injection Method for Analysis of Residual Chlorine by the DPD Procedure, Fresenius Z. Anal. Chem., 315 (1983) 47.
401 S. Motomizu, T. Wakimoto and K. Toei, Determination of Trace Amounts of Phosphate in River Water by Flow Injection Analysis, Talanta, 30 (1983) 333.
402 P. Marstorp, T. Anfält and L. Andersson, Determination of Oxidized Ketone Bodies in Milk by Flow Injection Analysis, Anal. Chim. Acta, 149 (1983) 281.
403 H. Wada, A. Yuchi and G. Nakagawa, Spectrophotometric Determination of Magnesium by Flow Injection Analysis with a Ligand Buffer for Masking Calcium, Anal. Chim. Acta, 149 (1983) 291.
404 U. J. Krull and M. Thompson, Flow Injection Analysis with a Bilayer Lipid Membrane Detector, Trends Anal. Chem., 2 (1983) 6.
405 A. K. Covington and A. Sibbald, Offset-Gate Chemical-Sensitive Field Effect Transistors with Electrolytically Programmable Selectivity, Eur. Pat. Appl. No. 821124, (1982).
406 T. Hara, M. Toriyama and K. Tsukagoshi, Determination of a Small Amount of Biological Constituent by Use of Chemiluminescence. 1. The Flow Injection Analysis of Protein, Bull. Chem. Soc. Jpn., 56 (1983) 1382.
407 G. B. Marshall and D. Midgley, Potentiometric Determination of Sulphite by Use of Mercury(I) Chloride—Mercury(II) Sulphide Electrodes in Flow Injection Analysis and in Air-gap electrodes, Analyst (London), 108 (1983) 701.
408 J. F. van Staden, Determination of Creatinine in Urine and Serum by Flow Injection Analysis Using the Jaffe Reaction, Fresenius Z. Anal. Chem., 315 (1983) 141.

409 B. Rössner and G. Schwedt, Methods for the Determination of Inorganic Anions. 1. Photometric Trace Analysis of Chloride in Air, Water and Technical Products in the Fe(II)/Hg-TPTZ-System. Manual Continuous-flow and Flow Injection Techniques, Fresenius Z. Anal. Chem., 315 (1983) 197.
410 A. G. Fogg, M. A. Ali and M. A. Abdalla, On-line Bromimetric Determination of Phenol, Aniline, Aspirin and Isoniazid using Flow Injection Voltammetry. Analyst (London), 108 (1983) 840.
411 M. Tamano and J. Keketsu, Flow Injection Determination of ppt Levels of Cobalt(II) in Water by the Use of Contact Catalytic Reaction (in Japanese), Nippon Kagaku Kaishi, 7 (1983) 1023.
412 J. Wang and B. A. Freiha, Selective Voltammetric Detection Based on Adsorptive Preconcentration for Flow Injection Analysis, Anal. Chem., 55 (1983) 1285.
413 D. Betteridge, T. J. Sly, A. P. Wade and J. E. W. Tillman, Computer-Assisted Optimization for Flow Injection Analysis of Isoprenaline, Anal. Chem., 55 (1983) 1291.
414 O. Åström, Ph.D. Thesis, New Approaches to Analytical Methods for Bismuth, Water, Acids and Bases using Flow Injection Analysis. Univ. of Umeå, Sweden, 1983.
415 F. J. Krug, B. F. Reis, M. F. Giné, E. A. G. Zagatto, A. O. Jacintho and J. R. Ferreira, Zone Trapping in Flow Injection Analysis. Spectrophotometric Determination of Low Levels of Ammonium Ion in Natural Waters, Anal. Chim. Acta, 151 (1983) 39.
416 M. Trojanowicz and W. Matuszewski, Potentiometric Flow Injection Determination of Chloride, Anal. Chim. Acta, 151 (1983) 77.
417 H. Kimura, K. Oguma and R. Kuroda, Atomic Absorption Spectrophotometric Determination of Calcium in Silicate Rocks by a Flow Injection Method (in Japanese), Bunseki Kagaku, 32 (1983) 179.
418 B. Karlberg, Automation of Wet Chemical Procedures using FIA, Am. Lab., 15 (1983) 73.
419 H. Ma and H. Yan, Study on Application of Flow Injection Analysis with an Amperometric Detector — Determination of Silver Ion in Wastewaters (in Chinese), Huanjing Huaxue, 1 (1982) 422.
420 T. Yamane, Determination of GOT and GPT in Blood Serum by Flow Injection Analysis using Pyruvate Oxidase (in Japanese), Mem. Fac. Liberal Arts Educ. (Univ. of Yamanashi), 32 (1981) 52.
421 O. Åström, Analysis of Substances which form Volatile Hydrides, Brit. U.K. Pat. Appl. No. 821208, (1982). Pat. No. 2,099,579.
422 R. Q. Thomson, The Characterization of Nylon Open-tubular Immobilized Enzyme Reactors Incorporated in Stopped-flow and Continuous Flow Systems, Diss. Abstr. Int. B: 43 (1983) 2893.
423 S. Motomizu, Fundamental Study of the Determination of Iron and Cobalt using 2-Nitroso-5-dimethylaminophenol as Colour Reagent by a Continuous Flow Stream Propelled by Gas Pressure (in Japanese), Bunseki Kagaku, 32 (1983) 191.
424 S. Xu and Z. Fang, Simultaneous Spectrophotometric Determination of Nitrate and Nitrite in Water and Soil Extracts by Flow Injection Analysis (in Chinese), Fenxi Huaxue, 11 (1983) 93.
425 J. F. van Staden, Simultaneous Determination of Protein (Nitrogen), Phosphorus and Calcium in Animal Feed Stuffs by Multichannel Flow Injection Analysis, J. Assoc. Anal. Chem., 66 (1983) 718.
426 J. Karlsson, I. Jacobs, B. Sjödin, P. Tesch, P. Kaiser, O. Sahl and B. Karlberg, Semi-Automatic Blood Lactate Assay. Experiences from an Exercise Laboratory, Int. J. Sports Med., 4 (1983) 52.
427 K. K. Stewart, Flow Injection Analysis — New Tool for Old Assays — New Approach to Analytical Measurements, Anal. Chem., 55 (1983) 931A.
428 S. Olsen, L. C. R. Pessenda, J. Růžička and E. H. Hansen, Combination of Flow Injection Analysis with Flame Atomic Absorption Spectrophotometry. Determination of Trace Amounts of Heavy Metals in Polluted Seawater, Analyst (London), 108 (1983) 905.

429 T. E. Edmonds and G. Coutts, Flow Injection Analysis System for Determining Soil pH, Analyst (London), 108 (1983) 1013.
430 W. E. van der Linden, Membrane Separation in Flow Injection Analysis. Gas Diffusion, Anal. Chim. Acta, 151 (1983) 359.
431 M. Valcarcel and M. D. Luque de Castro, Flow Injection Analysis. An Important Technical Invention in Analytical Chemistry (in Spanish), Quim. Anal., 1 (1983) 201.
432 N. Yoza, H. Hirano, M. Okamura, S. Ohashi, Y. Hirai and K. Tomokuni, Measurement of Enzymatic Activity of Inorganic Pyrophosphatase for Pyrophosphate by Flow Injection Analysis, Chem. Lett., 9 (1983) 1433.
433 T. Odashima, New Analytical Methods for Phosphorus (in Japanese), Mizu Shori Gijutsu, 23 (1982) 1063.
434 H. Baadenhuijsen and T. Zelders, The Use of a Microcomputer System for Peak Recognition, Data Processing and Representation in Continuous Flow Analysis, J. Autom. Chem., 5 (1983) 18.
435 E. H. Hansen and J. Růžička, Apparatus for Flow Injection Analysis, Brit. U.K. Pat. Appl. No. 830309, (1983). Pat. No. 2,104,657.
436 N. D. Byington, Flow Injection Atomic Absorption Assay of Copper and Zinc in the Plasma of Age-dependent Audiogenic Seizure-susceptible Mice, Diss. Abstr. Int. B: 43 (1983) 3228.
437 T. Mise, Determination of Anionic Surfactants by Flow Injection Analysis based on Solvent Extraction (in Japanese), Miyakojo Kogyo Koto Semmon Gakko Kenkyo Hokoku, 17 (1983) 7.
438 M. Hallas, Flow Injection Analysis — A New Environmentally Safe Analytical System for Future Laboratories (in Danish), Dan. Kemi, 64 (1983) 4.
439 S. Olsen, Trace Analysis of Heavy Metals in Seawater. Flow Injection Analysis and Atomic Absorption Spectrophotometry (in Danish), Dan. Kemi, 64 (1983) 68.
440 E. H. Hansen and J. Růžička, FIA is Already a Routine Tool in Brazil, Trends Anal. Chem., 2 (1983) 5.
441 J. Růžička, Flow Injection Analysis — From Test Tube to Integrated Microconduits, Anal. Chem., 55 (1983) 1040A.
442 R. A. Leach, J. Růžička and J. M. Harris, Spectrophotometric Determination of Metals at Trace Levels by Flow Injection and Series Differential Detection, Anal. Chem., 55 (1983) 1669.
443 A. P. Wade, Computer-assisted Optimisation of Chemical Systems, in particular Flow Injection Analysis, Anal. Proc., 20 (1983) 108.
444 C. B. Elliott, Application of Flow-injection Analysis to Enzymatic Fluorescence Kinetic Methods, Diss. Abstr. Int. B: 43 (1983) 3966.
445 K. Ogata, S. Tanabe and T. Imanari, Flame Atomic Absorption Spectrophotometry Coupled with Solvent Extraction/Flow Injection Analysis, Chem. Pharm. Bull., 31 (1983) 1419.
446 M. E. Meyerhoff and P. M. Kovach, An Ion-selective Electrode/Flow Injection Analysis Experiment. Determination of Potassium in Serum, J. Chem. Educ., 60 (1983) 766.
447 L. Fossey and F. F. Cantwell, Simultaneous Monitoring of Both Phases in the Solvent Extraction/Flow Injection Analysis of Dramamine Tablets, Anal. Chem., 55 (1983) 1882.
448 J. J. Donkerbroek, A. C. Veltkamp, C. Gooijer, N. H. Velthorst and R. W. Frei, Quenched Room-temperature Phosphorescence Detection for Flow Injection Analysis and Liquid Chromatography, Anal. Chem., 55 (1983) 1886.
449 N. Thøgersen, J. Janata and J. Růžička, Flow Injection Analysis and Cyclic Voltammetry, Anal. Chem., 55 (1983) 1986.
450 E. H. Hansen, The Early History of Flow Injection Analysis, In Focus, 6 (1983) 12.
451 B. Karlberg and S. Twengström, Applications Based on Gas Diffusion and Flow Injection Analysis, In Focus, 6 (1983) 14.

452 H. Ma, L. Jin and H. Yan, Flow Injection Analysis of Traces of Free Cyanide in Surface and Ground Waters with an Amperometric Flow-through Detector (in Chinese), Kexue Tongbao, 8 (1981) 1145.
453 H. Ma and H. Yan, An Amperometric Detector for Flow Injection Analysis (in Chinese), Yigi Yibiao Xuebao, 4 (1983) 44.
454 L. Wang, S. Zhang, Y. Zhu and Q. Wang, Rapid Determination of Sulphide in Waters by Flow Injection Analysis (in Chinese), Huanjing Huaxue, 2 (1983) 64.
455 H. Ma, L. Jin and H. Yan, Studies on the Application of an Amperometric Gold Tube Electrode Flow Through Detector. II. The Determination of Micro Quantities of Cyanide in Surface Waters (in Chinese), Huanjing Huaxue, 2 (1983) 58.
456 K. Kina, Flow Injection Analysis. A Review (in Japanese), Dojin, 25 (1983) 9.
457 J. Mortatti, F. J. Krug and H. Bergamin F°, Spectrophotometric Determination of Lead in Natural Waters and Plant Material by Flow Injection Analysis (in Portuguese), Energ. Nucl. Agric. (Piracicaba), 4 (1982) 82.
458 N. Zhou, W. Frech and E. Lundberg, Rapid Determination of Lead, Bismuth, Antimony and Silver in Steels by Flame Atomic Absorption Spectrometry Combined with Flow Injection Analysis, Anal. Chim. Acta, 153 (1983) 23.
459 R. C. Schothorst and G. den Boef, The Application of Strongly Reducing Agents in Flow Injection Analysis. Part 2. Chromium(II), Anal. Chim. Acta, 153 (1983) 133.
460 T. Yao, Flow Injection Analysis for Cholinesterase in Blood Serum by Use of a Choline-Sensitive Electrode as an Amperometric Detector, Anal. Chim. Acta, 153 (1983) 169.
461 H. Wada, G. Nakagawa and K. Ohshita, Spectrophotometric Determination of Traces of Iron with 2-(3,5-Dibromo-2-pyridylazo)-5-[N-ethyl-N-(3-sulfopropyl)amino]-phenol and its Application in Flow Injection Analysis, Anal. Chim. Acta, 153 (1983) 199.
462 J. L. Burguera and M. Burguera, Determination of Cadmium in Human Urine by Extraction with Dithizone in a Flow Injection System, Anal. Chim. Acta, 153 (1983) 207.
463 G. C. M. Bourke, G. Stedman and A. P. Wade, The Spectrophotometric Determination of Hydroxylamine Alone and in the Presence of Hydrazine by Flow Injection Analysis, Anal. Chim. Acta, 153 (1983) 277.
464 J. Wang and H. D. Dewald, Potential Scanning Voltammetric Detection for Flow Injection Systems, Anal. Chim. Acta, 153 (1983) 325.
465 T. Yao, Y. Kobayashi and M. Sato, Amperometric Determination of Phospholipids in Blood Serum with a Lecithin-sensitive Electrode in a Flow Injection System, Anal. Chim. Acta, 153 (1983) 337.
466 A. G. Fogg, G. C. Cripps and B. J. Birch, Static and Flow Injection Voltammetric Determination of Total Phosphate and Soluble Silicate in Commercial Washing Powders at a Glassy Carbon Electrode, Analyst (London), 108 (1983) 1485.
467 M. O. Babiker and J. A. W. Dalziel, Studies on the Determination of Sulphide Using *N,N*-Diethyl-*p*-phenylenediamine, Anal. Proc., 20 (1983) 609.
468 S. Motomizu, M. Oshima and K. Toei, Fluorimetric Determination of Boron with Chromatotropic Acid by Continuous Flow System (in Japanese), Bunseki Kagaku, 32 (1983) 458.
469 C. J. Patton, Design, Characterization and Applications of a Miniature Continuous Flow Analysis System, Diss. Abstr. Int. B: 44 (1983) 788.
470 H. Wada, T. Ishizuki and G. Nakagawa, Synthesis of 2-(2-Thiazolylazo)-4-methyl-5-(sulfopropylamino)benzoic Acid and the Application to the Flow Injection Analysis of Copper(II), Mikrochim. Acta, 3 (1983) 235.
471 J. C. Andrade, C. Pasquini, N. Baccan and J. C. van Loon, Cold-vapour Atomic Absorption Determination of Mercury by Flow Injection Analysis Using a Teflon Membrane Phase Separator Coupled to the Absorption Cell, Spectrochim. Acta, 38 (1983) 1329.

472 J. L. Burguera, M. Burguera and M. Gallignani, Direct Determination of Sodium and Potassium in Blood Serum by Flow Injection and Atomic Absorption Spectrophotometry, An. Acad. Bras. Cienc., 55 (1983) 209.
473 A. J. Frend, G. J. Moody, J. D. R. Thomas and B. J. Birch, Flow Injection Analysis with Tubular Membrane Ion-Selective Electrodes in the Presence of Anionic Surfactants, Analyst (London), 108 (1983) 1357.
474 B. P. Bubnis, M. R. Straka and G. E. Pacey, Metal Speciation by Flow Injection Analysis, Talanta, 30 (1983) 841.
475 H. Morita, T. Kimoto and S. Shimomura, Flow Injection Analysis of Mercury by Cold-vapour Atomic Fluorescence Spectrophotometry, Anal. Lett., 16 (1983) 1187.
476 M. H. Shah and J. T. Stewart, Amperometric Determination of Isoniazid in a Flowing Stream at the Glassy Carbon Electrode, Anal. Lett., 16 (1983) 913.
477 J. Thomsen, K. S. Johnson and R. L. Petty, Determination of Reactive Silicate in Sea Water by Flow Injection Analysis, Anal. Chem., 55 (1983) 2378.
478 C. W. Bradberry and R. N. Adams, Flow Injection Analysis with an Enzyme Reactor Bed for Determination of Ascorbic Acid in Brain Tissue, Anal. Chem., 55 (1983) 2439.
479 J. Harrow and J. Janata, Comparison of Sample Injection Systems for Flow Injection Analysis, Anal. Chem., 55 (1983) 2461.
480 K. S. Johnson, R. L. Petty and J. Thomsen, Flow Injection Analysis of Seawater Micronutrients, in A. Zirino (Ed.), Chemical Oceanography. Analytics for Mesoscale and Macroscale Processes, ACS Adv. Chem. Ser., 1983.
481 K. S. Jonson and R. L. Petty, Determination of Nitrate and Nitrite in Seawater by Flow Injection Analysis, Limnol. Oceanogr., 28 (1983) 1260.
482 C. D. C. Painton, Chemical Contributions to Dispersion. Their Analytical Impact in Flow Injection Sample Processing Systems, Diss. Abstr. Int. B: 44 (1983) 788.
483 D. E. Weisshaar, Application of Kelgraph to Electrochemical Detectors for Flow Injection Analysis and High Performance Liquid Chromatography, Gov. Rep. Announce. Index (U.S.), 83(20) (1983) 4961.
484 C. Macckoya, F. Mizuniwa, K. Usami and K. Osumi, Flow Injection Determination of Parts per Trillion Levels of Cobalt(II) in Water by the Use of Contact Catalytic Reaction (in Japanese), Nippon Kagaku Kaishi, 7 (1983) 1023.
485 M. Tachibana, T. Imamura, M. Saito and K. Kina, Rapid Determination of Copper in Serum by Flow Injection Analysis with a Water-soluble Azo Dye (in Japanese), Bunseki Kagaku, 32 (1983) 776.
486 N. H. Chen, Applications of Flow Injection Methods of Analysis, Diss. Abstr. Int. B: 43 (1983) 3581.
487 T. P. Tougas, An Electrochemical Detector for High Performance Liquid Chromatography and Flow Injection Analysis Based on a Reticulated Vitreous Carbon Working Electrode, Diss. Abstr. Int. B: 43 (1983) 3971.
488 P. J. Worsfold, Introduction to Flow Injection Analysis. Collective Summary of Five Papers Presented at a Meeting of the North East Region of SAC, December 8, 1982, in Sheffield, Anal. Proc., 20 (1983) 486.
489 J. F. Tyson, Flow Injection Methods and Atomic Absorption Spectrophotometry, Anal. Proc., 20 (1983) 488.
490 R. Eggli and R. Asper, Electrochemical Flow-through Detector for the Determination of Cysteine and Related Compounds, Anal. Chim. Acta, 101 (1978) 253.
491 J. Wang and B. A. Freiha, Flow Electrolysis at a Porous Tubular Electrode with Internal Stirring, Anal. Chim. Acta, 151 (1983) 109.
492 W. L. Caudill, A. G. Ewing, S. Jones and R. M. Wightman, Liquid Chromatography with Rapid Scanning Electrochemical Detection at Carbon Electrodes, Anal. Chem., 55 (1983) 1877.
493 P. Roehrig, C. M. Wolff and J. P. Schwing, Repetitive Enzymatic Determination of Glucose with Regeneration and Recycling of Coenzyme and Enzymes, Anal. Chim. Acta, 153 (1983) 181.

494 M. van Son, R. C. Schothorst and G. den Boef, Determination of Total Ammoniacal Nitrogen in Water by Flow Injection Analysis and a Gas Diffusion Membrane, Anal. Chim. Acta, 153 (1983) 271.
495 T. A. H. M. Janse, P. F. A. van der Wiel and G. Kateman, Experimental Optimization Procedures in the Determination of Phosphate by Flow Injection Analysis, Anal. Chim. Acta, 155 (1983) 89.
496 M. F. Giné, B. F. Reis, E. A. G. Zagatto, F. J. Krug and A. O. Jacintho, A Simple Procedure for Standard Additions in Flow Injection Analysis. Spectrophotometric Determination of Nitrate in Plant Extracts, Anal. Chim. Acta, 155 (1983) 131.
497 O. F. Kamson and A. Townshend, Ion-exchange Removal of some Interferences on the Determination of Calcium by Flow Injection Analysis and Atomic Absorption Spectrometry, Anal. Chim. Acta, 155 (1983) 253.
498 M. Yamada, T. Komatsu, S. Nakahara and S. Suzuki, Improved Chemiluminescence Determination of Traces of Cobalt(II) by Continuous Flow and Flow Injection Methods, Anal. Chim. Acta, 155 (1983) 259.
499 S. Nakashima, M. Yagi, M. Zenki, A. Takahashi and K. Toei, Spectrophotometric Determination of Nitrite in Natural Waters by Flow Injection Analysis, Anal. Chim. Acta, 155 (1983) 263.
500 W. E. van der Linden, The Optimum Composition of pH Sensitive Acceptor Solutions for Membrane Separation in Flow Injection Analysis, Anal. Chim. Acta, 155 (1983) 273.
501 J. M. Reijn, Ph.D. Thesis, Flow Injection Analysis, Univ. of Amsterdam, Holland, 1981.
502 S. M. Wolfrum, P. F. A. van der Wiel and P. C. Thijssen, A Computer-controlled System for Automated Flow Injection Analysis, Lab. Microcomput., 2 (1983) 4.
503 J. Wang and B. A. Freiha, Preconcentration and Differential Pulse Voltammetry of Butylated Hydroxyanisole at a Carbon Paste Electrode, Anal. Chim. Acta, 154 (1983) 87.
504 H. J. Wieck, Characterization of Immobilized Enzyme Chemically Modified Electrodes and Their Application in Flow Injection Analysis, Diss. Abstr. Int. B: 44 (1983) 1449.
505 J. N. Miller, Flow Injection Analysis — Flexible and Convenient Automation, Lab. Pract., Nov. (1983) 13.
506 A. P. Wade, Optimisation of Flow Injection Analysis and Polarography by the Modified Simplex Method, Anal. Proc., 20 (1983) 523.
507 H. W. van Rooijen and H. Poppe, Noise and Drift Phenomena in Amperometric and Coulometric Detectors for HPLC and FIA, J. Liq. Chromatogr., 6 (1983) 2231.
508 E. A. Jones, The Determination by Flow Injection Analysis of Iron, Sulphate, Silver and Cadmium, Techn. Rep. Mintek., M111 (1983) 32.
509 K. Kusube, K. Abe, O. Hiroshima, Y. Ishiguro, S. Ishikawa and H. Hoshida, Electrochemical Derivatization of Thiamine in a Flow Injection System — Application to Thiamine Analysis, Chem. Pharm. Bull., 31 (1983) 3589.
510 A. Schelter-Graf, H. Huck and H. L. Schmidt, A Rapid and Accurate Determination of Ethanol Using an Oxidase-Electrode in a Flow Injection System, Z. Lebensm. Unters. Forsch., 177 (1983) 356.
511 S. Nakashima, M. Yagi, M. Zenki, M. Doi and K. Toei, Determination of Sulphate in Natural Water by Flow Injection Analysis, Fresenius Z. Anal. Chem., 317 (1984) 29.
512 A. G. Fogg and N. K. Bsebsu, Sequential Flow Injection Voltammetric Determination of Phosphate and Nitrite by Injection of Reagents into a Sample Stream, Analyst (London), 109 (1984) 19.
513 J. F. Tyson and A. B. Idris, Determination of Chromium in Steel by Flame Atomic Absorption Spectrometry using a Flow Injection Standard Additions Method, Analyst (London), 109 (1984) 23.

514 D. Betteridge, N. G. Courtney, T. J. Sly and D. G. Porter, Development of a Flow Injection Analyser for the Post-Column Detection of Sugars Separated by High-Performance Liquid Chromatography, Analyst (London), 109 (1984) 91.
515 J. Wang and H. D. Dewald, Subtractive Anodic Stripping Voltammetry with Flow Injection Analysis, Anal. Chem., 56 (1984) 156.
516 G. Decristoforo and B. Danielsson, Flow Injection Analysis with Enzyme Thermistor Detector for Automated Determination of Beta-Lactams, Anal. Chem., 56 (1984) 263.
517 J. T. Vanderslice, G. R. Beecher and A. G. Rosenfeld, Determination of First-order Reaction Rate Constants by Flow Injection Analysis, Anal. Chem., 56 (1984) 268.
518 K. E. Lawrence, G. W. Rice and V. A. Fassel, Direct Liquid Sample Introduction for Flow Injection Analysis and Liquid Chromatography with Inductively-coupled Argon Plasma Spectrometric Detection, Anal. Chem., 56 (1984) 289.
519 J. T. Vanderslice, G. R. Beecher and A. G. Rosenfeld, Dispersion and Diffusion Coefficients in Flow Injection Analysis, Anal. Chem., 56 (1984) 292.
520 D. Zöltzer and G. Schwedt, Comparison of Continuous Flow and Flow Injection Techniques for the Photometric Determination of Traces of Aluminium in Water and Soil Samples. Fresenius Z. Anal. Chem., 317 (1984) 422.
521 G. Schulze, M. Husch and W. Frenzel, Flow Injection Potentiometric Stripping Analysis and Potentiometric Stripping Coulometry, Mikrochim. Acta, I (1984) 191.
522 N. Yoza, T. Miyaji, Y. Hirai and S. Ohashi, Determination of Complexing Abilities of Ligands for Metal Ions by Flow Injection Analysis and High Performance Liquid Chromatography. I. Principles of the Substitution Method, J. Chromatogr., 283 (1984) 89.
523 H. Imai, H. Yoshida, T. Masujima and T. Owa, Determination of Indole Derivatives by Flow Injection Method with Chemiluminescence Detection (in Japanese), Bunseki Kagaku, 33 (1984) 110.
524 T. Yamane and M. Kamijo, Determination of Water Hardness by Flow Injection Spectrophotometry (in Japanese), Bunseki Kagaku, 33 (1984) 110.
525 T. Zaitsu, M. Maehara and K. Toei, Flow Injection Analysis by using Turbidimetry for Chloride in River Water (in Japanese), Bunseki Kagaku, 33 (1984) 149.
526 J. F. Tyson, Extended Calibration of Flame Atomic Absorption Instruments by a Flow Injection Peak Width Method, Analyst (London), 109 (1984) 319.
527 K. Bäckström, L. G. Danielsson and L. Nord, Sample Work-up for Graphite Furnace Atomic Absorption Spectrometry using Continuous Flow Extraction, Analyst (London), 109 (1984) 323.
528 C. W. McLeod, P. J. Worsfold and A. G. Cox, Simultaneous Multi-element Analysis of Blood Serum by Flow Injection/Inductively Coupled Plasma Atomic Emission Spectrometry, Analyst (London), 109 (1984) 327.
529 F. L. Boza, M. D. Luque de Castro and M. Valcárcel, Cases, Catalytic-fluorimetric Determination of Copper at the Nanogram per Millilitre Level by Flow Injection Analysis, Analyst (London), 109 (1984) 333.
530 P. J. Worsfold and A. Hughes, A Model Immunoassay using Automated Flow Injection Analysis, Analyst (London), 109 (1983) 339.
531 M. Bos, J. H. H. G. van Willigen and W. E. van der Linden, Flow Injection Analysis with Tensammetric Detection for the Determination of Detergents, Anal. Chim. Acta, 156 (1984) 71.
532 C. Pasquini and W. A. De Oliveira, Comparison of Merging Zones, Injection of Reagent and Single-line Manifolds for Enthalpimetric Flow Injection Analysis, Anal. Chim. Acta, 156 (1984) 307.
533 E. A. Jones, Spectrophotometric Determination of Sulphate in Sodium Hydroxide Solutions by Flow Injection Analysis, Anal. Chim. Acta, 156 (1984) 313.
534 D. MacKoul, D. C. Johnson and K. G. Schick, Effect of Variation in Flow Rate on Amperometric Detection in Flow Injection Analysis, Anal. Chem., 56 (1984) 436.

535 A. S. Attiyat and G. D. Christian, Nonaqueous Solvents as Carrier or Sample Solvent in Flow Injection Analysis/Atomic Absorption Spectrometry, Anal. Chem., 56 (1984) 439.
536 D. J. Curran and T. P. Tougas, Electrochemical Detector based on Reticulated Vitreous Carbon Working Electrode for Liquid Chromatography and Flow Injection Analysis, Anal. Chem., 56 (1984) 672.
537 H. Müller and G. Wallaschek, Determination of Water in Organic Solvents by Means of the Karl Fischer Reagent with Flow Injection Analysis (in German), Z. Chem., 24 (1984) 75.
538 J. L. Burguera and M. Burguera, Determination of Sulphur Anions by Flow Injection with a Molecular Emission Cavity Detector, Anal. Chim. Acta, 157 (1984) 177.
539 M. Thompson, U. J. Krull and L. Bendell-Yuong, Biosensors and Their Uses in Flow Injection Systems, Anal. Proc., 20 (1984) 568.
540 M. D. Luque de Castro and M. Valcarcel Cases, Simultaneous Determinations in Flow Injection Analysis. A Review, Analyst (London), 109 (1984) 413.
541 C. C. Painton and H. A. Mottola, Kinetics in Continuous Flow Sample Processing. Chemical Contributions to Dispersion in Flow Injection Techniques, Anal. Chim. Acta, 158 (1984) 67.
542 H. J. Wieck, G. H. Heider, Jr. and A. M. Yacynych, Chemically Modified Reticulated Vitreous Carbon Electrode with Immobilized Enzyme as a Detector in Flow Injection Determination of Glucose, Anal. Chim. Acta, 158 (1984) 137.
543 M. Gallignani, J. L. Burguera and M. Burguera, Determination of Calcium and Magnesium in Blood Sera by Flow Injection Analysis and Atomic Absorption Spectrometry (in Spanish), Acta Cient. Venez., 33 (1982) 371.
544 S. Kato, M. Toyoshima, M. Washida and K. Sagisaka, Flow Injection Determination of Phosphorous in Phosphorous Deoxidized Copper (in Japanese), Sumitomo Keikinzoku Giho, 24 (1983) 108.
545 J. L. Burguera and M. Burguera, New Applications of Flow Injection Analysis in Analytical Chemistry (in Spanish), Acta Cient. Venez., 33 (1982) 375.
546 H. Lundbäck, G. Johansson and O. Holst, Determination of Hydrogen Peroxide for Application in Aerobic Cell Systems Oxygenated via Hydrogen Peroxide, Anal. Chim. Acta, 155 (1983) 47.
547 T. Yao, N. Nakanishi and T. Wasa, Flow Injection Analysis for Glucose with a Chemically Modified Enzyme Membrane Electrode (in Japanese), Bunseki Kagaku, 33 (1984) 213.
548 R. Kuroda, I. Ida and K. Oguma, Determination of Phosphorus in Silicate Rocks by Flow Injection Method of Analysis, Mikrochim. Acta, I (1984) 377.
549 T. Yamane, Catalytic Determination of Traces of Cobalt by the Protocatechuic Acid-Hydrogen Peroxide Reaction in a Flow Injection System, Mikrochim. Acta, I (1984) 425.
550 B. F. Rocks, R. A. Sherwood and C. Riley, Direct Determination of Calcium and Magnesium in Serum using Flow Injection Analysis and Atomic Absorption Spectroscopy, Ann. Clin. Biochem., 21 (1984) 51.
551 B. P. Bubnis, Flow Injection Analysis and Functionalized Crown Ethers for Trace Metal Analysis, Diss. Abstr. Int. B: 44 (1984) 2413.
552 R. Smith, R. J. Huber and J. Janata, Electrostatically Protected Ion-Sensitive Field Effect Transistors, Sens. Actuators, 5 (1984) 127.
553 T. Hara, M. Toriyama and K. Tsukagoshi, Determination of a Small Amount of a Biological Constituent by the Use of Chemiluminescence. II. Determination of Albumin as a Model Protein by Means of the Flow Injection Analysis using a Cobalt(III) Complex Compound as a Catalyst, Bull. Chem. Soc. Jpn., 57 (1984) 289.
554 J. M. Reijn, H. Poppe and W. E. van der Linden, Kinetics in a Single Bead String Reactor for Flow Injection Analysis, Anal. Chem., 56 (1984) 943.

555 J. C. de Andrade, J. C. Rocha and N. Baccan, On-line Oxidation of Cr(III) to Cr(VI) for Use with the Flow Injection Analysis Technique, Analyst (London), 109 (1984) 645.
556 C. C. Lee and B. D. Pollard, Determination of the Iodine Value of Fatty Acids by a Flow-injection Method, Anal. Chim. Acta, 158 (1984) 157.
557 P. W. Hansen, Determination of Fungal Alpha-Amylase by Flow Injection Analysis, Anal. Chim. Acta, 158 (1984) 375.
558 J. Wang and H. D. Dewald, Background-Current Subtraction in Voltammetric Detection for Flow Injection Analysis, Talanta, 31 (1984) 387.
559 H. Müller and V. Müller, Principles and Applications of Flow Injection Analysis (in German), Z. Chem., 24 (1984) 81.
560 R. S. Brazell, R. W. Holmberg and J. H. Moneyhun, Application of High-performance Liquid Chromatography. Flow Injection Analysis for the Determination of Polyphosphoric Acids in Phosphorus Smokes, J. Chromatogr., 290 (1984) 163.
561 H. Müller, Determination of Iodide, Cyanide, Molybdenum(VI) and Tungsten(VI) with the Flow-through Iodide-selective Electrode using the Flow Injection Method, Anal. Chem. Symp. Ser., 18 (1984) 353.
562 A. S. Attiyat and G. D. Christian, Flow Injection Analysis — Atomic Absorption Determination of Serum Zinc, Clin. Chim. Acta, 137 (1984) 151.
563 S. Ikeda, H. Satake and Y. Kohri, Flow Injection Analysis with an Amperometric Detector Utilizing the Redox Reaction of Iodate Ion, Chem. Lett., 6 (1984) 873.
564 A. Fernandez, M. D. Luque de Castro and M. Valcarcel, Comparison of Flow Injection Analysis Configurations for Differential Kinetic Determination of Cobalt and Nickel, Anal. Chem., 56 (1984) 1146.
565 Y. Israel and R. M. Barnes, Standard Addition Method in Flow Injection Analysis with Inductively-coupled Plasma Atomic Emission Spectrometry, Anal. Chem., 56 (1984) 1188.
566 L. Nondek, Band Broadening in Solid-Phase Derivatization Reactions for Irreversible First-order Reactions, Anal. Chem., 56 (1984) 1192.
567 H. Engelhardt and R. Klinkner, Phosphate Determination by Flow Injection Analysis with Geometrically Deformed Open Tubes (in German), Fresenius Z. Anal. Chem., 317 (1984) 671.
568 H. Engelhardt and R. Klinkner, Phosphate Determination by Flow Injection Analysis using Geometrically Deformed Open Tubes (in German), Fresenius Z. Anal. Chem., 319 (1984) 277.
569 A. Jensen and M. Hallas, Flow Injection Analysis. A New System of Analysis with Extensive Potential Applications for Pharmaceutically Relevant Analyses (in Danish), Farmaceut. Tidende., 26 (1984) 609.
570 H. Wada, G. Nakagawa and K. Ohshita, Synthesis of *o,o'*-Dihydroxyazo Compounds and Their Application to the Determination of Magnesium and Calcium by Flow Injection Analysis, Anal. Chim. Acta, 159 (1984) 289.
571 M. Yamada and S. Suzuki, Micellar Enhanced Chemiluminescence of 1,10-Phenanthroline for the Determination of Ultratraces of Copper(II) by the Flow Injection Method, Anal. Lett., A17 (1984) 251.
572 P. W. Alexander, M. Trojanowicz and P. R. Haddad, Indirect Potentiometric Determination of Metal Ions by Flow Injection Analysis with a Copper Electrode, Anal. Lett., A17 (1984) 309.
573 M. J. Medina, J. Bartroli, J. Alonso, M. Blanco and J. Fuentes, Direct Determination of Glucose in Blood Serum using Trinder's Reaction, Anal. Lett., B17 (1984) 385.
574 K. M. Korfhage, K. Ravichandran and R. P. Baldwin, Phthalocyanine-containing Chemically Modified Electrodes for Electrochemical Detection in Liquid Chromatography/Flow Injection Systems, Anal. Chem., 56 (1984) 1514.
575 M. R. Straka, G. E. Pacey and G. Gordon, Residual Ozone Determination by Flow Injection Analysis, Anal. Chem., 56 (1984) 1973.

576 F. Malamas, M. Bengtsson and G. Johansson, On-line Trace Metal Enrichment and Matrix Isolation in Atomic Absorption Spectrometry by a Column Containing Immobilized 8-Quinolinol in a Flow Injection System, Anal. Chim. Acta, 160 (1984) 1.
577 C. Silfwerbrand-Lindh, L. Nord, L.-G. Danielsson and F. Ingman, The Analysis of Aqueous Solutions with Ethanol-Soluble Reagents in a Flow Injection System. Spectrophotometric Determination of Uranium, Anal. Chim. Acta, 160 (1984) 11.
578 T. P. Lynch, Determination of Free Cyanide in Mineral Leachates, Analyst (London), 109 (1984) 421.
579 T. P. Lynch, N. J. Kernoghan and J. N. Wilson, Speciation of Metals in Solution by Flow Injection Analysis. Part 1. Sequential Spectrophotometric and Atomic Absorption Detectors, Analyst (London), 109 (1984) 839.
580 A. G. Fogg, A. Y. Chamsi, A. A. Barros and J. O. Cabral, Flow Injection Voltammetric Determination of Hypochlorite and Hypobromite as Bromine by Injection into an Acidic Bromide Eluent and the Indirect Determination of Ammonia and Hydrazine by Reaction with an Excess of Hypobromite, Analyst (London), 109 (1984) 901.
581 T. P. Lynch, N. J. Kernoghan and J. N. Wilson, Speciation of Metals in Solution by Flow Injection Analysis. Part 2. Determination of Iron(III) and Iron(II) in Mineral Process Liquors by Simultaneous Injection into Parallel Streams, Analyst (London), 109 (1984) 843.
582 A. G. Fogg and A. M. Summan, Simple Wall-jet Detector Cell holding either a Solid Electrode or a Sessile Mercury-Drop Electrode and an Illustration of Its Use in the Oxidative and Reductive Flow Injection Voltammetric Determination of Food Colouring Matters, Analyst (London), 109 (1984) 1029.
583 M. W. Brown and J. Růžička, Parameters Affecting Sensitivity and Precision in the Combination of Flow Injection Analysis with Flame Atomic Absorption Spectrophotometry, Analyst (London), 109 (1984) 1091.
584 T. M. Rossi, D. C. Shelly and I. M. Warner, Optimization of a Flow Injection Analysis System for Multiple Solvent Extraction, Energy. Res. Abstr., 9 (1984) No. 8101.
585 H. Weicker, Flow Injection Analysis is also for Lactate Determination, Labor Praxis, 8 (1984) 300.
586 C. Okumoto, M. Nagashima, S. Mizoiri, M. Kazama and K. Akiyama, Flow Injection Analysis of Cyanide in Wastewater from Metal Plating Processes (in Japanese), Eisei Kagaku, 30 (1984) 7.
587 T. Hara, M. Toriyama and K. Tsukagoshi, Determination of Small Amounts of Biological Constituents by use of Chemiluminescence. III. The Flow Injection Analysis of Protein by Direct Injection, Bull. Chem. Soc. Jpn., 57 (1984) 1551.
588 W. R. Seitz and M. L. Grayeski, Flow Injection Analysis: A New Approach to Laboratory Automation, J. Clin. Lab. Autom., 4 (1984) 169.
589 T. Chow, S. Yoshida, M. Itoh, S. Hirose and T. Takeda, Determination of Reduced Type Nicotinamide Adenine Dinucleotide by Flow Injection Analysis Using an Immobilized Enzyme Voltammetry System (in Japanese), Bunseki Kagaku, 33 (1984) 310.
590 N. Yoza, Flow Injection Analysis (in Japanese), Bunseki, 7 (1984) 513.
591 Hitachi Chemical Co., Reagent for Spectrophotometric Determination of Total Proteins (in Japanese), Kokai Tokkyo Koho, Pat. Appl. No. 8483059, (1984).
592 H. A. Mottola, C. M. Wolf, A. Iob and R. Gnanasekaran, Potentiometric and Amperometric Detection in Flow Injection Enzymatic Determination, Anal. Chem. Symp. Ser., 18 (1984) 49.
593 W. Kemula, J. Debrowski and W. Kutner, Flow Polarographic Detector, Pol. Pat. Appl. No. 831025, (1983). Pat. No. 119995.
594 F. Kikui and T. Hayakawa, Semiautomatic Method for Determination of Iron(II) and Iron(III) by using Flow Injection and a Coulometric Monitor (in Japanese). Sumito Tokushu Kinzoku Giho, 7 (1984) 33.
595 J. Wang and B. A. Freiha, Thin-layer Flow Cell with a Rotating Disk Electrode, J. Electroanal. Chem. Interfacial Electrochem., 164 (1984) 79.

596 H. Weicker, H. Hägele, B. Kornes and A. Werner, Determination of Alanine, Lactate, Pyruvate, Beta-Hydroxybutyrate and Acetoacetate by Flow Injection Analysis, Int. J. Sports Med., 5 (1984) 47.
597 M. H. Ho, Microprocessor-controlled Flow Injection Analyzer for Biochemical Applications, Biomed. Sci. Instrum., 20 (1984) 93.
598 R. A. Mowery, Jr., Flow Injection Analysis: Potential for Process Composition Measurement, InTech., 31 (1984) 51.
599 R. Kuroda, Flow Injection Analysis (in Japanese), Gendai Kagaku, 158 (1984) 48.
600 M. Trojanowicz, W. Augustyniak and A. Hulanicki, Photometric Flow Injection Measurements with Flow Cell Employing Light-emitting Diodes, Mikrochim. Acta, II (1984) 17.
601 Y. Baba, N. Yoza and S. Ohashi, Simultaneous Determination of Phosphate and Phosphonate by Flow Injection Analysis with Parallel Detection Systems, J. Chromatogr., 295 (1984) 153.
602 T. Yao and T. Wasa, Rapid Determination of Cholinesterase Activity in Blood Serum (in Japanese), Bunseki Kagaku, 33 (1984) 342.
603 T. Yamane, Flow Injection Determination of Hydrogen Peroxide by Means of the Manganese-Catalyzed Oxidation of Hydroxynaphthol Blue, Bunseki Kagaku, 33 (1984) E204.
604 N. Yoza, T. Shuto, Y. Baba, A. Tanaka and S. Ohashi, Determination of Complexing Abilities of Ligands for Metal Ions by Flow Injection Analysis and High-performance Liquid Chromatography. II. Copper(II) Complexes of Aminopolycarboxylic Acids, J. Chromatogr., 298 (1984) 419.
605 K. Matsumoto, K. Ishida, T. Nomura and Y. Osajima, Conductometric Flow Injection Analysis of the Organic Acid Content in Citrus Fruits, Agric. Biol. Chem., 48 (1984) 2211.
606 S. M. Harden and W. K. Nonidez, Determination of Orthophosphate by Flow Injection Analysis with Amperometric Detection, Anal. Chem., 56 (1984) 2218.
607 T. Braun and W. L. Lyon, The Epidemiology of Research on Flow Injection Analysis. An Unconventional Approach, Fresenius Z. Anal. Chem., 319 (1984) 74.
608 J. Růžička and E. H. Hansen, Integrated Microconduits for Flow Injection Analysis, Anal. Chim. Acta, 161 (1984) 1.
609 R. C. Schothorst, J. J. F. van Veen and G. den Boef, The Application of Strongly Reducing Agents in Flow Injection Analysis. Part 3. Vanadium(II), Anal. Chim. Acta, 161 (1984) 27.
610 F. J. Krug, O. Bahia F°. and E. A. G. Zagatto, Determination of Molybdenum in Steels by Flow Injection Spectrophotometry, Anal. Chim. Acta, 161 (1984) 245.
611 P. Linares, M. D. Luque de Castro and M. Valcarcel, Spectrofluorimetric Flow Injection Determination of Cyanide, Anal. Chim. Acta, 161 (1984) 257.
612 R. R. Liversage, J. C. van Loon and J. C. de Andrade, A Flow Injection/Hydride Generation System for the Determination of Arsenic by Inductively-Coupled Plasma Atomic Emission Spectrometry, Anal. Chim. Acta, 161 (1984) 275.
613 T. P. Tougas and D. J. Curran, Stopped-flow Linear Sweep Voltammetry at the Reticulated Vitreous Carbon Electrode in a Flow Injection System. Determination of Dopamine in the Presence of Ascorbic Acid, Anal. Chim. Acta, 161 (1984) 325.
614 J. L. Burguera and M. Burguera, Flow Injection Spectrophotometry followed by Atomic Absorption Spectrometry for the Determination of Iron(II) and Total Iron, Anal. Chim. Acta, 161 (1984) 375.
615 J. W. Keller, Enzyme Assay by Repetitive Flow Injection Analysis. Application to the Assay of Hog Kidney Aminoacylase, Anal. Lett., 17 (1984) 589.
616 P. W. Alexander, P. R. Haddad and M. Trojanowicz, Potentiometric Flow Injection Determination of Copper-complexing Inorganic Anions with a Copper Wire Indicator Electrode, Anal. Chem., 56 (1984) 2417.
617 H. Narasaki and M. Ikeda, Automated Determination of Arsenic and Selenium by Atomic Absorption Spectrometry with Hydride Generation, Anal. Chem., 56 (1984) 2059.

618 D. S. Austin, J. A. Polta, T. Z. Polta, A. P. C. Tang, T. D. Cabelka and D. C. Johnson, Electrocatalysis at Platinum Electrodes for Anodic Electroanalysis, J. Electroanal. Chem. Interfacial Electrochem., 168 (1984) 227.
619 J. F. van Staden and H. R. van Vliet, Flow Injection Analysis for Determining Total Alkalinity in Surface, Ground and Domestic Water Using the Automated Bromocresol Green Method (in Afrikaans), Water SA, 10 (1984) 168.
620 J. A. Wise, Flow Injection Anodic Stripping Voltammetry, Diss. Abstr. Int. B: 45 (1984) 176.
621 H. Cui, Z. Zhu and Z. Fang, Determination of Cyanide in Soil and Water by Flow Injection Analysis (in Chinese), Huanjing Huaxue, 3 (1984) 48.
622 S. Zhang, L. Sun, H. Jiang and Z. Fang, Determination of Copper, Zinc, Iron, Manganese, Sodium, Potassium and Magnesium in Plants and Soil by Flow Injection Analysis (in Chinese), Guangpruxe Yu Guangpu Fenxi, 4 (1984) 42.
623 Hitachi Chemicals Co., Reagent for Bilirubin Determination in Body Fluids (in Japanese), Jpn. Kokai Tokkyo Koho, Pat. No. 84109863, (1984).
624 Hitachi Chemicals Co., Reagent for Determination of Neutral Lipids (in Japanese), Jpn. Kokai Tokkyo Koho, Pat. No. 84109196, (1984).
625 Hitachi Chemicals Co., Reagent for Cholesterol Determination (in Japanese), Jpn. Kokai Tokkyo Koho, Pat. No. 84109100, (1984).
626 Hitachi Chemicals Co., Reagent for Glucose Determination (in Japanese), Jpn. Kokai Tokkyo Koho, Pat. No. 84109197, (1984).
627 H. Cui and Z. Fang, Flow Injection Analysis of Iron in Soil Extracts (in Chinese), Fenxi Huaxue, 12 (1984) 759.
628 Z. Fang, S. Xu and S. Zhang, The Determination of Trace Amounts of Nickel by On-line FIA Ion Exchange Preconcentration Atomic Absorption Spectrometry (in Chinese), Fenxi Huaxue, 12 (1984) 997.
629 T. Aoki, S. Uemura and M. Munemori, Flow Injection Analysis with Membrane Separation. Determination of Ammonia in Blood and Urine (in Japanese), Bunseki Kagaku, 33 (1984) 505.
630 K. Matsumoto, H. Ukede and Y. Osajima, Flow Injection Analysis of Reduced Nicotinamide Adenine Dinucleotide Using Beta-Naphthoquinone-4-sulfonate as a Mediator, Agric. Biol. Chem., 48 (1984) 1879.
631 K. L. Lu and Y. M. Chen, Catalytic Photometric Method for the Determination of Molybdenum in Plants with Flow Injection Analysis (in Chinese), Proc. Natl. Sci. Counc. Repub. China, Part A: 8 (1984) 85.
632 L. C. Davis and G. A. Radke, Chemically Coupled Spectrophotometric Assays Based on Flow Injection Analysis. Determination of Nitrogenase by Assays for Creatinine, Ammonia, Hydrazone, Phosphate and Dithionite, Anal. Biochem., 140 (1984) 434.
633 Hitachi Chemicals Co., Reagent for Uric Acid Determination (in Japanese), Jpn. Kokai Tokkyo Koho, Pat. No. 84109200, (1984).
634 Q. Wei, Spectrophotometric Determination of Calcium by Flow Injection Analysis (in Chinese), Jilin Daxue Kexue Xuebao, 3 (1984) 113.
635 M. Koupparis, P. Macheras and C. Reppas, Application of Automated Flow Injection Analysis to Dissolution Studies, Int. J. Pharm., 20 (1984) 325.
636 G. E. Pacey and B. P. Bubnis, Flow Injection Analysis as a Tool for Metal Speciation, Am. Lab., 16 (1984) 17.
637 R. C. Schothorst, M. van Son and G. den Boef, The Application of Strongly Reducing Agents in Flow Injection Analysis. Part 4. Uranium(III), Anal. Chim. Acta, 162 (1984) 1.
638 I. Nordin-Andersson, O. Åström and A. Cedergren, Determination of Water by Flow Injection Analysis with the Karl Fischer Reagent. Minimization of Effects Caused by Differences in Physical Properties of the Samples, Anal. Chim. Acta, 162 (1984) 9.
639 J. Wang and H. D. Dewald, Theoretical and Experimental Aspects of the Response of

Stripping Voltammetry in Flow Injection Systems, Anal. Chim. Acta, 162 (1984) 189.
640 A. Rios, M. D. Luque de Castro and M. Valcarcel, New Approach to the Simultaneous Determination of Pollutants in Waste Waters by Flow Injection Analysis. Part I. Anionic Pollutants, Analyst (London), 109 (1984) 1487.
641 S. Nakashima, M. Yagi, M. Zenki, A. Takahashi and K. Toei, Determination of Nitrate in Natural Waters by Flow Injection Analysis, Fresenius Z. Anal. Chem., 319 (1984) 506.
642 R. A. Leach and J. M. Harris, Thermal Lens Absorption Measurements by Flow Injection into Supercritical Fluid Solvents, Anal. Chem., 56 (1984) 2801.
643 B. C. Madsen and M. S. Kromis, Flow Injection and Photometric Determination of Hydrogen Peroxide in Rain Water with N-Ethyl-N-(sulfopropyl)aniline Sodium Salt, Anal. Chem., 56 (1984) 2849.
644 Y. Yang and R. E. Hairrell, Single Laser Crossed Beam Thermal Lens Detection for Short Path Length Samples and Flow Injection Analysis, Anal. Chem., 56 (1984) 3002.
645 C. Riley, B. F. Rocks and R. A. Sherwood, Flow Injection Analysis in Clinical Chemistry, Talanta, 31 (1984) 879.
646 Z. Feher, G. Nagy, L. Bezur, J. Szovik, K. Toth and E. Pungor, Use of a Novel Apparatus Based on the Injection Principle for Automatic Voltammetric Analysis, Hung. Sci. Instrum., 45 (1979) 1.
647 H. F. R. Reijnders, J. F. van Staden and B. Griepink, Flow-through Determination of Sulphate in Water Using Different Methods: A Comparison, Fresenius Z. Anal. Chem., 300 (1980) 273.
648 J. F. Brown, K. K. Stewart and D. Higgs, Microcomputer Control and Data System for Automated Multiple Flow Injection Analysis, J. Autom. Chem., 3 (1981) 182.
649 L.-G. Ekström, An Automated Method For Determination of Free Fatty Acids, J. Am. Oil Chem. Soc., 58 (1981) 935.
650 W. Huber, Mechanization of Photometric Analysis with the Component Parts of Liquid Chromatography. Fast Determination of Formaldehyde (in German), Fresenius Z. Anal. Chem., 309 (1981) 386.
651 L. Nord and B. Karlberg, An Automated Extraction System for Flame Atomic Absorption Spectrometry, Anal. Chim. Acta, 125 (1981) 199.
652 M. Vandeputte, Ph.D. Thesis, Fluor: Analyse en Voorkomen in Pollutieindikatoren (in Dutch), Vrije Univ., Brussels, Belgium, 1981/82.
653 N. Mertens, M.Sc. Thesis, Fluor: Bepaling in Commerciele Dranken. Een Preliminaire Studie van de Fluoride Elektrode in een F.I.A. System (in Dutch), Vrije Univ., Brussels, Belgium, 1981/82.
654 B. Karlberg and J. Möller, Flow Injection Analysis — A New Technique for the Automation of Wet-chemical Procedures, In Focus, 5 (1982) 5.
655 M. D. Lerique, F.I.A. — or Injection into a Continuously Moving Stream (in French), Chem. Mag., 6 (1982) 49.
656 P. W. Alexander, R. J. Finlayson, L. E. Smythe and A. Thalib, Rapid Flow Analysis with Inductively-coupled Plasma Atomic-Emission Spectroscopy Using a Micro-Injection Technique, Analyst (London), 107 (1982) 1335.
657 W. L. Caudill, J. O. Howell and R. M. Wightman, Flow Rate Independent Amperometric Cell, Anal. Chem., 54 (1982) 2532.
658 C. H. P. Bruins, D. A. Doornbos and K. Brunt, The Hydrodynamics of the Amperometric Detector Flow Cell with a Rotating Disk Electrode, Anal. Chim. Acta, 140 (1982) 39.
659 K. Brunt, Comparison Between the Performances of an Electrochemical Detector Flow Cell in a Potentiometric and an Amperometric Measuring System using Glucose as a Test Compound, Analyst (London), 107 (1982) 1261.
660 D. Pilosof and T. A. Nieman, Microporous Membrane Flow Cell with Nonimmobilized

Enzyme for Chemiluminescent Determination of Glucose, Anal. Chem., 54 (1982) 1698.
661 T. Ito, E. Nakagawa, H. Kawaguchi and A. Mizuike, Semi-automatic Microlitre Sample Injection into an Inductively Coupled Plasma for Simultaneous Multielement Analysis, Mikrochim. Acta, I (1982) 423.
662 P. W. Alexander and A. Thalib, Nonsegmented Rapid-Flow Analysis with Ultraviolet/Visible Spectrophotometric Determination for Short Sampling Times, Anal. Chem., 55 (1983) 497.
663 J. Růžička and E. H. Hansen, Flow Injection Analysis (in Japanese. Translation of Ref. 153, Translated by N. Ishibashi and N. Yoza), Kagakudonin, Kyoto, Japan, (1983) (ISBN 4-7598 0100-6).
664 K. Ueno and K. Kina, Introduction to Flow Injection Analysis. Experiments and Applications (in Japanese), Kodansha Scientific, Tokyo, Japan, (1983). (ISBN 4-06-139527-0).
665 M. Valcarcel Cases and M. D. Luque de Castro, Análisis por Inyección en Flujo (in Spanish), Imprenta San Pablo, Cordoba, Spain, (1984). (ISBN 84-7580-091-2).
666 H. Furuya and K. Nakayama, Flow Injection Analysis of Chloride Ion in Water Using Ion Selective Electrode (in Japanese), J. Jpn. Water Works Assoc., 52 (1983) 51.
667 D. Betteridge, Simulation and Modelling in Chemical Analysis, Anal. Proc., 21 (1984) 139.
668 J. A. Wise, Flow Injection Anodic Stripping Voltammetry, Diss. Abstr. Int. B: 45 (1984) 176.
669 A. Rios, M. D. Luque de Castro and M. Valcarcel, Spectrophotometric Determination of Cyanide by Unsegmented Flow Methods, Talanta, 31 (1984) 673.
670 K. Li and P. Hua, Flow Injection Catalytic Photometric Determination of Trace Iodine in Rock and Ore Samples (in Chinese), Yanshi Kuangwu Ji Ceshi, 3 (1984) 314.
671 K. G. Schick, High-Speed, On-Stream Acid-Base Titration utilizing Flow Injection Analysis, Adv. Instrum., 39 (1984) 279.
672 T. Odashima and K. Satoh, A New Analysis for Sulphur Compounds (in Japanese), Mizu Shori Gijutsu, 25 (1984) 647.
673 S. Xu and Z. Fang, Recent Developments in Flow Injection Analysis (in Chinese), Huaxue Tongbao, 12 (1984) 22.
674 H. Ishida, M. Maeda and A. Tsuji, Enzyme Immunoassay of Alpha-Fetoprotein based on Chemiluminescence Reaction using a Flow Injection Analysis System (in Japanese), Rinsho Kagaku, 13 (1984) 129.
675 T. Owa, T. Masujima, H. Yoshida and H. Imai, Determination of Tetracycline in Plasma by Flow Injection Method with Chemiluminescence Detection (in Japanese), Bunseki Kagaku, 33 (1984) 568.
676 H. Ma and H. Yan, Application of Amperometric Flow-Through Gold Tubular Detector. Determination of Trace Sulphide Ion by Flow Injection Analysis (in Chinese), Huanjing Huaxue, 3 (1984) 75.
677 T. Takeda, S. Yoshida, K. Oda and S. Hirose, Continuous Flow Injection Analysis of Total Bile Acid in Serum (in Japanese), Rinsho Kagaku, 13 (1984) 134.
678 M. Tabata, C. Fukunaga, M. Ohyabu and T. Murachi, Highly Sensitive Flow Injection Analysis of Glucose and Uric Acid in Serum Using an Immobilized Enzyme Column and Chemiluminescence, J. Appl. Biochem., 6 (1984) 251.
679 G. Decristoforo and F. Knauseder, Rapid Determination of Cephalosporins with an Immobilized Enzyme Reactor and Sequential Subtractive Spectrophotometric Detection in an Automated Flow-Injection System, Anal. Chim. Acta, 163 (1984) 73.
680 A. Schelter-Graf, H. L. Schmidt and H. Huck, Determination of the Substrates of Dehydrogenases in Biological Material in Flow-injection Systems with Electrocatalytic NADH Oxidation, Anal. Chim. Acta, 163 (1984) 299.

681 B. F. Rocks, R. A. Sherwood and C. Riley, Controlled-dispersion Flow Analysis in Clinical Chemistry: Determination of Albumin, Triglycerides and Theophylline, Analyst (London), 109 (1984) 847.
682 T. Sakai and N. Ohno, Flow Injection Analysis of Trace Amounts of Iron with 2-Nitroso-5-(N-ethyl-N-sulfopropylamino)phenol (in Japanese), Bunseki Kagaku, 33 (1984) 331.
683 Z. Fang, S. Xu and S. Zhang, The Determination of Trace Amounts of Heavy Metals in Waters by a Flow-injection System including Ion-exchange Preconcentration and Flame Atomic Absorption Spectrometric Detection, Anal. Chim. Acta, 164 (1984) 41.
684 Z. Fang, J. Růžička and E. H. Hansen, An Efficient Flow-injection System with On-line Ion-exchange Preconcentration for the Determination of Trace Amounts of Heavy Metals by Atomic Absorption Spectrometry, Anal. Chim. Acta, 164 (1984) 23.
685 R. A. Leach and J. M. Harris, Real-time Thermal Lens Absorption Measurements with Application to Flow-Injection Systems, Anal. Chim. Acta, 164 (1984) 91.
686 P. J. Worsfold, J. Farrelly and M. S. Matharu, A Comparison of Spectrophotometric and Chemiluminescence Methods for the Determination of Blood Glucose by Flow Injection Analysis, Anal. Chim. Acta, 164 (1984) 103.
687 S. Alegret, J. Alonso, J. Bartroli, J. M. Paulis, J. L. F. C. Lima and A. A. S. C. Machado, Flow-through Tubular PVC Matrix Membrane Electrode without Inner Reference Solution for Flow Injection Analysis, Anal. Chim. Acta, 164 (1984) 147.
688 L. Nord and B. Karlberg, Extraction based on the Flow-Injection Principle. Part 6. Film Formation and Dispersion in Liquid-liquid Segmented Flow Extraction Systems, Anal. Chim. Acta, 164 (1984) 233.
689 J. N. Miller, Flow Injection Analysis: Fundamentals and Recent Developments, Anal. Proc., 21 (1984) 372.
690 D. Betteridge, A. F. Taylor and A. P. Wade, Optimization of Conditions for Flow Injection Analysis, Anal. Proc., 21 (1984) 373.
691 A. Shaw, Practical Aspects of Flow Injection Analysis, Anal. Proc., 21 (1984) 375.
692 P. J. Worsfold, Clinical Applications of Flow Injection Analysis, Anal. Proc., 21 (1984) 376.
693 J. F. Tyson, Flow Injection Analysis combined with Atomic Absorption Spectrometry, Anal. Proc., 21 (1984) 377.
694 F. Morishita, Y. Hara and T. Kojima, Flow Injection Analysis of L-Lactate with Lactate Dehydrogenase Immobilized Open Tubular Reactor (in Japanese), Bunseki Kagaku, 33 (1984) 642.
695 T. Yamane and Y. Nozawa, Catalytic Determination of Trace Amounts of Manganese with a Flow Injection System (in Japanese), Bunseki Kagaku, 33 (1984) 652.
696 T. Korenaga and K. Okada, Automated System for Total Phosphorus in Waste Waters by Flow Injection Analysis (in Japanese), Bunseki Kagaku, 33 (1984) 683.
697 K. Ogata, S. Soma, I. Koshiishi, S. Tanabe and T. Imanari, Determination of Silicate by Flow Injection Analysis coupled with Suppression Column and Solvent Extraction System, Bunseki Kagaku, 33 (1984) E535.
698 C. Gooijer, N. H. Velthorst and R. W. Frei, Phosphorescence in Liquid Solutions. A Promising Detection Principle in Liquid Chromatography and Flow Injection Analysis, Trends Anal. Chem., 3 (1984) 259.
699 L. Nord, Ph.D. Thesis, Extraction in Liquid-liquid Segmented Flow Systems applied to the Mechanization of Sample Pretreatment. Royal Inst. Techn., Stockholm, Sweden, 1984.
700 F. Lázaro, M. D. Luque de Castro and M. Valcárcel, Stopped-flow Injection Determination of Copper(II) at the ng per ml Level, Anal. Chim. Acta, 165 (1984) 177.
701 A. Fernández, M. A. Gómez-Nieto, M. D. Luque de Castro and M. Valcárcel, A Flow-injection Manifold based on Splitting the Sample Zone and a Confluence Point before a Single Detector Unit, Anal. Chim. Acta, 165 (1984) 217.

702 D. Betteridge, C. Z. Marczewski and A. P. Wade, A Random Walk Simulation of Flow Injection Analysis, Anal. Chim. Acta, 165 (1984) 227.
703 T. Yao, M. Sato, Y. Kobayashi and T. Wasa, Flow Injection Analysis for Glucose by the Combined Use of an Immobilized Glucose Oxidase Reactor and a Peroxidase Electrode, Anal. Chim. Acta, 165 (1984) 291.
704 M. Masoom and A. Townshend, Applications of Immobilized Enzymes in Flow Injection Analysis, Anal. Proc., 22 (1985) 6.
705 A. T. Faizullah and A. Townshend, Flow Injection Analysis with Chemiluminescence Detection: Determination of Hydrazine, Anal. Proc., 22 (1985) 15.
706 A. Hughes and P. J. Worsfold, Monitoring of Immunoprecipitin Reactions Using Flow Injection Analysis, Anal. Proc., 22 (1985) 16.
707 J. F. Tyson and J. M. H. Appleton, Concentration Gradients for Calibration Purposes, Anal. Proc., 22 (1985) 17.
708 J. E. Newbery and M. P. Lopez Haddad, Amperometric Determination of Nitrite by Oxidation at A Glassy Carbon Electrode, Analyst (London), 110 (1985) 81.
709 M. G. Glaister, G. J. Moody and J. D. R. Thomas, Studies on Flow Injection Analysis with Sulphide Ion-selective Electrodes, Analyst (London), 110 (1985) 113.
710 O. K. Borggaard and S. S. Jørgensen, Determination of Silicon in Soil Extracts by Flow Injection Analysis, Analyst (London), 110 (1985) 177.
711 J. Carlos de Andrade, J. C. Rocha and N. Baccan, Sequential Spectrophotometric Determination of Chromium(III) and Chromium(VI) using Flow Injection Analysis, Analyst (London), 110 (1985) 197.
712 S. D. Hartenstein, J. Růžička and G. D. Christian, Sensitivity Enhancements for Flow Injection Analysis: Inductively-coupled Plasma Atomic Emission Spectrometry using an On-line Preconcentrating Ion-Exchange Column, Anal. Chem., 57 (1985) 21.
713 C. J. Yuan and C. O. Huber, Determination of Proteins and Denaturation Studies by Flow Injection with a Nickel Oxide Electrode, Anal. Chem., 57 (1985) 180.
714 F. F. Cantwell and J. A. Sweileh, Hydrodynamic and Interfacial Origin of Phase Segmentation in Solvent Extraction/Flow Injection Analysis, Anal. Chem., 57 (1985) 329.
715 J. A. Sweileh and F. F. Cantwell, Sample Introduction by Solvent Extraction/Flow Injection to Eliminate Interferences in Atomic Absorption Spectroscopy, Anal. Chem., 57 (1985) 420.
716 J. A. Polta, I.-H. Yeo and D. Johnson, Flow-injection System for the Rapid and Sensitive Assay of Concentrated Aqueous Solutions of Strong Acids and Bases, Anal. Chem., 57 (1985) 563.
717 P. Petak, Possible Applications of Electrochemical Methods for Detection of Substances in Flowing Liquids (in Czech), Rudy, 32 (1984) 173.
718 R. A. Mowery, Jr., The Potential of Flow Injection Techniques for On-stream Process Applications, Proc. Jt. Symp. Instrum. Control 80's, (1984) 51.
719 M. Masoom and A. Townshend, Determination of Glucose in Blood by Flow Injection Analysis and an Immobilized Glucose Oxidase Column, Anal. Chim. Acta, 166 (1984) 111.
720 P. W. Alexander and U. Akapongkul, Differential Pulse Voltammetry with Fast Pulse Repetition Times in a Flow-injection System with a Copper-Amalgam Electrode, Anal. Chim. Acta, 166 (1984) 119.
721 H. D. Dewald and J. Wang, Spectroelectrochemical Detector for Flow-injection Systems and Liquid Chromatography, Anal. Chim. Acta, 166 (1984) 163.
722 R. M. Smith and T. G. Hurdley, Spectrophotometric Determination of Copper as a Dithiocarbamate by Flow Injection Analysis, Anal. Chim. Acta, 166 (1984) 271.
723 I. Schneider, Determination of Penicillin V in Fermentation Samples by Flow Injection Analysis, Anal. Chim. Acta, 166 (1984) 293.
724 P. Linares, M. D. Luque de Castro and M. Valcárcel, Fluorimetric Determination of Pyridoxal and Pyridoxal-5-phosphate by Flow Injection Analysis, Anal. Lett. B, 18 (1985) 67.

725 K. Toda, I. Sanemasa and T. Deguchi, Flow Injection Analysis of Fluoride Ions Using Catalytic Reactions (in Japanese), Bunseki Kagaku, 34 (1985) 31.
726 Y. Suzuki and T. Inoue, Determination of Cyanide Ion as Its Fluorescent Derivative by Flow Injection Analysis (in Japanese), Bunseki Kagaku, 34 (1985) 53.
727 S. A. McClintock, J. R. Weber and W. C. Purdy, The Design of a Computer-controlled Flow-injection Analyzer: An Undergraduate Experiment, J. Chem. Educ., 62 (1985) 65.
728 N. Yoza, Flow Injection Analysis and Its Application to Environmental Analysis (in Japanese), Kankyo-to-Sokuteigijutsu, 10 (1982) 22.
729 P. Hemmings, Ph.D. Thesis, Automated Flow Injection Analysis for Anions in Waters, Univ. Birmingham, U.K., 1983.
730 P. Langer, M.Sc. Thesis, Investigations for Sulphate Determination in Natural Waters by Means of Flow Injection Analysis (in German), Tech. Univ. Berlin, Germany, 1983.
731 J. L. Burguera and M. Burguera, The Principles, Applications and Trends of Flow Injection Analysis for Monitoring Chemiluminescent Reactions, Acta Cient. Venez., 34 (1983) 79.
732 J. A. Polta and D. C. Johnson, The Direct Electrochemical Detection of Amino Acids at a Platinum Electrode in an Alkaline Chromatographic Effluent, J. Liq. Chromatogr., 6 (1983) 1729.
733 T. S. C. Wang, Analytical Chemistry of Bilirubins: New Methods, Caffeine Complexation, Stability, and Biosynthesis of Conjugates, Diss. Abstr. Int. B: 44 (1983) 1109.
734 M. Gallignani, J. L. Burguera and M. Burguera, Development and Comparison of Methods for the Determination of Selenium in Biological Tissues and/or Fluids (in Spanish), Acta Scient. Venez., 34 (1983) 449.
735 A. M. Gunn, An Automated Hydride Generation Atomic Absorption Spectrometric Method for the Determination of Total Arsenic in Raw and Potable Waters, Tech. Rep. TR-Water Res. Cent., No. TR191 (1983) 31.
736 R. F. Browner, Sample Introduction for Inductively Coupled Plasmas and Flames, Trends Anal. Chem., 2 (1983) 121.
737 J. Michel, M.Sc. Thesis, Investigations for the Determination of the Content of Ionized Materials in Water by means of Flow Injection Analysis, (in German), Tech. Univ. Berlin, Germany, 1984.
738 R. F. Browner and A. W. Boorn, Sample Introduction: The Achilles' Heel of Atomic Spectroscopy, Anal. Chem., 56 (1984) 786A.
739 R. F. Browner and A. W. Boorn, Sample Introduction Techniques for Atomic Spectroscopy, Anal. Chem., 56 (1984) 875A.
740 S. Honda, T. Konishi and H. Chiba, Evaluation of Dual-wavelength Spectrophotometry for Drug Level Monitoring, Anal. Chem., 56 (1984) 2352.
741 E. Anders, R. Voigtländer, H. W. Rüttinger and H. Matshiner, Determination of Ammonium in Water and in Blood Sera from Fish by Flow Injection Analysis (in German), Z. Binnenfischerei DDR, 31 (1984) 331.
742 G. Warren, An Introduction to Flow Injection Analysis, Lab. News., Nov. (1984) 33.
743 C. F. Mandenius, B. Danielsson and B. Mattiasson, Evaluation of a Dialysis Probe for Continuous Sampling in Fermentors and in Complex Media, Anal. Chim. Acta, 163 (1984) 135.
744 F. Winquist, A. Spetz and I. Lundström, Determination of Urea with an Ammonia Gas-sensitive Semiconductor Device in Combination with Urease, Anal. Chim. Acta, 163 (1984) 143.
745 F. Winquist, A. Spetz and I. Lundström, Determination of Ammonia in Air and Aqueous Samples with a Gas-sensitive Semiconductor Capacitor, Anal. Chim. Acta., 164 (1984) 127.
746 E. Watanabe, S. Tokimatsu and K. Toyama, Simultaneous Determination of Hypo-

xanthine, Inosine, Inosine-5'-phosphate and Adenosine-5'-phosphate with a Multielectrode Enzyme Sensor, Anal. Chim. Acta, 164 (1984) 139.
747 H. Lundbäck, Ph.D. Thesis, A Study of Some Methods Involving the Determination of Hydrogen Peroxide, in particular in Flow Injection Analysis. Univ. Lund, Sweden, 1984.
748 F. Lázaro, M. D. Luque de Castro and M. Valcárcel, Simultaneous Catalytic-fluorimetric Determination of Copper and Mercury by Flow Injection Analysis. Fresenius Z. Anal. Chem., 320 (1985) 128.
749 T. Greatorex and P. B. Smith, Flow Injection Analysis — A Review of Experiences in a Water Authority Laboratory, J. Inst. Water Eng. Sci., 39 (1985) 81.
750 K. H. Kroner and M. R. Kula, On-line Measurement of Extracellular Enzymes During Fermentation by using Membrane Techniques, Anal. Chim. Acta, 163 (1984) 3.
751 Y. Baba, N. Yoza and S. Ohashi, Simultaneous Determination of Phosphate and Phosphonate by Flow Injection Analysis and High Performance Liquid Chromatography with a Series Detection System, J. Chromatogr., 318 (1985) 319.
752 T. Yao, M. Sato and T. Wasa, Flow Injection Analysis for Uric Acid by the Combined Use of an Immobilized Uricase Reactor and a Peroxidase Electrode (in Japanese), Nippon Kagaku Kaishi, 2 (1985) 189.
753 M. Koupparis and P. Anagnastopoulou, An Automated Microprocessor-based Spectrophotometric Flow Injection Analyser, J. Autom. Chem., 6 (1984) 186.
754 M. A. Marshall and H. A. Mottola, Performance Studies under Flow Conditions of Silica-immobilized 8-Quinolinol and Its Application as a Preconcentration Tool in Flow Injection/Atomic Absorption Determinations, Anal. Chem., 57 (1985) 729.
755 K. G. Miller, G. E. Pacey and G. Gordon, Automated Iodometric Method for Determination of Trace Chlorate Ion using Flow Injection Analysis, Anal. Chem., 57 (1985) 734.
756 L. T. M. Prop, P. C. Thijssen and L. G. G. van Dongen, A Software Package for Computer-controlled Flow-injection Analysis, Talanta, 32 (1985) 230.
757 A. R. Rios, M. D. Luque de Castro and M. Valcárcel, New Approach to the Simultaneous Determination of Pollutants in Waste Waters by Flow Injection Analysis, Analyst (London), 110 (1985) 277.
758 B. Olsson, H. Lundbäck and G. Johansson, Galactose Determinations in an Automated Flow-injection System containing Enzyme Reactors and an On-line Dialyzer, Anal. Chim. Acta, 167 (1985) 123.
759 A. T. Faizullah and A. Townshend, Application of a Reducing Column for Metal Speciation by Flow Injection Analysis. Spectrophotometric Determination of Iron(III) and Simultaneous Determination of Iron(II) and Total Iron, Anal. Chim. Acta, 167 (1985) 225.
760 M. Maeda and A. Tsuji, Enzymatic Immunoassay of alpha-Fetoprotein, Insulin and 17-alpha-Hydroxyprogesterone based on Chemiluminescence in a Flow-injection System, Anal. Chim. Acta, 167 (1985) 231.
761 P. van Zoonen, D. A. Kamminga, C. Gooijer, N. H. Velthorst and R. W. Frei, Flow Injection Determination of Hydrogen Peroxide by means of a Solid-state Peroxyoxalate Chemiluminescence Reactor, Anal. Chim. Acta, 167 (1985) 249.
762 Y. Hirai and K. Tomokuni, Extraction—Spectrophotometric Determination of Anionic Surfactants with a Flow-injection System, Anal. Chim. Acta, 167 (1985) 409.
763 A. G. Cox, I. G. Cook and C. W. McLeod, Rapid Sequential Determination of Chromium(III) and Chromium(VI) by Flow Injection Analysis — Inductively Coupled Plasma Atomic Emission Spectrometry, Analyst (London), 110 (1985) 331.
764 A. G. Fogg, A. M. Summan and M. A. Fernández-Arciniega, Flow Injection Amperometric Determination of Ascorbic Acid and Dopamine at a Sessile Mercury Drop Electrode without Deoxygenation, Analyst (London), 110 (1985) 341.
765 A. G. Fogg, M. A. Fernández-Arciniega and R. M. Alonso, Flow Injection Amperometric Determination of Nitroprusside at a Glassy Carbon Electrode and at a Sessile Mercury Drop Electrode, Analyst (London), 110 (1985) 345.

766 T. Fukasawa, S. Kawakubo, T. Okabe and A. Mizuike, Catalytic Determination of Vanadium by Micro Ion Exchange Separation — Flow Injection Method and Its Application to Rain Water (in Japanese), Bunseki Kagaku, 33 (1984) 609.
767 M. Miyazaki, M. Okubo, K. Hayakawa and T. Umeda, Specific and Selective Determination Method for Halide Anions by a Flow Injection Technique, Chem. Pharm. Bull., 32 (1984) 3702.
768 S. Tanabe, T. Shiori, K. Murakami and T. Imanari, A New Method for Assay of Ferroxidase Activity and Its Application to Human and Rabbit Sera, Chem. Pharm. Bull., 32 (1984) 4029.
769 H. Ciu, L. Meng and Z. Zhu, Automatic Flow Injection Colorimetric Determination of Available Aluminum in Soils (in Chinese), Fenxi Huaxue, 12 (1984) 754.
770 M. Herrera, L. S. Kao, D. J. Curran and E. W. Westhead, Flow-injection Analysis of Catecholamine Secretion from Bovine Adrenal Medulla Cells on Microbeads, Anal. Biochem., 144 (1985) 218.
771 E. Martins, M. Bengtsson and G. Johansson, On-line Dialysis of Some Metal Ions and Metal Complexes, Anal. Chim. Acta, 169 (1985) 31.
772 K. Bäckström, L.-G. Danielsson and L. Nord, Design and Evaluation of a New Phase Separator for Liquid-Liquid Extraction in Flow Systems, Anal. Chim. Acta, 169 (1985) 43.
773 S. Storgaard Jørgensen, K. M. Petersen and L. A. Hansen, A Simple Multifunctional Valve for Flow Injection Analysis, Anal. Chim. Acta, 169 (1985) 51.
774 R. C. Schothorst and G. den Boef, The Application of Strongly Oxidizing Agents in Flow Injection Analysis. Part 1. Silver(II), Anal. Chim. Acta, 169 (1985) 99.
775 E. A. Jones, Spectrophotometric Determination of Uranium(VI) with 2-(5-Bromo-2-pyridylazo)-5-diethylaminophenol in a Flow-injection System, Anal. Chim. Acta, 169 (1985) 109.
776 F. Lazaro, M. D. Luque de Castro and M. Valcárcel, Sequential and Differential Catalytic—Fluorimetric Determination of Manganese and Iron by Flow Injection Analysis, Anal. Chim. Acta, 169 (1985) 141.
777 M. Gallego and M. Valcárcel, Indirect Atomic Absorption Spectrometric Determination of Perchlorate by Liquid-liquid Extraction in a Flow-Injection System, Anal. Chim. Acta, 169 (1985) 161.
778 C. Hongbo, E. H. Hansen and J. Růžička, Evaluation of Critical Parameters for Measurement of pH by Flow Injection Analysis. Determination of pH in Soil Extracts, Anal. Chim. Acta, 169 (1985) 209.
779 R. Appelqvist, G. Marko-Varga, L. Gorton, A. Torstensson and G. Johansson, Enzymatic Determination of Glucose in a Flow System by Catalytic Oxidation of the Nicotinamide Coenzyme at a Modified Electrode, Anal. Chim. Acta, 169 (1985) 237.
780 E. B. Milosavljevic, J. Růžička and E. H. Hansen, Simultaneous Determination of Free and EDTA-complexed Copper Ions by Flame Atomic Absorption Spectrometry with an Ion-exchange Flow-injection System, Anal. Chim. Acta, 169 (1985) 321.
781 Y. Hayashi, K. Zaitsu and Y. Ohkura, Flow Injection Analysis of Hydrogen Peroxide using Immobilized Horseradish Peroxidase and Its Fluorogenic Substrate 3-(p-Hydroxyphenyl)propionic Acid, Anal. Sci., 1 (1985) 65.
782 L. Fossey and F. F. Cantwell, Determination of Acidity Constants by Solvent Extraction/Flow Injection Analysis using a Dual-Membrane Phase Separator, Anal. Chem., 57 (1985) 922.
783 A. MacDonald and T. A. Nieman, Flow Injection and Liquid Chromatography Detector for Amino Acids based on a Postcolumn Reaction with Luminol, Anal. Chem., 57 (1985) 936.
784 F. L. Boza, M. D. Luque de Castro and M. Valcárcel Cases, Flow Injection Environmental Analysis. A Review. Quim. Anal., 13 (1985) 147.
785 T. Toyoda, S. S. Kuan and G. G. Guilbault, Determination of Lactate Dehydrogenase Isoenzyme Using Flow Injection Analysis with Electrochemical Detection after Immunochemical Separation, Anal. Lett., 18 (1985) 345.

786 M. H. Ho and M. U. Asouzu, Use of Immobilized Enzymes in Flow Injection Analysis, Ann. N. Y. Acad. Sci., 434 (1984) 526.
787 U. Jönsson, I. Rönnberg and H. Malmqvist, Flow Injection Ellipsometry: An in situ Method for the Study of Biomolecular Adsorption and Interaction at Solid Surfaces, Colloid. Sur., 13 (1985) 333.
788 T. Hara, M. Toriyama, T. Ebuchi and M. Imaki, Flow Injection Analysis of alpha-Amino Acids by a Chemiluminescence Method, Chem. Lett., 3 (1985) 341.
789 C. W. McLeod, I. G. Cook, P. J. Worsfold, J. E. Davies and J. Queay, Analyte Enrichment and Matrix Removal in Flow Injection Analysis/Inductively-coupled Plasma-Atomic Emission Spectrometry. Determination of Phosphorus in Steels, Spectrochim. Acta, 40 (1985) 57.
790 J. F. Tyson, Flow Injection Analysis Techniques for Atomic-absorption Spectrometry. A Review, Analyst (London), 110 (1985) 419.
791 J. F. Tyson, C. E. Adeeyinwo, J. M. H. Appleton, S. R. Bysouth, A. B. Idris and L. L. Sarkissian, Flow Injection Techniques of Method Development for Flame Atomic-absorption Spectrometry, Analyst (London), 110 (1985) 487.
792 R. A. Sherwood, B. F. Rocks and C. Riley, Controlled-dispersion Flow Analysis with Atomic-absorption Detection for the Determination of Clinically Relevant Elements, Analyst (London), 110 (1985) 493.
793 S. Lijing, S. Zheping, L. Lin and F. Zhaolun, The Determination of Soil Available Boron with Azomethine-H by a Flow Injection Spectrophotometric Method (in Chinese), Turang Tongbao, 5 (1983) 41.
794 R. Gnanasekaran and H. A. Mottola, Flow Injection Determination of Penicillins using Immobilized Penicillinase in a Single Bead String Reactor, Anal. Chem., 57 (1985) 1005.
795 P. K. Dasgupta and H. Hwang, Application of a Nested Loop System for the Flow Injection Analysis of Trace Aqueous Peroxides, Anal. Chem., 57 (1985) 1009.
796 K. Fujiwara and K. Fuwa, Liquid Core Optical Fiber Total Reflection Cell as a Colorimetric Detector for Flow Injection Analysis, Anal. Chem., 57 (1985) 1012.
797 M. Yamade, H. Kanai and S. Suzuki, Flavin Mononucleotide Chemiluminescence for Determination of Traces of Copper(II) by Continuous Flow and Flow Injection Methods, Bull. Chem. Soc. Jpn., 58 (1985) 1137.
798 J. B. Landis, Flow Injection Analysis (in Pharmaceutical Analysis), Drugs Pharm. Sci., 11 (1984) 217.
799 Z. Niegreisz, L. Szucs, J. Fekete, G. Horvai, K. Toth and E. Pungor, Modifications of the Wall-jet Electrochemical Detector for Liquid Chromatography and Flow Analysis, J. Chromatogr., 316 (1984) 451.
800 K. Hult, R. Fuchs, M. Peraica, R. Plestina and S. Ceovic, Screening for Ochratoxin A in Blood by Flow Injection Analysis, J. Appl. Toxicol., 4 (1984) 326.
801 C. B. Ranger, An Automated Ion Analyzer, Am. Lab., 17 (1985) 92.
802 M. A. Gómez-Nieto, A. D. Luque de Castro, A. Martin and M. Varcárcel, Prediction of the Behaviour of a Single Flow-injection Manifold, Talanta, 32 (1985) 319.
803 J. T. Vanderslice and G. R. Beecher, Comments on the Paper by Gómez-Nieto, Luque de Castro, Martin and Valcárcel, Talanta, 32 (1985) 334.
804 M. Valcárcel and M. D. Luque de Castro, Reply to the Comments by Vanderslice and Beecher, Talanta, 32 (1985) 339.
805 T. Braun and E. Bujdosó, CRC Crit. Rev. Anal. Chem., 13 (1982) 233.
806 M. Gisin, Paper presented at International Symposium on Flow Injection Analysis, Örenäs, Sweden, June 1985.
807 R. M. Wightman, C. Bright and J. N. Caviness, Life Sci., 288 (1981) 1279.
808 S. V. Olesik, S. B. French and M. Novotny, Anal. Chem., submitted.
809 J. Růžička and E. H. Hansen, Anal. Chim. Acta, 173 (1985) 3.
810 See, e.g., A. Zipp and W. E. Hornby, Talanta, 31 (1984) 863.
811 J. Hungerford, G. Christian, J. Růžička and C. Giddings, Anal. Chem., 57 (1985) 1794.

Analytica Chimica Acta, 179 (1986) 59—68
Elsevier Science Publishers B.V., Amsterdam — Printed in The Netherlands

TIME-BASED FLOW INJECTION ANALYSIS

KENT K. STEWART

Department of Biochemistry and Nutrition, Virginia Polytechnic Institute and State University, Blacksburg, VA 24061 (U.S.A.)

(Received 6th September 1985)

SUMMARY

Time-based flow-injection systems are novel measurement systems which use induced dispersion of the sample in the system and measurement of time to evaluate the concentration of the analyte in the sample. There are two types of time-based system. In the standard systems, assays are based on the chemistries of the classical intensity assays; in the pseudo-titration systems, the assays are based on classical titration chemistries. These systems are discussed in terms of basic theory, classification of the systems and their advantages.

As an automated or semi-automated process for the assay of discrete samples, flow injection analysis (f.i.a.) has become utilized in a wide variety of ways with a large number of detectors. It has been used with detectors involving spectrophotometry, fluorimetry, flame emission, atomic absorption or inductively-coupled plasma spectrometry, refractive index, chemiluminescence, ion-sensitive field effect transistors, thermochemistry and a variety of electrochemical techniques [1]. The field has grown dramatically since its inception in the early 1970s and continues to generate considerable attention. As Yoza has reported, there have been more than 200 papers published on various aspects of f.i.a. since the beginning of 1984 [2].

Standard measurement systems for f.i.a. can be viewed as extensions of liquid chromatographic (l.c.) systems. With both systems, the intensity of the signal from the detector is used in the direct computation of the original concentration of the analyte. Standard systems for l.c. and f.i.a. use peak height measurements, and/or peak area measurements for the determination of the concentration of the analyte.

While very powerful, these standard systems for f.i.a. have several limitations including a limited dynamic range, cost and complexity of the detector and data system, and inability to use classical titration chemistries. In this paper, a novel variant of f.i.a. is discussed; a quite different type of measurement system is used in which time is the variable related to the concentration of the analyte. These systems are discussed in terms of basic theory, classification of the systems, advantages of such systems, and their possible future development.

0003-2670/86/$03.50

TIME-BASED FLOW-INJECTION SYSTEMS

There is a category of flow-injection systems in which the sample is extensively dispersed in the flow stream. These are the "large dispersion" systems of Růžička and Hansen [3]. Among these systems are some of the first flow-injection systems [4, 5], the pseudo-titration systems [6—13], and the use of exponential dispersion chambers as scale expansion systems for f.i.a. [14]. (The use of the term "pseudo-titration" instead of "titration" in such systems has been discussed elsewhere [1].) The unusual aspect of this type of system is that time is the variable measured to determine the concentration of the analyte. The fundamental difference in the apparatus for these types of flow-injection systems is the addition of an exponential dispersion device (Fig. 1). When a bolus of analyte is injected into the inlet side of the exponential dispersion device and the concentration of the analyte is measured at the exit of this device, time/concentration curves like those shown in Fig. 2 are obtained. Under these conditions, the time/concentration curves can usually be described as an exponential increase of concentration followed by an exponential decrease. In such systems, the original concentration of the analyte is determined by measuring the time for the intensity of the signal from the detector to go above a predetermined level and then return to go below that level (Fig. 2). Under these conditions, the logarithm of the

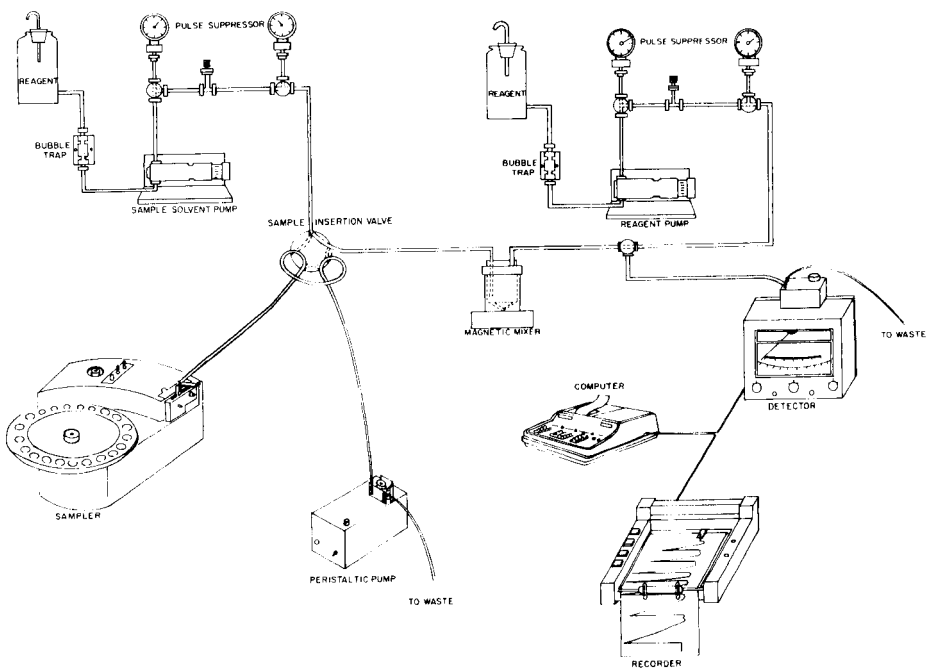

Fig. 1. Schematic diagram of an automated time-based flow-injection system [1]. Reprinted with permission.

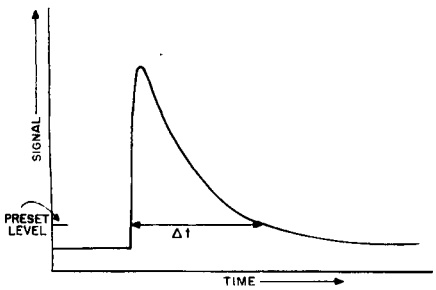

Fig. 2. Concentration profile at the exit of a dispersion chamber.

analyte concentration is usually proportional to the measured time [14] as shown by

$$\Delta t_{ep} = (V_g/f) \ln [\exp (V_s/V_g) - 1] C^{\circ}_{as} - (V_g/f) \ln [A]^{ep}_{g} \quad (1)$$

The symbols used are defined in Table 1.

Because time is the primary measurement for the determination of analyte concentration, these systems are called time-based flow injection analysis systems to distinguish them from the more standard flow-injection systems. While traditional systems are based directly or indirectly on the intensity of the measured signal, the time-based systems are not. In such systems, time is measured and the magnitude of the change in the intensity of the signal does not need to be measured. The classical assumptions about chemical measurements based on the concept of the measuring intensity and amount are not needed or, indeed, always valid with these time-based systems. The concepts inherent in the measurement of intensity are different than those in measurement of the time duration of a phenomenon. The key to successful operation of these time-based systems is that dispersion of the analyte will produce a mathematically predictable change in the detector signal such that the analyte concentration is proportional to some mathematical function of the

TABLE 1

List of symbols

Parameter	Symbol	Parameter	Symbol
Analyte concn. (mol l^{-1})		Flow rate (ml s^{-1})	f
initial	C°_{as}		
time-dependent in gradient chamber	C_{ag}	Time	
		for all sample to enter gradient chamber	t_2
Initial reagent concn. (mol l^{-1})	C°_{b}	equivalence	Δt_{ep}
Detected species concn. (mol l^{-1}) at end-point	A^{ep}_{g}	Volume (ml) gradient chamber	V_g
maximum	A^{max}_{g}	sample	V_s

time it takes for the detected species to pass through the detector. This is different than the situation for traditional flow-injection measurements.

There are two types of time-based f.i.a.: standard systems and pseudo-titration systems. Each has similarities to the other and each has some unique characteristics.

Standard time-based f.i.a.

The standard time-based flow-injection systems are analogous to the classical intensity assays, in which the intensity of some signal related to the analyte is measured directly, or the analyte is mixed with an excess of reagent and the intensity of the product is measured. In the time-based systems, the intensity is not measured, but the chemistries used for analyte detection are the same as the classical assays. Typically, the sample is inserted into a carrier stream, carried into and then out of the exponential dispersion device, and mixed with an excess of reagent; the mixture is allowed to react, and the product is monitored at the detector as the stream flows through it. When the detector signal exceeds a preset level, a timer is started and continues to run until the detector signal goes below a preset level. The logarithm of the analyte concentration is proportional to the measured time (Eqn. 1). The initial analyte concentration is obtained from a standard plot of the logarithm of the analyte concentration versus the equivalence time. Stewart and Rosenfeld [14] described this type of time-based flow-injection system with spectrophotometric, fluorimetric, conductometric, and flame emission detector systems. It appears that a standard time-based system could be developed for use with almost any detector.

Pseudo-titration time-based f.i.a.

The pseudo-titration systems are analogous to classical titrations. This type of system was first reported by Růžička et al. [6] and has been studied by several groups [7—13]. Typically, the sample is inserted into a carrier stream, carried into and then out of the exponential dispersion device, and mixed with the titrant; the mixture is allowed to react, and the analyte, titrant, or product concentration is monitored at the detector as the stream flows through it. Again, when the detector signal exceeds a preset level, a timer is started and continues to run until the detector signal goes below the preset level. In these pseudo-titrations, either the analyte is injected directly into the titrant stream and this mixture flows to the exponential dispersion device, or the analyte is injected into a carrier stream and the titrant is mixed with the effluent coming out of the device. Typical concentration profiles for the second type of system are shown in Fig. 3. Růžička et al. [6] used the following equation to describe the relationship of the "equivalence time" to the concentrations of the analyte and the titrant:

$$\Delta t_{ep} = (V_g/f) \ln C^{\circ}_{as} - (V_g/f) \ln C^{\circ}_{b} + \ln (V_s/V_g) \qquad (2)$$

The selection of the predetermined reaction equivalence points for the initia-

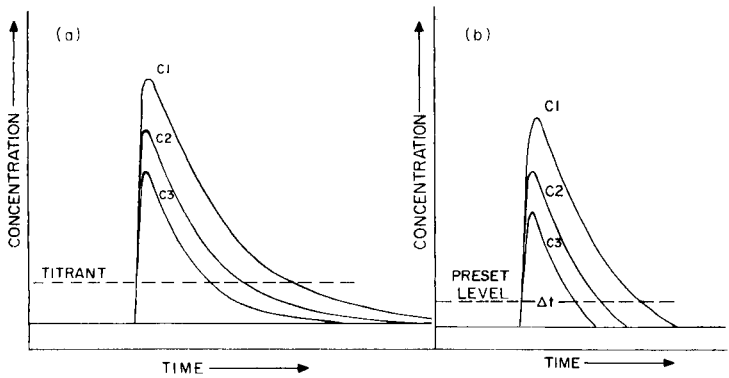

Fig. 3. Concentration profiles for time-based flow-injection systems [1]. (a) Concentration profiles for three different samples with original concentrations $C1$, $C2$, and $C3$ as the effluent emerges from the exponential dispersion device if no titrant is present; (b) pseudo-titration concentration profiles of the three samples after reacting with the titrant. The preset levels used for the Δt measurements are normally the inflection points of classical titration procedures. Reprinted with permission.

tion and cessation of the timing was based upon known inflection points determined in classical titration measurement systems. Essentially all the pseudo-titration systems have been developed for single end-point assays, although Růžička and Hansen [13] have reported the spectrophotometric pseudo-titration of dibasic acids. As with the above standard time-based systems, calibration curves are needed for the assay of unknowns.

Theory of time-based flow-injection systems

Pardue and Fields [15] expanded the theoretical basis for understanding high-dispersion systems beyond the early work of Nagy et al. [4] and Růžička et al. [6]. Their work provides an in-depth basis for the understanding of the relationship of the concentration of the sample and reagent to the "equivalence time" in the time-based pseudo-titration and standard systems. Pardue and Fields' equations for the concentration/time course, the maximum concentration produced by such a time course, and the time equivalence point for pseudo-titrations, respectively, are

$$C_{ag} = C^{\circ}_{as}[1 - \exp(-ft_2/V_g)] \exp[-f/V_g)(t - t_2)] \tag{3}$$

$$[A]_g^{max} = C^{\circ}_{as}[1 - \exp(-ft_2/V_g)] \tag{4}$$

$$\Delta t_{ep} = (V_g/f) \ln \left\{ C^{\circ}_{as} \frac{C^{\circ}_{as}[\exp(V_s/V_g)](zC^{\circ}_b + 1) - C^{\circ}_{as} - C^{\circ}_{bg}}{(C^{\circ}_{as} + zC^{\circ}_{bg})} \right\}$$
$$- (V_g/f) \ln \{[A]_g^{ep} + zC^{\circ}_b\} \tag{5}$$

Their work was an important advance in the understanding of time-based flow systems. However, as they noted, their procedure did not take into

account the effect of the laminar flow known to occur in such systems. The work of Vanderslice and coworkers [16—18] has demonstrated that when a bolus of analyte moves through a small-bore tubing, not only does the concentration of the analyte change along the length of the tubing with time, it also changes across the tubing with time; illustrative diagrams are given in another paper in this issue [18]. Obviously, the same phenomenon occurs after the analyte leaves the exponential dispersion chamber and more theoretical studies are needed for a better understanding of the present time-based systems.

The advantage of time-based flow-injection systems

Much has been said about the disadvantages of deliberately inserting an exponential dispersion device into a flow-injection system. For example, Růžička et al. [6] noted that the sensitivity of such systems is much lower than that of standard flow-injection systems and that the throughput is usually less. However, reducing the volume of the exponential dispersion device can significantly decrease the observed dilution of the sample and increase the throughput [12].

There are several reasons for continued interest in inserting a dispersion chamber into a flow-injection system. Among the more important is the potential ability to utilize the extensive numbers of chemistries developed for classical titrations in the proposed pseudo-titration assays. There is an enormous need for rapid automated titration systems. Properly designed time-based pseudo-titration flow systems could meet many of these needs. Another advantage of the time-based flow-injection systems is their large linear range. Such systems have been demonstrated to have a larger linear range than the standard flow-injection systems; scale expansions of 2—30-fold were obtained in the early studies by Stewart and Rosenfeld [14]. Linear ranges of six orders of magnitude might be possible for many assays planned around time-based f.i.a.

There are other potential advantages for these systems. For example, appropriate system design could lead to economies in the reagent used per assay and could utilize simpler detectors and data-acquisition systems and still be capable of sample through-puts of at least 100 h^{-1}. Possible losses in sensitivity would be of little practical importance in many routine laboratories compared to the advantages of expanded assay ranges, lower reagent use, and simpler instrumentation. The assay time of the system is reasonably insensitive to the concentration of the analyte. The incorporation of a microprocessor feed-back system [19] is a simple solution to the problem of the variable timing required when samples with widely varying concentrations are assayed in one batch of samples.

CLASSIFICATION OF SYSTEMS

All flow-injection systems fall under Pardue's classification of kinetic methods of analysis [20]. Pardue [21] has recently suggested that these time-based pseudo-titrations not be classified as such but rather as a variable-time kinetic method. While such a description is technically correct, it seems not sufficiently descriptive. It is useful to re-examine the categories of classical assays for better classification of normal flow-injection and time-based flow-injection systems. The information in Table 2 summarizes the following discussion.

Classical assays

There are important differences between classical assays done in mixed solutions ("beaker assays") and those done in flowing streams. Traditional assays have been classified in various ways, but usually the classification systems start with the concepts of equilibrium or kinetic assays. It is useful to approach the classification from the perspective of whether the assays are "intensity" assays or "trigger point" assays, and then to further classify them with regards to their kinetic or equilibrium characteristics.

Intensity assays. With many traditional assays based on chemical equilibria, the analyte concentration is proportional to some mathematical function of the intensity of the measured signal (e.g., weight, light intensity, voltage, volume). Such systems can be classified as "intensity assays". With equilibrium systems, physical equilibrium (i.e., concentration does not change with position in measurement device) and chemical equilibrium (i.e., total concentration does not change with time) are assumed and required. The assay conditions routinely require an excess of reagent. Standard curves are often not required and absolute measurements can be made.

TABLE 2

Classification of assays

	Classical "beaker" assays		Flowing stream assays			
	Photometric	Titrimetric	L.c.	F.i.a.	Time-based f.i.a.	
					Standard	Pseudo-titrations
Type	Intensity	Trigger point	Intensity	Intensity	Trigger point	Trigger point
Equilibrium						
chemical	+/—	+	+/—	+/—	+/—	+
physical	+	+	—	—	—	—
Reagent/ analyte ratio	R ≫ A	$nR = A$ (amount)	R ≫ A	R ≫ A	R ≫ A	$nR = A$ (Concn.)
Measurement point	Equilibrium	$nR = A$ (mole)	Time window Peak height Peak area	Time window Peak height Peak area	Time window Arbitrary	Time window $nR = A$ (Concn.)
Completely mixed at detector	Yes	Yes	No	No	No	No
Standard curve	No	No	Yes	Yes	Yes	Yes

With traditional kinetic assays (either fixed time or variable time), the analyte is also proportional to some mathematical function of the intensity of the signal acquired during the assay. Physical equilibrium is normally assumed and required and the assays routinely require an excess of reagent, but chemical equilibrium is not attained. Measurements are normally made either at fixed time intervals or after fixed concentration changes have occurred. Standard curves are usually required.

Trigger-point assays. There is a class of assays, here called trigger-point assays, in which the intensity of the signal from the detector is not proportional to a mathematical function of the concentration of the analyte. In these assays, a change in the detector signal is used as a trigger to indicate the beginning and/or the end of the measurement process. The signal itself is not quantified, but rather some quantity like volume or time is measured and used in the calculation of the analyte concentration. Spectrophotometric and potentiometric titrations are two examples of equilibrium trigger-point assays. In the classical assays, physical equilibrium normally exists at the point of measurement, and most of the chemical reactions associated with titrations also reach equilibrium at the point of measurement. The normal criterion for an end-point is that stoichiometrically equivalent molar amounts of the titrant and the analyte are present. Absolute measurements are possible; standard curves are normally not required.

Flowing liquid stream assays

Liquid chromatography. Liquid chromatographic systems with on-line detectors can be viewed as extensions of traditional intensity assays. Peak heights are single measurements of the intensity of a signal, and peak areas are the integrated intensity. Such measurements are usually made within time windows. Post-column reaction systems normally use an excess of reagent. Chemical equilibrium may or may not have occurred at the measurement point. In other ways, these systems are very different from traditional intensity assays. Physical equilibrium is not a feature of most chromatographic systems at the time of measurement. As seen above, the analyte and/or product is not usually completely mixed at the detector, and the best that can be done is to measure an apparent concentration inside a time window. Because all the factors that govern this apparent concentration are not fully understood theoretically, much less how the variables may interact, standard curves are essential in these assays.

Flow-injection analysis. Flow injection assays can be viewed as extensions of liquid chromatographic (l.c.) measurements. As in l.c., peak heights and/or peak areas are measured, and an excess of reagent is normally used. Chemical equilibrium may or may not be established at the time of measurement, and physical equilibrium is not achieved. As in l.c., the concentration of the analyte is usually a function of many variables. But, whereas in l.c. the time windows of measurement for the assay of individual components vary in both starting time and width, dependent on the retention times, in

f.i.a. the time windows are fixed both as to starting time from the point of sample injection and width. Standard curves are essential. (Stopped-flow systems and dilution systems are not discussed here.)

Time-based flow-injection analysis. The time-based assays are trigger-point assays. The detector signals are used only to initiate and switch off a timer. Like f.i.a., the time-based systems use time windows with a fixed starting point from sample injection, but these time windows vary in width. As in l.c. and flow-injection systems, physical equilibrium is not attained during the assay.

Standard time-based flow-injection systems have some characteristics similar to other flow systems and some similar to classical intensity assays. Chemical equilibrium may or may not have occurred at the point of measurement. The reagent concentration is in considerable excess at the point of measurement, but not necessarily throughout the bolus. The measurement points are usually some point of low concentration significantly above the background noise; thus far their selection has been rather arbitrary.

The time-based pseudo-titration systems are similar to classical titration systems; however, there are important differences. Chemical equilibrium usually has occurred at the point of measurement. As shown in Table 2, the concentration of the analyte is some multiple of the concentration of the reagent at the trigger points, but not necessarily throughout the entire bolus. Setting of the measurement points thus far has been based on the end-points in classical titration systems.

Conclusion

These novel time-based systems make it possible to utilize many of the traditional titration chemistries, thus considerably expanding the working concentration range of standard flow-injection assays in continuously flowing streams, and possibly simplifying the associated instrumentation. A great deal of work needs to be done, particularly on the design of instrumentation, the understanding of the theoretical aspects of the systems, and on the adaptation of classical chemistries.

In the development of this field, it is important to see time-based flow-injection systems for what they are. Analogies to "beaker" systems and intensity measurements may sometimes be acceptable, but the conditions in flowing streams and the conditions of trigger-point assays are quite different from those of the classical techniques. These differences must be recognized and classified if the development of this novel analytical tool is not to be hindered.

REFERENCES

1 K. K. Stewart, Anal. Chem., 55 (1983) 931A.
2 N. Yoza, J. Flow Inject. Anal., 1 (1984) 32, 49; 2 (1985) 61.
3 J. Růžička and E. H. Hansen, Flow Injection Analysis, J. Wiley and Sons, New York, 1981.

4 G. Nagy, Zs. Feher and E. Pungor, Anal. Chem. Acta, 52 (1970) 47.
5 H. U. Bergmeyer and A. Hagen, Fresenius Z. Anal. Chem., 261 (1972) 333.
6 J. Růžička, E. H. Hansen and H. Mosbaek, Anal. Chim. Acta, 92 (1977) 235.
7 G. Nagy, K. Toth and E. Pungor, Anal. Chem., 47 (1975) 1460.
8 G. Horvai, K. Toth and E. Pungor, Anal. Chim. Acta, 82 (1976) 45.
9 G. Nagy, Zs. Feher, K. Toth and E. Pungor, Anal. Chim. Acta, 91 (1977) 87; 91 (1977) 97; 100 (1978) 181.
10 O. Astrom, Anal. Chim. Acta, 105 (1979) 67.
11 A. U. Ramsing, J. Růžička and E. H. Hansen, Anal. Chim. Acta, 129 (1981) 1.
12 K. K. Stewart and A. G. Rosenfeld, J. Autom. Chem., 3 (1981) 30.
13 J. Růžička and E. H. Hansen, Anal. Chim. Acta, 161 (1984) 1.
14 K. K. Stewart and A. G. Rosenfeld, Anal. Chem., 54 (1982) 2368.
15 H. L. Pardue and B. Fields, Anal. Chim. Acta, 124 (1981) 39, 65.
16 J. T. Vanderslice, K. K. Stewart, A. G. Rosenfeld and D. J. Higgs, Talanta, 28 (1981) 11.
17 J. T. Vanderslice, G. R. Beecher and A. G. Rosenfeld, Anal. Chem., 56 (1984) 292.
18 J. T. Vanderslice, A. G. Rosenfeld and G. R. Beecher, Anal. Chim. Acta, 179 (1985) 119.
19 J. F. Brown, K. K. Stewart and D. Higgs, J. Autom. Chem., 3 (1981) 182.
20 H. Pardue, Clin. Chem., 23 (1977) 2189.
21 H. L. Pardue, in K. K. Stewart and J. R. Whitaker (Eds.), Modern Methods of Food Analysis, Avi, Westport, CT, 1984, pp. 1—28.

Analytica Chimica Acta, 179 (1986) 69—80
Elsevier Science Publishers B.V., Amsterdam — Printed in The Netherlands

CONTROLLED-DISPERSION FLOW ANALYSIS
Flow-Injection Analysis Applied to Clinical Chemistry

C. RILEY*

Centre for Medical Research, University of Sussex, Falmer, Brighton BN1 9RF (Great Britain)

B. F. ROCKS and R. A. SHERWOOD

Biochemistry Department, Royal Sussex County Hospital, Eastern Road, Brighton (Great Britain)

(Received 2nd September 1985)

SUMMARY

Mechanisation came early to clinical chemistry and has passed through a number of phases. Selective multichannel machines, usually discrete analysers with their associated mechanical complexities, have become popular; the simplicity and reliability of flow analysers has been lost. Flow injection offers new opportunities to develop simple selective machines. Sample waste is avoided in the controlled-dispersion flow analyser; the slug of sample is picked up by a probe, the volume being metered by the peristaltic pump driven by a stepping motor under computer control. Reagent waste is avoided by a similar system and use of merging zones. Very economical operation is thus possible and acceptable precision is attained. Various features of the technique, including prolonged incubation, use of kinetic methods to minimise the need for blanks, and application of different detectors are discussed in the context of clinical assays. Anomalous behaviour of particulate matter in flow streams and the changing shape of sample slugs in stationary streams are described. The application of flow-injection systems in clinical chemistry is extremely promising.

The progressive development of automatic analysis has alleviated the pressure on clinical laboratories, enabling them to cope with exponentially increasing workloads. Careful organisation has permitted the equipment to deal with irregular floods of samples on which multiple tests are required. Although most laboratories are equipped to conduct a wide range of analyses, a mere dozen tests account for 80—90% of the workload. For many years, this 80—90% has been entrusted to multichannel analysers which have been so designed that they perform a fixed set of tests (usually 12) on every specimen, irrespective of what was actually needed or requested. Of these multichannel analysers there have been two distinct types, namely the (gas-segmented) continuous flow typified by the Technicon SMA series and the so-called discrete analysers such as the AGA Autochemist or the Vickers M300. In the discrete analysers, each sample and its reagents are of course handled separately in a separate container and this confers a degree of

0003-2670/86/$03.50

versatility. Both types have their proponents but in truth there is not too much to choose between them. The continuous flow analyser is simpler, more reliable and easier to maintain. The discrete analyser is generally much faster but is bulkier and noisier and requires more highly skilled operators. The precision and accuracy of the two systems and their respective running costs are remarkably similar.

For most of the era of automatic analysers, economy in the use of reagents has been of limited importance but in the last few years, legislation in the United States, the imposition of strict budgetary control in the UK and similar happenings in continental Europe have influenced the design of machines. Now the preferred machine is a selective or discretionary analyser which will run only those tests which are specifically requested and will use a minimum of sample and reagent for such tests as are actually done.

A selective multichannel analyser must be so designed that its individual channels can remain on standby, often for prolonged periods, consuming no reagents but ready for immediate use. This excludes the simple and robust segmented continuous flow analyser which takes a considerable time to start and stop. Thus all the selective machines at present commercially available are discrete analysers. Discrete selective analysers are invariably costly and complex and this in part defeats the aims of their users. These considerable disadvantages led us to try to apply flow-injection to this field. Flow-injection, which can be left on standby for prolonged periods and which is simple, cheap and reliable, may well provide the perfect alternative.

There have always been particular difficulties in mechanisation of clinical tests and at first glance these seem to prohibit the use of flow-injection techniques. The major problem is the specimen. Most analyses are needed for blood plasma or serum which is always limited in volume and by virtue of its protein content (about 7% by weight) is sticky and viscous. These physical properties make volumetric measurement difficult and also make contamination between samples a serious hazard. A slightly lesser problem is the cost of reagents. Some, particularly those involved in enzyme assays, are so expensive that their use as carrier fluids is out of the question. Finally, there is the problem of the slow reaction; some of the reactions used in clinical tests proceed very slowly, for example, a commonly used manual technique for measuring acid phosphatase calls for incubation for 30 min. This does not suit conventional flow-injection techniques at all.

SAMPLE INTRODUCTION IN FLOW-INJECTION ANALYSIS

The earliest method of sample introduction, injection from a small syringe, either through the wall of the tube or through a septum [1] or a flap valve [2] was for some time the only method which did not waste precious sample. Rocks and co-workers [3, 4] used this technique together with atomic absorption spectrometry to measure concentrations of lithium, zinc and copper in serum. The technique is too slow to be useful in most areas of clinical chemistry but in this particular application it is quite satisfactory.

Injection valves of various forms have been used by many workers. The rotary valves with flat faces as described by Růžička and Hansen [5] and Anderson [6] are difficult to keep watertight; taps with tapered plugs are better in this respect. The bypass valves used in liquid chromatography are excellent but expensive. None of these valves is really suitable for clinical chemistry because an excess of sample must be used to ensure that the measuring space is cleaned. Other ingenious techniques, for example the hydrodynamic method of Růžička and Hansen [7] or the pinch valve system devised by Harrow and Janata [8] are also wasteful of sample. To avoid this waste, the alternative sampling method that we have called controlled-dispersion flow analysis was developed. In this, a probe is used for sampling. In the simplest form of the system (Fig. 1), the probe normally rests in reagent. When sampling takes place the (peristaltic) pump is stopped and the probe is transferred to the sample container. The pump then makes a predetermined precise angular movement, drawing sample into the probe. The probe is then returned to the reagent container and the pump is restarted so that the slug of sample is propelled onwards by a stream of reagent as in conventional flow-injection analysis (f.i.a.). More sophisticated versions were subsequently developed (Fig. 2); in these, reagent and sample were aspirated independently into distilled water as carrier and the concept of merging zones [9] was exploited. It was also possible to introduce two reagents by this method (Fig. 3). This version of f.i.a. thus provides the basic clinical requirements of strict economy of sample and reagents. It was described at some length in 1983 [10].

Some of the problems expected in using flow-injection to handle serum have failed to materialise. For example, viscosity, although it varies from

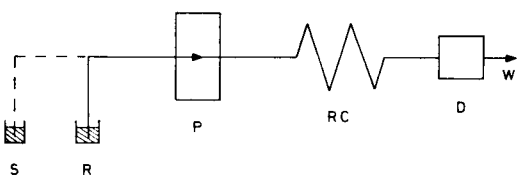

Fig. 1. Single-probe controlled-dispersion analyser: S, sample; R, reagent; P, peristaltic pump driven by a microcomputer-controlled stepper motor; RC, reaction coil; D, detector; W, waste. The broken line represents probe movements. These symbols are also used in Figs. 2—4 and Fig. 7.

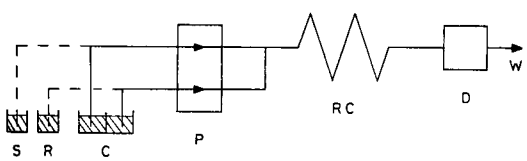

Fig. 2. Double-probed controlled-dispersion analyser. Both probes are attached to a single transfer arm; C, carrier solution (usually demineralised water).

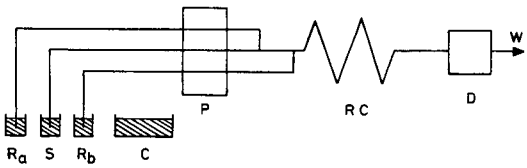

Fig. 3. Triple-probed controlled-dispersion analyser. The probes are shown in the sampling position. During the remainder of the analytical cycle, all three probes rest in the carrier solution.

sample to sample, does not seem to cause any variation in performance (although Betteridge et al. [11] have used f.i.a. to measure viscosity). Probably, the small volumes of sample are diluted with water so quickly that variation between samples is small. There were also fears that the stickiness of the sample might cause serious carryover. This problem has not arisen presumably because the entire system is so thoroughly washed by carrier fluid. An additional problem which caused concern was the possibly severe dispersion of the slug as it passed through the pump. This was tested by using the single-probe system shown in Fig. 1 but relocating the pump downstream of the detector and comparing the dispersion (calculated as described by Růžička and Hansen [12]) with that obtained with the original arrangement. Surprisingly, there was appreciably less dispersion when the slug passed through the rollers; we do not have a really satisfactory explanation for this.

Another great anxiety was whether the technique would provide adequate precision. In automatic analysers, an assortment of components including the samplers and dispensers, the readout devices (usually colorimeters) and the heating systems all make their own contribution to error. It has been our practice in the past to measure the reproducibility of each of these [13] and by using the sum-of-squares rule, to calculate the theoretical reproducibility of the whole system. Attempts to do this early in the present work were discontinued for the following reasons.

There are three methods for measuring the precision of a liquid-sampling device. One can aspirate a coloured solution, discharge it into a known volume of diluent and measure the absorbance in a photometer; but there is basic error in photometry (typically a relative standard deviation of 0.5%) and in any case the method does not lend itself well to f.i.a. where the slug is in dynamic contact with diluent at all times. In the second method, one can aspirate samples of distilled water from a small container, weighing the container before and after each aspiration. This method contributes its own error because it does not take account of the sample sticking to the outside of the probe and that lost by evaporation. The third method, that of measuring samples of radioactive material (usually a γ-emitter) gives all the reproducibility needed at the expense of counting perhaps a million counts, but requires the use of dangerously high levels of radioactivity if counting is not

to be impossibly prolonged. Weighing was actually used but was abandoned later when a relative standard deviation of less than 1% was achieved. It is in fact difficult to study individual parts of a flow-injection system; subsequently, only the performance of the system as a whole was measured either by conducting a simple chemical reaction or by pumping samples of stable coloured solutions. The exception to this is the study of temperature contol, which proved to be a great problem and which will be dealt with later.

In the course of this measurement exercise, several factors were found which are believed to have considerable bearing on precision. First, the design of the pumps. Custom-made pumps were used. These had closely spaced rollers and platens which were so designed that the rollers engaged and disengaged with them gradually giving relatively little pulsation. Minute errors of concentricity of the rotor are unavoidable with all pumps. To compensate for this, sampling always started with the same roller at the same angle, positioned so that it had just occluded the sample pump tube. To avoid "compression-set" of the pump tube, the pump tube was indexed a few degrees at frequent intervals when the system was on standby.

Another major contributor to imprecision is the occurrence of air bubbles in the system; these, of course, deform the peaks and can block the light path almost completely in an unpredictable manner as they pass through the cuvette. There are two distinct types of problem here: large solitary bubbles which appear in the probe and pass immediately through the system, and minute bubbles which appear on the inner surface of the conduits and slowly grow in size. With regard to the large solitary bubbles, it was not clear whether they were entering at the tip of the probe or whether the pressure drop inside the probe during aspiration of the sample was causing dissolved air to come out of solution. However, using a probe of larger diameter made matters worse and replacing the probe with a glass capillary enabled one to see bubbles entering at the tip. Careful positioning of the flexible tube connecting the probe to the pump eradicated the problem. The fine bubbles proved to be a subtler problem and one that can occur in all kinds of flow-injection systems. They are much more insidious than large bubbles; when conditions favour them they appear in large numbers, gradually grow and coalesce and are finally dislodged, producing erratic signals as described above. Inside the cuvette, they can gradually reduce the light path until a larger bubble dislodges them. These bubbles are obviously caused by dissolved air coming out of solution. Many of the reagents used clinically are unstable and must be stored cold. This aggravates the problem of air coming out of solution because the temperature of the reaction mixture must be raised inside the system and many reactions require incubation at raised temperatures. Various expedients were tried but the more obvious ones were only partly successful. Heating under reduced pressure is only acceptable with stable reagents; even ultrasound damages some reagents. Restricting the discharge of the cuvette to raise the internal pressure is

fairly effective but increases the tendency of the system to leak. Recently, shaking the reagents with helium, which retains its solubility at higher temperatures, was tested. This appears to be effective (Fig. 4) but it has not been used sufficiently for certainty that there are no serious disadvantages.

One contributor to precision which applies only to computerized systems is "working off the peak". In the software used here, the sampling system may not identify the actual tip of an extremely sharp peak. In order to improve this, the actual reading was taken after the apex of the peak had passed. This is discussed below.

HEATING AND TEMPERATURE CONTROL

Many reactions used in clinical chemistry call for incubation of the sample at temperatures above ambient, typically 30°C. Many enzymes are unstable at raised temperatures and proteins are denatured at about 55°C so that the lowest practicable temperatures should be used. Reactions are seldom

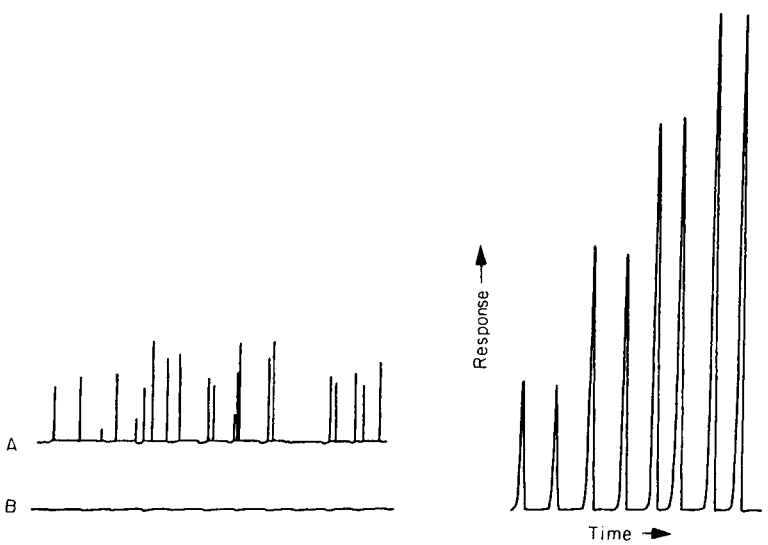

Fig. 4. Demineralised water (21°C) put through six analytical cycles involving a stopped-flow incubation period of 20 s at 37°C. The spikes result when small air bubbles pass through the colorimeter. (A) Untreated laboratory demineralised water; (B) helium-saturated demineralised water.

Fig. 5. Single standard calibration. The peaks were produced by duplicate introduction of different volumes (left to right 1.25, 2.50, 3.75 and 5.00 μl) of a single standard (1 mmol l^{-1} magnesium). The flow arrangement was the same as shown in Fig. 1 with the atomic absorption spectrometer as detector and an additional input of carrier solution between the pump and the mixing coil (see text).

carried to completion or are measured in the kinetic mode, thus precise temperature control and efficient heat transfer are mandatory; temperature variation of less than ±0.2°C in the reaction mixture is the usual aim. Calculation of heat transfer through the relatively thick walls of a plastic tube to a 0.5 mm diameter column of intermittently flowing liquid proved to be surprisingly difficult. Some simple experiments were therefore done. A coil (1.5 m) of PTFE tubing (0.5 mm i.d., 1 mm o.d.) was immersed in a water bath and the temperature of the emerging water was measured with a small thermistor probe. With the water bath held at 30°C and water at 20°C pumped continuously through the tube at 4 ml min^{-1}, the temperature of the emerging stream did not rise above 28°C. If the pump was halted for 30 s and restarted, the temperature of the emerging stream rose briefly to almost 30°C and then fell back to 28°C. Temperature fluctuations of this magnitude are unacceptable so the behaviour of metal tubing was examined. When PTFE was replaced by stainless steel tubing of the same dimensions, the temperature fluctuations became acceptably small. For subsequent work, the stainless steel tubing was embedded closely in a round-bottomed spiral groove machined in the surface of a cylindrical aluminium bar. The bar was heated by a cartridge heater and its temperature was controlled by a commercial 3-term controller.

Problems then appeared with the simple free-standing colorimeter originally in use. Unless care was taken to match the temperature of the cuvette with that of the reactor tubing, there were severe refractive-index effects which produced spurious signals. In addition, for enzyme assays it was necessary to hold the reaction mixture in the cuvette at controlled temperatures. Therefore, in the final version, the cuvette housing of the colorimeter was embedded in the cylindrical heater block and the reactor tubing was wound outside. The effectiveness of this was demonstrated by using the thermochromic solution devised by Blume [14] and Bowie et al. [15]. This is the only practicable way of measuring the temperature inside these small cuvettes.

Several simple colorimeters were constructed. All were single-beam instruments with tungsten halogen sources, fed from stabilised variable-voltage power supplies. Tungsten halogen lamps were chosen because they have a useful output in the long ultraviolet and most measurements of enzyme activity are made at 340 nm. The detectors used are photodiodes and if an output to a millivolt recorder is all that is needed, photodiodes with built-in pre-amplifiers are adequate without any additional amplification. Interference filters are used and these must be multilayer filters of very good quality for work at wavelengths below 450 nm.

SLOW REACTIONS

Achieving long incubation times is no problem when samples spend perhaps 10 min inside the machine as in most conventional machines, but the residence time is nearer 10 s in a basic flow-injection system. Of course, the

system can be halted for prolonged periods; e.g., Lim et al. [16] arrested the reaction mixtures for 6 min in order to achieve energy-transfer fluoroimmunoassays (a rate of ten tests per hour) but most clinical chemists seem to want a sample throughput of about 120 h^{-1}. This only allows sufficient time to permit the use of the simple kinetic approach [5] in which the sample is held in the cuvette whilst the rate of change of absorbance is observed, and it serves well for the simpler enzyme assays. Some enzymes however require pre-incubation and others are present in very small amounts, both of which require at least several minutes of treatment. As a first step, queueing samples one behind the other in an elongated reactor was tried. The most that could be achieved satisfactorily was three samples and then only by using very small volumes of sample which defeated the object. The single-bead-string reactor [17] and the knitted reactor [18] were both tried with some improvement but no increase in the number of specimens was possible. Růžička and Hansen [19] described a multichannel holding device for dealing with this problem but it is somewhat difficult to construct. Instead a small multiport tap was used, together with 100-cm long holding coils which were brought together at a junction downstream. This proved to be very effective and has been used for measuring acid phosphatase but it did present a problem in that each coil produced different-sized peaks. It would of course be possible to alter the length of the coils to compensate for this but in fact it is much easier to insert correction factors into the computer.

SOME APPLICATIONS OF THE CONTROLLED-DISPERSION FLOW ANALYSER

A list of assays achieved by means of controlled-dispersion flow analysis (c.d.f.a.) is given in Table 1. The type of detector used, the sampling frequency and the sample and reagent volumes are tabulated.

In its simple single-channel form, c.d.f.a. (Fig. 1) has been used to determine sodium and potassium with ion-selective electrodes (i.s.e's) and to measure magnesium, lithium, zinc and copper by atomic absorption spectrometry (a.a.s.). Sodium and potassium can be determined simultaneously by placing the two i.s.e.'s and the reference electrode close together and in such a way as to form a flow channel; a glass capillary sodium electrode and a valinomycin membrane electrode were used. The most reproducible response was obtained by stopping the flow and holding the sample slug in contact with the electrodes for about 30 s before taking the reading.

The use of conventional f.i.a. in conjunction with a.a.s. has already been mentioned. The controlled-dispersion flow analyser has proved to be an even better method of introducing serum samples into an atomic absorption spectrometer [20]. A given pump tube can be used to produce an almost infinite number of dispersion values simply by changing the sample volume. Serum copper and zinc assays require a dispersion of less than 2, while magnesium assays require a dispersion of 80. These vastly different

TABLE 1

Sample and reagent volumes and sample throughput for the controlled-dispersion flow analyser (photometric detection unless indicated otherwise)

Analyte	Sample volume (μl)	Reagent volume (μl)	Sample throughput (h^{-1})	Analyte	Sample volume (μl)	Reagent volume (μl)	Sample throughput (h^{-1})
Albumin (1)	0.24	360	120	Lactate dehydrogenase	16	130	80
Albumin (2)	2.4	16.6	180				
Aspartate transaminase	40	100	120	Phosphate	20	100	120
				Theophylline	9	120	80
Acid phosphatase	21	500	48	Total protein	12	260	180
Alkaline phosphatase	20	75	120	Triglycerides	7.5	115	120
Total bilirubin	20	100	120	Urea	12	180	100
Calcium	4	95	200	Uric acid	12	75	100
Cholesterol	6	150	120	Sodium/potassium[a]	120	—	80
Chloride	6	110	200	Copper[b]	120	—	120
Creatinine	30	120	120	Lithium[b]	13.5	—	180
γ-Glutamyl transferase	30	120	120	Magnesium[b]	2.5	—	150
Glucose	11	125	120	Zinc[b]	120	—	120

[a]With ion-selective electrodes. [b]By a.a.s.

dispersion requirements are achieved with the same pump tube by adjusting the volume of sample. In high-dispersion assays, the detector response is directly proportional to the sample volume. This often allows single standard calibration. In this case, the computer is programmed to sample three or more different volumes of an appropriate standard. For example, different volumes of a single magnesium standard can be used to produce a calibration graph (Fig. 5). This approach can also be used to dilute and re-analyse samples that produce readings above a preset concentration level. To prevent the nebuliser running dry during the probe transfer, a reservoir of carrier solution should be connected via a T-piece between the pump and the mixing coil in the manifold outlined in Fig. 1. The most stable flame conditions result when the pumping rate is matched to the aspiration rate.

The use of twin sampling probes and merging zones for simple colorimetric assays was described above. This type of arrangement was used to determine serum albumin by a dye-binding method [21]. If necessary, additional reagents can be added in a similar way.

Considerable use is made in clinical chemistry of enzyme-magnified immunoassays. For such assays, a two-reagent merging zone system is used. In this case three probes are attached to the transfer arm as shown in Fig. 3. The manifold tubing is arranged so that the reagent containing the antibody and enzyme substrate (Ra) is added to the sample slug before the second reagent containing the enzyme-labelled antigen (Rb). By this means the drug theophylline was determined in serum [22]. When merging zones were used in such applications, it was found easier to use a larger pump tube for reagent so that the reagent slug overlapped the sample slug and consequently small variations in relative flow rates were unimportant.

Measurement of reaction products

Most determinations in clinical chemistry are of course based on photometric measurements. Determinations in which the reagent reacts rapidly (e.g., albumin, chloride and calcium) are easily monitored by pumping the products of reaction straight through the system and measuring the resulting peak heights as seen by the detector. These sensitive determinations require high sample dispersion, which is best achieved by the introduction of very small volumes of sample, and because of the high dilution, serum blanks are usually negligible. When the merging-zones technique is used a reagent blank is usually run at the start of a batch of samples. For this type of assay, sample volumes are usually less than 10 μl and the within-batch precision (relative standard deviation) is typically 1—2%. With flow rates of between 2 and 4 ml min^{-1} an analytical cycle is complete in less than 30 s. The probe transfer and sampling phase take about 10 s and the remainder of the cycle about 20 s. In an effort to increase sample throughput, the flow rate was increased to about 7 ml min^{-1} but under these conditions the peak height measurements became less precise. It was noted, however, that taking the reading on the trailing edge rather than at the peak maxima gave much better reproducibility. This effect is illustrated in Fig. 6. To avoid losing too much sensitivity, the readings were taken at about 75% of peak maximum height. This was achieved by instructing the software to stop the pump after a fixed number of pulses. After a 0.5-s halt during which time the absorbance of the solution was integrated and the result printed, the pump restarted and rinsed the system.

Sample throughput can be increased further by introducing the succeeding sample before the previous sample has been completely washed out of the system. The number of motor steps separating the samples must be large enough to avoid carryover between samples. This approach was used in determining serum albumin with a bromocresol purple reagent at 180 samples h^{-1} [21]. This approach produces the unusual peak shapes shown in Fig. 7; the plateaux result from periods when the pump is at rest.

Finally, it seems appropriate to consider a surprising phenomenon, namely the increase in peak height observed when the sample slug is arrested in the reactor compared with that obtained when the slug passes directly through the system. This has already been observed by Růžička and Hansen [19] who suggested that dispersion decreases as a result of radial diffusion when the slug is arrested. There may be another explanation: travelling under ordinary dynamic conditions, the slug may become progressively more hollow, perhaps even completely so, and remains so as it passes through the cuvette. Some portion of the beam of light will then pass through the cuvette without being absorbed, producing a unique form of stray light. If, however, the slug is arrested in the reactor, radial diffusion ensures that the hollow centre is filled from the periphery. This state is likely to persist at least in part until the sample reaches the photometer so that in this case the absorbance will be higher. Some support for this view is lent by the

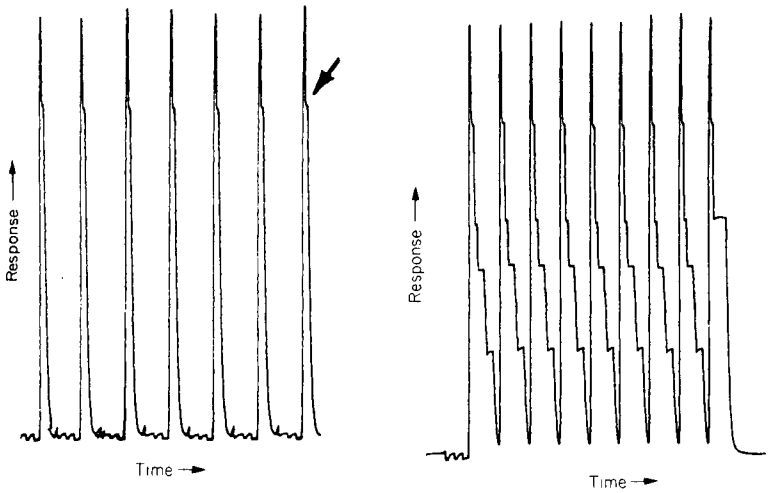

Fig. 6. In rapid photometric assays, taking readings on the peak shoulder (arrowed) gives better precision than readings taken at the peak maximum.

Fig. 7. Increased sample throughput obtained by introducing samples into the system before the previous one has been completely washed out.

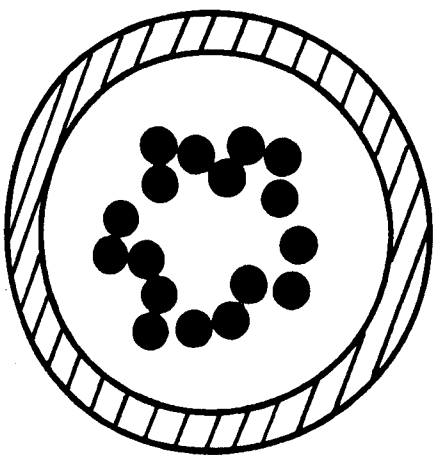

Fig. 8. Hollow tubular flow: cross-section of a tube through which suspended particles are flowing. Under certain flow conditions, particles originally near the tube wall move inward and those near the tube axis move outward producing an annular zone.

work of Repetti and Leonard [23] who studied the behaviour of suspended particles in flowing streams. Because of laminar flow, the outer and inner portions of the particles are in layers moving at different speeds and are thus caused to rotate. This propels them across the stream towards the centre; rotating particles in the exact centre are in a state of instability and tend to

move outwards. Thus there are constant movements away from the walls of the conduit and away from the centre, which tend to create a hollow tubular form (Fig. 8). It seems likely that most molecules, at least non-ionised species, will be affected by similar forces. If this be true, it represents an additional factor to be considered in attempts to explain dispersion on a mathematical basis.

So far, very few clinical chemists have interested themselves in flow-injection analysis and not many of them have either the time or the inclination to do their own instrument development. What is needed now is a commercially available machine with fully developed analytical methods and data-handling facilities. There is no doubt that this is readily achievable at a modest price.

REFERENCES

1 J. Růžička and E. H. Hansen, Anal. Chim. Acta, 78 (1975) 145.
2 D. Betteridge, Anal. Chem., 50 (1978) 832A.
3 B. F. Rocks, R. A. Sherwood, L. M. Bayford and C. Riley, Ann. Clin. Biochem., 19 (1982) 338.
4 B. F. Rocks, R. A. Sherwood and C. Riley, Clin. Chem., 28 (1982) 440.
5 J. Růžička and E. H. Hansen, Anal. Chim. Acta, 114 (1980) 19.
6 L. Anderson, Anal. Chim. Acta, 110 (1979) 123.
7 J. Růžička and E. H. Hansen, Anal. Chim. Acta, 145 (1983) 1.
8 J. J. Harrow and J. Janata, Anal. Chem., 55 (1983) 2461.
9 H. Bergamin F°, E. Zagatto, F. Krug and B. F. Reis, Anal. Chim. Acta, 101 (1978) 17.
10 C. Riley, L. H. Aslett, B. F. Rocks, R. A. Sherwood, J. D. McK. Watson and J. Morgon, Clin. Chem., 29 (1983) 332.
11 D. Betteridge, W. C. Cheng, E. C. Dagless, P. David, T. B. Goad, D. R. Deans, D. A. Newton and T. B. Pierce, Analyst (London), 108 (1983) 1.
12 J. Růžička and E. H. Hansen, Anal. Chim. Acta, 99 (1978) 37.
13 C. Riley, 7th Int. Congr. Clin. Chem. Geneva-Evian 1969, Karger, Basel, 1970, Vol. I, p. 214.
14 P. Blume, in P. Blume and E. F. Freier (Eds.), Enzymology in the Practice of Medicine, Academic Press, New York, 1974, p. 246.
15 L. Bowie, F. Esters, J. Bolin and N. Gochman, Clin. Chem., 22 (1976) 449.
16 C. S. Lim, J. N. Miller and J. W. Bridges, Anal. Chim. Acta, 114 (1980) 183.
17 J. M. Reijn, H. Poppe and W. E. Van der Linden, Anal. Chim. Acta, 145 (1983) 59.
18 H. Engelhardt and V. D. Neue, Chromatographia, 15 (1982) 403.
19 J. Růžička and E. H. Hansen, Flow Injection Analysis, Wiley-Interscience, New York, 1981, p. 66.
20 R. A. Sherwood, B. F. Rocks and C. Riley, Analyst (London), 110 (1985) 493.
21 B. F. Rocks, S. M. Wartel, R. A. Sherwood and C. Riley, Analyst (London), 110 (1985) 669.
22 B. F. Rocks, R. A. Sherwood and C. Riley, Analyst (London), 109 (1984) 847.
23 R. V. Repetti and E. F. Leonard, Trans. Am. Soc. Artif. Intern. Organs, 10 (1964) 311.

Analytica Chimica Acta, 179 (1986) 81—90
Elsevier Science Publishers B.V., Amsterdam — Printed in The Netherlands

STUDIES OF INTERACTING BIOCHEMICAL SYSTEMS BY FLOW INJECTION ANALYSIS

J. N. MILLER*, G. L. ABDULLAHI, H. N. STURLEY, V. GOSSAIN and P. L. McCLUSKEY

Department of Chemistry, Loughborough University of Technology, Loughborough, Leicestershire, LE11 3TU (Great Britain)

(Received 10th October 1985)

SUMMARY

Biochemical interactions of analytical importance can be investigated by heterogeneous and homogeneous techniques. In the former, small ligands are physically separated from macromolecular receptor molecules. This is technically complex but removes unwanted interferences. Homogeneous methods avoid the separation step and are rapid and convenient, but suffer more from background interferences. They also require the presence of suitable probe molecules. It is shown that flow injection analysis can be used advantageously with both heterogeneous and homogeneous techniques. Packed reactors containing group-specific receptors effectively reduce the background fluorescence of blood serum. Gradient flow-injection techniques are used with fluorescence probes in the rapid determination of ligand/protein binding parameters; the results agree well with those of slower, conventional procedures.

Specific non-covalent binding interactions between low-molecular-weight ions and molecules and macromolecular receptors are of great importance in analytical biochemistry [1]. In some cases, the interactions are of direct analytical value: enzymatic methods are based on the binding of substrates, cofactors, metal ions and inhibitors to enzymes, and immunoassays for small molecules (haptens) rely on the binding of the analyte molecules and/or their labelled analogues to antibodies. In other cases, the analytical implications of the ligand/receptor binding are indirect, but no less important. For example, the extent to which drug molecules in blood plasma are protein-bound influences both their pharmacological activity and the methods by which they can be quantified [2]. The suitability of an antibody preparation for use in an immunoassay is governed by the avidity with which it binds the corresponding hapten, and this avidity has to be separately evaluated before an immunoassay protocol is established [3].

In all the direct analytical applications, it is usually necessary to determine only the extent to which a ligand is bound to a receptor macromolecule. In indirect applications, two binding parameters must be measured, i.e., the association constant, K_A, of the interaction, and the apparent number of binding sites, n, on each macromolecular receptor. The binding parameters

0003-2670/86/$03.50

are determined by adding the ligand to the receptor over a wide range of concentration ratios (excess of receptor through to excess of ligand) and evaluating the extent of ligand binding that occurs at different concentration ratios.

Two distinct experimental schemes are available for ligand/receptor binding studies [1]. The most obvious approach involves the physical separation of the free and the receptor-bound ligand, and the subsequent determination of one or other ligand fraction. This "heterogeneous" mode of operation is universally applicable, but the techniques used (equilibrium dialysis, gel chromatography) are lengthy, unsuitable for large numbers of samples, and may affect the binding equilibrium itself. However, they have the notable advantage that the separation step allows the removal of endogenous sample molecules that would otherwise cause substantial background interferences at the measurement stage. The alternative, "homogeneous" approach utilises a probe molecule, the properties of which change when a ligand binds to the corresponding receptor. This removes the need for a separation step, and thus expedites the rapid and convenient handling of many samples; but the measurements may be subject to substantial background problems, and it may not be feasible in every case to identify a suitable probe.

Fluorescence detection techniques are readily combined with flow injection analysis (f.i.a.) [4, 5], and medium-dispersion flow-injection systems and appropriate fluorescence probes have previously been applied to study the protein binding of both acidic and basic drugs [5, 6]. In the present paper, it is shown that gradient flow-injection methods can be used advantageously to provide the range of concentrations required in such studies, and that gradient methods allow the complete processing of a ligand/receptor system in a few seconds. Several gradient systems are studied and compared. (A brief preliminary description of some of this work has been published [7].) The study of heterogeneous systems is exemplified by the use of packed-bed reactors to reduce substantially the fluorescence background signal from human blood plasma. It is demonstrated that quite large reactors can be used with little effect on the dispersion of medium-dispersion systems, and that moderate numbers of samples can be treated in rapid succession.

EXPERIMENTAL

Experiments were done at room temperature. Gilson or Ismatec peristaltic pumps propelled the flowing stream through polyethylene tubing of internal diameter 0.50—1.02 mm. Samples (30—100 μl) were injected through a loop injection valve. Perkin-Elmer Model 1000 and 2000 fluorescence spectrometers fitted with flow cells (45-μl volume, 1.1-mm i.d.) and connected to Bryans model 27000 recorders, were used as detectors. Excitation wavelengths were selected by using interference filters. Emission wavelengths were selected by using a continuous interference wedge and interference filters in the model 2000 and model 1000 instruments, respectively.

For gradient flow-injection experiments, mixing chambers with volumes of 0.4—7.0 ml were constructed of glass. Samples entered through the lower cylindrical portion of each chamber and exited through the domed upper portion. The contents of the chambers were continually stirred by miniature magnetic stirrer bars. Smaller mixing chambers (volumes <0.6 ml) were produced by using extended coils of flow tubing.

Two types of packed-bed reactor were used in heterogeneous experiments. The smaller reactors were made from teflon tubing fitted with polythene nipples, and contained gel columns ca. 30 mm long with internal diameter 2.79 mm (volume 183 μl). They were packed with gel at flow rates of ca. 4 ml min^{-1}, and the ends of the gel beds were protected with polythene frits or glass wool. Larger reactors were made from glass tubes with tapered ends, packed at ca. 1.5 ml min^{-1} and protected as before. Internal diameters of up to 6 mm were tested with volumes up to 1100 μl.

The fluorescence probes 1-anilinonaphthalene-8-sulphonic acid (ANS), and DL-*N*-[2-hydroxy-3-(1-naphthyloxy)propyl]-*N'*-dansylethylene diamine (DAPN) [8] were used as fluorescence probes for the binding of acidic drugs to albumin and of basic drugs to α_1-acid glycoprotein, respectively. All these materials were obtained from Sigma, except for DAPN (Molecular Probes, Portland, Oregon, USA). Human blood serum was obtained from Sigma and from Miles Laboratories (Stoke Poges, Buckinghamshire). Sepharose CL-6B was obtained from Pharmacia Biotechnology. Reactive Blue 2/Sepharose CL-6B was obtained from Sigma; this material contains the dye Cibacron blue covalently bound to the Sepharose gel and 1 g of the dry material swells to give a gel volume of ca. 3.5 ml, binding ca. 17.5 mg of human serum albumin. Protein A/Sepharose CL-4B was also obtained from Sigma; it contains *Staphylococcus aureus* Protein A covalently bound to the Sepharose. The conjugate swells to give a volume of ca. 4 ml g^{-1} of dry material, binding ca. 20 mg ml^{-1} of human immunoglobulin G (IgG). Both these affinity gels were stored at 4°C. Buffer salts and other reagents were of the purest obtainable grade, and water was twice-distilled in an all-glass apparatus.

RESULTS AND DISCUSSION

Homogeneous methods

Gradient flow-injection methods usually depend on the production of reproducible concentration gradients by mixing chambers. In the present work, mixing chambers were calibrated by using quinine sulphate solutions (1 μg ml^{-1}) in 0.05 M sulphuric acid. If the mixing chamber is first equilibrated with solvent, and this is then replaced by the quinine solution (concentration C_{max}) in a step-change, the concentration C_t of quinine emerging from the chamber after time t is given by $C_t = C_{max}[1 - \exp(-kt)]$, where the constant k is given by u/V, the ratio of the flow rate u and the mixing chamber volume V [9]. If the fluorescence intensity is proportional to the solute concentration over the concentration range in use, it may readily be

shown that $\ln (F_{max}/F_t) = kt$, where F_t and F_{max} are the fluorescence intensities corresponding to C_{max} and C_t, respectively [8]. Application of this equation to four mixing chambers, for a flow rate of 2 ml min^{-1} in each case, gave the results shown in Table 1. In each case, the correlation coefficient was evaluated for the plot of $\ln (F_{max}/F_t)$ vs. t. Larger mixing tanks clearly yielded more precise results and could be used over longer time periods. The smaller tanks were more economical in sample consumption but less precise, though the use of electronic rather than manual timing would provide more precise results in these cases also. The effective mixing chamber volume found was in each case very close to the geometrical volume.

The mixing chambers were used in several experimental arrangements. In the first system (Fig. 1), an ANS concentration gradient was established using the mixing chamber and was subsequently merged at a Y-junction with an albumin solution to study the ANS/albumin binding parameters. Mixing of the two solutions thus occurred in the flow tubing (<100 cm) between the merging point and the detector. Because the fluorescence of the free ANS under the experimental conditions was negligible, the fluorescence detected was a direct measure of ANS/albumin binding, an interaction that is accompanied by an ANS fluorescence enhancement of at least 100-fold. To study the binding of an acidic drug to albumin, a gradient of drug concentration was formed in the mixing chamber and subsequently merged with a solution of albumin/ANS complex. In this case, competitive displacement of the ANS from the protein molecule by the drug led to a decrease in fluorescence.

The second approach used a single-channel manifold (Fig. 2). The mixing chamber was first equilibrated with one reactant, and the second reactant was then injected into the chamber as a concentration step. The concentrations of the reactants thus varied simultaneously, one decreasing as the other increased. The result in a simple case when albumin was injected into a chamber containing ANS is shown. The third method (Fig. 3) was a variant of the second, in which a large sample of drug solution was injected into a mixing chamber containing the protein/fluorescence probe complex. Mixing of the drug with the complex, and consequent competition between the drug and the probe, then occurred at both ends of the sample zone. In practice, the second (trailing edge) mixing chamber was used in the calculations, and

TABLE 1

Calibration of mixing chambers for gradient f.i.a.

Type	Effective volume ml ± s.d.	Correlation coefficient	Working time range (s)
Mixing tank	6.99 ± 0.03	0.9999	300
Coiled tubing	0.55 ± 0.06	0.9997	80
Mixing tank	0.40 ± 0.04	0.9998	65
Coiled tubing	0.26 ± 0.04	0.9997	25

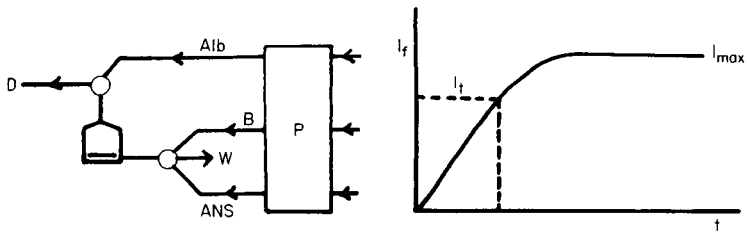

Fig. 1. Gradient system with a mixing chamber and merging streams. A gradient of ANS merges with a stream of albumin, giving a fluorescence signal of the type shown to the right. The fractional saturation by ANS of the albumin-binding sites is given at any time t by I_t/I_{max}.

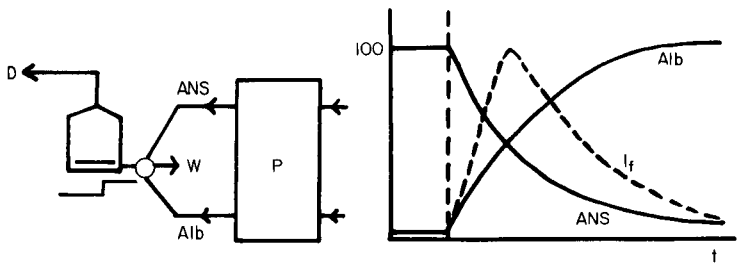

Fig. 2. Gradient system with a mixing chamber without merging. The mixing chamber produces an increasing gradient of one reactant and a simultaneously decreasing gradient of the second reactant, thereby generating a fluorescence signal of the type shown to the right.

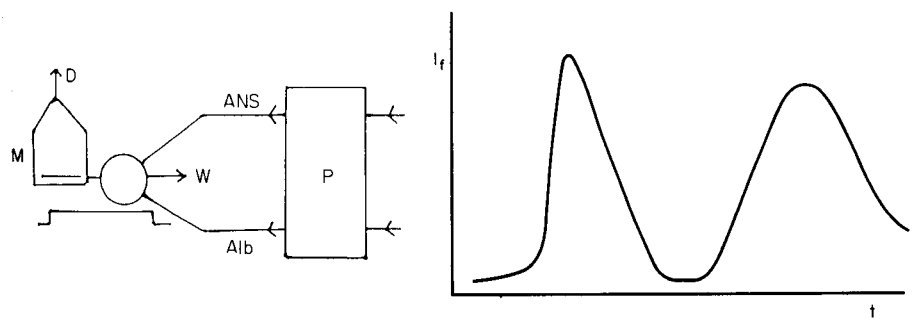

Fig. 3. Gradient system with a mixing chamber without merging. A large sample of (for example) albumin is injected into a stream of ANS. Mixing occurs at the leading and trailing ends of the sample zone, giving a fluorescence signal of the type shown to the right.

the method was applied only to small mixing chambers made from coiled flow tubing.

In each of these experimental arrangements, the binding parameters of the ligand/receptor interaction were evaluated by combining the equations describing mixing chamber behaviour [9] with those describing the interactions at different concentrations [10]. The theory of these methods will be described in detail in a later paper. Table 2 shows the results obtained for the binding of ANS and of two acidic drugs to albumin, and Table 3 provides similar data for the binding of three basic drugs to α_1-acid glycoprotein. In the latter case, the fluorescence enhancement when the probe molecule DAPN binds to the protein is only ca. 8-fold [8], so that a correction has to be made for the "background" fluorescence of the unbound probe. In all cases, the results obtained by the gradient flow-injection method agreed with those from a static fluorescence method using the same reagents. For example, the latter method yielded values of $K_A = 2.1 \times 10^6$ M^{-1}, $n = 0.93$ for the ANS/albumin interaction, and $K_A = 2.9 \times 10^6$ M^{-1}, $n = 1.10$ for the DAPN/α_1-acid glycoprotein binding. Comparison of the static, conventional flow-injection [5, 6], and gradient flow-injection approaches to such studies indicated the advantages of the gradient method in terms of speed and economy of reagents; the precision of the gradient method is also at least as good as those of the two other procedures [7]. Figure 4 shows the excellent coincidence of the results obtained when data from the three procedures are plotted according to the method described by Gutfreund [10]. The gradient method is simple to use, and the data can be processed rapidly by a microcomputer interfaced to the fluorescence spectrometer. Such a system is under development in this laboratory and will allow a complete calculation of the binding constants within a few seconds of the completion of the gradient experiment. Computer calculations will be of particular value in cases where multiple binding sites with different K_A values may be present [11]: for example, in the interactions discussed above, the data may be fitted better by a model that hypothesises one strong and several weaker binding sites.

TABLE 2

Binding of ANS and acidic drugs to human serum albumin

Ligand	Gradient system	K_A (M^{-1})	n
ANS	6.99-ml tank, merging	2.3×10^6	0.90
	0.26-ml tubing, merging	2.1×10^6	0.90
	6.99-ml tank, single channel	1.8×10^6	0.85
	0.55-ml tubing, single channel	2.0×10^6	0.80
Flufenamic acid	0.26-ml tubing, merging	1.0×10^6	—
	6.99-ml tank, merging	1.2×10^6	—
Warfarin	0.26-ml tubing, merging	3.0×10^5	—

TABLE 3

Binding of DAPN and basic drugs to α_1-acid glycoprotein[a]

Ligand	DAPN	Propanolol	Chloropromazine	Imipramine
K_A (M^{-1})	3.0×10^6	5.7×10^4	4.0×10^5	1.2×10^5

[a]In all cases, the gradient system comprised a 0.26-ml mixing tube and merging zones. [b]n = 1.06.

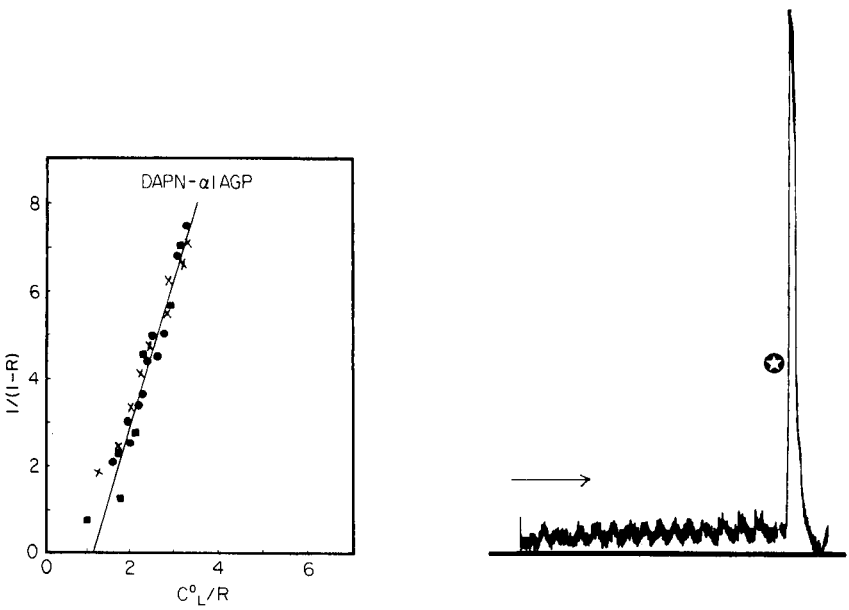

Fig. 4. Comparison of the results of different procedures in studies of the binding of DAPN to α_1-acid glycoprotein: (▪) static fluorimetry; (•) conventional f.i.a.; (×) gradient f.i.a. The data are plotted according to the method of Gutfreund [10].

Fig. 5. Use of a large packed-bed reactor containing immobilized Cibacron blue for the reduction of fluorescence of human serum (excitation and emission wavelengths were 369 and 452 nm, respectively). The arrow shows the intensity of untreated serum on the same scale; the asterisk indicates the point at which the eluent was changed from 0.05 M Tris buffer solution to the same buffer containing 0.2 M NaSCN.

Heterogeneous methods

The use of packed reactors, open-tube wall reactors and single-bead string reactors (SBSRs) has been a striking feature of recent developments in f.i.a. [12]. While SBSR systems are invaluable for control of dispersion in f.i.a., they may not be ideal for systems in which chemical interactions occur, because of the poor surface area offered by the large particles in the reactor. Open-tube and (especially) packed reactors, by contrast, have been frequently

applied to reacting systems. The immobilized activities used most commonly in practice have been ion-exchangers (for pre-concentration of analytes or the removal of interferences [13, 14]) and enzymes [15, 16]. Synthetic ion-exchangers have quite high capacities for binding charged species, and even small quantities of immobilized enzymes can be used for many successive determinations in flowing systems. Solid-phase reactors incorporating other activities have been relatively little studied, though immobilized affinity media and immobilized antibodies may be of great analytical utility.

The use of immobilized affinity media in the treatment of blood serum samples is described here. Fluorescence assays of materials in serum suffer from poor limits of detection compared with the corresponding assays in pure solution. These poor figures of merit are caused by the high background fluorescence of serum samples, which interferes seriously with assays over the whole visible and near ultraviolet region (200—600 nm). Of particular concern is the background level between 450 and 650 nm, the region of emission of the labels commonly used in fluorescence immunoassays. This fluorescence varies considerably from one serum sample to another [17], but its origin is not fully understood. Protein-bound bilirubin is known to be a major contributor, and studies in this laboratory [18—20] show that most of the fluorescence is associated with serum protein fractions. In static experiments, treatment of serum samples with immobilized affinity matrices such as Cibacron blue (which binds serum albumin and certain enzymes), *Staphylococcus aureus* Protein A (binding most antibodies), and concanavalin A (binding many glycoproteins) singly or in combination could remove up to 90% of serum fluorescence. Most of the studies described here used packed reactors containing immobilised Cibacron blue.

Preliminary experiments showed that packed columns could be introduced into the flow-injection manifold without large and damaging increases in the sample dispersion. Thus, a 185-μl column of Sepharose CL-6B gave dispersion values of ca. 6 when 44-μl samples of serum (diluted 5-fold in buffer) or quinine (1 μg ml^{-1}) were injected. The exact value naturally depended on the flow rate (<1.5 ml min^{-1}) and the pressure under which the reactor was originally packed, but was not much bigger than the dispersion value of ca. 4.0 obtained when a length of coiled flow tubing of similar volume replaced the reactor in the manifold.

A column of the same size, packed with Reactive blue/Sepharose CL-6B, achieved a reduction in the fluorescence of diluted serum of up to 67%; this value was in agreement with previous estimates obtained in static systems [19, 20]. However, only a few injections of serum were required to saturate the binding capacity of the reactor. This result was predictable; because the volume of reactive gel before packing was ca. 0.5 ml, it was expected from the manufacturers' specification to bind ca. 2.5 mg of serum albumin, corresponding to about 60 μl of undiluted serum, or about seven samples in the present work.

When a packed reactor with a volume of 1100 μl was used in place of the 185-μl reactor, a fluorescence reduction of 67% was again achieved for

normal serum, and the reactor could be used for at least 15 successive samples, with good reproducibility. Changing the eluent to include 0.2 M sodium thiocyanate rapidly removed the bound protein from the reactor (Fig. 5), giving a single large fluorescence peak. After washing with original buffer, the reactor could be used in further fluorescence reduction experiments of equivalent efficiency. Reproducible results were obtainable in repeated use over several days. Control experiments with Sepharose CL-6B without a bound affinity ligand showed no fluorescence reduction. Preliminary experiments were done with packed reactors containing 75% (v/v) Reactive blue/Sepharose CL-6B and 25% (v/v) Protein A/Sepharose CL-4B. The mixed bed presented no packing or flow problems, but the fluorescence reduction achieved was not significantly greater than that produced by the immobilized dye alone. This result accorded with data from static experiments [20], which suggested that the additional fluorescence reduction produced by the immobilized protein A at the wavelengths under study should not exceed ca. 3%.

CONCLUSIONS

The methods outlined above have considerable potential in several areas of biochemical analysis. The investigation of drug/protein binding interactions by homogeneous gradient flow-injection methods will be of particular value in pharmacology; at present, the in vivo consequences of such interactions are often neglected simply because there is a lack of rapid, simple and economical methods to study them. The study of interacting molecules can readily be extended to other systems. An obvious extension is the rapid characterisation of the monoclonal antibodies increasingly used in immunoassays. The gradient method may similarly be used to establish the "titration" curves used as the calibration plots in such immunoassays.

The heterogeneous methods described also show high promise. The packed reactors offer a real prospect of simple on-line clean-up methods for fluorescent samples prior to, for example, fluorescence immunoassays. Complete automation of such a system could be achieved by using two reactors in parallel, one being used to treat samples while the other is being regenerated. Extension of the principle to other stationary phases, including three-component reactors, hydroxyapatite, and Florisil should give even more complete reduction of serum fluorescence [19, 20]. Further applications will include the use of immobilized antibodies in solid-phase fluorescence and enzyme immunoassays for single and perhaps multiple analytes, and the possibility of using fibre-optic methods to study the fluorescence (or absorbance) of the reactor-bound material rather than the unbound sample components.

Finally, it is noteworthy that the two distinct experimental approaches described here could be advantageously combined. For example, gradient flow-injection methods could be used to study the binding of drugs to solid

matrices (e.g., tissue receptors); and a serum sample pretreated in a solid-phase reactor could subsequently be examined by a gradient flow-injection immunoassay. These applications, under study in this laboratory, will further enhance the extraordinary range of methods based on the simple and elegant concept of flow injection analysis.

This work was supported by the University of Maiduguri, Nigeria (leave of absence and financial support for G.L.A.), the Science and Engineering Research Council (Research and Advanced Course Studentships for H.T. and P.L.M. respectively), the Manpower Services Commission (financial support for V.G.) and the Medical Research Council (fluorimeters and financial support for H.N.S.).

REFERENCES

1 G. Scatchard, Ann. N.Y. Acad. Sci., 51 (1949) 460.
2 J. W. Bridges and A. E. G. Wilson, in J. W. Bridges and L. F. Chasseaud (Eds.), Progress in Drug Metabolism, Vol. 1, Wiley, Chichester, 1976.
3 P. M. Keane, W. H. C. Walker, J. Gauldie and G. E. Abraham, Clin. Chem., 22 (1976) 70.
4 J. I. Braithwaite and J. N. Miller, Anal. Chim. Acta, 106 (1979) 395.
5 J. N. Miller, Anal. Proc., 18 (1981) 227.
6 G. L. Abdullahi, J. N. Miller, H. N. Sturley and J. W. Bridges, Anal. Chim. Acta, 145 (1983) 109.
7 G. L. Abdullahi and J. N. Miller, Analyst (London), 110 (1985) 1271.
8 G. L. Abdullahi, Ph.D. Dissertation, Loughborough University of Technology, 1984.
9 J. F. Tyson, J. M. H. Appleton and A. B. Idris, Anal. Chim. Acta, 145 (1983) 159.
10 H. Gutfreund, Enzymes, Physical Principles, Wiley, New York, 1972.
11 H. N. Sturley, Ph.D. Dissertation, Loughborough University of Technology, 1983.
12 H. A. Mottola, Anal. Chim. Acta, 145 (1983) 27.
13 H. Bergamin, B. F. Reis, A. O. Jacintho and E. A. G. Zagatto, Anal. Chim. Acta, 117 (1980) 81.
14 Z. Fang, S. Xu and S. Zhang, Anal. Chim. Acta, 164 (1984) 41.
15 B. Olssen and L. Ogren, Anal. Chim. Acta, 145 (1983) 87.
16 M. Masoom and A. Townshend, Anal. Chim. Acta, 166 (1984) 111.
17 D. S. Smith, M. Hassan and R. D. Nargessi, in E. L. Wehry (Ed.), Modern Fluorescence Spectroscopy, Vol. 3, Plenum Press, NY, 1981.
18 H. Thakrar, Ph.D. Dissertation, Loughborough University of Technology, 1982.
19 H. Thakrar and J. N. Miller, J. Pharm. Biomed. Anal., in press.
20 V. Gossain, M.Sc. Dissertation, Loughborough University of Technology, 1984.

Analytica Chimica Acta, 179 (1986) 91—101
Elsevier Science Publishers B.V., Amsterdam — Printed in The Netherlands

FLOW INJECTION ANALYSIS IN ON-LINE PROCESS CONTROL

W. E. VAN DER LINDEN

Laboratory for Chemical Analysis, Department of Chemical Technology, Twente University of Technology, P.O. Box 217, 7500 AE Enschede (The Netherlands)

(Received 3rd July 1985)

SUMMARY

Flow injection systems are serious candidates for a new generation of chemical on-line analyzers because there is a growing interest in instruments that combine versatility with the possibility of attaining high sampling frequencies. For real on-line applications the instrument and its component parts have to meet the highest standards with respect to reliability and maintenance. These aspects are considered in some detail, and some industrial applications are briefly discussed.

Most process plants in operation today are still primarily controlled by monitoring operational variables such as temperature, pressure, flow and liquid level. These variables can be measured reliably and the equipment needed is relatively easy to install, calibrate and maintain. The failure rate and down-time of these devices is low, but, in general, this does not apply yet to the present generation of process analyzers, although a gradual improvement in the situation can be observed. The higher failure rate and the higher demands on maintenance of on-line analyzers is, of course, mainly due to the greater complexity of the equipment. Moreover, unlike temperature-measuring devices and pressure gauges, most of the sensing devices for chemical components cannot be installed directly in the process stream. This means that sampling and handling of sample streams form an integral part of the analyzing systems with all the complications inherent to it.

In spite of the difficulties encountered, there is a growing interest in process analyzers. The main reason is that by means of the analysis of the chemical composition of process streams the process operation can be "fine-tuned" to optimal levels not otherwise possible [1]. Optimization is of great importance for economic reasons, allowing better use of raw materials and energy as well as corrosion prevention; for environmental reasons, giving a check on the production of undesirable, toxic or otherwise hazardous by-products and continuous monitoring of waste streams required by stringent statutory regulations; and for quality reasons, the higher quality demanded for products leading to a narrowing of the out-of-specification limits.

Although these remarks apply to continuous bulk processes, on-line analysis may be of even greater importance for processes that cannot be considered

0003-2670/86/$03.50

as pure formulation processes in which components are simply mixed together to arrive at the final product. So, especially in most of the biotechnical production processes, chemical analyzers are essential.

Because the number of different component analyzers available on the market is quite limited and because it is not to be expected that this situation will improve dramatically in the near future, it is very attractive to focus on flexible modular systems that can easily be adapted to achieve the desired type of analysis. It is within this framework that such versatile methods as air-segmented continuous flow analysis (c.f.a.) and flow injection analysis (f.i.a.) come into the picture, but the use of completely automated titrators has also to be taken into consideration. Analyzers based on air-segmented c.f.a. are commercially available (e.g., Technicon Monitor 650). The very long experience with similar equipment, in particular in clinical laboratories, has led to the development of dependable parts with which a great variety of set-ups can be constructed. Although it is true that f.i.a. has shown explosive growth over the last six years, and most of the individual component parts needed to build a flow injection system have been well tested over longer periods of time, hardly any information on the application of these systems in process analysis can be found in the literature. No multipurpose process analyzer based on this principle is available commercially. The object of this paper is to present a concise discussion of the advantages and disadvantages of f.i.a. for on-line process control.

ANALYZER REQUIREMENTS

In some respects the requirements for a process analyzer are different from those of the corresponding laboratory instrument. Some of these aspects will be considered in more detail.

Sampling frequency and mechanical aspects

The quality of information gathered with an analyzer with respect to the possibilities for process control can be described by introduction of the concept of "measurability" [2, 3]. The mathematical expression for measurability (m) comprises the time lag between sampling and result (delay time, t_d), the time between consecutive samples ($t_s = 1/f$, in which f is the sampling frequency), the time constant of both the process (t_p) and the measuring device (t_a) as well as the standard deviations for the analyzer proper (σ_a) and the relevant process variable (σ_p):

$$m \approx \exp\left[-(t_d + 1/2t_s)/t_p\right]\left[1 - (\sigma_a/\sigma_p)(t_a/t_p)^{1/2}\right] \quad (1)$$

One of the important features of f.i.a. is its high sampling frequency. Therefore it has an advantage over, for instance, automated process titrators, if the process is subject to relatively rapid changes. A titrator might be preferable, however, for cases where process dynamics suggest that a somewhat lower sampling frequency ($f <$ ca. 6 samples h^{-1}) can be accepted but a higher precision of analysis is desirable.

To benefit fully from the high sampling frequency, the components of the set-up have to fulfil demanding mechanical requirements. It has to be realized that 24-h sampling at 1 sample per 3 min means 175 000 samples per annum. This emphasizes the general requirement that on-line analyzers should have as few moving parts as possible. In this respect, c.f.a. as well as f.i.a. compare favorably with titrators. In f.i.a., the injection valve is certainly the weakest part. A flow-injection analyzer for on-line process control should be constructed in such a way that maintenance and replacement of valves can easily be accomplished.

At present, reagent consumption in normal f.i.a. is generally of the order of 1 ml min^{-1}. However, on the basis of 24-h operation, this means a consumption of 500 l per annum, which can represent a considerable expenditure. Particularly when expensive reagents have to be used, it is worthwhile considering the possibility of reversed f.i.a. [4–6], for which the reagent is injected into a continuous sample stream. The application of merging zones can be an alternative way to decrease reagent consumption but it has the disadvantage that either the injection valve must be more complex or that two valves have to be used simultaneously, both of which are mechanically less attractive options.

Adjustment of temperature of sample and standards

In order to provide accurate quantitative measurements, process-stream data analyzers have to be calibrated regularly. In the laboratory environment and particularly with batch samples, such calibration procedures seldom cause difficulties because standards and samples will have approximately the same temperature. Process streams, in contrast, can have temperatures that deviate significantly from that of the analyzer environment in which the calibration solutions are stored, and so will the process samples if no adequate precautions are taken.

The influence of variation in temperature on f.i.a. can be of two kinds. First, it affects the dispersion process by changing the diffusion coefficient value and by introducing temperature gradients. Secondly, it affects the rate of chemical reactions. This latter effect has only to be taken into consideration for those cases in which the height of the transient signal is largely determined by reaction kinetics. Apart from a paper by Fernandez et al. [7], little or no attention has been paid in the literature to the influence of temperature on dispersion in f.i.a. systems; it has always been assumed implicitly that all experiments are done at the same uniform temperature.

For a prediction of the influence of fluctuations of temperature of the whole system, a mathematical expression is needed for peak profile or peak height as a function of parameters for which the temperature dependence is well established. No such universally applicable expression is available, but if the axial dispersion model is adopted as a suitable approximation the following expression is valid:

$$C_{max} = (M/\pi R^2)(\langle v \rangle / 4\pi L D_L)^{1/2} \qquad (2)$$

in which M is the mass of material injected, R is the tube radius, $\langle v \rangle$ is the mean linear flow velocity, L is the tube length and D_L is the so-called axial dispersion coefficient. At low Reynolds numbers, and for sufficiently long residence times to justify the assumption of Taylor flow conditions, D_L can be expressed as a function of the molecular diffusion coefficient, $\mathbb{D}$, by

$$D_L = R^2\langle v \rangle^2/48\,\mathbb{D} \tag{3}$$

Substitution in Eqn. 2 leads to

$$C_{max} = (2M/\pi^{3/2}R^3)(3\,\mathbb{D}/L\langle v \rangle)^{1/2} \tag{4}$$

Hence, $dC_{max}/dT \approx \mathbb{D}^{-1/2}\, d\mathbb{D}/dT$. Substitution of the Stokes-Einstein equation for the diffusion coefficient, $\mathbb{D} = kT/6\pi\eta r_o$, where η is the dynamic viscosity and r_o is the solute radius, yields the sought-for temperature dependence. However, it has to be realized that this does not present an unambiguous expression because viscosity also strongly depends on temperature as well as on the chemical composition of the fluid streams under study [8].

Difficult as it is to make some generally valid remarks on the influence of uniform temperature fluctuation of the whole assembly, even larger problems can be expected in making predictions when only the temperature of the sample plug is different to that of the rest of the equipment.

To conclude, it seems justified to state that in f.i.a. it is necessary to aim at the best possible uniformity of temperature between samples and standards. In c.f.a., where a steady-state situation exists at the moment of data collection, or in automatic process titrators, where equilibrium conditions prevail, fluctuations in temperature will have less influence. Moreover, in both latter methods the residence times are much longer, allowing for better heat exchange with the environment.

TECHNIQUES BASED ON DISCRETE SAMPLES VS. CONTINUOUS ON-LINE MEASURING DEVICES

In his discussion of the applications of f.i.a. in process analysis, Ranger [9] characterizes f.i.a. as a new approach for near real-time process monitoring. The expression near real-time might suggest that real-time measurement is an object to be pursued in process analysis. This is not generally true because it depends strongly on the time constant of the process, as discussed above. The faster the fluctuations in the process stream, the faster the analytical results have to be available. Nevertheless, it makes sense to raise this question in particular in relation to f.i.a. because, in principle, the same set-up can be used for real continuous measurements by leaving out the sample valve and introducing the sample stream continuously, giving an unsegmented continuous-flow system.

At first sight this might look an attractive proposal because it appears that the measurability will increase by decreasing t_s in Eqn. 1 to virtually zero. In fact, this is not true. By not using the transient character obtained with

discrete sample plugs, data have to be collected under steady-state conditions, i.e., at a later stage. Because the delay time, t_d, comprises both the time needed for transportation of the analyte from the process stream to the analyzer and the time spent inside the analyzer, data collection at a later stage means a corresponding increase in t_d. Thus the effect of decrease in t_s is counterbalanced by the increase in t_d and there is no profit with respect to time to be gained by introducing the sample stream continuously instead of intermittently.

One important feature is eliminated by omitting the injection valve and that is the constant check on baseline drift (Fig. 1). By a proper selection of the injection frequency, a nearly complete return to the baseline can be achieved between two successive injections. In this way, it is easy to correct for slow fluctuations of the background. Moreover, with the elimination of the injection valve an important diagnostic tool will be lost. The profile of the transient signal obtained with plug injection can provide a trained operator with valuable information about the correct functioning of any flow-injection system.

SAMPLING, SAMPLE TRANSPORT AND SAMPLE CONDITIONING

Although f.i.a. is very well suited, in principle, for "continuous" on-line monitoring of liquid process streams, very few examples can be found in the literature. Most of them apply to the field of water quality and pollution monitoring; hardly any example deals with real process analysis. This is at least partly due to problems associated with the design and construction of adequate sampling and sample conditioning systems. In an excellent textbook on sampling systems for process analyzers, Cornish et al. [10] have presented a comprehensive survey of almost all the aspects related to sampling. In their introduction, they state that "... the complexities associated with sampling have often resulted in inadequate designs or have held back the use of on-line analysis, even though this may otherwise have been preferred to manual sampling and laboratory analysis procedures."

Some important requirements that the sampling system has to meet can

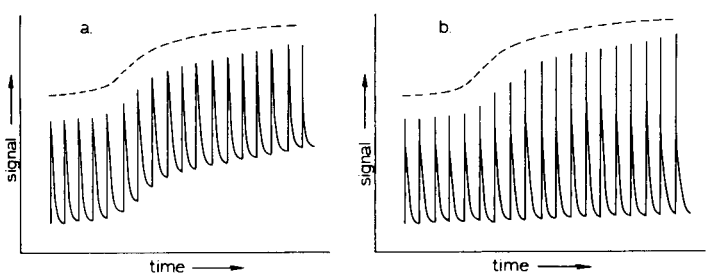

Fig. 1. Analyzer response vs. time: (——) flow-injection device; (-----) continuous monitoring device. (a) No concentration change; drift of baseline. (b) Concentration variation; constant baseline.

be summarized as follows: removal of representative samples from the process stream and maintenance of the representativeness throughout the whole transport line; regulation of pressure and temperature of the sample provided to the analyzer; prevention of any vaporization, loss or contamination of the sample; quantitative transportation of the sample to the analyzer within a specified time period; provision of a means of introducing, when necessary, a calibration sample or standard; in a multi-stream application, provision of the ability to switch between sample streams without cross-contamination; provision of a means of returning part or all the sample to the process or to a waste container; removal of dirt and any other extraneous material from the sample; and provision of a quantitative means of sample dilution when necessary. Of course, not all these aspects are of interest for every analysis and for every case a thorough evaluation is necessary to assess which aspects deserve special attention, but the optimum design for a case at hand should be as simple as possible consistent with the required functions.

If the analyzer cannot be installed close to the process stream, a longer transport line with a correspondingly longer delay time may be necessary. To diminish this time lag and to speed up the response time, so-called fast loops have been constructed (Fig. 2). A fast loop is a bypass in the process stream in which the fluid is propelled with increased velocity. By the introduction of a self-cleaning bypass filter, a virtually particulate-free sample stream can be introduced into the analyzer. The appropriate dimensions of the fast loop line depend on the delay time that can be accepted, on viscosity, etc., and can be calculated by means of the Hagen-Poisseuille equation.

In a preceding section, the influence of temperature was discussed. It would be possible to change the temperature by adjustment of the dimensions of the fast loop line in order to get the best possible heat exchange. However, there are two reasons to avoid such an approach: first, it will always be at

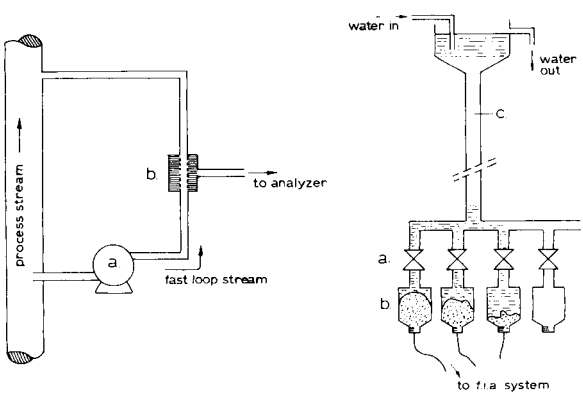

Fig. 2. Fast loop system: (a) pump; (b) self-cleaning bypass filter.

Fig. 3. Constant head device: (a) wide-bore water valve; (b) polythene bottle provided with flexible plastic bag containing carrier, reagent(s), etc.; (c) wide-bore pipe.

the expense of transportation time, and secondly, from the process operation point of view, it might not be advisable to reintroduce a fast loop stream at a greatly different temperature into the main process stream. Therefore, any adjustment of temperature has to proceed in the sample stream between the fast loop system (e.g., bypass filter in Fig. 2) and the analyzer.

COMPONENT PARTS OF A FLOW-INJECTION SYSTEM

In a recent review on the application of flow-injection techniques to atomic absorption spectrometry (a.a.s.), Tyson [11] has made some noteworthy remarks on the components of flow-injection systems. Some of his remarks apply specifically to the use of a.a.s. as a detection system but others have a much broader scope, at least for applications in the laboratory. As discussed above, the situation may be somewhat different for process analyzers.

Pumps

It is common practice in f.i.a. to use multi-roller peristaltic pumps. The slight flow fluctuations that may occur are damped to some extent by the use of flexible and somewhat elastic tubing and, if necessary, an additional pulse-dampening device can be used. When in daily use, pump tubing gradually loses its flexibility, accompanied by a slow decrease in pumping capacity. Depending on the quality of the tubing, and the kind of fluids pumped through it, the tubes have to be replaced at certain intervals. Peristaltic pumps are sufficiently robust and reliable for use in process analysis. The vital parts can easily be protected against corrosive environmental attack. In an explosive environment, special precautions have to be taken to meet existing safety requirements.

The advantage of peristaltic and similar pumps is that they are capable, in principle, of maintaining a constant volumetric flow rate and correspondingly a constant residence time independent of minor changes in viscosity or variations in back-pressure because of restriction changes in the remainder of the system. This does not apply to the use of gas-pressurized reservoirs for reagents and carrier or to the use of constant-head vessels. However, both are cheap alternatives to pumping, and apart from the benefit of an almost completely pulse-free fluid flow, their main advantages are simplicity and the lack of any moving parts. As long as the geometry of the whole set-up is fixed and clogging or just narrowing of the conduits is avoided, a continuous and very constant flow can be guaranteed. In the author's laboratory, a flexible and essentially maintenance-free assembly has been tested (Fig. 3).

The same advantages apparently apply to the use of gas-pressurized reservoirs. They seem to be less attractive, however, because of the increased chance of formation of gas bubbles in the conduits; this is due to gradually decreasing gas solubility in proportion to the continuous pressure drop across the flow system.

Injection devices

During the last decade, many home-made injection valves have been described. Many, particularly those from Bergamin's group [12], are ingenious but also rather complex. Most important from the point of view of process analysis is that such valves probably do not yet meet high standards of long-term reliability, and that valves which are not commercially available are of little interest for process analyzers.

At this moment a good, simple rotary valve with external sample loop seems to be a suitable choice. In tests, it has been proved that after 50 000 switches, such valves still function properly, and no wear or tear was noticeable provided that the sample and carrier stream were virtually free from particles [13]. The "hydrodynamic" injection proposed by Růžička and Hansen [14] is of interest for process analysis, but it has the drawback that two independent pumps are needed. Another valveless injection procedure, "controlled dispersion analysis" suggested by Sherwood et al. [15], seems less attractive for the purposes of process analysis.

Detection systems

It is beyond the scope of this article to review the types of sensing devices suitable for use in flow-injection systems. Only a few comments will be made on some general aspects of importance in process analysis. In addition to obvious criteria such as sensitivity, limit of detection and response time, the selection of an appropriate detection system strongly depends on factors that influence long-term uninterrupted operation. Media that exhibit a tendency to deposit formation will cause problems with optical detectors because deposits on optical windows will affect the transmission of light, and with electrochemical detectors because the nature or rate of electron-transfer reactions at the electrode surface can be changed. Thermistors are less sensitive to deposits and enthalpimetric detection should be of interest for this reason. The use of an enthalpimetric flow-through detector is being studied in the author's laboratory. Electrochemical as well as enthalpimetric detectors are essentially insensitive to turbidity or colour. For this reason, they should be preferable to spectrophotometric detectors for many applications.

The signals obtained from optical, enthalpimetric and some electrochemical (amperometric and conductometric) detectors exhibit a linear dependence on concentration. In these cases, the magnitude of the transient signal can be measured from the baseline, thus allowing for correction of drift. This does not apply to the important category of potentiometric detectors, which exhibit a logarithmic response. This means that it is not the peak height but the absolute value at the peak that is of interest. The baseline can be rather indeterminate and often shows large fluctuations. Because this can be rather confusing when low concentrations are involved, it is often recommended that the carrier stream be maintained at a relatively low but constant concentration of the species to be determined. Another possibility for circumventing this problem is computational on-line transformation of the potentials measured to their corresponding concentrations.

To conclude this section, the concept and design of integrated micro-conduits recently introduced by Růžička and Hansen [16, 17] has to be mentioned. There is no doubt that this approach will contribute positively to the reliability of flow-injection systems; the possibility of replacement is a very attractive feature, comparable to the use of single boards or cards in microelectronics.

PRACTICAL APPLICATIONS OF FLOW-INJECTION SYSTEMS IN PROCESS ANALYSIS

Hardly any reference can be found to the industrial applications of f.i.a. for real continuous monitoring or control of processes. Even in a chapter entirely devoted to this subject, Ranger [9] does not give any example. Only very recently were some applications in the field of water quality surveillance reported. Gisin and Jardas [18] described a single-channel sequential monitoring method for phosphate and sulfate in industrial effluents by means of reversed f.i.a., using hydrodynamic injection and photometric detection. During a two-month run with a sampling frequency of 15 samples h^{-1}, neither clogging nor significant baseline drift caused by deposition on the cell windows were observed because a proper wash cycle was used. Another unattended operation of f.i.a. was reported by Smith et al. [19]; by splitting the sample stream, nitrate, phosphate and sulfate in rivers could be monitored simultaneously. Finally, Petty and Johnson [20] described continuous monitoring by means of reversed f.i.a.; optimized methods were reported for the determination of nitrate, nitrite, phosphate, silicate, ammonia and primary amines.

In the author's laboratory, experience has been gathered with the long-term reliability of a flow-injection determination of sulfide in di-isopropanolamine (DIPA) solutions. Such DIPA or related amine solutions are used for the removal of hydrogen sulfide from, for instance, natural gas. The set-up, shown in Fig. 4, was used for several months in a test of suitable reactors. The use of the gas-diffusion membrane module provides selective transfer of some gaseous compounds from sample to detector stream but excludes contamination of the detector stream by all involatile compounds present in the sample stream. Detection was by a silver sulfide-based ion-selective electrode. The detector stream is forced through a nozzle at a short distance perpendicular to the electrode surface. By using such a wall-jet configuration a very short response time was obtained.

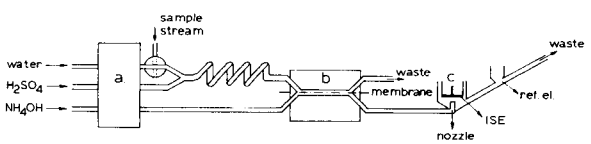

Fig. 4. Assembly for the measurement of sulfide content of di-isopropylamine solution with potentiometric detection: (a) peristaltic pump; (b) membrane gas-diffusion module; (c) ion-selective sulfide electrode.

The use of membranes for dialysis, gas diffusion, etc., deserves more attention particularly for on-line process analysis because it offers a very elegant way of avoiding interferences from many components and it protects the detector stream from undesirable contamination. As far as gas diffusion is concerned, it allows the determination of ammonia, carbon dioxide, cyanide (HCN) and sulfur dioxide (see e.g. [21]). Some preliminary experiments [22] have shown that hydrophilic microporous polypropylene membranes (Celgard 3501; Celanese Corp.) can be used in the determination of the water content of organic solvents. Water from the organic sample stream is transferred across the membrane to methanol and subsequently at the outlet of the membrane module is mixed with pyridine-free Karl Fischer reagent. Biamperometric detection in a flow-through cell is used.

Conclusion

Theoretically, f.i.a. has many features that should make it a valuable technique for on-line process control. The slow introduction in process analysis of flow injection-based analyzers, and indeed chemical analyzers in general, is caused by the stringent requirements for correct and uninterrupted operation. For some time to come, it is to be expected that applications will be found primarily in areas where possible failure of the monitoring function is unlikely to have serious short-term consequences. Surveillance of water quality can be considered as one such area.

REFERENCES

1 L. J. Wachel in D. P. Manka (Ed.), Automated Stream Analysis for Process Control, Academic Press, New York, 1984, Vol. 2, Chap. 15.
2 D. L. Massart, A. Dijkstra and L. Kaufman, Evaluation and Optimization of Laboratory Methods and Analytical Procedures, Elsevier, Amsterdam, 1978.
3 G. Kateman and F. W. Pijpers, Quality Control in Analytical Chemistry, Wiley, New York, 1981.
4 K. S. Johnson and R. L. Petty, Anal. Chem., 54 (1982) 1185.
5 A. G. Fogg and N. K. Bsebsu, Analyst (London), 109 (1984) 19.
6 A. Ríos, M. D. Luque de Castro and M. Valcárcel, Analyst (London), 109 (1984) 1487.
7 A. Fernández, M. A. Gómez-Nieto, M. D. Luque de Castro and M. Valcárcel, Anal. Chim. Acta, 165 (1984) 217.
8 E. L. Cussler, Diffusion; Mass Transfer in Fluid Systems, Cambridge University Press, Cambridge, 1984.
9 C. B. Ranger in D. P. Manka (Ed.), Automated Stream Analysis for Process Control, Academic Press, New York, 1982, Vol. 1, Chap. 2.
10 D. C. Cornish, G. Jepson and M. J. Smurthwaite, Sampling Systems for Process Analyzers, Butterworths, London, 1981, p. 3.
11 J. F. Tyson, Analyst (London), 110 (1985) 419.
12 E. A. G. Zagatto, A. O. Jacintho, L. C. R. Pessenda, F. J. Krug, B. F. Reis and H. Bergamin F°., Anal. Chim. Acta, 125 (1981) 37.
13 H. J. van den Dolder, private communication.
14 J. Růžička and E. H. Hansen, Anal. Chim. Acta, 145 (1983) 1.
15 R. A. Sherwood, B. F. Rocks and C. Riley, Analyst (London), 110 (1985) 493.
16 J. Růžička and E. H. Hansen, Anal. Chim. Acta, 161 (1984) 1.

17 J. Růžička, Anal. Chem., 55 (1983) 1041A.
18 M. Gisin and Z. Jardas, FACCS 11th Annual Meeting, Philadelphia, 1984, Abstr. no. 354.
19 B. Smith, A. Sherry and A. Cherdak, FACCS 11th Annual Meeting, Philadelphia, 1984, Abstr. no. 355.
20 R. L. Petty and K. S. Johnson, FACCS 11th Annual Meeting, Philadelphia, 1984, Abstr. no. 356.
21 W. E. van der Linden, Anal. Chim. Acta, 151 (1983) 359.
22 L. M. M. Cristóva and W. E. van der Linden. Unpublished results.

Analytica Chimica Acta, 179 (1986) 103—118
Elsevier Science Publishers B.V., Amsterdam — Printed in The Netherlands

COMMUTATION IN FLOW INJECTION ANALYSIS

F. J. KRUG*, H. BERGAMIN F° and E. A. G. ZAGATTO

Centro de Energia Nuclear na Agricultura — Universidade de São Paulo, C.P. 96, 13400 Piracicaba, S. Paulo (Brazil)

(Received 7th August 1985)

SUMMARY

Recent advances in flow injection analysis, including the introduction of zone-sampling and zone-trapping processes and the incorporation of ion exchangers, have involved electronically operated injector/commutators. Other techniques based on manual commutation, such as manifold modifications and intermittent and alternating streams, have been reported. A comprehensive review of these techniques is given. The use of commutation for different injection procedures (loop-based, time-based, hydrodynamic, sequential and nested injection) is emphasized. An alternative stopped-flow approach without stopping the pump is suggested.

There is a clear linkage between the development of flow injection analysis (f.i.a.) [1] and that of commutating devices. This link was not clear when the first of these devices, termed stream sampling valves [2], rotary valves [3] or proportional injectors [4], were used to inject samples instead of syringes with [5] or without [6] needles. When the merging-zones approach was proposed [7], the commutation feature of the double proportional injector was not emphasized because at that time the only function of the commutator was to introduce samples and reagents into the flow-injection system. The increased analytical path length caused by the placement of a sampling loop in the sample carrier stream [8] was also of interest.

The commutation principle became clearer when a flow-injection system with two analytical paths, one of which included a reductor column, was proposed for the simultaneous determination of nitrate and nitrite in natural waters [9]. The "injector-commutator" was used for both sample and reagent injections and for commutation of some components of the manifold. The application of intermittent [10] and alternating [11] streams without stopping the peristaltic pump, the sequential injection process [12] and the concept of monosegmented flow-injection systems [13] have all been achieved successfully with manual commutation.

Time-controlled commutation, applied in the first work on incorporating ion-exchange in flow injection analysis [14], greatly expanded the possibilities of f.i.a., allowing the development of new processes such as zone sampling [15], zone trapping [16], time-based injection, etc. In this paper, the value of commutation in flow injection analysis is discussed.

0003-2670/86/$03.50

THE FLOW-INJECTION SYSTEM

For the spectrophotometric model systems discussed in the present work, dye solutions were prepared by diluting a 0.1% (w/v) bromocresol green stock solution in 0.01 M sodium tetraborate with more 0.01 M tetraborate. The same tetraborate solution was always applied as carrier stream. For detection, absorbances were measured at 617 nm with a Varian 634-S spectrophotometer provided with a Hellma 178-OS flow cell (80-μl inner volume, 10-mm optical path) and connected to a Radiometer REC-61 recorder with a REA-112 high-sensitivity unit.

A three-piece commutator was preferred to the original two-piece design [7] because its construction is simpler, although both commutators offer the same possibilities. The commutator is made from perspex and consists of two fixed external plates with a movable central bar, all held tightly together by two screws with springs. Holes (1-mm bore) are made through the pieces of the commutator in accordance with the related flow diagram. For insertion of the polyethylene connecting tubes, either tygon bushings were used or the holes were drilled so as to be slightly conical near the surface. Silicone rubber sheets with holes (ca. 0.5-mm diameter) corresponding to those of the external plates were placed between the commutator pieces to avoid leakage. A metal lever, which can be operated manually or electronically, is used to move the central bar of the commutator between the two resting positions associated with the two states of the manifold. Electronic operation requires two solenoids controlled by a microprocessor system based on an Intel SDK-85. Details of interfacing, hardware and software are available upon request.

The volume-selecting devices used for hydrodynamic injection and the Y-shaped connectors are also made from perspex, the internal diameter of the drillings being 0.7 mm.

The open tubular helical reactors (with a coil diameter of ca. 1.5 cm), the sampling loops and the transmission lines were made from firm-walled polyethylene tubing (0.8 mm i.d.). Tygon pump tubes were used with an Ismatec mp-13-GJ4 peristaltic pump.

SAMPLE INJECTION

In flow injection analysis, a precise sample volume must be selected and transferred reproducibly into the sample carrier stream. Sample metering is usually achieved by controlling either the internal volume of a small container (usually an external loop) or the sampling time. Recently, hydrodynamic injection [17] and nested injection [13, 18] have been proposed. All these injection procedures, including simultaneous injections, are easily done with commutation devices.

Loop-based injection

The flow diagram of the simplest loop-based injection procedure is shown in Fig. 1(a) which corresponds to the position for taking a sample state. The sample is aspirated to fill the sampling loop which defines the volume to be injected, the excess being discarded. The commutator is then operated to introduce the sample into the carrier stream. This produces a well defined and reproducible zone which undergoes continuous dispersion while being transported through the analytical path. After an interval of time compatible with the acceptable carry-over level, the commutator is switched back to the sampling position, in order to start another cycle. With this approach, therefore, one injection is performed per commutation cycle.

There are situations, however, where two injections per cycle are required, so that the sample zone may be processed in two different ways, according to the manifold characteristics associated with the two commutator positions. This possibility has been exploited mainly for simultaneous determinations [9, 19, 20]; the flow diagrams of the injection processes are shown in Fig. 2. An example is the flow-injection system proposed for the simultaneous spectrophotometric determination of nitrogen and phosphorus in plant digests based on the indophenol blue and molybdenum blue reactions [19]. As shown in Fig. 3, the sample and the alkaline phenate and hypochlorite reagents required for the nitrogen determination are filling the corresponding

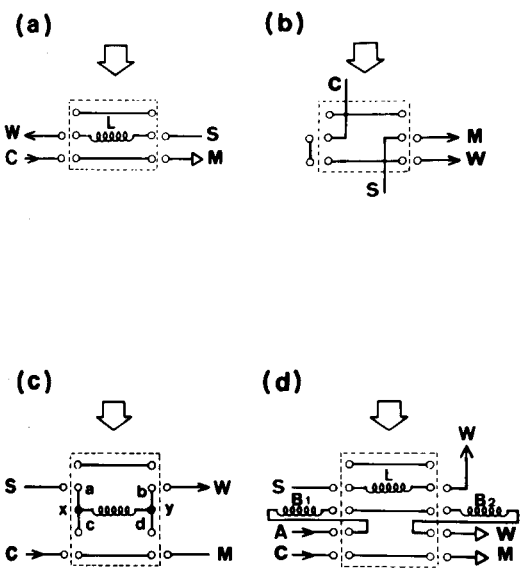

Fig. 1. Flow diagrams for loop-based (a), time-based (b), hydrodynamic (c) and nested (d) injections: S, sample; L, loop; C, carrier solution; M, outlet towards detector; W, waste; xy, duct; a, b, c and d, duct arms; B_1 and B_2, volume-selecting coils; A, air (or a solution to be added). The components within the dashed lines are linked to the movable central bar of the commutator, the movement being indicated by the big arrows. The sites where pumping is applied are indicated by arrows. Triangles indicate flow directions.

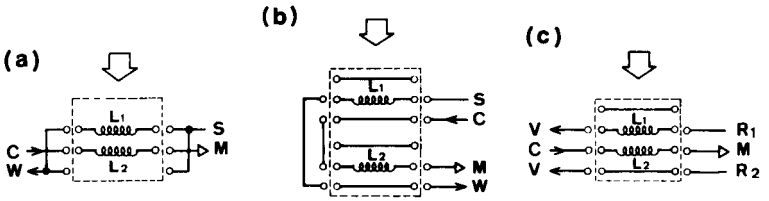

Fig. 2. Flow diagrams for two loop-based injections per commutation cycle related to single (a, b) or independent (c) solutions to be introduced. Subscripts 1 and 2 refer to the two positions of the system. R is a reagent. For other symbols, see legend to Fig. 1.

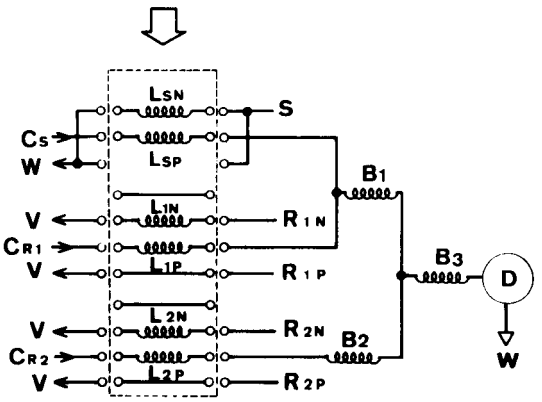

Fig. 3. Flow diagrams of the system for the simultaneous determination of nitrogen and phosphorus in plant digests. L_{1N}, L_{1P}, L_{2N} and L_{2P} are the sampling loops associated with the alkaline phenate (R_{1N}), molybdate (R_{1P}), hypochlorite (R_{2N}) and ascorbic acid (R_{2P}) reagents, respectively. L_{SN} and L_{SP} are sampling loops for the nitrogen and phosphorus determinations. B_1, B_2 and B_3, coils; V, recovery vessels; D, spectrophotometer. For other symbols, see legends to Figs. 1 and 2. For system dimensions, see [19].

loops while the reactions related to the phosphate determination proceed in the analytical path. Commutation inverts this situation, allowing the metering of the sample and reagent volumes required for the phosphate determination, and the development of the modified Berthelot reaction in the analytical path. As both methods yield coloured species quantifiable at 630 nm, only one spectrophotometer is needed. The same basic manifold without stream splitting can be used for both methods, despite the acidity and alkalinity inherent to the reactions involved. The introduction of two different sample volumes per commutation cycle in order to diminish the number of "out-of-range" samples in routine work is common practice in this laboratory.

Another possibility is to replace the sampling loop by an ion-exchange resin column, as originally proposed by Bergamin et al. [14] for the determination of ammonium ion in natural waters at the $\mu g\ l^{-1}$ level. In this approach, the sample is aspirated through an Amberlite IRA-120 resin column, and the depleted sample passes to waste, thus minimizing any matrix effects. After commutation, the resin column is switched into a flowing sodium hydroxide

solution which acts as eluent and as carrier stream. The Nessler reagent is introduced by the commutator and added downstream, allowing the coloured zone to be measured at 410 nm. With the ion-exchange resin column as the sampling loop, electronic operation of the commutator is needed because the sample volume is proportional to the loading time. This limitation can be avoided with the zone-sampling process, as discussed below. The sampling frequency can be speeded up by using two resin columns [20, 21], the system being set up as in the injection configurations of Fig. 2.

Loop-based injection is most effective when small injected volumes are required. As the injected volume increases, the increase in the analytical path length caused by placement of the sampling loop in the carrier stream produces a pronounced decrease in the sampling frequency. This drawback can be overcome partly by switching the commutator back to the sampling position before the loop is emptied completely, in order to lessen the tailed portion of the sample zone. This procedure, applied by Jacintho et al. [22] when i.c.p./a.e.s. was used for detection in flow injection analysis, was critically investigated by Reijn et al. [23] who pointed out that a time-based injection is approximated.

Time-based injection

The flow diagram related to the simplest time-based injection procedure is outlined in Fig. 1(b), in which the electronically operated commutator is shown in the sampling position. The sample is directed to the detector and the carrier solution is discarded. After the time interval corresponding to the required injected volume, the commutator is operated so that the carrier solution is directed through the analytical path in order to push the sample and wash out the system. In this situation, replacement of the sample is done. The commutation cycle is completed when the commutator is switched back to the position specified in Fig. 1(b). Time-based injection with a two-piece commutator was recently described [24]. It should be stressed that, if the commutator is stopped in the injection position, which corresponds to the injection of an "infinite volume" of sample, a steady-state situation is reached, and it is not necessary to pass the sample through the peristaltic pump. Switching the pump off is thus a simple way of acquiring useful information about the trends of the development of the chemical reactions involved [9, 11].

Time-based injection is particularly attractive when large sample volumes are needed. Its advantage over loop-based injection can be illustrated by the flow-injection system proposed for the spectrophotometric determination of boron in plants [25]. In the original system, about 1.8 ml of sample is needed to fill the 1-ml sampling loop completely; this required volume can be decreased slightly with reverse aspiration. The injected sample undergoes some dispersion in the analytical path, so that the absorbance measured is about 80% of the absorbance in the infinite-volume situation. With time-based injection, only 1.1 ml of sample is needed to achieve the same absorbance level.

In addition, the procedure is speeded up by about 40% because, with time-based injection, the length of the analytical path is not increased by commutation. Alternatively, by maintaining the original sampling frequency of 60 h^{-1}, the procedure can be optimized in terms of sensitivity. This improved procedure with time-based injection has been adopted for routine work; details are available on request.

For small volumes, however, time-based injection can be limited by fluctuations in flow rates which lead to a decline in reproducibility of the selected volume, particularly when small injection times or high flow rates are used. Fortunately, this limitation becomes less severe in confluence flow-injection systems in which the injected volume can also be decreased, without a marked drop in sampling rate, by lowering the flow rate of the sample carrier stream. Lowering the flow rate for the analysis of more concentrated samples was investigated in designing a procedure for the spectrophotometric determination of aluminium in steel. The consumption of the carrier solution (6000 mg Fe l^{-1} plus 0.12 M HCl, prepared with highly pure iron oxide) was reduced, a more favourable final pH could be adjusted, and a smaller blank value was observed with a decrease in the flow rate of the sample carrier stream. Steel samples with higher aluminium contents could thus be analyzed in a more stable system.

Hydrodynamic injection

Hydrodynamic injection, proposed by Růžička and Hansen [17], can also be achieved with the commutation device (Fig. 1c). In the specified situation, the sample is aspirated through the xy duct via the a and b arms, the excess being discarded. The other duct arms are filled with trapped portions of the carrier solution. After commutation, the trapped solutions start moving, pushing forward the selected sample volume. The sample portions inside the a and b arms become trapped. Thus, the injected volume is selected in a region with no moving parts. Only one peristaltic pump under continuous operation is needed. As the sample carrier stream flows continuously, a steady-state situation is maintained for the flow system. Positioning of the sampling duct is not critical because three of its four arms are outside the analytical path, and their dimensions are not relevant.

When this injection procedure was investigated in detail for application to steel analysis [26], the slight sacrifice in reproducibility reported earlier [17], which was probably due to the inertia of the peristaltic pump, was not observed. Sample volumes as small as 1 μl could be injected precisely, the relative standard deviations of peak-height measurements after successive injections being 0.6%. With electronic operation of the commutator, the dead-volume effects caused by diffusion and by the non-rigidity of the system were kept constant. No comparison between the procedures for obtaining hydrodynamic injection was made because of the difficulty in achieving two identical flow rates, as required in the previous procedure [17].

Nested injection

The concept of the monosegmented flow-injection systems [13] includes some useful aspects of unsegmented flow-injection systems and of multisegmented continuous-flow systems. The sample is injected together with two air plugs, which limits the established sample zone, thus minimizing the interaction between sample and carrier solutions. The mean sample residence time can be increased without impairing the sampling rate, as several samples are processed in the analytical path. The air plugs are removed pneumatically before detection. The injection procedure is depicted in Fig. 1(d). The sample is aspirated to fill the sampling loop while air passes through the B_1 and B_2 lines. When the commutator is switched, the sampling loop is placed between the B_1 and B_2 lines, and the entire assembly is introduced into the carrier stream, being directed towards the detector. A critical comparison with the unsegmented system was possible [13] when both systems were applied to spectrophotometric determinations of boron, chromium and ammonium. In all situations, the reagents were added to the sample before the injection. The use of this idea in confluence systems and the feasibility of zone sampling to avoid the awkward air removal is being investigated.

Recently [18], nested injection with a reactor packed with manganese dioxide as one of the loops has been used for hydrogen peroxide/organic peroxide assays. Also, a merging-zones approach is possible by using different solutions to feed the outer loop and the B_1 and B_2 lines.

Simultaneous injections

Only one commutator device is needed for simultaneous injections, regardless of the injection procedure involved. Figure 4(a) shows the sample solution filling three sampling loops which are later introduced into different carrier streams of separate flow systems to permit simultaneous determinations [27].

Another possibility is to introduce several sample plugs into the same carrier stream (Fig. 4b) to achieve overlapping zones. This sequential injection process was critically investigated [12] and applied as an alternative to gradient exploitation, for the determination of a wide range of manganese contents in rocks and for the determination of copper in ethanol. Matrix effects on the atomic absorption spectrometry of copper were overcome by using an automated standard addition method. Hansen et al. [28] used intercalation of the sample and another solution with a potential interfering species into the same carrier stream in order to evaluate selectivities. Although they used two rotary valves, this procedure would be possible with only one commutator (Fig. 4c). Similarly, with simultaneous injections of sample and reagent solutions into the same carrier stream, the merging-zones approach [7] can be incorporated in straight flow-injection systems.

The merging-zones approach has often been used in confluence systems, the sample and reagents being introduced into separate carrier streams flowing towards a confluence point (Fig. 4d). The two established zones merge

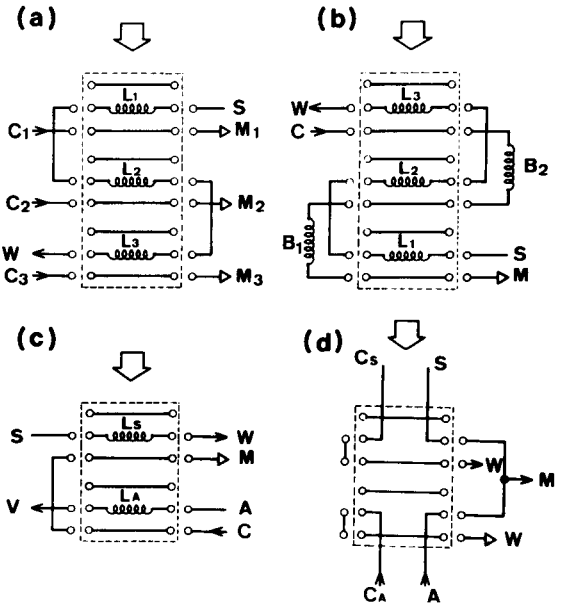

Fig. 4. Flow diagrams for simultaneous injections into independent (a), single (b, c) and merging (d) carrier streams: L_1, L_2, L_3, L_S and L_A, sampling loops; C_1, C_2 and C_3, independent carrier streams; B_1 and B_2, transmission lines; A, solution to be added to the sample zone. For other symbols, see legends of Figs. 1—3.

and are processed downstream. This approach was used originally to reduce the consumption of reagents [7, 9, 10, 29, 30]. Futher developments revealed other useful aspects, e.g., providing initial neutralization of samples [30], determining high concentrations of analytes in samples without prior dilution [31], allowing simultaneous determinations [9, 19], avoiding baseline drift [14, 32], and simplifying standard additions [22, 33—35]. Zone-sampling processes [34, 36, 37] and stopped-flow procedures [38] have also been applied with merging zones. All these procedures are possible with only one commutator. Furthermore, the commutator can provide an intermittent reagent stream to achieve coalesced zones [39] with incomplete overlap between them.

ZONE SAMPLING

The zone-sampling process [15] consists of selecting a portion of a dispersed zone and introducing it into another carrier stream (Fig. 5). This aliquoting process is possible with the commutation device and can be used in conjunction with any flow-injection configuration or approach so far proposed; it is compatible with all the injection procedures.

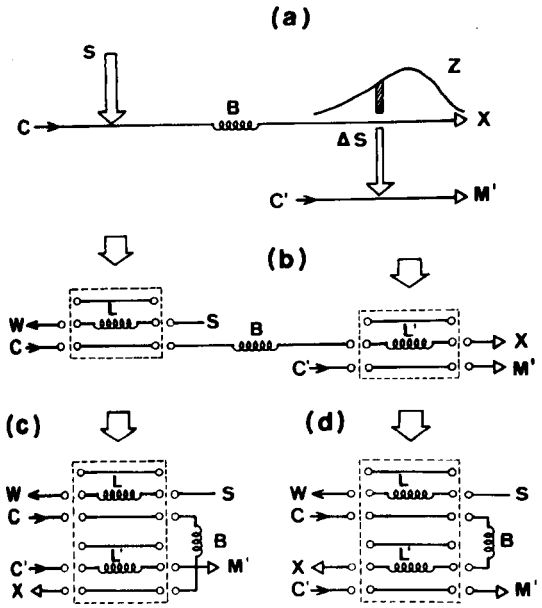

Fig. 5. The zone-sampling process represented schematically (a) and conducted with two commutators (b) or one (c, d). B, Dispersion coil; Z, dispersed zone; ΔS, aliquot of the sample zone; X, waste (or an independent manifold); C', L', M', referred to the second carrier stream. For other symbols, see legend to Fig. 1.

Controlled dispersion

The zone-sampling process is very efficient in achieving a high degree of dispersion, as emphasized by Reis et al. [15], who used the system outlined in Fig. 5(c) to avoid manual sample dilution prior to the atomic absorption spectrometric determination of potassium in plant digests. In this system, when the commutator rests in the injection position, the sample zone defined by the first sampling loop is allowed to flow through the second loop which is placed in the same path. After a time interval t_s (here $t_s = t_1$, the resting time of the commutator in the injection position), when the portion of the sample zone to be sampled is passing through the second loop, the commutator is switched back to the position specified in Fig. 5(c). This introduces the sampled aliquot into the second carrier stream, originating another sample zone which is thereafter processed and measured. With this approach, about 120 plant digests per hour could be analyzed accurately in spite of the high degree of dispersion involved (dispersion factor [15] = 0.0076). Actually, the t_s values can be defined as $t_1 + NT$, where N is an integer (usually 0, 1 or 2) and T is the flow-injection period. Also, when the zone-sampling process is conducted as in Fig. 5(d), the t_s value is defined as NT, where N is usually 1 or 2. These different ways of conducting the same process are sometimes needed when t_1 or t_2 (the resting time of the commutator in the sampling position) are not easily modified. It should be stressed that with two commutators (Fig. 5b), there is no dependence between the t_s value and t_1 or t_2.

Flow-injection systems with zone sampling provide the efficient control of dispersion required for analyzing materials with widely different analyte contents. This advantage has been exploited by Jacintho et al. [37], who determined calcium spectrophotometrically in waters, soils and plants using the same basic manifold. The required analytical ranges were adjusted by suitable selection of the t_s values.

Simultaneous determinations

After the zone-sampling process, while the selected portion of the sample zone is being analyzed for one chemical species, the remainder of the zone can be used for other determinations. This is particularly useful when the required dispersions are very different and was exploited for simultaneous determinations of aluminium and iron in plant digests [36]. A 500-μl sample volume was introduced by loop injection into a perchloric acid solution at 6.0 ml min^{-1} directed to an atomic absorption spectrometer in which iron was determined under the conditions of limited [1] sample dispersion. Eight seconds after the injection, a small fraction (200 μl) of the sample zone, located at its tail, was resampled and introduced into another carrier stream; the reagents needed for the spectrophotometric determination of aluminium with eriochrome cyanine R were then added successively to this zone. For this determination, large dispersion was easily attained (dispersion factor = 0.022) without stream splitting and with very reproducibile results.

Programmable additions

Different t_s values select different portions of the dispersed zone, each with a given mean concentration. Therefore, by choosing suitable values for t_s, it is possible to provide small volumes of known mean concentrations to be added to the sample zone. The usefulness of this approach became evident when a flow-injection procedure with standard additions was developed for the spectrophotometric determination of nitrate in plant extracts [34]. Twelve known amounts of nitrate were selected by using zone sampling, their addition to the sample zone being attained with merging zones (Fig. 6). After the standard additions, the reagents required for the nitrate reduction and for the modified Griess reaction were added, and the complex formed was quantified at 535 nm. In this way, the standard additions were made under constant conditions of any sample matrix effects, as the sample dispersion was always the same, regardless of the addition level involved. Presently, a similar approach is used for routine multi-element determinations in rocks by atomic emission spectrometry, for which the generalized standard addition method is needed to overcome spectral interferences.

With programmable additions based on zone sampling and merging zones, it should not be necessary to prepare large sets of solutions with different concentrations, which are used in the factorial experiments needed in the development of new procedures for f.i.a. Also, this approach permits the achievement of a calibration curve by applying only one standard solution,

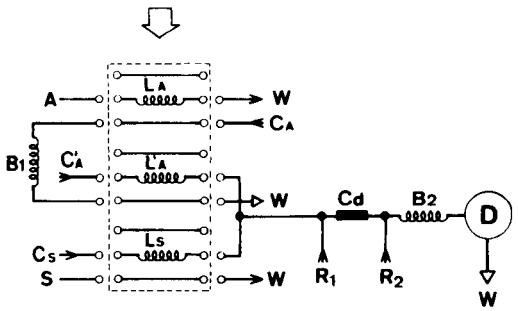

Fig.6. Flow diagram of the flow-injection system for nitrate determinations in plant extracts: L_A and L'_A, sampling and resampling loops for the standard solution, A, to be added; B_1, dispersion coil; B_2, reaction coil; R_1, buffer/masking reagent; R_2, colour-forming reagent; Cd, copperized cadmium reductor. Other symbols as in Figs. 1—4. For system dimensions, see [34].

as an alternative to "electronic dilution" [1]. These possibilities have not been studied fully so far.

Concentrations and separations

A very useful system for ion-exchange results from the replacement of the resampling loop L' (Fig. 5c, d) by an ion-exchange resin column. This variation of the zone-sampling process permits resin cycles involving three steps to be applied in flow-injection systems. Resin conditioning (or rinsing) is done by the first carrier stream, loading occurs when the first sample zone flows through the resin column, and elution is achieved after commutation, by the second carrier stream. The entire depleted sample zone is discarded, minimizing problems associated with matrix effects, especially the "schlieren" pattern [40]. Manual operation of the commutator is possible with loop-based injection, as the selected amount of sample is defined by the first sampling loop. This approach, with two injection devices, was proposed originally by Olsen et al. [41] who determined zinc, lead and cadmium in waters by atomic absorption spectrometry after sample concentration on a Chelex-100 ion-exchanger. For this purpose, only one commutator could be used, as demonstrated by Fang et al. [20] in the determination of heavy metals in waters. When time-based injection is used to introduce the first sample volume, the system approaches that originally proposed for the incorporation of ion-exchange in flow injection analysis [14].

Detailed study of dispersion

Scans based on different t_s values enable the entire dispersed zone to be transferred stepwise to a second carrier stream, allowing the detector to build an image which represents the concentration/time profile of the dispersed zone at the resampling loop [12, 15, 34]. Therefore, this loop can be regarded as an intermittent monitor which acts during the passage of the dispersed

zone through it [12]. This recorded profile is chopped because t_s may assume only discrete variations. The general shape of this profile is independent of the parameters linked to the second analytical path, including the dead volume of the detector and its response time. Zone sampling, therefore, can be used to investigate dead-volume effects associated with flow-through sensors, the inner volume of the resampling loop corresponding to the dead volume of the simulated detector. It this loop is small enough, nearing a point sampler, it can be regarded as an ideal monitor, allowing a detailed study of the boundaries of the dispersed zone and carrier stream.

Zone sampling involving t_s scans was applied to confirm that in the first f.i.a./a.e.s. systems, the characteristics of the spectrometer had little influence on sample dispersion [22]. With this approach, it was also possible to demonstrate that in flow injection analysis, the reproducibility of measurements depends on the region of the dispersed zone to which it is referred [12, 15, 34]. When measurements are made in a region of the sample zone with pronounced concentration gradients, the reproducibility drops. This drawback can be overcome by using a sequential injection process [12] as an alternative to flow-injection procedures based on gradient exploitation.

When zone sampling with t_s scans is done with only one commutator [12, 15, 22, 34], another injection of the initial solution is required after each variation of t_s. With two commutators (Fig. 5b), only one injection of the solution to be aliquoted is needed.

Zone-sampling processes involving L scans, L being the length of the dispersion coil in Fig. 5, are being studied. This will help to obtain an image which will represent the true axial distribution of the dispersed zone after a time interval t_s.

ZONE TRAPPING

This process consists of the removal of the central portion of a processed sample zone, leaving it for a pre-established period of time under defined conditions, and later re-introducing it into the same carrier stream [16]. Zone trapping is easily achieved with an electronically operated commutator (Fig. 7). When the commutator is operated, the sample is injected and the trapping coil is placed in the same path. The chemical reactions are initiated

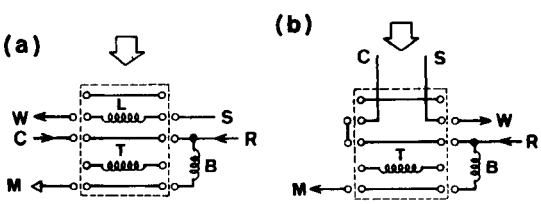

Fig. 7. Flow diagrams for the zone-trapping process involving loop-based (a) or time-based (b) injection: R, required reagents; B, transmission line; T, trapping coil; other symbols as in Fig. 1.

at the confluence point where the reagents are added. After a time interval t_s (here $t_s = t_1$), the commutator is operated again, trapping the most concentrated portion of the sample zone for a period t_2, which corresponds to the sampling period. When the next commutation occurs, the following sample is introduced and the first is pushed towards the detector. This approach is particularly suitable for procedures based on relatively slow chemical reactions in which sensitivity and/or sampling rate is critical. It has some advantages over the stopped-flow and the intermittent-flow approaches [16], and was applied to the spectrophotometric determination of ammonium ion [16] and silica [42] in natural waters. Although in both applications one loop-based injection was used per commutation cycle (as in Fig. 7a), the sampling rate can be doubled by using two injections per commutation cycle (Fig. 2) into a system with two parallel equivalent trapping coils. It should be emphasized that time-based injection seems to be more attractive for use with zone trapping (Fig. 7b).

MANIFOLD MODIFICATIONS

For any flow-injection system, one commutation device defines two states. With two injections per commutation cycle (Fig. 2), each established sample zone can be processed according to requirements. This aspect is useful for simultaneous determinations, as confirmed by Giné et al. [9] who determined nitrate and nitrite in natural waters with the system shown in Fig. 8(a). Commutation to the state specified in Fig. 8(a) causes the introduction of both sample and colour reagent into their merging streams as well as introduction of a reductor column in the analytical path. The recorded signal is then proportional to the total nitrate and nitrite in the sample. With the next commutation, the reductor is removed from the analytical path, so that the measured signal reflects only the nitrite content of the sample.

Recently, manifold modifications, made possible by commutation devices, led to the development of a procedure for simultaneous spectrophotometric

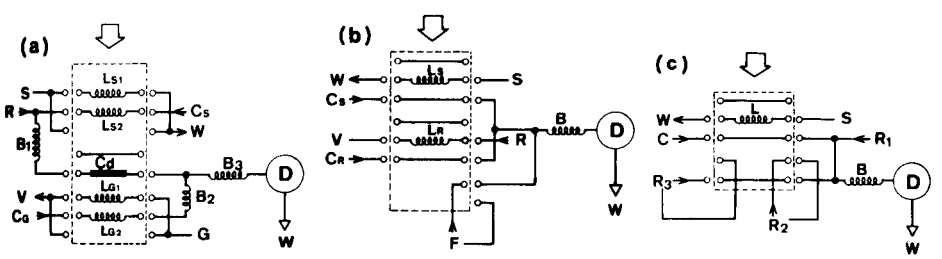

Fig. 8. Flow diagrams for the simultaneous determination of nitrate and nitrite (a), for the nitrite determination with intermittent flow (b), and for the turbidimetric determination of sulphate with alternating streams (c). G, Modified Griess reagent; F, fast intermittent flow; R, buffer/masking reagent (a) or colour-forming reagent (b); R_1, sulphate standard solution; R_2, barium chloride reagent; R_3, alkaline EDTA wash solution. Other symbols as in Fig. 1. For system dimensions, see [9], [10] and [11], respectively.

determination of silica and phosphate based on differential kinetics. Two different mean available times for the reactions were achieved simply by switching the reaction coils during commutation; the method will be reported at a later date.

Intermittent and alternating streams

Some flow-injection procedures are improved by using a fast intermittent flow during the wash period [39]. Also, an intermittent reagent stream flowing only when the sample zone reaches the confluence point can be useful for merging zones [39]. Commutation permits intermittent flows to be achieved without stopping the peristaltic pump as emphasized in an improved procedure for nitrite determination in waters [10]. Figure 8(b) shows the flow diagram of this system in the state corresponding to the wash period, the fast flow being directed towards the analytical path in order to speed up washing of the system. When the commutator is operated, the sample and reagent solutions are injected while the wash solution recycles outside the analytical path. With intermittent streams, therefore, the mean available time for the reactions can be increased without impairing sampling frequency.

Similarly, commutation can provide alternating streams (Fig. 8c); this possibility was studied for turbidimetric determination of sulphate in natural waters and plant digests [11] based on barium sulphate precipitation. During the sampling period, an alkaline EDTA solution flowing at high speed was used to wash out the system, thus avoiding gradual accumulation of barium sulphate in the manifold.

Stopped-flow procedures and other trends

Stopped-flow procedures with intermittent pumping have often been described [38, 43]. With commutation (Fig. 9), stopping the peristaltic pump

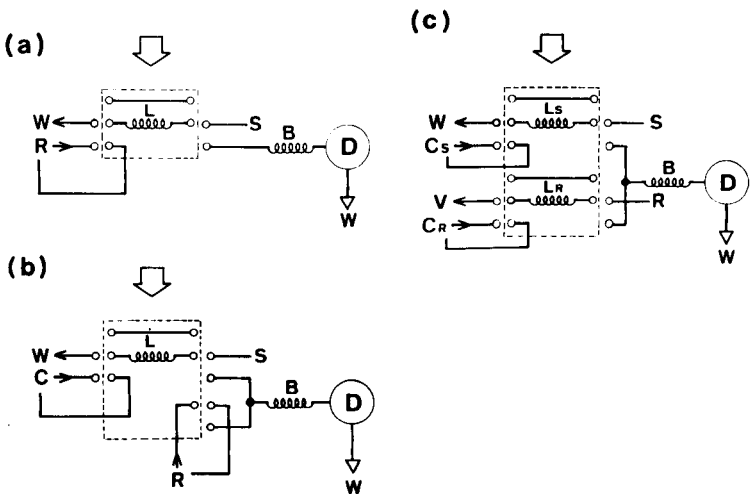

Fig. 9. Flow diagrams of the stopped-flow systems in the straight (a), confluence (b) and merging-zones (c) configurations. Symbols as in Figs. 1—4.

is avoided, resulting in a simple system which is in use in this laboratory. Stopped-flow procedures with the commutator have not yet been described in the literature.

The commutator devices can be considered as a main component of the hardware for f.i.a. With commutators operated by microprocessors, new system configurations, feed-back mechanisms and improved data processing will become possible further to improve sampling, aliquoting, diluting, adding, separating, timing, and the other steps required in automated analytical procedures. The flow-injection systems will then become fully automated processing systems for the handling of solutions.

The authors express their gratitude to the staff of the Analytical Chemistry Division of CENA, and thank Mrs. Diva Athié for her assistance with the manuscript. Financial support by CNPq (Conselho Nacional de Desenvolvimento Cientifico e Tecnológico) and by FAPESP (Fundacao Para o Amparo a Pesquisa do Estado de Sao Paulo).

REFERENCES

1 J. Růžička, Phil. Trans. R. Soc. London, A305 (1982) 645.
2 K. K. Stewart, G. R. Beecher and P. E. Hare, Anal. Biochem., 70 (1976) 167.
3 J. Růžička, E. H. Hansen and H. Mosbaek, Anal. Chim. Acta, 92 (1977) 235.
4 H. Bergamin F°, J. X. Medeiros, B. F. Reis and E. A. G. Zagatto, Anal. Chim. Acta, 101 (1978) 9.
5 J. Růžička and E. H. Hansen, Anal. Chim. Acta, 78 (1975) 145.
6 J. W. B. Stewart, J. Růžička, H. Bergamin F° and E. A. G. Zagatto, Anal. Chim. Acta, 81 (1976) 371.
7 H. Bergamin F°, E. A. G. Zagatto, F. J. Krug and B. F. Reis, Anal. Chim. Acta, 101 (1978) 17.
8 A. U. Ramsing, J. Růžička and E. H. Hansen, Anal. Chim. Acta, 129 (1981) 1.
9 M. F. Giné, H. Bergamin F°, E. A. G. Zagatto and B. F. Reis, Anal. Chim. Acta, 114 (1980) 191.
10 E. A. G. Zagatto, A. O. Jacintho, J. Mortatti and H. Bergamin F°, Anal. Chim. Acta, 120 (1980) 399.
11 F. J. Krug, E. A. G. Zagatto, B. F. Reis, O. Bahia F°, A. O. Jacintho and S. S. Jørgensen, Anal. Chim. Acta, 145 (1983) 179.
12 E. A. G. Zagatto, M. F. Giné, E. A. N. Fernandes, B. F. Reis and F. J. Krug, Anal. Chim. Acta, 173 (1985) 289.
13 C. Pasquini, Ph.D. Thesis, Campinas, Universidade Estadual de Campinas, 1984.
14 H. Bergamin F°, B. F. Reis, A. O. Jacintho and E. A. G. Zagatto, Anal. Chim. Acta, 117 (1980) 81.
15 B. F. Reis, A. O. Jacintho, J. Mortatti, F. J. Krug, E. A. G. Zagatto, H. Bergamin F° and L. C. R. Pessenda, Anal. Chim. Acta, 123 (1981) 221.
16 F. J. Krug, B. P. Reis, M. F. Giné, E. A. G. Zagatto, J. R. Ferreira and A. O. Jacintho, Anal. Chim. Acta, 151 (1983) 39.
17 J. Růžička and E. H. Hansen, Anal. Chim. Acta, 145 (1983) 1.
18 P. K. Dasgupta and H. Hwang, Anal. Chem., 57 (1985) 1009.
19 B. F. Reis, E. A. G. Zagatto, A. O. Jacintho, F. J. Krug and H. Bergamin F°, Anal. Chim. Acta, 119 (1980) 305.
20 Z. Fang, S. Xu and S. Zhang, Anal. Chim. Acta, 164 (1984) 41.

21 Z. Fang, J. Růžička and E. H. Hansen, Anal. Chim. Acta, 164 (1984) 23.
22 A. O. Jacintho, E. A. G. Zagatto, H. Bergamin F°, F. J. Krug, B. F. Reis, R. E. Bruns and B. R. Kowalski, Anal. Chim. Acta, 130 (1981) 243.
23 J. M. Reijn, W. E. van der Linden and H. Poppe, Anal. Chim. Acta, 114 (1980) 105.
24 S. S. Jørgensen, K. M. Petersen and L. A. Hansen, Anal. Chim. Acta, 169 (1985) 51.
25 F. J. Krug, J. Mortatti, L. C. R. Pessenda, E. A. G. Zagatto and H. Bergamin F°, Anal. Chim. Acta, 125 (1981) 29.
26 E. A. G. Zagatto, O. Bahia F°, M. F. Giné and H. Bergamin F°, Anal. Chim. Acta, in press.
27 J. Slanina, F. Bakker, A. Bruyn-Hes and J. J. Möls, Anal. Chim. Acta, 113 (1980) 331.
28 E. H. Hansen, J. Růžička, F. J. Krug and E. A. G. Zagatto, Anal. Chim. Acta, 148 (1983) 111.
29 E. A. G. Zagatto, F. J. Krug, H. Bergamin F°, S. S. Jørgensen and B. F. Reis, Anal. Chim. Acta, 104 (1979) 279.
30 B. F. Reis, H. Bergamin F°, E. A. G. Zagatto and F. J. Krug, Anal. Chim. Acta, 107 (1979) 309.
31 J. Mindegaard, Anal. Chim. Acta, 104 (1979) 185.
32 E. A. G. Zagatto, B. F. Reis, H. Bergamin F° and F. J. Krug, Anal. Chim. Acta, 109 (1979) 45.
33 E. A. G. Zagatto, A. O. Jacintho, F. J. Krug, B. F. Reis, R. E. Bruns and M. C. U. Araújo, Anal. Chim. Acta, 145 (1983) 169.
34 M. F. Giné, B. F. Reis, E. A. G. Zagatto, F. J. Krug and A. O. Jacintho, Anal. Chim. Acta, 155 (1983) 131.
35 M. C. U. Araújo, C. Pasquini, R. E. Bruns and E. A. G. Zagatto, Anal. Chim. Acta, 171 (1985) 337.
36 E. A. G. Zagatto, A. O. Jacintho, L. C. R. Pessenda, F. J. Krug, B. F. Reis and H. Bergamin F°, Anal. Chim. Acta, 125 (1981) 37.
37 A. O. Jacintho, E. A. G. Zagatto, B. F. Reis, L. C. R. Pessenda and F. J. Krug, Anal. Chim. Acta, 130 (1981) 361.
38 J. Růžička and E. H. Hansen, Anal. Chim. Acta, 106 (1979) 207.
39 J. Růžička and E. H. Hansen, Anal. Chim. Acta, 114 (1980) 19.
40 F. J. Krug, H. Bergamin F°, E. A. G. Zagatto and S. S. Jørgensen, Analyst (London), 102 (1977) 503.
41 S. Olsen, L. C. R. Pessenda, J. Růžička and E. H. Hansen, Analyst (London), 108 (1983) 905.
42 F. J. Krug, B. F. Reis and S. S. Jørgensen, Proc. Workshop on Locally Produced Laboratory Equipment for Chemical Education, Copenhagen, Denmark, 1983, p. 121.
43 B. Rocks and C. Riley, Clin. Chem., 28 (1982) 409.

Analytica Chimica Acta, 179 (1986) 119—129
Elsevier Science Publishers B.V., Amsterdam — Printed in The Netherlands

LAMINAR-FLOW BOLUS SHAPES IN FLOW INJECTION ANALYSIS

JOSEPH T. VANDERSLICE,* A. GREGORY ROSENFELD† and GARY R. BEECHER

U.S. Department of Agriculture, Agricultural Research Service, Beltsville Human Nutrition Research Center, Nutrient Composition Laboratory, Beltsville, MD 20705 (U.S.A.)

(Received 30th September 1985)

SUMMARY

Bolus shapes for injected samples have been calculated for times of interest in experiments on flow injection analysis. The effect of both system and molecular parameters on the shapes and the dispersion of samples is considered. The implications for merging-zone experiments are discussed briefly.

The movement of a solvent in a flowing stream through a cylindrical tubing under laminar flow conditions is controlled by convective forces and is a well understood phenomenon [1]. When a solute dissolved in an appropriate solvent is injected into the flowing stream, the dispersion of that solute in the absence of any chemical reaction is controlled by the twin processes of diffusion and convection [2]. The relative magnitude of these two effects defines the concentration profiles of the solute in the stream at any instant in time and also determines the shape of the observed peaks as the solute moves past the detector.

A knowledge of the concentration profiles within a solute bolus provides not only some insight into the relative effects of convection and diffusion in a moving stream but also introduces some "caveats" that an experimentalist should at least consider when designing a flow injection system. In this paper, bolus shapes and concentration profiles are calculated as a function of time for flow in straight cylindrical tubing under laminar flow conditions. Calculations are restricted to laminar flow in straight tubing for three reasons. First, the Reynolds numbers under normal flow-injection conditions are such that the flow should be laminar if no turbulence is introduced by experimental imperfections; second, it is possible to solve the appropriate equation governing the dispersion of solute under these conditions; third, molecular parameters such as diffusion coefficients and rate constants can be directly related to measured parameters.

Solute concentration profiles are first presented as a function of time under the conditions normally used in flow injection analysis. A discussion

†Present address: Medical College of Northern Virginia, Richmond, VA, U.S.A.

then ensues on the effect of a system parameter, the internal radius of the tubing, on the dispersion of the solute and finally, the effect of different diffusion coefficients on the concentration profiles is delineated. Possible ramifications of these results to merging-zone experiments are briefly addressed.

THEORETICAL CONSIDERATIONS

As shown in Fig. 1, the initial configuration of an injected sample is that of a slug (Fig. 1a) which is then distorted into the shape shown in Fig. 1(b). Downstream at the observation point, a peak is observed which for purposes of the present discussion is characterized by an initial appearance time, t_a, and a baseline to baseline time, Δt_B. The concentration profile in the bolus shown in Fig. 1(b) is governed by the convection-diffusion equation [2] shown in Fig. 2. This has to be solved subject to the initial boundary conditions as shown where the injected bolus is of finite length. The solution of

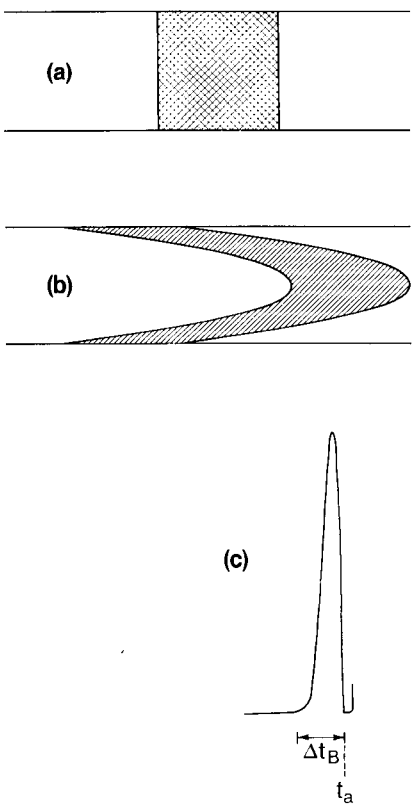

Fig. 1. Bolus shapes at injection (a) and after injection (b). Observed peak shape at detector (c).

Convection-Diffusion Equation:

$$D\left(\frac{\partial^2 C}{\partial x^2} + \frac{\partial^2 C}{\partial r^2} + \frac{1}{r}\frac{\partial C}{\partial r}\right) = \frac{\partial C}{\partial t} + u_0\left(1 - \frac{r^2}{a^2}\right)\frac{\partial C}{\partial x}$$

Initial Boundary Conditions:

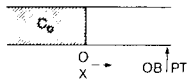

Reduced Units:

$$P_e = \frac{au_0}{D} ; X = \frac{Dx}{a^2 u_0} ; \tau = \frac{Dt}{a^2}$$

Fig. 2. Convection-diffusion equation to be solved along with initial boundary conditions. Convenient dimensionless parameters P_e, τ, and X are used in the numerical solution.

this equation has been exhaustively studied over the period 1965—1973 by Gill and coworkers in the United States [3—6] and by Bate et al. in Great Britain [7, 8]. The methods used by these workers were applied here to solve the convection-diffusion equation to obtain extensive results in those regions of interest appropriate for flow injection analysis. It was convenient to introduce the units of Anathakrishnan et al. [3] shown in Fig. 2, namely, the reduced velocity or Peclet number $P_e = au_0/D$, the reduced distance $X = Dx/a^2u_0$, and the reduced time $\tau = Dt/a^2$, where D is the diffusion coefficient ($cm^2\ s^{-1}$), x is the axial distance downstream (cm), t is the time (s), a is the radius of the tubing (cm), and u_0 is the maximum velocity of the fluid at the center of the tubing, equal to twice the average velocity, $\bar{u}$. As Gill and coworkers have shown, the convection-diffusion equation has to be numerically integrated for all values of $\tau < 0.8$, which is the region of interest in flow injection analysis [9]. The numerical methods of solution have been extensively discussed by both Gill and coworkers [3—6] and by Bate et al. [7, 8].

For a given value of the reduced time, τ, the relative concentration of solute was calculated at each point in the moving stream. The initial sample size for each calculation was kept constant. The calculated concentrations were then grouped in eight equal intervals depending on the maximum concentration, $C_{max\,\tau}$, calculated for a given τ (i.e., the concentrations were grouped in intervals of (7/8—1)C_{max}, (6/8—7/8) C_{max}, ..., (0—1/8) C_{max}. The first seven intervals are plotted while the last interval with the lowest concentration of solute was deleted for purposes of illustration. An expert draftsman was then given the contours along with the average concentration within each contour and the relative color intensities were chosen to correspond as closely as possible to the calculated concentrations in each interval. The results of this procedure are shown in Fig. 3 (shaded but not in color) for a particular bolus which is plotted as a function of the reduced radial distance r/a, and the reduced axial distance. The deeper shades of gray in this half-tone figure correspond to the higher relative concentrations in the bolus.

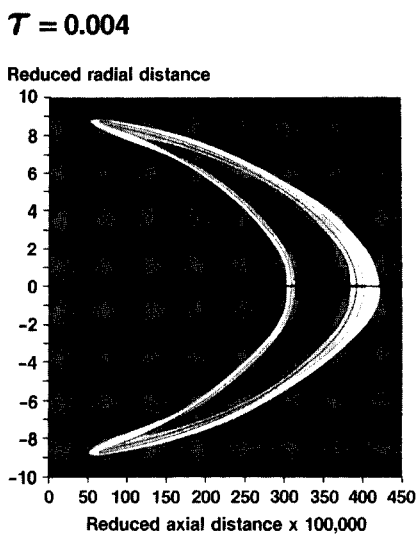

Fig. 3. Half-tone display of a calculated bolus concentration distribution. The darker tones of gray correspond to higher concentrations (see text for more detail).

RESULTS

In Fig. 4, the bolus shapes are shown for values of $\tau \leqslant 0.01$. These are plotted as a function of the reduced radial and axial distances. The relative color intensities of the solute concentrations for the four boluses have been normalized to the darkest shading in the bolus at $\tau = 0.002$. For this range of τ values, the boluses are essentially crescent-shaped and show the increased dispersion and diminution of intensity in the bolus as τ increases. Figure 5 shows the corresponding bolus shapes for values of $0.01 \leqslant \tau \leqslant 0.10$. Here, the reduced axial distance scale was increased by a factor of 10 compared to what it was in Fig. 4 and the color intensities were renormalized to the darkest shading in the bolus at $\tau = 0.01$ which was increased compared to what it was in Fig. 4. These changes in axial distance and intensity were done so as not to lose too much resolution. In this region of τ, the boluses show rather unusual shapes which lead to double-humped peaks as will be explained later. In Fig. 6, the bolus shapes are displayed for values of $0.10 \leqslant \tau \leqslant 0.704$. Again, the reduced axial distance scale was increased and the intensities were renormalized to the maximum color intensity in the bolus at $\tau = 0.10$ so as not to lose resolution. In this region of τ, the boluses are more uniformly spread over the axial distance and show less unusual shapes than those observed in Fig. 5. The three ranges of τ shown in Figs. 4—6 were chosen with a particular point in mind. For $\tau < 0.01$, the dispersion of the solute in the stream is dominated by convection while for $\tau > 0.1$, diffusion dominates. For $0.01 \leqslant \tau \leqslant 0.1$, both convection and diffusion are equally important and their interplay leads to the unusual shapes shown in Fig. 5.

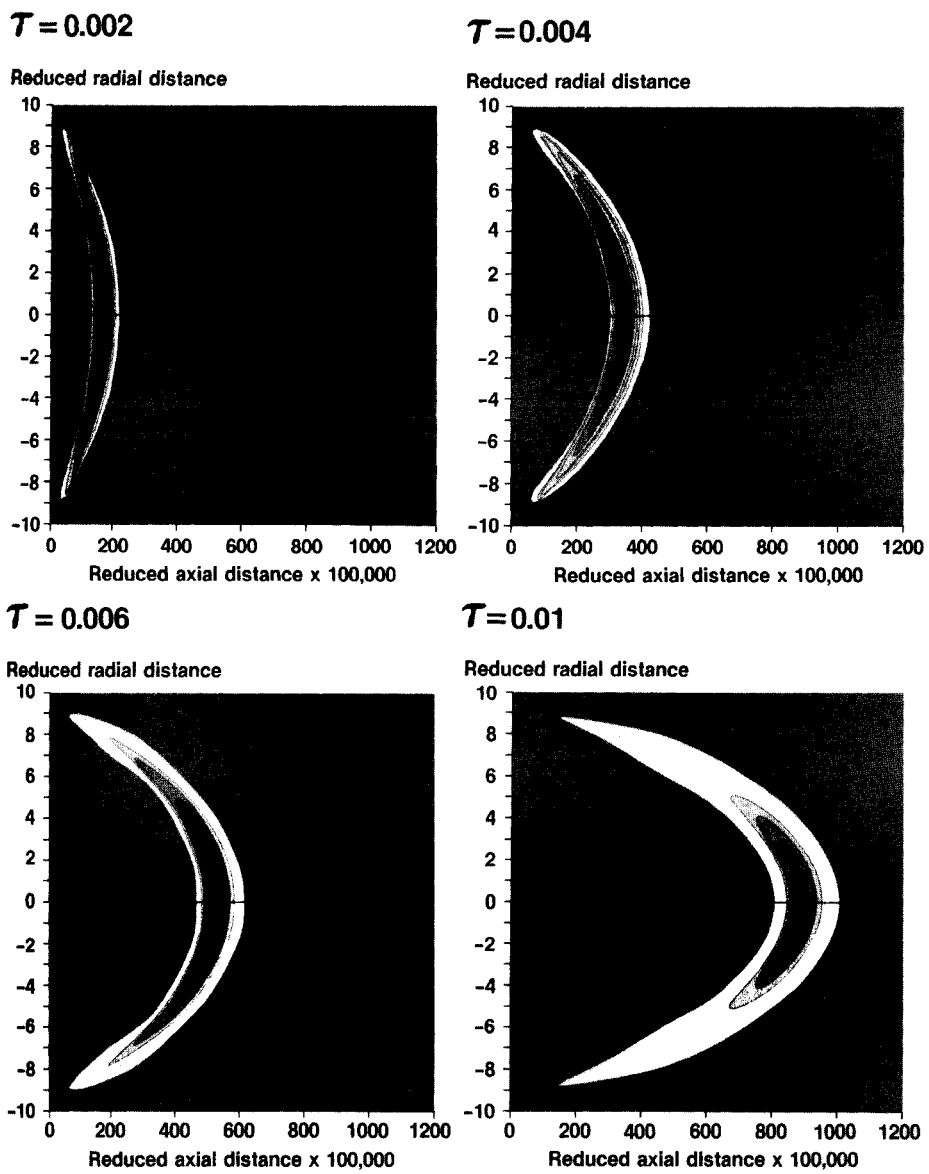

Fig. 4. Bolus shapes for values of $\tau \leqslant 0.01$ (0.002—0.01).

In Fig. 7, three types of experimental curves expected as the bolus passes the detector are shown for the different ranges of τ. For $\tau < 0.01$, the usual sharp rise and exponential decay associated with convective dispersion are observed, while for $\tau > 0.1$, "skewed" Gaussian curves typical of diffusion-controlled phenomena are observed. For $0.01 \leqslant \tau \leqslant 0.1$, one expects to see double-humped peaks with the rounded hump increasing as τ increases and

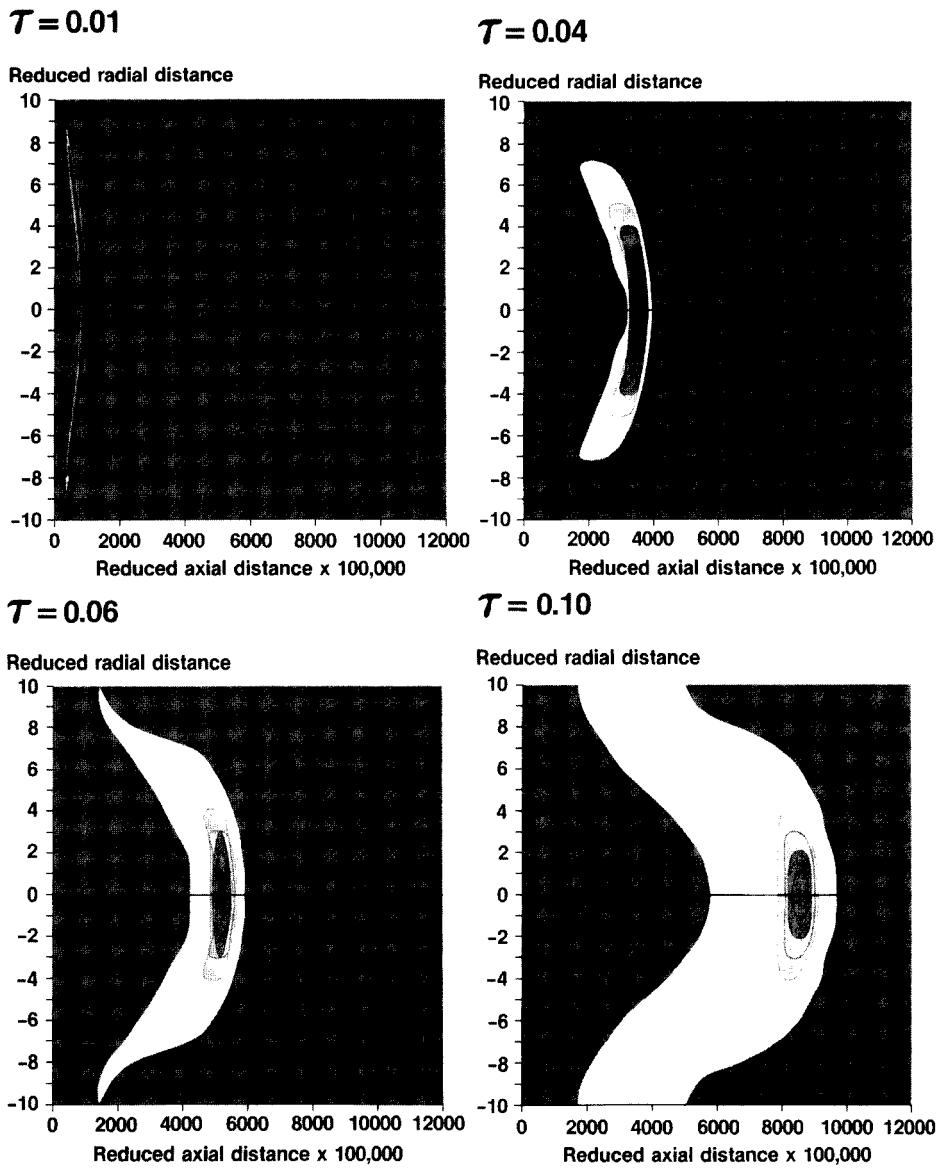

Fig. 5. Bolus shapes for values of $0.01 \leqslant \tau \leqslant 0.1$.

this hump dominates as τ increases beyond $\tau = 0.1$ [9]. All of these curves were experimentally observed in this laboratory at the expected times under laminar flow conditions.

The effect of the variation of a system parameter, the tubing radius, on dispersion is shown in Fig. 8, where the radius in one case is assumed to be twice the other case. Here, the axial distance along the tube is no longer

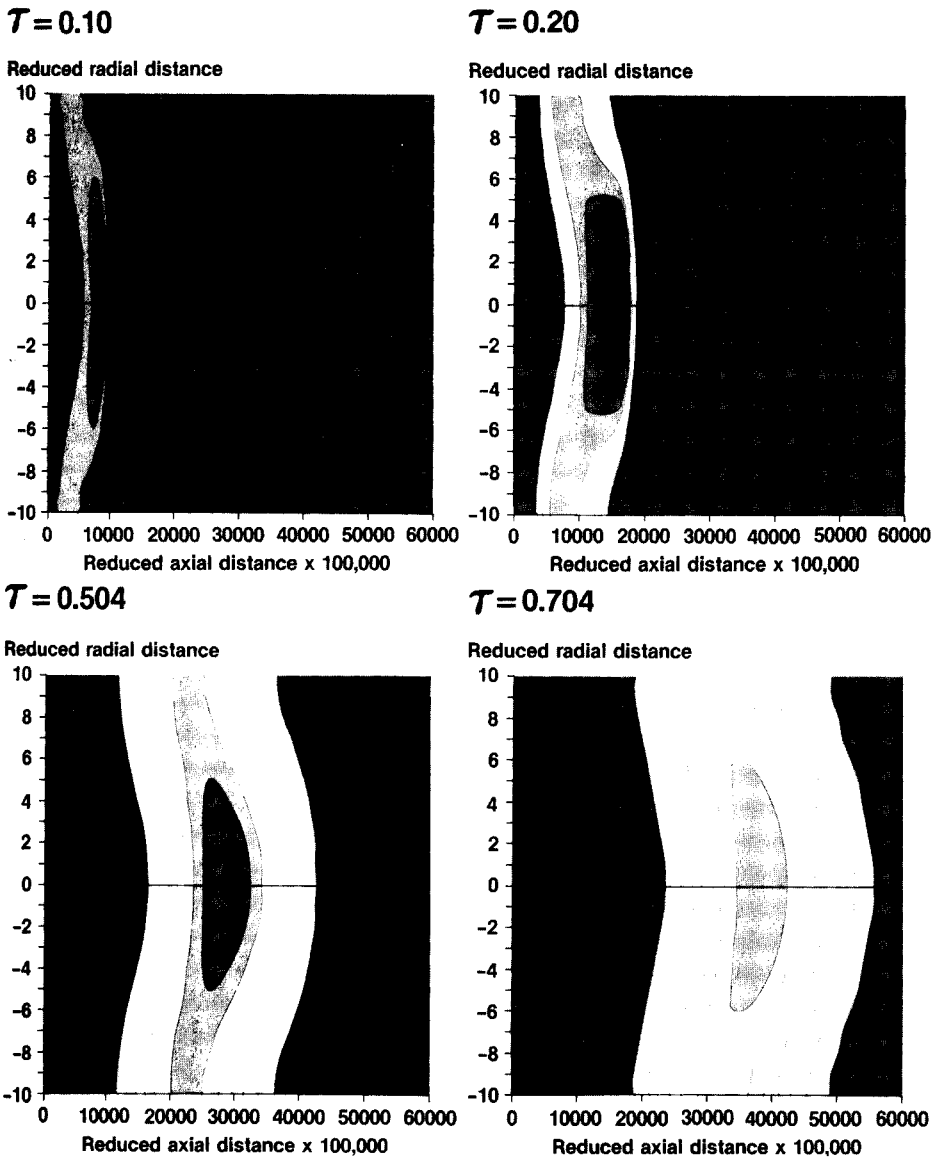

Fig. 6. Bolus shapes for values of $0.1 \leqslant \tau \leqslant 0.704$.

given in reduced units but in centimetres. Two comparisons are given, one where the flow rates are the same (Fig. 8a,c) and one where the appearance times are the same (Fig. 8b,d). The dispersion in the former case is the same in both tubings because for the same size of sample, the initial length of the sample injection in the smaller tubing is four times as long. However, for the case in which the appearance times are the same, the dispersion in the larger tubing is greater, as is well known [10].

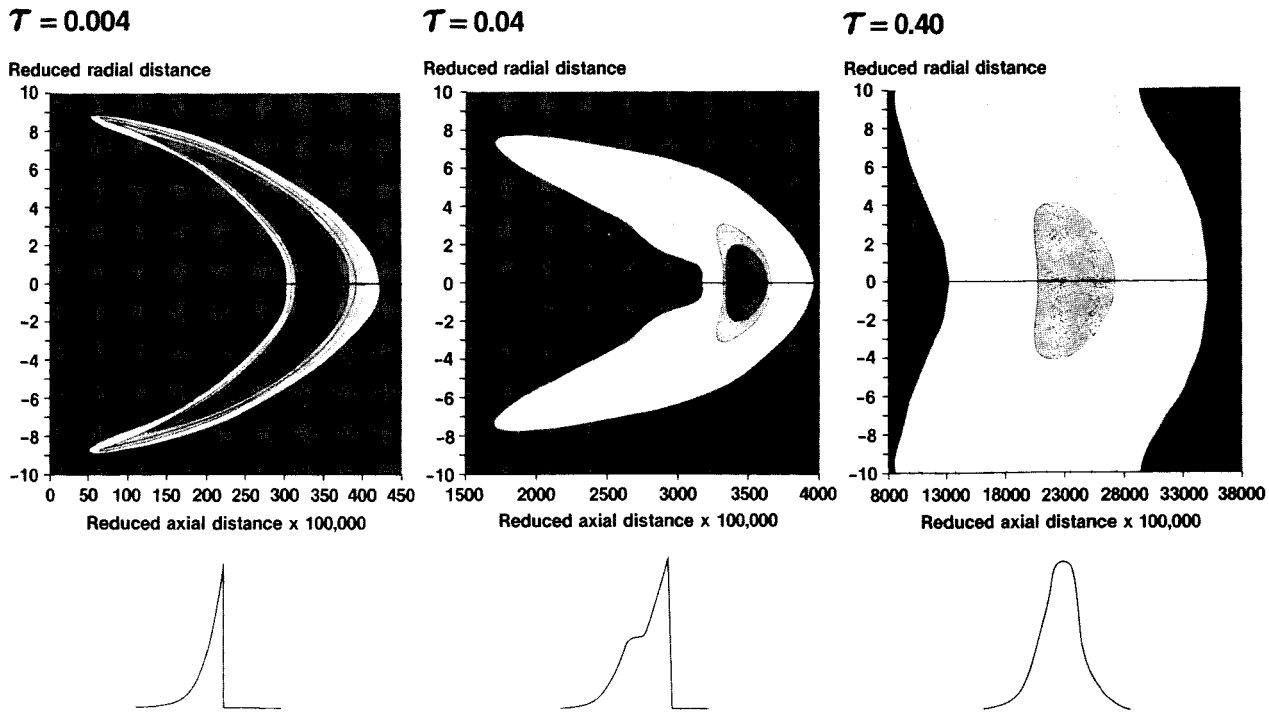

Fig. 7. Experimental curves to be expected for different values of τ (see discussion in text).

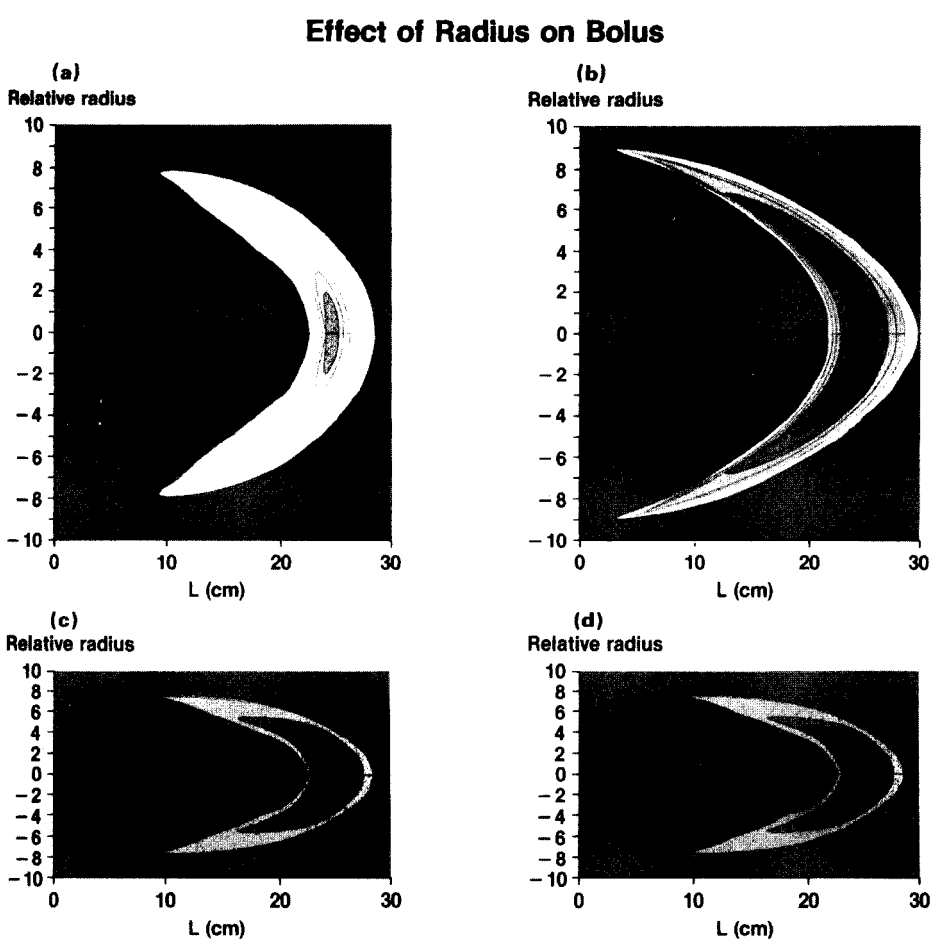

Fig. 8. The effect of tubing radius (a) on concentration profiles. Conditions: (a) a = 0.040 cm, t = 4.24 s, q = 1.00 ml min^{-1}; (b) a = 0.040 cm, t = 1.06 s, q = 4.00 ml min^{-1}; (c) a = 0.020 cm, t = 1.06 s, q = 1.00 ml min^{-1}; (d) a = 0.020 cm, t = 1.06 s, q = 1.00 ml min^{-1}; D = 7.55 × 10^{-6} cm^2 s^{-1}; in all cases, q is the flow rate in ml min^{-1} and L is the distance along the tube. Parts (a) and (c) show the effect on the bolus of halving the tubing radius with other parameters held constant. Parts (b) and (d) show comparable boluses when the appearance time is the same from the different sized tubing.

The effect of different diffusion coefficients is shown in Fig. 9 where boluses are compared for cases in which these coefficients differ by a factor of five. With all the system parameters being equal, Fig. 9(a,b) shows that the two boluses are radically different at a given point downstream, and the relative concentrations vary differently in different parts of the stream. Thus, if, in a merging-zones experiment, one were interested in an enzyme/substrate reaction for which diffusion coefficients can vary by a factor of ten or more, one should have some legitimate concern that the two reagents

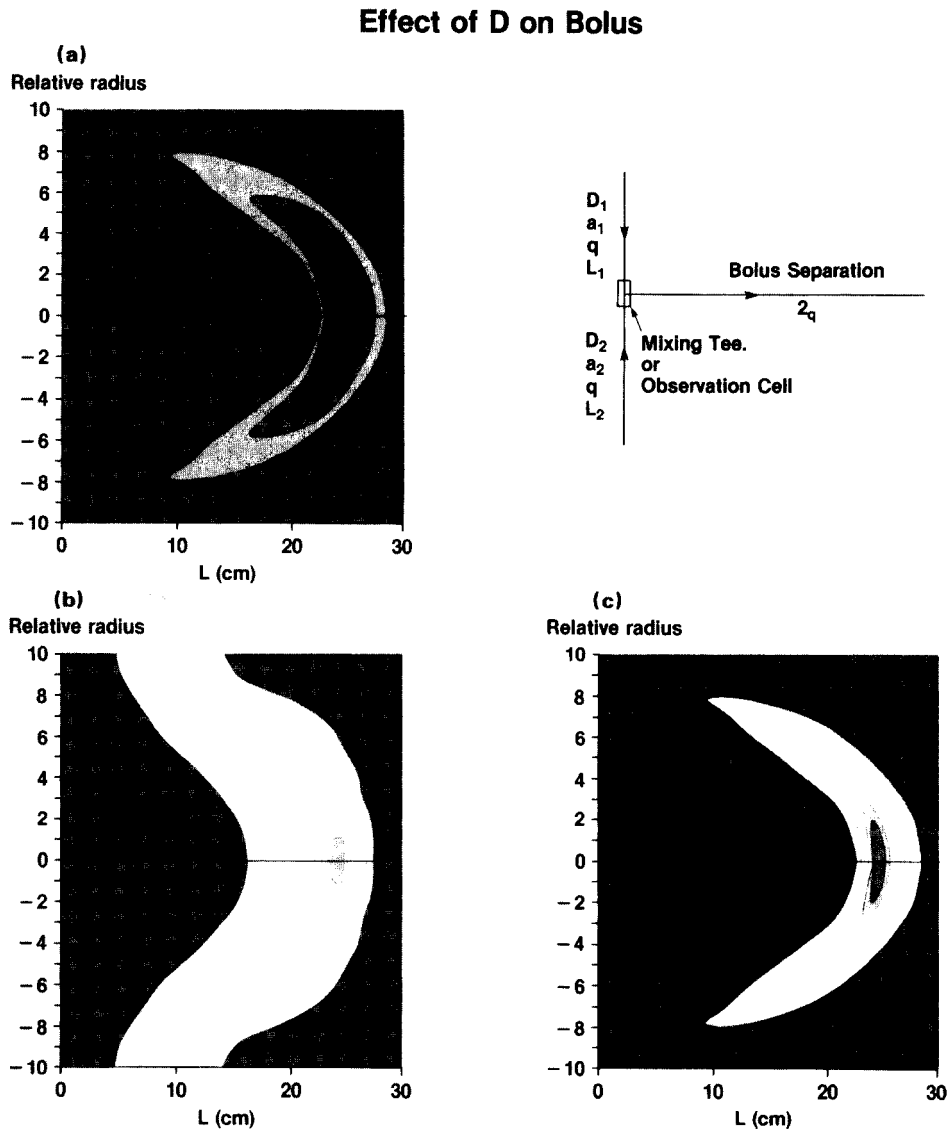

Fig. 9. The effect of different diffusion coefficients on the bolus. Conditions: (a) D_2 = 7.55×10^{-6} cm^2 s^{-1}, L_2 = 30 cm, a_2 = 0.020 cm; (b) D_1 = 3.78×10^{-5} cm^2 s^{-1}, L_1 = 30 cm, a_1 = 0.020 cm; (c) L_1 = 6.03 cm, a_1 = 0.045 cm, D_1 as in (b); appearance time is 1.06 s in all cases. Parts (a) and (b) show the effect of a five-fold difference in diffusion coefficient on the concentration profile; (c) shows how the distribution can be changed by varying the system parameters. The upper right-hand illustration outlines a typical merging-zones experiment.

are not being uniformly mixed at the same relative concentrations. For analytical experiments, where one might be interested in determining an average substrate concentration, this apparent mismatch of the boluses may not be a serious problem. However, if one were interested in determining

total enzyme activity, where the relative concentrations of enzyme and substrate are important, then the mismatch of the boluses may lead to errors. Fortunately, the system parameters can be adjusted to compensate for the differences in the diffusion coefficients as shown in Fig. 9(c); if a and L are adjusted as shown, then the two boluses can be made to match just prior to mixing. Unfortunately, after mixing, even ideal mixing, there is no guarantee that the boluses will remain matched as the solutes move further downstream. The parameters a and L can be adjusted to compensate for differences in diffusion coefficients of two solutes in a merging-zones experiment by using previously published equations [9, 11] for initial appearance and baseline to baseline times. Thus, if $D_1 = 5D_2$, then $a_1 = 2.23\ a_2$ and $L_1 = 0.201\ L_2$; if $D_1 = 10D_2$, then $a_1 = 3.15\ a_2$ and $L_1 = 0.101\ L_2$. These values were calculated from the equations $t_{app} = 109\ a^2\ D^{0.025}\ (L/q)^{1.025}$ and $\Delta t_b = (35.4a^2/D^{0.36})\ (L/q)^{0.64}$.

In summary, the calculation of bolus profiles in regions of interest for flow injection analysis gives added insight into the behavior of a sample after injection into a moving stream and raises questions concerning the validity of the merging-zones approach for certain types of experiments where molecular parameters are to be determined.

The authors greatly appreciate the skill and work of Gene Hanson of Heritage Arts, Inc., Greenbelt, MD, in constructing the bolus density contours shown.

REFERENCES

1 J. G. Knudsen and D. L. Katz, Fluid Dynamics and Heat Transfer, McGraw-Hill, New York, 1958, Chap. 4, p. 75.
2 G. Taylor, Proc. R. London, Soc. Ser. A: 219 (1953) 186; 225 (1954) 473.
3 V. Anathakrishnan, W. N. Gill and A. J. Barduhn, J. Am. Inst. Chem. Eng., 11 (1965) 1063.
4 W. N. Gill and V. Anathakrishnan, J. Am. Inst. Chem. Eng., 12 (1966) 906; 13 (1967) 801.
5 N. S. Reejhsinghani, W. N. Gill and A. J. Barduhn, J. Am. Inst. Chem. Eng., 12 (1966) 916.
6 N. S. Reejhsinghani, A. J. Barduhn and W. N. Gill, J. Am. Inst. Chem. Eng., 14 (1968) 100.
7 H. Bate, S. Rowlands, J. A. Sirs and H. W. Thomas, J. Phys. D: 2 (1969) 1447.
8 H. Bate, S. Rowlands and J. A. Sirs, J. Appl. Physiol., 34 (1973) 866.
9 J. T. Vanderslice, K. K. Stewart, A. G. Rosenfeld and D. Higgs, Talanta, 28 (1981) 11.
10 J. Růžička and E. H. Hansen, Anal. Chim. Acta, 99 (1978) 37.
11 J. T. Vanderslice, G. R. Beecher and A. G. Rosenfeld, Anal. Chem., 56 (1984) 292.

Analytica Chimica Acta, 179 (1986) 131—148
Elsevier Science Publishers B.V., Amsterdam — Printed in The Netherlands

PEAK WIDTH AND REAGENT DISPERSION IN FLOW INJECTION ANALYSIS

JULIAN F. TYSON

Department of Chemistry, University of Technology, Loughborough, Leicestershire, LE11 3TU (Great Britain)

(Received 6th September 1985)

SUMMARY

Accurate equations are derived for relating peak width to injected concentration for single-line and merging-stream manifolds in which a well stirred mixing chamber is used to generate concentration gradients. The consequences of making an approximation to produce a linear relationship between peak width and the natural logarithm of the injected concentration are evaluated and shown to have little practical effect. The concept of reagent dispersion coefficient, D^R, is used in certain derivations and a relationship between this and the conventional dispersion coefficient is derived and investigated experimentally. The use of D^R to evaluate the likely performance of other flow-injection modes is illustrated for the calculation of reagent-to-sample concentration ratios and the case of reversed f.i.a. (reagent injected into sample carrier stream). An extension of the usual peak-width method is in f.i.a. described; a low-dispersion coefficient manifold is used and the product concentration profile is monitored. The analytical information in the double peaks obtained is discussed and illustrated for the peak-width mode by the injection of copper(II) ions (1.6×10^{-6}—0.16 M) into a carrier stream of 10^{-4} M EDTA. The single well stirred mixing chamber model is used as a basis for the evaluation of the results and is applied to discussion of other manifolds not containing a real mixing chamber, in particular for the calculation of peak base-widths.

Although the most commonly used quantitative parameter in flow injection analysis (f.i.a.) is the peak maximum, the originators of the technique, Růžička and Hansen have shown that analytical information is available from other properties of the response curve (see, e.g. [1]). The peak maximum has the advantage of being very easily located on the recording of detector response vs. time and its use is thus more in keeping with the general philosophy of f.i.a. than, for example, peak area or a point on the peak tail which require additional signal-processing devices. However, the use of peak height suffers from the same limitations as for conventional steady-state analyses, namely that an upper limit to the working range is set. This may be due to the response being "off-scale" or into a very non-linear part of the calibration function or because there is insufficient reagent to produce the appropriate amount of product.

These disadvantages may be overcome if the width of the peak is measured. Under appropriate circumstances, the points between which the peak

0003-2670/86/$03.50

width is to be measured may be identified accurately using only a chart recorder. Previously, such methods have been referred to as "titrations" [2], "pseudotitrations" [3], "variable-time kinetic" methods [4] and "scale expansion" methods [5]. Some of these terms are misleading and all obscure the basis of the quantification, namely measurement of peak width, which must be confusing to newcomers to the technique. It is proposed here that all methods encompassed by the terminology above be known as "peak-width" methods and that these form a subset of all "time-based" methods in f.i.a. This latter set would also include methods based on "electronic dilution" [6], "gradient calibration" (both decreasing [6] and increasing [7]), "stopped flow" [8], "gradient scanning" [9] and "zone sampling" [10] amongst others.

In order to obtain a relationship between peak width and the concentration of the material injected, the concentration/time (C, t) equations for the rise and fall curves must be known. If the C, t equations are exponentials, as produced by a well-stirred mixing chamber, then the peak width is related to the logarithm of the concentration. Two groups of workers have previously derived peak-width equations, several of which are inaccurate. Růžička and co-workers [2, 6] assumed that the injected sample volume was instantly dispersed throughout the mixing chamber and then washed out. This is the tanks-in-series model for dispersion behaviour [11] with the number of tanks reduced to one and does not correspond to the situation, often adopted in practice, in which a real mixing chamber is introduced into the manifold and the sample slug flows into the tank. It is also possible in practice for the injected volume to be larger than the tank volume, a situation not covered by this version of the tanks-in-series model. Olsen et al. [6] considered that, for a system without a real mixing chamber, the dispersion produced was equivalent to wash out from a tank comprising the reactor volume plus half the injected volume. This situation is possibly covered better by the "one-tank" model but examination of their experimental results shows the rise time to occupy a significant proportion of the total peak time, at variance with the prediction of an infinitely fast rise time. This paper [6] also corrects an error in the equivalence condition made in the earlier paper [2], but perpetuates the hidden approximation in deriving the equation for the single-line manifold.

Pardue and Fields [4] adopted a model based on slug flow up to a well stirred tank, but make unnecessary approximations in deriving their final peak-width equation and also perpetuate the error in the equivalence condition.

Here, exact equations are derived for the passage of an injected slug through a well stirred mixing chamber for a single-line manifold for the conditions (a) no reagent in the carrier stream and (b) reagent in the carrier stream. The equations are also applied to a merging stream manifold in which the dispersed sample zone is merged with a stream of reagent. The potential of the peak-width method for extending the working range of a technique,

particularly when a manifold with a low dispersion coefficient is used and the product of the reaction is followed, is demonstrated. The derivation of the equations makes use of the concept of reagent dispersion coefficient and the usefulness of this concept in other f.i.a. situations is discussed.

DERIVATION OF PEAK-WIDTH EQUATIONS

Physical dispersion in a well stirred mixing chamber

The manifold and underlying assumptions are shown in Fig. 1A. An abbreviated version of this derivation has been given [12]. A fuller version is given in Appendix 1 together with some other useful equations relating to this model [13]. The resulting equation (all symbols are explained in Table 1) is

$$\Delta t = (V/u^s) \ln [(C^s_m/C') - 1] - (V/u^s) \ln (D - 1) \quad (1)$$

Thus the width of the peak is not directly proportional to the logarithm of the injected concentration but to the function $\ln [(C^s_m/C') - 1]$. The former relationship is only obtained if the approximation $C^s_m/C' \gg 1$ is valid and hence $(C^s_m/C') - 1 \approx C^s_m/C'$. The extent to which this approximation is valid will be discussed later.

Physical dispersion of sample and reagent

Just as the dispersion coefficient based on the injected sample material is given by

$$D = C^s_m/C^s_p \quad (2)$$

it is proposed that the reagent dispersion coefficient be defined by

$$D^R = C^R_m/C^R_p \quad (3)$$

These definitions are valid for any single-line manifold, of course, and can be extended to any point on the reagent or sample profile:

$$D_g = C^s_m/C^s_g \quad (4)$$

$$D^R_g = C^R_m/C^R_g \quad (5)$$

The concentrations involved are indicated in Fig. 2A.

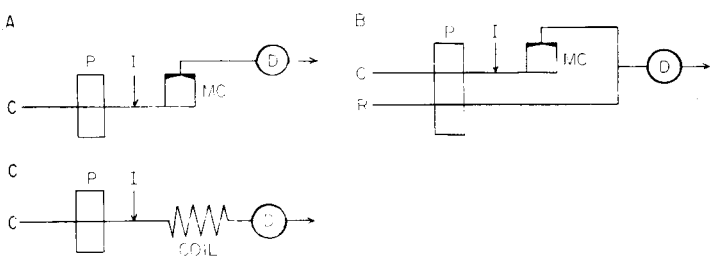

Fig. 1. Manifolds for peak-width methods: C, water carrier stream; D, detector; I, injector; MC, mixing chamber; P, pump; R, reagent stream. Manifolds A and B are hypothetical. It is assumed that the injected sample plug is not dispersed between I and MC nor is there any dispersion between MC and D, nor in D itself.

TABLE 1

List of symbols

Symbol	Definition
C	Concentration
C'	Concentration at which peak width is measured
C_{bl}	Concentration indistinguishable from baseline
C_{eq}	Concentration at equivalence point (before reaction)
C_g	Concentration at any point on dispersed profile
C_m	Steady-state concentration
C_p	Peak concentration
C^R	Reagent concentration
C^s	Sample concentration
D	Dispersion coefficient for injected material ($D = C^s_m/C^s_p$)
D^R	Dispersion coefficient for carrier stream material ($D^R = C^R_m/C^R_p$)
D_g	Dispersion coefficient for injected material at any point on peak profile
D^R_g	Dispersion coefficient for carrier stream material at any point on inverse peak profile
f^R	Fraction of total flow rate caused by merged reagent stream [$f^R = u^R/(u^R + u^s)$]
f^s	Fraction of total flow rate caused by merged sample stream [$f^s = u^s/(u^R + u^s)$]
R	Reagent (carrier stream material)
$R^{R/s}$	Ratio of reagent to sample concentrations (subscripts m and p also apply)
S	Sample (injected material)
t	Time
t_1, t_2	Time taken to reach C' on rising profile and falling profile, respectively
t_p	Time to reach peak maximum ($t_p = V_i/u$)
Δt	Peak-width ($\Delta t = t_2 - t_1$)
Δt_{eq}	Peak-width when $C' = C_{eq}$
Δt_b	Peak base width
u	Volumetric flow rate
u^R	Volumetric flow rate of reagent stream
u^s	Volumetric flow rate of injected sample carrier stream
V	Volume of mixing chamber
V_i	Volume injected
∂V	Hypothetical detector volume
∂V_r	Hypothetical volume of sample removed from ∂V and hypothetical volume of reagent replaced to account for sample and reagent dilution at point of measurement

In order to derive the relationship between D and D^R, it is first assumed that the concentration is monitored in a finite volume ∂V. This avoids the difficulties associated with considering concentrations at a point or in an infinitely thin slice across the tube. Secondly, it is assumed that a diluted sample concentration has been obtained in ∂V by replacement of a volume ∂V_r by an equal volume of reagent solution. The resulting concentrations of the sample and reagent are given by $C^s_g = C^s_m\,(\partial V - \partial V_r)/\partial V$ and $C^R_g = C^R_m\,\partial V_r/\partial V$, respectively. For the sample, substitution from Eqn. 4 gives $1/D_g = 1 - (\partial V_r/\partial V)$. For the reagent, substitution from Eqn. 5 gives $1/D^R_g = \partial V/\partial V_r$.

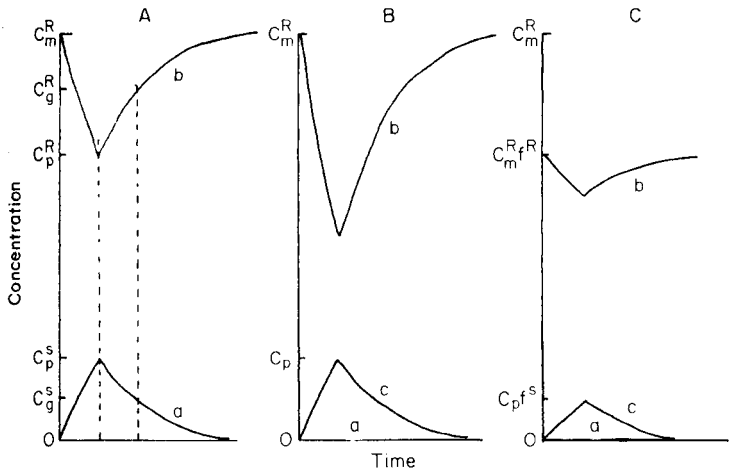

Fig. 2. Concentration profiles of dispersed sample and reagent without and with chemical reaction for C^R always greater than C^s. A, the sample (a) and reagent (b) profiles for manifold 1A with no chemical reaction; B, the sample (a), reagent (b) and product (c) profiles when chemical reaction occurs; C, the same profiles for manifold 1B in which C is a water carrier stream and R is the reagent carrier stream.

Reorganization of these last two equations gives $1/D_g = 1 - 1/D_g^R$ and $1/D_g^R = 1 - 1/D_g$. Thus

$$D_g = D_g^R/(D_g^R - 1) \tag{6a}$$

$$D_g^R = D_g/(D_g - 1) \tag{6b}$$

The corresponding equations for the dispersion coefficients at the peak maxima are obtained by dropping the subscript g. An experimental verification of Eqns. 6(a) and 6(b) will be described later, as will some other applications of the equations. The equations are in agreement with that derived previously for the well stirred mixing chamber model [13].

Chemical reaction between sample and reagent in a well stirred mixing chamber

If C^R is always greater than C^s across the profile (as shown in Fig. 2A), then the peak width of the product profile (Fig. 2B) will be as given in Eqn. 1 for the single-line manifold (Fig. 1A) and will be modified (Fig. 2C) by the inclusion of the flow rates of the sample carrier stream and merging reagent stream to account for the dilution at the confluence point, for the manifold shown in Fig. 1B:

$$\Delta t = (V/u^s) \ln [(C_m^s/C') - 1/f^s] - (V/u^s) \ln (D - 1/f^s) \tag{7}$$

The equation is derived in full in Appendix 2.

Taking the single-line manifold case first, if the dispersion produced is

such that $C^s > C^R$ in the profile centre (the reagent is in deficit, as shown in Fig. 3A), then there are points on the rising and falling profiles at which the concentrations are in the stoichiometric ratio for the reaction between R and S. Here it is assumed that this ratio is 1:1 (the full equations for a ratio $m:n$ are given in Appendix 4). These profiles represent the situation properly described as a "titration", as there are equivalence points on the rise and fall curves.

The concentration of reagent and sample at these points if reaction occurs, C_{eq}, may be found from either version of Eqn. 6. For example, from Eqn. 6(b), at an equivalence point $C^R_{eq} = C^s_{eq}$ for a 1:1 reaction

$$C^R_m/C^s_{eq} = (C^s_m/C^s_{eq})/[(C^s_m/C^s_{eq}) - 1]$$

thus $C^s_m/C^R_m = (C^s_m/C^s_{eq}) - 1$, and $C^s_m/C^s_{eq} = (C^s_m + C^R_m)/C^R_m$, so

$$C^s_{eq} = C^s_m C^R_m/(C^s_m + C^R_m) \tag{8}$$

As Eqn. (8) is derived from Eqn. 6, its validity is independent of the curve shape and shows that, provided all elements of the sample and reagent zones are subject to the same dispersion effects, the line joining the two equivalence points is parallel to the time axis. The peak width at the equivalence point, Δt_{eq}, is obtained by substituting C_{eq} for C' in Eqn. 1 and for C_{eq} from Eqn. 8. This gives

$$\Delta t_{eq} = (V/u^s) \ln (C^s_m/C^R_m) - (V/u^s) \ln (D - 1)$$

$$= (V/u^s) \ln C^s_m - (V/u^s) \ln C^R_m(D - 1) \tag{9}$$

Thus, without any approximation, Δt_{eq} is a linear function of $\ln C^s_m$. The corresponding equation for the manifold shown in Fig. 1B is derived in Appendix 3 and is

$$\Delta t_{eq} = (V/u^s) \ln [(C^s_m/C^R_m) - (u^R/u^s)] - (V/u^s) \ln [Df^R - (u^R/u^s)] \tag{10}$$

In the situation where the flow rates are equal ($u^R = u^s$), Eqn. 10 reduces to

$$\Delta t_{eq} = (V/u^s) \ln [(C^s_m/C^R_m) - 1] - (V/u^s) \ln [(D/2) - 1] \tag{11}$$

It should be noted that Δt_{eq} represents a real peak width only for the product profile (which has now become a double peak as shown in Fig. 3B) and represents a hypothetical width for the reagent and sample profiles (physical dispersion without chemical reaction). If the real reagent or sample profile is followed, as is often the case in reports of the application of this type of peak-width method in f.i.a., then there is a practical problem of locating the equivalence points. As they are at points in which the gradients of the profiles show the greatest change, this is often taken as the criterion for their location. It should also be noted that the equivalence concentration in the single-line manifold case is a function of the injected concentration and thus the corresponding concentration level of reagent or sample at the equivalence points varies with C^s_m. Thus selection of a single measurement level, as

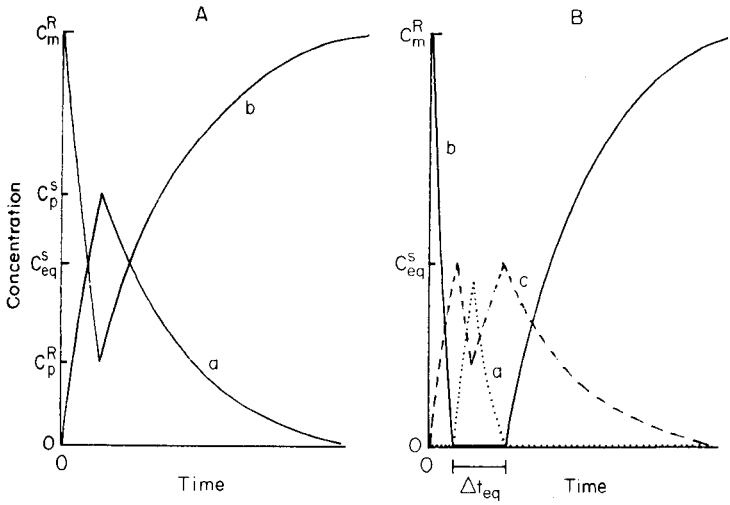

Fig. 3. Concentration profiles of dispersed sample and reagent without and with chemical reaction for C^S greater than C^R in the profile centre. A, The sample (a) and reagent (b) profiles for manifold 1A with no chemical reaction; B, the sample (a), reagent (b) and product (c) profiles when chemical reaction occurs.

is invariably done in practice, represents a further approximation in the method.

Equations 9—11 may also be used to calculate a limiting concentration for a given set of experimental conditions at which Δt_{eq} becomes zero and thus the "limit of detection" has been reached. However, the equations also clearly show that it is easy to arrange matters so that this limit is never reached. Putting $\Delta t_{eq} = 0$ for Eqn. 9, for example, shows that the limit is reached when $C_m^S/C_m^R = D - 1$. And thus, no matter how small the ratio C_m^S/C_m^R is, a peak width will be obtained provided that D is small enough. In practical terms, the easiest way to achieve this is to inject a sufficiently large volume. Such a volume is readily calculated from the equation $V_i = V \ln [D/(D - 1)]$ (Eqn. A1.7, Appendix 1) for any given volume of mixing chamber; substituting from the peak maximum version of Eqn. 6 gives

$$V_i = V \ln D^R \qquad (12)$$

This is a further example of the use of the reagent dispersion coefficient concept.

There is thus no reason to limit the concentration of the injected material to values greater than the concentration of the reagent in the carrier stream as seems to be common practice [14]. The larger the volume injected, the smaller the sampling frequency and so speed of analysis is a trade-off for decreasing the C_m^S/C_m^R ratio. This aspect will be discussed later.

It is suggested here that the full potential of the peak-width method is realised only with a single-line manifold of small dispersion coefficient in

which the concentration of the product is monitored. This produces doublet peaks as illustrated in Fig. 3B. There is then no difficulty in locating the equivalence points. The limit of detection is set by the ability of the detector to detect a product peak above the baseline noise. Furthermore, there is no need for the detector response to be linearly related to concentration and no need to maintain the same response parameters for each sample injected. An example in which the sample concentration was varied over five orders of magnitude is given later.

EXPERIMENTAL

Two types of experimental work are described. First, illustrative calculations based on some of the equations derived above are given, using, where appropriate, data based closely on results reported in the literature. Secondly, experiments illustrative of the validity and use of some of the above concepts are described.

Physical dispersion with no chemical reaction

Values of the appropriate parameters of V_i = 50 μl, V = 200 μl, u^s = 50 μl s^{-1} and C_m = 10 to 10 000 μg l^{-1} were taken from Stewart and Rosenfeld [5] and used to calculate points for a plot of Δt vs. ln $[(C_m^s/C') - 1]$ and Δt vs. ln C_m^s. A linear regression analysis of the data was made. A value of C' was not given and was taken here to be 2 μg l^{-1}.

Reagent dispersion

The manifold shown in Fig. 1C was used in which P was a Gilson Minipuls-2 peristaltic pump, the injection valve was an Altex type 201-25 eight-port, double-loop (44 and 63 μl) valve, the coil was 100 cm of teflon tubing (0.71 mm i.d.) and the detector was a Pye-Unicam PU4020 u.v. detector for liquid chromatography incorporating an 8-μl flow cell. Peaks were recorded on a Pye-Unicam PM8251 chart recorder. The test solution was 10^{-4} M potassium nitrate, the wavelength was 200 nm and the flow rate was measured by collecting and weighing the detector effluent when distilled water was used as the carrier stream over intervals of ten minutes. The mean and 95% confidence interval were calculated with no correction for density.

With water as the carrier stream, 10^{-4} M potassium nitrate was injected from each loop and the resulting peaks were recorded at a chart speed of 300 mm min^{-1}. The carrier was changed to 10^{-4} M potassium nitrate, the chart recorder rewound and water injected from each loop at the same point on the chart as injections for the first experiment. Values of D_g and D_g^R were calculated from measurements taken directly from the chart recording (a linear absorbance/concentration relationship was assumed), the corresponding values of D_g^R and D_g were calculated from Eqns. 6(b) and 6(a), respectively, and linear regression was applied to the data. The 95% confidence intervals for the slope and intercept were also calculated.

A plot of D^R vs. D based on Eqn. 6 was constructed, as was a plot of C_m^R/C_m^s vs. D to illustrate the use of the reagent dispersion coefficient concept in calculating C_p^R/C_p^s ratios. The latter is necessary in conventional f.i.a. based on peak-height measurement to ensure an adequate excess of reagent over sample to drive the desired reaction to an appropriate extent.

To illustrate the use of some of the concepts described earlier to assess the features of reversed f.i.a. (reagent injected into sample carrier stream), calculations were done with values based on those of Johnson and Petty [15]: $V = 100\ \mu l$, $D = 5$ and $u = 33.3\ \mu l\ s^{-1}$.

Dispersion and chemical reaction

The manifold shown in Fig. 1C was used as described above except that one of the sample loops was replaced by a 500-μl loop. The carrier reagent stream was 10^{-4} M EDTA (disodium salt) and sample solutions covering the range 0.1—10 000 mg l^{-1} copper(II) (1.6×10^{-6}—0.16 M). The absorbance was monitored at appropriate wavelengths to obtain the double peaks of the type shown in Fig. 3B. This was necessary because reagent, sample and product all absorb to some extent over the usable wavelength range. The wavelengths used were 270 nm (0.1 mg l^{-1}), 340 nm (1, 10, 100 mg l^{-1}), 290 nm (1000 mg l^{-1}) and 320 nm (10 000 mg l^{-1}).

Values of the "mixing chamber volume" and dispersion coefficient for the experimental results obtained with the manifold (Fig. 1C) were estimated from the slope and intercept of the plot of Δt_{eq} against ln C_m^s. Some representative calculations of the sampling frequency for the low dispersion mode and the variation of C_{eq} with C_m^s for a given value of C_m^R of 10^{-4} M was calculated according to Eqn. 8.

RESULTS AND DISCUSSION

Physical dispersion with no chemical reaction

The results of the calculations based on Eqn. 1 are given in Table 2. The parameters of the linear regression for the plot of Δt vs. ln $[(C_m^s/C') - 1]$ were slope 3.999 s, intercept —5.036 s and correlation coefficient 0.999995; the values for the corresponding plot of Δt vs. ln C_m (the approximation commonly used) were slope, 4.081 s, intercept —8.414 s and correlation coefficient 0.999796. Values of Δt were calculated to 3 significant figures as were the values of the logarithmic functions. These results show that the approximation of neglecting 1 compared with C_m^s/C' introduces very little error; the error would not be significant for a plot resulting from real values as the experimental uncertainties would be greater than the rounding errors introduced here. Visual inspection of large scale plots of the appropriate data in Table 2 showed curvature only at low values of C_m^s.

Reagent dispersion

The recorder traces are shown in Fig. 4. Values of D_g and D_g^R are given in Table 3 for ten points on each of the two curves. Linear regression on the

TABLE 2

Data for plots of peak width vs. ln (function of concentration)

C_m^s	ln C_m^s	$(C_m^s/C') - 1$	ln $[(C_m^s/C') - 1]$	Δt
10	2.30	4	1.39	0.52
20	3.00	9	2.20	3.76
40	3.69	19	2.94	6.75
50	3.91	24	3.18	7.68
60	4.09	29	4.37	8.44
80	4.38	39	3.66	9.62
100	4.61	49	3.89	10.5
500	6.21	249	5.52	17.0
1,000	6.91	499	6.21	19.8
5,000	8.52	2499	7.82	26.3
10,000	9.21	4999	8.51	29.0

data for Eqn. 6a gave slope 1.10 ± 0.10, intercept −0.40 ± 0.72 and correlation coefficient 0.994. The ± terms are 95% confidence intervals. The corresponding treatment for Eqn. 6b gave slope 0.97 ± 0.07, intercept 0.037 ± 0.095 and correlation coefficient 0.996. In both cases, the 95% confidence intervals for the slope and intercept include the theoretical values of 1 and 0. The experimental data thus fit the theoretical expressions.

The experimental flow rate was measured to be 2.05 ± 0.05 (95% confidence interval) ml min^{-1}.

A plot of D^R vs. D is given in Fig. 5A. This clearly shows the rapid decrease in D^R as D increases from 1 to 3 (so-called low dispersion systems). For D values between 3 and 10 (medium dispersion systems), D^R changes very little.

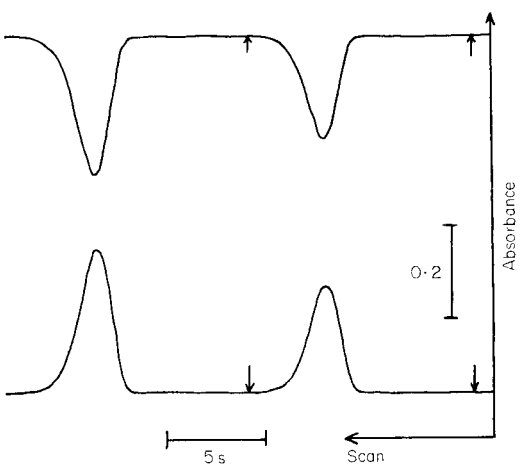

Fig. 4. Recorder traces for injection of 10^{-4} M KNO_3 into water (lower trace) and of water into 10^{-4} M KNO_3 (upper trace). The arrows on the traces show the points of injection.

TABLE 3

Values for D_g and D_g^R obtained from recorder traces shown in Fig. 4 and the corresponding calculated values based on Eqn. 6 (the measured values of C_m^s and C_m^R were both 191 mm)

C_g^s (mm)	D_g	$D_g/(D_g-1)$	C_g^R (mm)	D_g^R	$D_g^R/(D_g^R-1)$
26.0	7.35	1.16	167.7	1.14	8.14
55.5	3.44	1.41	135.7	1.41	3.43
23.8	8.03	1.14	164.6	1.16	7.25
21.2	9.01	1.12	167.8	1.14	8.24
76.8	2.49	1.67	116.1	1.65	2.55
44.5	4.29	1.30	145.0	1.32	4.15
11.5	16.61	1.06	178.0	1.07	15.3
56.6	3.37	1.42	135.5	1.41	3.44
35.5	5.38	1.23	157.5	1.21	5.70
64.5	2.96	1.51	125.0	1.53	2.89

As it is the values of D and D^R which govern the peak concentrations of sample and reagent, respectively (for any given initial concentrations), it is of interest to see how the ratio of peak concentrations varies with D. If $R^{R/s}$ is the ratio of reagent to sample, then at the peak maximum $R_p^{R/s} = C_p^R/C_p^s$, and substituting from Eqns. 2, 3 and the peak version of 6b gives

$$R_m^{R/s} = R_p^{R/s}/(D-1) \tag{13}$$

The relationship between $R_m^{R/s}$ and D is illustrated in Fig. 5B for the case where $R_p^{R/s}$ is 10. It can be seen from this plot (and from Eqn. 13) that provided $D > 2$, then $R_m^{R/s} < R_p^{R/s}$; i.e., if a desired concentration ratio is required at the peak maximum to obtain a particular degree of reaction, it is not necessary to have as high a ratio between the reagent carrier and injected sample. For example, in this case, if the value of D was 5, an initial concen-

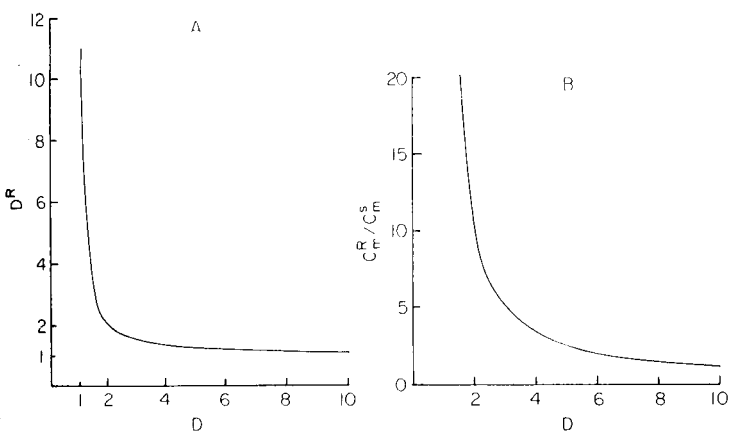

Fig. 5. Relationship between D^R and D (curve A) and C_m^R/C_m^s and D (curve B). For curve B, a value of C_p^R/C_p^s of 10 was taken.

tration ratio of 2.5 produces a peak concentration ratio of 10. To maximize the advantage to be obtained from this relationship (i.e., to economize on reagent as much as possible) requires a large value of D which in turn reduces the sensitivity.

The use of the reversed f.i.a. configuration (injection of reagent into sample) has been claimed as a means of increasing the sensitivity [15]. The basis of this claim may be examined by applying the relationships derived above. In the example discussed, it is required that at the peak maximum the sample material shall be diluted to not more than 0.8 times its original concentration and that to obtain the required degree of reaction a 10-fold excess of reagent is required at the peak maximum. For conventional f.i.a., D must be 1/0.8 = 1.25 and thus, from Eqn. 13 a 40-fold concentration excess of reagent (over the sample concentration) is needed in the carrier stream. For reversed f.i.a., a value of D (based on injected material dispersion) of 5 is required and again a 40-fold concentration excess of reagent (injected) to sample (in the carrier stream) is required. On the basis of the single-line well stirred mixing chamber model for dispersion behaviour, if V = 100 μl then to obtain D = 1.25 for conventional f.i.a. the volume injected needed can be calculated from Eqn. 12 to be 161 μl. For reversed f.i.a., the volume injected required is 22 μl. At first sight it would appear that the theoretical sampling frequency for reversed f.i.a. will be higher than for conventional f.i.a. for manifolds which achieve comparable sensitivity. However, it should be borne in mind that the peak-width at the baseline is set by the time taken for the product concentration to reduce to some acceptable value, say 0.03, of the peak value. In conventional f.i.a., the product profile follows the sample profile and thus on the basis of the well stirred mixing chamber model, the baseline peak-width is calculated to be 15 s. In the case of reversed f.i.a., the product profile follows the injected reagent profile. As in this example, the reagent is 10-fold more concentrated at the peak than the sample, the product profile returns to within the same value of the baseline as for the conventional f.i.a. case when the reagent concentration has fallen to 0.003 of its peak value, giving a total width of 18 s. Of course, if discrete samples are used in reversed f.i.a., the sampling frequency is limited. However, reversed f.i.a. does conserve reagent and, for the identical manifold (including volume injected), is more sensitive.

Dispersion and chemical reaction

Typical double peaks are shown in Fig. 6A, the results for the peak separations for the range 0.1—10 000 mg l^{-1} are given in Table 4, and a plot of Δt_{eq} vs. ln C_m^s is shown in Fig. 6B. The line shown is the best fit on the basis of linear regression. The results for this were slope 2.89 ± 0.50 s, intercept 11.4 ± 2.6 s and correlation coefficient 0.992. From the flow rate of 2.05 ± 0.05 ml min^{-1} and the slope of the plot, the volume, V, of the equivalent mixing chamber is calculated to be 99 ± 17 μl and the dispersion coefficient as 1.008 ± 0.006. From the intercept, $-(V/u^s) \ln C_m^R (D - 1)$, the dispersion

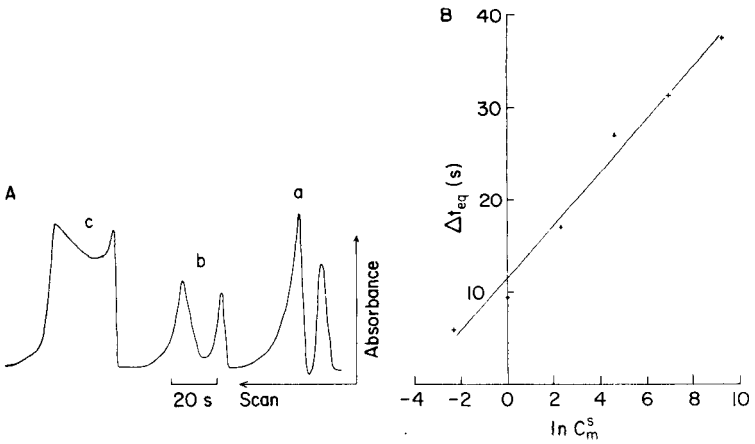

Fig. 6. Peak width when reagent concentration is deficient. A, The recorder traces obtained when 500 μl of 1, 10 and 100 mg l^{-1} Cu^{2+} (traces a, b and c) were injected into a 10^{-4} M EDTA carrier stream (the vertical scale is not the same for all peaks); the minimum between the peaks decreases as the Cu^{2+} injected increases because Cu^{2+} absorbs at the wavelength used. B, A plot of peak width against natural logarithm of the injected concentration.

TABLE 4

Results for peak-width (separation between doublets) as a function of injected concentrations (carrier 10^{-4} M EDTA, sample Cu^{2+})

C_m^s (mg l^{-1})	ln C_m^s	Δt_{eq} (s)	Baseline to baseline peak-width[a] (s)
0.1	−2.303	6.0	21
1	0	9.5	28
10	2.303	17.0	35
100	4.605	27.0	41
1000	6.908	31.2	48
10 000	9.210	37.5	55

[a]Calculated values on the basis of the well-stirred mixing chamber model.

coefficient is calculated to be 1.009 ± 0.007. (All the deviations given are for 95% confidence intervals.)

Taking 0.01 mg l^{-1} as the level indistinguishable from the baseline, the base-widths can be estimated from Eqn. A1.9 (see Appendix 1) and values of V_i, V and u for the above experiment. The results of the calculation are shown in Table 4. Thus the base-width increases by about 7 s for every 10-fold increase in sample concentration as does the doublet peak separation. Thus five orders of magnitude change in concentration can be accommodated on one calibration graph without the base-width becoming impractically large. As time measurements may be made, with fairly simple data logging

equipment, to the nearest 0.01 s [14] and precisions of well under 1% RSD may be obtained, it should be possible to distinguish between small relative differences in concentration. At high concentrations of analyte, this may provide a satisfactory measurement of the analyte concentration or, if not, it will give the dilution factor required to bring the concentration onto a more accurate restricted range calibration. For low concentrations of analyte compared with reagent, such a calibration may be obtained from the doublet peak chart recording with no further experimental work other than measuring peak height.

The reason for this is embodied in Eqn. 8. If essentially complete reaction is assumed, C_{eq} represents the product concentration at the peak maximum. The way in which this is related to sample concentration C_m^s is illustrated in Fig. 7 for a reagent concentration of 10^{-4} M. It can be seen from Fig. 7 that, assuming that peak height could be measured, almost linear calibrations would be obtained over the ranges 0—10^{-8} M, 0—10^{-7} M, 0—10^{-6} M and 0—10^{-5} M. The calibration would be curved over the range 0—10^{-4} M but probably usable. However, above 10^{-4} M all peaks have almost the same height and peak height could no longer be used as a quantitative parameter. The reason for this can be seen from Eqn. 8; when $C_m^s > C_m^R$ so that C_m^R can be neglected in comparison, then $C_{eq}^s \approx C_m^R$, and when C_m^s can be neglected in comparison with C_m^R ($C_m^s < C_m^R$), $C_{eq}^s \approx C_m^s$.

CONCLUSIONS

The derivation of equations relating peak-width to concentration for the peak shapes produced by passage through a well stirred mixing chamber

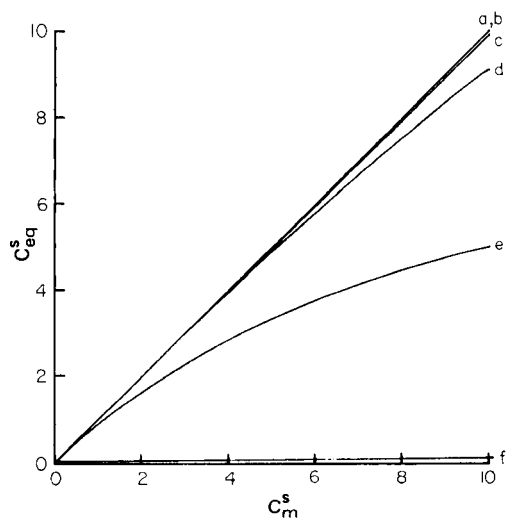

Fig. 7. Plots of C_{eq}^s against C_m^s according to Eqn. 8 for $C_m^R = 10^{-4}$. Curves (a)—(f) cover the ranges 0—10^{-8}, 10^{-7}, 10^{-6}, 10^{-5}, 10^{-4}, 10^{-3}, respectively.

needs no approximations or simplifications. In the absence of chemical reaction, peak-width is not simply a logarithmic function of concentration but a function which approximates very closely to it. For the case in which chemical reaction occurs, the simple ln(concentration) relationship is exact (but only for the single-line manifold). For the merging stream manifold, an equation similar to the case for no chemical reaction applies and a similar approximation may be made to restore the ln(concentration) relationship. The concept of reagent dispersion coefficient is useful in deriving the equations for the case involving chemical reaction and may be applied to other situations in f.i.a., as the relationship with dispersion coefficient is independent of peak shape. Together with the single mixing chamber model of dispersion behaviour, the reagent dispersion coefficient can be used to predict the performance of particular manifolds for systems based on both normal f.i.a. and reversed f.i.a., i.e., the model may be usefully applied to manifolds which do not contain a real mixing chamber.

The peak-width mode in which the reagent concentration is deficient at the centre of the profile has a number of features capable of exploitation for analytical purposes, particularly when the reaction product is monitored rather than one of the reactants. The product peaks occur when the equivalence condition is achieved in the flowing stream and thus there is no difficulty in locating the time values associated with this condition. The only limit to the lowest concentration detectable by this method is set by the ability of the detector to distinguish the product profile from the baseline. Equivalence points can always be achieved by injecting a large enough volume. As this produces a low dispersion coefficient, some caution is needed in the use of terms such as "high dispersion" to describe peak-width methods in f.i.a. The peaks are broader than those obtained in conventional peak-height f.i.a. but the method covers a much wider range of concentrations, so that dilution and re-injection of off-range samples are avoided. The double-peak mode is not restricted to samples of greater concentration than the reagent and contains information to allow peak height to be used as a quantitative parameter, if desired, when the sample concentration is less than the reagent concentration.

This method has considerable potential for investigating chemical reactions, as a manifold designed to give peaks on a scale of minutes or even hours could be used to provide information about the stoichiometry of a reaction and the deviation of the product profile from the theoretically expected profile could be used to calculate the equilibrium constant of the reaction. Each rise and fall of the sample profile provides information analogous to that obtained from the various methods available for determining equilibrium constants (e.g., Job's method, mole-ratio method, Bjerrum's method [16]). A variety of detectors in series could give essentially simultaneous monitoring of a variety of species in the solution.

Financial support from the SERC to purchase the PU4020 detector is gratefully acknowledged.

APPENDIX 1. Physical dispersion in a well stirred mixing chamber

The basis of this model for dispersion behaviour is that the injected plug is transported undispersed to the mixing chamber and that no further dispersion occurs between the mixing chamber exit and the detector. The resulting C, t profile can be described in three stages.

(1) The injected plug flows into mixing chamber. The change in concentration with time is given by $dC/dt = C^s_m u^s/V - Cu/V$. Separating the variables and integrating gives $\ln (C^s_m - C) = -u^s t/V + k$, where k is a constant of integration which may be found, from substituting the initial conditions $C = 0$, $t = 0$, to be $\ln C^s_m$. Thus

$$t = (V/u^s) \ln [C^s_m/(C^s_m - C)] \tag{A1.1}$$

which can be rearranged to give

$$C = C^s_m[1 - \exp(-u^s t/V)] \tag{A1.2}$$

(2) The trailing edge of plug enters the mixing chamber. At this instant, t_p, the concentration in the tank is at its maximum and C^s_p is given by substituting $t_p = V_i/u^s$ in Eqn. A1.2:

$$C^s_p = C^s_m[1 - \exp(-V_i/V)] \tag{A1.3}$$

(3) Material washed out of the mixing chamber. The change in concentration with time (from the peak maximum) is given by $dC/dt = -C^s_p(u^s/V)$. Integration as described under (1) gives

$$t = (V/u^s) \ln (C^s_p/C) \tag{A1.4}$$

Reverting to time measured from when the plug started to enter the mixing chamber gives

$$t - t_p = (V/u^s) \ln (C^s_p/C) \tag{A1.5}$$

which can be rearranged to $C = C^s_p \exp [-u^s(t - t_p)/V]$.

The time interval, Δt, between any two points on the rise and fall curves corresponding to C' can be calculated from $\Delta t = (t_p - t_1) + (t_2 - t_p)$ (see Fig. A1a). Substituting for t_p and t, from Eqn. A1.1 and $(t_2 - t_p)$ from Eqn. A1.5 gives

$$\Delta t = (V_i/u^s) - (V/u^s) \ln [C^s_m/(C^s_m - C')] + (V/u^s) \ln (C^s_p/C')$$

As $D = C^s_m/C^s_p$, rearrangement of Eqn. A1.3 gives

$$D = [1 - \exp(-V_i/V)]^{-1} \tag{A1.6}$$

and

$$V_i = V \ln [D/(D - 1)] \tag{A1.7}$$

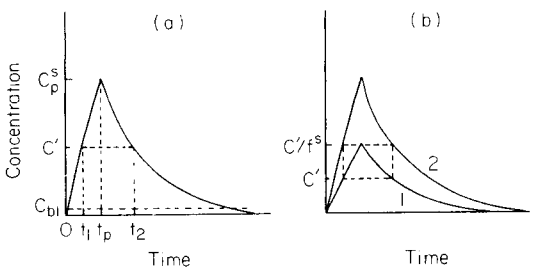

Fig. A1. (a) Concentration profile produced by plug flow through a well stirred mixing chamber. (b) Concentration profile of (1) sample after confluence point and (2) before confluence point. The product profile follows curve 1.

Analytica Chimica Acta, 179 (1986) 149—167
Elsevier Science Publishers B.V., Amsterdam — Printed in The Netherlands

HYDRODYNAMICALLY LIMITED PRECISION OF GRADIENT TECHNIQUES IN FLOW INJECTION ANALYSIS

M. GISIN* and C. THOMMEN
Central Analytical Department, CIBA-GEIGY Ltd., CH-4002 Basel (Switzerland)
K. F. MANSFIELD
University of Rhode Island, P.O. Box 1595, Kingston, RI 02881 (U.S.A.)
(Received 26th July 1985)

SUMMARY

Based on the law of error propagation, a general expression is derived to study theoretically the hydrodynamically limited precision associated with each single element of fluid in a concentration profile in flow injection analysis. Convolution of the injection and residence time distribution functions is used to obtain response functions for a homogeneously stirred mixing chamber and for a straight capillary tube. The effects of stochastic variations on overall precision by sample introduction, pumping and timing are elucidated and compared with experimental findings. Resulting practical implications for the use of these two dispersing elements are outlined.

After pioneering experiments by Nagy et al. [1], flow injection analysis (f.i.a.) has been developed by two independent research groups [2, 3] to a widely appreciated concept of analytical automation on a cost-effective microscale [4]. The technique is based on reproducible injection of samples into an unsegmented and continuously flowing stream of carrier or reagent solution, controlled (and controllable) dispersion of the sample zone on its way downstream to the detector and precise timing. The absence of air bubbles in the flow streams, which eliminates compressibility, makes fast transient concentration profiles possible with excellent reproducibility of peak heights of 1% r.s.d. or less. Because of restricted band broadening, quite high injection frequencies of up to several hundred per hour can be obtained which allows for sample throughput in the order of 100 h^{-1} or more.

Such features were stressed at the very beginning of the enthusiastic period of development, but it was the development of gradient techniques [5] that set a landmark for f.i.a. It is a strict consequence of the concept of controlled dispersion and precise timing that elements of fluid can be probed reproducibly not only at the peak maximum but at any arbitrarily selected time along the concentration profile. This has opened up a tremendous conceptual and analytical potential which is not feasible with air-segmented flow systems. So far, gradient techniques have successfully been applied to titrations [4] for process control [6] and to scale expansion to extend the range of detection

0003-2670/86/$03.50

[7]; for on-line sample pretreatment using gradient dilution [8] and zone sampling [9]; in studies of selectivity [10] and its efficient increase by kinetic discrimination under stopped-flow conditions [11]; and for significant improvement of throughput and cost effectiveness by gradient calibration [8], zone trapping [12], merging zones [13] and sequential multicomponent analysis within the same dispersed sample zone [5]. Rather surprisingly, there is little published information on the precision attained with gradient experiments, especially when large dispersion coefficients, say $D = 100$ and more, or the steeply ascending part of the peak are involved [9, 14]. Neither an experimental nor a theoretical study seems to be available which would provide some insight into the effect of various experimental parameters on the attainable precision of such experiments.

It is the main objective of the present work to investigate theoretically the hydrodynamically limited precision associated with each single element of fluid of a concentration gradient created in a well stirred mixing chamber and a straight capillary tube. Several hydrodynamic models at various levels of sophistication have so far been worked out. However, only moderately simple models will be consulted to gain qualitative insight into the dynamics of the effect of those parameters which significantly limit hydrodynamic precision and thus the precision of gradient experiments per se.

EXPERIMENTAL

Calculations

Gradient functions $G(\nu, \theta)$ were calculated on a microcomputer (HP 9816). Each 2D surface was represented by a total of 10^4 points partitioned into 50 increments of unit length 0.01 along the reduced volume coordinate, ν, and 200 increments of unit length 0.05 along the reduced time coordinate, θ. The surfaces were stored in files and single projections along either coordinate could be retrieved for graphical representation, print-outs and subsequent calculation of derived functions. Transformation of the θ-axis to a coordinate of dispersion coefficients $D(\nu, \theta)$ allowed for proper comparisons between different models or conditions within the scope of the same model.

Apparatus and reagents

The flow-injection manifold used was composed of a pneumatically driven variable loop rotary valve (Rheodyne 5020), a peristaltic pump (Ismatec Mini-S-820) for sample loop filling and a syringe type of pump (Metrohm 655 Dosimat) to provide constant and pulse-free flow in the carrier stream. In all experiments, the precision of pumping was optimized by operating the carrier pump in a single stroke mode such that a specific position of the piston corresponded to the same residence time between subsequent injections. Measurements of the absorbance in the range 0.02—2.0 were made by means of a variable-wavelength flow-through detector (Kratos Spectroflow 783) equipped with a 12-μl cell of 8-mm path length. The mixing chamber

was home-made from perspex with a 10-mm internal bore of 30-mm depth. Dome-shaped stop-cocks (teflon) of variable length allowed adjustment of the effective internal volume. The stirring bar was driven by an external magnetic field. Data acquisition/reduction was done by means of a computing integrator (Spectra Physics SP-4100) supported by user-written software.

Distilled water served as the carrier together with 0.02 M potassium permanganate tracer stock solution in the set of experiments to elucidate the predictive power of the "tanks-in-series" model. A carrier solution consisting of 0.015 M disodium tetraborate, 0.021 M sodium hydroxide and 10 mg l^{-1} Brij-35 in water, or a 1:1 mixture of water and ethanol, was used in gradient experiments. A 0.1% (w/v) stock solution of bromothymol blue in a 1:1 mixture of water and ethanol was injected either directly or after dilution by a factor of 10. All solutions were vacuum-filtered before use.

GENERAL THEORY

From the various conceivable ways of describing a concentration profile (gradient) in f.i.a., its mathematical representation as a distribution $G(\nu, \theta)$ of the reciprocal dispersion coefficients $D^{-1}(\nu, \theta)$, in terms of reduced time θ and reduced injection volume ν, is one of the most general forms (Eqn. 1).

$$G(\nu, \theta) = D^{-1}(\nu, \theta) = C(\nu, \theta)/C_0 \tag{1}$$

Here, C_0 is the concentration of the injected sample and $C(\nu, \theta)$ is the concentration of an element of fluid within the gradient at specific experimental conditions (ν, θ). The dimensionless variables ν and θ are arbitrarily defined for convenience as follows:

$$\theta = (Q/V_t)t \tag{2a}$$

$$\nu = V_i/V_t; \nu \lesssim 0.2 \tag{2b}$$

$$V_t = V_i + V_g \tag{2c}$$

where t is the residence time for an element of fluid of the dispersed sample zone, or alternatively, the gradient sampling time, Q is the volume flow rate, V_i the injection volume and V_g the volume of the dominant dispersing element. The dead volume of the transfer lines and the (cup mixing) detector are neglected. No upper limit is imposed on the reduced time θ (Eqn. 2a). A reduced injection volume ν of 0.2 (Eqn. 2b) is considered a reasonable upper limit in order to remain within the C-curve approximation [15].

The precision of the gradient $G(\nu, \theta)$ at a particular experimental condition (ν, θ) is estimated by the associated relative standard deviation $\sigma[G(\nu, \theta)]/G(\nu, \theta)$. A given gradient (model) function $G(\nu, \theta)$ may also depend on parameters other than ν and θ, e.g., the molecular diffusion coefficient, dynamic viscosity, skewness factor N, etc. However, it is the reduced variables ν and θ which are related to the most relevant experimental parameters (Eqns. 2) and these in turn are very susceptible to variations significantly affecting the

performance of a gradient-forming setup. Therefore, the precision of $G(\nu, \theta)$ has to be related to the individual variations of these reduced variables. Conceivable contributions of other origin are neglected at this point. From the law of error propagation, the equation obtained is

$$\{\sigma[G(\nu, \theta)]/G(\nu, \theta)\}^2 = K_\theta^2(\nu, \theta)[\sigma(\theta)/\theta]^2 + K_\nu^2(\nu, \theta)[\sigma(\nu)/\nu]^2 \quad (3)$$

The statistical weight functions $K_\theta(\nu, \theta)$ and $K_\nu(\nu, \theta)$ are dependent on their respective first partial differential of $G(\nu, \theta)$, the dispersion coefficient $D(\nu, \theta)$ and their respective reduced variables

$$K_\theta(\nu, \theta) = [\partial G(\nu, \theta)/\partial\theta]\theta D(\nu, \theta) \quad (4a)$$

$$K_\nu(\nu, \theta) = [\partial G(\nu, \theta)/\partial\nu]\nu D(\nu, \theta) \quad (4b)$$

From Eqns. 4(a) and 4(b) it becomes evident that the precision of the gradient at any arbitrarily selected experimental condition (ν, θ) is a very sensitive function of the slope of the profile, i.e., of the effective flow pattern per se. Therefore, it must be expected that the precision of a gradient generated in a mixing chamber differs significantly from that created in a capillary tube.

The relative standard deviations of the reduced variables ν and θ are dependent on the individual precision of the gradient sampling time $[\sigma(t)/t]$, the flow rate $[\sigma(Q)/Q]$ and the injection volume $[\sigma(V_i)/V_i]$. Two assumptions faithfully meeting experimental reality are introduced at this point: (a) the volume V_g of the dominant dispersing element is constant and (b) variations of the effective injection volume V_i are caused by axial diffusion at both interfaces between the carrier/reagent and the uniform sample plug at the very instant of the injection process. From Eqn. 2 it follows that

$$[\sigma(\theta)/\theta]^2 = [\sigma(t)/t]^2 + [\sigma(Q)/Q]^2 + \nu^2[\sigma(V_i)/V_i]^2 \quad (5a)$$

$$[\sigma(\nu)/\nu] = (1 - \nu)[\sigma(V_i)/V_i] \quad (5b)$$

By combining Eqn. 3 and Eqns. 5, a general expression is obtained which describes the dependence of the precision associated with a specific element of fluid on the precision of the gradient sampling time t, the flow rate Q and the effective injection volume V_i. Thus:

$$\{\sigma[G(\nu, \theta)]/G(\nu, \theta)\}^2 = K_f^2(\nu, \theta)\{[\sigma(Q)/Q]^2 + [\sigma(t)/t]^2\} + K_i^2(\nu, \theta)[\sigma(V_i)/V_i]^2 \quad (6a)$$

$$K_f(\nu, \theta) = K_\theta(\nu, \theta) \quad (6b)$$

$$K_i^2(\nu, \theta) = \nu^2 K_\theta^2(\nu, \theta) + (1 - \nu)^2 K_\nu^2(\nu, \theta) \quad (6c)$$

Some detailed studies of the dynamic effects influencing overall precision are rendered possible by applying Eqns. 6 on selected model functions and thus still being independent of specific experimental conditions. These equations also imply some general conclusions which will be discussed later.

MODEL FUNCTIONS

The diffusion-convection mechanism operating under the conditions of f.i.a. is quite well understood on a heuristic level for laminar flow in a straight capillary tube. However, its physical and mathematical treatment is still rather complex even if a minimum set of restrictions is imposed on the diffusion-convection equation. Comprehensive studies have been published by Vanderslice et al. [16]; the most restrictive approximation imposed on their diffusion-convection model is a delta input function to represent sample introduction. The Taylor(-Aris) approach [4, 17, 18, 19] is exclusively valid within the diffusion-controlled domain, i.e., for small reduced injection volumes and rather long mean residence times. In a recent publication [20], a random walk simulation procedure has been described to mimic peak profiles for a single-channel flow-injection system. It illuminates the effect of various physical variables while also giving detailed mechanistic insight into the mixing process. The phenomenological "tanks-in-series" model [15] allows the simulation of experimental conditions from low to large dispersion by continuously adjusting the skewness factor N, or the number of tanks. Although the model suffers from a low degree of physical significance, it predicts fairly faithfully the dependence of the axial dispersion on the most relevant physical parameters in the full range of practical conditions in f.i.a. [4].

The introduction of a well-stirred mixing chamber into a single-channel flow-injection system brings about homogeneous, radial distribution and an exponential residence time distribution (r.t.d.) at the exit of the chamber. In this particular case, a simple yet physically significant and accurate mathematical description of the dispersion process is possible.

It has been pointed out [21] that the convolution of the sample injection function $I(\nu, \theta)$ with the residence time distribution $E(\nu, \theta)$

$$G(\nu, \theta) = \int_0^\infty I(\nu, \tau)E[\nu, (\theta - \tau)]\,d\tau \qquad (7)$$

should not be neglected if the effect of the sample volume on the shape of the observed gradient $G(\nu, \theta)$ is to be accounted for properly. The emphasis of the present study is on elucidating, on a semi-quantitative level, the influence on the precision of the gradient by subtle variations of pumping, timing and injection. In this regard, phenomenological models are considered sufficient to provide some insight into these interrelations and to derive guidelines for proper design of flow-injection systems subject to given constraints.

Mixing chamber

Model MC1. Plug injection into a mixing chamber has been studied theoretically in great detail with regard to flow-injection titrations [22, 23]. By

convolution of the plug injection function $I(\nu, \theta)$

$$I(\nu, \theta) = 1 \ (0 < \theta \leqslant \nu) \tag{8a}$$

$$I(\nu, \theta) = 0 \ (\theta > \nu) \tag{8b}$$

with the normalized exponential residence time distribution

$$E_M(\nu, \theta) = (1 - \nu)^{-1} \exp [-\theta/(1 - \nu)] \tag{8c}$$

an identical solution for the descending part of the gradient $G(\nu, \theta)$ can be obtained

$$G(\nu, \theta) = G_{max}(\nu) \exp [-\theta/(1 - \nu)] \tag{9a}$$

$$G_{max}(\nu) = \exp [\nu/(1 - \nu)] - 1 \tag{9b}$$

The maximum of the gradient lies at the origin of the coordinate θ—CO; this is an artefact of the present approach which has no adverse effect at all on the statistical relations. The gradient transforms into a simpler form for small reduced injection volumes:

$$G(\nu, \theta) \approx \nu \exp [-\theta] \tag{9c}$$

Combining Eqns. 9(a) and 4 yields the corresponding statistical weight functions:

$$K_\theta(\nu, \theta) = -\theta/(1 - \nu) \tag{10a}$$

$$K_\nu(\nu, \theta) = \nu(1 - \nu)^{-2} \{(1 - \exp [-\nu/(1 - \nu)])^{-1} - \theta\} \tag{10b}$$

The root of $K_\nu(\nu, \theta)$ (Eqn. 10b) occurs at larger θ values with decreasing ν values. For small reduced injection volumes, these expressions simplify to

$$K_\theta(\nu, \theta) \approx \theta \quad \text{and} \quad K_\nu(\nu, \theta) \approx 1 - \nu\theta \tag{10c}$$

Model MC2. Plug injection is one of the ideal models to simulate a real injection process, say by means of a fixed sample loop rotary valve or by hydrodynamic injection [8]. However, there is little experimental or theoretical indication that an exponential "single-tank" wash-out function may apply as an alternative [24]. In analogy to the previously treated model, the injection function

$$I(\nu, \theta) = \exp [-\theta/\nu] \tag{11}$$

convoluted with the inherent r.t.d. of the mixing chamber (Eqn. 8c) yields

$$G(\nu, \theta) = \nu(1 - 2\nu)^{-1} \{\exp [-\theta/(1 - \nu)] - \exp [-\theta/\nu]\} \tag{12}$$

with the associated maximum

$$G_{max}(\nu) = \exp (-\theta_{max}/\nu) \tag{13a}$$

$$\theta_{max}(\nu) = \nu(1 - \nu)(1 - 2\nu)^{-1} \ln [(1 - \nu)/\nu] \tag{13b}$$

For $\nu \to 0$, Eqns. 12 and 13(a) collapse into Eqn. 9(c) and the peak maximum is shifted to the origin $\theta_{max} = 0$, i.e., models MC1 and MC2 become identical. From Eqn. 12, the statistical weight functions are found to be

$$K_\theta(\nu, \theta) = \theta(1 - \nu)^{-1}(\rho\epsilon - 1)(1 - \epsilon)^{-1} \tag{14a}$$

$$K_\nu(\nu, \theta) = (1 - 2\nu)^{-1} - \theta\nu^{-1}\rho^{-2}(1 + \rho^2\epsilon)(1 - \epsilon)^{-1} \tag{14b}$$

where $\rho = (1 - \nu)/\nu$ and $\epsilon = \exp[-(\theta/\nu)(1 - 2\nu)/(1 - \nu)]$. These functions are very complex and their qualitative interpretation is rendered difficult. However, it must be concluded from a comparison with model MC1, that the two statistical weight functions (Eqns. 14a and 14b) must be similar to Eqns. 10(a) and (b), respectively. In fact, Eqns. 14(a) and 14(b) transform to Eqns. 10(c) for small reduced injection volumes.

Capillary tube

Model CT1. The "tanks-in-series" r.t.d. is considered sufficiently appropriate for elucidating general guidelines to optimize overall precision in a gradient experiment using a capillary tube. A general solution based on the convolution (Eqn. 7) has been given by Rein et al. [21] for plug injection. The representation of the gradient given here

$$G(\nu, \theta) = E_c(N, \theta) \int_0^\nu [1 - (\tau/\theta)]^{N-1} \exp[N\tau]\, d\tau \tag{15}$$

is but an explicit form of Eqn. 48 in [21] using the injection function (Eqn. 8a, b) along with the normalized r.t.d.

$$E_c(N, \theta) = N^N\theta^{N-1} \exp[-N\theta]/(N - 1)! \tag{16}$$

and with our reduced variables and the skewness factor N, i.e., the number of mixing stages. The gradient function (Eqn. 15) and the associated statistical weight functions (Eqns. 4a, b) must now be subjected to numerical evaluation by means of a computer. A simple analytical expression

$$\theta_{max}(\nu) = \nu\{1 - \exp[-N\nu/(N - 1)]\}^{-1} \tag{17a}$$

has been derived from the solution in the Laplace domain [21] which, in the delta input limit, yields the well-known relation between the reduced time of the peak maximum and the number of mixing stages in the system

$$\theta_{max}(\nu) \approx 1 - 1/N \tag{17b}$$

Model CT2. The complexity of model CT1, which sufficiently accounts for the influence of the reduced injection volume on the shape of the gradient, despite its low physical significance, prompts a comparison with a less sophisticated model. The delta injection convoluted with the "tanks-in-series" residence time distribution (Eqn. 16) obviously reproduces the r.t.d. of the system [15]. In order to take into account the influence of the reduced injection volume ν by an approximation, an empirical correction on Eqn. 16

is applied, which is derived exclusively from the mass balance

$$\int_0^\infty G(\nu, \theta)\mathrm{d}\theta = \nu \tag{18}$$

This yields a simple expression for the gradient:

$$G(\nu, \theta) = \nu E_c(N, \theta) \tag{19}$$

The θ_{max} thus obtained is identical to the θ_{max} of Model CT1 in the delta input limit (Eqn. 17b). An analytical expression can be derived for the maximum of the gradient:

$$G_{max}(\nu) = \nu N(N-1)^{N-1} \exp\,[-(N-1)]/(N-1)! \tag{20a}$$

which, on applying Stirling's approximation, further simplifies for skewness factors $N > 5$ (i.e., in the region of medium to large dispersion in f.i.a.) to

$$G_{max}(\nu) \approx \nu N[2\pi(N-1)]^{-1/2} \qquad (N > 5) \tag{20b}$$

The statistical weight functions (Eqn. 4) of the present model are

$$K_\theta(\nu, \theta) = N(\theta_{max} - \theta) = N(1-\theta) - 1 \tag{21a}$$

$$K_\nu(\nu, \theta) = 1 \tag{21b}$$

So far, it has tacitly been assumed that the skewness factor N is an independent parameter of peak shape which simply transforms an exponential ($N = 1$) to a Gaussian profile ($N = \infty$). In fact, N is a sensitive function of various experimental parameters. This can be demonstrated formally, e.g., by comparing the first ($\bar{t}$) and second moment (σ^2) of the peak profile with the Taylor-Aris approximation. From the "tanks-in-series" model, $N = (\bar{t}/\sigma)^2$ is obtained [15]. The mean residence time is related to the total volume of the system as well as the volume flow rate by $\bar{t} = V_t/Q$ and the Taylor-Aris axial time variance is given by $\sigma^2 = \bar{t}R^2(24D_m)^{-1}$ [4], where R is the inner radius of the capillary tube and D_m is the molecular diffusion coefficient. Combining these expressions yields

$$N = 24D_m V_t R^{-2} Q^{-1} \tag{22}$$

The interrelations between N and the various experimental parameters are, however, far more complex than is implied by Eqn. 22 (vide infra). Though these interrelations are not known in detail, predictions on the effect of variations of N on the precision of the gradient are obtained by constructing cross-sections of $G(\nu, \theta)$ along a N-coordinate at otherwise fixed conditions (ν, θ). Thus, the neglect of such interacting variations between the variables ν, θ and N is corrected to some extent.

RESULTS AND DISCUSSION

Numerical calculations

General aspects. The expression derived for the overall precision (Eqns. 6) generally applies for any gradient created in a flow-injection system. The pertinent statistical weight functions (Eqns. 4, 6b, c) may be evaluated from theoretical gradient functions (vide supra) or from experimental peak profiles; as for the latter, relative considerations between different experimental conditions are of more practical value than attempts to predict quantitatively the overall precision for a specific situation. Some general conclusions can be drawn at this point without knowledge of the individual precision of pumping, timing and injection which, unless otherwise stated, are considered constant. First, pumping and timing increasingly affect the precision with increasing dispersion coefficient and/or increasing steepness associated with the probed gradient element (Eqn. 4a). Thus, gradient experiments within the fast rising branch of the profile must be conducted cautiously whenever good precision is desired. Secondly, the contribution of the precision of injection to the overall precision is increasingly affected by pumping and timing with increasing injection volume (Eqn. 6c), particularly at points remote from the peak maximum (Eqn. 4a). The implication that injection volumes should be kept rather small in gradient experiments aiming for large dispersion coefficients (e.g., gradient dilutions) is contradicted by the frequently observed loss of precision with decreasing injection volume. Thirdly, the precision of the dispersion coefficient at peak maximum (D_{max}) is limited only by the precision of sample introduction (Eqns. 6a, c), because the first derivative along θ does vanish (Eqn. 4a) but that along ν does not (Eqn. 4b). Therefore, experimental evaluation of the precision of D_{max} reflects the precision of injection. Unfortunately, the experimental evaluation of the precision of pumping and timing is not as straightforward.

Mixing chamber. Numerical calculations corroborate the analytical finding that the post-maximum peak profiles of the two models MC1 (Eqn. 9a) and MC2 (Eqn. 12) are quite similar and become identical for small reduced injection volumes, i.e., for flow-injection systems of medium to large dispersion (Fig. 1). Significant deviations are only observed close to and at the peak maximum. Yet, both models predict the dispersion coefficient D_{max} to be independent of flow rate, which has been experimentally verified (Table 1). The data in Table 1 also reveal that model MC2 has superior predictive power for D_{max}, particularly in the realm of large injection volumes ($\nu = 0.2$). As a result, the gradient function (Eqn. 12) sufficiently describes the hydrodynamic flow conditions in a single-line flow-injection system incorporating a mixing chamber. More importantly, Eqns. 12 and 13 may be appreciated as reliable guidelines for planning and constructing flow-injection systems which have to meet specific requirements such as D_{max}, throughput, total dispersion coefficient and precision.

Capillary tube. Extensive numerical calculations have shown that the peak shapes predicted by models CT1 (Eqn. 15) and CT2 (Eqn. 19) are almost

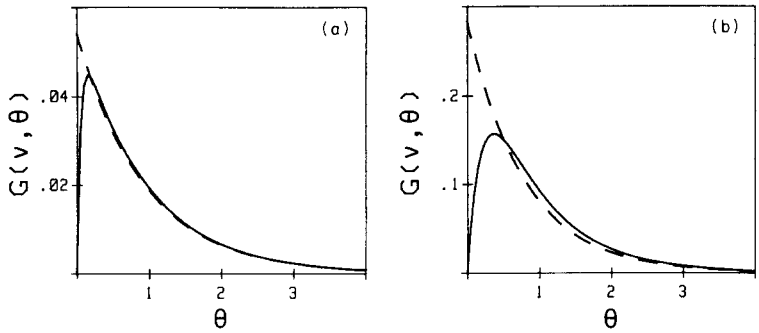

Fig. 1. Calculated gradient functions $G(\nu, \theta)$ for a mixing chamber: (– – – – –) model MC1 (Eqn. 9a); (———) model MC2 (Eqn. 12). (a) $\nu = 0.05$; (b) $\nu = 0.2$.

TABLE 1

Comparison of experimental and calculated D_{max} values for a mixing chamber

ν[a]	Q (ml min^{-1})	D_{max}[b] exp.	D_{max}, MC1 (Eqn. 9a)	D_{max}, MC2 (Eqn. 12)	D_{max}, CT2 (Eqn. 19)	
					$N = 1$	$N = 2$
0.06	0.5	18.2	15.51	19.25	16.67	22.65
	1.0	18.4				
	2.0	18.1				
	2.9	18.1				
0.11	0.5	12.1	7.51	10.77	9.00	12.23
	1.0	12.3				
	2.0	12.2				
	2.9	12.1				
0.20	0.5	8.0	3.52	6.35	5.00	6.79
	1.0	8.1				
	2.0	8.1				
	2.9	8.0				

[a]Mixing chamber volume $V_g = 800$ µl. [b]Potassium permanganate tracer.

identical, regardless of the skewness factor N as well as the reduced injection volume ν (Fig. 2). Only a slight difference is observed between the calculated D_{max} values. The relative shift of the peaks (θ_{max}), as a consequence of convolution, expectedly diminishes for low reduced injection volumes. Hence, model CT2 is acceptable as a sufficient description of hydrodynamic flow conditions to gain some insight into the dynamics of attainable precision. The resulting expressions for the statistical weight functions $K_f(\nu, \theta)$ and $K_i(\nu, \theta)$ thus become very simple (Eqns. 6 and 21). They show their (linear) dependence on the skewness factor N as well as the relative location ($\theta_{max} - \theta$)

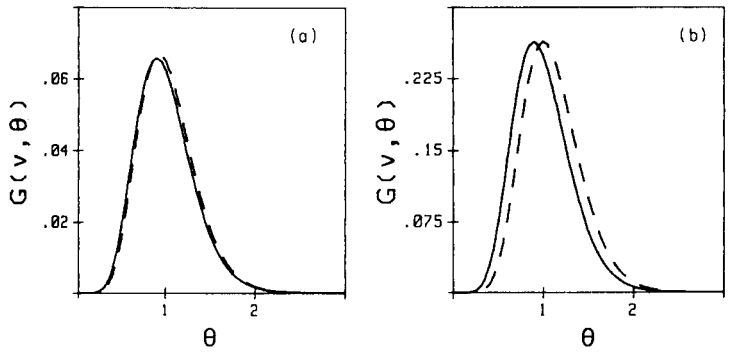

Fig. 2. Calculated gradient functions $G(\nu, \theta)$ for a capillary tube: (— — — —) model CT1 (Eqn. 15); (———) model CT2 (Eqn. 19). (a) $\nu = 0.05$; (b) $\nu = 0.2$.

of the probed gradient element. However, attempts to elucidate experimentally some reliable correlations between the skewness factor N and experimental parameters such as flow rate, total dead volume, reduced injection volume etc. have plainly failed. From a total of 48 experimental conditions (Q = 0.5—3.0 ml min^{-1}, V_t = 125—1000 μl, ν = 0.05—0.61), values for N were calculated according to four different methods: (1) from the first and second moment of the peak profile ($N = [\bar{t}/\sigma]^2$); (2) from Eqn. 17(a), i.e., taking into account the effect of convolution; (3) from Eqn. 17(b), i.e., neglecting convolution; and (4) by evaluation from D_{max} (Eqn. 20a). The most precise values were obtained by method (4) whereas the values derived by method (1) exhibited tremendous scatter (±20%). The skewness factors obtained from the four methods differed by as much as a factor of 3 under identical experimental conditions. At any rate, two significant trends became apparent: (a) at constant total volume V_t, N decreases with increasing flow rate Q; and (b) at constant flow rate Q, N increases with increasing total volume V_t. These findings conform qualitatively with the implication of Eqn. 22. They also reflect the thorough inefficiency of the "tanks-in-series" model for predicting the hydrodynamic behaviour of a given flow-injection manifold. Similar findings have recently been published [25] concerning the predictive power of the diffusion-convection model of Vanderslice et al. [16].

Influence of pumping and timing on precision

As depicted in Fig. 3, the post-maximum peak shape of model MC2 (Eqn. 12) can be approximated roughly by model CT2 (Eqn. 19) if the skewness factor is assigned a value of $N = 1$ at low injection volumes ($\nu = 0.05$) and $N = 2$ at large injection volumes ($0.1 \leqslant \nu \leqslant 0.2$). In other words, $N \leqslant 2$ represents the limit of an ideally mixed gradient chamber whereas $N > 2$ is associated with a capillary tube as a dominant dispersing element. In certain instances, apparent skewness factors of $N \leqslant 2$ can also be obtained by using low dead volume capillaries at high flow rates [24]. Rather surprisingly,

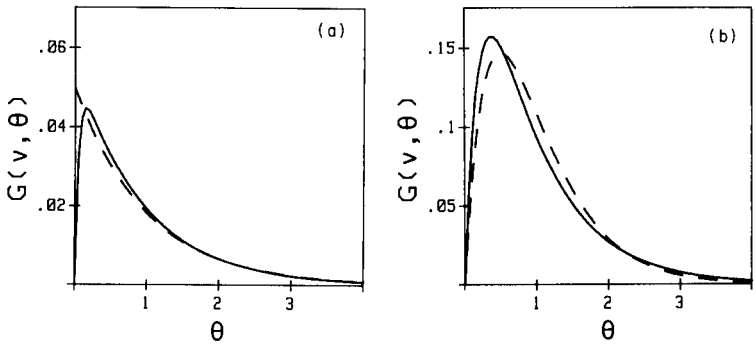

Fig. 3. Comparison of model CT2 (– – – – –) with model MC2 (———): (a) $\nu = 0.05$, $N = 1$; (b) $\nu = 0.2$, $N = 2$. See text.

D_{max} values predicted by the above approximation for the mixing chamber conform with those from model MC2 or are of superior accuracy when the proper skewness factor N is chosen with respect to the reduced injection volume (Table 1). It becomes qualitatively self-evident from Eqn. 21(a) that under specified experimental conditions (ν, θ), i.e., total dispersion coefficient $D(\nu, \theta)$ as well as constant precision of pumping and timing, the contribution to overall precision (Eqn. 6a) is generally larger for a capillary tube than for a mixing chamber of the same dead volume V_g. This behaviour is represented in Fig. 4. The plotted $K_f^2(\nu, \theta)$ functions were calculated for model MC2 (Eqn. 12) and model CT2 (Eqn. 19). From the same figure, it can be inferred that the relative improvement of precision, by a decrease in the injection volume at a given dilution $D(\nu, \theta)$, is more efficient for the mixing chamber. More importantly, it follows from Eqns. 14(a, b), 10(c, d) and 6(a, b), that a specific dispersion coefficient $D(\nu, \theta)$ can be created at constant precision over a large range of chamber volumes V_g and flow rates Q as long as θ (Eqn. 2a) is constant and changes of ν (Eqn. 2b) are minute. This is in sharp contrast to the hydrodynamic behaviour of a capillary tube. The corresponding $K_f(\nu, \theta)$ depends on peak shape, i.e., on the skewness factor N (Eqns. 6b and 21a). Because N has been demonstrated to react sensitively to variations of the dead volume V_t of the system and the flow rate Q (vide supra), precision of a specific $D(\nu, \theta)$ is strongly affected. Thus, the operational dynamic range of a flow-injection manifold based on a capillary tube is rather restricted. This statement, though theoretically deduced from the standpoint of precision, is supported by findings from scale expansion experiments [7].

A decrease in the precision of pumping and timing inevitably worsens the overall precision of gradient experiments no matter what kind of dispersing element is used. Therefore, careful selection of the pumping system is indispensable, in particular for gradient experiments involving complex chemistry at low to moderate dispersion ($D(\nu, \theta) \lesssim 50$, e.g., stopped flow kinetics [26]) or excessive dilutions ($D(\nu, \theta) \lesssim 2000$, e.g., in process control [27]). Pulse-free

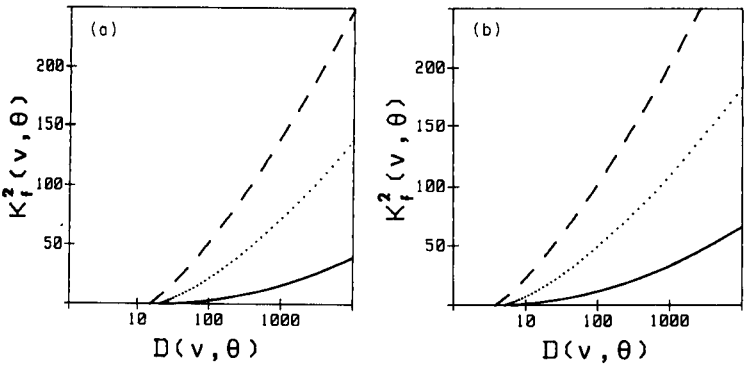

Fig. 4. Calculated statistical weight functions $K_f^2(\nu, \theta)$: (— — — —) model CT2, $N = 10$; (· · · · ·) model CT2, $N = 5$; (———) model MC2. (a) $\nu = 0.05$; (b) $\nu = 0.2$.

and constant flow rates are optimal, i.e., a syringe type of pump is superior to a pulse-damped reciprocating pump or the commonly used peristaltic pumps; for the latter, numerous actively driven rollers are obviously needed. Precise timing presents no serious problem if flow-injection experiments are run under microcomputer control. Further improvement of overall precision may be achieved by identifying the gradient sampling time t of the probed gradient element with respect to the time t_{max} of the peak maximum, which is easily detected on-line. Such a procedure efficiently compensates for flow rate fluctuations which cause irregular shifts of the gradient along the time axis. Although such subtle shifts do not seriously affect peak shape, they would allocate the wrong element of the gradient to a specified time t after sample injection.

Influence of sample injection on precision

Flow injection analysis is a process subject to convolution of the injection function with the residence time distribution, thus each element of fluid along the gradient must carry some memory on the mode and precision of sample introduction. Within the scope of the present models, there are two promoting mechanisms; first, a direct effect by variations of the sample volume V_i (Eqns. 4b and 6c), and secondly, an amplification and transfer of such variations into each gradient element by pumping and timing (Eqns. 4a and 6c). Both effects are dependent on the reduced injection volume ν. The latter is proportional to ν^2, and the associated statistical weight function $K_\theta^2(\nu, \theta)$ increases monotonically along θ (vide supra). The influence of pumping and timing will be negligible unless the injection volume is large and/or the gradient element is located remote from the peak maximum. The direct effect is proportional to $(1 - \nu)^2$ and characterized by $K_\nu^2(\nu, \theta)$. This function decreases monotonically along the post-maximum concentration profile in a mixing chamber operated under normal flow-injection conditions, say $\nu \ll 1$ and $D(\nu, \theta) < 10^4$ (Eqns. 14b and 10c). [The root $K_\nu(\nu, \theta) = 0$ of Eqn. 14(b)

is immaterial in this regard, because it occurs at $D(\nu, \theta) > 10^3$ within the range of reduced volumes considered in the present discussion.] In other words, homogeneous mixing instantaneously destroys the integrity of the sample zone entering the chamber and thus efficiently attenuates fluctuations of the effective injection volume. In contrast, the direct influence of the precision of injection provides a constant contribution to the overall precision along the complete gradient generated by a capillary tube (Eqn. 21b). As a result, the net contribution to the overall precision by the injection process is quite different for the two dispersing elements (Fig. 5). At small reduced injection volumes, the attenuating effect of the gradient chamber prevails far beyond $D(\nu, \theta) = 1000$, whereas the amplifying transfer effect by pumping and timing dominates in the capillary tube, particularly for more symmetric peak shapes (e.g., $N = 10$, Fig. 5). However, in both cases, the relative change of $K_i^2(\nu, \theta)$ is quite small. The capillary tube appears to perform competitively at and close to the peak maximum and at dispersion coefficients of up to ca. 100. At moderate-to-large reduced injection volumes ($\nu \leqslant 0.2$), the amplifying transfer effect promoted by the mixing chamber roughly compensates the direct attenuating effect. Thus, the use of a mixing chamber under such conditions is advantageous within the full range of accessible dispersion coefficients. This recommendation is corroborated by the comparatively sensitive dependence of $K_i^2(\nu, \theta)$ on variations of ν for a gradient generated in a capillary tube. For instance, when the reduced injection volume is increased from 0.05 to 0.2, the statistical weight function for the capillary tube ($N = 10$) increases by a factor of ca. 7 vs. ca. 2 for the mixing chamber at $D(\nu, \theta) = 1000$.

It has already been pointed out that the precision of the gradient at its maximum is limited only by the precision of injection, i.e., $K_\theta(\nu, \theta_{max}) = 0$. Combining Eqns. 6(a, c) with Eqn. 10(d) or Eqn. 21(b) and assuming $\nu\theta \ll 1$, yields a simple relation between the experimentally observed precision of

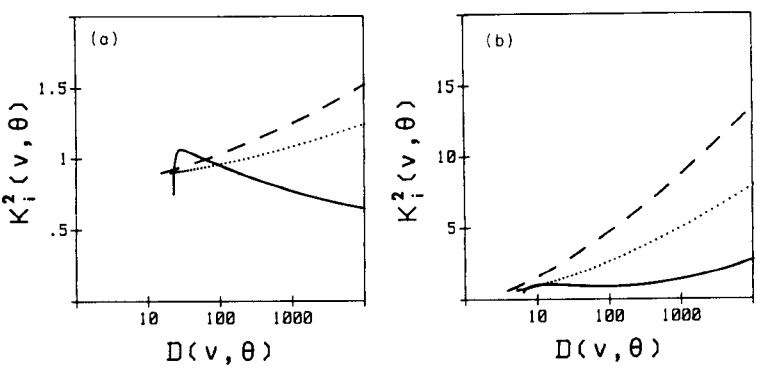

Fig. 5. Calculated statistical weight functions $K_i^2(\nu, \theta)$: (— — — —) model CT2, $N = 10$; (· · · · ·) model CT2, $N = 5$; (———) model MC2. (a) $\nu = 0.05$; (b) $\nu = 0.2$.

$G_{max}(\nu)$ and the precision of injection $[\sigma(V_i)/V_i]$:

$$[\sigma(V_i)/V_i] \approx (1-\nu)^{-1}\{\sigma[G_{max}(\nu)]/G_{max}(\nu)\}$$

Under optimal instrumental conditions (e.g., microcomputer control as well as pulse-free constant pumping), it is known from experience that $[\sigma(t)/t] < [\sigma(Q)/Q] \ll [\sigma(V_i)/V_i]$. Thus, the mode and precision of injection is obviously a limiting experimental parameter.

Hydrodynamic injection [8] represents a practical alternative to sample loop rotary valves, especially with regard to process control [27]. Acceptable precision is obtained by this mode of sample introduction in experiments exploiting elements of fluid at or near the peak maximum. However, in order to take advantage of the gradient at acceptable precision ($\leqslant$2% r.s.d.) and large dispersion coefficients, rotary valves or devices of similar or superior precision should be used in flow-injection manifolds.

The predicted improvement of overall precision by decreasing the injection volume ν (Fig. 5) is frequently contradicted by a concomitant loss of precision of injection. Therefore, specific experimental requirements must dictate the optimal injection volume.

Experimental results

The precision of various dispersion coefficients of up to ca. 2000 was evaluated on a single-line flow-injection system with the bromothymol blue tracer. Except for replacing mixing chambers by capillary tubes, the construction of the manifold was kept constant, i.e., the experimental data reflect the performance of the dominant dispersing element used.

The data presented in Tables 2 and 3 qualitatively corroborate the theoretical predictions outlined in the previous sections. Relative standard deviations of 1% or less are obtained over a much larger dynamic range of accessible dispersion coefficients with a gradient chamber (Table 2) than with a capillary tube (Table 3), particularly when small sample volumes are injected. (The precision of dispersion coefficients larger than ca. 1000 is impaired to some extent by signal-to-noise limitations of the detector). Given the presumption that the precision of injection is the limiting factor, variations of sample introduction appear to be attenuated efficiently even at fairly large injection volumes (e.g., $\nu = 0.2$). The observation that the precision at a specific $D(\nu, \theta)$ at $\nu = 0.06$ is similar to the precision obtained at $\nu = 0.2$ is a strong indication of the previously mentioned loss of precision on injection of small sample volumes.

From the theoretical angle, better precision is expected for low sample volumes injected into a capillary tube rather than large volumes. Yet, the reverse is observed experimentally (Table 3). Although the poor performance of small sample volume injections is undoubtedly implicated, the drastic change of peak shape from $N = 6$ at $\nu = 0.2$ to $N = 13$ at $\nu = 0.06$ is, according to theoretical predictions, the major cause of the inferior precision.

TABLE 2

Experimental precision obtained with a mixing chamber

ν[a]	$D(\nu, \theta)$[b] exp.	R.s.d.[c] exp. (%)	$K_f^2(\nu, \theta)$[d] calc.	$K_i^2(\nu, \theta)$[d] calc.
0.06	20	0.07	0.05	0.98
	50	0.05	1.51	0.99
	99	0.15	3.69	0.92
	197	0.12	6.83	0.86
	497	0.26	12.47	0.78
	995	0.30	17.85	0.73
	2040	0.56	24.38	0.68
0.20	20	0.08	3.52	1.01
	49	0.09	7.91	0.91
	100	0.10	12.31	0.89
	200	0.09	17.66	0.95
	498	0.15	26.21	1.14
	1000	0.25	33.79	1.38
	1980	1.12	42.21	1.69

[a]Mixing chamber volume V_g = 800 μl. [b]At a constant flow rate of 2 ml min^{-1}. [c]Evaluated from 17 consecutive injections and subsequent elimination of the lowest and highest value. [d]Calculated from model MC2 (Eqn. 12).

TABLE 3

Experimental precision obtained with a capillary tube

ν[a]	N[b]	$D(\nu, \theta)$[c] exp.	R.s.d.[d] exp. (%)	$K_f^2(\nu, \theta)$[e] calc.	$K_i^2(\nu, \theta)$[e] calc.
0.06	13	20	0.72	16.86	0.94
		48	1.20	49.82	1.06
		105	1.34	78.01	1.16
		208	1.60	109.51	1.28
		538	1.49	154.23	1.44
		1020	2.38	190.75	1.57
		2100	2.01	229.27	1.71
0.20	6	20	0.61	23.19	1.57
		49	0.60	43.03	2.36
		98	0.55	60.09	3.04
		185	1.21	78.70	3.79
		496	1.75	105.86	4.87
		1090	1.51	128.02	5.76
		1850	2.25	151.78	6.71

[a]Capillary tube volume V_g = 800 μl. [b]From θ_{max} (Eqn. 17b). [c]At a constant flow rate of 2 ml min^{-1}. [d]Evaluated from 17 consecutive injections and subsequent elimination of the lowest and highest value. [e]Calculated from model CT2 (Eqn. 19) using listed N values.

In summary, the presented experimental results confirm qualitatively the implication of the models studied that a mixing chamber represents a preferable gradient-forming element whenever good precision is a critical performance criterion. Although the capillary tube allows for quite precise experiments close to peak maximum, its restricted dynamic range of operation at acceptable precision imposes a serious limitation on its use.

Throughput with gradient experiments

The preference for a mixing chamber as a precise gradient-forming device inevitably raises the question of how throughput is affected by its inclusion in a flow-injection system. To answer this question, a mixing chamber and a capillary tube are compared under identical experimental conditions, e.g., Q = 2 ml min^{-1}, V_t = 800 μl, V_i = 200 μl (ν = 0.2), N = 6 (see Tables 2 and 3). The corresponding calculated peak profiles are represented in Fig. 6, from which three distinct sections on the θ axis can be recognized. Gradient elements are accessible from the mixing chamber with good precision starting at the peak maximum down to point A, i.e., within the time period of the sharply rising peak generated in the capillary tube. Thus, in terms of access of gradient elements to be probed, throughput is unequivocally superior. Proceeding from A to B, throughput is again much better, not only in terms of rapid access of elements of fluid with identical dispersion coefficients, but also in terms of their related precision (slope). It is only beyond point B where the capillary tube becomes efficiently competitive in creating extensively dispersed gradient elements, but at the expense of good or acceptable precision. The lengthy washout behaviour of the gradient chamber, after the desired gradient element has been probed, can be overcome by intermittent pumping with an additional pump propelling wash solution (carrier) at a high

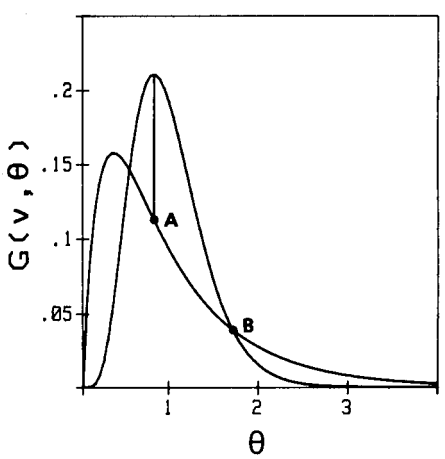

Fig. 6. Throughput with gradient experiments: comparison of a mixing chamber (model MC2) with a capillary tube (model CT2, N = 6). See text.

flow rate. Operating the mixing chamber at high flow rates without significantly impairing precision (vide supra) is an efficient alternative which simplifies the construction of the system. In summary, if acceptable precision is required in gradient experiments of medium to extensive dispersion, the mixing chamber does not impose a serious loss of throughput. In this laboratory, it is now common practice to use mixing chambers to create dispersion coefficients of up to 1500 with a precision better than 2% r.s.d. and still have chemistry involved and cycle times of less than 2 min [27].

Mixing chamber vs. capillary tube

The skewness factor N is a simple expression of peak shape within the scope of the "tanks-in-series" model and, as a consequence, ultimately governs the hydrodynamically limited precision. Variations of N completely transform a purely exponential gradient ($N = 1$) to a Gaussian profile ($N = \infty$). From this general consideration, there is no compelling difference between a capillary tube and a mixing chamber which represent nothing but an experimental means of generating such gradients. In fact, low dead-volume capillaries operated in a flow-injection system with high flow rates create almost ideal exponential concentration profiles, as has earlier been mentioned. However, practical limitations of the use of a capillary tube under such extreme conditions mean that use of a mixing chamber is advantageous for five reasons. First, substantial variations of injection volume, hold-up volume of the chamber and flow rate do not adversely affect precision over a large dynamic range of dispersion coefficients [$D(\nu, \theta) \lesssim 2000$]. Secondly, most flow-injection applications involve chemical reactions and thus impose widespread restrictions on the minimum residence time to assure sufficient sensitivity. Because of the large dynamic operational range, hydrodynamic conditions can easily be adjusted to such chemical constraints. Thirdly, sample zone conditioning (density, viscosity, ionic strength, buffer capacity, etc.) is very efficient because active stirring provides better compensation of matrix effects rather than the confluence technique commonly used with capillaries (see also [22]). The latter is subject to a fairly low dynamic range (D_{max}, ratio of flow rates) together with an inevitable influence on peak shape and thus precision. Fourthly, subtle variations of the sample injection process are efficiently attenuated. Finally, the performance of a flow-injection system with a mixing chamber is completely predictable in terms of D_{max}, throughput and precision.

In conclusion, experiments exploiting the gradient at or near its maximum can be done by means of a capillary tube. Optimal precision is obtained by optimizing the asymmetry of the concentration profile. For gradient experiments exploiting elements of fluid with dispersion coefficients beyond ca. 50 up to as large as 2000, a mixing chamber is recommended in order to assure optimal throughput as well as acceptable precision.

REFERENCES

1 G. Nagy, Zs. Fehér and E. Pungor, Anal. Chim. Acta, 43 (1970) 47.
2 J. Růžička and E. H. Hansen, Anal. Chim. Acta, 78 (1975) 145.
3 K. K. Stewart, G. R. Beecher and P. E. Hare, Anal. Biochem., 70 (1976) 167.
4 J. Růžička and E. H. Hansen, Flow Injection Analysis, Wiley, New York, 1981.
5 D. Betteridge and B. Fields, Anal. Chem., 50 (1978) 654.
6 D. K. Wolcott and D. G. Hunt, paper presented at the 11th Meeting of the Federation of Analytical Chemistry and Spectroscopy Societies, Philadelphia, 1984.
7 K. K. Stewart and A. G. Rosenfeld, Anal. Chem., 54 (1982) 2368.
8 J. Růžička and E. H. Hansen, Anal. Chim. Acta, 145 (1983) 1.
9 B. F. Reis, A. O. Jacintho, J. Mortatti, F. J. Krug, E. A. G. Zagatto, H. Bergamin Fº and L. C. R. Pessenda, Anal. Chim. Acta, 123 (1981) 221.
10 E. H. Hansen, J. Růžička, F. J. Krug and E. A. G. Zagatto, Anal. Chim. Acta, 148 (1983) 111.
11 J. Růžička and E. H. Hansen, Anal. Chim. Acta, 99 (1978) 37.
12 F. J. Krug, B. F. Reis, M. F. Giné, E. A. G. Zagatto, J. R. Ferreira and A. O. Jacintho, Anal. Chim. Acta, 151 (1983) 39.
13 H. Bergamin Fº, E. A. G. Zagatto, F. J. Krug and B. F. Reis, Anal. Chim. Acta, 101 (1978) 17.
14 F. Lazaro, M. D. Luque de Castro and M. Valcárcel, Anal. Chim. Acta, 165 (1984) 177.
15 O. Levenspiel, Chemical Reaction Engineering, 2nd edn., Wiley, New York, 1972.
16 J. T. Vanderslice, K. K. Stewart, A. G. Rosenfeld and D. J. Higgs, Talanta, 28 (1981) 11.
17 G. Taylor, Proc. Roy. Soc. London, Ser. A: 219 (1953) 186; 223 (1954) 446.
18 R. Aris, Proc. Roy. Soc. London, Ser. A: 235 (1956) 67.
19 H. A. Mottola and C. C. Painton, Anal. Chim. Acta, 154 (1983) 1.
20 D. Betteridge, C. Z. Marczewski and A. P. Wade, Anal. Chim. Acta, 165 (1984) 227.
21 J. M. Rein, W. E. van der Linden and H. Poppe, Anal. Chim. Acta, 114 (1980) 105.
22 E. Pungor, Z. Fehér, G. Nagy, K. Tóth, G. Horvai and M. Gratzl, Anal. Chim. Acta, 109 (1979) 1.
23 H. L. Pardue and B. Fields, Anal. Chim. Acta, 124 (1981) 39, 65.
24 A. U. Ramsing, J. Růžička and E. H. Hansen, Anal. Chim. Acta, 129 (1981) 1.
25 M. A. Gomez-Nieto, M. D. Luque de Castro, A. Martin and M. Valcárcel, Talanta, 32 (1985) 319.
26 M. Gisin, A. Demaurex, paper presented at the 11th Annual Meeting of the Federation of Analytical Chemistry and Spectroscopy Societies, Philadelphia, 1984.
27 M. Gisin, paper presented at the Symposium on Flow Injection Analysis, Oerenäs, Sweden, June 1985.

Analytica Chimica Acta, 179 (1986) 169—179
Elsevier Science Publishers B.V., Amsterdam — Printed in The Netherlands

KINETIC TREATMENT OF UNSEGMENTED FLOW SYSTEMS
Part 3. Flow-Injection System with Gradient Chamber Evaluated with a Linearly Responding Detector

HARRY L. PARDUE* and PAUL JAGER
Department of Chemistry, Purdue University, West Lafayette, IN 47907 (U.S.A.)
(Received 25th September 1985)

SUMMARY

A variable-time kinetic model is evaluated for a flow-injection sample-processing system that includes a gradient chamber. Quantification of triiodide, including reaction with thiosulfate, is used as the model system. A thin-layer electrochemical detector consisting of a platinum working electrode and glassy carbon counter electrode with a 200-mV difference imposed between them yields linear current response for triiodide concentrations between 0.01 and 1.2 mM. Equations based on the kinetic model are evaluated for situations in which neither the flow stream nor gradient chamber contain reactant (thiosulfate) initially, only the flow stream contains reactant, and both the flow stream and gradient chamber contain reactant. Both calibration data and response curves exhibit very good agreement between theory and experiment except for the situation in which only the flow stream contains reactant. In this case, the theoretical treatment accurately predicts the general nature of responses but predicts slightly longer time intervals for completion of the process than are observed experimentally.

An earlier paper by Růžička et al. [1] described a flow-injection sample-processing system with a gradient chamber in which a portion of the species of interest reacted with a reactant present in the flow stream that was pumped into the gradient chamber at a fixed rate. The time interval, t_{ep}, required for a detector signal to rise above and return to a predetermined level was used to quantify the component of interest. Two subsequent papers from this laboratory [2, 3] suggested that this system is a physicochemical analog of the variable-time approach to chemical kinetic methods [4, 5]. The papers [2, 3] included a detailed mathematical treatment based on the variable-time kinetic model and some experimental verification of the model and equations. However, because the response of the detection system consisting of an acid-base indicator and a photodiode detector was not a linear function of concentration, that work was not completely conclusive, especially regarding the time-dependent response for the system. This paper extends the earlier work to include an electrochemical detection system that responds linearly to the concentration of the species of interest.

The reaction of triiodide with thiosulfate is used as a model for this study. Triiodide concentration is monitored amperometrically with a thin-layer

0003-2670/86/$03.50

electrochemical detector. Current from the detector varies linearly with triiodide concentration between 0.01 and 1.2 mM. Standard solutions of triiodide were used as samples and thiosulfate was used as the reactant in the flow stream. This chemical system was used to evaluate the equations developed earlier [2, 3] for a variety of conditions.

EXPERIMENTAL

The flow system was essentially the same as the single-channel system described earlier (Fig. 1A in [2]). Volumes, flow rates, concentrations, etc. are described in connection with individual experiments.

The detector was a thin-layer electrochemical cell (Electrode no. TL-10A Bioanalytical Systems, West Lafayette, IN) with a platinum working electrode and a glassy carbon counter electrode. A fixed potential of 200 mV was applied between the electrodes with the platinum electrode being negative relative to the glassy carbon electrode. A conventional operational amplifier circuit in a current-to-voltage configuration was used to monitor cell current. A strip-chart recorder was used to monitor the output from the amplifier circuit.

All reagents were prepared in deionized distilled water with reagent-grade chemicals. All solutions, including the flow stream, consisted of 0.122 M KH_2PO_4, 0.026 M $Na_2HPO_4 \cdot 7H_2O$, and 0.15 M KI at pH 6.0. Desired amounts of sodium thiosulfate and iodine were dissolved in this solution.

GENERAL CONSIDERATIONS

Background information

In the original paper describing this general approach [1], the detector system used produced very sharp changes as the concentration of the species being detected exceeded and dropped to (or near) zero in the gradient chamber. Figure 1A illustrates such a signal obtained in the present work with the sensitivity of the electrochemical detection system set very high. The time interval, Δt, between the rapidly rising and falling portions of the response was measured and related to concentration. For a variety of reasons, including the facts that a reaction took place in the flow stream and an acid-base indicator was used to produce the abrupt signal changes, the procedure was identified as a continuous flow titration.

The high sensitivity of the detection system used to produce Fig. 1A and the response curves in the earlier work [1] tend to obscure time-dependent (kinetic) changes in concentration in the gradient chamber. Figure 1B shows a response curve obtained when the sensitivity of the detection system was adjusted to permit the time-dependent concentration changes to be monitored. This plot emphasizes the kinetic nature of the process in the gradient chamber.

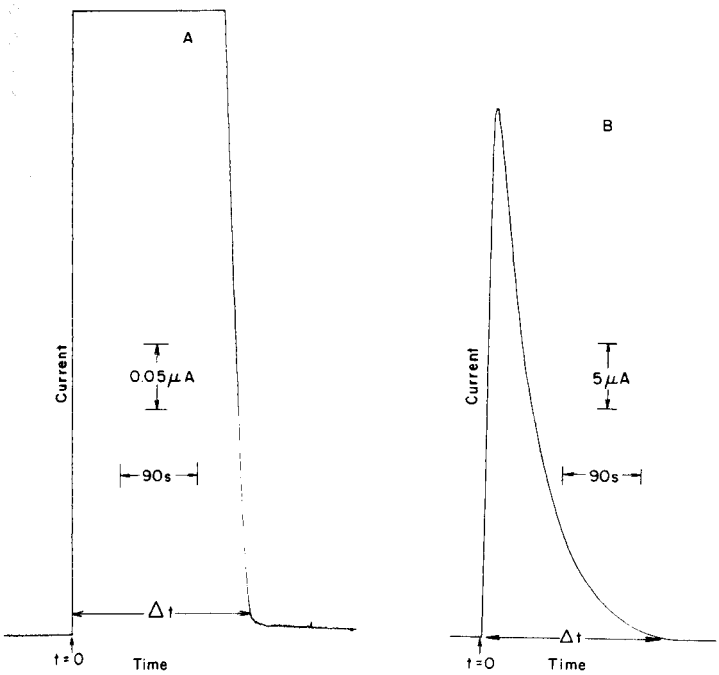

Fig. 1. Effects of detector sensitivity on shapes of response curves. Conditions: 2 mM triiodide, 10 μm thiosulfate in flow stream; 0.033 ml s^{-1} flow rate; V_s = 0.1858 ml; V_g = 1.618 ml. (A) 0.5 μA full scale; (B) 50 μA full scale.

Figure 2 shows a series of response curves obtained without any reactant in the flow stream. These plots are similar in shape to the plot in Fig. 1B that included a reactant; if the detector sensitivity were set very high, they would be virtually identical to that in Fig. 1A. The time intervals, Δt_a, Δt_b, Δt_c, etc., obtained from an experiment without reactant can be used the same way as time intervals with reactant can be used to determine concentration [2, 3]. Because the experiment does not require a reactant to be successful, and because variable time measurements, Δt, are made on a kinetic system, the process was identified as a variable-time kinetic method [4, 5] and treated mathematically according to that model [2, 3].

Mathematical treatment

It is assumed that the species to be determined (A) reacts rapidly and completely with a reactant (B) in the flow stream to give products, P:

$$A + zB \rightarrow P \qquad (1a)$$

In this case, the species to be determined, A, is triiodide, the reactant, B, is thiosulfate, and z is 2:

$$I_3^- + 2S_2O_3^{2-} \rightarrow 3I^- + S_4O_6^{2-} \qquad (1b)$$

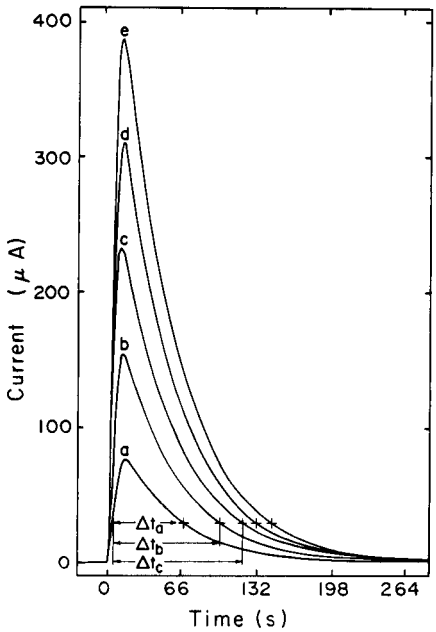

Fig. 2. Response curves obtained with no reactant (thiosulfate) in flow stream or gradient chamber. V_s = 0.366 ml, V_g = 1.618 ml, f = 0.0328 ml s^{-1}. Concentration of triiodide (mM): (a) 2; (b) 4; (c) 6; (d) 8; (e) 10.

A volume, V_s, of sample with concentration C^o_{as}, is introduced into a flow stream, with a flow rate f, and containing a reactant with concentration C^o_b. The sample aliquot is flushed into a gradient chamber with volume V_g, where the species to be determined reacts with reactant already in the chamber and/or in the flow stream. Time-dependent concentrations of the species to be determined and the reactant in the gradient chamber are represented as C_{ag} and C_{bg}, respectively. Instantaneous concentrations at the "end-point" in the process are represented as $[A]_g$ and $[B]_g$.

Depending on the nature of the experiment, there can be up to three distinct phases in the process from the time the sample begins to enter the gradient chamber, t_o, until the "end-point", t_3 or t_{ep} (see Figs. 2 and 3A in [2]). As the sample begins to enter the gradient chamber at t_o, the required species in the sample aliquot will begin to react with the reactant that is in the chamber; this process will continue until time t_1, when all reactant in the chamber is consumed. At time t_1, the concentration of the species to be determined will begin to increase in the gradient chamber, and will continue to increase until time t_2, when all the sample has entered the chamber. After time t_2, the concentration of the species to be determined in the gradient chamber will decrease as a result of dilution and reaction with reactant in the flow stream (if the flow stream contains reactant). Kinetically, the process during the first phase (t_o to t_1) is a pseudo-zero-order process because the

sample aliquot is flowing in at a fixed rate and the volume of the gradient chamber is large relative to the volume of sample used; the process during the second phase (t_1 to t_2) is pseudo-first-order, and the process during the third phase (t_2 to t_3) is either first order if the reactant concentration is zero in the flow stream ($C_b^o = 0$) or combined zero-order/first-order if the reactant concentration in the flow stream is finite ($C_b^o > 0$).

This physical model was used to develop the equation (see [3])

$$\Delta t_{ep} = (V_g/f) \ln \{C_{as}^o [C_{as}^o \exp (V_s/V_g)(1 + C_b^o/zC_{as}^o) - C_{as}^o - C_{bg}^o/z]/(C_{as}^o + C_{bg}^o/z)\} - (V_g/f) \ln \{[A]_g^{ep} + C_b^o/z\} \quad (2)$$

in which all symbols have been defined above and earlier (see Table 1 in [2]). This is the primary equation to be evaluated, but it will be useful to present some alternative forms. First, Eqn. 2 can be rearranged into the form

$$\exp [(f/V_g)\Delta t_{ep}] = \{[C_{as}^o \exp (V_s/V_g)(1 + C_b^o/zC_{as}^o) - C_{as}^o - C_{bg}^o/z]/[(C_{as}^o + C_{bg}^o/z)([A]_g^{ep} + C_b^o/z)]\} C_{as}^o \quad (3)$$

which has the potential to yield a relationship that is linear in the concentration of the species to be determined, C_{as}^o, under certain conditions.

These equations were evaluated for three general sets of conditions, namely with no reactant in the flow stream or gradient chamber ($C_b^o = C_{bg}^o = 0$), reactant in the flow stream but no reactant in the gradient chamber initially ($C_b^o > 0$, $C_{bg}^o = 0$) and reactant in both the flow stream and gradient chamber initially ($C_b^o = C_{bg}^o > 0$). Simplified forms of Eqns. 2 and 3 can be developed for these conditions that both simplify calculations and permit special features to be visualized more easily.

For the special case when there is no reactant in the flow stream or gradient chamber ($C_b^o = C_{bg}^o = 0$), Eqn. 2 reduces to

$$\Delta t_{ep} = (V_g/f) \ln C_{as}^o + (V_g/f) \ln \{[\exp (V_s/V_g) - 1]/[A]_g^{ep}\} \quad (4)$$

which predicts that the measured time interval, Δt_{ep}, is linear in $\ln C_{as}^o$. For these conditions, Eqn. 3 can be simplified to

$$\exp [(f/V_g)\Delta t_{ep}] = \{[\exp (V_s/V_g) - 1]/[A]_g^{ep}\} C_{as}^o \quad (5)$$

which predicts that the exponential function on the left side of Eqn. 5 is proportional to the concentration of the species to be determined.

For the special case when there is reactant in the flow stream ($C_b^o > 0$) but none in the gradient chamber initially ($C_{bg}^o = 0$), Eqn. 2 reduces to

$$\Delta t_{ep} = (V_g/f) \ln \{[C_{as}^o(\exp (V_s/V_g) - 1) + (C_b^o/z) \exp (V_s/V_g)]\} - (V_g/f) \ln ([A]_g^{ep} + C_b^o/z) \quad (6)$$

This situation results in an expected nonlinear relationship between Δt_{ep} and $\ln C_{as}^o$, and Eqn. 3 can be simplified to

$$\exp [(f/V_g)\Delta t_{ep}] = [(\exp (V_s/V_g) - 1)/([A]_g^{ep} + C_b^o/z)] C_{as}^o + [(C_b^o/z) \exp (V_s/V_g)/([A]_g^{ep} + C_b^o/z)] \quad (7)$$

which predicts a linear relationship between the exponential function and the concentration of the species determined.

For the situation when both the flow stream and gradient chamber contain reactant ($C_b^o = C_{bg}^o > 0$), Eqn. 2 reduces to

$$\Delta t_{ep} = (V_g/f) \ln C_{as}^o + (V_g/f) \ln [(\exp (V_s/V_g) - 1)([A]_g^{ep} + C_b^o/z)] \quad (8)$$

and Eqn. 3 can be simplified to

$$\exp [(f/V_g)\Delta t_{ep}] = [(\exp (V_s/V_g) - 1)/([A]_g^{ep} + C_b^o/z)]C_{as}^o \quad (9)$$

Both equations predict linear relationships between the dependent variable and concentration.

RESULTS AND DISCUSSION

In all plots presented below, points represent experimental results and solid lines represent theoretical results calculated with appropriate equations.

Detector response

The thin-layer electrochemical cell exhibited excellent linearity for triiodide concentrations between 0.01 and 1.2 mM. A least-squares fit of current (I, μA) vs. triiodide concentration ($C_{I_3^-}^o$, mM) in this concentration range gave the equation

$$I = (220.7 \pm 0.2)C_{I_3^-}^o + (0.07 \pm 0.09)\mu A$$

with a standard error of estimate (S_{yx}) of 0.20 μA and a correlation coefficient (r) of 0.9999.

Calibration results

Nineteen solutions containing triiodide concentrations between 0.8 and 8.0 mM were used to evaluate the simplified equations presented above.

Figure 3A presents results for Δt_{ep} vs. ln C_{as}^o. Excellent agreement is observed between experiment and theory for the situations in which $C_b^o = C_{bg}^o$. For the situation in which $C_b^o > 0$ and $C_{bg}^o = 0$, Eqn. 6 correctly predicts the general (nonlinear) shape of the calibration plot; however, in every case, the measured time interval, Δt_{ep}, is lower than the predicted value. Despite this fixed offset, it is satisfying to note that the theoretical treatment correctly predicts the curvature observed experimentally. The offset may be an experimental artifact resulting from the fact that there may have been some residual reactant (thiosulfate) in the gradient chamber or more likely, in the tubing between the sample loop and the gradient chamber. This reactant would reduce some triiodide, causing experimentally measured values of Δt_{ep} to be less than expected. If this were indeed the problem, then experiments with lower thiosulfate concentrations relative to the concentration of triiodide should give better agreement because less triiodide would be consumed per unit volume of reactant in the line and/or gradient chamber. To

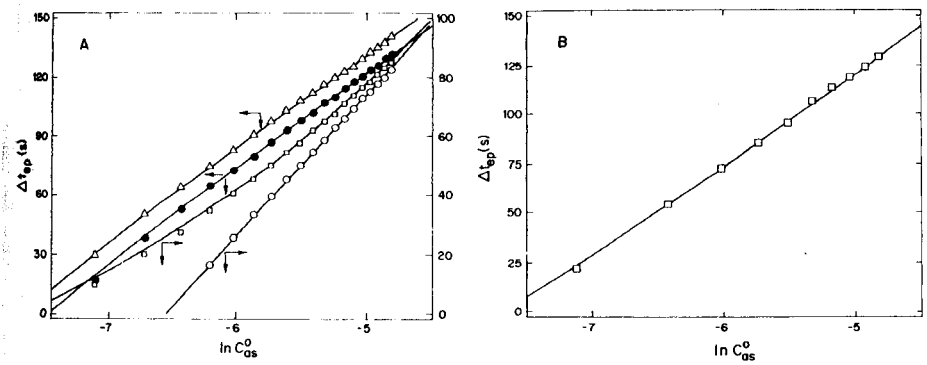

Fig. 3. Logarithmic calibration plots for different conditions. For both frames, V_s = 0.1858 ml; V_g = 1.618 ml. For frame A: (△) $C^o_b = C^o_{bg} = 0$, f = 0.03379 ml s^{-1}, $[A]^{ep}_g$ = 0.0526 mM; (•) $C^o_b = C^o_{bg}$ = 0.03008 mM, f = 0.03333 ml s^{-1}, $[A]^{ep}_g$ = 0.0506 mM; (○) $C^o_b = C^o_{bg}$ = 0.2473 mM, f = 0.03317 ml s^{-1}, $[A]^{ep}_g$ = 0.0537 mM; (□) C^o_b = 0.2516 mM, C^o_{bg} = 0, f = 0.03378 ml s^{-1}, $[A]^{ep}_g$ = 0.0540 mM. For frame B: C^o_b = 0.03010 mM, C^o_{bg} = 0, f = 0.03328 ml s^{-1}, $[A]^{ep}_g$ = 0.0556 mM.

test this, experiments were done with C^o_b = 0.0301 mM and C^o_{bg} = 0. Results in Fig. 3B show very good agreement between theory and experiment. It should be noted that less curvature is expected in Fig. 3B because the lower thiosulfate concentration causes the first term involving C^o_b/z in Eqn. 6 to be much smaller relative to the term containing C^o_{as}, and under this condition Eqn. 6 approaches Eqn. 8.

Figure 4 presents results for experimental and predicted data for the exponential function in Eqns. 5, 7 and 9 vs. concentration. Again, there is excellent agreement for the two situations in which $C^o_b = C^o_{bg}$, with both plots exhibiting the expected proportional relationship. Again, agreement between experiment and theory is not so good for the situation in which $C^o_b > 0$, $C^o_{bg} = 0$, probably for the same reasons as discussed above. However, the data exhibit near linearity and a nonzero intercept as predicted by Eqn. 7. Thus although exact agreement is not achieved, the kinetic model permits prediction of the correct form of the response.

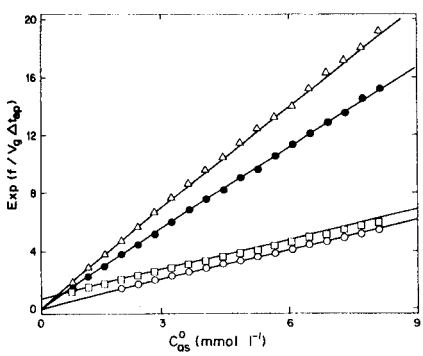

Fig. 4. Exponential calibration plots for different conditions (as in Fig. 3A).

TABLE 1

Comparison of least-squares slopes and intercepts for experimental data with values predicted with equations based on a kinetic model

Situation			Slopes[a]		Intercepts[a]		Std. error	Corr. coeff.	Eqn. no.
Fig. and plot	C_b^o (mM)	C_{bg}^o (mM)	Pred.	Exp.[b]	Pred.	Exp.[b]			
3A (△)	0	0	47.9	47.9 ± 0.15	371	372 ± 0.9	0.43	0.9999	4
3A (•)	0.030	0.030	48.5	49.4 ± 0.2	365	370 ± 1	0.56	0.9999	8
3A (○)	0.247	0.247	48.8	47.4 ± 0.2	319	311 ± 1	0.29	0.9999	8
4 (△)	0	0	2.31	2.35 ± 0.01	0	0.003 ± 0.05	0.09	0.9999	5
4 (•)	0.030	0.030	1.85	1.87 ± 0.008	0	−0.10 ± 0.04	0.08	0.9999	9
4 (○)	0.247	0.247	0.686	0.662 ± 0.003	0	0.10 ± 0.18	0.02	0.9999	9
4 (□)	0.252	0	0.677	0.628 ± 0.007	0.785	0.789 ± 0.03	0.07	0.9990	7

[a]Pred. is predicted value; Exp. is experimental value. [b]Experimental value ± one standard deviation.

Least-squares statistics for all the plots are summarized in Table 1. Although there are modest differences among predicted and experimental values of slopes and intercepts, values are sufficiently close to add credibility to the validity of the kinetic model and resulting equations.

Response curves

The kinetic equations can be used to predict the shapes of the response curves in the different phases of the process for different conditions.

For the situation in which there is no reactant in either the flow stream or the gradient chamber ($C_b^o = C_{bg}^o = 0$), the rising and falling portions of the curve should follow first-order kinetics. Between t_1 and t_2 (rising portion), the expected response can be rearranged into the form

$$-\ln [(C_{as}^o - C_{ag})/C_{as}^o] = (f/V_g)(t - t_1) \tag{10}$$

Between t_2 and t_3, the expected response can be rearranged into the form

$$-\ln (C_{ag}/[A]_g^{max}) = (f/V_g)(t - t_2) \tag{11}$$

Figure 5 includes plots of these functions along with experimental data. Agreement between theory and experiment is very good except in the region of the maximum. The most probable reason for this discrepancy is that the kinetic model used to develop Eqns. 10 and 11 included an assumption of plug flow for the sample. The curvature near the peak most likely results from the fact that the trailing edge of the sample aliquot does not enter as a "plug", but rather is highly dispersed. This would cause the curvature observed and would prevent the peak from reaching the maximum predicted value.

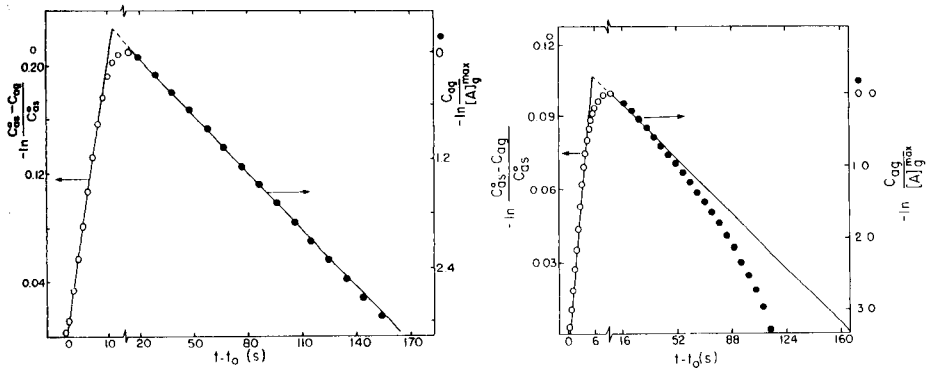

Fig. 5. Comparison of computed and experimentally observed response curves with no reactant in the flow stream. V_s = 0.3660 ml, V_g = 1.618 ml, f = 0.03255 ml s^{-1}, C^o_{as} = 1.001 mM, $C^o_b = C^o_{bg} = 0$.

Fig. 6. Comparison of computed and experimentally observed response curves with reactant in the flow stream and gradient chamber, assuming first-order behavior throughout the process. V_s = 0.1858 ml, V_g = 1.618 ml, f = 0.033383 ml s^{-1}, C^o_{as} = 2.026 mM, $C^o_b = C^o_{bg}$ = 0.03101 mM.

In the original treatment [1] of this system for the situation in which both the flow stream and gradient chamber contained reactant, the entire process was assumed to follow first-order kinetics. If this were the case, Eqns. 10 and 11 should be applicable. Figure 6 compares experimental and computed results for this situation. Clearly, the ascending part of the plot is accurately described by the first-order model, but the descending portion of the plot is not. The first-order model predicts a longer time for the process to reach the end-point than is observed experimentally. Treating the descending portion of the curve solely as a first-order process ignores the fact that the reactant is flowing into the gradient chamber at a constant rate, which corresponds to a zero-order process. Thus, the dilution process contributes first-order behavior and the reaction process contributes zero-order behavior. This mixed zero-order/first-order kinetic behavior can be represented by

$$-\ln\left[(C_{ag} + C^o_b/z)/([A]^{max}_g + C^o_b/z)\right] = (f/V_g)(t - t_2) \qquad (12)$$

These functions (Eqns. 10 and 12) are plotted in Fig. 7 along with experimental data. Again, agreement is very good except at the peak of the curve as discussed above.

These results lend additional support to the validity of the kinetic equations except for the region at which the final portions of sample are entering the gradient chamber at which the assumption of plug flow is not valid.

Reproducibility

Reproducibility was studied with five injections of six different solutions with $C^o_{I_3^-}$ between 0.8 and 8 mM and no thiosulfate in either the flow stream

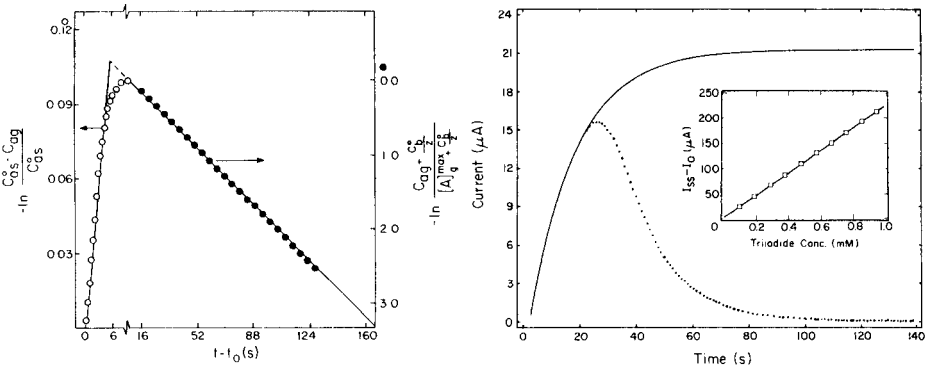

Fig. 7. Comparison of computed and experimentally observed response curves with a combined zero-order/first-order model. Conditions as in Fig. 6.

Fig. 8. Results of the predictive kinetic method applied to current vs. time data: (···) experimental; (—) fitted (3—23 s fitting range). Conditions: V_s = 0.93 ml, V_g = 0.484 ml, f = 0.0337 ml s^{-1}, C^o_{as} = 0.095—0.95 mmol l^{-1}; data rate, 2 points per second. The inset is explained in the text.

or gradient chamber, and for five injections each of eight solutions with $C^o_{I_3^-}$ between 2 and 8 mM and a thiosulfate concentration of 0.251 mM in the flow stream and gradient chamber initially. The pooled standard deviations of Δt_{ep} for the two sets of data were 0.71 s and 0.35 s, respectively, for Δt_{ep} between 30.2 s and 141.4 s for the first set ($C^o_b = C^o_{bg} = 0$) and Δt_{ep} between 16.0 s and 82.3 s for the second set ($C^o_b = C^o_{bg} = 0.251$ mM). Least-squares equations for the two data sets were

$$\Delta t_{ep} = (48.2 \pm 0.18) \ln C^o_{as} + (374 \pm 1) \text{ s}$$

with $S_{yx} = 0.79$ and $r = 0.9998$, and

$$\Delta t_{ep} = (47.8 \pm 0.13) \ln C^o_{as} + (313 \pm 0.7) \text{ s}$$

with $S_{yx} = 0.35$ and $r = 0.9999$.

These equations can be used to convert Δt_{ep} errors to concentration errors.

Predictive kinetic method

As a further test of the kinetic nature of the response, a predictive kinetic method developed and applied earlier for chemical reactions [6, 7] was evaluated for the rising portion of the response curve. In this approach, time-dependent data (current vs. time in this case) collected early in a kinetic process are used with a suitable kinetic model to predict the total signal change that would occur if the process were monitored to completion. The concept is illustrated in Fig. 8. The dotted curve represents experimental data (i vs. t) and the solid curve represents a predicted curve based on a fit of data collected during the period from 3 to 23 s to a first-order model. The maximum predicted steady-state current, $\hat{I}_{ss}$, represents the current expected

if sufficient sample were used to flush all reagent from the gradient chamber. Accordingly, the total current change, $\Delta\hat{I}_{ss} = \hat{I}_{ss} - \hat{I}_0$, is expected to vary linearly with concentration. Values of $\Delta\hat{I}_{ss}$, computed in this way for ten triiodide concentrations between 0.1 and 1 mmol l^{-1} exhibited excellent linearity (inset, Fig. 8) with virtually no deviation of experimental data from a least-squares line represented by the equation

$$\Delta\hat{I}_{ss} = (223 \pm 1.2)C^{o}_{as} + (1.8 \pm 0.7)\ \mu A$$

with $S_{yx} = 1.1\ \mu A$ and $r = 0.9998$. A fit of computed values of $\Delta\hat{I}_{ss}$ with values measured when sufficient sample was used to flush all diluent from the gradient chamber yielded the equation

$$\Delta\hat{I}_{ss} = (1.03 \pm 0.006)\ \Delta I_{ss} + (1.3 \pm 0.7)\ \mu A$$

where $\Delta\hat{I}_{ss}$ and ΔI_{ss} are the computed and measured values of current change, with $S_{yx} = 1.1\ \mu A$ and $r = 0.9999$. The near-unity slope, and the small values of intercept and standard error suggest excellent agreement between the computed and measured values of the steady-state current.

Recognition of the kinetic nature of these processes permits other data-processing approaches to be identified and evaluated.

This work was supported by Grant No. CHE 8319014 from the National Science Foundation.

REFERENCES

1 J. Růžička, E. H. Hansen and H. Mosbaek, Anal. Chim. Acta, 92 (1977) 235.
2 H. L. Pardue and B. Fields, Anal. Chim. Acta, 124 (1981) 39.
3 H. L. Pardue and B. Fields, Anal. Chim. Acta, 124 (1981) 65.
4 W. J. Blaedel and G. P. Hicks, in C. N. Reilley (Ed.), Advances in Analytical Chemistry and Instrumentation, Vol. 3, Wiley, New York, 1964, pp. 105.
5 H. L. Pardue, Clin. Chem., 23 (1977) 2189.
6 G. E. Mieling and H. L. Pardue, Anal. Chem., 50 (1978) 1611.
7 Y. R. Tahboub and H. L. Pardue, Anal. Chim. Acta, 173 (1985) 23.

Analytica Chimica Acta, 179 (1986) 181—188
Elsevier Science Publishers B.V., Amsterdam — Printed in The Netherlands

SAMPLE DISPERSION WITH CHEMICAL REACTION IN A FLOW-INJECTION SYSTEM

H. WADA*, S. HIRAOKA, A. YUCHI and G. NAKAGAWA
Nagoya Institute of Technology, Gokiso-cho, Showa-ku, Nagoya 466 (Japan)
(Received 29th July 1985)

SUMMARY

Computer simulations of signals based on a dispersion equation involving diffusion, convection and chemical reaction terms are reported for systems with and without chemical reaction. 2-(2-Thiazolylazo)-4-methyl-5-(sulfomethylamino)benzoic acid (TAMSMB) is used as the reagent because it reacts very quickly with copper(II) and much more slowly with nickel(II). Comparison of experimental signal profiles with the simulated ones enables sample dispersion from the reaction rates to be elucidated. Concentration profiles of the reaction product in a straight narrow tube were also simulated; they explain satisfactorily the signal profiles obtained experimentally.

The development of theoretical expressions for sample dispersion in flow-injection systems has been approached in several ways [1]. In many flow-injection systems, the sample injected reacts with a reagent in an unsegmented flow, so that the effects of sample dispersion and reaction rate on the shape and height of the signal must be important. However, only a few studies in which chemical kinetics is directly considered have been reported. Haagensen [2] studied the dependence of peak height on the tube length and the reaction rate. Painton and Mottola [3] described a computer simulation based on a laminar dispersion equation and rate equation, which was evaluated with experimental studies of a moderate reaction rate (oxidation of ascorbic acid by dichromate). However, their experimental device did not satisfy the theoretical conditions, and the deviation between experimental and simulated signal profiles required the use of correction factors. Betteridge et al. [4] discussed computer simulations based on a random-walk model, which provided some insight into mixing processes.

In order to obtain more insight into sample dispersion when a chemical reaction is involved, computer simulations of signals based on an equation involving diffusion, convection and reaction terms were examined here. Sample dispersions without reaction, with a fast reaction and with a slower reaction were studied. Comparison of experimental and computed signals for sample dispersion with chemical reaction is discussed. The computed concentration profiles of the reaction product in the narrow tube are presented.

0003-2670/86/$03.50

EXPERIMENTAL

Reagents

2-(2-Thiazolylazo)-4-methyl-5-(sulfomethylamino)benzoic acid (TAMSMB), synthesized and purified as described previously [5], was dissolved in acetate buffer pH 5.0 (see below). Copper(II) nitrate and nickel(II) nitrate solutions were also prepared in the acetate buffer. The 0.05 M acetic acid/sodium acetate buffer (pH 5.0) was adjusted to an ionic strength of 0.1 M with potassium nitrate. The water used was redistilled from hard glass vessels.

Five pairs of carrier and sample were selected for the experiment and computation as shown in Table 1.

Equilibria of the dissociation and complex formation of TAMSMB, and measurement of rate constants

The acidity constants of TAMSMB are $pK_{NH} = 1.28$ and $pK_{COOH} = 3.44$ [6]:

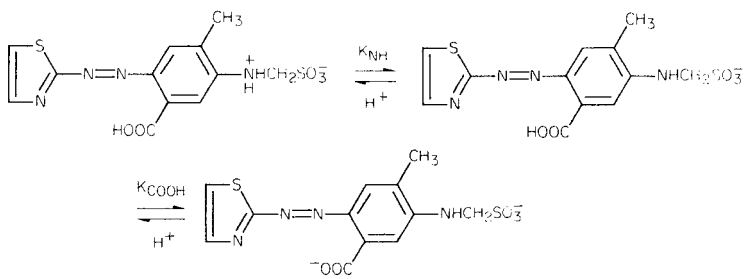

The formation constants of the copper(II) and nickel(II) complexes of TAMSMB are $\log K^{R}_{CuR} = 7.36$, $\log K^{R}_{NiR} = 5.19$, $\log K^{R}_{NiR_2} = 3.86$ [6].

The rate of reaction between copper(II) and TAMSMB was too fast to be measured by the usual stopped-flow method. According to the literature, the reaction rate of copper(II) ion with a ligand is generally fast, and the rate constant is about 10^8 l mol^{-1} s^{-1}.

TABLE 1

Experimental conditions

Experiment no.	Sample (A) (5.0×10^{-5} M)	Carrier (B) (5.0×10^{-4} M)	Experiment no.	Sample (A) (5.0×10^{-5} M)	Carrier (B) (5.0×10^{-4} M)
Cu(II)/TAMSMB system			*Ni(II)/TAMSMB system*		
1	Cu(II)	TAMSMB	1	Ni(II)	TAMSMB
2	Cu(II)/ TAMSMB[a]	TAMSMB	2	TAMSMB	Ni(II)
3	TAMSMB	Cu(II)			

[a] TAMSMB 5.0×10^{-4} M in excess.

The rate of complex formation between nickel(II) ion and TAMSMB was measured in 0.01—0.1 M acetic acid/sodium acetate (pH 5.0, μ = 0.1 M) by the stopped-flow method. The rate constants of the second-order reaction ($v = k_{H_2O}[Ni^{2+}][R^{2-}] + k_{AcO}[Ni(AcO)^{+}][R^{2-}]$) were estimated as k_{AcO} = 8.9×10^3 l mol^{-1} s^{-1} and as $k_{H_2O} = 5.1 \times 10^3$ l mol^{-1} s^{-1} by extrapolation, where R^{2-} is the anionic form of TAMSMB and k_{H_2O} and k_{AcO} are the rate constants of the reaction with hexaaquonickel(II) and pentaaquoacetatonickel(II) with R^{2-}, respectively. Under the present experimental conditions (in 0.05 M acetate buffer), the conditional rate constant was evaluated as 5.9×10^3 l mol^{-1} s^{-1}.

Apparatus

The flow-injection manifold used is shown in Fig. 1. The reaction tube and the sample tube, both of translucent polyethylene (0.5 mm i.d.), were kept straight. The length of the reaction tube was fixed at 50 cm. The detector was placed at the end of the reaction tube, and there was no joint between point S2 and valve V_5, though the reaction tube was curved at the entrance to the flow-cell block.

A JASCO (Japan Spectroscopic Co.) Uvidec-100IIW spectrophotometer with a response time of 0.1 s, was used with a Hitachi 056 recorder (chart speed 240 mm min^{-1}). An Ismatec IP-4 peristaltic pump was used. A HITAC M-260D (Hitachi Co.) computer was used for the simulation.

Procedure

Sample was filled into the sample tube by hydrodynamic injection [7]: valves V_4 and V_5 were closed, and sample solution was delivered to the sample tube (S1—S2) of fixed length L by nitrogen pressure. After sample solution had overflowed from W_1, valves V_1, V_2 and V_3 were closed. Then valve V_5 was switched to the water reservoir and the peristaltic pump was started. When the flow rate became constant, valves V_4 and V_5 were switched to the carrier. The absorbance of the product above the baseline was recorded.

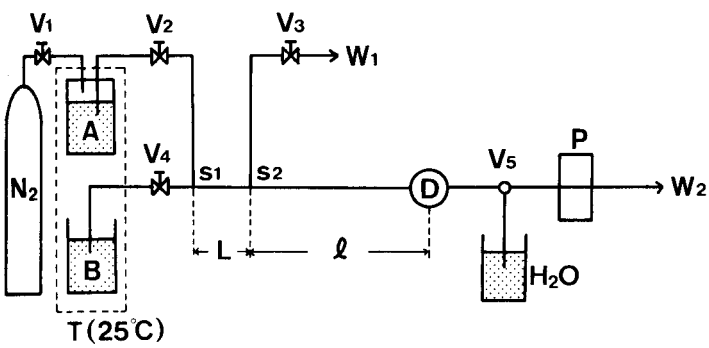

Fig. 1. Flow diagram: S1—S2, sample tube (L cm); S2—D, reaction tube (l = 50 cm); V_1, V_2, V_3, V_4, two-way valves; V_5, three-way valve; D, spectrophotometer (light path 0.5 mm); T, thermostat (25°C); P, peristaltic pump; W_1, W_2, waste; A, sample; B, carrier.

The detecting wavelength was 585 nm for copper(II)/TAMSMB systems and 554 nm for nickel(II)/TAMSMB systems.

Flow rates were varied in the range 0.12– 0.58 ml min^{-1}. The sample tube length was varied in the range 10– 50 cm.

COMPUTER SIMULATIONS

When a sample (A) is injected as a plug into a laminar flow (Fig. 2), and reacts with a reagent (B) to yield a product (P), A + B → P, the change in the concentrations of A, B and P can be calculated by solving Eqn. 1 based on diffusion and convection with chemical reaction:

$$\partial C_i/\partial t = -U_{max}(1 - r^2/R^2)(\partial C_i/\partial Z) + (D_i/r)\partial(r\partial C_i/\partial r)/\partial r \pm kC_AC_B \quad (1)$$

where the plus sign in the last term of the right-hand side refers to the product; C_i is the concentration of species where i is A, B or P (mol l^{-1}), D_i is the diffusion coefficient of a species (cm^2 s^{-1}), U_{max}(= 2 $\bar{U}$) is the maximum velocity and $\bar{U}$ the mean velocity (cm s^{-1}); Z is the axial distance (cm), R the reaction tube radius (cm) and r the radial distance from the tube axis (cm); t is time (s) and k the rate constant of the reaction (l mol^{-1} s^{-1}).

Equation 1 was solved numerically, subject to the initial conditions (t = 0),

$$\left.\begin{array}{l} C_A = C_{A0},\ C_B = 0,\ C_p = 0, \text{ at } 0 \leqslant Z \leqslant L \\ C_A = 0,\ C_B = C_{B0},\ C_P = 0, \text{ at } L < Z < \infty \\ \text{and } -\infty < Z < 0 \end{array}\right\} \quad \text{at } 0 < r < R$$

and the boundary conditions ($t > 0$),

$\partial C_i/\partial r = 0$ (i = A, B, P) at $r = 0$ and $r = R$

$C_A = 0,\ C_B = C_{B0},\ C_P = 0$ at $Z = \infty$

The following parameters calculated under the experimental conditions and the diffusion coefficients were introduced into the program: $K = U_{max}R^2/LD_A$, $t^* = tU_{max}/L$ (reduced time), $k' = kR^2C_{i0}/D_A$ and $k^* = k'/K$. The other input values were the concentration ratio C_{B0}^* (= C_{B0}/C_{A0}) and the diffusion coefficient ratios D_B/D_A and D_P/D_A. Diffusion coefficients for Cu^{2+} and Ni^{2+} are available; the values for TAMSMB, and the two TAMSMB complexes were estimated from the Wilke equation as a first approximation. Thus for Cu^{2+} and Ni^{2+} 7.0×10^{-6} cm^2 s^{-1}, for TAMSMB 4.5×10^{-6} cm^2 s^{-1}, for the Cu(II)/TAMSMB (1:1) complex 4.15×10^{-6} cm^2 s^{-1}, and for the Ni(II)/

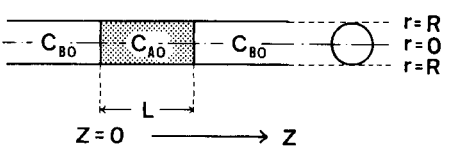

Fig. 2. Initial state of the sample plug.

TAMSMB (1:1) complex 4.1×10^{-6} cm^2 s^{-1}. The estimated coefficients had to be corrected to obtain a better fit of the simulated to the experimental signals: for TAMSMB 5.6×10^{-6} cm^2 s^{-1}, for Cu(II)/TAMSMB 5.4×10^{-6} cm^2 s^{-1}, and for Ni(II)/TAMSMB 5.1×10^{-6} cm^2 s^{-1}.

For the copper(II)/TAMSMB system, the reaction term in Eqn. 1 was omitted and an additional boundary condition was introduced, i.e., the mass fluxes of A and B are equal at the reaction surface.

In the case of the nickel(II)/TAMSMB system, TAMSMB in the carrier has appreciable absorbance at the wavelength used (554 nm). Apparent molar absorptivities (l mol^{-1} cm^{-1}) in these experiments were 1800 for TAMSMB and 54000 for the nickel complex. Therefore, the decrease in absorbance corresponding to decreased concentration of free TAMSMB on formation of the complex should lower the experimental peak heights. Actually, the experimental signals were smaller than the simulated signals of P, because the baseline was set at the absorbance of the carrier solution. Thus the simulated signal was obtained by correcting the concentration of P corresponding to decreased concentration of B by taking into account the molar absorptivities of B and P. As the absorbance of TAMSMB at 585 nm was very small, the correction was not needed in the case of copper(II)/TAMSMB system.

The peak height was calculated in the range of $r/R = 0$—0.5, because the detection did not cover the entire section of the reaction tube.

The computer program was based on the FCT method [8].

RESULTS AND DISCUSSION

Copper(II)/TAMSMB system

First, copper(II) solution was injected into the TAMSMB solution. The experimental signals (plots of C/C_0 vs. t^*) are shown in Fig. 3(a). The simulated signals are shown in Fig. 3(b). All the peak profiles were in fairly good agreement with those simulated, but the initial appearance times obtained experimentally were delayed at lower flow rates. Figure 3(c) shows the simulated concentration profiles in the reaction tube; the black areas indicate where the concentration of the complex produced is greatest in the reaction tube at any given time. When the reduced time is small, the absorbance of the complex near the front must be detected. As t^* becomes larger, the concentration of the product increases near the center and the wall of the tube; this corresponds to the double-humped peak. As t^* increases further, the product spreads in the tube and the peak profile becomes that obtained by Taylor's model. The simulated concentration profiles explain the peak profiles obtained experimentally.

In further studies, a solution of the copper(II)/TAMSMB complex prepared by mixing 10^{-4} M copper(II) and 1.1×10^{-3} M TAMSMB solution at pH 5 was injected into the TAMSMB solution, so that chemical reaction was not involved. The experimental results and the simulated peaks are shown in Fig. 4. The peak profiles are similar to those in Fig. 3, but there are differ-

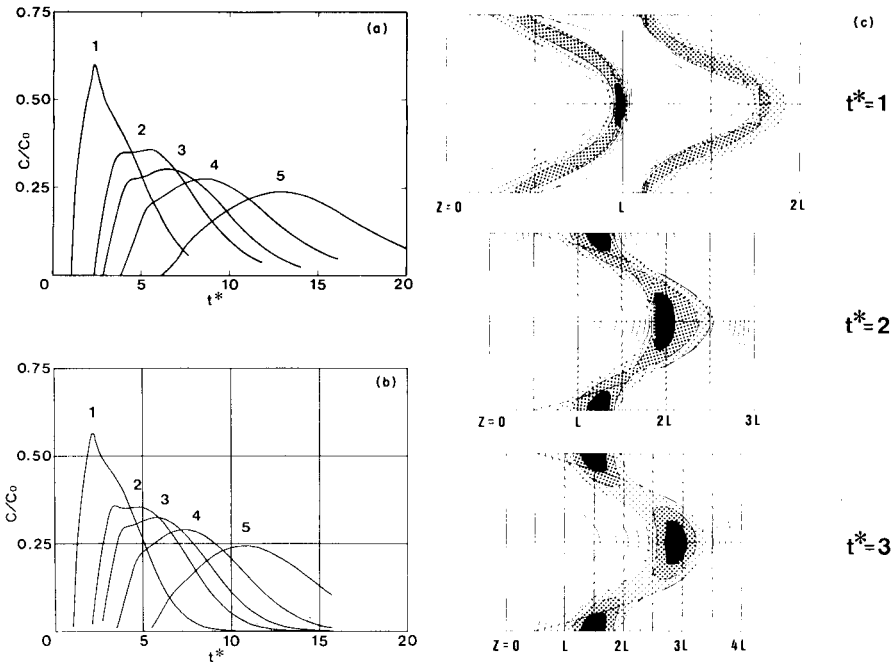

Fig. 3. The Cu(II)/TAMSMB system with copper injected into TAMSMB solution. (a) Experimental signals. (b) Simulated signals. Values of $(L + l)/L$ and flow rate (ml min^{-1}): (1) 2.0, 0.58; (2) 3.0, 0.29; (3) 3.5, 0.23; (4) 4.3, 0.17; (5) 6.0, 0.12. (c) Simulated concentration profiles in the reaction tube (see text for explanation). K = 17.6.

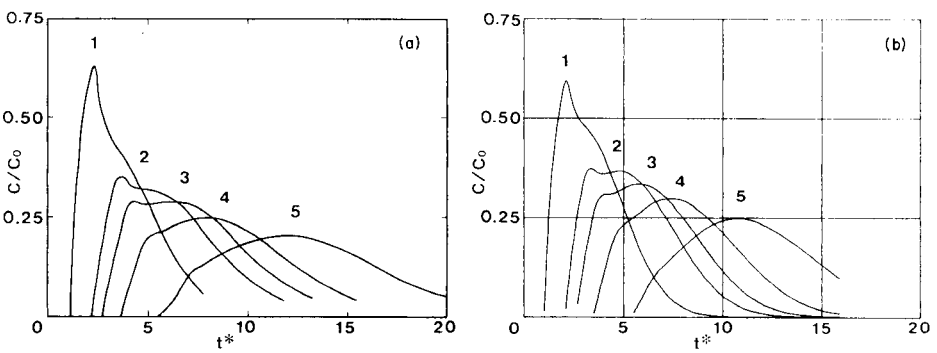

Fig. 4. The Cu(II)/TAMSMB system with the complex injected into TAMSMB solution. (a) Experimental signals. (b) Simulated signals. Values of $(L + l)/L$ and flow rate as in Fig. 3; K = 22.8.

ences in the shapes of the double-humped peak at $(L + l)/L$ = 3.0 and 3.5. The difference in diffusion coefficients between copper(II) ion and the copper/TAMSMB complex may be responsible for this. In this case, the initial appearance times were in good agreement with those of the simulated signals.

In further tests, the TAMSMB solution was injected into the copper(II)

solution. The experimental peak profiles were almost the same as those obtained when the complex was injected into the TAMSMB carrier, and the simulated signals were identical with those shown in Fig. 4(b).

Nickel(II)/TAMSMB system

In the first tests, nickel(II) solution was injected into the TAMSMB solution. Compared with the copper/TAMSMB system, the experimental signals are lower (Fig. 5a), because the reaction of nickel(II) with TAMSMB is incomplete at the detection point and there is an appreciable negative baseline shift as described above. The simulated signals with correction for the baseline shift are shown in Fig. 5(b). The double-humped peak can be seen at lower t^* values. As shown in Fig. 5(c) for $t^* = 2$, the concentration of the nickel/TAMSMB complex is small near the front of the plug and much smaller behind that; this must cause the double-humped peak. As t^* increases to 3, the concentration profile becomes similar to the second case ($t^* = 2$) in the copper/TAMSMB system. In further tests, the TAMSMB solution was injected into the nickel(II) solution. The general shapes of the curves were similar to those shown in Fig. 4, but with lower absorbances. The simulated signals without the correction for baseline shift were similar to the experimental ones. In the nickel/TAMSMB systems there is a problem: when the TAMSMB

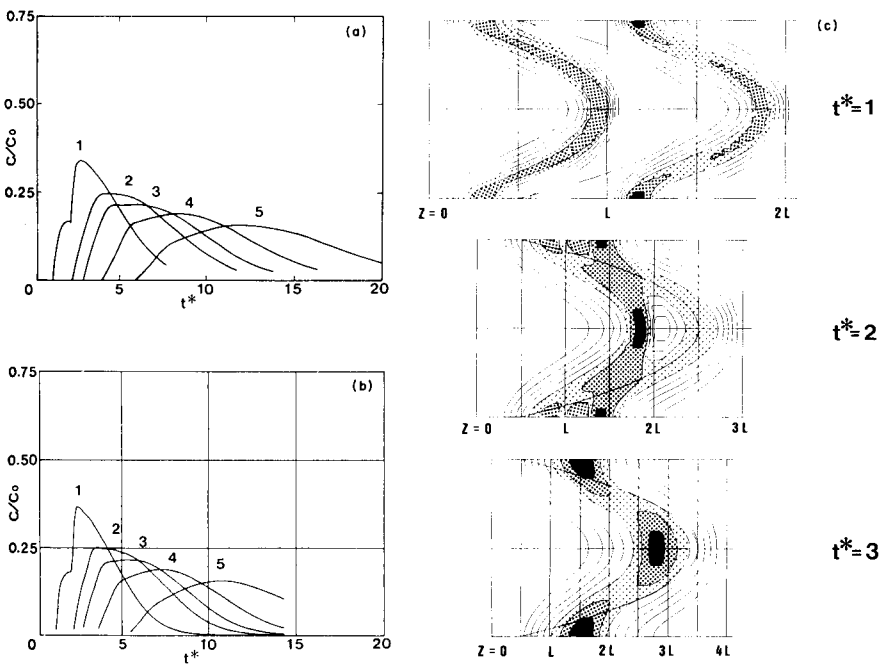

Fig. 5. The Ni(II)/TAMSMB system with nickel injected into TAMSMB solution. (a) Experimental signals. (b) Simulated signals. Values of $(L + l)/L$ and flow rate as for Fig. 3. (c) Simulated concentration profiles in the reaction tube. $K = 17.6$.

is in large excess, the NiR_2 complex can be formed and its molar absorptivity is twice that of the NiR complex. The possible formation of the NiR_2 complex was not included in the present computations.

Conclusions

The results described above give some further insight on the dispersion of injected samples when chemical reactions are involved. It has long been recognized implicitly in the general construction of flow-injection systems that reaction kinetics contribute significantly to signal profiles. The simulated concentration profiles reported above are based on a dispersion equation involving diffusion, convection and chemical reaction terms. The simulated signals corresponded fairly well to the signal profiles which were encountered in practical flow-injection analysis, although the fit of the experimental and simulated signals cannot be described as excellent, even although great attention was given in the experimental work to maintaining laminar flow conditions. In actual practice, small curves in the reaction tube, secondary flow at connecting points and even small flow pulsations caused by the pump must have significant effects on signal profiles.

When fast reactions are utilized, small l/L ratios and high flow rates can be used, whereas with relatively slow reactions, the optimum set of l/L and flow rate must be sought empirically.

In practical flow-injection analysis, the peak profile will be affected by many factors such as the geometries of the reactor, mixing point, sample injector, connecting point, and flow cell, and the type of pump; secondary flow can decrease axial dispersion. Further studies of the effects of such factors on peak profiles are in progress. But it should be emphasized that each particular manifold will have its own individual characteristics of total dispersion. Thus a generalized theoretical approach to this problem is likely to provide only rough guidance in the choice of practical conditions.

We are grateful to Mr. Y. Sawa and Mr. K. Ando for assistance with the computer simulations and the experiments. This work was supported by the Grant-in-Aid for Scientific Research (No. 59340035 and No. 58549356) from the Ministry of Education, Science and Culture, Japan.

REFERENCES

1 C. C. Painton and H. A. Mottola, Anal. Chim. Acta, 154 (1983) 1.
2 P. Haagensen, cited in J. Růžička and E. H. Hansen, Flow Injection Analysis, Wiley, New York, 1981, pp. 26—29.
3 C. C. Painton and H. A. Mottola, Anal. Chim. Acta, 158 (1984) 67.
4 D. Betteridge, C. Z. Marczewski and A. P. Wade, Anal. Chim. Acta, 165 (1984) 227.
5 H. Wada, T. Ishizuki and G. Nakagawa, Anal. Chim. Acta, 135 (1982) 333.
6 H. Wada, T. Ishizuki and G. Nakagawa, Mikrochim. Acta, III (1983) 235.
7 J. Růžička and E. H. Hansen, Anal. Chim. Acta, 145 (1983) 1.
8 D. L. Book, Finite Difference Techniques for Vectorized Fluid Dynamics Calculations, Springer-Verlag, New York, 1981, pp. 29—55.

Analytica Chimica Acta, 179 (1986) 189—201
Elsevier Science Publishers B.V., Amsterdam — Printed in The Netherlands

EXPERIMENTAL COMPARISON OF FLOW-INJECTION ANALYSIS AND AIR-SEGMENTED CONTINUOUS FLOW ANALYSIS

C. J. PATTON† and S. R. CROUCH

Department of Chemistry, Michigan State University, East Lansing, MI 48824 (U.S.A.)

(Received 8th August 1985)

SUMMARY

A miniature continuous flow analyzer that can be configured for either air-segmented continuous flow analysis (c.f.a.) or flow-injection analysis (f.i.a.) was used to compare the performance of the two techniques in terms of sampling rates, sample and reagent consumption factors and analytical precision. Details of simple dye dispersion experiments and spectrophotometric chloride determinations are presented. Chloride determinations at rates of up to 360 determinations per hour could be achieved with either technique; sample and reagent consumption was less for the air-segmented flow system than for flow-injection systems equipped with either coiled open tubular reactors (0.05 cm i.d.) or single-bead-string reactors. The advantages of single-bead-string reactors for determinations by merging-zones f.i.a. are demonstrated. The c.f.a. and f.i.a. techniques are shown to be complementary, and the relative merits of each for various applications are discussed.

The challenge to gas-segmented continuous flow analysis (c.f.a.) [1] presented by flow-injection analysis (f.i.a.) [2, 3] has led to several lively exchanges in the literature [4—7] concerning the relative performance (rates of data production, sample and reagent consumption, and precision of analytical results) of the two techniques. In addition, a theoretical comparison of c.f.a. and f.i.a. presented by Snyder [8] predicted that for equilibrium-based spectrophotometric determinations requiring more than a few seconds of reaction time, faster rates of sample throughput and lower reagent consumption should be achieved with c.f.a. than with f.i.a. Exactly the opposite conclusion was reached in a recent review [9] on the basis of figures of merit for f.i.a. and c.f.a. determinations published in the literature. To date, however, there has been no direct experimental comparison of the two techniques, perhaps because ground rules to minimize bias in such a comparison are difficult to establish, and also because until recently, a single-channel, technologically up-to-date c.f.a. instrument necessary for such a comparison was unavailable commercially.

A miniature continuous flow analyzer developed in this Department [10] that can be configured either for f.i.a. or c.f.a. made it possible to compare

---

†Present address: Alpkem Corporation, Clackamas, OR 97015, U.S.A.

0003-2670/86/$03.50

these two techniques with minimal bias because the same pump, flow cell, and detectors were used for all experiments. In the first set of experiments, dispersion of dye slugs in open tubular reactors (OTRs), single-bead-string reactors (SBSRs) [11], and air-segmented reactors (ASRs) was compared under identical operational conditions. Because chemical reaction was not required for detection in these experiments, recorded peak profiles provided an indication of the extent of dispersion that occurred in each reactor. A more complex situation exists when chemical reaction is required for detection, as is the case for spectrophotometric continuous flow determinations. The recorded peak profiles depend not only on the dispersion characteristics of the reactor, but also on the kinetics of the chemical reactions involved. Analytical reactions with relatively slow kinetics were expected to bias the comparison in favor of c.f.a. For this reason, a spectrophotometric reaction that requires only a few seconds to reach equilibrium was chosen to compare the relative performance of f.i.a. and c.f.a. in the second set of experiments. It must be emphasized that this comparison pertains only to equilibrium-based spectrophotometric determinations. Conclusions drawn from data presented here should not be extrapolated to analytical schemes in which the formation of concentration gradients is a prerequisite.

EXPERIMENTAL

Instrumentation

The modified model IP-12 variable-speed peristaltic pump (Brinkmann Instruments, Westbury, NY) that was used for all work reported here has been described [12]; SMA flow-rated pump tubes (Technicon Instruments, Tarrytown, NY) were used for all experiments. Table 1 lists pump tube delivery factors as a function of pump speed. In c.f.a. experiments, proportioning errors were minimized by introducing air segments into the analytical

TABLE 1

Segmentation frequencies and delivery factors as a function of speed control settings on the modified Brinkmann IP-12 peristaltic pump

Speed control setting	Delivery factor[a]	Segmentation frequency (s^{-1})
14	0.33	0.5
28	0.67	1.0
42	1.00	1.5
56	1.33	2.0
70	1.67	2.5
84	2.00	3.0
98	2.33	3.5

[a]Factor by which nominal pump tube flow rate must be multiplied to estimate actual flow rate in ml min^{-1}.

stream in phase with the pump pulsations that occur each time a roller leaves the platen. This was accomplished by the dual pump tube method which was first described by Habig et al. [13]. The segmentation frequency associated with each pump speed used can also be found in Table 1.

Sample injection valves used in this study were of two types: a four-way slider valve (Alltech Associates, Deerfield, IL), and a Type 50, six-port rotary valve (Rheodyne, Cotati, CA). The slider valve was used for both f.i.a. and c.f.a. experiments on dye dispersion. It was pneumatically actuated and microprocessor-controlled [14]. The volume of dye injected into the carrier stream was a function of the pump speed and the valve actuation time as shown in Table 2. The rotary valve was used for chloride determinations by f.i.a. It was equipped with a 60-μl sample loop. Chloride samples were introduced into the system for c.f.a. by manual "pecked" sampling as described previously [12]. The sweep hand on a wrist watch was used to time "sample" and "wash" (c.f.a.) or "inject" and "load" (f.i.a.) intervals. Reaction coils for f.i.a. experiments were of two types: open tubular reactors (OTRs) which were made from 0.5-mm i.d. teflon tubing, and single-bead-string reactors (SBSRs) [11] which were made by packing 0.8-mm i.d. teflon tubing with 0.5-mm diameter glass beads (Propper Manufacturing Co., Long Island City, NY). Both reactor types were terminated with 1/4-28 flangeless gripper fittings (Omnifit, New York, NY) and then wrapped into tight, overlapping coils around a 1.0-cm diameter rod. The resulting coils were then slipped off the rod and secured at two points with plastic cable ties. Helical reaction coils (ASRs) of various lengths for c.f.a. experiments were made from 1.0-mm i.d. Micro-line tubing (Thermoplastics Scientific, Warren, NJ) by a procedure similar to the one reported by Amador [15]. All ASRs were formed around a glass rod with a diameter of approximately 8 mm. The lengths of all OTRs, SBSRs, and ASRs used in these studies can be found in Table 3. Letters in parentheses in this table are used to identify each reactor in the discussions that follow.

A functional diagram of the dual-beam, fiber-optic photometer used for all experiments is shown in Fig. 1. The light source consisted of a miniature

TABLE 2

Sample volume as a function of sample time for experiments on dye dispersion

Pump speed	Flow rate (ml min^{-1})	Sampling time (s) for different sample volumes (μl)					
		25	50	100	200	400	800
21[a], 45[b]	0.5	3.0	6.0	12.0	24.0	48.0	96.0
42[a], 90[b]	1.0	1.5	3.0	6.0	12.0	24.0	48.0
63[a]	1.5	1.0	2.0	4.0	8.0	16.0	32.0
84[a]	2.0	0.75	1.5	3.0	6.0	12.0	24.0

[a]Pump tubes with nominal flow rate of 1.0 ml min^{-1} at standard speed. [b]Pump tubes with nominal flow rate of 0.42 ml min^{-1} at standard speed, used with ASRs only.

TABLE 3

Reactor lengths used for experiments on dye dispersion

Reactor type	Length (cm)			
OTR	10 (A)	50 (B)	100 (C)	200 (D)
SBSR	10 (E)	25 (F)	50 (G)	100 (H)
ASR	10 (I)	30 (J)	50 (K)	75 (L)

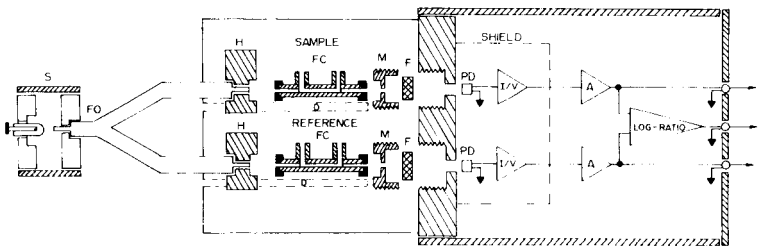

Fig. 1. Schematic representation of the dual-beam, fiber-optic filter photometer used for all experiments: S, source; FO, randomized, bifurcated fiber-optic bundle; H, fiber optic/flow cell holder; D, dovetailed slide; FC, flow cell; M, flow cell/interference filter mount; F, interference filter; PD, photodiode; I/V, operational amplifier current-to-voltage converter; A, second stage amplifier.

tungsten-halogen lamp (Welch-Allyn, Skanenteles Falls, NY) and a randomized, bifurcated fiber-optic assembly (Dolan-Jenner, Woburn, MA). Flow cells with path lengths of 1.0 cm and an internal volume of approximately 2 μl were obtained commercially (Gamma Enterprises, Mt. Vernon, NY), as were the narrow bandwidth (ca. 10 nm), three-cavity interference filters (Ditric Optics, Hudson, MA). Silicon photodiodes (E.G. & G., Electro-optics Division, Princeton, NJ) that were operated without bias served as photodetectors. Simple operational amplifier circuits served as fixed gain (ca. 2×10^8 VA^{-1}) current-to-voltage converters and variable gain ($\times 2$ to $\times 100$) second stage amplifiers for these detectors. A log-ratio amplifier (Analog Devices, Norwood, MA) was used to provide a final output of 1.0 V for an absorbance of 1.000. In routine operation, the drift of the log-ratio output was less than 1% per hour. The electronic bubble gate used to eliminate the air-segment artifact in c.f.a. has been described previously [12].

Data were recorded with a model SR-255 10-in. strip chart recorder (Heath Company, Benton Harbor, MI).

Reagents and standards

Borate buffer (0.025 M, pH 9.5) was prepared as described in the "Handbook of Chemistry and Physics" [16]. Brij-35 surfactant (Atlas Chemical Industries, Wilmington, DE) was added to this buffer in the amount of 1 ml l^{-1}.

A stock solution (ca. 0.001 M) of phenol red was prepared by dissolving 0.1 g of the dye in 250 ml of 0.001 M sodium hydroxide. A working solution

(ca. 10^{-5} M) used for dye dispersion experiments was prepared by suitable dilution of the stock with pH 9.5 borate buffer.

The reagent solution for chloride determinations [17] was prepared by dissolving 0.625 g of mercury(II) thiocyanate, 30.3 g of iron(III) nitrate, 3.3 ml of concentrated nitric acid, and 150 ml of methanol in about 500 ml of deionized-distilled water contained in a 1-l volumetric flask. The solution was diluted to the mark with the water, mixed, and transferred to an amber glass bottle. Then 1 ml of Brij-35 surfactant was added.

The primary chloride standard (100 mg l^{-1}) was prepared by dissolving 1.648 g of dried sodium chloride (analytical reagent grade) in 1 l of deionized-distilled water. Working standards in the concentration range of 5 to 45 mg l^{-1} chloride were prepared by dilution of the primary standard.

RESULTS

Experiments on dye dispersion

The simple flow system used for these experiments is shown schematically in Fig. 2. A four-way slider valve was used to direct either the working phenol red solution or the carrier solution (pH 9.5 borate buffer) into the reactors. Pump tubes with nominal flow rates of 1.0 ml min^{-1} were used for all experiments with OTRs and SBSRs. For experiments with ASRs at the two lower flow rates, however, pump tubes with nominal flow rates of 0.42 ml min^{-1} were used. This was necessary to achieve segmentation frequencies of at least 1.5 s^{-1} at all flow rates (see Tables 1 and 2). Reactor lengths were chosen such that the dwell time of the dye slug in each reactor type would be about the same in each set of experiments.

Signals that resulted when 25, 50, 100, 200, 400, and 800 μl of dye were injected sequentially into each of the twelve reactors at four different flow rates were recorded with a strip-chart recorder. In addition, five replicate determinations for one sample volume (usually 50 μl) were obtained at each flow rate for each reactor. The average and the standard deviation for each set of replicate determinations can be found in Table 4. Relative standard deviations of 1% or less were calculated for all data sets except those obtained with ASRs at the two higher flow rates. The higher relative standard deviations calculated for these data (3—5%) resulted from unfavorable experimental conditions that could not be avoided. At the two lower flow rates, the

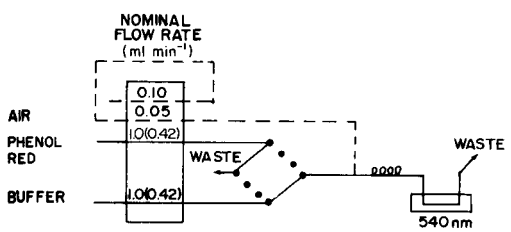

Fig. 2. Composite diagram of flow systems used for f.i.a. and c.f.a. experiments on dye dispersion.

TABLE 4

Precision (standard deviation) of experiments on dye dispersion[a]

Reactor	Flow rate (ml min^{-1})			
	0.5	1.0	1.5	2.0
OTR				
A	0.217 ± 0.003	0.241 ± 0.002	0.258 ± 0.007	0.274 ± 0.004
B	0.232[b] ± 0.001	0.280[b] ± 0.000	0.170 ± 0.002	0.164 ± 0.002
C	0.153[b] ± 0.001	0.150[b] ± 0.001	0.160[b] ± 0.001	0.204[b] ± 0.001
D	0.124[b] ± 0.001	0.227[c] ± 0.002	0.257[c] ± 0.001	0.305[c] ± 0.000
SBSR				
E	0.323 ± 0.002	0.334 ± 0.002	0.350 ± 0.003	0.364 ± 0.003
F	0.247 ± 0.002	0.254 ± 0.002	0.273 ± 0.003	0.285 ± 0.003
G	0.173 ± 0.002	0.183 ± 0.002	0.194 ± 0.002	0.203 ± 0.001
H	0.128 ± 0.001	0.138 ± 0.001	0.148 ± 0.002	0.146 ± 0.002
ASR				
I	0.436 ± 0.004	0.430 ± 0.000	0.408 ± 0.004	0.392 ± 0.015
J	0.424 ± 0.002	0.422 ± 0.003	0.371 ± 0.007	0.364 ± 0.009
K	0.440 ± 0.002	0.435 ± 0.001	0.368 ± 0.008	0.352 ± 0.014
L	0.433 ± 0.002	0.431 ± 0.002	0.354 ± 0.009	0.309 ± 0.017

[a]Sample volume is 50 μl unless otherwise indicated. [b]100-μl sample volume. [c]200-μl sample volume.

injected dye slug was divided into about ten segments while at the two higher flow rates, the dye slug was divided into only about five segments. For this reason, proportioning errors were more pronounced at the higher flow rates. Under normal operating conditions used for c.f.a., this situation would not arise. In any case, the precision of these two data sets is sufficient for qualitative comparisons.

Tracings of peaks recorded when 50 μl of dye was injected into each reactor are shown in Fig. 3. This figure provides qualitative insight into the dispersion characteristics of the three reactor types. Examination of the peak profiles obtained with the four OTRs (A, B, C, D) reveals that peak heights decrease and peak widths broaden as the reactor length increases. Of course, reactor length (or volume) and dwell time of the sample slug in the reactor are two sides of the same coin. A general rule of thumb [18] states that dispersion in OTRs increases with the square root of either the reactor length (volume) or the mean dwell time of the sample slug in the reactor. This relationship was found to hold to a fair approximation under all experimental conditions. As the reactor lengths increase, the peaks become more sym-

Fig. 3. Curve tracings of peaks from experiments on dye dispersion with open tubular reactors, single-bead-string reactors, and air-segmented reactors at flow rates of 0.5—2.0 ml min^{-1}. The four peaks in each set correspond to lengths A—D for the OTR, E—H for the SBSR, and I—L for the ASR (see Table 3).

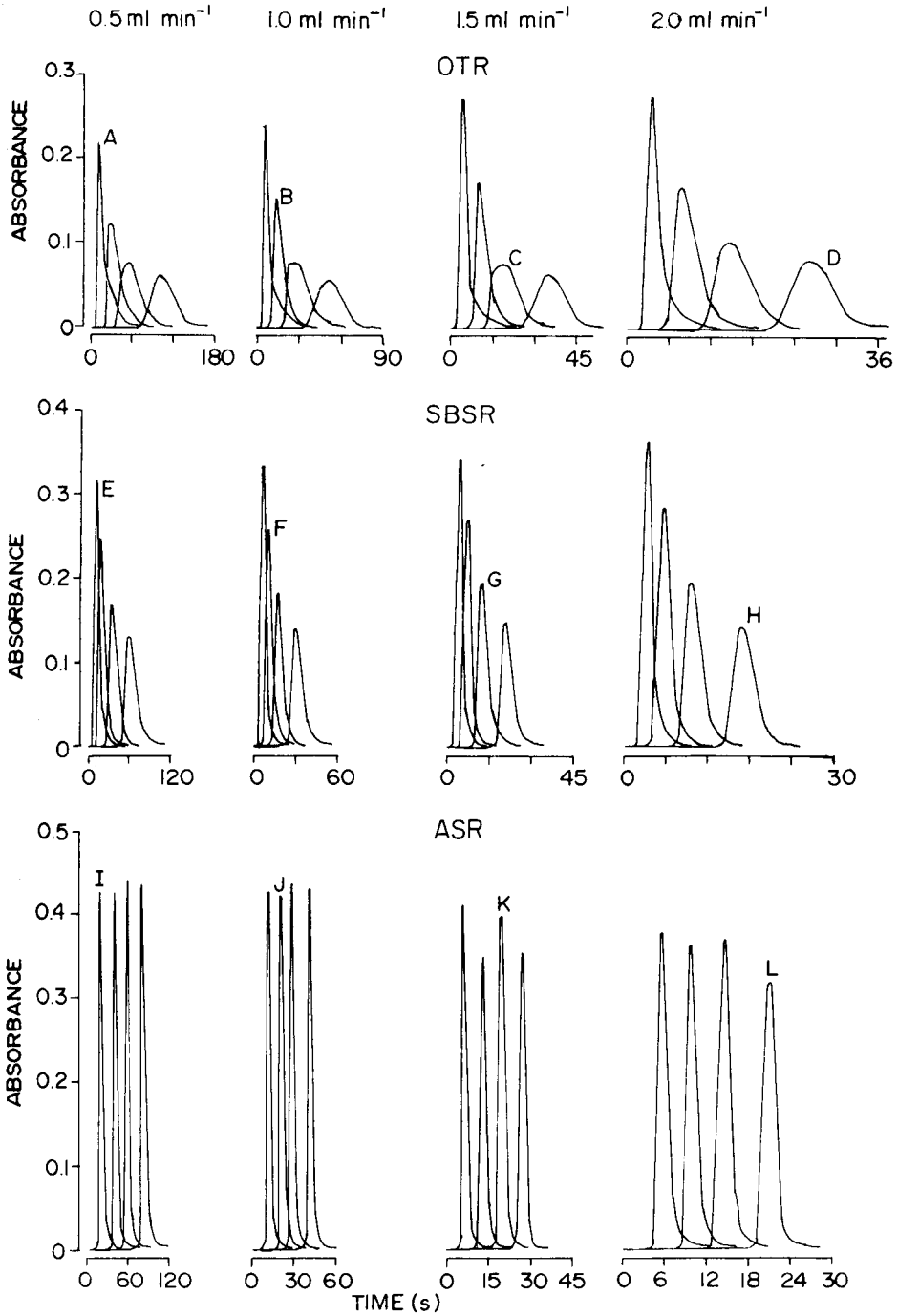
0.5 ml min⁻¹
1.0 ml min⁻¹
1.5 ml min⁻¹
2.0 ml min⁻¹
OTR
SBSR
ASR
ABSORBANCE
TIME (s)
A
B
C
D
E
F
G
H
I
J
K
L
0.3
0.2
0.1
0
0.4
0.5
180
90
45
36
120
60
30
15
6
12
18
24

metrical as predicted by the "tanks-in-series" model of dispersion in OTRs [19]. Another clearly visible trend is the increase in peak heights and decrease in peak widths that occur as the flow rate increases. This trend is due primarily to the decreased residence time of the dye slug in the reactor, but it may also, to a lesser extent, reflect an increase in secondary flow effects. These same trends hold for peaks recorded for the four SBSRs (E, F, G, H). However, at comparable residence times, peak widths for SBSRs were about half those recorded for OTRs. Also tailing, which was particularly noticeable in peaks recorded for the shortest OTR (A), was much less pronounced in the SBSR (E) of comparable length, especially at lower flow rates. In general, peaks recorded for SBSRs were more symmetrical than those recorded for OTRs. This suggests that the mixing efficiency of SBSRs is better than in OTRs, as reported by Reijn et al. [11] who stressed that dispersion is not synonymous with adequate mixing, especially in OTRs. The peaks recorded for the four ASRs (I, J, K, L) exhibited very different characteristics. First, reactor length had very little effect on either peak heights or peak widths at a given flow rate. Peak heights also decreased slightly as the flow rate increased in keeping with theory [20], although mixing effects that occurred in the sampling valve before the dye slug was segmented with air would tend to obscure this effect. Under normal operating conditions for c.f.a. where pecked sampling is used, sharper peaks would have been recorded. Nonetheless, the ability of air segments to minimize dispersion is readily apparent. This study shows very clearly that under comparable experimental conditions the extent of dispersion in the three reactor types can be ranked as follows: ASR < SBSR < OTR.

Determination of chloride

In the second set of experiments, the three reactor types were evaluated in terms of their performance in the simple spectrophotometric determination of chloride by its reaction with mercury(II) thiocyanate in the presence of iron(III) [17, 21, 22]. The f.i.a. and c.f.a. manifolds used for these experiments are shown schematically in Figs. 4 and 5, respectively.

When chloride standards in the concentration range 5—35 mg l^{-1} were injected into the single-line f.i.a. manifold (Fig. 4) at 30 s intervals, the peaks shown in Fig. 6A were recorded. As can be seen, there is a large blank signal

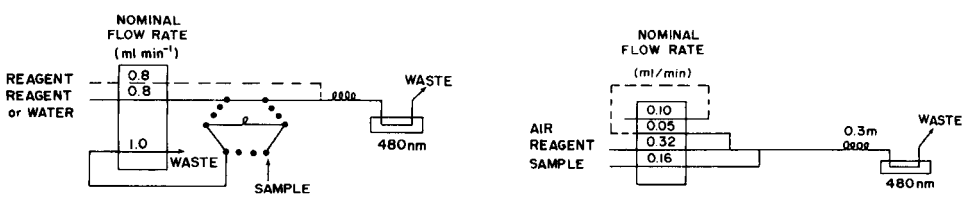

Fig. 4. Composite diagram of flow systems used for the determination of chloride by f.i.a.

Fig. 5. Diagram of the flow system used for determination of chloride by c.f.a. Pump speed 56, $n = 2$.

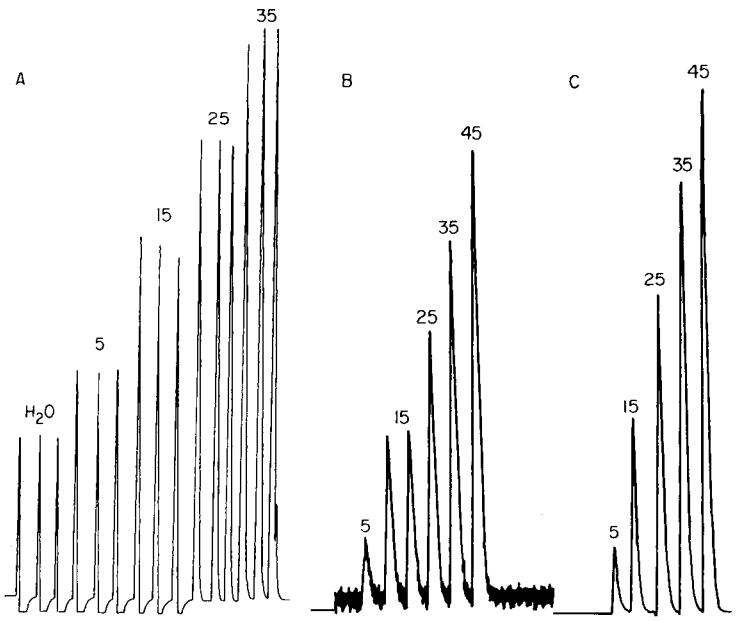

Fig. 6. Peaks recorded for chloride determinations by f.i.a.: (A) with the single-line manifold; (B) with a merging-zones manifold including a 50-cm open tubular reactor; (C) with a merging-zones manifold including a 50-cm single-bead-string reactor. The numbers on the peaks relate to chloride concentrations (mg l^{-1}) injected.

(i.e., injection of deionized-distilled water produced a peak), and each positive peak is followed by a negative peak before the signal returns to baseline. These effects are frequently observed when an aqueous sample is injected into a partly non-aqueous reagent stream [18] or when there are large differences between the viscosities of the sample and the reagent stream [23]. The effects are due to temporal changes in refractive index and concentration along the dispersed sample slug. This behavior was not observed in an almost identical experiment described by Hansen and Růžička [17], probably because they used a flow cell with an internal volume of 18 μl and a sample volume of 30 μl. The 2-μl flow cell and 60-μl sample volume used in the experiments reported here would be expected to increase these effects.

The above problem was eliminated by adding a second pump tube to the flow-injection system (dashed line in Fig. 4). Here samples were injected into a distilled water carrier stream that merged with the reagent stream in a tee-mixer in order to eliminate changes in the refractive index of the flow stream through the detector. Peaks obtained with the merging-zones system (50-cm OTR) are also shown in Fig. 6. As expected, no response was observed when distilled water was injected into the system, but peaks and the baseline signal were noisy (Fig. 6B); this was due to poor mixing between the reagent and sample carrier streams. When the 50-cm OTR was replaced with a 50-cm

SBSR, the peaks shown in Fig. 6C were recorded; here the baseline noise was reduced to negligible levels, peak heights increased, and the time required to return to baseline from peak maxima decreased. This illustrates the benefits of using SBSRs for routine f.i.a. The decreased dispersion permits sampling frequency to be increased, while the mixing efficiency is actually improved relative to an OTR of comparable volume. Further experiments showed that good results were still obtained when the length of the SBSR was reduced to 25 cm. At a flow rate of 1.6 ml min^{-1} (carrier, 0.8 ml min^{-1}; reagent, 0.8 ml min^{-1}, pump speed 42), sampling rates of 180 h^{-1} were achieved with interaction of 1% or less. When the pump speed was doubled (total flow rate $\approx$ 3.2 ml min^{-1}), it was possible to increase the sampling rate to 360 h^{-1}. Peaks recorded at this sampling rate are shown in Fig. 7A; interaction was estimated at $\approx$2%.

The same chloride standards were determined with the c.f.a. manifold (see Fig. 5). The pump speed and segmentation frequency (n) were 56 and 2 s^{-1}, respectively, which resulted in a total liquid flow rate of approximately 0.6 ml min^{-1}. Peaks recorded with this system at a sampling rate of 360 h^{-1} (sample time = wash time = 5 s) are shown in Fig. 7B. Data from chloride determinations with both the flow systems are compiled in Table 5. In all cases, less reagent and sample were required for the continuous-flow determinations, while linearity of the standard curves and precision of analytical results were similar for both.

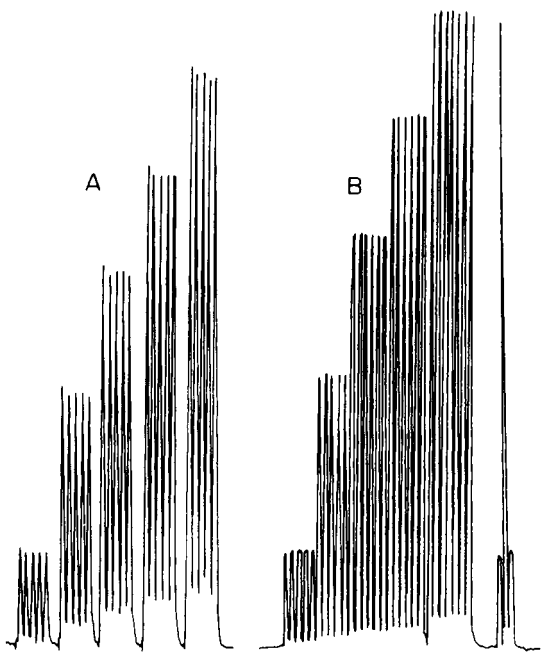

Fig. 7. Peaks recorded for chloride determinations at a sampling rate of 360 h^{-1}: (A) f.i.a. with merging zones and a 25-cm single-bead-string reactor; (B) c.f.a.

TABLE 5

Comparison of c.f.a. and f.i.a.: spectrophotometric chloride determinations

	C.f.a.[a]			F.i.a.[b]		
Sample rate (h^{-1})	360	240	180	360	240	180
Sample time (s)	5	10	15	—	—	—
Wash time (s)	5	5	5	—	—	—
Sample volume (μl)	18	36	54	60	60	60
Reagent volume (μl)[c]	71	107	142	267	400	533
Precision (% RSD)[d]	0.43	0.25	0.34	1.72	0.44	0.67
% Interaction	0.6	0.6	0.5	$\simeq$1—2	>1	>1
Slope	0.020	0.021	0.021	0.018	0.019	0.019
Y intercept	0.032	0.034	0.033	0.036	0.040	0.037
r_{xy} (correl. coeff.)	0.998	0.998	0.998	0.997	0.997	0.997

[a]Pump speed 56, n = 2, t = 30 s, d_t = 0.1 cm. [b]Pump speed 84, 25-cm SBSR. [c]C.f.a.: the volume of reagent delivered during one sample and wash interval. F.i.a.: the volume of reagent delivered during the time interval between sample injections. [d]Calculated from 5 replicate determinations of the 15 mg l^{-1} chloride standard.

DISCUSSION

The foregoing experiments underscore the fundamental differences between f.i.a. and c.f.a. In f.i.a. the sample enters the reactor as a slug and begins to disperse into the carrier stream at the moment of injection. The sample loop is itself a mixing stage, as is the flow cell. Except in cases where samples are not required to undergo chemical reaction prior to detection, some dispersion of the sample slug is necessary. In single-line flow-injection systems, in fact, dispersion is the only mechanism by which the sample and reagent can interact. In dual-line flow-injection systems where the sample and reagent are merged in a tee-connector, mixing is improved, but may still be incomplete. This can be a drawback to the f.i.a. approach for spectrophotometric determinations, especially those that require more than about 30 s to reach an appreciable degree of completion because it is generally necessary to compromise between adequate mixing of the sample and reagent on the one hand, and excessive broadening of the sample slug on the other. There are several techniques, however, that enhance mixing and minimize dispersion in f.i.a. which can make this compromise more favorable. These include inducing secondary flow by using tightly coiled or "wavy" tubes [24] rather than loosely coiled OTRs, and by using SBSRs rather than OTRs. Both these approaches are successful because they disrupt the parabolic velocity profile normally associated with laminar flow. Another effective way to increase residence time without excessive dispersion is simply to inject the sample into the carrier stream and then stop the pump [18]. To a close approximation when the flow stops, dispersion stops. After sufficient reaction time has elapsed, the pump is restarted, and the reacted sample is propelled

into the detector. This approach is effective, but operationally cumbersome, and it often decreases sample throughput rates.

The situation is quite different for c.f.a. because the process of mixing the sample with reagent is not dependent on sample dispersion. In c.f.a. the sample slug is divided into a number of nominally identical segments before it enters the reactor. Then each segment is proportioned with reagent, and mixing within each segment is enhanced by the microcirculation pattern that develops naturally in a segmented, flowing stream [25]. Furthermore, air segments provide barriers to the establishment of parabolic velocity profiles in all zones of the system: pecked sampling greatly reduces dispersion that would otherwise arise during the sampling process; segmented flow greatly reduces dispersion in the reactor; and bubble-through flow cells reduce dispersion associated with detection. In addition, other factors being equal, dispersion decreases as the flow rate decreases which leads to conservation of samples and reagents.

The foregoing experiments demonstrate that for equilibrium-based spectrophotometric determinations, c.f.a. competes favorably with f.i.a. even for relatively simple chemistries with fast reaction rates. It cannot be denied, however, that in the limit f.i.a. is simpler, operationally, than c.f.a. Consider the case where a sample is treated with a single reagent and detected. The minimum requirements for a flow-injection system are a single-channel pump, an injection valve, and a recording detector. The same determination with c.f.a. would require three pump channels (one each for sample, air, and reagent), and the detector signal would have to be gated to eliminate the air bubble artifact; otherwise a fourth pump channel would be required to debubble the flow stream prior to detection. Also, for operation without an automatic sampler, introduction of samples with a valve in f.i.a. is much less taxing than the manual, pecked sampling used for c.f.a., which requires precise and continuous timing. Thus for single-reagent determinations where the differences in performance between c.f.a. and f.i.a. are small, f.i.a. may be preferred because of the relative ease and simplicity with which determinations can be done. However, for spectrophotometric determinations that require multiple reagent additions, or reaction times that exceed about 30 s, the increased complexity of c.f.a. may be offset by virtue of its high mixing efficiency, low dispersion, and conservation of samples and reagents. The point at which this trade-off is reached is not clear-cut, and the choice between these two complementary continuous flow techniques will be strongly influenced by the ingenuity of the operators and their predisposition to c.f.a. or f.i.a.

This work was partly supported by National Science Foundation grant No. CHE 83-20620.

REFERENCES

1 L. T. Skeggs, Am. J. Clin. Pathol., 28 (1957) 311.
2 K. K. Stewart, G. R. Beecher and P. E. Hare, Fed. Proc., 33 (1974) 1439.
3 J. Růžička and E. H. Hansen, Anal. Chim. Acta, 78 (1975) 145.
4 M. Margoshes, Anal. Chem., 49 (1977) 17, 1861.
5 J. Růžička, E. H. Hansen, M. Mosbaek and F. J. Krug, Anal. Chem., 49 (1977) 1858.
6 M. Margoshes, Anal. Chem., 54 (1982) 678A, 1106A.
7 C. B. Ranger, Anal. Chem., 54 (1982) 1106A.
8 L. R. Snyder, Anal. Chim. Acta, 114 (1980) 3.
9 B. Rocks and C. Riley, Clin. Chem., 28 (1982) 409.
10 C. J. Patton, Ph.D. Dissertation, Michigan State University, East Lansing, MI, 1982.
11 J. M. Reijn, W. E. Van Der Linden and H. Poppe, Anal. Chim. Acta, 123 (1981) 229.
12 C. J. Patton, M. Rabb and S. R. Crouch, Anal. Chem., 54 (1982) 1113.
13 R. L. Habig, B. W. Schlein, L. Walters and R. E. Thiers, Clin. Chem., 15 (1969) 1045.
14 R. Q. Thompson, Ph.D. Dissertation, Michigan State University, East Lansing, MI, 1982.
15 E. Amador, Clin. Chem., 18 (1972) 164.
16 R. C. Weast (Ed.), Handbook of Chemistry and Physics, 48th edn., Chemical Rubber Corp., Cleveland, OH, 1967.
17 E. H. Hansen and J. Růžička, J. Chem. Educ., 56 (1979) 677.
18 J. Růžička and E. H. Hansen, Flow Injection Analysis, Wiley, New York, 1981, pp. 20, 21, 144.
19 O. Levenspiel, Chemical Reaction Engineering, 2nd edn., Wiley, New York, 1972.
20 L. R. Snyder, J. Chromatogr., 125 (1976) 287.
21 D. M. Zall, D. Fisher and M. Q. Garner, Anal. Chem., 28 (1956) 1665.
22 L. T. Skeggs and H. Hochstrasser, Clin. Chem., 10 (1964) 918.
23 D. Betteridge, Talanta, 23 (1976) 409.
24 K. Hofman and I. Halasz, J. Chromatogr., 199 (1980) 3.
25 L. R. Snyder and H. J. Adler, Anal. Chem., 48 (1976) 1022.

Analytica Chimica Acta, 179 (1986) 203—208
Elsevier Science Publishers B.V., Amsterdam — Printed in The Netherlands

DETERMINATION OF SUCROSE IN THE PRESENCE OF GLUCOSE IN A FLOW-INJECTION SYSTEM WITH IMMOBILIZED MULTI-ENZYME REACTORS

BO OLSSON, BERIT STÅLBOM and GILLIS JOHANSSON*

Department of Analytical Chemistry, University of Lund, P.O. Box 124, S-221 00 Lund (Sweden)

(Received 30th July 1985)

SUMMARY

Sucrose is determined by its reactions in a packed-bed enzyme reactor containing co-immobilized invertase, mutarotase and glucose oxidase. The hydrogen peroxide produced is measured spectrophotometrically after a chromogenic reaction. Glucose in the samples is decomposed in a pre-reactor containing co-immobilized mutarotase, glucose oxidase and catalase. The response is linear over more than three decades. The detection limit is 0.1 μM sucrose for injection volumes of 80 μl. The sample frequency is 80 h^{-1} with an r.s.d. of 0.3%. The response for glucose is 0.7% that for sucrose.

Sucrose can be determined by a number of different methods, e.g., by polarimetry, density or refractive index measurements, chromatography, or by chemical reactions [1]. The physical methods are very fast and precise but may be less correct because of the presence of other compounds. Most samples contain optically active interferents but it is often tacitly assumed that errors will compensate each other. Corrections can be made by measuring the difference in polarization before and after inversion of the sucrose. Determination by gas chromatography relies on an imprecise derivatization and determination by liquid chromatography would benefit from further development of columns and detection methods. The chemical methods for sucrose can be made very selective by using enzymatic reagents, but they are at present less reproducible than the physical methods and most give much the same response for glucose as for sucrose. A separate glucose determination is therefore often made so that a correction can be applied. A direct determination with an enzyme electrode with an outer glucose-eliminating layer has been described [2].

A flow-injection method with immobilized enzymes should be able to provide increased speed, precision and convenience compared with previous enzymatic procedures. Immobilized enzymes have been used in flow systems for sucrose determinations [3—6] and a recent report also uses flow-injection methodology [7].

0003-2670/86/$03.50

EXPERIMENTAL

Chemicals

Invertase (EC.3.2.1.26) from *Candida utilis* (Sigma grade X, 500 U mg^{-1}), mutarotase (EC.5.1.3.3) from porcine kidney (Sigma, 5700 U mg^{-1}), glucose oxidase (EC.1.1.3.4) from *Aspergillus niger* (Serva, 300 U mg^{-1}), catalase (EC.1.11.1.6) from bovine liver (Sigma, 65000 U mg^{-1}), and peroxidase (EC.1.11.1.7) from horseradish (Sigma, type VI, 300 U mg^{-1}) were used as received. 2,4-Dichlorophenol-6-sulphonate (DCPS) was synthesized as described before [8]; it contained unreacted dichlorophenol which acts as a mediator in the colour-forming peroxidase reaction.

The reagent contained 20 mM DCPS, 1 mM 4-aminoantipyrine (BDH Chemicals) and 1 mM EDTA in 0.1 M citrate buffer, pH 6.0. It can be used for up to a week if kept in a dark bottle. The buffer used in the flow system was 0.1 M citrate, pH 6.0. The azide buffer contained 60 mg l^{-1} sodium azide.

Preparation of reactors

Sucrose reactor. Controlled-pore glass (Serva, CPG-10, pore diameter 66.8 nm, particle size 75—125 μm) was alkylamino derivatized and activated with glutaraldehyde as described before [9]. Invertase (8.6 mg), mutarotase (0.5 mg) and glucose oxidase (5.2 mg) were dissolved in 2.4 ml of 0.1 M sodium phosphate buffer, pH 7.0, and thoroughly dialyzed against the same buffer. The activated glass (0.20 g) was suspended in the chilled enzyme solution and the reaction was allowed to proceed overnight at 8°C. The preparation was packed into nylon tubing (i.d. 2.4 mm, length 80 mm) provided with retaining polypropylene nets and Altex screw fittings. A solution of 0.5 M sodium chloride was pumped through the reactor for 1 h, and the reactor was stored filled with phosphate buffer.

Glucose-eliminating reactor. Mutarotase (0.5 mg), glucose oxidase (5.2 mg) and catalase (0.5 mg) were co-immobilized on controlled-pore glass (0.20 g) by the procedure described above. The sodium chloride solution was pumped through the nylon tubing reactor (length 90 mm) for 12 h to desorb any loosely bound catalase.

Peroxidase reactor. Peroxidase (5 mg) was diazo-coupled to 0.10 g of arylamino-derivatized controlled-pore glass, CPG-glucophase-G (Pierce, pore diameter 46 nm, particle size 37—74 μm) as described before [10] and the material was packed into a nylon tubing reactor (length 40 mm).

The flow-injection system

A four-channel peristaltic pump (Gilson Minipuls 2) was used to deliver the solutions to the manifold at the flow rates indicated (in ml min^{-1}) in Fig. 1. The sample, normally 80 μl, was introduced into the carrier stream by means of a pneumatically actuated loop injector (Cheminert SVA 8031). Each confluence point was followed by a short single-bead string reactor (length 50 mm, i.d. 0.8 mm, bead diameter 0.5 mm) to improve the mixing. All

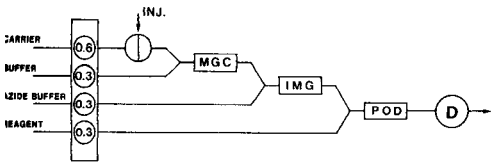

Fig. 1. Diagram of the flow injection system. MGC, glucose eliminating reactor; IMG, sucrose reactor; POD, peroxidase reactor. For details, see text.

connecting lines were of 0.5 mm i.d. teflon tubing and were kept as short as possible. The flow-through spectrophotometer (LKB, model 2051) was set at 514 nm.

RESULTS AND DISCUSSION

Sucrose reactor

Enzymatic determination of sucrose is commonly done by a sequence of reactions:

$$\text{sucrose} + H_2O \xrightarrow{\text{invertase}} \alpha\text{-D-glucose} + \text{D-fructose}$$

$$\alpha\text{-D-glucose} \xrightleftharpoons{\text{mutarotase}} \beta\text{-D-glucose}$$

$$\beta\text{-D-glucose} + O_2 + H_2O \xrightarrow[\text{oxidase}]{\text{glucose}} \text{D-gluconic acid} + H_2O_2$$

Invertase acts selectively on terminal, unsubstituted β-D-fructofuranosides [11]. Glucose oxidase is very selective for β-D-glucose and the combination will therefore only act on glucose and sugars which leave a free glucose after one or more fructose units have been split off. The hydrolysis produces α-D-glucose which will mutarotate slowly (half-life = 4 min at 30°C, pH 6.5 [12]) to β-D-glucose until an equilibrium is reached, with 27% α-D-glucose and 63% β-D-glucose. Mutarotase speeds up the reaction so that equilibrium is reached in a very short time.

The immobilization and particularly the co-immobilization of the three enzymes necessary for sucrose determination has been studied in detail previously [12]. It has also been shown that the values of the apparent first-order rate constants for the three enzymes in a reactor should be about the same for optimum performance [13]. Glutaraldehyde immobilization was selected for this work, and it was found that dialysis of the enzyme solution before coupling was essential. Each enzyme was first immobilized separately and packed in a reactor so that the rate constant of the material could be evaluated. The data were used to estimate the proportion of the enzymes necessary for co-immobilization on porous glass.

The stoichiometry of the conversion of sucrose to hydrogen peroxide in the sucrose reactor was determined at different flow rates. The results showed

that a 360-μl reactor can produce hydrogen peroxide quantitatively from 0.2 ml min^{-1} to the flow rate used in the analytical system (1.2 ml min^{-1}). The conversion drops to 96% at 1.4 ml min^{-1} and 93% at 1.6 ml min^{-1} as the residence time in the reactor becomes too short. Experiments in which auxiliary reactors with a single enzyme were also inserted in the flow indicated that invertase and glucose oxidase were limiting the overall rate to about the same extent. There was an excess of mutarotase activity in spite of the small amount taken for co-immobilization.

Glucose-eliminating reactor

Glucose is perhaps the commonest sugar other than sucrose in food samples and it will also give hydrogen peroxide in stoichiometric amounts in the sucrose reactor, as shown above. Two possibilities are available for the determination of sucrose in the presence of glucose: one in which the glucose is decomposed prior to the sucrose reactor and one based on a simultaneous determination of glucose and glucose plus sucrose, with subsequent subtraction of glucose equivalents from the total [5, 7]. Masoom and Townshend [7] split the flow so that one half of the sample reached a glucose oxidase reactor directly and one half after passing through an invertase/mutarotase reactor.

The approach used in this work was to decompose glucose in a reactor containing co-immobilized glucose oxidase and mutarotase, as well as catalase to destroy hydrogen peroxide:

$$H_2O_2 \xrightarrow{\text{catalase}} H_2O + 1/2\ O_2$$

A glucose-eliminating reactor with a volume of 400 μl was inserted in the flow upstream from the sucrose reactor (Fig. 1). Glucose samples were injected and any α-D-glucose, β-D-glucose or hydrogen peroxide which emerge from the first reactor will produce a detector response. It was found that 99.3% of the response to glucose was eliminated by the reactor at a flow rate of 0.9 ml min^{-1}.

Analytical results

The peak shapes obtained by injection of different volumes of a sucrose standard are shown in Fig. 2. The peak width at half maximum height is almost constant at 15 s, up to a sample volume of 80 μl. The sample frequency at 1% carry-over was 80 h^{-1}.

Sucrose produced a linear calibration graph (Fig. 3) from the detection limit, 0.1 μM, up to 500 μM, where the peak absorbance (1.5) became limiting. The sensitivity for glucose was 0.7% of that for sucrose up to at least 1 mM glucose (Fig. 3).

Table 1, which reports on some sucrose determinations with samples containing increasing amounts of glucose, verifies that the glucose elimination works equally well in the presence of sucrose. The relative standard deviation

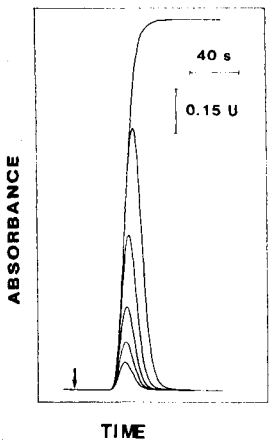

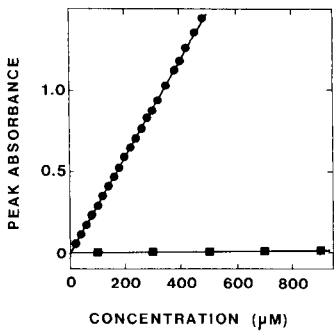

Fig. 2. Response injections of 10, 20, 40, 80, 160 and 2000 μl of a 200 μM sucrose standard.

Fig. 3. Peak height absorbance as a function of sugar concentration: (•) sucrose; (▪) glucose.

TABLE 1

Error in the determination of 200 μM sucrose caused by the presence of glucose in the sample

[Glucose] (μM)	Peak absorbance	Error (%)
0	0.480	—
100	0.480	0.0
300	0.488	1.7
500	0.493	2.7
700	0.496	3.3
900	0.498	3.8

was 0.3% for 200 μM sucrose (n = 20). The mean systematic error from glucose was less than 1% at equimolar concentrations of glucose and sucrose. The enzyme reactors were stable during the course of this work and no measurable decrease in activity could be observed after 6 months in a refrigerator.

Properties of the method

Mutarotase should be present in a sucrose reactor intended for a fast analytical system because of the slowness of the spontaneous mutarotation; without mutarotase, the signal became 5% of its previous value in the present system. The mutarotase will also make the response immune to factors (pH, temperature, etc.) which affect the rate of spontaneous mutarotation. The

robustness of the system is greatly improved by the selection of reactors with essentially 100% conversion because this makes the system more independent of factors that affect the activity of the enzymes, such as pH, temperature, ionic strength, and inhibitors or activators in the samples [14]. Mutarotase in the sucrose reactor also makes it necessary to include this enzyme in the glucose-eliminating reactor, as α-D-glucose otherwise would pass and be converted to the β-form in the sucrose reactor. It is necessary to co-immobilize the mutarotase and the glucose oxidase so that the α-form can continuously be transformed to the β-form as the latter is consumed.

Oxygen depletion through consumption in the enzymatic reactions sets an upper limit to the glucose and sucrose concentrations that can be determined. If the reaction rate or conversion decreases in the first reactor, a break-through of glucose will occur which can give a large positive error. Lack of oxygen in the sucrose reactor may give negative errors. Table 1 shows that the present system has been designed so that no effects of oxygen depletion are noticeable within the specified range. The method has a large linear dynamic range and a decrease in the injection volume would make it possible to cover a higher range. Dilution in the flow system will automatically adjust the oxygen requirements in the reactors.

Many of the enzymatic methods for sucrose determinations which have been described have produced curved calibration graphs. The linear calibration of the present method arises both because the conversion is high and because the substrate concentrations in the enzyme reactors are well below the corresponding Michaelis constants [13] so that the reactions are first order [14]. The selectivity for sucrose over glucose can easily be improved by increasing the size of the glucose-eliminating reactor. A doubling should theoretically decrease the interference level to the square of the present value, i.e., to 5×10^{-3}%. The increased reactor volume would cause additional peak broadening, and thus a decreased sample throughput, but would not impair the precision.

REFERENCES

1 Kirk-Othmer Encyclopedia of Chemical Technology, Vol. 21, 3rd edn., Wiley, New York, 1983, p. 871.
2 F. Scheller and R. Renneberg, Anal. Chim. Acta, 152 (1983) 265.
3 J. W. Finley and A. C. Olson, Cereal Chem., 52 (1974) 500.
4 D. J. Inman and W. E. Hornby, Biochem. J., 137 (1974) 25.
5 J. A. Burns, Cereal Food World, 21 (1976) 594.
6 Y. Y. Kulis, E. V. Ralis and R. S. Penkova, Appl. Biochem. Microbiol., 15 (1979) 215.
7 M. Masoom and A. Townshend, Anal. Chim. Acta, 171 (1985) 185.
8 D. Barham and P. Trinder, Analyst (London), 97 (1972) 142.
9 G. Johansson and L. Ögren, Anal. Chim. Acta, 84 (1976) 23.
10 B. Olsson, H. Lundbäck and G. Johansson, Anal. Chim. Acta, 167 (1985) 123.
11 S. Hestrin, D. S. Feingold and M. Schramm, in S. P. Colowick and N. O. Kaplan (Eds.), Methods in Enzymology, Vol. 1, Academic Press, New York, 1955, p. 251.
12 M. V. Morkyavichene, A. A. Dikchyuvene, A. B. Paulyukonis and D. A. Kazlavskas, Appl. Biochem. Microbiol., 18 (1982) 557.
13 M. V. Morkyavichene, A. A. Dikchyuvene, A. B. Paulyukonis and D. A. Kazlavskas, Appl. Biochem. Microbiol., 20 (1984) 60.
14 G. Johansson, L. Ögren and B. Olsson, Anal. Chim. Acta, 145 (1983) 71.
15 H. Ooshima, M. Sakimoto and Y. Harano, Biotechnol. Bioeng., 22 (1980) 2155.

Analytica Chimica Acta, 179 (1986) 209—216
Elsevier Science Publishers B.V., Amsterdam — Printed in The Netherlands

MEASUREMENTS OF KINETIC PARAMETERS OF INORGANIC PYROPHOSPHATASE BY FLOW-INJECTION PROCEDURES

HISANOBU HIRANO*, YOSHINOBU BABA, NORIMASA YOZA and SHIGERU OHASHI

Department of Chemistry, Faculty of Science, Kyushu University, Hakozaki, Higashiku, Fukuoka, 812 (Japan)

(Received 24th July 1985)

SUMMARY

Two flow-injection systems were designed for characterizing the enzymatic hydrolysis of pyrophosphate by inorganic pyrophosphatase (EC 3.6.1.1). By using a molybdenum(VI) reagent the selective determination of a product, orthophosphate, in the presence of pyrophosphate was made. An anion exchange column was employed for the simultaneous determination of both the substrate and the product with a molybdenum(V)/molybdenum-(VI) reagent. The effects of magnesium concentration and reaction temperature on the enzyme activity were determined. The Michaelis constant and maximum velocity at 25° C and pH 7.2 were evaluated. K_m was ca. 3 μM.

Inorganic pyrophosphatase (P_2ase or PP_iase, EC 3.6.1.1) is the enzyme that catalyzes the hydrolysis of inorganic pyrophosphate (diphosphate) to orthophosphate in a neutral medium [1—7]:

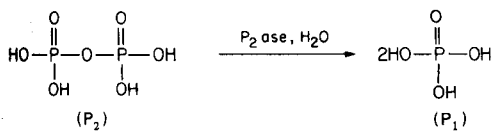

Pyrophosphatase is widely distributed in nature (in micro-organisms, mammalian tissues, plants and soils) and is likely to be indispensable to all living systems with nucleotides. The pyrophosphatase isolated from baker's yeast has been well characterized by x-ray crystallography [2] and amino-acid sequence analysis [3]. The molecular weight of the pyrophosphatase with two identical subunits is 64084.

Pyrophosphatase is considered to play an important role in controlling the pyrophosphate concentration in various biological reactions associated with nucleotides and to regulate the formation of cyclic adenosine monophosphate, ATP → cAMP + pyrophosphate and the formation of RNA [5]. Therefore, much attention has been focussed on the reaction mechanisms and the substrate specificity of pyrophosphatase in the presence of various metal ions [1—7]. The interesting possibility of using pyrophosphatase as a marker

0003-2670/86/$03.50

enzyme in cancer research has been suggested [6]. A current project in this laboratory is investigating the fate of polyphosphates in environmental waters. Activities for hydrolysis of polyphosphates in environmental waters are monitored, with a view to evaluating the role of free enzymes and enzyme carriers such as micro-organisms, cells and cell fragments that may control the lifetimes of polyphosphates and the process of eutrophication.

In order to proceed with such kinetic researches, analytical techniques are required for evaluation of the kinetic parameters for the above reaction. Two flow-injection systems, with molybdenum(VI) and molybdenum(V)/molybdenum(VI) as chromogenic reagents, are described in this paper. A normal flow-injection system with two lines was used for selective determination of the product (orthophosphate) in the presence of the substrate (pyrophosphate). For the simultaneous determination of orthophosphate and pyrophosphate at low concentrations of pyrophosphate, a medium-pressure liquid chromatographic system or a flow-injection system combined with an anion exchange column was successfully used. The effects of magnesium concentration and reaction temperature on the pyrophosphatase activity were established, and the Michaelis constant, K_m, and maximum velocity, V_{max}, at 25°C and pH 7.2 were evaluated.

EXPERIMENTAL

Samples and reagents

Potassium dihydrogen phosphate and tetrasodium pyrophosphate decahydrate were used (Wako, Osaka). Inorganic pyrophosphatase (EC 3.6.1.1) isolated from baker's yeast was purchased (Sigma Chemical Co.). The specific activity of the lyophilized enzyme as specified by Sigma was 500—600 U mg^{-1} of protein at pH 7.2 and 25°C.

The molybdenum(VI) reagent for the flow-injection measurement of V_{max} was prepared by dissolving 5.3 g of ammonium molybdate [$(NH_4)_6Mo_7O_{24}\cdot 4H_2O$] in 1 l of 0.3 M sulfuric acid. The molybdenum(VI) concentration was ca. 0.03 M. The molydenum(V)/(VI) reagent for the liquid chromatographic measurement of K_m and V_{max} was prepared as follows: 1 l of ca. 0.03 M molybdenum(VI) solution was prepared by dissolving ammonium molybdate in 1.8 M H_2SO_4, and 0.65 g of zinc dust (free from arsenic) was added. Some molybdenum(VI) was reduced to molybdenum(V) during the complete dissolution of the zinc. The resultant reagent was stable at least for a month, and was used for the determination of orthophosphate and polyphosphates.

Equipment and procedures

The apparatus for the construction of the flow systems was the same as that used in previous papers [4, 7—11]. The main equipment included reciprocating pumps with four plungers (Jasco, RP-4F), a spectrophotometer with an 8-μl flow cell (Jasco, Uvidec-100W) and an h.p.l.c. system (Jasco, Trirotar). An anion-exchange separation column (4 mm i.d. × 5 cm, TSK-gel SAX,

10 μm) was used. Isocratic elutions were made at a flow rate of 1.0 ml min^{-1} with an eluent composed of 0.21 M potassium chloride/1 mM disodium EDTA/10 mM ammonia.

All incubation experiments with pyrophosphatase were done at pH 7.2 (5 mM Tris-HCl buffer), at various magnesium concentrations and at reaction temperatures from 10 to 40° C.

Careful preparation of pure water to be used as a solvent was needed. A Milli-Q system with a Millipore filter was used throughout. All glass vessels used for the incubation of reaction mixtures had been autoclaved at 121° C. Without such treatment, pseudo-enzymatic hydrolysis of pyrophosphate was often observed even in the absence of pyrophosphatase.

RESULTS AND DISCUSSION

Measurement of V_{max} in the flow-injection system

The system in Fig. 1 was designed so that the enzymatic hydrolysis could be stopped instantly and the orthophosphate detected in the presence of the pyrophosphate. Sample solution was injected into the water stream via a loop valve injector (100 μl). The molybdenum(VI) reagent was acidic enough to stop the enzymatic hydrolysis by acidifying the sample zone at the confluence point. Only orthophosphate reacted with the molybdenum(VI) reagent in the reaction coil to form 12-molybdophosphoric acid. The absorbance of this yellow species was monitored at 380 nm. The two-line system permitted the reproducible detection of orthophosphate without the appearance of a negative peak even at zero sample concentration despite the strong u.v. absorption of the reagent.

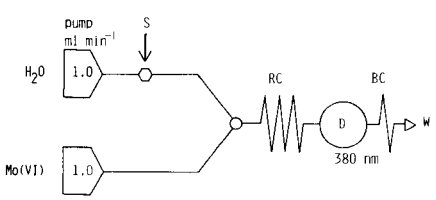

Fig. 1. Flow-injection system for the selective determination of orthophosphate in the presence of pyrophosphate: S, sample injection; RC, reaction coil (0.5 mm i.d. × 5 m, PTFE, 30° C); D, detector; BC, back-pressure coil (0.25 mm i.d. × 1 m, PTFE); W, waste.

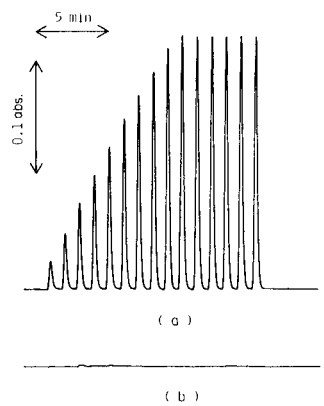

Fig. 2. Kinetic flow-injection profiles for the enzymatic hydrolysis of pyrophosphate: (a) with magnesium ions (1.0 mM); (b) without magnesium ions. Initial conditions: 0.5 mM pyrophosphate, 3.0 × 10^{-9} M pyrophosphatase, pH 7.2, 25° C (see text).

Figure 2 shows the kinetic flow-injection profiles for the enzymatic hydrolysis of pyrophosphate at constant initial concentrations of substrate and enzyme, in the presence and absence of magnesium ions. Aliquots (each 100 μl) of the reaction mixtures incubated at 25°C were successively injected at 1-min intervals into the manifold (Fig. 1). In the presence of magnesium ions (Fig. 2a), the peak height corresponding to the amount of orthophosphate increased linearly with time until it became constant toward the end of enzymatic hydrolysis. In the absence of magnesium ion, the formation of orthophosphate was not observed (Fig. 2b), which indicated the requirement of magnesium ions as a pyrophosphatase activator.

The hydrolysis of pyrophosphate (P_2) by the enzyme (P_2ase) can be represented as follows in the Michaelis-Menten expression [5]:

$$1/2(d[P_1]/dt) = -d[P_2]/dt = k_2 [P_2ase]_0 [P_2]/(K_m + [P_2])$$
$$= V_{max}[P_2]/(K_m + [P_2]) \quad (1)$$

where subscript 0 denotes the initial concentration. At $[P_2] \gg K_m$, the peak height in the kinetic flow-injection profile was expected to increase linearly with time and $d[P_1]/dt$ was regarded as equal to $2V_{max}$ (a constant). The linear increase of orthophosphate concentration suggested a low K_m value ($\ll$0.5 mM) which is consistent with the literature values (ca. 0.005 mM) [6, 12–20]. The value of $2V_{max}$ at 25°C was evaluated directly from the slope in Fig. 2(a) to be 0.11 mM min^{-1}, corresponding to a specific activity of 580 U mg^{-1} of protein.

Effect of magnesium ion concentration and temperature on pyrophosphatase activity

In the absence of magnesium ions, pyrophosphatase activity was not observed (Fig. 2b). To understand the effect of magnesium ions in more detail, pyrophosphatase activities, i.e., the slopes ($d[P_1]/dt$) of the kinetic profile in Fig. 2, were measured at 25°C over a wide range of magnesium concentrations. In all experiments pyrophosphatase concentration was 1.5×10^{-9} M. The pyrophosphate concentration was varied from 0.1 mM to 0.5 mM at 0.1-mM intervals. At all pyrophosphate concentrations, the orthophosphate concentration increased linearly with time, indicating that the slope is equal to $2V_{max}$ and $K_m \ll 0.1$ mM. With an increase in magnesium ion concentration the pyrophosphatase activity increased, to a maximum at 1 mM magnesium (Fig. 3). Unless otherwise stated, subsequent experiments were made with 1.0 mM magnesium chloride.

Figure 4 shows the effect of temperature (T) on pyrophosphatase activity. The activities were measured by the system in Fig. 1. Because the activity is equal to $2k_2[P_2ase]_0$, k_2 can easily be calculated. The value of k_2 at 25°C was 1.8×10^4 min^{-1}. From the linear Arrhenius plot, log k_2 vs. $1/T$, with correlation coefficient 0.998 (5 points), the activation energy was evaluated to be 9.6 kcal mol^{-1}. This is markedly less than that for chemical hydrolysis of pyrophosphate (30 kcal mol^{-1} at pH 7.0 [21]).

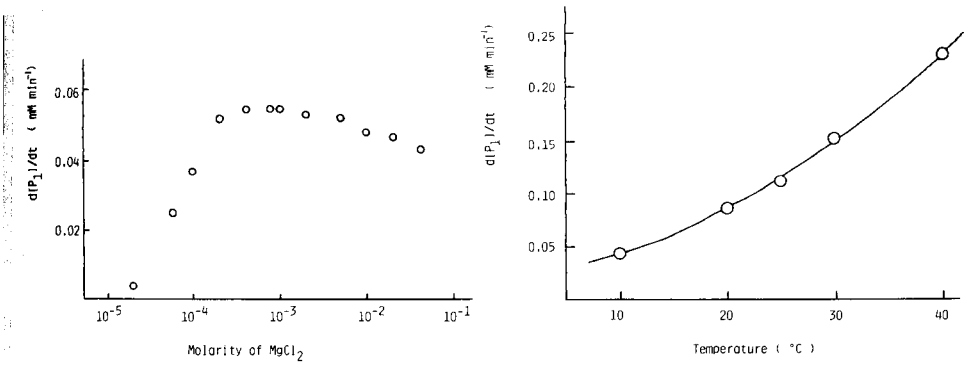

Fig. 3. Effect of magnesium concentration on the production of orthophosphate (P_i). In all runs, the initial pyrophosphatase concentration was 1.5×10^{-9} M; the pyrophosphate concentration was varied from 0.1 mM to 0.5 mM at 0.1-mM intervals (pH 7.2, 25°C).

Fig. 4. Effect of temperature on pyrophosphatase activity. Initial conditions: 3.0×10^{-9} M pyrophosphatase, 0.5 mM pyrophosphate, 1.0 mM magnesium, pH 7.2, 25° C.

Measurement of K_m *and* V_{max} *by liquid chromatography*

The molybdophosphate method based on the flow-injection system in Fig. 1 was advantageous for measuring V_{max} under the condition $[P_2] \gg K_m$. However, the yellow color was too insensitive to evaluate K_m, because the measurement of activity in Eqn. 1 had to be done under the condition $K_m \approx [P_2]$. To monitor the orthophosphate produced at low concentrations of pyrophosphate (0.01 mM), the more sensitive heteropoly molybdenum blue method based on the molybdenum(V)/(VI) reagent was used.

The liquid chromatography system in Fig. 5 was designed so that both P_2 and P_i at low concentrations (0.01 mM) could be monitored simultaneously. This system is based on a post-column reaction with the molybdenum (V)/(VI) reagent and an anion-exchange separation. By shortening the column to 5 cm, the pressure drop at the inlet of the column became less than 10 kg cm^{-2}. This improvement enabled the use of PTFE flow lines and a loop valve sample injector that had not been suitable for high-pressure experiments. The pumping line P_b was installed for multi-purpose use and was not always necessary.

The reagent reacted with orthophosphate to form a heteropoly blue species which could sensitively be detected at its absorption maximum, 820—830 nm. The hydrolysis of pyrophosphate to orthophosphate and the color reaction proceeded simultaneously in the reaction coil maintained at 140° C.

Aliquots (300 μl) of the mixture of the two phosphates were successively injected into the manifold (Fig. 5) at 3-min intervals. The resultant profile in Fig. 6 shows the reproducible detection of orthophosphate and pyrophosphate. The recoveries of orthophosphate and pyrophosphate were confirmed by peak-area measurement with a Chromatopac (Shimadzu).

Aliquots (300 μl) of the reaction mixture of pyrophosphate with the enzyme incubated at 25° C were successively injected into the manifold

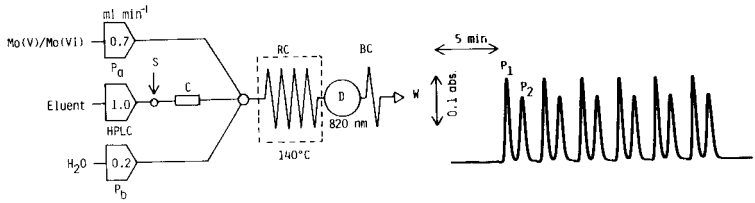

Fig. 5. Flow-injection system for the simultaneous determination of orthophosphate and pyrophosphate. P_a and P_b, pumps; HPLC, pumping system for h.p.l.c.; S, automatic sample injector; C, separation column; RC, reaction coil (0.5 mm i.d. × 20 m, PTFE, 140°C); BC, back-pressure coil (0.25 mm i.d. × 1.5 m, PTFE); other notations as in Fig. 1.

Fig. 6. Reproducibility of successive peaks for orthophosphate (initially 2×10^{-5} M) and pyrophosphate (initially 1×10^{-5} M).

(Fig. 5) at 3-min intervals, with the first injection 2 min after the start of the reaction (Fig. 7). Pyrophosphate was confirmed to be stable at least for 2 h in the buffered solution when pyrophosphatase was absent. The enzymatic reaction was initiated by adding the enzyme solution to the buffered pyrophosphate solution. By using this chromatographic system, the hydrolysis of P_2 with a half-life of the order of 10 min could easily be monitored. The peak area or the amount of orthophosphate in Fig. 7 increased with time at the expense of pyrophosphate and tended to become constant toward the end of enzymatic hydrolysis, as is also shown in Fig. 2. A marked difference between the kinetic profiles in Figs. 2 and 7 was that orthophosphate in Fig. 2 increased linearly with time under the condition $[P_2] \gg K_m$, while orthophosphate in Fig. 7 increased non-linearly with time when the pyrophosphate concentration became comparable to or less than the K_m value. The results in Fig. 7 are useful for evaluating not only V_{max} but also K_m on the basis of the above Michaelis-Menten equation.

The Michaelis constant and maximum velocity have usually been evaluated by making the measurements of the initial velocities at various substrate concentrations [5]. An alternative approach for evaluating kinetic parameters is based on the analysis of a progress curve obtained at a fixed substrate concentration. The progress curve method [22] was used in this work to determine the kinetic parameters of pyrophosphatase. The basic equation for the progress curve method is

$$([P_2]_0 - [P_2])/t = V_{max} - K_m\{\ln([P_2]_0/[P_2]\}/t \quad (2)$$

where $[\ ]_0$ and $[\ ]$ are the concentrations at time zero and t, respectively. From the linear plots of $([P_2]_0 - [P_2])/t$ vs. $\ln([P_2]_0/[P_2])/t$, K_m and V_{max} values can be evaluated as the slope and intercept, respectively.

Table 1 shows the K_m and V_{max} values at various enzyme concentrations. As would be expected from the relation, $V_{max} = k_2[P_2ase]_0$, the V_{max} values in Table 1 were approximately proportional to the pyrophosphatase concentrations. The V_{max} value at 1.5×10^{-11} M pyrophosphatase was in close

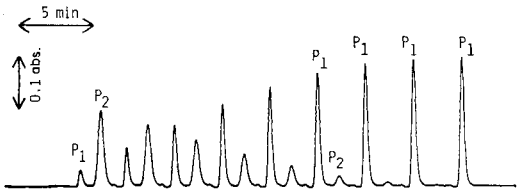

Fig. 7. Kinetic flow-injection profile for the enzymatic hydrolysis of pyrophosphate (1×10^{-5} M) in presence of 6.0×10^{-11} M pyrophosphatase and 1.0 mM magnesium ions.

TABLE 1

Michaelis constants and maximum velocities evaluated for different pyrophosphatase concentrations at 25°C and pH 7.2 ($[P_2]_0 = 1.0 \times 10^{-5}$ M and $[Mg^{2+}]_0 = 1.0$ mM)

Pyrophosphatase (10^{-11} M)	K_m ± s.d.[a] (μM)	V_{max} ± s.d.[a] (μM min^{-1})
1.5	4.1 ± 0.5	0.28 ± 0.01
3.0	3.7 ± 0.3	0.46 ± 0.04
4.5	3.3 ± 0.6	0.64 ± 0.02
6.0	2.6 ± 0.3	0.74 ± 0.03
7.5	2.7 ± 0.3	1.11 ± 0.08

[a]Standard deviation ($n = 4$).

agreement with the expected value, 0.27 μM min^{-1}, which was calculated on the basis of the k_2 value (1.8×10^4 min^{-1}) given in the previous section. However, there is no reasonable explanation for the gradual decrease of the K_m values in Table 1 with increasing pyrophosphatase concentrations. The K_m value at 1.5×10^{-11} M pyrophosphatase is somewhat lower than the K_m value, ca. 5 μM, in the literature [6, 12—20]. Such an uncertainty and discrepancy seem to be tolerable, because the experiments to determine K_m values as small as 10^{-6} M involve various difficult problems concerning analytical techniques and data analysis.

REFERENCES

1 B. S. Cooperman, Methods Enzymol., 87 (1982) 526.
2 G. Bunick, G. P. McKenna, F. E. Scarbrough, E. C. Uberbacher and D. Voet, Acta Crystallogr., Sect. B: 34 (1978) 3210.
3 S. A. Cohen, R. Sterner, P. S. Kein and R. L. Heinrickson, J. Biol. Chem., 253 (1978) 889.
4 N. Yoza, H. Hirano, Y. Baba and S. Ohashi, J. Chromatogr., 325 (1985) 385.
5 R. W. McGilvery and G. W. Goldstein, Biochemistry; A Functional Approach, Saunders, New York, 1983.
6 J. B. Shatton, A. Williams and S. Weinhouse, Cancer Res., 43 (1983) 3742.
7 N. Yoza, H. Hirano, M. Okamura, S. Ohashi, Y. Hirai and K. Tomokuni, Chem. Lett., (1983) 1433.
8 Y. Baba, N. Yoza and S. Ohashi, J. Chromatogr., 295 (1984) 153.

9 Y. Hirai, N. Yoza and S. Ohashi, Anal. Chim. Acta, 115 (1980) 269.
10 Y. Hirai, N. Yoza and S. Ohashi, J. Chromatogr., 206 (1981) 501.
11 N. Yoza, K. Ishibashi and S. Ohashi, J. Chromatogr., 134 (1977) 497.
12 K. M. Welsh and B. S. Cooperman, Biochemistry, 23 (1984) 4947.
13 W. B. Knight, S.-J. Ting, S. Chauang, D. Dunaway-Mariano, T. Haromy and M. Sundaralingam, Arch. Biochem. Biophys., 227 (1983) 302.
14 J. B. Shatton, C. Ward, A. Williams and S. Weinhouse, Anal. Biochem., 130 (1983) 114.
15 S. E. Volk, A. A. Baykov, E. B. Kostenko and S. M. Avaeva, Biochim. Biophys. Acta, 744 (1983) 127.
16 J. W. Ridlington, Y. Yang and L. Butler, Arch. Biochem. Biophys., 153 (1972) 714.
17 Y. A. Shakkov and P. Nyren, Acta Chem. Scand., Ser. B: 36 (1982) 689.
18 D. D. Hackney, J. Biol. Chem., 255 (1980) 5320.
19 T. A. Rapoport, W. E. Hohme, J. Reich, P. Heitman and S. M. Rapoport, Eur. J. Biochem., 26 (1972) 237.
20 J. Josse, J. Biol. Chem., 241 (1965) 1948.
21 J. R. Van Wazer, E. J. Griffith and J. F. McCullough, J. Am. Chem. Soc., 77 (1955) 287.
22 T. Spector, Anal. Biochem., 138 (1984) 242.

Analytica Chimica Acta, 179 (1986) 217—223
Elsevier Science Publishers B.V., Amsterdam — Printed in The Netherlands

THE KINETIC DETERMINATION OF CLINICALLY SIGNIFICANT ENZYMES IN AN AUTOMATED FLOW-INJECTION SYSTEM WITH FLUORESCENCE DETECTION

M. MASOOM and P. J. WORSFOLD*
Department of Chemistry, University of Hull, Hull, HU6 7RX (Great Britain)
(Received 14th June 1985)

SUMMARY

An automated flow-injection manifold is described for the kinetic determination of enzyme activities by a stopped-flow procedure with fluorescence detection. The linear calibration range for alkaline phosphatase is 0—250 U l^{-1} with a precision of 2%; sample throughput is 35—40 h^{-1}. Linear responses were also obtained for lipase (0—100 U l^{-1}), acetylcholinesterase (0—500 U l^{-1}) and chymotrypsin (0—200 U l^{-1}). The advantages of this approach to the determination of plasma enzyme activities include sensitivity and the small sample and reagent volumes needed.

The determination of enzyme activities in biological fluids has become an important diagnostic aid and constitutes a significant fraction of the workload in clinical laboratories. In some cases, organ-specific enzymes can be released from the organ cells into the blood plasma during the course of a disease, resulting in short-term elevated plasma enzyme levels. In other cases, the supply of plasma-specific enzymes normally secreted by particular organs into the blood plasma can be depressed as a result of cellular damage. The most important organ-specific indicator enzymes include lipase, α-amylase and chymotrypsin (pancreas), alkaline phosphatase (bone), cholinesterase, γ-glutamyltranspeptidase and glutamate—pyruvate transaminase (liver) and creatine kinase, lactate dehydrogenase and glutamate—oxaloacetate transaminase (cardiac muscle).

Enzyme activities are normally determined by a kinetic or two-point method under zero-order reaction conditions [1] with u.v.-visible spectrophotometric detection. Detection limits would be improved by using fluorescence techniques, provided that background interference from the protein matrix could be removed and that suitable fluorogenic substrates were available [2].

This paper describes an automated flow-injection manifold based on merging zones, stopped-flow and fluorescence detection, for the determination of enzyme activities by an initial rate method. Four important diagnostic enzymes, alkaline phosphatase, lipase, acetylcholinesterase (AChE) and chymotrypsin, are assayed.

0003-2670/86/$03.50

EXPERIMENTAL

Reagents

Alkaline phosphatase determination. Alkaline phosphatase (orthophosphoric-monoester phosphohydrolase; E.C. 3.1.3.1, from bovine kidney; Sigma) was obtained as a lyophilized powder with an activity of 5 U mg^{-1}. Standards covering the range 0—250 U l^{-1} were prepared in cold deionized water and stored at 4° C when not in use. Umbelliferone (7-hydroxycoumarin; Sigma) was phosphorylated as described by Guilbault et al. [3] and used as the substrate. A working substrate solution (1×10^{-4} M) was prepared in Tris buffer (0.1 M) at pH 8.

Lipase determination. Lipase (triacylglycerol lipase, triacylglycerol acyl hydrolase; E.C. 3.1.1.3, from *candida cylindracia*; Sigma) was obtained as a lyophilized powder with an activity of 670 U mg^{-1}. Standards covering the range 0—250 U l^{-1} were prepared in cold deionized water and stored at 4°C when not in use.

Dibutyryl fluorescein was used as the substrate and was prepared as follows. A solution of butyric anhydride (0.2 mol) in dry benzene was added slowly to a solution of fluorescein (0.1 mol) in pyridine at 0° C. The mixture was stirred overnight and poured over an ice/concentrated hydrochloric acid mixture. After vigorous shaking, the organic phase was dried over anhydrous magnesium sulphate and the solvent removed. The resulting solid (m.p. 117—118°) was recrystallized four times from methanol to minimize residual fluorescence. A working substrate solution (5×10^{-5} M) was made by dissolving dibutyrylfluorescein (2.4 mg) in 2-methoxyethanol (5 ml) and diluting to 100 ml with Tris buffer (0.1 M) at pH 8.

Acetylcholinesterase determination. Acetylcholinesterase (acetylcholine acetyl hydrolase; E.C. 3.1.1.7, from electric eel; Sigma) was obtained as a lyophilized powder with an activity of 1355 U mg^{-1}. Standards covering the range 0—500 U l^{-1} were prepared in cold deionized water and stored at 4°C when not in use. *N*-Methylindoxyl acetate was used as the substrate after preparation by the method of Guilbault et al. [4]. A stock solution was made by dissolving *N*-methylindoxyl acetate (0.1 g) in 2-methoxyethanol (5 ml) and standards over the range 0—4 mM were prepared by diluting appropriate volumes of the stock solution to 25 ml with water.

Chymotrypsin determination. Chymotrypsin (E.C. 3.4.21.1, from bovine pancreas; Sigma) was obtained as a lyophilized powder with an activity of 40 U mg^{-1}. Standards covering the range 0—200 U l^{-1} were prepared in cold deionized water and stored at 4°C when not in use. *N*-Glutaryl-glycylglycyl-L-phenylalanine β-naphthylamide (GGPNA; Sigma) was used as the substrate. Aqueous buffered standards over the range 0—5 mM were prepared from a stock solution (0.1 M) in Tris buffer (pH 8.0).

Instrumentation and procedures

The flow-injection manifold used is shown in Fig. 1. Enzyme (20 μl) and substrate (20 μl) were injected simultaneously into separate carrier streams

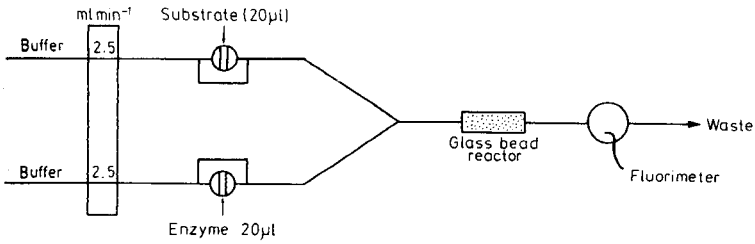

Fig. 1. Stopped-flow merging-zones manifold for the fluorescence determination of plasma enzymes. Substrate and enzyme are simultaneously injected into buffer streams and synchronously merged. Distance from injection valves to confluence point, 12 cm; from confluence point to detector, 50 cm. Glass bead reactor, 2.5 cm × 1.5 mm i.d.

from two low-pressure injection valves (Rheodyne 5020) and synchronously merged 12 cm downstream. The carrier streams (see below for composition) were pumped at 2.5 ml min^{-1}; poly(vinyl chloride) pump tubing was used with a peristaltic pump (Ismatec Mini-S 820). Teflon tubing (0.5 mm i.d.) was used for the remainder of the system. The distance from the confluence point to the detector was 50 cm, inclusive of a packed reactor (2.5 cm × 1.5 mm i.d.) containing glass beads (0.5—0.75 mm diameter) to ensure complete mixing of enzyme and substrate. The detector was a filter spectrofluorimeter (Perkin-Elmer LS2) equipped with a 7-µl flow-through cell; the excitation and emission wavelengths used for determination of each enzyme are given below. The signals from the fluorimeter (1 V full scale) were fed directly to the analogue-to-digital (A/D) converter of a microcomputer (BBC model B), at a rate of 1 s^{-1}, with 10-bit resolution.

The rate of reaction was determined by stopping a segment of the merged enzyme and substrate zones in the flow cell for moving-point kinetic analysis. This was achieved by switching off the pump 14.2 s after sample injection, waiting 10 s for the reaction zone to settle in the flow cell, and then taking fluorescence readings for a predetermined measurement time. The measurement time was divided into three equal periods and readings were taken at 1 s^{-1} over the first and third periods. A set of reaction rates was obtained from the difference between corresponding readings in each period and the mean reaction rate was determined. All results reported are from triplicate injections unless otherwise stated.

A microcomputer (BBC model B) was used to control the operation of the two injection valves, the switching of the peristaltic pump, the reproducible timing of events, and the collection and treatment of data. The timing was controlled by an on-board elapsed-time clock, reproducible to within 10 ms. The switching of the valves and the pump was controlled by three optically isolated a.c. output modules (Radio Spares 348-469), capable of switching output loads operating on a.c. supplies between 48 and 240 V a.c., at currents up to 3 A, from a TTL open collector compatible input signal. The a.c. modules were connected to the user port of the BBC via a 7407 hexadecimal

driver chip (RS 75492) to protect the user port from reverse voltages. Two injection valves were connected to a modified pneumatic actuator (Rheodyne 5701) such that simultaneous injection was achieved when the actuator was activated. The pneumatic arm was driven by compressed air (60 psi) via two solenoid valves (RS 348-380) connected to two a.c. output modules. The third a.c. output module was used to control the peristaltic pump.

A block diagram of the automated flow-injection system is shown in Fig. 2.

RESULTS AND DISCUSSION

Alkaline phosphatase

Alkaline phosphatase (AP) catalyses the hydrolysis of a variety of phosphate esters and plays an important role in the diagnosis of bone and liver diseases. The recommended method for determining alkaline phosphatase activity in clinical laboratories is to measure the rate of formation of *p*-nitrophenol from *p*-nitrophenyl phosphate at 405 nm [5]. For this work a more sensitive fluorescence procedure was used, with umbelliferone phosphate as the substrate. It is stable in aqueous solution, highly selective for alkaline phosphatase, has a fast enzymatic hydrolysis rate and yields the highly fluorescent umbelliferone as product [3]:

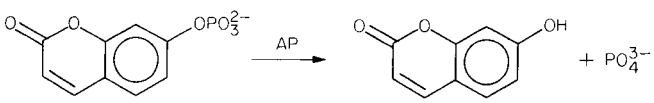

For the flow-injection procedure, λ_{ex} was 340 nm and λ_{em} was 450 nm; the carrier streams were both Tris buffer (0.1 M) at pH 8.0, and the measurement time during the stopped-flow procedure was 60 s. The effect of substrate concentration was investigated by using a 250 U l^{-1} alkaline phosphatase standard; concentrations greater than 1×10^{-4} M gave a high background fluorescence because of the presence of free umbelliferone. Hence 1×10^{-4} M

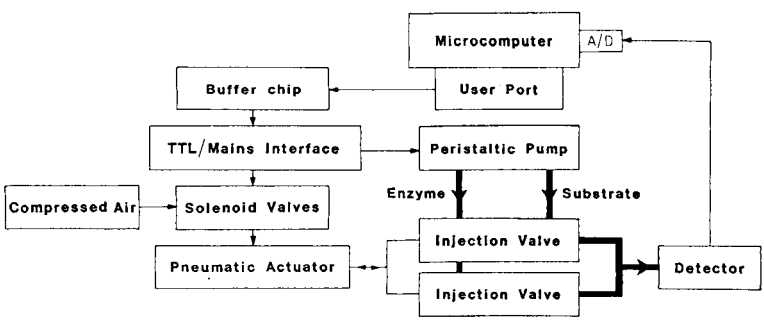

Fig. 2. Block diagram of the automated flow injection system. Bold lines indicate the flow-injection manifold; thin lines indicate electrical or mechanical signals.

umbelliferone phosphate was used for all further work, prepared daily to minimise non-enzymatic hydrolysis.

Nine alkaline phosphatase standards covering the normal and elevated levels found in serum (0—250 U l^{-1}) were analysed; a linear calibration graph (r = 0.9989) was obtained. The within-batch precision for the 100 U l^{-1} standard, injected ten times, was 2.0%. Two control sera (Versatol Hi and Versatol Lo; General Diagnostics) were analysed in triplicate and gave mean results of 245 U l^{-1} and 59 U l^{-1} respectively, compared with the quoted values of 256 ± 11 U l^{-1} and 53 ± 11 U l^{-1}. The total analysis time was 85 s per sample, giving a realistic sample throughput of 35—40 h^{-1}.

Lipase

Lipase is an important enzyme in digestion processes and as a diagnostic indicator for pancreatitis. It cleaves a variety of esters (e.g., triglycerides). It is distinct from other esterases in that it acts on emulsified rather than water-soluble substrates [6]. Several chromogenic and fluorogenic substrates have been used for the determination of lipase activity [7] but the method of Kramer and Guilbault [8] was used for this work. It involves the hydrolysis of dibutyrylfluorescein by lipase to fluorescein:

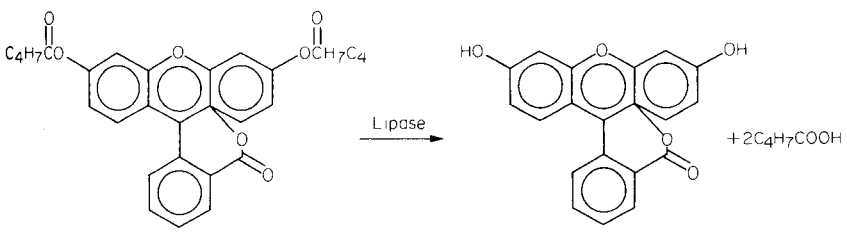

For the flow-injection procedure, λ_{ex} was 480 nm and λ_{em} was 520 nm, the carrier streams were both Tris buffer (0.1 M) at pH 8.0, and the measurement time during the stopped-flow procedure was 240 s (because of the slow reaction). 2-Methoxyethanol, which was used to dissolve the substrate, can cause a decrease in enzyme activity and therefore the substrate concentration used (5×10^{-5} M) was the highest that would form a clear emulsion in 5:95 2-methoxyethanol/water. This restricted the linear range for lipase to 0—100 U l^{-1}; the linear regression equation for seven lipase standards covering this range had a correlation coefficient of 0.9987.

Acetylcholinesterase

Cholinesterases are a group of esterases that have a marked affinity for quaternary ammonium salts [9], and acetylcholine is the primary substrate for acetylcholinesterase (AChE); AChE is one of several indicator enzymes for liver disease and its inhibition by certain pesticides can also be used analytically. The preferred fluorogenic substrate for AChE is *N*-methylindoxyl acetate [4]:

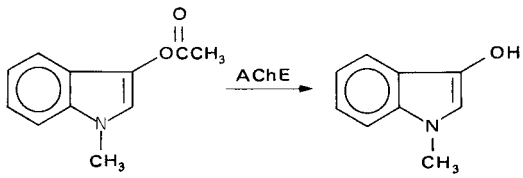

For the flow-injection procedure, λ_{ex} was 400 nm and λ_{em} was 470 nm both carrier streams were phosphate buffer (0.1 M) at pH 7.5 and the measurement time during the stopped-flow procedure was 60 s. A substrate concentration of 2×10^{-3} M was found to be sufficient to give zero-order reaction conditions for aqueous AChE solutions up to 500 U l^{-1}. Seven standards covering the range 0—500 U l^{-1} gave a linear calibration graph (r = 0.9996). Samples in the normal range (1900—3800 U l^{-1}) could be accommodated if parameters such as measurement time or substrate concentration were changed or an asynchronous merging technique was used.

Chymotrypsin

Chymotrypsin is a relatively inselective enzyme that cleaves peptide linkages in which the carbonyl function derives from an aromatic amino-acid residue, and is one of three indicator enzymes used for the diagnosis of pancreatic diseases. A stable, water-soluble substrate for the fluorimetric determination of chymotrypsin, for which the reaction is both sensitive and selective, has been reported by Rinderknecht and Fleming [10], and was used in the present study. *N*-Glutaryl-glycylglycyl-L-phenylalanine-β-naphthylamide (GGPNA) releases fluorescent β-naphthylamine upon cleavage by chymotrypsin.

For the flow-injection procedure, λ_{ex} was 375 nm and λ_{em} was 415 nm; both carrier streams were Tris buffer (0.1 M) at pH 8.0, and the measurement time was 120 s. A substrate concentration of 5×10^{-3} M was sufficient to prevent substrate depletion in the flow system and was not affected by non-enzymatic hydrolysis. The response was linear up to 200 U l^{-1}, but because the clinically significant range in adult serum is 1—6 U l^{-1} (abnormal) or 10—27 U l^{-1} (normal) [10], six standards covering the range 0—50 U l^{-1} were measured. The linear regression equation on these results had a correlation coefficient of 0.9991.

Conclusions

This paper demonstrates the well-documented attractions of flow injection systems, particularly their high throughput, rapid readout, flexibility, low cost and ease of automation. Of particular importance for the determination of plasma enzyme levels are the small sample and reagent volumes required in the merging-zones manifold and the sensitivity achieved by the stopped-flow procedure with fluorescence detection.

The authors thank Ian Whiteside for the construction of the automated system. One of us (M.M.) thanks the Ministry of Education, Government of

Pakistan, for a research grant and the University of Baluchistan, Quetta, for study leave.

REFERENCES

1 H. U. Bergmeyer, Methods of Enzymatic Analysis, Vol. 2, Academic Press, London, 1974, p. 840.
2 G. G. Guilbault, Enzymatic Methods of Analysis, Pergamon Press, Oxford, 1970.
3 G. G. Guilbault, S. H. Sadar, R. Glazer and J. Haynes, Anal. Lett., 1 (1968) 333.
4 G. G. Guilbault, M. H. Sadar, R. Glazer and C. Skou, Anal. Lett., 1 (1968) 365.
5 D. F. Davidson, Enzyme Microbiol. Technol., 1 (1979) 9.
6 L. Sarda and P. Desnuelle, Biochim. Biophys. Acta, 30 (1958) 513.
7 R. G. Jensen, Lipids, 18 (1983) 650.
8 D. N. Kramer and G. G. Guilbault, Anal. Chem., 35 (1963) 588.
9 E. Silk, J. King and M. Whittaker, Ann. Clin. Biochem., 16 (1979) 57.
10 H. Rinderknecht and R. M. Fleming, Clin. Chim. Acta, 59 (1975) 139.

Analytica Chimica Acta, 179 (1986) 225—231
Elsevier Science Publishers B.V., Amsterdam — Printed in The Netherlands

THE USE OF HOLDING COILS TO FACILITATE LONG INCUBATION TIMES IN UNSEGMENTED FLOW ANALYSIS
Determination of Serum Prostatic Acid Phosphatase

B. F. ROCKS* and R. A. SHERWOOD

Biochemistry Department, Royal Sussex County Hospital, Brighton (Great Britain)

M. M. HOSSEINMARDI and C. RILEY

Centre for Medical Research, Mantell Building, University of Sussex, Brighton (Great Britain)

(Received 24th July 1985)

SUMMARY

Conventional unsegmented flow analysis is best suited to determinations involving rapid chemical reactions. Analyses requiring relatively long reaction times necessitate stopping the flow to allow sufficient reaction product to accumulate, which significantly decreases sampling frequency. An automated distribution valve is described which directs samples into one of four holding coils where they remain for a predetermined time. Because one parallel coil may be filled with a sample while the others hold other samples for reaction, throughput is increased fourfold compared with a comparable single tube system. This technique is applied to the determination of prostatic acid phosphatase in human blood sera. The method is compared with a manual procedure.

Although many determinations of interest to clinical chemists are possible with flow injection analysis (f.i.a.) [1, 2], the technique has not found many routine applications in hospital laboratories. One reason is that injection valves waste sample, and because the volume of specimen is limited in the hospital laboratory, conventional f.i.a. has been ignored by the majority of clinical chemists.

It was chiefly to overcome this demerit that Riley et al. [3] devised a different system of sample introduction that does not waste sample. In this system, a probe connected to a peristaltic pump tube is used to aspirate a small volume of sample into the analytical conduits. The pump is driven by a microcomputer-controlled stepper motor which allows very fine control over the movement of the pump. The pump can be programmed to start, pump and stop with great precision and at a variety of speeds. The movement of the sampling probe, which normally rests in a trough of demineralised water, is also under microcomputer control. Because this technique uses the flow of liquids to control the dispersion of the sample as it passes through the system, but does not use injection valves, it is referred to as controlled-dispersion flow analysis (c.d.f.a.). The low sample consumption of this technique has been demonstrated for several assays of clinical interest [3—6].

0003-2670/86/$03.50

A second disadvantage, which is common to both unsegmented flow systems (f.i.a. and c.d.f.a.), is that they are not well suited to assays involving slow reactions. For this type of assay, the flow can be stopped and the product of the reaction allowed to build up, but for very slow reactions this drastically decreases the rate of sample throughput [7]. This type of reaction could be processed more quickly if a number of separate reaction lines were provided in which individual samples could be stopped for a time before being pumped to the detector. Růžička and Hansen [8] have described systems with two holding coils and with an eight-channel revolving drum in which samples could be held for reaction before being directed to the detector. The recorder traces, obtained when these devices were tested with dye solutions, suggested that the method would work with reacting systems but no application was described.

An increased activity of acid phosphatase (orthophosphoric monoester phosphohydrolase, EC 3.1.3.2) is often found in malignant disease of the prostate, particularly when there are secondary deposits in the bone. The particular acid phosphatase which is clinically important is derived from mature prostatic epithelium, but other acid phosphatases are present in erythrocytes and in platelets, and escape into the serum if the blood is haemolysed or during clotting. The prostatic isoenzyme can be distinguished from acid phosphatase from other sources by its inhibition by L-tartrate. Assays in the presence and absence of L-tartrate can be employed to distinguish the fraction of serum acid phosphatase that is prostatic in origin. Estimation of serum prostatic acid phosphatase is of value both in diagnosis and in monitoring the treatment of patients suffering from carcinoma of the prostate [9].

There are no rapid methods for determining the activity of acid phosphatase in serum. Single-tube unsegmented flow systems would suffer from the disadvantage of low sample throughput because it would take several minutes for measurable reaction products to accumulate. This paper describes the incorporation of a distribution valve and four holding coils into a c.d.f. system. Because each of the coils may be used to incubate sample slugs, the sampling frequency is increased compared with a single-tube system. This technique is applied to the assay of prostatic acid phosphatase in human sera.

EXPERIMENTAL

Samples and reagents

Because acid phosphatase is extremely labile, particularly at alkaline pH, the serum, which was removed from the cells soon after clot formation, was collected into 5-ml glass bottles containing 10 mg of disodium hydrogencitrate. The treated serum specimens were stored at 4°C and assayed on the same day as collection.

A commercially available acid phosphatase reagent was used (Sigma

Diagnostics, procedure no. 435). The method is similar in principle to that described by Fabiny-Byrd and Ertingshausen [10]. The acid phosphatase activity is determined by hydrolysis of α-naphthyl phosphate in pH 5.3 buffer and coupling of the liberated α-naphthol with Fast Red TR to form a yellow diazo dye, the absorbance of which is measured at 405 nm.

In order to measure total acid phosphatase activity, the reagent was reconstituted with demineralised water, as instructed by the manufacturer. To measure non-prostatic acid phosphatase the reagent was reconstituted with 50 mM L-tartaric acid. The non-prostatic acid phosphatase was subtracted from the total acid phosphatase value to yield the prostatic acid phosphatase activity. The tartrate-inhibited reaction also served as a reagent blank and eliminated all nonenzymatic contributions to substrate hydrolysis. Both reagents and the demineralised water were degassed before use.

Apparatus and instrumentation

The controlled-dispersion analyser in its single-line mode was described previously [3]. The arrangement for use with the four holding coils is outlined in Fig. 1. Each of the tygon pump tubes (0.5-mm bore) was fitted with a stainless steel probe (0.3-mm bore). The other end of each tube was attached to a T-piece (Elkay Laboratories; no. PT 2) and the exit from the T-piece was connected to the bottom port of a small Hamilton miniature valve (no. 86788). The valve enabled a stream joining at the bottom to be directed through one of the four ports spaced at 90° intervals in the horizontal plane. The rotating plug of the valve was driven by a stepper motor (Astrosyn Ltd., model no. 23LM-L002) under microcomputer control. On system startup, the valve was driven to the home position, detected by a magnet mounted on an aluminium disc attached to the motor shaft. Four small holes, drilled near the edge of the disc, activated an optical sensor used to detect the index position (i.e., one of the four valve channels). To the valve exits were connected four 1-m lengths of 0.5-mm bore teflon

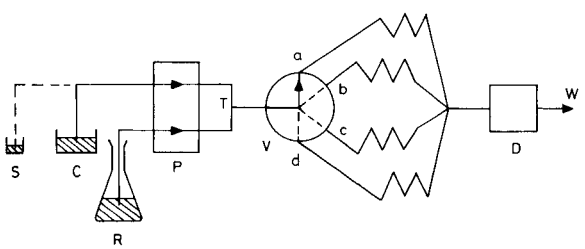

Fig. 1. Controlled dispersion analyser fitted with four holding coils. (S) sample cup; (C) demineralised water carrier solution; (R) reagent; (P) peristaltic pump fitted with two pump tubes of the same nominal diameter; (T) T-piece connector; (V) valve capable of directing the flowing streams through any one of four (a—d) similar teflon reaction tubes; (D) spectrophotometer fitted with flow-through cuvette; (W) waste. The broken lines indicate alternative positions for the probe and valve. Movements of the probe, pump and valve are under microcomputer control.

tubing, coiled (4-cm diameter coils) and submerged in a thermostatically regulated water bath at 37°C. A part intended as a stream divider for gas-segmented continuous flow systems (Elkay Laboratories; no. PT13) was used to join the coils to the flow-through cuvette. This connector consisted of four channels joining a straight-through channel at right angles. One end of the straight-through channel was blocked off and the other connected to the cuvette. The coils were joined to the side connectors. The photometer was fitted with a Hellma flow-through cuvette with an optical volume of 8 μl (no. 178.31) and a 405-nm interference filter.

Preliminary evaluation of the valve and coils was done by aspirating potassium dichromate solutions into a water carrier solution. The resulting peak shapes showed that although peaks from a single coil were reproducible there was a small difference in the height of the peaks from the various coils. The mean relative peak heights for the coils were 95, 96, 99 and 100%. It is not surprising that the tubes produced different dispersion patterns because the connection points and geometry of each coil were not identical. Identical dispersion could be obtained for each coil by adjusting the lengths of the tubes until completely overlapping peaks were obtained. However, when more than two coils were involved this was tedious and a more satisfactory method of compensation was to apply a correction factor to the peak-height measuring software. In the system described here, the valve always started from the same position and the software kept track of which coil was in use at any given time. (Further details of the control processes and data processing algorithms may be obtained from the authors.)

Analytical mechanism and performance

An analytical cycle involves the following microcomputer-controlled operations. First, the valve is turned to the first coil position, e.g., (a) in Fig. 1. Secondly, water and reagent are pumped through the system at a preset flow rate for a fixed number of motor steps. During the initial four cycles this flushes each coil through with reagent which has been diluted 1 + 1 with water from the water trough in which the sample probe normally rests. During subsequent cycles this phase serves to transport the reaction products from the coil through the detector where the concentration is computed from the peak height measurement; the pump then stops. Thirdly, the sample probe is moved from the water trough to the sample cup (broken line, Fig. 1); the pump aspirates a small volume of sample into the pump tube and again stops, and the probe is returned to the water trough. Fourthly, the pump restarts, causing the slug of sample to be carried through the system. As it moves the sample slug disperses into the water carrier and at the T-piece it is mixed with reagent before entering one of the reaction coils; during this phase the number of pump steps is such that the slug of sample is transported to the middle of the coil. The pump then stops and after a predetermined time another cycle begins.

The time between cycles may be used to produce different incubation

periods. When there is no halt between cycles, the minimum incubation period of 3 min is achieved, as each cycle takes 45 s. In this situation, maximum sample throughput is obtainable. However, for the acid phosphatase assay an incubation time of 5 min was chosen as a compromise between an acceptable absorbance reading and sampling frequency. Under these conditions, the absorbance change was 0.009 per IU of enzyme activity and a sample was aspirated into the system every 75 s. Reagent and water consumption were 0.5 ml each per cycle. The aspirated sample volume was 21 μl and the dispersion coefficient [8] for the system was calculated to be 8.

The system was calibrated by using two reference sera, Versatol-EN and Versatol-E (General Diagnostics), with prostatic acid phosphatase activities of 1 and 20 IU l^{-1}, respectively.

RESULTS AND DISCUSSION

The within-batch precision for the method was evaluated by replicate analyses (n = 10) of two different batches of pooled serum. These gave relative standard deviations for acid phosphatase of 8.0% at a mean activity of 4.2 IU l^{-1}, and 2.0% at a mean activity of 23.5 IU l^{-1}. This reproducibility is acceptable for diagnostic purposes.

Comparison of methods

A batch of ten serum samples was assayed for prostatic acid phosphatase activity by a commercial manual procedure (General Diagnostics Acid Phosphastrate) which is used routinely in this laboratory. Five of the samples were then spiked with known amounts of acid phosphatase of prostatic origin (Sigma Diagnostics; product P1774) to give a range of samples with activities covering the pathological range. These spiked samples were also assayed by the routine method currently in use here and immediately afterwards the complete batch was assayed by the proposed holding-coil procedure.

The General Diagnostics method uses α-naphthyl phosphate as substrate. After an incubation period of 30 min, the liberated α-naphthol is coupled with diazotised 4-nitro-*o*-anisidine and the colour is developed by the addition of sodium hydroxide [11]. The absorbance is measured at 590 nm and the enzyme activity is evaluated by comparison with the calibrators, Versatol-E and Versatol-EN. As with the c.d.f. method the prostatic acid phosphatase fraction is calculated from assays done in the presence and absence of the prostatic acid phosphatase inhibitor L-tartrate. Figure 2 shows a comparison of the results obtained by the two methods. The agreement was good (r = 0.98).

Previously the determination of acid phosphatase has proved to be one of the most difficult of clinical analyses to automate. In serum, the enzyme has a very low concentration and there are no rapid sensitive reagents for its

detection. Most of the methods in use involve a relatively long incubation of serum with a buffered substrate followed by the addition of further reagents to produce a colour [9]. The method marketed by Sigma makes automation easier because no additional reagents are required for colour development.

The routine method used at present in this laboratory is labour-intensive, requires 30-min incubation and the preparation of four reagents, and consumes 200 μl of serum. The c.d.f. method based on the Sigma reagent is more convenient and requires little manual intervention. Sample consumption is 42 μl per prostatic acid phosphatase determination. Both methods yield very similar results and the precision of the c.d.f. system is adequate for the assay of pathological specimens. If necessary, the precision for samples with low activity samples could be improved by increasing the incubation period. This would, however, decrease sample throughput unless more holding coils were added. With the 4-coil system described above, 48 samples h^{-1} can be aspirated, producing about 20 prostatic acid phosphatase results per h.

This practical demonstration validates Růžička and Hansen's suggestion [8] that holding coils could be used in this way and opens up another area of tests that are now amenable to automation by unsegmented flow analysis.

We thank Mr P. Thrush for carrying out the acid phosphatase assays by the current routine method. We also thank Mr A. D. Coombe for constructing the valve assembly.

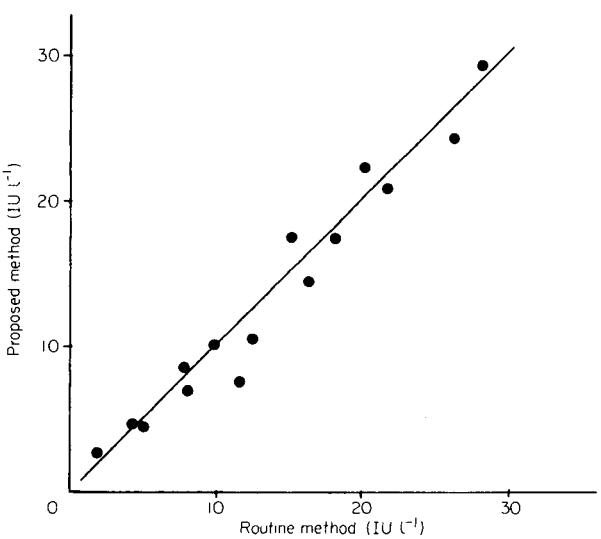

Fig. 2. Comparison of results obtained by c.d.f.a. and a commercially available manual procedure.

REFERENCES

1 B. F. Rocks and C. Riley, Clin. Chem., 28 (1982) 409.
2 C. Riley, B. F. Rocks and R. A. Sherwood, Talanta, 31 (1984) 879.
3 C. Riley, L. H. Aslett, B. F. Rocks, R. A. Sherwood, J. D. McK. Watson and J. Morgon, Clin. Chem., 29 (1983) 332.
4 B. F. Rocks, R. A. Sherwood and C. Riley, Analyst (London), 109 (1984) 847.
5 B. F. Rocks, S. M. Wartel, R. A. Sherwood and C. Riley, Analyst (London), 110 (1985) 669.
6 R. A. Sherwood, B. F. Rocks and C. Riley, Analyst (London), 110 (1985) 493.
7 C. S. Lim, J. N. Miller and J. W. Bridges, Anal. Chim. Acta, 114 (1980) 183.
8 J. Růžička and E. H. Hansen, Flow Injection Analysis, Wiley, New York, 1981, pp. 65–71, 115.
9 H. Varley, A. H. Gowenlock and M. Bell, Practical Clinical Biochemistry, Vol. 1, Heinemann, London, 1980, p. 913.
10 D. L. Fabiny-Byrd and G. Ertingshausen, Clin. Chem., 18 (1972) 841.
11 A. Babson and G. Phillips, Clin. Chim. Acta, 13 (1966) 264.

Analytica Chimica Acta, 179 (1986) 233—244
Elsevier Science Publishers B.V., Amsterdam — Printed in The Netherlands

APPLICATIONS OF ION-EXCHANGE MINICOLUMNS IN A FLOW-INJECTION SYSTEM FOR THE SPECTROPHOTOMETRIC DETERMINATION OF ANIONS

AZAD T. FAIZULLAH and ALAN TOWNSHEND*
Department of Chemistry, University of Hull, Hull HU6 7RX (Great Britain)
(Received 11th July 1985)

SUMMARY

Displacement of thiocyanate from a strongly basic ion-exchange resin by other anions is used to determine common anions at the 10^{-5}—10^{-4} M level by spectrophotometric detection of the iron(III)/thiocyanate complex. Chloride and sulphate can be removed by incorporating a pre-column containing a cation-exchange resin in the silver form followed by a zinc reductor, thus allowing the determination of nitrate in their presence. Binary mixtures (e.g., chloride and nitrate) can be determined simultaneously by splitting the sample in the flow system so that part goes through the chloride suppressor (giving a nitrate response only) and part by-passes it giving a response to both chloride and nitrate.

In flow injection analysis (f.i.a.), the use of solid ion-exchangers in the form of packed reactors is of particular interest [1—10]. An example is their use in the determination of the sum of either anions or cations in aqueous solution [1]; the method is based on measuring the pH change caused by the hydroxide ion (or hydrogen ion) released from a strongly basic anion exchanger (or strongly acidic cation exchanger) by the anions (or cations) in the flowing stream. The pH is detected by the change of colour of an indicator.

On-line preconcentration methods in f.i.a. have been developed, with use of a minicolumn of chelating resin for heavy metal determinations in sea water by atomic absorption spectrometry (a.a.s.) [3, 5—7] and for increasing the sensitivity of multielement measurements by inductively-coupled plasma emission spectrometry [4]. The incorporation of a miniature column of chelating resin in a flow-injection system for monitoring the chemiluminescence of hydrazine was found to be suitable for removing interfering metal ions from hydrazine samples [8]. An on-line anion-exchange column has been used to eliminate the interfering effects of phosphate and sulphate on the determination of calcium by a.a.s. [9]. A strongly basic anion-exchange resin was used for separation of iron(II) and iron(III) before their determination by a.a.s. [10]; with 6 M hydrochloric acid as eluent, iron(II) was retained on the resin column while iron(III) was eluted, and iron(II) was eluted later with water.

0003-2670/86/$03.50

Many of the common anions (e.g., sulphate, chloride, oxalate and nitrate) form few useful coloured species, so that there is a dearth of direct spectrophotometric methods for their determination. Indirect methods often depend on the displacement of a chromogenic species from insoluble compounds such as the mercury(II) thiocyanate/iron(III) method for the determination of chloride [11] and the barium chloranilate method for sulphate [12]. Ion-exchange has been used for separating these anions, and for their determination via another anion which can readily be determined spectrophotometrically. An example of this latter concept is the work of Ducret and Ratouis [13] in which sulphate displaced thiocyanate from a strongly basic anion-exchange column in the thiocyanate form, the thiocyanate being determined by extracting its methylene blue ion-pair into 1,2-dichloroethane.

The aim of the work described here was to combine ion-exchange with spectrophotometric detection in a flow system in order to develop methods for those anions which are not easily determined by direct spectrophotometric methods. These anions include sulphate, chloride and nitrate. The reactions investigated were displacement from an ion-exchange resin of thiocyanate, dihydrogenphosphate or iodide, spectrophotometric determinations of which are straightforward. Thiocyanate rapidly forms a red complex with iron(III) which can be measured at 465 nm [14], phosphate forms a blue colour with a mixture of ascorbic acid and ammonium molybdate [15] and iodide complexes with palladium(II) can be measured at 400 nm [16]. All these procedures are accomplished in aqueous media, which is advantageous for f.i.a.

EXPERIMENTAL

Reagents and solutions

All chemicals were of analytical-reagent grade, and distilled-deionized water was used throughout. Standard solutions of the anions examined were prepared from their sodium or potassium salts. Solutions of different pH values were prepared by mixing 25 ml of 0.2 M potassium chloride and 67.0 ml, 26.6 ml, 10.2 ml or 3.9 ml of 0.2 M hydrochloric acid to give solutions of pH 1.0, 1.4, 1.8 and 2.2, respectively, after dilution to 100 ml with water [17]. These solutions were used to prepare 2.5×10^{-3} M iron(III) solutions for the study of pH effects.

Preparation of columns

Preparation of the exchanger column. The strongly basic anion-exchange resin Dowex 1-X4 (200—400 mesh) in the chloride form was used and converted to the thiocyanate form in the following way [13]. A 2-g portion of resin was placed in a 100-ml round-bottomed flask and shaken twice with 50 ml of 0.1 M potassium thiocyanate for 20 min and 3 times with 50 ml of 2 M potassium thiocyanate for 20 min. The resin was filtered off and washed

with water between each shaking. The resin was twice shaken for 10 min with 50 ml of water, filtered off and left for 24 h in water. The resin was filtered off and added to a glass tube (3 cm long, 2 mm i.d.) until the required packing was achieved. A thin layer of glass wool was put at both ends of the column to prevent movement of the resin particles by the carrier stream. A small piece of silicone rubber tubing (0.8 mm i.d.) was pushed into each of the columns so as to achieve a very tight connection, and a suitable adhesive (Bostik 1) was applied from outside onto the column/silicone tube joint. When the flow injection system shown in Fig. 1 was used, water was passed through the exchanger column until a stable baseline was obtained, and the column was stored in this condition until required for use.

A similar procedure was used to convert the resin to the iodide or phosphate form by shaking the resin with potassium iodide or potassium dihydrogenphosphate, respectively. The packed columns were also prepared as above.

Preparation of the interference suppressor columns. A silver-form resin column was prepared from Dowex 50W-X8 (4% cross-linked) by passing 25 ml of 1 M silver nitrate through the H^+-form column (1.5 cm long, 2 mm i.d.) for 25 min at 1 ml min^{-1}. Water was passed until a test (with chloride) showed the absence of silver ions in the effluent. A Jones reductor (amalgamated zinc), 1.5 cm long, 2 mm i.d., was prepared as described previously [18]. The bodies of the suppressor columns were made from a Perspex rod (1.5 cm o.d., through which a 2 mm i.d. hole had been bored centrally). Suppressor columns could be combined by screwing together two (or three) columns, each 1.5 cm long, 2 mm i.d. (see below). Glass wool was used to separate the contents of each column. This combination facilitates the separate regeneration of each column.

Flow manifold

The system used for the determination of anions is shown in Fig. 1. A 4-channel peristaltic pump (Gilson Minipuls 2) was used, and anion solutions were introduced by means of a Rheodyne 5020 injection valve (Anachem) with a 40-μl sample loop. Teflon tubing (0.5 mm i.d.) was used for all connections. The absorbance was measured at a suitable wavelength (465 nm for thiocyanate, 660 nm for phosphate and 400 nm for iodide) with a Cecil

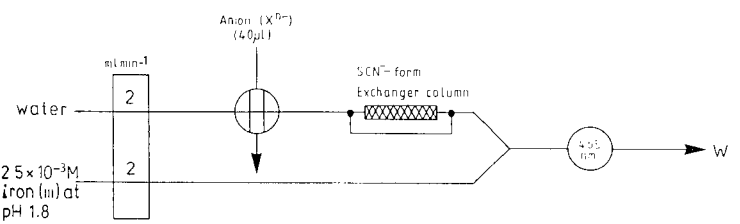

Fig. 1. Flow diagram of the system used for the determination of anions. W, waste.

CE373 linear-readout spectrophotometer incorporating a 18-μl flow cell, and connected to a Tekman Labwriter TE-200 chart recorder.

RESULTS AND DISCUSSION

Thiocyanate exchange

When standard solutions of different anions (sulphate, oxalate, nitrate, chloride, dihydrogenphosphate) were injected into the carrier stream in Fig. 1, with the exchanger column bypassed, no signals were obtained, but with the column on-line all anions gave rise to sharp peaks.

The procedure was optimized by using sulphate. The effect of iron(III) concentration in the range 5×10^{-5}—1×10^{-2} M was examined. The results obtained are shown in Fig. 2. A 5×10^{-3} M solution was used for further studies. Formation of iron(III)/thiocyanate complexes takes place predominantly at pH < 1.5 [15]. Above pH 2.0, there is hydrolysis of iron(III), and therefore less complex formation. The effect of pH in the range 1.0—2.2 is shown in Fig. 3. The absorbance increased with pH up to pH 1.8 and decreased on further increase in pH. In the solutions of lower pH the chloride concentration is also greater, so that protonation of thiocyanate and iron(III)/chloride complex formation may both contribute to the decrease in the concentration of iron(III)/thiocyanate complex produced, and therefore the smaller absorbance. When the pH exceeds 1.8, hydrolysis of iron(III) becomes significant and causes a decrease in absorbance; pH 1.5 was used in further experiments.

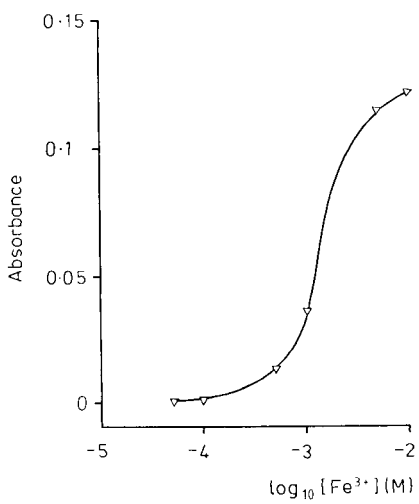

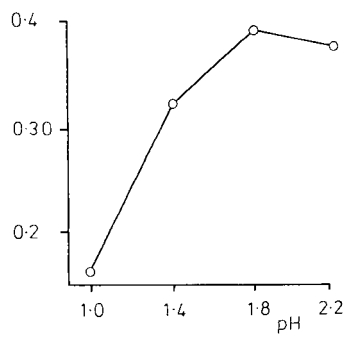

Fig. 2. Effect of iron(III) concentration. Conditions: 5×10^{-4} M sulphate, flow rate 1.5 ml min^{-1}, pH 1.0.

Fig. 3. Effect of pH on the determination of 5×10^{-4} M sulphate.

The effect of flow rate in the sample stream was also studied. Increasing the flow rate through the exchanger column from 0.5 to 5 ml min^{-1} was accompanied by an increase in the peak height absorbance, as well as the expected peak broadening (in volume terms) up to 4 ml min^{-1}. To avoid excessive reagent consumption, a flow rate of 2 ml min^{-1} each through the exchanger and reagent lines (4 ml min^{-1} total) is recommended.

It was also of interest to study the effect of column parameters on the exchange of thiocyanate by sulphate. Five columns were prepared having lengths of 1.5, 3.0, 4.5, 7.5 and 10.0 cm, all with an internal diameter of 2 mm. The results obtained for each column by injecting different sulphate concentrations are shown in Fig. 4. At all sulphate concentrations a column length of 3 cm gave the greatest peak height. Increase in column length caused some increase in dispersion of the sample which resulted in the slight decrease in peak height. The effects of using resins with different degrees of cross-linking were investigated. The results (Fig. 5) show that 4% cross-linking gives greatest sensitivity, although all columns gave reasonable sensitivity and linear calibration graphs.

A calibration graph for sulphate obtained under the optimized conditions was linear over the range 5×10^{-6}—2.5×10^{-4} M. A typical recording for calibration is shown in Fig. 6. The resulting graph had a linear regression coefficient of 0.9970, and a least squares equation of Abs. = 2340 $[SO_4^{2-}]$ $- 5 \times 10^{-3}$. The limit of detection (2 × blank noise) was 5×10^{-6} M sulphate. The mean r.s.d. of these measurements was 1%.

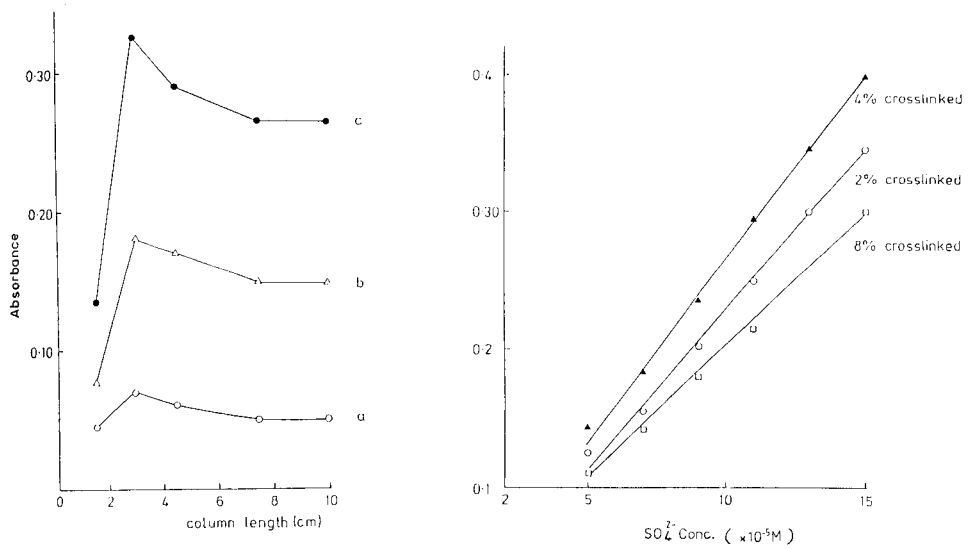

Fig. 4. Effect of length of exchanger column for different sulphate concentrations: (a) 4×10^{-5} M, (b) 9×10^{-5} M, (c) 15×10^{-5} M. Conditions: pH 1.8, total flow rate 4 ml min^{-1}.

Fig. 5. Effect of degree of resin crosslinking.

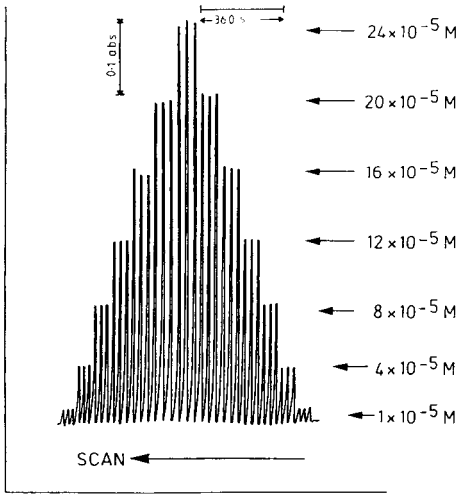

Fig. 6. Peaks obtained by injecting triplicate sulphate standards of the concentrations shown. Sampling rate, 120 h^{-1}.

Determination of other anions

Once the optimum conditions for the determination of sulphate had been established, the behaviour of some other common anions (oxalate, phosphate, nitrate and chloride) was tested under these conditions. The results, summarized in Table 1, show that each anion displaced equivalent amounts of thiocyanate according to their charge. For example, oxalate and sulphate gave similar signals which are twice the signals given by equimolar amounts of nitrate and chloride, while phosphate (therefore as $H_2PO_4^-$) gave similar results to chloride or nitrate. Therefore the procedure can also be used for the determination of these other anions. Linear calibration graphs were obtained in each instance. For example, for phosphate the graph satisfied the equation Abs. = 1024 $[H_2PO_4^-]$ — 0.0025 with a regression coefficient of 0.9989 (8 points).

A mixture of anions gave a single additive peak, according to the charge and concentration of the anions in the mixture. For example, the peak height from a mixture of sulphate and chloride (both 1×10^{-5} M) was 3 times that of 1×10^{-5} M chloride alone.

The present development provides a very simple, rapid and sensitive method for anion determinations. However, it is essential to improve its selectivity so that one or two anions can be determined in the presence of others. Some attempts to do this are described below.

Use of other anions on the exchanger

Dowex 1 (Cl^- form, 4% crosslinked, 200—400 mesh) was converted to its phosphate or iodide forms as described above. Minicolumns, 3 cm long, 2 mm i.d., were made of each, as for the thiocyanate form. Spectrophoto-

TABLE 1

Results obtained for the exchange of thiocyanate by some common anions

Anion	Absorbance[a]		Anion	Absorbance[a]	
	Anion concn. (M)			Anion concn. (M)	
	5×10^{-5}	1×10^{-4}		5×10^{-5}	1×10^{-4}
$C_2O_4^{2-}$	0.15	0.30	Cl^-	0.06	0.14
SO_4^{2-}	0.14	0.29	NO_3^-	0.06	0.15
$H_2PO_4^-$	0.06	0.14			

[a]Mean of three results.

metric detection of phosphate was based on 12-molybdophosphoric acid formation and its reduction to molybdenum blue [19], that of iodide on complexation with palladium chloride [16]. The manifold and conditions for the exchanger in the phosphate form are shown in Fig. 7. The manifold with the exchanger in the iodide form was identical with Fig. 1; 1×10^{-4} M palladium(II) chloride in 0.1 M hydrochloric acid was pumped instead of the iron(III) solution and detection was at 400 nm. Both systems behaved similarly to the thiocyanate system in exchanging all other anions tested in accordance with their charge. Therefore no increase in selectivity was found, but either system could be used for the determination of anions in the same way as the thiocyanate column.

Use of interference suppressor columns

The fundamentals of suppressor columns used for improving the selectivity of anion determinations have been described extensively, especially for use in ion chromatography [20—22]. They can involve one of a number of types of reactions. One is the conversion of an ionic species to a molecular form, e.g., hydroxide to water, or hydrogencarbonate to carbon dioxide and water. Another is replacement of all anions or cations by a single species, e.g., release of hydrogen ion on uptake of different metal ions. Suppression via precipitation has also been used for ion chromatography [23, 24]. One example is the precipitation of chloride from a hydrochloric acid eluent with silver ions on a cation-exchange column and insertion of hydrogen ions onto the vacant resin site. The silver chloride precipitate is held in the resin network. Regeneration can be done by dissolving the silver chloride with ammonia, or can be avoided if a commercial disposable plastic column is used, the expended portion being cut off as required [22].

It should be possible, therefore, to design a flow-injection manifold similar to that used in ion chromatography in which two columns are used in the operation for anion determination, a suppressor column to remove interferences and a second column to release the ion needed for colour formation.

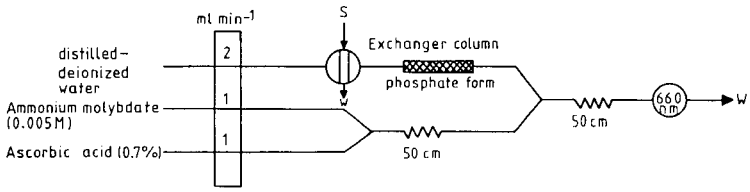

Fig. 7. Flow-injection manifold for the determination of anions with Dowex 1 (phosphate-form) as the exchanger (S, sample; W, waste).

A variety of these columns was tested depending on the anion to be suppressed.

In various studies of the removal of anion interferences, the sample has been passed through a small conventional ion-exchange column in a particular cationic form before the required analytical exchange reaction. For example, a cation-exchange column in the lead form has been used to remove sulphate, leaving nitrate unaffected; lead sulphate was precipitated and retained on the column and nitrate was eluted as lead nitrate [25]. A cation-exchange resin in the silver form has been used widely as a post-suppressor column in ion-chromatographic systems to remove anions such as sulphate, carbonate, halides, oxalate and phosphate [22—26]. A resin column in the cadmium form has been used for removing sulphide, oxalate, carbonate and hydroxide from sulphate or phosphate solutions, and a resin column in the barium form has been used to remove sulphate [15]. These devices can easily be modified and applied to the present system.

Two methods of increasing selectivity were examined here. These involved the simultaneous determination of two anions (e.g., nitrate and chloride or sulphate) and the selective determination of nitrate.

Simultaneous determination of chloride and nitrate

For this determination, it is necessary to use a suppressor which removes chloride while allowing nitrate to reach the exchanger column. A suppressor column (3 cm long, 2 mm i.d.) in the silver form was incorporated after the sample injection port into the system in Fig. 1. When chloride/nitrate solutions were injected, no signals were obtained. Similar investigations had indicated that when a mixture of sulphate and nitrate ions was passed through a cation-exchange column in the lead form [25], nitrate and a stoichiometric amount of lead ion were eluted. Thus it was thought that silver ions were being eluted from the suppressor column under these conditions and were affecting the release of thiocyanate.

Removal of such silver ions from the eluted nitrate solution was achieved by trapping on a Jones reductor minicolumn (2.0 cm long, 2 mm i.d.); nitrate then displaced thiocyanate from the exchanger column to give a characteristic peak. The effectiveness of this method of removing silver ions has been demonstrated by Siemer [27]. The additional column had little effect on dispersion and it could be regenerated simply by passing a 0.25 M mercury(II) nitrate solution through it.

A combined column (4 cm long, 2 mm i.d.) for removing chloride and trapping silver was prepared from two Perspex columns, each 2 cm long, 2 mm i.d., screwed firmly together to form a compact continuous unit, the first column packed with the silver-form resin, and the second with amalgamated zinc; the packings were held in position with short wads of glass wool. The effect of flow rate on the efficiency of the combined suppressor when incorporated into the system shown in Fig. 1 was investigated by injecting a chloride/nitrate solution. The results are shown in Fig. 8. Generally, the peak height decreases as the flow rate increases, most probably because of incomplete trapping of silver ions. The efficiency of the Jones reductor for reduction of iron(III) was also found to decrease at higher flow rates [18].

The simultaneous determination of chloride and nitrate can be achieved by splitting the injected sample into two streams. The manifold is shown in Fig. 9. One stream passes through the suppressor columns and the thiocyanate column. This produces a peak which is a measure of the concentration of nitrate only. The other portion flows through a 200-cm delay coil (0.5 mm i.d.), bypassing the suppressor columns and thence through the thiocyanate column to give a second peak, completely resolved from the nitrate peak. This peak is a measure of chloride and nitrate concentration. Because

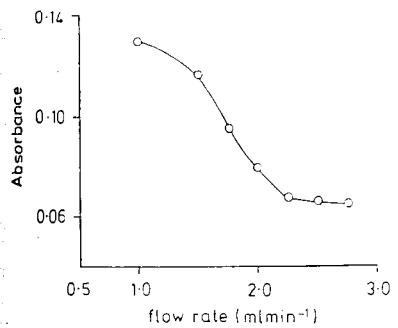

Fig. 8. Effect of flow rate on the peak heights obtained by use of the combined suppressor minicolumn.

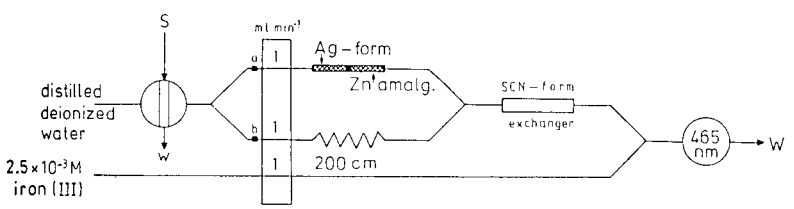

Fig. 9. Manifold used for simultaneous spectrophotometric determination of chloride and nitrate. S, sample; a and b, pulse suppressors; W, waste.

the combined suppressor requires a slow flow rate (1 ml min^{-1}), splitting was achieved by situating the pump after the splitter, as described previously [18]. The 1:1 peak height splitting achieved is shown in Fig. 10, together with typical calibration results for 40-μl injections of standards. The sample throughput was about 60 h^{-1}. The calibration graphs obtained from these results were linear for nitrate and chloride with regression coefficients of 0.999 and 0.997, respectively. The least-squares equations were Abs. = 521 $[NO_3^-]$ + 7.5 × 10^{-3} and 870 $[Cl^-]$ — 2.3 × 10^{-2}.

The system in Fig. 9 was also used to determine sulphate and nitrate simultaneously. Table 2 shows the results for a typical range of sulphate and nitrate concentrations. The calibration graphs obtained have regression coefficients of 0.980 (sulphate) and 0.999 (nitrate) (5 points). The least-squares equations were Abs. = 540 $[NO_3^-]$ — 1.3 × 10^{-2} and 855 $[SO_4^{2-}]$ —3.2 × 10^{-2}. Sampling throughput was 60 h^{-1} with a midrange r.s.d. for 5 injections of 1.5% for nitrate.

Removing interfering effects of carbonate and chloride (or sulphate) in the determination of nitrate

Ion exchange can readily be used to separate nitrate from chloride, hydrogencarbonate and organic anions [26]. Two cation-exchange resins were used. The first, in the silver form, removes chloride and the second, in the hydrogen form, removes the silver displaced from the first column.

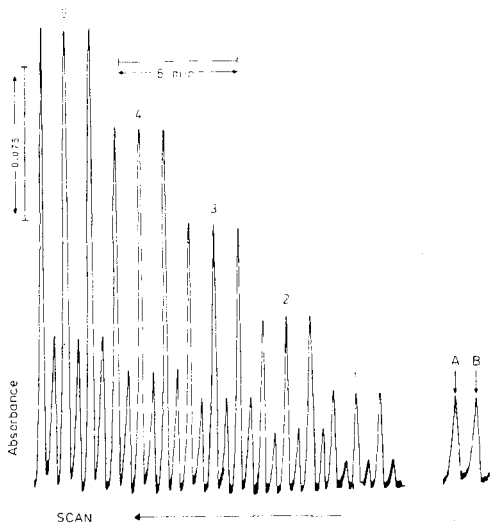

Fig. 10. Typical calibration responses for simultaneous determination of chloride and nitrate at the following respective concentrations: (1) 5 × 10^{-5}, 2 × 10^{-5} M; (2) 8 × 10^{-5}, 5 × 10^{-5} M; (3) 11 × 10^{-5}, 8 × 10^{-5} M; (4) 14 × 10^{-5}, 11 × 10^{-5} M; (5) 17 × 10^{-5}, 14 × 10^{-5} M. Peaks A and B were obtained for an 8 × 10^{-5} M nitrate injection, corresponding to the peak from the delay coil and the peak from the suppressor columns, respectively.

TABLE 2

Peak-height absorbance for simultaneous determination of sulphate and nitrate

Sample	Anion concn. (M)		Absorbance	
	SO_4^{2-}	NO_3^-	NO_3^-	$SO_4^{2-} + NO_3^-$
1	2×10^{-5}	5×10^{-5}	0.018	0.06
2	4×10^{-5}	8×10^{-5}	0.028	0.09
3	6×10^{-5}	11×10^{-5}	0.045	0.12
4	8×10^{-5}	14×10^{-5}	0.060	0.15
5	10×10^{-5}	17×10^{-5}	0.083	0.20

Solutions leaving the second column are acidic, thus eliminating hydrogencarbonate. This possibility was investigated for the determination of nitrate in the presence of chloride and hydrogencarbonate.

When such a suppressor column (two minicolumns of equal length containing successively the silver-form resin and the hydrogen-form resin) was introduced into the flow injection system shown in Fig. 1 between the injection valve and the thiocyanate column, the arrangement was reasonably effective for removing the effect of carbonate, but chloride caused decreased nitrate peaks, because the displaced silver ions were inefficiently trapped by the resin. This problem was overcome by introducing a third minicolumn (1.5 cm long, 2 mm i.d.) packed with amalgamated zinc to trap any silver ions eluted from the Ag^+-form and H^+-form resin columns. This completely restored the nitrate signal obtained in the presence of chloride. Therefore the combined suppressor column was suitable for the determination of nitrate in the presence of sulphate, chloride and carbonate.

Determination of nitrate in tap water

The low solubility of most silver salts gave an opportunity for the determination of nitrate in tap water. It was assumed that the incorporation of the combined suppressor columns (Ag^+-form resin, H^+-form resin and Jones reductor) into the system in Fig. 1 was capable of removing most of the anions present in tap water. Injections of tap water into the system gave a peak height ratio of 7:1 in the absence and presence of the suppressor column, respectively, indicating that the suppressor removes an appreciable amount of the anions present in the water sample. Nitrate, however, should not be affected. A standard addition method was used to determine nitrate in tap water; 23.7 μg ml^{-1} nitrate was found. The same water was also analysed by the u.v. spectrophotometric method of Hoather and Rackam [28]; the concentration found was 22.5 μg ml^{-1}. These preliminary experiments indicated that the common anions present in tap water, with the exception of nitrate, are removed by the suppressor column, thus allowing the rapid determination of nitrate, and without the need to revert to u.v. measurements.

Azad T. Faizullah thanks the Ministry of Higher Education and Scientific Research and the University of Salahaddin, Iraq, for a Scholarship.

REFERENCES

1 A. Ramsing, J. Růžička and E. H. Hansen, Anal. Chim. Acta, 114 (1980) 165.
2 H. Bergamin F°, B. F. Reis, A. O. Jacintho and E. A. G. Zaggato, Anal. Chim. Acta, 117 (1980) 81.
3 S. Olsen, L. C. R. Pessenda, J. Růžička and E. H. Hansen, Analyst (London), 108 (1983) 905.
4 S. D. Hartenstein, J. Růžička and G. D. Christian, Anal. Chem., 57 (1985) 21.
5 J. Růžička and E. H. Hansen, Anal. Chim. Acta, 161 (1984) 1.
6 Z. Fang, J. Růžička and E. H. Hansen, Anal. Chim. Acta, 164 (1984) 23.
7 Z. Fang, S. Xu and S. Zhang, Anal. Chim. Acta, 164 (1984) 41.
8 A. T. Faizullah and A. Townshend, Anal. Proc., 22 (1985) 15.
9 O. F. Kamson and A. Townshend, Anal. Chim. Acta, 155 (1983) 253.
10 G. E. Pacey and B. P. Bubnis, Int. Lab., 14 (1984) 253.
11 I. Iwasaki, S. Utsumi, K. Hageno and T. Ozowa, Bull. Chem. Soc. Jpn., 29 (1956) 860.
12 R. J. Bertolacini and J. E. Barney, Anal. Chem., 29 (1957) 281.
13 L. Ducret and M. Ratouis, Anal. Chim. Acta, 21 (1959) 91.
14 E. B. Sandell, Colorimetric Determination of Traces of Metals, 3rd edn., Interscience, New York, 1959.
15 W. J. Williams, Handbook of Anion Determination, Butterworths, London, 1979, p. 233.
16 J. Novak and I. Slama, Collect. Czech. Chem. Commun., Engl. Edn., 37 (1972) 2907.
17 D. D. Perrin and B. Dempsey, Buffers for pH and Metal Ion Control, Chapman and Hall, London, 1974, p. 128.
18 A. T. Faizullah and A. Townshend, Anal. Chim. Acta, 167 (1985) 225.
19 E. H. Hansen and J. Růžička, J. Chem. Educ., 56 (1979) 677.
20 D. R. Crow, Lab. Pract., 29 (1979) 1211.
21 F. C. Smith and R. C. Chang, CRC Crit. Rev. Anal. Chem., 9 (1980) 197.
22 F. C. Smith and R. C. Chang, The Practice of Ion Chromatography, Wiley-Interscience, New York, 1983.
23 H. Small, T. S. Stevens and W. C. Bauman, Anal. Chem., 47 (1975) 1801.
24 F. R. Nordmeyer, L. D. Hansen, D. J. Eatough, D. K. Rollins and J. D. Lamb, Anal. Chem., 52 (1980) 852.
25 A. I. Ryabinin and V. L. Bogatyrev, Zh. Anal. Khim., 23 (1968) 894; Anal. Abs., 18 (1970) 875.
26 J. L. Paul and R. M. Carlson, J. Agric. Food Chem., 16 (1968) 766.
27 D. D. Siemer, Anal. Chem., 52 (1980) 1874.
28 R. C. Hoather and R. F. Rackman, Analyst (London), 84 (1959) 548.

Analytica Chimica Acta, 179 (1986) 245—257
Elsevier Science Publishers B.V., Amsterdam — Printed in The Netherlands

A SUBMERSIBLE FLOW ANALYSIS SYSTEM

KENNETH S. JOHNSON*, CARL L. BEEHLER
and CAROLE M. SAKAMOTO-ARNOLD

Marine Science Institute, University of California, Santa Barbara, CA 93106 (U.S.A.)

(Received 6th September 1985)

SUMMARY

A submersible chemical analyzer (SCANNER) has been developed which can perform analyses in situ in the ocean. The SCANNER is based on a modified flow-injection system and can be used to automate virtually any spectrophotometric determination that can be done by flow injection analysis. The SCANNER consists of a multichannel peristaltic pump, solid-state colorimeters, manifold tubing, valves, and an electronic module. All of the components are pressure-tolerant, except the electronics module, which is placed in a pressure housing. Typical detection limits are of the order of 0.1 μM. Sample introduction is continuous. The SCANNER has been tested successfully to pressures of 3300 dbar in the laboratory and to depths of 2500 m in the ocean. Examples of silicate and sulfide determinations around animal communities in a deep-sea hydrothermal vent field are presented.

Chemical oceanographers study the processes that control the composition of the ocean by measuring the spatial and temporal distribution of elements in sea water. However, the resolution of chemical measurements in the ocean is rather coarse and subject to systematic error. The limitations of conventional sampling techniques and analytical methods preclude the collection and analysis of more than a few samples per hour [1]. In addition, the sampling process greatly increases the possibility of contamination and chemical or biological reaction. Chemical analyses done in situ avoid these problems. Only electrochemical-based sensors for oxygen and pH have been successfully developed for high-resolution measurements in situ [2—4].

Recent advances in analytical chemistry make it feasible to perform a variety of chemical analyses in situ. The development of flow injection analysis (f.i.a.) [5, 6] and light-emitting diode (LED) photometric detectors [7] have been particularly important in this respect. Prior to the development of f.i.a., automated chemical analyses of sea water required air bubbles in the sample stream [8]. The bubbles made these analyses unsuitable for use underwater at high pressure. Only one design of an air-segmented continuous flow analysis system for use in situ has been reported [9]. It was apparently unsuccessful as no further work appeared. The absence of air bubbles in a flow-injection apparatus permits the analysis to be carried out at the high pressure of the deep sea (up to 1000 bar). In addition, the development of

0003-2670/86/$03.50

LED photometers [7] greatly simplifies the measurement of color changes because pressure-tolerant, solid-state light sources and detectors are used.

The instrument described here is based on a modification of f.i.a. that can operate in situ. This submersible chemical analyzer (SCANNER) has been used to depths of 2500 m in the ocean with excellent results [10]. Measurements of silicate and sulfide in a deep-sea hydrothermal vent field in the Galapagos Rift are presented. These results are the first in situ chemical measurements made in the deep sea, other than electrochemical determinations of oxygen and pH.

Principles

The SCANNER runs two photometric determinations simultaneously. Determinations of dissolved silicate and sulfide are discussed here. Silicate was determined by a molybdenum blue method [11] based on the f.i.a. adaptations previously described [12]. Sulfide was measured with a methylene blue method [13]. The methylene blue technique was adapted to f.i.a. by Sakamoto-Arnold et al. [14]. In addition, the SCANNER has sensors for measuring dissolved oxygen, temperature, and pressure.

Nitrate, nitrite, phosphate and hydrogen peroxide have also been determined photometrically in sea water with the SCANNER. Many other determinations are suitable for such use. However, the chemistries used with the SCANNER must produce a color change at wavelengths compatible with the LED photometers. Light-emitting diodes are currently available only at wavelengths greater than 560 nm.

EXPERIMENTAL

Instrumentation

A block diagram of the SCANNER is shown in Fig. 1. Although the design of this instrument is based on the principles of f.i.a. [5], injection was not used to introduce the sample into the reaction manifolds (Fig. 2). In a submersible system, the mechanical complexities of sample injection outweigh any advantages that are gained. Therefore, the sample is added continuously to the reagent stream with a T-fitting. The detector baseline is determined by periodically analyzing a blank solution in situ. The system is also calibrated in situ by pumping a standard solution. Two valves placed in the sample line allow switching between sample, blank, and standard (Fig. 1).

The electronics module used to control the SCANNER and record data is protected from pressure with an aluminum pressure housing. The remaining components of the SCANNER are pressure-tolerant; however, the motors, valves and detectors must be electrically isolated from sea water. This is accomplished by placing them in pressure-compensated, oil-filled vessels. Electrical signals are transmitted between the electronics module and the oil-filled vessels by underwater cables and connectors.

Pump. A peristaltic pump propels the sample and reagents. A Rainin

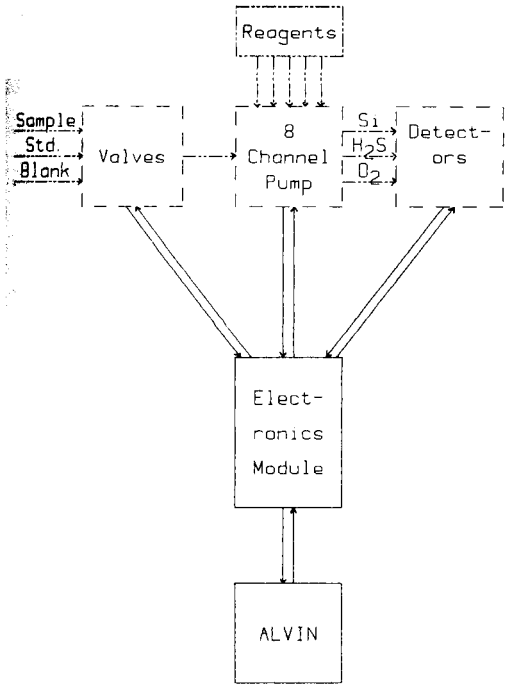

Fig. 1. Block diagram of the SCANNER. Solid boxes are pressure-tight. Dashed boxes are pressure-compensated and oil-filled. Solid lines are electrical cables. Dashed lines are teflon manifold tubing.

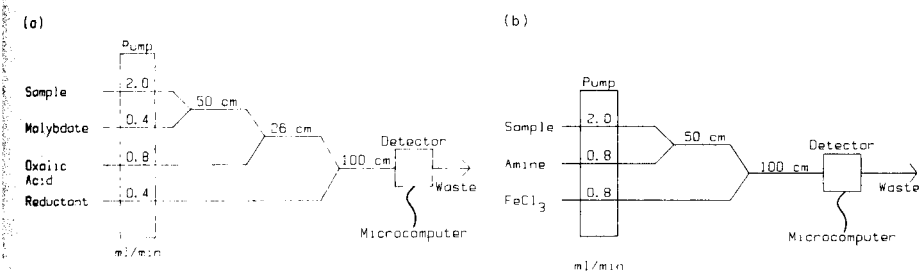

Fig. 2. Flow-injection manifolds used for determinations with the SCANNER: (a) silicate; (b) sulfide.

8-channel pump head (39-613) was used in this work without any modification. The pump is driven with a 27-V d.c. gear motor (TRW EM-15 with 180:1 reduction gear) that has an integral a.c. tachometer. The spring pressure on the motor brushes is approximately doubled to ensure reliable motor operation in oil. No other modifications to the motor were needed.

The entire gear motor and pump head is placed in a pressure-compensated container filled with LPS-1 lubricant. The container has inlet and outlet ports for each of the eight pump tubes. The tubing (viton or solvent-flexible

tygon) lasts for at least 5 days of intermittent use even when pressure is not released on the pump tubes while the motor is off.

Valves. Two Neptune Research solenoid pinch valves (225P082-11) were used to select between the sea-water inlet, blank and standard. Viton tubing (0.8 mm i.d.) is used in the valves. The valves are placed in a pressure-compensated, oil-filled container. The container has six ports for the inlet and outlet of the sea water and standards.

Detectors. In each manifold, a LED photometer is used to detect color change. The detector design is similar to that described by Betteridge et al. [7]. Each flow cell, with its LED and phototransistor, is placed in a pressure-compensated, oil-filled vessel. The phototransistors are Siemens LPT-100. A Radio-Shack 276-143 infrared LED (880 nm maximum emission) is used for the silicate manifold. A Hewlett-Packard HEMT-3300 near-infrared LED (675 nm maximum emission) is used for the sulfide manifold.

The oxygen concentration in the sample line is monitored with a pressure-tolerant amperometric oxygen electrode [15]. Temperature is measured with a thermistor (Sea Data Corp.). Pressure is evaluated with a Kulite ITQ-1000 transducer whenever the SCANNER is used to measure vertical profiles of chemical concentrations in the ocean.

Manifold. The reaction manifolds for silicate and sulfide are shown in Fig. 2. The manifolds are constructed from flanged teflon tubing (0.8 mm i.d.) and threaded fittings with viton O-rings behind the flange. Ports into the oil-filled chambers are made from Omnifit adapters that have O-ring grooves machined into their base to prevent oil from flowing around the threads.

Electronics

The electronics package performs three primary functions: controlling the chemical determinations, logging data, and communicating with the experimenter to establish operational parameters and to give real-time updates of the data. The package is comprised of eight 11.5-cm square circuit boards plugged into a ten-slot mother board based on the Onset Computer Co. C-44 bus (Fig. 3). The boards are modular in function to simplify modifications and troubleshooting. Components within the system can be easily updated as technology improves. The boards use low-power components when applicable. The mother board is sawn in half and the halves joined back to back with ribbon cable to reduce its diameter.

The electronics package fits into an aluminum cylinder (15.2 cm i.d. by 63 cm with a 2.54-cm wall) for protection from high pressure. Double O-ring end caps seal the cylinder on both ends. Four 12-wire penetrators transmit up to 48 electrical signals through the end cap attached to the electronics package.

Power. The SCANNER uses two power supplies with separate grounds. One source supplies low power for the digital logic and analog signals. The other source drives the variable-speed gear motor and valve actuators. The isolated dual supplies protect the sensitive logic and analog circuits from voltage spikes and power interruptions.

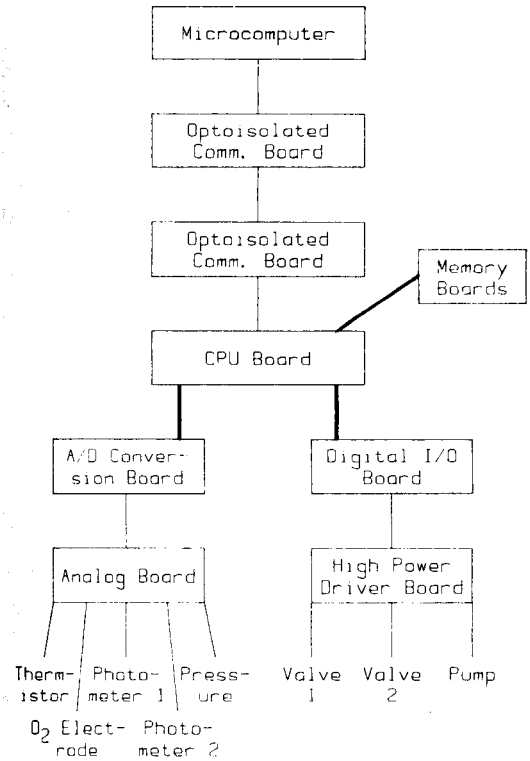

Fig. 3. Block diagram of the electronics of the SCANNER. Heavy lines indicate connections on the C-44 bus.

A Sea Data, SDB-4, dry cell battery package provides 8—18 V for the low power circuits. Voltage regulators on the individual boards control the required voltages for the circuitry. Average power drain on the battery is less than 50 mA with all boards activated. The microprocessor turns off power to specific boards when they are not in use to save power. The battery is placed inside the electronics pressure housing.

The control circuitry for gear motor and valve actuation require power from an 18—38 V d.c. supply voltage. This voltage range allows the SCANNER to utilize power from a variety of sources, depending on the required operating conditions. We have used power from the deep-submersible Alvin and from a submersible battery pack. A shipboard power supply can also be used when the SCANNER is tethered to a conducting hydrowire. The average load on this power supply is 0.5 A at 24 V.

Microprocessor system. The microprocessor board is the control, communications, and timing unit. A Hitachi HD6303R microprocessor is the central processing unit. It has a built-in serial interface for communication with a terminal or another computer by a simplified, 3-wire serial communi-

cations protocol. The microprocessor uses a Hitachi HD146818 real-time clock to keep track of event timing. This clock also provides starting and ending times for the SCANNER data record. The system program resides on the microprocessor board in an 8-kbyte erasable programmable read-only memory.

Two Onset Computer Corporation MEM-64 boards provide the SCANNER with 90 kbyte of addressable memory. These boards use 8 kbyte CMOS static random-access memory integrated circuits. Transducer measurements are stored in this memory and also transmitted over the serial communications interface.

Communication signals generated by the microprocessor board and the device it communicates with are conditioned by boards in the electronics package and at the target communications device. The boards form an optically isolated interface between the SCANNER and the target device. This interface protects both systems against hazardous voltage spikes that may be introduced on the communications lines.

Mechanical control. The peristaltic pump and sample selection valves are regulated by a high-power driver board. The driver board uses MOSFET power transistors to control power to the pump and sample selection valves. The tachometer of the gear motor provides feedback to control the duty cycle of the power transistors and regulate the pump speed. Speed regulation is better than 99% accurate. An analog multiplexer selects four programmable pump speeds.

Communications between the microprocessor and the high-power driver board are buffered with an optically isolated digital input/output (I/O) board. This protects the digital and analog circuits from power line spikes and inductive spikes caused by the gear motor and solenoid valves.

Analog signals. The SCANNER uses a QADC-12 analog/digital (A/D) converter board (Quartec Systems). The QADC-12 board has a 12-bit resolution A/D converter integrated circuit. A programmable amplifier with six gains allows the board to handle a range of analog signals from plus or minus 0.1 V to plus or minus 5.0 V. The board accommodates 16 single-channel or 8 dual-channel analog signals. A multiplexer selects the analog signal to amplify and digitize.

Driving circuitry and signal amplification circuitry for the thermistor, oxygen electrode, pressure transducer and two LED photometer cells are contained on an analog signal-conditioning board. Data signals are preamplified before transmission to the A/D conversion board.

Reagents

All solutions were prepared from reagent-grade salts and distilled-deionized water (Millipore Milli-Q System). The silicate reagent solutions [12] were modified for use with flow analysis. The oxalic acid reagent solution [12] was diluted (1 + 1) with deionized water to avoid precipitation problems at the low temperatures encountered in the deep sea. The molybdate reagent

was prepared with less of the molybdate (30 g l^{-1} instead of 50). Both ascorbic acid and tin(II) chloride were tested as reductants. A portion (3 ml) of the tin(II) chloride stock solution (5.5 g $SnCl_2$ in 100 ml of 6 M HCl) was diluted with 500 ml of deionized water. The ascorbic acid solution [12] was diluted (2 + 5) with deionized water. The reductant solutions were diluted with deionized water because there is much less dispersion in the manifold described here than in the system used by Thomsen et al. [12]. The reagents for the sulfide determination were prepared exactly as described elsewhere [14]. Standard solutions were deoxygenated with nitrogen to retard sulfide oxidation.

RESULTS AND DISCUSSION

Laboratory tests

Initial tests of the SCANNER were done in a high-pressure test facility. The water-filled test tank could be cooled to 2°C and pressurized to 650 bar. The entire instrument was placed in the tank for these tests. Figure 4 shows recordings for three silicate and three sulfide standard solutions; for these runs, the equipment was held in the test tank at a pressure of 3300 dbar (1 dbar is nearly equal to 1 m depth in the ocean) and 19°C. The data were evaluated by converting the detector signals, which are proportional to transmittance, to absorbance values. A 2-point calibration line was calculated from the mean value of the absorbances measured on the plateaus of each pair of blanks and high standards and their known concentrations. Sulfide and silicate concentrations at each data point were calculated by linear interpolation between the adjacent calibration lines. This procedure treats the intermediate sulfide and silicate standards as unknowns.

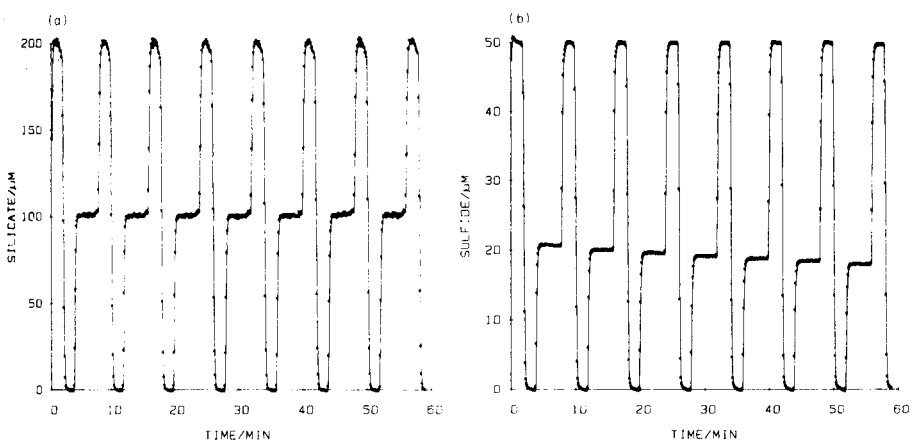

Fig. 4. Repeated determinations of standards with the SCANNER: (a) 0, 100 and 200 μM silicate standards; (b) 0, 25 and 50 μM sulfide standards. The SCANNER was used in a laboratory test tank at 3300 dbar and 19°C. The high and low standards were each pumped for periods of 2 min, while the intermediate standards were pumped for 4 min. Data were recorded at 6-s intervals.

The absorbances of the high and low standards were extremely stable over time at constant temperature and pressure; the absorbances changed by less than 0.0004 over a 1-h period. The relative standard deviations of the calculated concentration of the intermediate sulfide and silicate standards were 0.5% and 0.6%.

The accuracy of each determination can be estimated by comparing the known values of the intermediate standards with the calculated concentrations. The silicate values agree to within 1.5%. The concentration of the intermediate sulfide standard decreased continuously with time and agreement with the expected value was not as good. The drift in its concentration was almost certainly due to sulfide oxidation. In a laboratory experiment, a 25 μM sulfide standard in oxygenated sea water decreased in concentration at a rate of 8% per hour, similar to the rate of decrease in Fig. 4(b). Apparently the intermediate standard was not deoxygenated or air was dissolved into the solution during compression.

It is common in flow injection analysis for the extent of a reaction to be less than 100% at the time the analyte species is detected [5]. Incomplete reaction increases the susceptibility of a procedure to effects of temperature and pressure. The effects of changes in temperature and pressure on the absorbance of silicate and sulfide standard solutions are shown in Table 1. The absorbances of standard solutions increase significantly with increasing

TABLE 1

Effects of pressure and temperature on the absorbances of a 50 μM sulfide standard and a 200 μM silicate standard.

(For the sulfide and Si-AA[a] procedures 2-cm path length flow cells were used; for the Si-Sn method[b], a 0.5-cm path length was used. The results are not corrected for the differences in path length.)

Analysis	Pressure (dbar)	Absorbance		Ratio (19/5)
		5°C	19°C	
Sulfide	10	0.0584	0.1725	2.95
	3300	0.0921	0.1771	1.92
	Ratio (3300/10)	1.58	1.03	
Si-AA[a]	10	0.0277	0.1603	5.79
	3300	0.0408	0.2545	6.24
	Ratio (3300/10)	1.47	1.59	
Si-Sn[b]	10	0.114[c]	0.170	1.49
	3300	0.185[c]	—	
	Ratio (3300/10)	1.62		

[a]Determination of silicate with ascorbic acid as reductant. [b]Determination of silicate with tin(II) chloride as reductant. [c]Temperature was 2°C.

temperature and pressure. The absorbance of the silicate standards increased 6-fold over a 14°C range when ascorbic acid was used as the reductant. Temperature changes of 5 or 10°C, which may occur in a few tens of meters in the seasonal thermocline of the ocean, would lead to large changes in the calibration factor.

The determination of silicate by the molybdenum blue method with ascorbic acid involves two slow steps: formation of the molybdosilicate complex and reduction of the complex by ascorbic acid [12]. The extent of both reactions is less than 50% in the present flow system. These two slow steps are responsible for the large effect of temperature on the sensitivity. The influence of temperature on the silicate determination can be reduced significantly by using tin(II) chloride as the reductant. The molybdosilicate complex is reduced within a few seconds with this reductant [12]. Consequently, the effect of a 14°C temperature change on absorbances from silicate standards in the tin(II) chloride procedure is reduced to from 600% to 41% (Table 1). Therefore, tin(II) chloride was used as the reducing agent in all field work. If necessary, the effect of temperature can be further decreased by lengthening the time available for the formation of the molybdosilicate complex.

The sensitivity of both determinations increases with higher pressure (Table 1). This pressure-dependence indicates that the rate-limited steps involve the formation of transition states that have a smaller volume than that of the reactants (negative volume of activation). Slow bimolecular reactions are generally characterized by large negative volumes of activation [16]. Most of the reactions used in spectrophotometric analyses, particularly the reactions used to measure dissolved nutrients in sea water, fall into this class. An increase in sensitivity with pressure should, therefore, be expected for most analyses done with the SCANNER.

The combined effects of temperature and pressure on the sensitivity of the methods complicate the calculation of concentrations from detector voltages. If the extent of reaction is less than 100%, then it is imperative that the system be calibrated in situ. The influence of temperature and pressure can be reduced by increasing the extent of the reaction. For example, the extent of formation of the methylene blue used to quantify sulfide is 96% at 1 bar and 20°C [14]. An increase in the rate of reaction caused by an increase in the pressure can, at most, increase the sensitivity by only 3—4% (Table 1) at 19°C, barring any change in the molar absorptivity. However, the extent of reaction is less at 5°C and the effect of pressure is proportionately greater. The reaction manifold could be maintained at a higher temperature to increase the reaction rate if higher power consumption is acceptable. Further work is needed to find the optimum conditions for each chemistry and the frequency of in situ calibration that is required when working in environments with large temperature gradients, such as the seasonal thermocline.

Applications

The extensive communities of animals living in close proximity with hydrothermal springs in the deep sea [17] are one example of an area where high-resolution measurements must be made in situ. These dense communities at depths greater than two kilometers are remarkable because the deep sea is usually characterized by a low abundance of animals [18]. Physiological measurements [19, 20] demonstrate that the animals in hydrothermal vents have the capability to metabolize reduced compounds, primarily sulfide, that are present in high concentrations in the venting water [21]. Knowledge of the distributions of reduced chemicals around these animals is essential to an understanding of the community metabolism and structure. Relatively few measurements have actually been made because technology has limited the collection of water samples to a few per dive with manned submersibles.

The SCANNER has been used to measure silicate, sulfide, oxygen and temperature in the Rose Garden hydrothermal vent field of the Galapagos Rift [10]. These vents lie at a depth of 2450 m. The SCANNER was mounted on the outside of the submersible Alvin during this work. The sample inlet was placed on a probe attached to the starboard manipulator of the submersible. Data from the SCANNER were transmitted into the pressure hull of the submersible and displayed graphically on a battery-powered Hewlett-Packard HP-110 microcomputer.

More than 10,000 measurements of silicate, sulfide, oxygen and temperature were made in the Rose Garden vent field. Figure 5 shows the changes

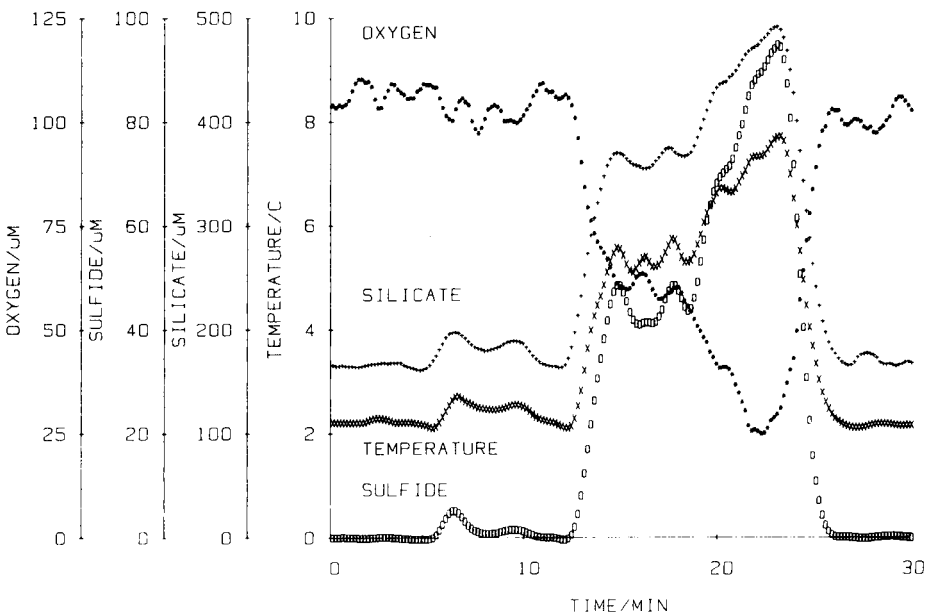

Fig. 5. Silicate, sulfide, oxygen and temperature values measured in situ with the SCANNER on Alvin dive 1528 in the Rose Garden vent field at site C [10].

measured in silicate, sulfide, oxygen and temperature over a 30-min period around a clump of hydrothermal vent animals. The sample inlet was moved a distance of about 1 m during the time period shown in the figure. The SCANNER responds rapidly (ca. 4 min) to step changes in chemical concentrations as the probe is moved through the sharp gradients around the vents. The 90% rise time for a step change is 40 s. There is some lag time for the sample to be transported along 5 m of 0.8 mm i.d. tubing from the inlet at the end of the manipulator to the LED photometers.

The precision of the determinations done in situ with the SCANNER was estimated from replicate analyses of ambient sea water at 2450 m (0 μM sulfide, 160 μM silicate). These measurements have a precision (1 standard deviation) of 0.05 μM sulfide and 1 μM silicate. The relative precisions of these measurements are comparable to those found in the laboratory. The dynamic range of the determinations extends to 300 μM sulfide and 800 μM silicate. At higher concentrations, the calibration curves become too flat for useful work. The sulfide calibration curve reverses itself at concentrations above 500 μM [14].

The accuracy of these procedures can be assessed by comparison with data that were obtained with previous measurements on discrete samples collected in the Galapagos Rift hydrothermal system. Linear regressions of temperature and silicate measurements on discrete samples collected in 1977 in the Galapagos Rift have a slope of 0.0160°C μM^{-1} [22]. Present measurements at a number of sites have slopes in the range 0.015—0.017°C μM^{-1} (Fig. 6) in agreement with the earlier measurements. However, sites with significantly higher (up to 0.0238°C μM^{-1}) slopes have also been found. These differences probably reflect real variability between sites, perhaps because of different

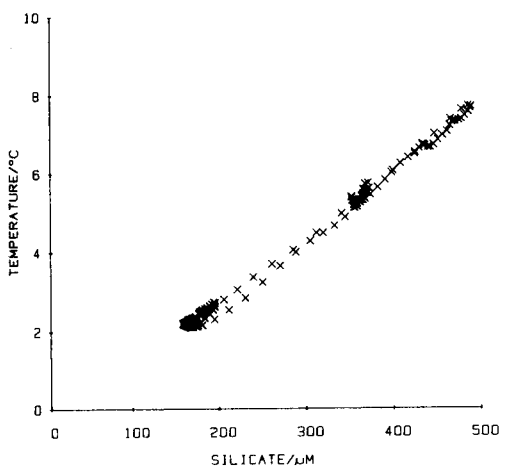

Fig. 6. Temperature plotted versus silicate from the data shown in Fig. 5. A least-squares linear regression through the data fits the equation T (°C) = —0.62 + 0.0165 C_{Si} (μM); r^2 = 0.996.

flow rates from the vents. Sulfide measurements made in situ with the SCANNER are also in general agreement with the concentrations found in discrete samples [10, 14]; there is no detectable bias in measurements made with the SCANNER, therefore.

Conclusions

The SCANNER has proven to be an effective tool for providing quantitative data on chemical concentrations in the ocean. It is capable of high-resolution measurements at depths greater than 2500 m. The versatility of flow analysis allows the SCANNER to be adapted to a variety of procedures. It can produce measurements in situ that might otherwise be difficult because of sampling artifacts [22]. Time-series analyses are also possible by tethering the SCANNER to a mooring. A broad suite of in situ measurements will greatly expand the capabilities of oceanographers to study ocean circulation. The combination of SCANNER data and the inverse techniques pioneered by Wunsch [23] would be a particularly valuable tool for tracing the flow of water. The SCANNER will lend itself to many innovative applications in oceanography.

This work was supported by NSF Grant OCE 83-11256 and ONR Contract N00014-82-K-0740. We thank Joel Edelman, Oscar Kirsten, Rudi Stuber and Stewart Willason for their advice and assistance. Dan Chabot graciously assisted with the Maripro, Inc., high-pressure test facility. James Childress provided the encouragement to initiate and complete this project.

REFERENCES

1 K. Grasshoff, in K. Grasshoff, M. Ehrhardt and K. Kremling (Eds.), Methods of Seawater Analysis, 2nd edn., Verlag Chemie, Weinheim, 1983, p. 1.
2 E. Foyn, in M. Sears (Ed.), Progress in Oceanography, Vol. 3, Pergamon, New York, 1965, p. 137.
3 D. R. Kester, K. T. Crocker and G. R. Miller, Jr., Deep-Sea Res., 20 (1973) 409.
4 S. Ben-Yaakov and I. R. Kaplan, Limnol. Oceanogr., 13 (1968) 688.
5 J. Růžička and E. H. Hansen, Flow Injection Analysis, Wiley-Interscience, New York, 1981.
6 K. K. Stewart, Anal. Chem., 55 (1983) 931A.
7 D. Betteridge, E. L. Dagless, B. Fields and N. F. Graves, Analyst (London), 104 (1978) 897.
8 H. P. Hansen and K. Grasshoff, in K. Grasshoff, M. Ehrhardt and K. Kremling (Eds.), Methods of Seawater Analysis, 2nd edn., Verlag Chemie, Weinheim, 1983, p. 347.
9 M. Bernhard, E. Torti, M. Ghibaudo, G. Rossi and A. Bruschi, in E. Kawerau (Ed.), Automation in Analytical Chemistry, Vol. 2, Mediad, White Plains, 1967, p. 391.
10 K. S. Johnson, C. L. Beehler, C. M. Sakamoto-Arnold and J. J. Childress, Science, in press.
11 J. D. H. Strickland and T. R. Parsons, A Practical Handbook of Seawater Analysis, Bull. 167, Fish. Res. Bd. Canada, Ottawa, 1972, p. 41.
12 J. Thomsen, K. S. Johnson and R. L. Petty, Anal. Chem., 55 (1983) 2378.
13 J. D. Cline, Limnol. Oceanogr., 14 (1969) 454.

14 C. M. Sakamoto-Arnold, C. L. Beehler and K. S. Johnson, Limnol. Oceanogr., in press.
15 T. J. Mickel, L. B. Quetin and J. J. Childress, in E. Gnaiger and H. Forstner (Eds.), Polarographic Oxygen Sensors, Springer-Verlag, Berlin, 1983, p. 81.
16 K. J. Laidler, Chemical Kinetics, McGraw-Hill, New York, 1965, p. 231.
17 J. B. Corliss, J. Dymond, L. I. Gordon, J. M. Edmond, R. P. von Herzen, R. D. Ballard, K. Green, D. Williams, A. Bainbridge, K. Crane and T. H. van Andel, Science, 203 (1979) 1073.
18 D. Desbruyeres and L. Laubier, in P. A. Rona, K. Bostrom, L. Laubier and K. L. Smith, Jr., (Eds.), Hydrothermal Processes at Seafloor Spreading Centers, Plenum, New York, 1983, p. 711.
19 H. Felbeck, Science, 213 (1981) 336.
20 J. J. Childress, A. J. Arp and C. R. Fisher, Jr., Mar. Biol., 83 (1984) 109.
21 J. M. Edmond, C. Measures, B. Mangum, B. Grant, F. R. Sclater, R. Collier, A. Hudson, L. I. Gordon and J. B. Corliss, Earth Planet. Sci. Lett., 46 (1979) 19.
22 J. W. Murray, S. Emerson and R. Jahnke, Geochim. Cosmochim. Acta, 44 (1980) 963.
23 C. Wunsch, Rev. Geophys. Space Phys., 16 (1978) 583.

Analytica Chimica Acta, 179 (1986) 259—267
Elsevier Science Publishers B.V., Amsterdam — Printed in The Netherlands

SELECTIVITY ENHANCEMENT BY FLOW INJECTION ANALYSIS

G. E. PACEY*, D. A. HOLLOWELL, K. G. MILLER, M. R. STRAKA and G. GORDON
Department of Chemistry, Miami University, Oxford, OH 45056 (U.S.A.)
(Received 9th August 1985)

SUMMARY

Flow injection analysis offers numerous possibilities for significantly increasing the selectivity of existing methods by utilizing knowledge of the chemistry of those methods. It also enables new selective methods to be created by utilizing kinetic methods and fast separation techniques such as gas diffusion, dialysis, extraction and ion-exchange columns. Selectivity enhancements and increased sensitivity can be achieved by incorporating the kinetic techniques of kinetic discrimination and/or kinetic enhancement into the timing of the system or the reagent concentrations and conditions for a given method. Methods have been developed for quantifying ozone, chlorine dioxide, chlorate ion, and chlorite and chlorate ions sequentially. A dual-phase gas diffusion system for hydride generation provides significant decreases in the interferences observed for transition metals.

Flow injection analysis (f.i.a.) is unquestionably an excellent technique for the automation of existing methods. Rapid throughput and high reproducibility are now expected of any flow-injection method. However, the most promising advantage of f.i.a. lies in the utilization of the gradients and the incorporation of separation techniques in order to develop improved methods. This aspect makes it possible to increase the selectivity of existing methods significantly by utilizing knowledge of the chemistry of those methods. It also offers possibilities of creating new selective methods by utilizing separation techniques such as gas diffusion, dialysis, extraction, column separations, and kinetic methods. Selectivity enhancements and increased sensitivity can be achieved by incorporating the techniques of kinetic discrimination and/or kinetic enhancement into the timing of the system or the reagent concentrations and conditions for a given method.

In this paper, several improved or new methods are discussed for selectively or specifically quantifying a given analyte. Evaluation of the selectivity factor contributed by a given technique for selectivity enhancement is derived.

EXPERIMENTAL

For all the experiments, the Tecator 5020 flow injection analyzer was used with Chemifolds I—V. The detectors used were a Tecator 5023 spectro-

0003-2670/86/$03.50

photometer for visible measurements, an ISCO-V4 flow-through spectrophotometer for u.v. measurements, a Perkin-Elmer 560 atomic absorption unit for atomic absorption measurements and a spiral T-cell mounted on a GCA-McPherson photomultiplier housing unit. A Keithley 601 or 617 electrometer was used to amplify signals in the chemiluminescence system.

All reagents were of analytical grade except for some primary standards. The chlorine dioxide and ozone samples were prepared by established procedures [1, 2]. All water was prepared by passing through a Barnstead ion-exchange system followed by a Barnstead double-distillation system.

RESULTS AND DISCUSSION

Flow-injection methods provide excellent opportunities to take advantage of the chemistry being used. Two techniques that can easily be incorporated into a flow-injection system are kinetic discrimination and kinetic enhancement. In kinetic discrimination the differences in the rates of reactions with the reagent between the analyte of interest and the interferents are exploited. In kinetic enhancement, an understanding of the rate equation allows the chemical reactions involved to be driven in the direction appropriate to the analyte of interest. Obviously, both techniques are dependent on an understanding of the chemistry of the analytical reagent. Very few reagents react instantaneously with all potential analytes, but in batch chemistry measurements are made at equilibrium conditions where any kinetic difference is lost. However, under the conditions of f.i.a., the reagents appear to react reproducibly but with different sensitivities. These differences in sensitivity result from the different kinetics of the reaction between reagent and analyte and/or interferent.

Kinetic discrimination in the determination of ozone and chlorine dioxide

Two examples of kinetic discrimination are the determination of ozone with indigo blue and the determination of chlorine dioxide based on luminol chemiluminescence. Both reagents are capable of reacting with chlorine. Even though ozone and chlorine dioxide are considered as alternative water disinfectants, chlorine will still be present in a water sample. Therefore, the determination of residual ozone or chlorine dioxide in the presence of residual chlorine is important.

For the batch determination of ozone with indigo blue, the equilibrium measurements do not discriminate between ozone, chlorine, and manganese-(VII) [3]. Investigation of the reaction rate between chlorine with indigo blue and ozone with indigo blue showed that ozone reacts much faster than chlorine or manganese with indigo blue. Therefore, it appeared that this reagent system would be an excellent candidate for kinetic discrimination by means of f.i.a.

The manifold that is used is a limited dispersion system (Fig. 1). The decolorization of the indigo blue is measured at 600 nm. The results of the

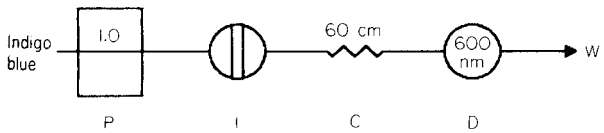

Fig. 1. Manifold for the determination of ozone by observing the bleaching of indigo blue reagent at 600 nm: P, pump; I, injector; C, 60-cm coil; D, visible spectrophotometer. Flow rate 1.0 ml min^{-1}; all tubing was 0.5 mm i.d. teflon. The concentration of indigo depends on the sensitivity needed; for these experiments, 15 mg l^{-1} and 77 mg l^{-1} were the concentrations used.

manual and flow-injection methods are compared in Table 1. As can be seen, the flow-injection system increased the selectivity for ozone over chlorine by a factor of about 3, and that over Mn(VII) by a factor of about 2. Although the method described is not considered selective, this does demonstrate that kinetic discrimination can be useful and can enhance the selectivity of a method, particularly when combined with a preseparation technique (e.g., gas diffusion).

In the case of the chemiluminescence determination of chlorine dioxide with luminol, the differences in the signal produced for chlorine dioxide and chlorine depend on time and pH. Chlorine dioxide reacts extremely quickly with luminol while chlorine reacts more slowly and with longer lifetimes. By using a flow-injection system, the chemistry and timing can be controlled in such a way as to minimize the signal for chlorine. The additional use of pH 13 makes the reagent even more selective, under flow-injection conditions, toward chlorine dioxide. The observed selectivity factor between chlorine dioxide and chlorine is over 500.

It is difficult at best to attempt to use these methods in a segmented flow system because of analyte decomposition and diffusion of analyte into the gas segmentation. Therefore, the only real comparison is with batch methods. In both cases, the selectivities are improved.

TABLE 1

Comparison of analytical properties of the manual and automated ozone determination based on indigo blue

		Manual	Flow-injection
Indigo solution consumed per sample (ml)		10	0.5
Sampling frequency		20	120
Precision (%)		5	<1
Interferences:	H_2O_2	None	None
	Mn(VII)	1 mg l^{-1} ≡ 0.8 mg l^{-1} O_3 (apparent)	1 mg l^{-1} ≡ 0.44 mg l^{-1} O_3 (apparent)
	Cl_2	1 mg l^{-1} ≡ 0.9 mg l^{-1} O_3 (apparent)	1 mg l^{-1} ≡ 0.36 mg l^{-1} O_3 (apparent)

Kinetic enhancement

Kinetic enhancement involves driving the chemical reactions of a system toward the production of the signal-producing species. This technique is needed when the chemical reactions used in a procedure do not meet the requirements for sensitivity or selectivity. In the example given below, other limitations such as the presence of air (oxidation) or the health hazard of high reagent concentration (12 M hydrochloric acid) precludes the utilization of this chemistry in batch methods.

The example discussed is the determination of chlorate below concentrations of 0.125 mg l^{-1} with a relative standard deviation (RSD) better than ±5%. The reaction of chlorate with iodide ions is extremely slow; the rate shows that it is a second-order reaction with respect to acid concentrations. Therefore, the approach is to use 6—12 M hydrochloric acid to enhance the production of the iodine. Unfortunately, the fumes are objectionable and the air oxidation of iodine is increased at high acid concentrations. Cumbersome precautions must be taken in batch methods to eliminate these problems [4]. However, under flow-injection conditions (Fig. 2), the rate of the reaction can be increased by using 12 M hydrochloric acid because the flow system excludes air and contains the hydrogen chloride fumes. When standard f.i.a. is used, the detection limit for chlorate is 1×10^{-5} M. By using a stopped-flow system, the detection limit is improved to 1×10^{-6} M. Overall, the kinetically enhanced flow-injection method improved the detection limit of the chemical system from 1×10^{-4} M (batch) to 1×10^{-6} M. The reproducibility was improved to less than 1% versus 25—50% (batch). Table 2 shows the results for the determination of chlorate in samples. It is important to note that there is no batch method suitable for comparison; the best batch method cannot detect chlorate at these concentrations. The kinetic enhancement technique provided a significant increase in the sensitivity of the method.

The increase in selectivity that can be achieved by the use of kinetic discrimination can be used in conjunction with another technique such as chasing zones. The reaction that releases iodine from chlorate ion will also produce iodine from chlorite ions. However, chlorite reacts easily with iodide at pH 4. This means that a selective iodimetric method for chlorite in the presence of chlorate can easily be developed. But by using kinetic enhancement and chasing zones, sequential chlorite and total chlorite/chlorate determinations are also possible.

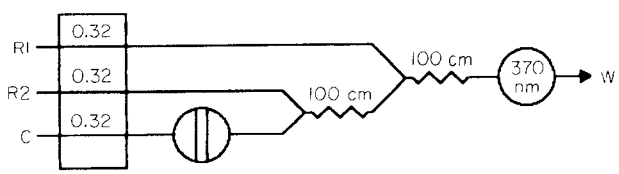

Fig. 2. Manifold for the determination of chlorate: R_1, 12 M HCl; R_2, 0.3 M potassium iodide; C, water carrier stream; 0.32 ml min^{-1} flow rate for all streams; 0.5 mm i.d. teflon tubing was used; detection at 370 nm.

TABLE 2

Accuracy of the determination of chlorate samples

Chlorate concn. (M)		Error (%)	Chlorate concn. (M)		Error (%)
Actual	Found		Actual	Found	
Straight f.i.a.			*Stopped-flow f.i.a.*		
1.6×10^{-5}	1.6×10^{-5}	0	2.6×10^{-6}	2.4×10^{-6}	7.7
9.2×10^{-5}	9.3×10^{-5}	1.1	3.2×10^{-6}	3.2×10^{-6}	0
4.8×10^{-5}	4.8×10^{-5}	0	4.0×10^{-6}	3.7×10^{-6}	7.5
			6.0×10^{-6}	6.0×10^{-6}	0
			7.0×10^{-6}	7.0×10^{-6}	0

By injecting a 12 M hydrochloric acid plug in front of the injected sample stream followed by the usual pH 4 carrier, a chasing zone situation is established (Fig. 3). As the plugs flow down the tube and dispersion occurs, the first plug and the front edge of the sample plug overlap while the back of the sample plug and the pH 4 carrier stream overlap. The result is a double peak. The first peak corresponds to total chlorate and chlorite. The second peak is for chlorite only. Although the chlorate is determined indirectly, the two peaks are measured under exactly the same conditions, which makes the indirect determination more acceptable. The manifold can be constructed in such a way as to insure that the peaks exhibit the same sensitivity for equal concentrations of chlorite and chlorate.

Separation techniques

The separation techniques of f.i.a. are becoming well established. By utilizing extraction, columns, gas diffusion, and dialysis, many classical separation chemistries can readily be automated. However, the real advantages of these methods are the increase in selectivities that can be realized. In particular, gas diffusion has been studied here.

By incorporating gas diffusion into a flow-injection system, several selec-

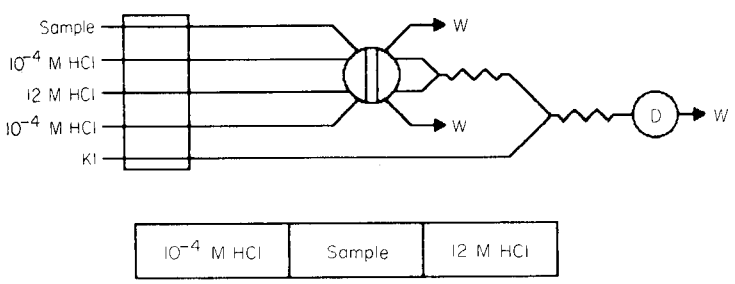

Fig. 3. Manifold for the sequential determination of chlorite and chlorate with 0.3 M potassium iodide. Both 12 M and 1×10^{-4} M HCl were used; coil lengths were 60 cm each; detection was at 370 nm. The bottom blocks show the initial positions of the plugs immediately after the first confluence point.

tivity factors can be exploited. The most obvious is that when teflon micrc porous membranes are used, aqueous solutions do not wet the membran surface. Therefore, ionic interferences such as that of manganese(VII) in th ozone determination will not pass through the membrane and so will be eliminated. The second, less obvious, advantage is the difference between gases in terms of their permeability through the membrane. Although gas diffusion is based on physical properties such as vapor pressure [5], the membrane used will add some selectivity to the system. As an example, although the vapor pressure of chlorine is three times that of chlorine dioxide, the selectivity between the two gases based on the teflon membrane only is 3.1 in favor of chlorine dioxide [6]. When these selectivity factors are multiplied by those of kinetic discrimination, the resulting selectivities can be very impressive.

Three examples of this type of advantage are provided by the gas-diffusion methods for ozone based on indigo blue, chlorine dioxide based on straight absorbance measurements, and chlorine dioxide based on chemiluminescence. Once again, the interference that is most troublesome is chlorine, followed by several ionic species.

In the case of the gas-diffusion method for ozone with indigo blue, the diffusion membrane totally eliminated the manganese(VII) interferences. The interference from chlorine was significantly decreased from 1 mg of chlorine corresponding to 0.36 mg l^{-1} ozone (apparent) for the manual method to 0.008 mg l^{-1} ozone (apparent) in the gas-diffusion method (Table 3). The reagent has a selectivity factor of 2.5 from kinetic discrimination while the inclusion of the gas-diffusion membrane to the system enhanced the selectivity by a factor of 45, giving a total selectivity factor for the method of about 112. In the case of the determination of ozone in the presence of chlorine, this selectivity factor is sufficient for a method used to determine residual ozone in disinfected water samples. The combination of kinetic discrimination and gas diffusion make this method possible.

TABLE 3

Comparison between the standard flow-injection method and the gas-diffusion method for ozone determinations with indigo blue

	Standard f.i.a.	Gas diffusion
Sample frequency	120	65
Linear range (mg l^{-1} O_3)	2—4.0	0.03—0.4
Sensitivity (Abs./mg l^{-1})	0.04	0.1191
Interference		
H_2O_2	None	None
Mn(VII)	1 mg l^{-1} ≡ 0.44 mg l^{-1} O_3[a]	None
Cl_2	1 mg l^{-1} ≡ 0.36 mg l^{-1} O_3[a]	1 mg l^{-1} ≡ 0.008 mg l^{-1} O_3[a]

[a]Apparent.

The determination of chlorine dioxide by means of gas-diffusion f.i.a. and absorbance detection has been described [6]. The use of gas diffusion again eliminates both ionic and organic materials that absorb light in the ultraviolet region. Experiments run to evaluate the selectivity enhancement between chlorine dioxide and chlorine created by the membrane produced a selectivity factor of 3.1. When this selectivity factor is multiplied by the selectivity factor created by the difference in molar absorptivity for Cl_2 and ClO_2 at the wavelength used, a factor of 175, the total selectivity is over 550. When this selectivity is multiplied by the masking effect of oxalic acid on chlorine [6] then the overall selectivity is over 5500.

In the case of the luminol chemiluminescence method for the determination of chlorine dioxide (Fig. 4), the addition of the gas diffusion cell produces an extremely selective method without the use of masking agents. The gas-diffusion cell with a 3.1 selectivity factor multiplied by the 500 selectivity factor arising from kinetic discrimination gives a method with a selectivity factor of over 1500. Table 4 shows the good accuracy of this method. By eliminating masking agents, any side-reactions that may be created by these reagents are no longer a problem, thereby simplifying the system. This simplification is extremely important in dealing with readily decomposing analytes like ozone and chlorine dioxide.

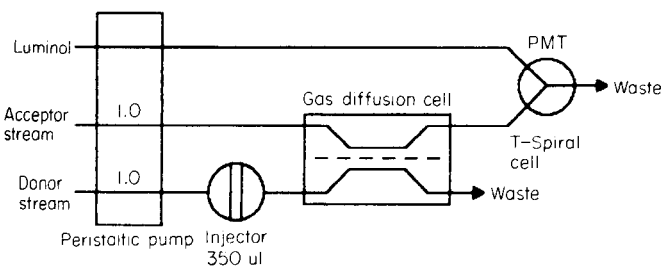

Fig. 4. Manifold for the determination of chlorine dioxide based on luminol chemiluminescence. Donor and acceptor streams are water at pH 2; the pH is adjusted with sulfuric acid. Luminol (1×10^{-3} M) is the reagent mixed in front of the PMT in the spiral T-cell. The membrane is 0.45-μm teflon (Gore); 0.5 mm i.d. teflon tubing is used. Flow rates are 1 ml min^{-1} for all streams.

TABLE 4

Determination of chlorine dioxide in the presence of a large excess of chlorine based on luminol chemiluminescence

Chlorine concn. (mg l^{-1})	Chlorine dioxide concn. (mg l^{-1})		
	Taken	Found	Error
0.42	0.016	0.0174	0.0014
4.2	0.016	0.0206	0.0046
0.42	0.16	0.165	0.005
4.2	0.16	0.171	0.011
42.0	0.16	0.192	0.032

Dual-phase gas diffusion

Gas diffusion can be extended even further to take advantage of those selectivity factors. The development of the dual-phase gas diffusion system allows the process of gas diffusion to occur from liquid to gas phase in order to utilize gas-phase reactions for detection.

The best example is the use of the dual-phase gas diffusion cell to generate hydrides for their detection by atomic absorption spectrometry. Hydride generation procedures suffer from interference in both the liquid and gas phases. The interferences in the gas phase involve the atomizer and have essentially been eliminated by Dedina [7]. However, the interferences in the liquid phase still pose a problem

The interferences in the liquid phase are in two categories. The transition metals precipitate during hydride generation and adsorb the hydrides on their surface, thereby decreasing the signal. The second type of interference is the competition between hydride-forming metals. Both these types of interference are a function of the residence time of the hydride in solution. Although attempts have been made to use f.i.a. to automate the process in the hope that the kinetics would be in their favor, no one seems to have incorporated gas diffusion into the hydride system.

The use of the dual-phase gas diffusion cell allows the hydride to pass immediately through the membane into a hydrogen acceptor stream. The effect of this process is to decrease the contact time between the hydride and any transition metal precipitate. The end result is that the interference levels observed for this system versus other flow methods are similar or better (Table 5). The hydride competition interference is also effective but in a very sporadic way (Table 5). The observed reductions are really a combination of the separation techniques of f.i.a. and kinetic discrimination.

TABLE 5

Permissible levels[a] of interfering ions in arsenic hydride generation using a dual-phase gas diffusion cell

Ion	Continuous flow method [8]	Dual-phase gas diffusion	Ion	Continuous flow method [8]	Dual-phase gas diffusion
Fe(III)	—	10,000	Bi(III)	3000	200
Cu(II)	1000	10,000	Sb(III)	20	100
Ni(II)	300	2500	Te(IV)	100	25
Co(II)	500	10,000	Se(IV)	5	5
Sn(II)	50	1250			

[a]Permissible amounts (weight ratio) correspond to the concentrations that give an error of $\leqslant 10\%$.

Conclusion

The advantage of f.i.a. is the possibility of combining gradients, separation techniques and kinetics to improve the selectivity and sensitivity of a given method. Without question, f.i.a. allows the development of new methods with excellent selectivity, reproducibility and accuracy.

The dual-phase gas diffusion method has many potential uses because many gas-phase reactions at room-temperature produce strong measurable signals. One such example for future work is the determination of ozone with nitrous oxides.

REFERENCES

1 J. Benga, Dissertation, Miami University, Oxford, OH, 1980.
2 D. H. Rosenblatt, A. J. Hayes, Jr., B. L. Harrison, R. A. Streaty and K. A. Moore, J. Org. Chem., 28 (1963) 2790.
3 H. Bader and J. Hoigne, Water Res., 15 (1981) 449.
4 Y. Ikeda, T. F. Tang and G. Gordon, Anal. Chem., 56 (1984) 71.
5 W. E. Van der Linden, Anal. Chim. Acta, 151 (1983) 359.
6 D. H. Hollowell, Dissertation, Miami University, Oxford, OH, 1985.
7 J. Dedina, Anal. Chem., 54 (1982) 2097.
8 M. Ikeda, Anal. Chim. Acta, 167 (1985) 289.

Analytica Chimica Acta, 179 (1986) 269—278
Elsevier Science Publishers B.V., Amsterdam — Printed in The Netherlands

THE RAPID DETERMINATION OF CHEMICAL OXYGEN DEMAND IN WASTE WATERS AND EFFLUENTS BY FLOW INJECTION ANALYSIS

J. M. H. APPLETON and J. F. TYSON

Department of Chemistry, University of Technology, Loughborough, Leicestershire, LE11 3TU (Great Britain)

R. P. MOUNCE

British Gas Corporation, London Research Station, Michael Road, London, SW6 2AD (Great Britain)

(Received 6th September 1985)

SUMMARY

Chemical oxygen demand (COD) and the limitations of the standard method of determination are discussed. A fully automated method based on a commercial flow injection analyzer is described. The results obtained with a processing time of 3 min are comparable with those given by the standard method for a wide range of types of effluent. Good agreement was achieved between the results for various standard materials. Mercury(II) is added to the sample to prevent chloride interference. Silver(I) catalyst can be incorporated into the reagent. A limitation to performance is caused by the maximum cycle time of 198 s of the analyzer.

The discharge of polluting organic matter to water-courses is strictly controlled by water authorities. When an ecological balance is maintained, natural waters are purified by biochemical oxidation by micro-organisms which utilize the polluting substances as sources of carbon whilst consuming dissolved oxygen for respiration. The rate of purification depends on many conditions, including the water temperature and the nature of the pollutants.

In Europe and the U.S.A., a widely-used index of waste water quality is chemical oxygen demand (COD) which relates to the oxygen required for complete oxidation of the sample. The COD is an arbitrary empirical measurement obtained by subjecting the sample to oxidation by chromic acid under prescribed conditions. Despite its importance, the manual method has several disadvantages. It is complicated and time-consuming, requiring toxic reagents; precision depends heavily on operator skill, and about 3 h is required to obtain a result. This delay presents holding and discharge problems for industries producing large volumes of effluents. As a result of these shortcomings, improvements or alternatives to the traditional COD method have been sought. The major considerations in this are the extent to which the traditional method is entrenched in industrial and analytical practice and in legislation, the extreme range of effluent types, and the fact that most

0003-2670/86/$03.50

effluents are complex mixtures of substances with varying susceptibilities to oxidation. Present and planned schedules dealing with effluent analysis require many COD determinations and considerable manpower commitment. The development of an automated method would improve the efficiency of pollution control and the operation of biofermentors and effluent treatment plants.

An AutoAnalyzer procedure for the determination of COD was described by Adelman [1] in 1966. More recently, extensive work on the determination of COD by flow injection analysis (f.i.a.) has been reported by Korenaga and Ikatsu who used permanganate [2] or dichromate [3] as the oxidant. The latter method gave about 75% of the result by the conventional method in 20 min. However, labour-saving versions of the traditional apparatus remain widely used and there are continued research efforts in the same direction [4]. When an alternative method for COD is based on milder conditions than those employed in the standard method, more stable compounds in the samples may resist oxidation, leading to low results. The use of correction factors to derive standard COD values from such results is questionable, because those probably relate to the masses of readily-oxidizable material in the samples, which is not a simple measure of COD. Therefore, an alternative COD method is valid only if it achieves the same degree of oxidation of the sample as the standard method. Hence conditions and chemistry should correspond as closely as possible to those conventionally used.

In the standard procedure, the interference of chloride is reduced to acceptable levels by the addition of mercury(II) sulphate. The degree of suppression depends on the ratio of mercury(II) to chloride ions [5]. Dobbs and Williams [6] recommended a ratio of at least 5:1. Certain compounds, notably those containing an aromatic nucleus, may be only partly and irreproducibly oxidized. Heterocyclic compounds, such as pyridine, are particularly resistant to oxidation. Conventionally, silver sulphate (about 0.5% in the refluxing mixture) is added to catalyse the oxidation of straight-chain alcohols and acids. The oxidation of acetic acid, for example, is improved from about 2% to about 95% of the theoretical value by the use of silver sulphate [7]. Thus any procedure which omits mercury(II) and silver(I) ions cannot be expected to reproduce standard COD values for all samples.

Ideally, then, a method suitable for automated determination of COD should be quick, simple, cheap, and as effective as the standard method in oxidizing the samples. This paper describes an attempt to realize these objectives with conventional f.i.a. equipment. In the proposed method, a reagent stream, containing potassium dichromate and sulphuric acid, is merged with a distilled water carrier into which samples are injected. After the merging point, whilst the stream flows through a suitable reactor, the sample is oxidized and Cr(VI) species in the reagent are reduced to Cr(III). Downstream, the absorbance of chromate is monitored at 445 nm. Reagent consumption is indicated by a transient negative departure from the steady-state absorbance. In this paper, response is shown as the magnitude ΔV (in mV) of this negative peak.

EXPERIMENTAL

Reagents

Analytical-grade chemicals and distilled water were used unless specified otherwise.

Potassium dichromate/sulphuric acid reagent. About 600 ml of sulphuric acid, obtained from a newly opened 2.5-l bottle, was placed in a beaker in a sink. A solution of 3.0 g of potassium dichromate in 25 ml of distilled water was added dropwise down the inside of the beaker with vigorous stirring (addition of the acid to the solution precipitates chromium trioxide). After cooling, the contents of the beaker were returned to the bottle and mixed to yield approximately 2.5 l of reagent.

Reference solutions for COD determinations. Solutions with a theoretical 800 mg l^{-1} COD were prepared containing potassium hydrogenphthalate (0.680 g l^{-1}), D-glucose (0.750 g l^{-1}), sodium oxalate (6.70 g l^{-1}), sodium salicylate (0.571 g l^{-1}) and sodium acetate (1.025 g l^{-1}).

A 1000 mg l^{-1} chloride solution was prepared from sodium chloride. The mercury(II) sulphate was Fisons SLR grade.

Instrumentation

A Tecator 5020 flow injection analyzer was used with a 5032 spectrophotometer (detector/controller/printer) equipped with a 5000-0428 Flow-cell (volume 18 μl, 10-mm path length) and a 5007 autosampler. Some work involved the use of an external Gilson Minipuls 2 peristaltic pump. The peaks were recorded with a Tekman TE200 chart recorder. The manifold represented schematically in Fig. 1 is the final version resulting from considerable preliminary development and optimization, as described below.

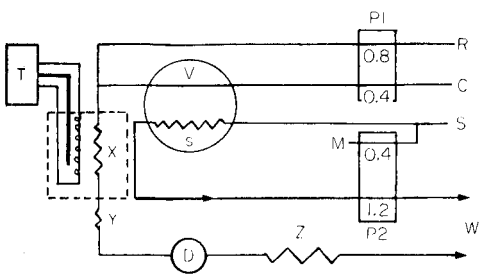

Fig. 1. Flow-injection manifold for the determination of COD. P1, an external Gilson Minipuls II peristaltic pump operated continuously on speed setting 700; P2, right-hand pump of the Tecator 5020 Analyzer; V, injection valve fitted with a sample loop of volume s; X, Y and Z, coils of 0.58 mm i.d. teflon tubing (Anachem) of lengths 3.0, 0.75 and 1.5 m, respectively. Reaction coil X is housed in an oven equipped with a temperature control T; Y is a water-cooled coil and Z a back-pressure coil. R, C, S and M are streams of chromic acid reagent, water, sample and mercury(II) sulphate, respectively. R is pumped via Acidflex tubing; the other pump tubes are Tygon. The figures indicate the flow rates quoted in ml min^{-1} for the pump tubes used. The thumb wheel settings were 99/99/99/30/9/6, the left-hand pump being switched off.

Procedures

Development of apparatus. The first manifold was based on an appraisal of the chemistry involved, the instrumentation available and the experiences of earlier workers [1—3]. The major object was to obtain rapid and effective oxidation of the sample using simple apparatus. The effects of temperature, flow rates, reagent composition and manifold geometry were investigated. By varying parameters within the instrumental limitations, conditions giving acceptable sensitivity and calibration linearity were identified.

Determination of COD. Initially the performance of the method was investigated using solutions with equivalent theoretical COD's of various substances. Sodium acetate was included, in order to demonstrate the catalytic action of silver sulphate. Investigation of the suppression of chloride interference by mercury(II) sulphate necessitated incorporation of this substance into the test solutions because it is only sparingly soluble in the chromic acid reagent. The responses to injections of potassium hydrogenphthalate, with and without mercury(II) sulphate, were compared. Samples for analysis were industrial effluents supplied by the British Gas Corporation and trade effluents obtained locally. Their COD values, determined routinely by independent authorities using the standard method, were compared with the results obtained by the flow-injection method.

RESULTS AND DISCUSSION

Development of apparatus

The Tecator 5020 Analyzer has the advantages of a ready-made automated system with programmable pumping and built-in signal evaluation. It also has some limitations. The analytical cycle is limited to just over 3 min (198 s). As the standard method for COD involves refluxing for 2 h, this limitation represents a considerable challenge. Initially, the coils X and Y (Fig. 1) were 5 m and 2 m, respectively, and the injected volume of sample was 260 μl; the reaction coil X was immersed in an oil bath. This system performed well but required an analytical cycle time of about 7 min, which could not be automated with the 5020 Analyzer.

As reported by Korenaga and Ikatsu [3], pumping the reagent presents a problem. Some difficulty in maintaining baseline stability was experienced with the 5020 peristaltic pump when tubes of different bores and/or materials were fitted over a common pump wheel. Pumping efficiency is a function of the tension in the compression band. The optimum tension for one tube may be quite unsuitable for another. Also relative movement and wear of the tubes tend to alter the flow rates. Better results were obtained when the multichannel Gilson pump replaced pump P1 (Fig. 1) because this pump restricts lateral movement of the tubes on the rollers and allows independent optimization of the compression of each tube. Even so, the useful lifetime of the Acidflex pump tube was only 3—4 h of continuous operation.

The temperature of the heating bath must be constant, because it influ-

ences the steady-state absorbance (increased temperature gives lower absorbance). An ordinary commercial thermostat, providing 160 ± 8°C, produced a sinusoidal baseline and was replaced by a purpose-built analogue controller which gave a thermal stability better than ±1°C at 160°C. In the first trials, conducted at 120°C, bubbles formed in the stream and were removed by splitting the stream immediately before the flow cell. An inverted glass Y junction was used; the stream entered by one arm and 20% flowed out to the detector via the other while the rest, together with the bubbles, flowed up the vertical stem to waste. As expected, the signal was very noisy.

However, from the outset it was intended to achieve reaction conditions in the manifold at least as aggressive as those used in the standard method. In order to achieve the required temperature (160°C) in the stream without it boiling, the proportion of sulphuric acid was increased above that used conventionally. If carefully degassed distilled water was used as the carrier, for the preparation of standards and for the dilution of the concentrated samples, the reaction proceeded, even at a bath temperature of 200°C, with no bubble formation. Baseline noise, caused largely by the formation of minute bubbles as the stream approached boiling point, was drastically reduced. The debubbling device was thus redundant. As a final development, the oil bath was replaced by a purpose-built oven.

The optimization of response

An attempt to reduce the analytical cycle time by increasing the carrier and reagent flow rates led to increased reagent consumption and higher manifold pressures, with reduced baseline stability and increased risk of reagent spillage. A cycle time compatible with the performance of the 5020 was therefore achieved by adjusting the flow rates and decreasing the manifold dimensions to those described in Fig. 1.

The variation of response with sample volume, carrier flow rate and reaction temperature is summarized in Figs. 2—4. The most powerful of these effects is changing the sample volume (s). Increasing this volume leads to increased sensitivity and reduced linear calibration range (Fig. 2). For fixed flows of reagent (R), the carrier flow rate (C) determines both the sample-to-reagent ratio and the initial length of the sample zone at the confluence point. Figure 3 illustrates results obtained by varying C by means of an external Gilson peristaltic pump. Optimum sensitivity occurs around the 400 speed setting. Under the chosen operating conditions, baseline absorbance increased with heating bath temperature in a manner which suggested increasing thermal decomposition of the reagent (Fig. 4). However, stopping the flow for 1—2 min produced no further reagent depletion, so some other thermal change must be involved. Mere mixing of the reagent and carrier streams generates a stream temperature of about 100°C, so the use of a lower bath temperature actually cools the mixture. The net peak response reaches a maximum at a bath temperature of about 180°C.

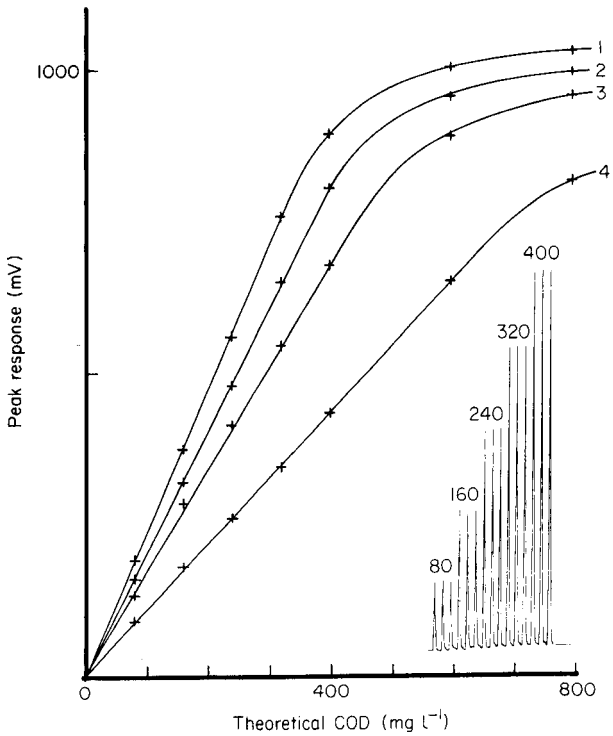

Fig. 2. The effect of sample volume on sensitivity and linear range of calibration. Curves: (1) 130 μl; (2) 110 μl; (3) 90 μl; (4) 60 μl. Conditions: potassium hydrogenphthalate as reference substance; 176°C oven; 18 cycles per hour. The inset shows the 90-μl peaks for 80, 160, 240, 320, 400 mg l^{-1} COD solutions.

The determination of COD

Various pure substances were used as reference materials for COD. Even in the absence of silver sulphate catalyst, glucose, sodium salicylate, sodium oxalate and potassium hydrogenphthalate produced calibration plots that were identical within 4% (Table 1), which suggested that these substances were completely oxidized. In contrast, the peak responses produced by equivalent (COD) solutions of sodium acetate were scarcely distinguishable from the baseline noise (Fig. 5A). Incorporation of silver sulphate (7.5 g l^{-1}) into the reagent (i.e., 0.5% after merging with the carrier) produced a dramatic increase (to more than 90% of the theoretical value) in these responses. The responses of the industrial samples 3 and 4 were unchanged (Fig. 5B).

The masking of chloride interferences was investigated by using solutions of potassium hydrogenphthalate (200 mg l^{-1} COD), containing 5.0 g l^{-1} of mercury(II) sulphate and chloride levels between 0 and 500 mg l^{-1} (Fig. 6). Introduction of the mercury salt by saturating the reagent with it, effective up to 50 mg l^{-1} chloride, would be suitable for the determination of the

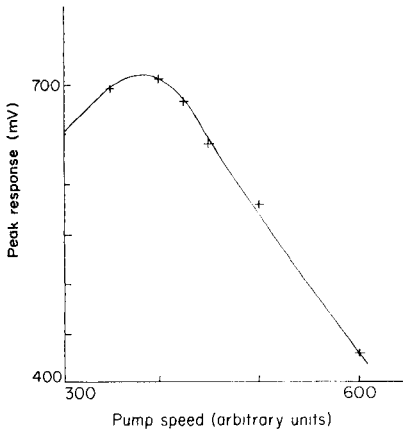

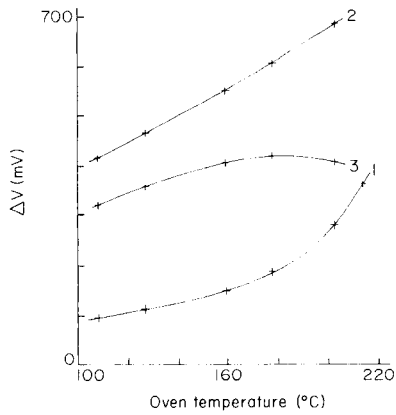

Fig. 3. The effect of increasing the carrier flow rate (C) for a constant reagent flow. C was pumped at various rates using the Gilson pump with O/W coded tubing (0.8 ml min^{-1}) whilst R was pumped at a constant rate by the pump of the 5020 Analyzer using B/B coded tubing (1.2 ml min^{-1}). Potassium hydrogenphthalate solution (200 mg l^{-1} COD) was injected (160 μl); temperature was 160°C.

Fig. 4. The effect of heating bath temperature on baseline and peak response. The baseline was initially set at 950 mV at ambient temperature (24°C). Curves 1 and 2 show the interval ΔV from this level to the baseline and peak, respectively, as temperature increases. Plot 3 shows the net interval ΔV between baseline and peak response. Potassium hydrogenphthalate solution (240 mg l^{-1} COD) was injected (110 μl). Injection at a bath temperature of 214°C produced bubbles in the stream, which disrupted the output.

COD of river water, which usually contains about 10 mg l^{-1} chloride. The results demonstrate serious chloride interference in the determination of COD when no mercury(II) sulphate is added.

Reproducible performance of the apparatus was restricted chiefly by base-

TABLE 1

Peak responses (mV) for different substances

Substance	Theoretical COD (mg l^{-1})					Least-squares regression[a]		
	80	160	240	320	400	Slope	Intercept	r
Glucose	156	310	463	625	754	1.90	4.0	0.9996
Salicylate[b]	159	320	485	651	794	2.00	0.7	0.9998
Oxalate[b]	159	321	484	659	792	2.01	0.9	0.9996
KHP[c]	153	313	482	654	806	2.04	−6.0	0.9998
Mean	157	316	478	647	784	1.983	0.4	0.9997

[a]Origin included in data, because peaks are measured from baseline which corresponds to the blank; r is Pearson's correlation coefficient. Sample volume 110 μl; reactor temperature 176°C. [b]As sodium salt. [c]Potassium hydrogenphthalate.

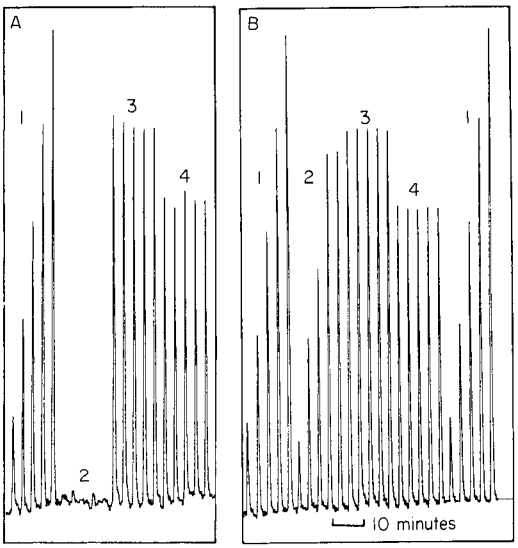

Fig. 5. The catalytic action of silver(I). A, No silver(I) added; B, 7.5 g l^{-1} silver sulphate added to reagent. Peaks: (1) potassium hydrogenphthalate (80, 160, 240, 320, 400 mg l^{-1} COD); (2) sodium acetate solutions of the same theoretical COD values; (3) gas works effluent, diluted 100-fold; (4) chemical factory effluent, diluted 20-fold.

line instability. A relative standard deviation of about 0.65% was attainable for 20 injections of 240 mg l^{-1} COD potassium hydrogenphthalate solution when new pump tubes were fitted. The deviation increases to 2—3% as the tubes wear.

Although, with the present system, reaction time is severely limited, the determinations on real samples (Table 2) frequently produced COD values greater than 90% of those obtained by the standard method. In some cases,

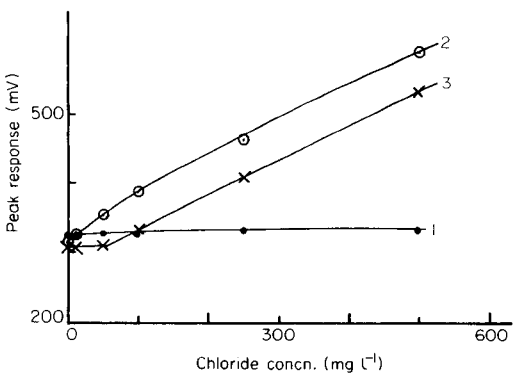

Fig. 6. The masking of chloride interference by mercury(II) sulphate in the measurement of 200 mg l^{-1} COD (potassium hydrogenphthalate): (1) 5.0 g l^{-1} mercury(II) sulphate added to sample; (2) no mercury(II) sulphate added; (3) reagent saturated with mercury(II) sulphate. Conditions: sample volume 110 μl; 160°C.

TABLE 2

Comparison of COD values (mg l^{-1}) obtained by the standard and proposed methods

Sample	Sample type	COD found		Sample	Sample type	COD found	
		Standard[a]	F.i.a.[b]			Standard[a]	F.i.a.[b]
1	Dye waste	672	560	12	Brewery waste	1621	1555
2	Dye waste	1591	1400	13	Chemical manufacture	2055	2052
3	Dye waste	296	268	14	Fabric washing	2372	2057
4	Dye waste	435	413	15	Circuit board manufacture	899	890
5	Dye waste	467	443				
6	Brewery waste	2006	1818	16	Chemical manufacture	5070	5000
7	Cattle market waste	2530	2528	17	Gas-works effluent	22000	23300
				18	Gas-works effluent	28000	27900
8	Dye waste	1571	1379	19	Gas-works effluent	31000	28500
9	Dye waste	356	302	20	Gas-works effluent	34000	31000
10	Dye waste	399	270	21	Gas-works effluent	37000	32000
11	Dye waste	597	584				

[a]Values determined by the standard method by Severn-Trent Water Authority, Wanlip (Samples 1—15), Fison's Scientific Equipment, Loughborough (Sample 16) and British Gas Corporation, Fulham (Samples 17—21). [b]With silver sulphate (7.5 g l^{-1}) added to the reagent.

the agreement is quite good, but overall accuracy would be further improved by the use of longer reaction times. Nevertheless, these results compare favourably with those of Korenaga and Ikatsu [3].

Conclusions

The results of this feasibility study indicate that the determination of COD is possible with conventional equipment for f.i.a. without the need for an expensive high-pressure system and a 50-m manifold [3]. A significantly higher degree of sample oxidation has been achieved by raising the temperature. The reaction proceeds without the formation of bubbles, and without excessive decomposition of the reagent, owing to the brief exposure and the absence of local overheating. Silver sulphate is incorporated into the reagent when necessary, or when there is doubt. The interference of chloride ions is prevented by merging the sample with mercury(II) sulphate solution before injection into the manifold.

In order to obtain the best agreement with results obtained by the standard method, certain restrictions imposed by the apparatus used here need to be relaxed. The 5020 Analyzer restricts the analytical cycle to 198 s (2 × 99 s), which limits the sample residence time in the reaction coil to about 2 min. This is inadequate for the complete oxidation of many samples, even when the more aggressive reagent and elevated temperature are used. More time would permit the use of a longer manifold, slower flow and larger sample volumes, giving better reproducibility of results, as revealed during preliminary work with a 7-m manifold and manual injection of samples.

Peristaltic pumps are unsuitable for pumping the viscous chromic acid reagent. Pump tubes become quickly fatigued, leading to excessive baseline

drift and variation in the carrier/reagent ratio. The method requires a fixed displacement pump capable of operating at 30—40 psi. The study again emphasizes the great value and versatility of f.i.a. in analytical chemistry. Over the last 10 years the technique has been used with imagination and ingenuity to improve the performance and efficiency of countless analyses. Slow reactions were a major challenge. Stopped flow is one answer. This paper has presented the more traditional solution of increasing the concentration and temperature of the reacting species.

The authors express their sincere thanks to Mr. A. F. Bower (Electronics Engineer, Department of Chemistry, LUT) who designed the oven and thermistor-controlled analogue power supply; and to Messrs. P. Child (Fisons Scientific Equipment, Loughborough), P. Kirkwood (British Gas Corporation, London Research Station), R. Yates and G. Boorman (Severn Trent Water Authority) for kindly providing analysed effluent samples. Financial support for J. M. H. A. by the British Gas Corporation is gratefully acknowledged.

REFERENCES

1 M. H. Adelman, Automation in Analytical Chemistry, Vol. 1, Technicon Symposia 1966, Mediad, New York, 1967.
2 T. Korenaga and H. Ikatsu, Analyst (London), 106 (1981) 653.
3 T. Korenaga and H. Ikatsu, Anal. Chim. Acta, 141 (1982) 301.
4 S. J. Edwards and M. Allen, Analyst (London), 109 (1984) 671.
5 Department of the Environment Standing Committee of Analysts, Chemical Oxygen Demand (Dichromate Value) of Polluted and Waste Waters, H.M.S.O., London, 1977.
6 R. A. Dobbs and R. T. Williams, Anal. Chem., 35 (1963) 1064.
7 W. A. Moore, F. J. Ludzack and C. C. Ruchhoft, Anal. Chem., 23 (1951) 1297.

Analytica Chimica Acta, 179 (1986) 279—287
Elsevier Science Publishers B.V., Amsterdam — Printed in The Netherlands

SIMULTANEOUS MULTIWAVELENGTH DETECTION IN FLOW INJECTION ANALYSIS

F. LÁZARO, A. RÍOS, M. D. LUQUE DE CASTRO and M. VALCÁRCEL

Department of Analytical Chemistry, Faculty of Sciences, University of Córdoba, Córdoba (Spain)

(Received 17th July 1985)

SUMMARY

The potential of the use of the diode-array detector in conjunction with flow injection analysis is outlined. Methods for multicomponent resolution can be based on the formation of complexes absorbing at different wavelengths. The example given is the determination of mixtures of copper(II) and iron(III) with a mixed 1:10-phenanthroline/neocuproine reagent. Amplification and dilution methods are based on the sum of the absorbances at several wavelengths and on monitoring absorbances at wavelengths away from the absorption maximum, respectively. The determination of nitrite via the Griess reaction is used as an example; the viable determination range is extended to 0.002—60.0 μg ml^{-1} nitrite. Software for the implementation of the suggested methods is outlined.

Multiwavelength diode arrays have become quite widely used as detectors in high-performance liquid chromatography (h.p.l.c.). The possibility of monitoring the different components of an eluate at the characteristic wavelength for each of them represents an important improvement in mixture resolution [1—3], which has been exploited in the development of quantitative methods in industrial [4], clinical [5, 6] and environmental [7, 8] chemistry. Several firms now provide these detectors along with sophisticated software for their use in conjunction with h.p.l.c. Nevertheless, the possibilities of a detection system of this type can be of more interest from a practical point of view when they are used directly without a prior separation technique.

Flow injection analysis (f.i.a.) has been compared with h.p.l.c. [9, 10], but it differs essentially in that there is no column to separate individual components of a sample. Nevertheless, f.i.a. has various possibilities for simultaneous determinations of several species [11]. A logical step in the development of f.i.a. is therefore its association with fast-scan detectors as a means of augmenting its value in multicomponent determinations. This association has been implemented with use of a fast-scan electrochemical detector [12], but there seem to be few practical applications.

In the context of a general research program on simultaneous determinations by f.i.a., the present paper deals with the use of a diode-array detector

0003-2670/86/$03.50

in conjunction with f.i.a. The combination is shown to be valuable in applications of dilution and amplification methods, which allow determination limits to be manipulated over very broad ranges.

Commercial software developed for use in h.p.l.c. is not suitable for the purposes of f.i.a.; its sophistication complicates rather than facilitates troubleshooting. Thus two programs were written for multicomponent resolution as well as for dilution and amplification methods, which allow the fast and convenient resolution of mixed samples.

EXPERIMENTAL

Apparatus

A Hewlett-Packard 8451A diode-array detector was used with the HP-9121 floppy-disk unit, HP-98155A keyboard and HP-7470A plotter. Other equipment included a Gilson Minipuls-2 peristaltic pump, Hellma 178.12-QS flow cell (inner volume 18 μl), Tecator L-100-1 injection valve and Tecator TM-II chemifold.

Simultaneous determination of iron(II) or iron(III) and copper(II)

The reagent solution is a mixture of 1,10-phenanthroline (0.1% w/v) and neocuproine (0.15% w/v) in 4:1 water/ethanol. The buffer solution contains 25 g of sodium acetate and 25 g of hydroxylammonium chloride in 250 ml of water. Standard solutions (1.00 g l^{-1}) of Fe(III) and Cu(II) were prepared.

The manifold is shown in Fig. 1(a). The sample is injected into the buffered reducing stream, which ensures the reduction of the metal ions to Fe(II) and Cu(I) along the coil L_1. This stream then merges with the reagent stream, producing the indicator reactions in coil L_2.

The wavelengths of maximum absorption are 454 nm and 512 nm for copper and iron, respectively and the detector monitors these two wavelengths simultaneously.

The optimization of variables yielded the results given above for the chemical variables. The optimum values found for the variables in f.i.a. were: q_1 = 1.7 ml min^{-1}, q_2 = 1.1 ml min^{-1}, L_1 = 40 cm, L_2 = 110 cm (0.5 mm i.d.), and V_i = 156.8 μl.

The basis for the calculation program used for the resolution of these mixtures (MIXFIA program) is the establishment of n equations in m unknowns ($n > m$), where n is the number of wavelengths at which the reaction is monitored and m is the number of components in the mixture. A flow diagram of this program is shown in Fig. 2. It works by collecting the maximum absorbance of the flow peak at n wavelengths per unknown sample. Prior to this, one calibration curve is run per n value for each component (overall, $n \times m$ equations).

Nitrite determination

The reagent solutions contain 0.95 g of sulphanilamide dissolved in 10 ml of concentrated hydrochloric acid and diluted to 250 ml with water, and

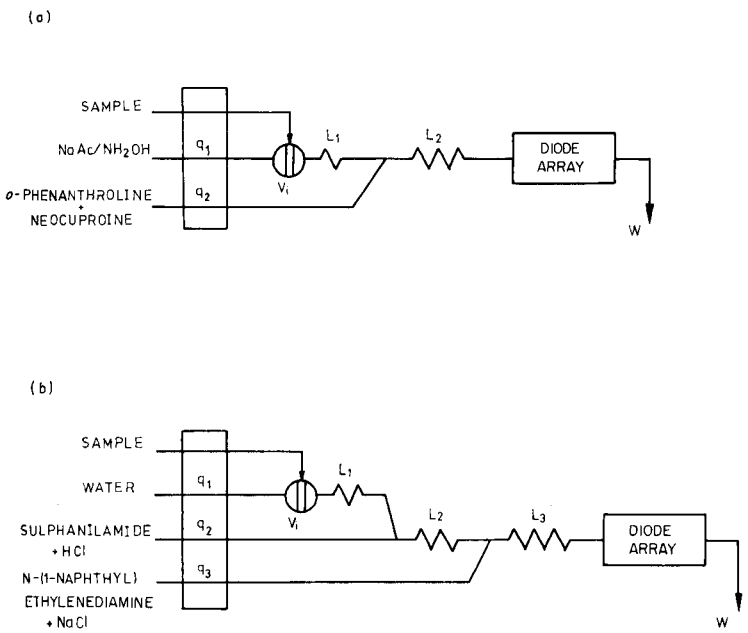

Fig. 1. Manifolds used: (a) for resolution of Fe(III)/Cu(II) mixtures; (b) for nitrite determination. (For q, V_i and L values, see text.)

0.36 g of *N*-(1-naphthyl)ethylenediamine dihydrochloride and 2.9 g of NaCl in 250 ml of water. A 1.00 g l^{-1} nitrite standard solution was prepared.

The manifold is shown in Fig. 1(b). The sample (aqueous nitrite solution) is injected into an aqueous stream which merges with the sulphanilamide solution, yielding the diazonium salt in coil L_2; this forms the monitored azo dye when mixed with the *N*-(1-naphthyl)ethylenediamine stream in coil L_3. The optimisation of variables yielded the above data for the chemical variables and the following for the variables in the manifold: $q_1 = q_2 = q_3 = 1.3$ ml min^{-1}, $L_1 = 20$ cm, $L_2 = 120$ cm, $L_3 = 250$ cm (0.5 mm i.d.), $V_i = 137.3$ μl.

RESULTS AND DISCUSSION

Simultaneous determination

The resolution of the mixture of iron(III) or iron(II) and copper(II) ions is based on the use of mixed selective reagents; 1,10-phenanthroline and neocuproine were chosen for Fe(III) and Cu(II), respectively. The working conditions are similar for both complexes, whereas their u.v.-visible absorption spectra are different.

The calibration equations obtained at the maximum absorption wavelengths for the two complexes (454 and 512 nm) were: for iron(II) or

TABLE 1

Definition of variables (MIXFIA program)

Variable	Meaning
A∅ (I, Y)	Intercepts of the calibration graphs
*A*1 (I, Y)	Slopes of the calibration graphs
*A*2 (Y, M1)	Sum of the maximum absorbances of the peaks obtained for each standard at each wavelength chosen
*A*3 (J, Y)	Average of the absorbances for each standard and wavelength
*A*4 (Y)	This stores the absorbances at the maximum at the different working wavelengths
A∅$	Symbol of each component in the mixture
B$	Different from "Y" when no more injections of the standard are necessary
C (I, J)	Concentration of standard J for component I of the mixture
C$	When equal to "S", standard measurements are made; if equal to "M" mixture measurements are made
L(Y)	Wavelengths at which the absorbances at the maximum of the f.i.a. peak are obtained
*L*1, *L*2	Initial and final wavelengths of the useful measurement range
M	Number of wavelengths corresponding to the desired absorbance at the maximum of the f.i.a. peak
*M*1	Number of injections for each standard
*M*4$	Different from "Y" when no more samples are analyzed
P (I)	Number of standards used
*T*1, *T*2	Initial and final measurement time from the moment of injection
*T*3	Integration time
*T*4	Interval between measurements
X (I)	Results of the equation systems
*Y*1, *Y*2	Minimum and maximum absorbance values taken as the end of the *y*-axis of the f.i.a. peak plot

iron(III) in the range 1.0—8.0 μg ml^{-1},

$A_{454} = 0.0626[Fe^{3+}] - 0.0305$ ($r^2 = 0.995$)

$A_{512} = 0.0858[Fe^{3+}] - 0.0326$ ($r^2 = 0.996$)

and for copper(II) in the range 15.0—30 μg ml^{-1},

$A_{454} = 0.0267[Cu^{2+}] - 0.0907$ ($r^2 = 0.999$)

$A_{512} = 0.0044[Cu^{2+}] - 0.0306$ ($r^2 = 0.955$)

It can be seen that the sensitivity for the Cu(II) determination is much lower than that of the conventional method. This is due partly to the fact that in the conventional method, extraction of the chelate into chloroform is used to increase sensitivity [13] and partly to the fact that the presence of 1,10-phenanthroline dramatically diminishes the absorbance of the Cu(I)/neocuproine system (by about 55%), because it competes for the Cu(I).

In the resolution of the mixture, it was necessary to take into account

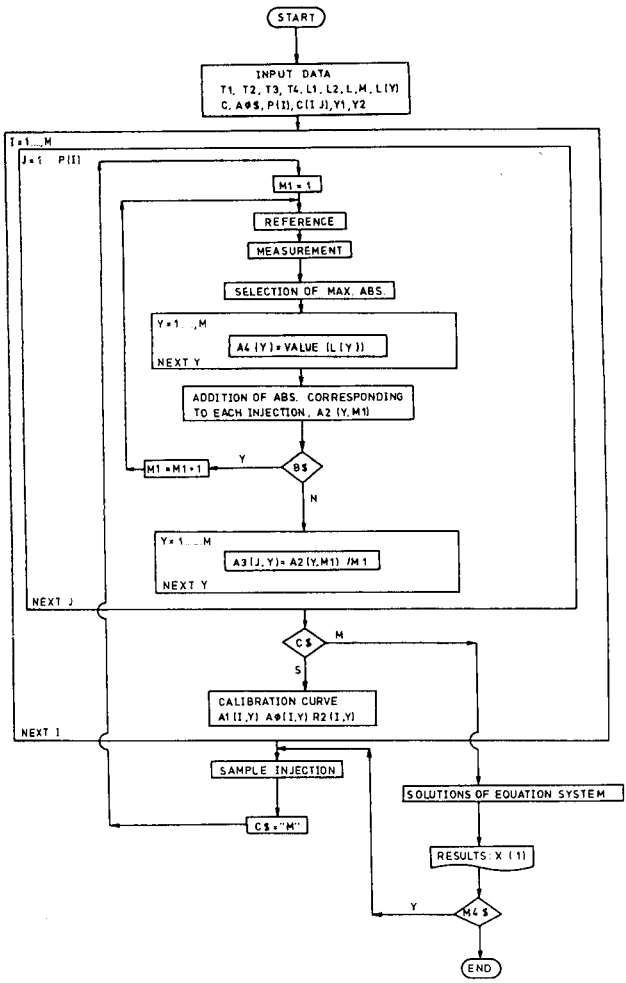

Fig. 2. Flow diagram of the MIXFIA program used for resolution of Fe(III)/Cu(II) mixtures. Variables are defined in Table 1.

that the individual absorbances are not additive in the mixture; the overall absorbance is slightly higher than the sum of the individual values (8—10%). This synergic effect required mathematical study and clarification. For this purpose, calibration graphs were constructed for copper(II) in the presence of different iron(III) concentrations. The slopes and intercepts of these straight lines were a linear function of the iron(III) concentration. Finally expressions were established similar to those found in other cases of synergy [14, 15], but this time at the two different wavelengths:

$$A_{454} = -0.0025[Fe^{3+}][Cu^{2+}] + 0.1307[Fe^{3+}] + 0.03407[Cu^{2+}] - 0.2776$$

$$A_{512} = -0.0033[Fe^{3+}][Cu^{2+}] + 0.1628[Fe^{3+}] + 0.01493[Cu^{2+}] - 0.2836$$

From these equations, it is possible to solve synthetic iron(III)/copper(II) mixtures satisfactorily, as shown in Table 2. The r.s.d. values for 11 samples containing 5 μg ml^{-1} Fe(III) and 19 μg ml^{-1} Cu(II) were ±1.69% and ±1.07%, respectively.

Dilution and amplification methods

The Griess reaction (Shinn's modification [16]) was chosen for the development of these methods. The calculation program (DINAFIA) used for the

TABLE 2

Resolution of synthetic mixtures of iron(III) and copper(II) by the suggested method

Added (μg ml^{-1})		Found (μg ml^{-1})		Errors (%)	
Fe(III)	Cu(II)	Fe(III)	Cu(II)	Fe(III)	Cu(II)
3.00	16.00	3.08	16.10	2.7	0.6
5.00	16.00	5.00	16.03	0.0	0.2
7.00	22.00	7.13	21.79	1.8	−0.9
3.00	19.00	2.86	18.85	−4.6	−0.8
3.00	25.00	3.05	25.04	1.6	0.1
5.00	25.00	5.00	25.06	0.0	0.2
1.00	19.00	1.01	19.12	1.0	0.6

TABLE 3

Definition of variables (DINAFIA program)

Variable	Meaning
A∅ (1)	Intercept of calibration graph I
*A*1 (I)	Slope of calibration graph I
*A*3 (I)	Average absorbance for the injection made
*A*4 (Y)	Values of the maximum absorbance at the wavelengths chosen
A$	Analyte formula
B$	"Y" if another injection is made
C (J)	Concentration of standard J
C$	"Y" when the standards are injected, "M" when the sample is injected
*L*1, *L*2	Initial and final wavelengths of the interval used
L (Y, I)	Wavelengths corresponding to the desired maximum absorbance for calibration graph I
*M*1	Counter of the number of injections
M (I)	Number of wavelengths corresponding to the desired maximum absorbance
N$	"*Y*" if another sample is injected
P (I)	Number of standards injected for the construction of calibration graph I
*R*2 (I)	Correlation coefficient of the calibration graph I
*T*1, *T*2	Initial and final measurement times taken from the moment of injection
*T*3	Integration time
*T*4	Interval between measurements
*Y*1, *Y*2	Minimum and maximum absorbances used for plotting the f.i.a. peak

automated nitrite determination over a very wide concentration range (2.0—60 000 ng ml^{-1}) is based on measurement of the absorbances provided by the analyte at different wavelengths depending on its concentration. If the nitrite concentration is high (>4.0 $\mu g\ ml^{-1}$), medium (0.2—4.0 $\mu g\ ml^{-1}$) or low (<0.2 $\mu g\ ml^{-1}$), the reaction product is monitored at a wavelength distant from the absorption maximum (λ_{dil}), at the absorption maximum (λ_{max}) or at a series of wavelengths around the absorption maximum ($\Sigma\lambda$), respectively. In the third case, the absorbances measured are added.

The program (Fig. 3) starts by asking for the working conditions (integration time, interval between measurements, initial and final time, λ_{dil}, λ_{max},

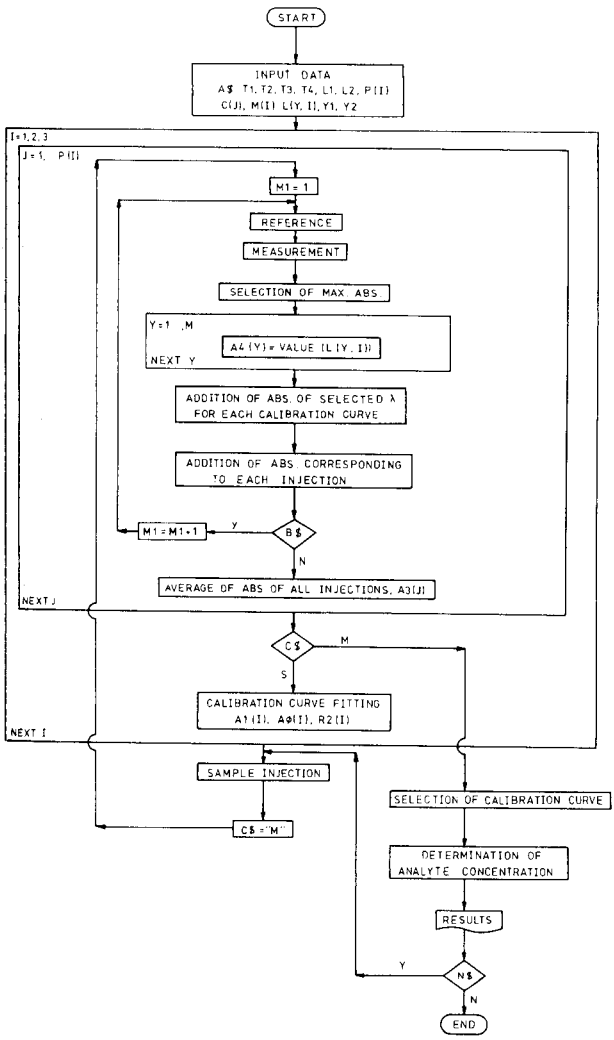

Fig. 3. Flow diagram of the DINAFIA program for normal, dilution and amplification methods. Variables are defined in Table 3.

$\Sigma\lambda$), then it requests the injection into the flow-injection system of each of the standards for the three calibration graphs (dilution, normal and amplification method in the above-mentioned ranges). Afterwards, the features of each calibration graph are calculated and, finally, the program evaluates the nitrite concentration in the unknown samples, using the appropriate calibration graph in each case.

The calibration graphs used for nitrite determination were obtained by monitoring the reaction product at 450 nm (dilution method), 542 nm (normal method) and the set of $\Sigma\lambda_{15}$ = 528, 530, ... 554, 556 nm (amplification method). Table 4 lists the characteristic of these graphs and several others for the dilution and amplification methods. The following conclusions can be drawn. The range of determinations is extended from 0.2—4.0 μg ml^{-1} for the conventional method to 0.002—60.0 μg ml^{-1} for the method suggested here. Although the possible range of determination is considerably shortened as a result of using the amplification plots instead of the dilution plots, the linearity ratio (quotient between the upper and lower determination limits) is very similar in every case. The sensitivity of the procedure, as well as the manipulation factor (ratio between the slopes of the dilution or amplification calibration graphs and the normal graphs) in the dilution calibration increases with the proximity of λ_{dil} to λ_{max}, whereas in the amplification calibration it increases with the number of wavelengths considered.

The relative errors found on injecting 15 samples with concentrations lying over a very wide range into the flow-injection system, are listed in Table 5. Such errors are small for all the samples, but even smaller in the normal method (average relative error ±0.28%) than in the dilution method (±1.58%) or the amplification method (±1.50%). The precision of the method was calculated separately from 11 different samples for each curve. The relative standard deviations obtained and the concentrations used were

TABLE 4

Manipulation of sensitivity in the determination of nitrite

Method	λ (nm)	Determination range[a] (μg ml^{-1})	Sensitivity (μg ml^{-1})$^{-1}$	Manipulation factor
Dilution	450	2.0—60.0	0.019	0.10
	470	0.8—20.0	0.048	0.20
	510	0.4—8.0	0.172	0.75
Normal	542	0.2—4.0	0.226	1.00
Amplification	$\Sigma\lambda_3$[b]	0.06—2.0	0.686	3.00
	$\Sigma\lambda_{15}$[c]	0.004—0.2	3.504	15.00
	$\Sigma\lambda_{25}$[d]	0.002—0.1	5.484	24.00

[a]The regression coefficient was 0.999 in all cases. [b]$\Sigma\lambda_3$ = 540, 542, 544 (nm). [c]$\Sigma\lambda_{15}$ = 528, 530, ..., 554, 556 (nm). [d]$\Sigma\lambda_{25}$ = 518, 520, ..., 564, 566 (nm).

TABLE 5

Relative errors in the determination of nitrite over a wide concentration range

Added (μg ml^{-1})	Found (μg ml^{-1})	Error (%)	Added (μg ml^{-1})	Found (μg ml^{-1})	Error (%)
0.0066	0.0067	1.5	2.000	2.005	0.2
0.020	0.0202	1.0	3.060	3.075	0.5
0.0673	0.0688	2.2	4.000	3.950	−1.2
0.080	0.078	−2.5	10.000	9.840	−1.6
0.100	0.1003	0.3	12.000	11.770	−1.9
0.600	0.597	−0.5	20.000	19.720	−1.4
0.800	0.801	0.1	30.600	31.150	1.8
1.200	1.201	0.1			

as follows: dilution, ±0.40% (25 μg ml^{-1}); normal method, ±0.13% (2.0 μg ml^{-1}); amplification method, ±0.10% (0.15 μg ml^{-1}).

REFERENCES

1 B. Vandeginste, R. Essers, T. Bosman, J. Reijn and G. Kateman, Anal. Chem., 57 (1985) 971.
2 S. A. George and A. Maute, Chromatographia, 15 (1982) 419.
3 A. C. J. Drouen, H. A. H. Billiet and L. de Galan, Anal. Chem., 57 (1985) 962.
4 K. W. Jost, T. Crispin and I. Halasz, Erdoel Kohle, Erdgas, Petrochem., 37 (1984) 178.
5 T. Takeuchi and D. Ishii, Chromatogr. Commun., 7 (1984) 151.
6 A. Fell, B. J. Clark and H. P. Scott, J. Chromatogr., 297 (1984) 203.
7 D. J. Desilets, P. T. Kissinger, F. E. Lytle, M. A. Horne, M. S. Ludwiczak and R. B. Jacko, Environ. Sci. Technol., 18 (1984) 386.
8 J. L. Anderson, K. K. Whiten, J. D. Brewster, T. Y. Ou and W. K. Nonidez, Anal. Chem., 57 (1985) 1366.
9 J. Růžička and E. H. Hansen, Flow Injection Analysis, Wiley, New York, 1981.
10 M. Valcárcel and M. D. Luque de Castro, Flow Injection Analysis: Principles and Applications, Ellis Horwood, Chichester, in press.
11 M. D. Luque de Castro and M. Valcárcel, Analyst (London), 109 (1984) 413.
12 J. Janata and J. Růžička, Anal. Chim. Acta, 139 (1982) 105.
13 A. R. Gahler, Anal. Chem., 26 (1954) 577.
14 A. Ríos and M. Valcárcel, Talanta, 32 (1985) 851.
15 A. Ríos, M. Silva and M. Valcárcel, Z. Anal. Chem., 320 (1985) 762.
16 M. B. Shinn, Ind. Eng. Chem. Anal. Ed., 13 (1941) 33.

Analytica Chimica Acta, 179 (1986) 289—297
Elsevier Science Publishers B.V., Amsterdam — Printed in The Netherlands

BATCH AND FLOW-INJECTION DETERMINATION OF ETHYLENEDIAMINE IN PHARMACEUTICAL PREPARATIONS

M. MILLA*, R. M. DE CASTRO, M. GARCIA-VARGAS and J. A. MUÑOZ-LEYVA

Department of Analytical Chemistry, Faculty of Sciences, University of Cádiz, Cádiz (Spain)

(Received 9th August 1985)

SUMMARY

The ethylenediamine/pyridine-2-carbaldehyde/copper(I) system is used in a new spectrophotometric method for the determination of ethylenediamine. The batch procedure involves the formation of an orange chelate between the Schiff's base and copper(I) ions at pH 8.5 (borate buffer) and measurement of the absorbance at 475 nm against water after 10—15 min; Beer's law is obeyed over the range 0.5—11.2 $\mu g\ ml^{-1}$ and the molar absorptivity is 6.21×10^3 $l\ mol^{-1}\ cm^{-1}$. Tolerance limits for different amines [36] and other organic compounds [12] are reported. In the optimized flow-injection system, ethylenediamine (1.4—84.6 $\mu g\ ml^{-1}$) is determined at a sample throughput of 55 h^{-1}. The method is sensitive and selective and is satisfactory for the determination of the diamine in aminophylline and pharmaceutical preparations (ethylenediamine contents from 0.031 to 3.23%) with relative errors ranging from —7.4 to +11.1% and relative standard deviations of about 0.65% for both procedures.

Ethylenediamine finds application in the electrochemical industry, as an antioxidant, and as a swelling agent in the manufacture of resins and polymers. It may have to be determined in electroplating baths, in degradation products of resins and polymers, and in factory air. The presence of ethylenediamine in soils and plants can be a measure of contamination by residual pesticides, and its determination in these samples is also of interest. In pharmaceutical use, ethylenediamine is associated with theophylline to give aminophylline, a water-soluble powder with anti-asthmatic properties.

Apart from the numerous titrimetric and chromatographic methods that have been reported for the determination of ethylenediamine, various spectrophotometric procedures have been described. These generally exhibit rather poor sensitivity and selectivity, being based on the formation of copper(II) and nickel(II) ethylenediamine complexes [1] or on the reaction of the diamine with different organic compounds [2—6]. The in-situ synthesis of Schiff's bases has been used to determine amines by titrimetry and spectrophotometry [7]. However, the presence of a suitable metal ion improves both sensitivity and selectivity, providing useful methods for the determination of either organic compound involved in the reaction. Critchfield and Johnson [8] first reported the use of amine/carbonyl compound/

0003-2670/86/$03.50

metal ion systems to determine primary amines spectrophotometrically. Only a few procedures have been described for the evaluation of ethylenediamine in pharmaceutical preparations, e.g., aminophylline [9, 10], tablets [11] and suppositories [7, 12]. A simple, fast spectrophotometric method for determining ethylenediamine is described below. It is based on formation of the copper(I) chelate of the Schiff's base produced by reaction of ethylenediamine with pyridine-2-carbaldehyde. This assay of ethylenediamine is sensitive and selective and is applicable to aminophylline and pharmaceutical preparations by either a batch procedure or flow injection analysis (f.i.a.).

EXPERIMENTAL

Reagents and equipment

Ethylenediamine solutions were prepared from the analytical-grade reagent and standardized against hydrochloric acid (bromophenol blue indicator). The pyridine-2-carbaldehyde used was 99% pure. Copper(I) solutions were prepared from copper(II) nitrate pentahydrate standardized by titration with EDTA, by addition of ascorbic acid. The aldehyde solutions were stable for at least a week, whereas the copper(I) solutions had to be prepared daily. Borate buffer was prepared by adjusting 0.1 mol l^{-1} boric acid to pH 8.5 with sodium hydroxide pellets. Aminophylline, standardized like ethylenediamine, and alkaloids (pharmacopoeial grade) were used. All other chemicals were of analytical grade and distilled water was used throughout.

A Perkin-Elmer Coleman 575 spectrophotometer was used for recording spectra and measuring absorbance at 475 nm. A Hellma QS-1000 18-μl flow cell was used in the flow-injection system. A Metrohm 620 pH meter and a Beckman J2-21 centrifuge were used. The flow manifold was based on a FIAstar (Bifok) with an Eyela MP-3 peristaltic pump and 0.5 mm i.d. teflon tubing. All solutions were degassed in a Selecta ultrasonic bath and samples and standards were injected in triplicate at least. An Apple-II desk computer was used for statistical calculations and for running the optimization program.

Procedures

Dissolution of the samples. For aminophylline and syrup, an appropriate amount was dissolved in water. For injections, the preparation (2.5 ml) was diluted to the mark in a 25-ml volumetric flask with water. Tablets (2—10) were finely powdered; a portion (0.2—0.5 g) was treated with 20—30 ml of distilled water in a ultrasonic bath and centrifuged for 15 min at 15 000 rpm. The solution was transferred to an 100-ml volumetric flask and the precipitate was treated again in the same way. The combined aqueous portions were diluted to the mark. All these working solutions contained between 50 and 150 μg ml^{-1} ethylenediamine.

Batch method for ethylenediamine. The necessary solutions were: (a) 0.1 ml of 99% pyridine-2-carbaldehyde diluted to 50 ml with distilled water; (b) a 500 μg Cu(II) ml^{-1} solution containing 0.4% (w/v) ascorbic acid; (c) a 4.000 g l^{-1} solution of disodium ethylenediaminetetraacetate (EDTA).

For the determination, the sample solution containing up to 110 μg of ethylenediamine was placed in a 10-ml volumetric flask; 2 ml of solution (a), 2.5—5.0 ml of the buffer solution, 0.6 ml of solution (b) and 0.5 ml of solution (c) were added and the mixture was diluted to the mark. After 10—15 min, the absorbance was measured at 475 nm against water.

Flow-injection procedure. The aldehyde stream was 1 ml of pyridine-2-carbaldehyde diluted to 100 ml with the buffer solution. The Cu(I) stream was a 1 + 12 (v/v) dilution of solution (b) of the batch procedure. The manifold is described in Fig. 1. The injected sample (116 μl) contained up to 840 μg of EDA. Peak heights were measured.

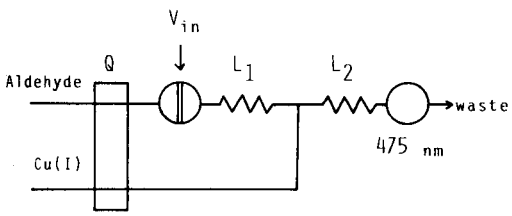

Fig. 1. Flow diagram. Optimum values of Q, V_{in}, L_1 and L_2 are 1.1 ml min^{-1}, 116 μl, 80 cm and 95 cm, respectively.

RESULTS AND DISCUSSION

Study of the ethylenediamine/pyridine-2-carbaldehyde/Cu(I) system

The feasibility of the in situ synthesis of the Schiff's base derived from ethylenediamine and pyridine-2-carbaldehyde was reported previously [13]. In this study, it was found that copper(I) ions offered advantages of sensitivity and stability of the coloured chelate. The maximum absorption wavelength of the system was 475 nm.

The system chosen for the determination of ethylenediamine (en) was optimized. The best pH range was 7.5—11.5 and a borate buffer of pH 8.5 was selected. The optimum molar ratios of the reagents were 1:80 en/pyridine-2-carbaldehyde, 1:12 en/Cu(I) and 1:1 Cu(II)/ascorbic acid. The preferred order of addition was en/aldehyde/buffer/Cu(I). Under these conditions, the chelate attained maximum absorbance within 10—15 min after mixing of the reagents and remained stable for at least 2 h. Attempts were made to increase the sensitivity of the procedure by adding 5—20% (v/v) ethanol, dimethylformamide and dioxane; the maximum wavelength remained 475 nm in all cases and the absorbance was not significantly increased. Heating had little effect on the reaction time, hence room temperature was preferred for convenience.

The chelate was extracted into isoamyl alcohol (λ_{max} = 475 nm; ϵ = 7.6 × 10^3 l mol^{-1} cm^{-1}), isobutyl methyl ketone (partially) and chloroform (λ_{max} = 475 nm; ϵ = 7.5 × 10^3 l mol^{-1} cm^{-1}) in the presence of perchlorate. This offers the possibility of extraction-photometric or atomic-absorption (measuring at the copper line) determinations of ethylenediamine.

The continuous-variations method was applied to ascertain the ethylenediamine/copper molar ratio in the chelate. Two complex species of 2:1 and 1:1 en/metal ion stoichiometric ratios were observed, the latter predominating when Cu(I) was in excess. The electrical charge of the chelate formed under the optimum conditions was studied; the chelate was retained by a cationic resin, thus proving it to be a positively charged species.

Spectrophotometric determination of ethylenediamine

Beer's law was obeyed between 0.5 and 11.2 μg ml^{-1} ethylenediamine, the molar absorptivity, calculated from the calibration graph by least squares, being 6.21 × 10^3 l mol^{-1} cm^{-1}. The Sandell sensitivity was 0.0097 μg cm^{-2}. The relative standard deviation was ±0.61% for eleven samples, each containing 4.6 μg ml^{-1} (P = 0.05). A Ringbom plot showed that the optimum range for accurate determinations was between 1.9 and 9.3 μg ml^{-1} ethylenediamine.

A systematic study of possible interferences from inorganic and organic substances showed that EDTA, up to a final concentration of 200 μg ml^{-1}, not only did not interfere, but also reduced substantially the interfering effects of other species. The presence of EDTA also prevented the precipitation of any Cu(I) excess, thus making centrifugation or filtration unnecessary. Table 1 lists the tolerated levels for some common cations and anions. The organic compounds tested were primary, secondary and tertiary amines, quaternary ammonium salts and alkaloids and other substances accompanying ethylenediamine in the pharmaceutical preparations. The histograms in Fig. 2 show the tolerated levels, expressed as molar ratios, for various organic compounds.

Batch determination of ethylenediamine in pharmaceutical preparations

The method was applied to the evaluation of ethylenediamine in samples of medicines containing aminophylline. Samples containing an exact amount of ethylenediamine were specially prepared from the components of the commercial preparation (see footnotes to Table 2). All the sample solutions were prepared as described under Procedures. A decrease in ethylenediamine content was observed for all prepared solutions stored for some time at room temperature; this is in agreement with the other experimental observations on the stability of aminophylline solutions [14] and of preparations containing ethylenediamine [9, 12]. The fate of the ethylenediamine is not known in most cases. Owing to this, all sample solutions were analyzed within a week after preparation. The calibration equation was $A = 0.0986C$ (μg ml^{-1}) + 0.016, where A is absorbance.

TABLE 1

Tolerance limits[a] for some cations and anions in the determination of 4.6 μg ml^{-1} ethylenediamine

Tolerated amount (μg ml^{-1})		Ion
No EDTA	With EDTA	
10 000	10 000	Alkali metals, SO_4^{2-}, NO_3^-, acetate, As(III), As(V)
750	1000	Ca(II)
500	10 000	Cl^-, Br^-
200	1000	Mn(II)
100	200	Ba(II), Zn(II), Cd(II)
100	1000	Tartrate, oxalate, citrate, PO_4^{3-}, CO_3^{2-}
50	200	I^-
—	200	EDTA
—[b]	100	Bi(III), Al(III), Cr(III), Ag(I), Pb(II), Mg(II), Sr(II)
—[b]	10	Fe(III), Co(II), CN^-

[a]Maximum concentration tested was 10 000 μg ml^{-1}. [b]Turbidity appeared even at low concentrations.

For the determination of ethylediamine in aminophylline, 0.3—0.5 g of aminophylline was dissolved in 50 ml of water and appropriate aliquots were taken; the mean result obtained by the photometric procedure was 14.80 ± 0.10% (n = 3), which agreed well with the mean result obtained by titration with acid (14.57 ± 0.08%). The amounts of ethylenediamine in specially prepared and commercial drugs were evaluated by the standard-additions method as well as from calibration graphs. Details are given in Table 2 which shows good agreement between the two methods of evaluation. Of the commercial samples tested, only the results for tablets are reported. The analysis of commercial syrups and injections gave ethylenediamine contents much below the nominal amounts, possibly because of reaction of ethylenediamine with other ingredients of the preparation on storage at room temperature and exposure to light.

Flow injection method for ethylenediamine in pharmaceutical preparations

Flow injection analysis was used for the determination of ethylenediamine based on the above chemical system. The flow system was optimized and then utilized for the rapid assay of the ethylenediamine content in the pharmaceutical preparations listed in Table 2. In order to simplify the manifold, the buffer was incorporated into the aldehyde reagent. The sample was injected into the aldehyde stream (buffered at pH 8.5) and then mixed with the copper(I) reagent stream (Fig. 1). In numerous preliminary tests, the reagents were mixed following the same order as in the batch procedure, the sample was injected into the copper(I) stream rather than the aldehyde stream, and a 200-μl mixing chamber was used instead of coil L_2 to increase the extent of reaction. Flow rates from 1.0 to 5.0 ml min^{-1} in

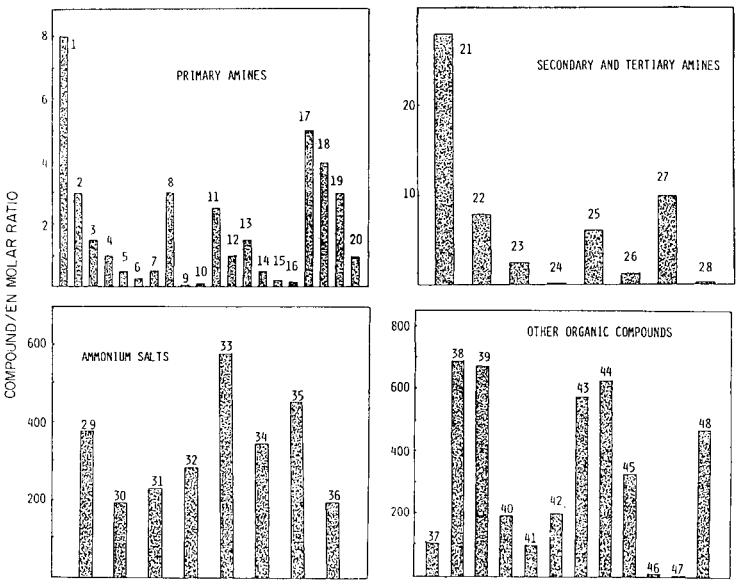

Fig. 2. Interference histograms for some amines and other organic compounds in the determination of 4.6 μg ml^{-1} ethylenediamine: (1) methylamine; (2) ethylamine; (3) n-propylamine; (4) n-butylamine; (5) *p*-phenetidine; (6) benzylamine; (7) *p*-anisidine; (8) 1,3-diaminepropane; (9) 1,4-diaminebutane; (10) benzidine; (11) naphthylamine; (12) hydrazine; (13) aniline; (14) ethanolamine; (15) anthranilic acid; (16) 4-nitroaniline; (17) glycine; (18) alanine; (19) L-serine; (20) hydroxylammonium chloride; (21) diethanolamine; (22) diphenylamine; (23) diethylenetriamine; (24) *N,N*-dimethyl-*p*-phenylendiamine; (25) n-trioctylamine; (26) aminoethylethanolamine; (27) *N,N'*-dimethylaniline; (28) hexamine; (29) trimethylphenylammonium chloride; (30) benzyltri-*N*-butylammonium bromide; (31) tetrabutylammonium chloride; (32) benzyltriethylammonium chloride; (33) triethylammonium chloride; (34) benzyltrimethylammonium chloride; (35) *N*-2-chloroethyl-*N,N*-diethylammonium chloride; (36) *N*-acetyl-*N,N,N*-trimethylammonium bromide; (37) atropine; (38) ephedrine; (39) guaiacol; (40) papaverine; (41) codeine; (42) phenobarbital; (43) caffeine; (44) glucose; (45) fructose; (46) starch; (47) theophylline; (48) mannitol. For ammonium salts and non-amines the ratio shown is the maximum tested.

each stream were tested; the length of coils L_1 (75 cm) and L_2 (85 cm) and the volume of the injected sample (60 μl of 1.8×10^{-3} M ethylenediamine) were kept constant in these tests. These preliminary experiments indicated that a manifold similar to that shown in Fig. 1 would be satisfactory.

In the optimization process, the influence of the buffer solution in the aldehyde stream was examined; tests with three percentages (25, 50 and 100%, v/v) of buffer solutions suggested that the aldehyde reagent should be prepared in 100% buffer solution, i.e., in 0.1 mol l^{-1} borate buffer, pH 8.5. A modified simplex method [15] was used to optimize the interdependent variables, i.e., overall flow rate (Q), volume of injected sample (V_{in}), lengths of the first (L_1) and the second (L_2) coils and the aldehyde (PCA) and Cu(I) concentrations. The maximum value of the absorbance

TABLE 2

Determination of ethylenediamine (en) in pharmaceutical preparations by the batch procedure

Sample	Amount taken	Ethylenediamine content (%)[a]		
		Calibration graph	Standard additions	True value
Tablets[b]	(g/100 ml)			
	0.5270	2.47 ± 0.08 (−2.0)	2.68 (+6.3)	2.52
	0.4900	2.50 ± 0.10 (−0.4	2.52 (+0.4)	2.51
	0.4487	2.44 ± 0.11 (−2.9)	2.38 (−5.2)	2.51
	0.5235	2.60 ± 0.03 (+3.2)	2.47 (−2.0)	2.52
	0.5200	2.28 ± 0.05 (−0.4)	2.12 (−7.4)	2.29
	0.5757	2.26 ± 0.04 (−1.3)	2.19 (−4.4)	2.29
Injections[c]	(ml)			
	0.5	$7.80(\pm0.04)\times10^{-2}$ (−2.13)	8.19×10^{-2} (+2.76)	7.97×10^{-2}
	0.4	$6.92(\pm0.10)\times10^{-2}$ (−4.15)	6.89×10^{-2} (−4.57)	7.22×10^{-2}
	0.3	$8.24(\pm0.06)\times10^{-2}$ (+3.39)	7.91×10^{-2} (−0.75)	7.97×10^{-2}
	0.4	$8.35(\pm0.08)\times10^{-2}$ (+4.47)	8.07×10^{-2} (+1.25)	7.97×10^{-2}
	0.2	$8.31(\pm0.05)\times10^{-2}$ (+4.26)	8.21×10^{-2} (+3.00)	7.97×10^{-2}
Syrups[d]	(g/ml)			
	8.4881/100	$4.00(\pm0.05)\times10^{-2}$ (+11.1)	4.00×10^{-2} (+11.1)	3.63×10^{-2}
		$3.71(\pm0.02)\times10^{-2}$ (+3.05)	3.58×10^{-2} (−1.38)	
	4.1300/25	$3.77(\pm0.02)\times10^{-2}$ (+3.86)	3.79×10^{-2} (+4.40)	3.63×10^{-2}
		$3.66(\pm0.02)\times10^{-2}$ (+0.83)	3.55×10^{-2} (+2.20)	
	5.1093/50	$3.54(\pm0.02)\times10^{-2}$ (−2.48)	3.66×10^{-2} (+0.83)	3.63×10^{-2}
		$3.64(\pm0.04)\times10^{-2}$ (+0.28)	3.63×10^{-2} (0)	
Tablets[e]	(g/100 ml)			
	0.5235	2.71 ± 0.01	2.68	
	0.5311	2.58 ± 0.03	2.78	2.7—3.1
	0.5200	2.85 ± 0.02	2.93	

[a]Results are given as percentage found (average of 3—5 measurements) with standard deviation and, in parentheses, the relative error. [b]Composition: aminophylline, 0.6000 g; ephedrine hydrochloride 0.1045 g; papaverine hydrochloride, 0.1600 g; phenobarbital, 0.1000 g; atropine hydrochloride 0.0010 g; excipients to 2.500 g. Relative standard deviations for the standard additions method were from 1.2 to 12.2%. [c]Composition: aminophylline, 12.4—13.9 mg; guaifenesine, 150.0 mg; chlorphenamine maleate, 1.0 mg; bromhexine chloride, 2.0 mg; lydocaine hydrochloride, 25.0 mg; aqueous solution, 2.50 ml. An aliquot (2.5 ml) of this preparation was diluted to 25 ml. Data are given as weight % in the original preparations. Relative standard deviations for the standard additions method were in the range 0.65—10.69%. [d]Composition: aminophylline, 0.2500 g; ephedrine hydrochloride, 0.1000 g; thyme extract, 3.0000 g; ammonium benzoate, 1.500 g; excipients to 100.0 g. Relative standard deviations for the standard additions method were from 0.18—4.07%. [e]Commercial tablets. The nominal (true) value is based on the calculated content for an aminophylline content of 12—14%.

at 475 nm was attained after 18 experiments, seven of which were used to construct the initial matrix of the simplex. Table 3 shows the optimum values obtained.

The influence of the temperature on the peak height was then studied by heating the second reaction coil at 40, 60 or 80°C (±1°C) in a thermostated bath. The stream was then cooled to room temperature before entering the flow cell. Heating at 80°C resulted in a two-fold increase of sensitivity, but reproducibility was poor. Further, sample throughput decreased because of

TABLE 3

Optimum values of the variables in the flow-injection system

Variable	Q (ml min^{-1})	V_{in} (μl)	L_1 (cm)	L_2 (cm)	PCA[a]	Cu[a]
Value	1.1	116	80	95	5	0,08

[a]Given as molar ratios for the flow method to the batch method.

the longer residence time of the sample in the system, and the manifol became more complicated. Given the choice between sensitivity and repr ducibility/simplicity, the optimized system was operated at room tempe ature.

With the optimized flow-injection system, linear response was obtaine between 1.4 and 84.6 μg ml^{-1} ethylenediamine (Fig. 3). The least-squar calibration equation (n = 16) was A = 0.0122 C + 0.043 with r^2 = 0.999 Precision (r.s.d.) was 0.68% for eleven injections of a 36.2 μg ml^{-1} ethylen diamine solution. A theoretical injection rate of 55 h^{-1} was calculate Reagent consumption per injection was 8.4 × 10^{-2} mmol of aldehyde an 39 μg of copper(I).

Finally, the flow-injection system was used for the semi-automated dete mination of ethylenediamine in aminophylline and in pharmaceutical prepa ations. The results given in Table 4 show good agreement with the tr values, confirming the reliability of the new method.

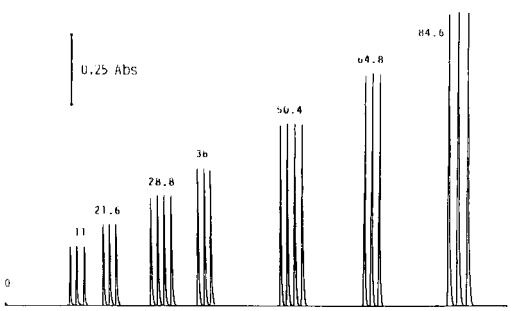

Fig. 3. Peaks obtained by injection of standard solutions of ethylenediamine; the numbe on the peaks are μg ml^{-1} ethylenediamine.

TABLE 4

Flow-injection determination of ethylenediamine in aminophylline and pharmaceutical preparations

Preparation	Solution taken (g/ml)	Ethylenediamine found[a]		True value (%)
		$\mu g\ ml^{-1}$	%	
Aminophylline	0.4644/50	51.4 ± 0.7	13.9 ± 0.5	14.57[b]
	0.3319/50	19.1 ± 0.5	14.4 ± 0.6	
	0.4970/50	56.1 ± 0.8	14.1 ± 0.5	
Tablets	0.4991/100	11.2 ± 0.3	2.79 ± 0.08	2.52
	0.2032/50	45.6 ± 0.8	2.35 ± 0.06	2.36
Injections	—	70.7 ± 0.5	$(7.6 \pm 0.1) \times 10^{-2}$	7.63×10^{-2}
	—	9.4 ± 0.5	$(7.1 \pm 0.1) \times 10^{-2}$	7.02×10^{-2}
Syrup	0.1434/100	15.4 ± 0.8	$(3.3 \pm 0.1) \times 10^{-2}$	3.12×10^{-2}
	0.1128/50	80.2 ± 0.5	$(3.3 \pm 0.1) \times 10^{-2}$	3.12×10^{-2}

[a]With standard deviation for $n = 3$—6. [b]Calculated from acid-base titration.

The authors express their gratitude to ELMU Pharmaceutical Laboratories (Madrid) for their generous provision of chemicals and samples.

REFERENCES

1 See, e.g., A. Budniok and J. Gala, Chem. Anal. (Warsaw), 21 (1976) 1283.
2 B. P. Lugovkin and E. T. Zemlyanitskaya, Nauchn. Rab. Inst. Okhr. Tr. Vses. Tsentr. Sov. Prof. Soyuzov, 64 (1970) 78.
3 I. Zalnierius and H. Laumenskas, Issled. Obl. Elektroosazhdeniya Met., 2 (1973) 210.
4 T. S. Al-Ghabsha, S. A. Rahim and A. Townshend, Anal. Chim. Acta, 85 (1976) 189.
5 G. Hihara, H. Miyamae and M. Nagata, Bull. Chem. Soc. Jpn., 54 (1981) 2668.
6 J. A. Vinson, J. F. Evans and H. E. Holets, Mikrochim. Acta, 3 (1983) 301.
7 See, e.g., S. Siggia and J. G. Hanna, Quantitative Organic Analysis via Functional Groups, 4th Edn., Wiley, New York, 1979, pp. 579.
8 F. E. Critchfield and J. B. Johnson, Anal. Chem., 28 (1956) 436.
9 Y. Ishiguro, T. Tamegai, M. Sawada, Y. Tanaka and K. Kawabe, Yakugaku Zasshi, 100 (1980) 576.
10 V. A. Popkov, V. Reshetnyak and E. V. Gurenkova, Khim. Farm. Zh., 17 (1983) 373.
11 J. W. Turczan, B. A. Goldwitz and J. Nelson, Talanta, 19 (1972) 1549.
12 C. Van Dop, G. M. Overvliet and H. M. Smits, Pharm. Acta Helv., 56 (1981) 281.
13 J. A. Muñoz Leyva and P. Salazar, Microchem. J., 31 (1985) 332.
14 Y. Ishiguro, M. Sawada, Y. Tanaka and K. Kawabe, Yakugaku Zasshi, 100 (1980) 1048.
15 J. A. Nelder and R. Mead, Comput. J., 7 (1965) 308.

Analytica Chimica Acta, 179 (1986) 299—305
Elsevier Science Publishers B.V., Amsterdam — Printed in The Netherlands

THE APPLICATION OF STRONGLY OXIDIZING AGENTS IN FLOW INJECTION ANALYSIS
Part 2. Manganese(III)

R. C. SCHOTHORST, O. O. SCHMITZ and G. DEN BOEF*

Laboratory for Analytical Chemistry, University of Amsterdam, Nieuwe Achtergracht 166, 1018 WV Amsterdam (The Netherlands)

(Received 30th May 1985)

SUMMARY

The application of manganese(III) as a powerful oxidizing agent in flow injection analysis is described. Manganese(III) is generated electrochemically in the flowing system at a working electrode consisting of a packed bed of gold powder. Spectrophotometric detection is used at 490 nm, where manganese(III) in sulphuric acid solution absorbs strongly. Under the experimental conditions, the generation of manganese(III) can be accompanied by generation of manganese(IV) and permanganate; manganese(III) alone can be generated by a proper selection of the generating current and the flow rate. Results are presented for the determination of various organic and inorganic substances by means of manganese(III), usually at concentrations in the 10^{-4}—10^{-2} mol l^{-1} range. Unlike permanganate and manganese(IV), manganese(III) does not react with chloride, so that oxidizable compounds can be determined in the presence of large amounts of this species.

Manganese(III), a strong oxidizing agent like silver(II), has only been occasionally applied in titrimetric analysis, probably because of its disproportionation to manganese(II) and manganese dioxide, which makes the storage of reagent standard solutions rather complicated. However, as with silver(II) [1], generating the reagent and conducting the analytical reaction in a flowing system provides new and fast applications of this oxidimetric reagent.

The standard potential of the half-reaction $Mn^{3+} + e^- \leftrightharpoons Mn^{2+}$ in 7.5 mol l^{-1} sulphuric acid is 1.49 V [2]. The standard potential is lower than the corresponding value for Ag^{2+}/Ag^+, hence manganese(III) is a milder oxidizing agent than silver(II). The standard potentials in acidic solution for some half-reactions involving manganese are [2, 3]:

$Mn^{3+} + e^- \leftrightharpoons Mn^{2+}$	$E = 1.49$ V
$Mn^{4+} + 2e^- \leftrightharpoons Mn^{2+}$	$E = 1.57$ V
$MnO_4^- + 8H^+ + 5e^- \leftrightharpoons Mn^{2+} + 4H_2O$	$E = 1.49$ V
$Mn^{4+} + e^- \leftrightharpoons Mn^{3+}$	$E = 1.64$ V
$MnO_4^- + 8H^+ + 3e^- \leftrightharpoons Mn^{4+} + 4H_2O$	$E = 1.68$ V

0003-2670/86/$03.50

These standard potentials are very similar, hence the electrochemical generation of manganese(III) from manganese(II) can easily result in the generation of manganese(IV) and permanganate as well. It must, however, be kept in mind that the electrochemical generation of manganese(III) and the analytical reactions proceed in 3.6 mol l^{-1} sulphuric acid and that under these circumstances the formal potentials of the half-reactions mentioned above will be different.

The stability of solutions of manganese(III) is adversely affected by disproportionation into Mn^{2+} and manganese(IV), but this reaction can be suppressed by adding substances that form complexes with manganese(III) or by increasing the concentration of manganese(II) or hydrogen ions. Complexing agents often employed are phosphoric acid, sulphuric acid and acetic acid [4]. However, too strongly complexing agents must be avoided if the oxidizing properties of manganese(III) are to be maintained.

The commonest procedures for the preparation of solutions of manganese(III) described in the literature are as follows: Chemical oxidation of manganese(II) to manganese(III) is quite easy; suitable oxidizing agents are summarized by Barek and Berka [4]. Belcher and West [5] prepared solutions of manganese(III) by dissolution of manganese(III) phosphate. Several workers have studied the electrochemical oxidation of manganese(II). Selim and Lingane [6] investigated the influence of the temperature, current density and the sulphuric acid and manganese(II) concentrations on the current efficiency for the electrochemical generation of manganese(III) at a platinum working electrode. The current efficiency is not dependent on the sulphuric acid concentration between 2 and 7 mol l^{-1}, but is dependent on the manganese(II) concentration and on the current density. When the temperature is increased, the current efficiency falls, probably because of the disproportionation of manganese(III). The same behaviour was found by Fenton and Furman [7] for the generation of manganese(III) at a gold working electrode. For sulphuric acid concentrations below 2 mol l^{-1}, a brown deposit of manganese dioxide was visible on the working electrode. At high current densities permanganate was formed. Buck [8] generated manganese(III) at carbon and boron carbide working electrodes. Of these three methods only the electrochemical generation of manganese(III) is suitable for generation in flow. Determinations of a great number of inorganic and organic substances by means of titration with manganese(III) are summarized by Barek and Berka [4]. Detection can be done at 490 nm, the wavelength of maximum absorption of manganese(III) in 2 mol l^{-1} sulphuric acid solution [9].

Selim and Lingane [6] found that the wavelength of the absorbance maximum of manganese(III) and the molar absorptivity increases with increasing sulphuric acid concentration. The molar absorptivity at the wavelength of maximum absorption increases from about 100 l mol^{-1} cm in 3 mol l^{-1} sulphuric acid to about 190 l mol^{-1} cm in 18 mol l^{-1} sulphuric acid.

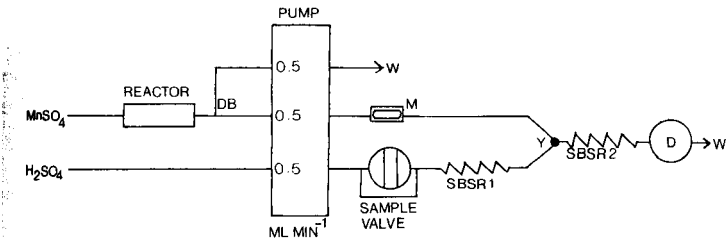

Fig. 1. Flow diagram. Length of single bead string reactors (SBSR): (1) 0.2 m; (2) 0.4 m; DB, debubbler; D, detector; M, mixing chamber; W, waste. All connecting and SBSR tubing is of 0.75 mm i.d. polyethylene. SBSRs are packed with 0.6 mm glass beads.

The present paper describes the electrochemical generation of manganese(III) in a flow-injection system at a working electrode consisting of a packed bed of gold powder. Detection is done spectrophotometrically.

EXPERIMENTAL

Apart from the spectrophotometric flow-through cell, the instrumentation and the dimensions of the flow system (Fig. 1) were identical with those in the paper on silver(II) [1]. A Hellma flow-through cell was used (optical path length 10 mm, volume 8 μl). Detection was done at 490 nm. The flow rate in each stream is indicated in the figure. The loop volume of the injection valve was 35 μl. The manganese(II) sulphate concentration entering the electrochemical flow-through reactor was 5×10^{-3} mol l^{-1} in 3.6 mol l^{-1} sulphuric acid. The sample stream was 3.6 mol l^{-1} sulphuric acid. All sample solutions were also made 3.6 mol l^{-1} in sulphuric acid. The counter and reference electrode of the electrochemical flow-through reactor were continuously rinsed (1.5 ml min^{-1}) with 3.6 mol l^{-1} sulphuric acid.

RESULTS AND DISCUSSION

Preliminary experiments

The stability of manganese(III) and the molar absorptivity increase with increasing sulphuric acid concentration. The sulphuric acid concentration should, however, be as low as possible for practical applications in a flow system. Therefore, absorption spectra resulting from a solution of manganese(II) after passage of a fixed amount of charge in batch were recorded as a function of the sulphuric acid concentration. Under the experimental conditions used, manganese(II) is only partly converted to manganese(III) and neither manganese(IV) nor permanganate were found. The results are presented in Table 1. The maximum light absorption increases with increasing sulphuric acid concentration, which can mainly be ascribed to an increasing manganese(III) concentration. At sulphuric acid concentrations below 2.0 mol l^{-1}, a brown deposit of probably manganese dioxide [7, 10] was

TABLE 1

The dependence of the maximum absorption at about 490 nm of generated manganese(II) on the sulphuric acid concentration
(Initial manganese(II) sulphate concentration was 10^{-2} mol l^{-1}; generating current 10 mA; generating time 15 min.)

H_2SO_4 (mol l^{-1})	1.8	2.7	3.6	4.5
Absorbance	0.39	0.54	0.62	0.72

visible on the working electrode. A sulphuric acid concentration of 3.6 mol l^{-1} was chosen for further work. The wavelength of maximum absorption for manganese(III) in 3.6 mol l^{-1} was found to be 490 nm.

Dependence of the solution composition on the generating current

Because the standard potentials of the Mn(III)/Mn(II), Mn(IV)/Mn(III), Mn(IV)/Mn(II), Mn(VII)/Mn(II) and Mn(VII)/Mn(IV) redox couples in acidic solution are very similar, the electrochemical generation of manganese(III) can easily be accompanied by the generation of manganese(IV) and permanganate. On generating manganese(III) in the flowing system at the packed bed gold powder working electrode, at a flow rate of 0.95 ml min^{-1}, the colour of the resulting solution turned from pink through brown to purple for generating currents changing from 2 to 20 mA, indicating that manganese(IV) and permanganate were generated at higher generating currents.

As manganese(IV) and permanganate are also strong oxidants, the solution leaving the electrochemical reactor must not contain these species. Therefore, the composition of the solution leaving the electrochemical reactor at different generating currents was investigated. As the molar absorptivity of manganese(II) is negligible between 220 and 600 nm, the composition of the solution leaving the reactor can be calculated by recording the absorbance of this solution at three different wavelengths at which the molar absorptivities of manganese(III), manganese(IV) and permanganate are known. The selected wavelengths were 405, 450 and 490 nm; 490 nm is the wavelength of maximum absorption of manganese(III) and manganese(IV) absorbs strongly at 405 nm where the absorption of manganese(III) and permanganate is minimal. The molar absorptivities of manganese(III), manganese(IV) and permanganate at these three wavelengths, under the experimental conditions, were measured from solutions of known concentrations. For permanganate this caused no problems. Manganese(IV) sulphate solutions were prepared by the method described by Mandal and Sant [11]; the manganese(IV) concentration was determined by a bipotentiometric titration with standard diammonium iron(II) sulphate solution. Manganese(III) sulphate solutions were prepared in the flowing system with a generating current of 4 mA and a flow rate of 0.95 ml min^{-1}. Under these conditions, neither manganese(IV) nor permanganate was generated. The manganese(III)

concentration was also determined by a bipotentiometric titration with standard diammonium iron(II) sulphate solution [12]. The experimentally evaluated molar absorptivities of manganese(III), manganese(IV) and permanganate at 405, 450 and 490 nm are summarized in Table 2.

The composition of the solution leaving the electrochemical reactor was determined for generating currents between 2 and 20 mA at a flow rate of 0.95 ml min^{-1}. The results are presented in Fig. 2. For generating currents up to 8 mA, the amount of generated manganese(III) increases continuously. Above 8 mA, manganese(IV) and above 12 mA permanganate are also generated. For practical applications of manganese(III), generating currents of 7 mA or less can be used.

Dependence of the solution composition on the flow rate

In an electrochemical reactor as described, the oxidation efficiency as well as the composition of the oxidation products are dependent on the electrode parameters and on the flow rate. Thus by changing the flow rate the composition of the solution leaving the electrochemical reactor may alter. For a generating current of 7 mA, the dependence of the solution composition on the flow rate is presented in Fig. 3A. At flow rates lower than 1 ml min^{-1}, manganese(IV) is also generated, but no permanganate is formed.

TABLE 2

Molar absorptivity in 3.6 mol l^{-1} sulphuric acid

Substance	Molar absorptivity (l mol^{-1} cm)		
	490 nm	450 nm	405 nm
Manganese(III)	100	80	45
Managanese(IV)	175	390	845
Permanganate	1130	185	45

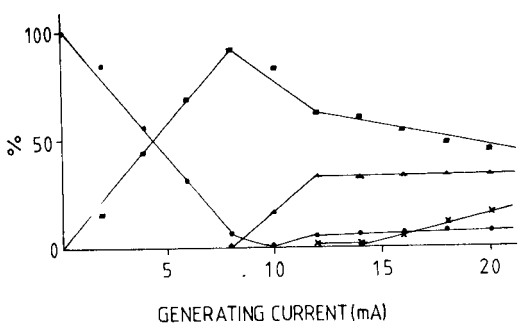

Fig. 2. Solution composition as a function of the generating current: (•) Mn^{2+}; (▪) Mn^{3+}; (▲) Mn^{4+}; (×) MnO_4^-. Flow rate 0.95 ml min^{-1}; initial manganese(II) sulphate concentration 5 × 10^{-3} mol l^{-1}.

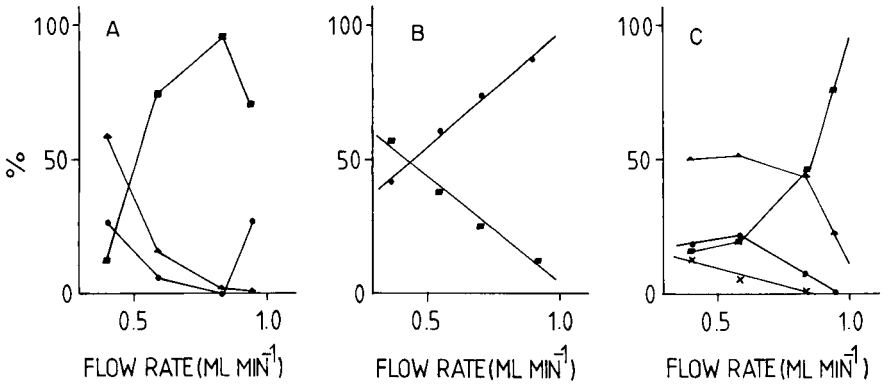

Fig. 3. Solution composition as a function of the flow rate at different generating currents: (•) Mn^{2+}; (▪) Mn^{3+}; (▲) Mn^{4+}; (×) MnO_4^-. Generating current: (A) 7 mA; (B) 2 mA; (C) 11 mA. Initial manganese(II) sulphate concentration 5×10^{-3} mol^{-1} in all cases.

Only at very low generating currents (2 mA) can the flow rate be varied over a wide range without generating manganese(IV) and permanganate as well (Fig. 3B). Permanganate can be generated by using high generating currents and low flow rates (Fig. 3C). In the experiments, a generating current of 5 mA and a flow rate of about 1 ml min^{-1} were used. It must be kept in mind, however, that the described situation is only valid for the electrochemical reactor used in this work, and may be different for other reactors.

Analytical applicability

The substances examined to test the analytical applicability of manganese(III) were the same as those used for Silver(II) [1]. The successful results for the determination of the chosen substances are summarized in Table 3. The correlations for the absorbance (A) and the concentration of the analyte in the sample solution (C) show good linearity over about one decade change in concentration The limit of determination is defined here as the analyte concentration for which the absorbance change was ten times the peak-to-peak noise.

Chromium(III) could not be determined by this method, because the product of the reaction with manganese(III), dichromate, itself absorbs strongly at 490 nm. No signals were obtained from formic acid, propan-1-ol, propan-2-ol or 2-methylpropan-2-ol in the concentration range 10^{-3}—10^{-2} mol l^{-1}. In non-flowing systems, alcohols also show no reaction and formic acid reacts only very slowly with manganese(III) [4].

Injections of 10^{-2} mol l^{-1} chloride caused no absorbance changes. However, as soon as manganese(IV) or permanganate were present in the solution, injections of chloride produced large absorbance changes. Hence determinations with manganese(III) are possible in the presence of a large amount of chloride ions as contrasted with manganese(IV) and permanganate, which quickly react with chloride.

TABLE 3

Calibration lines for the flow-injection system (initial manganese(II) sulphate concentration 5×10^{-3} mol l^{-1})

Sample	Concentration range (mol l^{-1})	Regression line	r^a	Limit of determination (mol l^{-1})
Gold powder working electrode				
$NaNO_2$	10^{-4}—5.4×10^{-4}	$A = (38.7 \pm 0.7)C$	0.9959	3×10^{-4}
$VOSO_4$	4×10^{-4}—2×10^{-3}	$A = (20.7 \pm 0.4)C$	0.9987	5×10^{-4}
$(NH_4)_2Fe(SO_4)_2$	10^{-3}—5×10^{-3}	$A = (11.3 \pm 0.1)C$	0.9995	9×10^{-4}
$Ce(NO_3)_3$	1.7×10^{-3}—7×10^{-3}	$A = (3.9 \pm 0.1)C$	0.9991	3×10^{-3}
KIO_3	2×10^{-3}—7×10^{-3}	$A = (5.1 \pm 0.1)C$	0.9967	2×10^{-3}
			—	—
$(COONa)_2$	2×10^{-3}—6×10^{-3}	$A = (13.4 \pm 0.2)C$	0.9979	8×10^{-4}
C_6H_5COOH	4×10^{-4}—1.4×10^{-3}	$A = (17.7 \pm 0.1)C$	0.9968	6×10^{-4}
Glassy carbon powder working electrode				
$NaNO_2$	10^{-3}—4×10^{-3}	$A = (30.5 \pm 0.2)C$	0.9994	3×10^{-4}
$VOSO_4$	10^{-3}—5×10^{-3}	$A = (16.3 \pm 0.2)C$	0.9988	6×10^{-4}
$Ce(NO_3)_3$	2×10^{-3}—5×10^{-3}	$A = (2.7 \pm 0.2)C$	0.9984	4×10^{-3}

[a]Regression coefficient.

Instead of gold powder, glassy carbon powder (particle diameter < 0.6 mm) can be used for the working electrode. The results for the determination of nitrite, vanadium(IV) and cerium(III) by means of manganese(III) generated at a glassy carbon working electrode are also presented in Table 3. The generating current was 8 mA and neither manganese(IV) nor permanganate was generated. The limits of determination are about of the same order as with generation at the gold working electrode. The glassy carbon electrode was, however, quickly deactivated, probably by manganese dioxide, and had to be cleaned regularly, so the gold electrode has to be preferred.

When the results of the determinations with silver(II) and manganese(III) are compared, the conclusion is that the determinations with silver(II) achieve lower limits of determination for all the substances tested. This must be ascribed to the high molar absorptivity of silver(II). However, manganese(III) is more selective and can be applied in sulphuric acid and hydrochloric acid solution.

REFERENCES

1 R. C. Schothorst and G. den Boef, Anal. Chim. Acta, 169 (1985) 99.
2 K. J. Vetta and G. Manecke, Z. Physik. Chem., 195 (1950) 270.
3 G. Grube and H. Huberich, Z. Electrochem., 29 (1923) 8.
4 J. Barek and A. Berka, CRC Crit. Rev. Anal. Chem., 9 (1980) 55.
5 R. Belcher and T. S. West, Anal. Chim. Acta, 6 (1952) 322.
6 R. G. Selim and J. J. Lingane, Anal. Chim. Acta, 21 (1959) 536.
7 A. J. Fenton and N. H. Furman, Anal. Chem., 32 (1960) 748.
8 R. P. Buck, Anal. Chem., 35 (1963) 692.
9 I. M. Issa, M. M. G. Honeim, A. A. El-Samahy and M. Tharwat, Electrochim. Acta, 17 (1972) 1251.
10 G. Davies, Coord. Chem. Rev., 4 (1969) 199.
11 S. K. Mandal and B. R. Sant, Talanta, 23 (1976) 485.
12 T. J. Pastor and M. M. Antonijević, Analyst (London), 109 (1984) 235.

Analytica Chimica Acta, 179 (1986) 307—313
Elsevier Science Publishers B.V., Amsterdam — Printed in The Netherlands

BIOLUMINESCENT ASSAYS WITH IMMOBILIZED FIREFLY LUCIFERASE BASED ON FLOW INJECTION ANALYSIS

P. J. WORSFOLD* and A. NABI
Department of Chemistry, University of Hull, Hull, HU6 7RX (Great Britain)
(Received 29th July 1985)

SUMMARY

A flow-injection manifold incorporating immobilized firefly luciferase is described. The detector design and reaction conditions are discussed and results are presented for the determination of adenosine-5′-triphosphate over the range 1×10^{-12}—1×10^{-5} M. Modifications for creatine phosphokinase (10—400 U l^{-1}) and creatine phosphate (10^{-5}—10^{-1} M), both determined indirectly via ATP, are also described.

The phenomenon of bioluminescence, whereby an enzyme catalyses the oxidation of a substrate by oxygen or hydrogen peroxide, occurs extensively in nature [1]. One of the most useful bioluminescence reactions for analytical purposes is the firefly luciferase (*Photinus pyralis*)/luciferin system, which requires adenosine-5′-triphosphate (ATP) as a cofactor [2], and can therefore be used to monitor any reaction that produces or consumes ATP. Green light (562 nm) is emitted during the reaction, probably by an excited anionic form of oxyluciferin [3], and detection limits of 10^{-17} mol ATP have been reported [4].

The conventional procedure for monitoring bioluminescence reactions is to inject luciferase and luciferin into a discrete, light-tight tube containing the sample and to monitor the emitted light intensity vs. time. Recently, however, a continuous-flow procedure has been reported by Worsfold and Nabi [5] that facilitates rapid analysis with minimal reagent and sample consumption, but most importantly, provides reproducible mixing of sample and reagent and therefore gives improved precision. One limitation of the above methods is the irrecoverable use of an expensive enzyme. Several workers have reported bioluminescence analyses using immobilized firefly luciferase or immobilized bacterial luciferase and oxidoreductase. Of the immobilization techniques used, covalent attachment of the enzyme to Sepharose 4B via cyanogen bromide appears to offer the best retention of enzyme activity [6]. Immobilized bacterial luciferase/oxidoreductase has been used instead of the free enzymes in a conventional discrete analyser [7] and in a single channel continuous-flow system with septum injection [8], and immobilized firefly luciferase has been used in a continuous-flow manifold with a modified commercial photometer and continuous pumping of luciferin [9].

0003-2670/86/$03.50

This paper describes a purpose-built flow injection analyser for the determination of ATP with immobilized firefly luciferase. The determination of creatine phosphokinase (CPK) and creatine phosphate by a coupled reaction is also investigated and the advantages of the flow injection method are discussed.

EXPERIMENTAL

Reagents

For ATP determination. D-Luciferin was synthesized according to the method of Seto et al. [10]. A stock solution (5×10^{-4} M) was prepared in Tris acetate buffer (0.1 M) at pH 7.5 and stored in the dark at 4°C. A stock solution of ATP (1×10^{-4} M; Sigma) was made in the same buffer and stored at 4°C; ATP standards covering the range 10^{-5}—10^{-12} M were prepared daily from the stock solution. Both carrier streams (see below) were Tris acetate buffer (0.1 M) at pH 7.5 containing magnesium acetate (1 mM). Firefly luciferase (5 U mg^{-1}) was obtained as a lyophilized powder (Sigma) and immobilized according to the procedures given below.

For creatine phosphokinase determination. Creatine phosphokinase (CPK; EC 2.7.3.2) from rabbit muscle was obtained as a lyophilized powder (190 U mg^{-1}; Sigma) and standards covering the range 0—400 U l^{-1} were prepared in imidazole buffer (0.1 M) at pH 6.7 containing bovine serum albumin (1 g l^{-1}) and *N*-acetyl-L-cysteine (10 mM). The CPK control sera (Sigma) were reconstituted with deionized water before use. The carrier stream for the CPK standards and samples consisted of partially purified [11] adenosine-5′-diphosphate (ADP; Sigma; 1×10^{-6} M), creatine phosphate (5×10^{-3} M) and EDTA (1 mM) in Tris acetate buffer (0.1 M) at pH 6.7. The carrier stream for the luciferin consisted of Tris acetate buffer (0.1 M) at pH 8.2.

For creatine phosphate determination. Creatine phosphate standards covering the range 10^{-1}—10^{-5} M were prepared in Tris acetate buffer (0.1 M) at pH 6.7. The carrier stream for the creatine phosphate standards consisted of CPK (100 U l^{-1}), partially purified ADP (1×10^{-6} M) and EDTA (1 mM) in Tris acetate buffer (0.1 M) at pH 6.7. The carrier stream for the luciferin consisted of Tris acetate buffer (0.1 M) at pH 8.2.

Immobilization of luciferase

On Sepharose 4B. Cyanogen bromide-activated Sepharose 4B (0.5 g; Sigma) was added to 2 ml of sodium hydrogencarbonate buffer (0.1 M) at pH 8.0 containing lyophilized firefly luciferase (2 mg) and bovine serum albumin (10 mg) [7]. The mixture was gently stirred at 4°C for 20 h, filtered through a G3 sintered glass filter, washed with 50 ml of cold phosphate buffer (0.1 M) at pH 7.0 containing dithiothreitol (DTT; 0.5 mM) and finally washed with 50 ml of phosphate buffer (0.1 M) at pH 7.0 containing sodium chloride (1 M) and DTT (0.5 mM). The beads were stored at

4°C in 3 ml of a phosphate buffer (0.1 M) at pH 7.0 containing DTT (0.5 mM), bovine serum albumin (2 g l^{-1}) and sodium azide (0.2 g l^{-1}).

On controlled porosity glass (CPG). Controlled porosity glass beads (120—200 mesh; 25.3-nm mean pore size; Sigma) were washed with nitric acid, silanized with γ-aminopropyltriethoxysilane and derivatized with glutaraldehyde according to the method of Weetall and Filbert [12]. The derivatized glass beads (0.5 g) were added to 2 ml of phosphate buffer (0.1 M) at pH 7.0 containing lyophilized firefly luciferase (2 mg) and kept at 4°C for 3 h. The washing and storage of the CPG-immobilized enzyme was as described above for Sepharose.

Instrumentation and procedures

Determination of ATP. The merging zones manifold used for the determination of ATP is shown in Fig. 1. The Tris acetate buffer carrier streams were pumped at 0.75 ml min^{-1} using a peristaltic pump (Ismatec Mini S-820) with poly(vinyl chloride) pump tubing. Teflon tubing (0.5 mm i.d.) was used throughout the remainder of the system. An ATP standard (30 μl) and luciferin (30 μl) were simultaneously injected into separate Tris acetate buffer carrier streams at pH 7.5 using a rotary PTFE valve. The two injected zones were synchronously merged 12.5 cm downstream at a T-piece and travelled 2.2 cm before passing into a glass coil (2.5 mm i.d. × 60 mm length) containing immobilized enzyme (0.1 g of beads) held in place by plugs of glass wool (Fig. 2). The coil was placed directly in front of an end-window

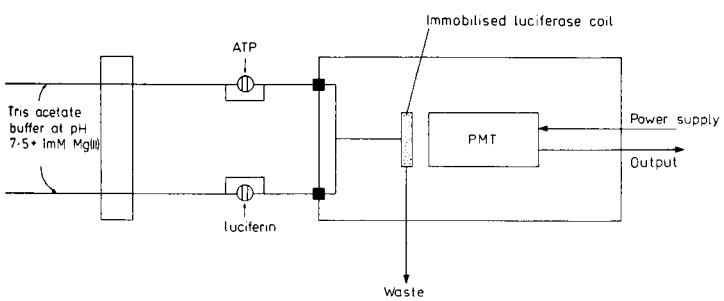

Fig. 1. Manifold for the bioluminescent determination of ATP. ATP standards (30 μl) and luciferin (30 μl) are injected into the buffered carrier streams, each pumped at 0.7 ml min^{-1} and synchronously merged 12.5 cm downstream. Distance from confluence point to immobilized enzyme coil, 2.2 cm.

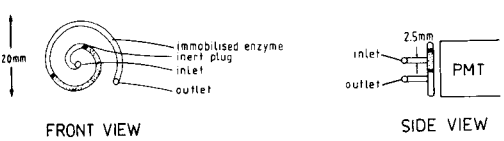

Fig. 2. Design of the glass coil containing immobilized luciferase.

photomultiplier tube (Thorn EMI 9789QB) and a reflective plate was placed behind the coil. The photomultiplier tube, immobilized enzyme coil and T-piece were enclosed in a light-tight housing, as shown in Fig. 3. All results are the means of three injections unless otherwise stated.

Determination of CPK and creatine phosphate. The instrumentation and procedures were as described above except that the pH values of the buffer streams were modified to optimize both the CPK reaction (pH 6.7) and the luciferase reaction (pH 7.5).

RESULTS AND DISCUSSION

Optimization of the ATP manifold

The optimum flow rate for maximum bioluminescence emission was 1.7 ml min^{-1} in each channel. The decreased signal observed at higher flow rates was due to the shorter residence time of the substrates within the immobilized enzyme coil coupled with the slow turnover rate of the enzyme. The reason for the decreased signal observed at lower flow rates is less obvious; probably, less efficient mixing of the injected ATP with the magnesium-containing carrier stream resulted in decreased ATP/magnesium complex formation [13].

The composition of the carrier streams and the concentrations of reagents used had a significant effect on the quantum yield of the bioluminescence reaction. The signal increased with increasing magnesium concentration up to 1×10^{-3} M, above which the ionic strength of the carrier stream had an inhibiting effect on luciferase activity. The anion of the magnesium salt used can also affect enzyme activity [14] and the extent of inhibition by the three anions studied was found to be chloride > sulphate > acetate. The concentration of luciferin used (5×10^{-4} M) was sufficient to give an excess of substrate within the detector coil without prohibitively affecting the cost of the analysis. Certain surfactants have been shown to stimulate bioluminescence emission in solution [15] but the use of a non-ionic surfactant (Triton X-100) over the range 0.0—4.0% v/v in the immobilized

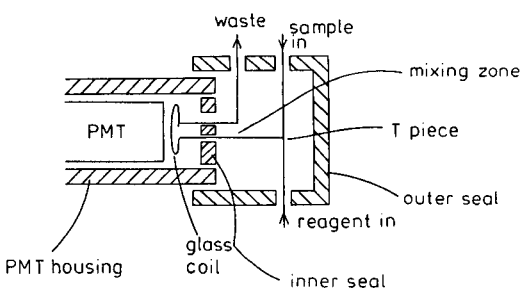

Fig. 3. Design of the light-tight housing containing the T-piece and the immobilized enzyme coil.

enzyme system gave a progressively diminishing signal with increasing concentration.

A comparison of Sepharose 4B and CPG for the immobilization of firefly luciferase showed that the Sepharose system had a limit of detection three orders of magnitude better and a sensitivity two orders of magnitude greater than the CPG system. The pH optimum for the Sepharose-bound enzyme was 7.5, compared with a reported value of 7.8 for the free enzyme [16], the shift being due to changes in the microenvironment of the active site of the enzyme. Previous workers [6] have indicated that 84% of the protein fraction is bound to Sepharose during the immobilization step. For CPG-bound enzyme the pH shift was more pronounced, with a pH optimum of 7.2. This agrees with previously reported results [17], and the corresponding lack of sensitivity is due in part to a loss of enzyme activity on binding and in part to a shift in the emission maximum to a longer wavelength where the detector is less sensitive.

Calibration for ATP

The results obtained from triplicate injections of ATP standards over the range 10^{-12}—10^{-5} M are shown in Table 1. The relative standard deviation is generally <2% over the whole range, and the limit of detection is governed by background luminescence from the blank rather than by any absolute limitation in the detection of the bioluminescence. This could therefore be improved by the use of more highly purified reagents. A log-log plot of the calibration results (Fig. 4) shows that the dynamic range of the present system is 10^{-12}—10^{-7} M ATP.

TABLE 1

Calibration data for the bioluminescent determinations of ATP, CPK and creatine phosphate

ATP conc. (M)	Output voltage (V)	R.s.d.[a] (%)	CPK conc. ($U\ l^{-1}$)	Output voltage (V)	R.s.d.[a] (%)	Creatine phosphate conc. (M)	Output voltage (V)	R.s.d.[a] (%)
0	0.10	—	0	0.40	0.0			
1×10^{-12}	0.12	—	10	0.48	4.4	0	0.95	9.1
1×10^{-11}	0.25	5.6	20	0.70	3.0	1×10^{-5}	1.06	4.0
1×10^{-10}	0.51	1.6	30	0.99	2.0	1×10^{-4}	2.14	4.3
1×10^{-9}	1.22	4.1	50	1.47	1.0	1×10^{-3}	5.68	1.4
1×10^{-8}	4.08	0.7	80	2.13	3.6	1×10^{-2}	6.53	1.4
1×10^{-7}	7.13	1.3	100	2.80	3.8	1×10^{-1}	6.83	1.3
1×10^{-6}	8.30	1.7	200	3.77	2.6			
1×10^{-5}	9.40	1.5	300	4.43	2.0			
			400	4.73	4.2			

[a] $n = 3$.

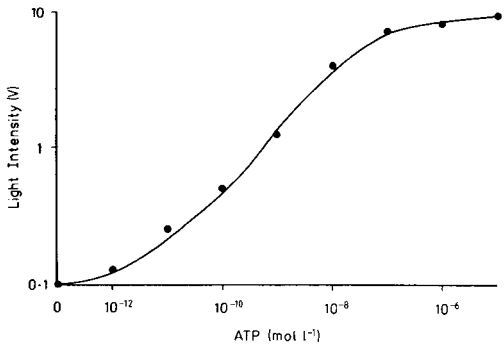

Fig. 4. Log-log calibration curve for ATP.

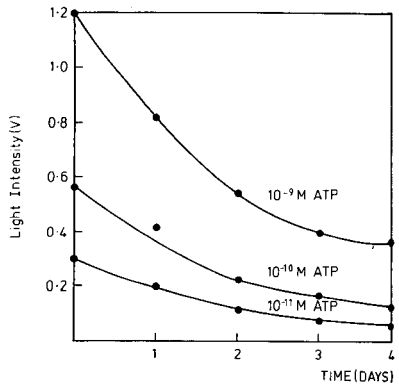

Fig. 5. Stability of immobilized firefly luciferase at room temperature in the flow-injection manifold. The response of one coil to daily injections of three ATP standards is shown.

The Sepharose-bound enzyme showed no loss of activity over a two month period when stored at 4°C; Fig. 5 shows the gradual loss of activity over 4 days when the immobilized enzyme was kept continuously at room temperature within the flow-injection manifold. The activity loss is probably due to degradation by micro-organisms and could be decreased by the periodic injection of sodium azide solution.

Calibration for CPK and creatine phosphate

The manifold used for the CPK assay was the same as for the ATP assay except that CPK was injected into a carrier stream containing ADP and creatine phosphate, and ATP was produced in situ. As with the ATP assay, the limit of detection was governed by the reagent blank, which was amplified by the presence of ATP in the ADP, even after purification by anion-exchange chromatography. To minimise the blank signal, 1×10^{-6} M ADP was used, which is less than the K_M value; this caused substrate depletion at higher CPK activities.

The pH of the two carrier streams was such that both enzyme reactions took place at their optimum pH values (6.7 for CPK and 7.5 for luciferase). Results for CPK standards over the range 0—400 U l^{-1} are given in Table 1; they demonstrate good precision and excellent sensitivity. The accuracy of the technique was evaluated by injecting two control sera with reported values of 40 and 60 U l^{-1}. The results obtained (n = 3) were 35 U l^{-1} (r.s.d. = 5.4%) and 57 U l^{-1} (r.s.d. = 2.5%), respectively.

For the determination of creatine phosphate, the manifold was as above except that creatine phosphate was injected into a carrier stream containing CPK. The results for creatine phosphate over the range 1×10^{-5}—0.1 M are given in Table 1; again, they demonstrate good precision and excellent sensitivity.

Conclusions

The results obtained demonstrate that flow injection is an excellent tool for the study of bioluminescence processes and that firefly luciferase can be immobilized and used on-line for several days whilst remaining active. The manifold can easily be modified to monitor reactions which produce or consume ATP, and a similar system involving bacterial luciferase could be developed for NADH. The technique is rapid, simple and economical and has considerable potential for the development of highly selective and sensitive assays of clinical and biological samples.

The authors thank Mrs. B. Worthington for the synthesis of firefly luciferin.

REFERENCES

1 A. Thore, Sci. Tools, 26 (1979) 30.
2 W. D. McElroy, Proc. Nat. Acad. Sci. U.S., 33 (1947) 342.
3 E. H. White, E. Rapaport, H. H. Seliger and T. A. Hopkins, Bioorg. Chem., 1 (1971) 92.
4 E. W. Chappelle and G. V. Levin, Biochem. Med., 2 (1968) 41.
5 P. J. Worsfold and A. Nabi, Anal. Chim. Acta, 171 (1985) 333.
6 G. K. Wienhausen, L. J. Kricka, J.. E. Hinckley and M. DeLuca, Appl. Biochem. Biotech., 7 (1982) 463.
7 J. Ford and M. DeLuca, Anal. Biochem., 110 (1981) 43.
8 K. Kurkijarvi, R. Raunio and T. Korpela, Anal. Biochem., 125 (1982) 415.
9 L. J. Kricka, G. K. Wienhausen, J. E. Hinkley and M. DeLuca, Anal. Biochem., 129 (1983) 392.
10 S. Seto, K. Ogura and Y. Nishiyama, Bull. Chem. Soc. Jpn., 36 (1963) 332.
11 A. Lundin, in M. DeLuca (Ed.), Methods in Enzymology, Vol. 57, Academic Press, New York, pp. 56—65, 1978.
12 H. H. Weetall and A. M. Filbert, in W. B. Jakoby (Ed.), Methods in Enzymology, Vol. 34, Academic Press, New York, pp. 59—72, 1974.
13 W. D. McElroy, J. W. Hastings, J. Coulombre and V. Sonnenfeld, Arch. Biochem. Biophys., 46 (1953) 399.
14 R. Gilles, A. Pequeux, J. J. Saive, A. C. Spronck and G. Thorne-Lentz, Arch. Int. Phys. Biochim., 84 (1976) 807.
15 L. J. Kricka and M. DeLuca, Arch. Biochem. Biophys., 217 (1982) 674.
16 L. Yu. Brovko, N. V. Kost and N. N. Ungarova, Biochemistry (Moscow), 45 (1981) 1199.
17 Y. Lee, I. Jablonski and M. DeLuca, Anal. Biochem., 80 (1977) 496.

Analytica Chimica Acta, 179 (1986) 315—323
Elsevier Science Publishers B.V., Amsterdam — Printed in The Netherlands

AN UNSEGMENTED EXTRACTION SYSTEM FOR FLOW INJECTION ANALYSIS

YLVA SAHLESTRÖM

Department of Analytical Chemistry, Royal Institute of Technology, S-100 44 Stockholm (Sweden)

BO KARLBERG*

Bifok AB, Box 124, S-191 22 Sollentuna (Sweden)

(Received 29th July 1985)

SUMMARY

In the system described, the two phases are fed into a module containing a PTFE membrane so that no segmentation takes place, i.e., each phase is fed to only one side of the membrane. The groove depth on the "aqueous" side of the membrane is 0.4 mm and on the "organic" side 0.8 mm. This latter groove is filled with a porous support of polyethylene. Caffeine, sodium dodecyl sulphate and sodium dioctylsulphosuccinate samples (40—500 μl) were injected into an aqueous carrier stream which was merged and mixed with an aqueous reagent before it was fed into the module. The maximum extraction efficiency varied with the flow rate but was in the range 8—18% and was obtained by injecting sample volumes larger than 400 μl. By injecting 40 μl of sample, the efficiency dropped by a factor of 1.5—7, depending on the character of the analyte. The system is suitable for coarse liquid-liquid extraction of concentrated samples because neither segmentation nor separation of the phases is required.

Liquid-liquid extraction based on flow injection analysis (f.i.a.) was described some years ago [1] and has been used for a variety of applications mainly in the determination of drugs. In most cases, the sample solution is injected into an aqueous phase and then mixed with a reagent, whereafter the aqueous stream is segmented by an organic phase so that analyte transfer can take place. The separated fraction of organic phase is led through the detector and the resulting peak is evaluated. Technically, three main problems must be solved in the construction of an extraction system of this kind, namely segmentation of the two immiscible phases, selection of suitable dimensions and material for the extraction coil and separation of the two phases. The last problem is probably the most complicated one, judged from the number of papers which have given attention to this subject [2].

Phase separators for extraction systems must be able completely to remove all traces of the unwanted phase while they must also be able to isolate a large fraction, preferably close to 100%, of the required phase. The construction of phase separators is also critical with respect to the peak broadening which may arise in this part of the extraction system [3]. Recent studies have

0003-2670/86/$03.50

shown that a thin film is formed in the extraction coil by the phase which has the largest affinity to the coil material [4]. This film plays an important role in the broadening of the peak, i.e., in the dispersion (or dilution) process of the analyte. The film thickness depends on the flow velocity, the coil material and on the viscosity and interfacial tension of the solvent. The thicker the film, the greater the peak broadening. Because of this film, the contact area between the two phases becomes very large in relation to the phase volumes involved and this can make the transfer of analyte more efficient. The size of the contact area is influenced by the segment length in the extraction coil, which means that segmentation pattern must be controllable. It must also be kept constant during the entire analytical cycle. Thus, in a given situation there are many possibilities, as well as difficulties, in optimizing the extraction conditions with respect to kinetic efficiency, total extraction yield and analyte dispersion. For uncomplicated and coarse extraction processes, there is a need for simpler systems in which the requirement of a high extraction yield can be relaxed.

This paper describes the evaluation of an unsegmented extraction system which from a fundamental point of view works like a dialysis system: the sample is injected into the aqueous phase which is then led into an extraction cell together with an organic recipient stream. The two streams are separated by a membrane across which transfer of the analyte can take place. Thus both segmentation and separation problems are avoided because the unsegmented recipient stream is led directly to the detector flow cell. Furthermore, the contact area between the two phases is kept constant throughout.

EXPERIMENTAL

The extraction system

A schematic diagram of the extraction system is shown in Fig. 1. A peristaltic pump (Ismatec mp13-GJ-4) with variable pump speed was used together with standard Tygon pump tubes of different sizes. All connecting tubes were of PTFE (0.5 mm i.d.). Pure chloroform was pumped from a displacement bottle arrangement (Tecator, Sweden) as indicated in Fig. 1. Chloroform/methanol mixtures were pumped directly by Acidflex pump tubings. Aqueous test solutions were injected into the aqueous carrier stream by a rotary valve with variable volume (L-100-1, Tecator). The normal injection volume was 40 μl. The samples were filled into the injector by aspiration using the peristaltic pump. The carrier and the reagent streams were merged at a conventional T-piece with a uniform inner diameter of 0.7 mm. The extractor is depicted in Fig. 2; it consists of two halves made from poly(vinyl difluoride) (PVDF), each half having one inlet and one outlet. Different groove dimensions and membrane types were investigated (see below). The groove in the bottom half was filled with support material of a porous polyethylene. The gasket consisted of a PTFE tape in which a rectangular cut was made, adapted to the grooves. The two PVDF halves were sandwiched between two aluminium plates (not shown in Fig. 2).

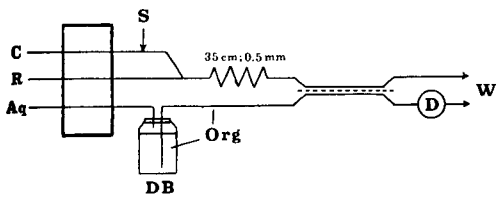

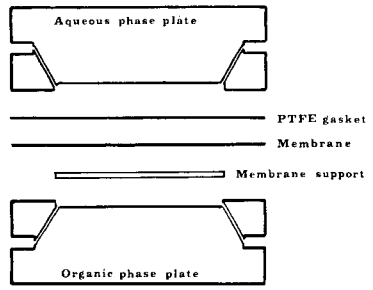

Fig. 1. Flow scheme of the unsegmented extraction system. Streams: C, carrier; R, reagent; Aq, water fed to displacement bottle (DB); Org, organic phase; S, sample; W, waste; D, detector.

Fig. 2. The extraction cell. The recommended dimensions of the organic groove are 40 mm long, 2 mm wide and 0.8 mm deep. The diameter of the inlet and outlet tubes is 0.5 mm.

The flow cell (Hellma) had a volume of 8 μl and a light path length of 10 mm. It was used with an ultraviolet/visible spectrophotometer (Pye-Unicam SP6-550) connected to a strip-chart recorder.

Chemicals and solutions

Test compounds. Caffeine (Astra, Sweden), sodium dodecyl sulphate (Merck) and sodium dioctyl sulphosuccinate (Rohm & Haas, USA) were selected as test substances for the extraction. Their molecular weights are 194, 288, and 444, respectively. These substances were of high-purity grade. Commercial surfactants were obtained from Nordtend, Berol and Astra (Sweden). Aqueous stock solutions (1 mM) were prepared and stored for a maximum of one week. All other standard solutions were prepared daily by dilution.

Reagent solutions and solvents. For the determination of caffeine, R and C in Fig. 1, consisted of distilled water. For the determination of the two test surfactants, the reagent stream (R, Fig. 1) was a solution prepared as follows: 0.05 g of methylene blue and 28.3 g of sodium dihydrogenphosphate dihydrate were dissolved in about 200 ml of distilled water, 6.8 ml of concentrated sulphuric acid and 400 ml methanol were added and the solution was diluted to 1 l with distilled water. This solution can be stored at room temperature and used for about one week. The carrier stream (C) was distilled water. Chloroform (Merck) was shaken to equilibrium with distilled water before use. Methanol was used without any pretreatment. All reagents and solvents were of analytical grade.

Procedure

Before starting up the system, the displacement bottle was filled to 90—95% of its volume with chloroform. The remaining 5—10% of the volume was filled with distilled water. It is important that no air is trapped beneath

the cap, to ensure smooth delivery of the organic solvent. This arrangement is to be preferred to the direct pumping of organic phase by Acidflex pump tubes, which are expensive, have a short lifetime, and can produce large variations of the flow rate. However, for chloroform/methanol mixtures, Acidflex pump tubes must be used. The aqueous and the organic phases should enter the extractor unit simultaneously. It is important that no water droplets are present in the flow cell because they are not easily rinsed out by the chloroform phase. Ethanol was used to remove traces of water in such instances. Normally, a steady baseline was obtained after a few minutes, and injections of test solutions could be started almost immediately. For system performance tests, 40 μl of a 1 mM sodium dodecyl sulphate solution was injected. The flow rates of C, R, and O in Fig. 1 were 0.44, 1.3, and 1.0 ml min^{-1}, respectively. Evaluation of peak heights was done manually.

Optimization of the extractor design

Different groove depths, 0.4, 0.8 and 1.5 mm, in the lower "organic" half were investigated for a constant groove length (40 mm) and a constant width (2 mm). The extraction efficiency increased by a factor of almost two when the groove depth was increased from 0.4 to 0.8 mm. The counter pressure was rather substantial for the 0.4-mm depth and this resulted in penetration of organic phase through the membrane into the aqueous phase. Such penetration was not observed when the 0.8-mm depth was investigated. A groove depth of 1.5 mm gave only a very low extraction efficiency, far below any practical level. Consequently, a groove depth of 0.8 mm was used in all subsequent investigations. The best groove depth for the water stream was 0.4 mm.

Several types of membranes were tested but only two were found to be satisfactory, namely PTFE membranes with porosity of 0.45 and 1.0 μm (Millipore). The 1.0-μm porosity was preferred because it gave the largest extraction yield, about a factor of two better than the 0.45-μm porosity.

RESULTS AND DISCUSSION

Extraction efficiency and flow rates

Figure 3 shows the extraction efficiency for the three test compounds as a function of the total flow rate. The flow ratic between the organic and the joined aqueous streams, Q_{org}/Q_{aq}, was kept constant at about 0.4. The flow manifold is depicted in the upper part of Fig. 3. Each test solution was pumped as carrier (C in Fig. 1) and the steady-state signals were recorded at different total flow rates. These steady-state values were related to the theoretical extraction yield which could be obtained by manual batch extraction with volume proportions in agreement with those selected for the flow system. The efficiency profiles did not change when the concentration of the test compounds was varied within reasonable limits. For the compounds tested, the concentration range was 0.05—0.20 mM. Three important conclu-

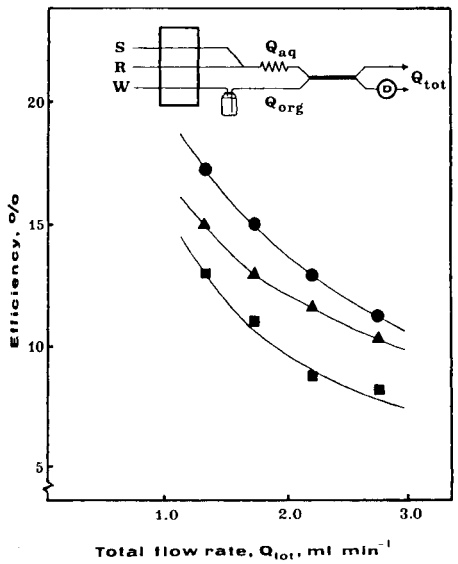

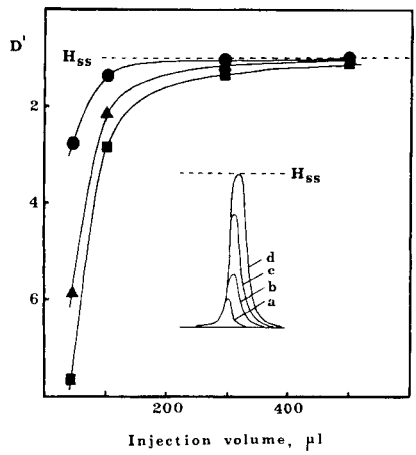

Fig. 3. Extraction efficiency as a function of total flow rate: (•) caffeine; (▲) sodium dodecyl sulphate; (■) sodium dioctyl sulphosuccinate. Concentration range is 0.05—0.20 mM.

Fig. 4. Peak profiles and D' as a function of injection volume: (•) caffeine; (▲) sodium dodecyl sulphate (SDS); (■) sodium dioctyl sulphosuccinate. Peaks: (a) 40, (b) 85, (c) 200, (d) 500 µl of 0.125 mM SDS. For explanation of symbols, see text.

sions can be drawn from the results in Fig. 3. First, the efficiency of the unsegmented extraction system seems to be typically 8—18% of that for batch extraction. Secondly, there is a significant individual difference in extraction efficiency between the three test compounds which might be explained by the difference in molecular structure. Thirdly, there is a practical lower limit for the total flow rate; below this limit, the accuracy and precision of an analysis cannot be maintained because small variations in the flow rate produce large variations of the extraction efficiency.

Kawase et al. [5] have shown that the extraction efficiency of anionic surfactants can be improved in a continuous flow system by an appropriate choice of buffer capacity and methanol content of the aqueous reagent (R). The enhanced extraction is due to the solvating effect of methanol. For the present type of system, a significant increase of the signal was observed when the methanol content in the reagent stream was increased from 0 to 40%. The order and profile of this increase were in close agreement with the data reported by Kawase et al. [5]. A methanol content of at least 20% in the reagent stream is recommended in this system because adsorption effects (i.e., peak tailing) were observed at lower values.

The extraction efficiency was also studied in several situations when the individual flow rates Q_R and Q_{org} were varied. All other flows were kept

constant. Sample was pumped as carrier. Table 1 shows the variation of H_{ss}, i.e., the steady-state signal, as a function of Q_{org}. The phase volume ratio in the system is defined by $(Q_C + Q_R)/Q_{org}$. The sample dilution factor for the aqueous phase is $Q_C/(Q_C + Q_R)$. When the sample is pumped as carrier, the overall "dilution" of the sample in the system is easily derived to be

$$\text{"dilution" factor} = [Q_C/(Q_C + Q_R)]\,[(Q_C + Q_R)/Q_{org}]f_{eff} = (Q_C/Q_{org})f_{eff}$$

where f_{eff} is the extraction efficiency factor. The dilution factor would consequently be proportional to the inverse flow rate of the organic phase if f_{eff} is a true constant when Q_{org} is varied. As can be seen in Table 1, the product $H_{ss}Q_{org}$ is fairly constant (H_{ss} is proportional to the dilution factor) which indicates that the extraction efficiency factor is constant when the organic flow rate, Q_{org}, is varied. This result is to be expected because the analyte transfer process up to the membrane on the aqueous side as well as the analyte transfer across the membrane should not be influenced by variation of the recipient flow rate.

The expression for the dilution factor above does not account for variation of the reagent flow rate, Q_R. It is, however, reasonable to assume that the extraction efficiency factor, f_{eff}, will vary when the total flow rate of aqueous phase is varied even if this is achieved without varying the flow rate of the reagent, Q_R. Table 2 confirms this view. The variation in flow rate of the joined aqueous stream leads to different conditions for the analyte compounds to reach the membrane area.

TABLE 1

The steady-state value, H_{ss}, obtained at different flow rates of organic phase, Q_{org}. Q_R and Q_C were kept constant, at 1.21 and 0.43 ml min^{-1}, respectively; C was 0.5 mM caffeine, and R water

Q_{org} (ml min^{-1})	1.21	0.99	0.64	0.54
H_{ss}[a]	0.190	0.236	0.368	0.448
$Q_{org} \times H_{ss}$	0.23	0.23	0.24	0.24

[a]Given as absorbance.

TABLE 2

The steady-state value, H_{ss}, obtained at different flow rates of reagent, Q_R. Flow rates Q_C and Q_{org} were kept constant at 0.43 and 0.99 ml min^{-1}, respectively; C was 0.5 mM caffeine, and R water

Q_R (ml min^{-1})	1.21	0.99	0.64	0.54	0.43
H_{ss}[a]	0.236	0.270	0.319	0.338	0.348

[a]Given as absorbance.

Injection volumes and peak shapes

The set of peaks depicted in the centre section of Fig. 4 was obtained by injecting different volumes of a standard solution of sodium dodecyl sulphate. As expected, the peaks become smaller when smaller volumes are injected. For large volumes, a steady-state level is reached and a further increase of the injection volume only results in an increased cycle time. All peak heights can be related to this steady-state level, H_{ss}, via the quantity D', defined as $D' = H_{ss}/H_{max}$, where H_{max} is the peak height; D' is thus analogous to the dispersion coefficient, D, defined for single-phase systems [6]. H_{ss} values were recorded for the three test substances by replacing the carrier by the respective standard solution. The D' values obtained are plotted in Fig. 4 as a function of injected volume. All flow rates were kept constant.

As can be seen, there is a significant difference in the D' values for the three compounds which can be expected because of differences in diffusion coefficients and in the kinetics of the phase transfer process. Table 3 shows the variation of H_{ss} and H_{max} for an injected volume of 40 μl as a function of the total flow rate. The proportions between the C, R and O flows were kept constant. Corresponding D' values were calculated; D' seems to be unaffected by the variation of the total flow rate, while both H_{ss} and H_{max}, of course, vary in such a way that larger values are obtained at lower flow rates.

Combinations of solvents

A fundamental question was whether the unsegmented system would be able to cope with aqueous and organic phases which had been modified by addition of a third phase miscible with both phases, e.g., methanol, which is miscible with both water and chloroform. Batch extractions or continuous flow extractions based on segmented streams involving a chloroform/methanol organic phase and water would end up with complete transfer of methanol from the organic phase to the aqueous phase, i.e., the organic/aqueous phase ratio would change continuously during the course of the extraction. With the present system, however, the methanol transfer is minimized. Table 4 shows the different combinations of chloroform, water and methanol

TABLE 3

The steady-state value, H_{ss}, and peak height value, H_{max}, at different total flow rates. The ratio of the organic/aqueous flow rates was kept at 0.4; the injected volume was 40 μl

Q_{tot} (ml min^{-1})	0.1 mM caffeine			0.125 mM SDS			0.1 mM SDOSS		
	H_{ss} (mm)	H_{max} (mm)	D'	H_{ss} (mm)	H_{max} (mm)	D'	H_{ss} (mm)	H_{max} (mm)	D'
2.76	18	12	1.5	92	15	6.1	80	11.5	7.0
2.22	20	13	1.5	107	17	6.3	84	12.3	6.8
1.75	25	15	1.7	135	21	6.4	121.5	15.2	8.0
1.36	30	19.5	1.5	158	26	6.1	131	18	7.3

TABLE 4

The effect of different combinations of water/methanol and methanol/chloroform on the absorbance values obtained by injecting 1 mM SDS into the extraction system. Flow rates: (C) 0.43, (R) 1.21, (Org) 0.94 ml min^{-1}. 40 μl was injected

Organic phase	Aqueous phase	Absorbance	Batch
$CHCl_3$	H_2O	0.310	possible
$CHCl_3$	20% CH_3OH	0.479	possible
$CHCl_3$	40% CH_3OH	0.471	possible
1:1 $CHCl_3/CH_3OH$	H_2O	0.538	not possible
1:1 $CHCl_3/CH_3OH$	40% CH_3OH	0.365	not possible

tested and the corresponding results obtained for extraction of a 1 mM sodium dodecyl sulphate test solution. The improved extraction yield obtained at 20 and 40% methanol in the reagent stream confirms the view that the extraction rate is improved when methanol is present in the aqueous phase. When the organic phase consists of a chloroform/methanol mixture while the aqueous phase contains no methanol, the extraction yields are large. However, the peaks were skewed with large tails and the baseline was not completely stable. In a batch procedure, such an increase of the analyte concentration in the chloroform phase would be explained by the reduced volume of the organic phase, caused by transfer of methanol to the water phase, thereby concentrating the analyte. In this case, however, no significant methanol transfer was detected in either of the different solvent combinations shown in Table 4.

The chloroform/methanol/water system was used here only as a test system for the unsegmented extraction principle. This principle seems to be practical and important in applications where short contact times between the two phases are required or when the change in phase volume ratio that occurs in batch extraction, is unacceptable.

Practical applications

Several anionic surfactants were determined by means of the system outlined in Fig. 1; the injected volume was 40 μl. Table 5 shows a comparison of different surfactants extracted batchwise and by the unsegmented system. The extraction efficiency was calculated for each substance and normalized by using sodium dodecyl sulphate as a standard. All these surfactants contained one sulphonic group except for sodium dioctyl sulphosuccinate (SDOSS) which contains two groups. This may explain the significantly lower extraction efficiency for this substance. To reduce this difference, a larger injection volume can be used (see Fig. 4). The working concentration range was 20—2000 μM. The repeatability was typically 2% (r.s.d.).

TABLE 5

Comparison of batch and flow-injection extractions of different commercial surfactants. Samples 1—9 are commercial SDS-related surfactants

Sample	Normalized ratio of extraction efficiency f.i.a./batch	Molecular weight	Sample	Normalized ratio of extraction efficiency f.i.a./batch	Molecular weight
SDS	1.00	288	6	0.92	260
1	1.00	320	7	0.97	232
2	0.97	328	8	0.94	348
3	0.92	428	9	0.99	316
4	0.96	302	SDOSS	0.86	444
5	0.96	273			

Conclusions

The unsegmented flow-injection extraction system allows coarse liquid-liquid extractions to be achieved with small volumes (30—200 μl) and a consumption of organic phase of typically 1 ml min^{-1}. The extraction cell, in construction similar to a dialysis cell, replaces the segmentor, the extraction coil and the separator usually needed in flow-injection extraction systems. Because there is no segmentation, the contact area between the aqueous and the organic phases is reduced to a "stagnant" zone in the extraction cell. Extractions involving miscible phases can be achieved without significant change in the proportions of the solvents in the phases.

REFERENCES

1 B. Karlberg and S. Thelander, Anal. Chim. Acta, 98 (1978) 1.
2 K. Bäckström, L. G. Danielsson and L. Nord, Anal. Chim. Acta, 169 (1985) 43.
3 L. Nord and B. Karlberg, Anal. Chim. Acta, 118 (1980) 285.
4 L. Nord and B. Karlberg, Anal. Chim. Acta, 164 (1984) 233.
5 J. Kawase, A. Nakae and M. Yamanaka, Anal. Chem., 51 (1979) 1640.
6 E. H. Hansen, J. Růžička, F. J. Krug and E. A. G. Zagatto, Anal. Chim. Acta, 148 (1983) 111.

Analytica Chimica Acta, 179 (1986) 325—340
Elsevier Science Publishers B.V., Amsterdam — Printed in The Netherlands

COMBINATION OF FLOW-INJECTION TECHNIQUES WITH ATOMIC SPECTROMETRY IN AGRICULTURAL AND ENVIRONMENTAL ANALYSIS

ZHAOLUN FANG,* SHUKUN XU, XIU WANG and SUCHUN ZHANG
Institute of Forestry and Soil Science, Academia Sinica, P.O. Box 417, Shenyang (China)
(Received 31st July 1985)

SUMMARY

Combinations of flow-injection techniques with flame atomic absorption spectrometry (a.a.s.) and inductively-coupled plasma/atomic emission spectrometry (i.c.p./a.e.s.) are reviewed in the general context of agricultural and environmental analysis. The flow-injection systems are valuable for sample introduction; appropriate dispersion control allows the analysis of solutions containing as much as 40% (w/v) urea or phosphate in fertilizers. A study on the determination of cadmium in soil extracts by on-line ion-exchange preconcentration and flame a.a.s. detection is described. The interpolative standard-addition method with i.c.p./a.e.s. detection is outlined. Improvements in the determinations of selenium in environmental samples by hydride-generation a.a.s. and of mercury by cold-vapour a.a.s. are reported.

During the last ten years, flow injection analysis (f.i.a.) has developed rapidly as a new technique of solution handling. Although most of the developments have involved spectrophotometric detection, the technique should also have much to contribute to such systems as flame atomic absorption spectrometry (a.a.s.) and inductively-coupled plasma/atomic emission spectrometry (i.c.p./a.e.s.). However, earlier developments in the combination of f.i.a. with atomic spectrometry were limited mostly to applications of flow injection as an efficient technique for sample introduction. More recent advances have shown that the combination can provide broader advantages, extending significantly the capabilities of well-established techniques in atomic spectrometry and providing methods with higher efficiencies, better sensitivities, fewer interferences and smaller sample and/or reagent consumption. These merits have been exploited in this Institute to provide better results in the analysis of agricultural and environmental samples. Examples are the combination of f.i.a. with flame a.a.s. for efficient sample introduction, involving merging zones [1] and the direct aspiration of samples with high solute concentrations, applications of flow-injection systems with on-line ion-exchange preconcentration and flame a.a.s. detection [2], the determination of selenium, arsenic and other elements by hydride-generation a.a.s. [3], standard additions for an i.c.p./a.e.s. system, and the determination of mercury by cold-vapour a.a.s. [5].

0003-2670/86/$03.50

The purpose of the present paper is to outline these applications and to provide a general overview of the combination of f.i.a. with atomic spectrometry to illustrate its potential in agricultural and environmental analysis and related fields.

SAMPLE INTRODUCTION AND DILUTION SYSTEMS FOR FLAME AND PLASMA SPECTROMETRY

The flow-injection manifolds for sample introduction into flame a.a.s. or i.c.p. systems reported in the literature are usually very simple, consisting of an injection port or valve and a single, often very short line; the samples injected into the carrier stream are propelled either by a peristaltic pump or by the suction of the nebulizer. Simple as they are, these systems provide several important advantages over the conventional mode of sampling; these have been discussed by Tyson [6] and Greenfield [7]. In this laboratory, these simple sample introduction systems have been used with both flame a.a.s. and i.c.p./a.e.s. detectors for the analysis of soil extracts and plant digests. The merits of the simple combination can be summarized as follows: (a) high sampling frequencies of over 500 h^{-1} can be attained with little or no loss in precision [1, 8]; (b) samples with high solute contents (up to 40% w/v) can be tolerated without blocking of the nebulizer or burner (see below); (c) introduction of the sample by a peristaltic pump located before the injection valve decreases matrix effects caused by differences in viscosity; (d) there is no intermediate introduction of air into the nebulizer between samples, a feature which is especially important for improving the stability of plasmas [9]; (e) the optimum concentration range for the analyte can often be attained by controlling the dispersion of the sample zone; (f) in flame a.a.s., water-immiscible organic solvents can be used as carrier to limit sample dispersion and enhance sensitivity through solvation effects [10]; (g) the small sample consumption in the range 30—300 μl, is an important feature in clinical analysis but is of minor importance in agricultural and environmental analyses where the samples are rarely limited.

Several groups using sample introduction by flow-injection techniques with flame a.a.s. or i.c.p. detection have reported inferior relative detection limits compared to conventional sample introduction although the absolute detection limits were better [1, 11, 12]. However, Brown and Růžička [8] reported recently that the precision of the flow-injection sampling process could be improved by making the carrier flow rate higher than the natural aspiration rate of the nebulizer. With copper as a model element, a precision (r.s.d.) of 0.44% was obtained with the flow-injection system, compared to 0.78—0.89% for continuous aspiration. As the response of the peak in f.i.a. can reach 80—90% of the steady-state signal with 150-μl injections, the sensitivity would be very similar and a lower detection limit could be obtained with f.i.a. These observations were made without using electronic integration; conclusions would be different if integration were used for both

approaches, as the integration period for continuous aspiration could be made much longer. Yet careful control of the carrier flow rate and the natural aspiration rate of the nebulizer, makes it possible to achieve comparable detection limits. An important advantage of flow-injection sample introduction is that much higher salt concentrations can be tolerated [13] so that actual detection limits can be lowered by introducing more concentrated sample solutions. Zhou et al. [14] have reported an increase in sensitivity by introducing sample solutions containing 8% iron instead of the 1% needed with conventional aspiration.

This feature has been utilized here in the determination of trace elements in soluble fertilizers. Sample solutions containing as much as 40% (w/v) urea or potassium hydrogenphosphate were analyzed for copper with a flow-injection/flame a.a.s. system (as reported earlier [1] except that a peristaltic pump was used). As the tolerable concentration was limited to 10% with conventional sample aspiration, a three-fold gain in sensitivity was obtained for the flow-injection mode using 150-μl samples. The 40% solutions could be injected sequentially for extended periods without any sign of blocking the nebulizer or burner, and without affecting the precision, whereas continuous aspiration extinguished the flame in about 5 min (Fig. 1).

Dilution systems

With a single-line flow-injection system, the sensitivity of any determination can be suppressed by decreasing the sample volume without affecting the sampling frequency, but there is a practical limit to this approach. More effective flow-injection systems for dilution have been proposed to simplify volumetric manipulation when samples with off-range concentrations are involved [13, 15].

In the system of Mindel and Karlberg [13], part of the flow stream containing the dispersed sample zone is withdrawn from the conduit and

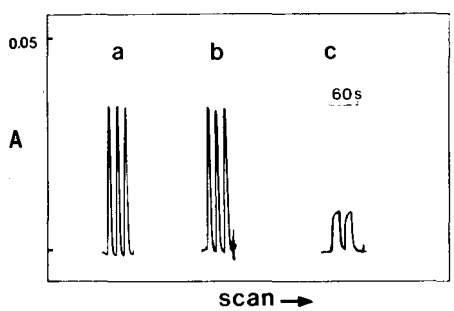

Fig. 1. Determination of copper in aqueous 40% (w/v) urea solutions in a single-line flow-injection system with an aqueous carrier at 5 ml min^{-1} (sample volume 80 μl; copper content in urea 1.25 $\mu g\ g^{-1}$). (a) Recordings obtained at the start of a series of injections; (b) recordings after 100 successive injections at 15-s intervals; (c) recordings by conventional aspiration of a 10% (w/v) solution of the same sample (highest concentration tolerable).

replaced by an equal amount of carrier diluent downstream at the same flow rate. In the system proposed by Reis et al. [15], more effective dilution was achieved by a zone-sampling process; the dispersed sample zone flows into a second sample loop on the injection valve instead of flowing directly into the nebulizer. By precise timing, a predetermined "slice" of the dispersed sample zone is sampled for a second time on a turn of the valve and dispersed again in a second carrier before entering the nebulizer. In the determination of potassium in plants by flame photometry, Reis et al. were able to achieve 100-fold dilutions of the plant digests at a sampling frequency of 120 h^{-1}. The flow-injection dilution system will be very useful in cases where multi-element determinations requiring different degrees of dilution are needed in a single plant digest or soil extract.

MERGING-ZONES SYSTEMS AND CALIBRATION TECHNIQUES

The merging-zones principle is extremely useful in saving reagents; instead of maintaining a constant reagent flow, the addition of reagent is controlled to merge with the sample zone only. A merging-zones system was proposed by Zagatto et al. [16] for the determination of calcium and magnesium in plant materials by flame a.a.s., where the addition of lanthanum as a releasing agent was necessary. The consumption of lanthanum was decreased dramatically to only 1% of the amount needed in conventional operation. This was verified in the authors' laboratory with a similar system [1] for the determination of calcium and magnesium in soil extracts and plant digests.

The merging-zones principle was also used for the addition of internal standards by Jacintho et al. [17] for the i.c.p./a.e.s. determination of calcium and magnesium in dolomitic limestones. Zagatto et al. [18] applied the principle to develop a multi-element i.c.p./a.e.s. procedure based on the generalized standard addition method. The manipulations for standard additions involved in these applications were significantly simplified.

Calibration techniques based on f.i.a. in connection with flame a.a.s. detection have been studied extensively by Tyson et al. [19—21]. Apart from the standard addition mode of calibration achieved by merging zones as mentioned above, various other calibration modes were proposed. The exponential flask calibration method is based on the use of the well-defined exponential concentration/time profile generated by the passage of a step concentration change through a mixing chamber. When the response of the detector is recorded as a function of time, the resulting curve can be used as a calibration graph and only a single standard is needed for the calibration [19]. In the interpolative standard-addition method proposed by Tyson [19, 20], the sample is used as the carrier stream and the standards are injected into this stream; standards which have a higher concentration than the sample produce positive peaks whilst those which are of lower concentration produce negative peaks. If the interference effects are within certain limits, identical concentrations of sample and standard produce no peaks.

When the concentrations of the standards (C_s) are plotted against the peak height (ΔA), the intercept on the C_s axis gives the unknown concentration, C_x. Obviously, the dispersion of the standards has to be controlled carefully and steps must be taken to ensure that interference effects are the same for samples and standards. In an application of the method to the determination of chromium in steels, excellent results were obtained [19]. Interference control is more difficult in agricultural and environmental samples where the matrices are more varied, yet the method would be well suited to a system with i.c.p. detection where interferences are less and the interpolative mode of calibration would be advantageous in compensating for source or wavelength drift. The wide dynamic range of i.c.p./a.e.s. helps in simplifying the procedure further. Assuming a linear emission intensity/concentration relationship, Israel and Barnes [22] deduced an equation for the standard addition method: $C_x^0 = I^m C_s^0/(I^m + I^p)$, where C_x^0 and C_s^0 are the concentrations of the sample and standard solution added, and I^m and I^p are the peak heights of the blank and standard relative to the sample baseline response. For optimum results, large injection volumes for the standard, corresponding to a dispersion of $D = 4$ for the sample, and a C_s^0/C_x^0 ratio between 2 and 2.5 were recommended. The method is simple in that only two injections are necessary for a determination, yet the method was not expected to compensate spectral and chemical interferences. The method was tested in this laboratory with a few standard reference materials; the above criteria for dispersion and standard concentration were adopted. The results were satisfactory (Table 1).

An even simpler standard addition method for atomic emission spectrometry was recently proposed by Fang et al. [4]. The method is based on the gradient-scanning technique and will be discussed below. In order to extend the calibration range of flame a.a.s. determinations to higher concentration levels, Tyson [21] introduced a peak-width calibration method. The relationship developed was verified up to a concentration of 1000 mg l^{-1} for magnesium.

TABLE 1

Results obtained by the interpolative standard addition method with i.c.p. detection

Standard sample	Certified value (μg g^{-1})		Found (μg g^{-1})[a]	
	Ba	Cr	Ba	Cr
River sediment	375 ± 22	90 ± 8	369 ± 13	86 ± 1
Coal fly ash[b]	—	196 ± 6	—	198 ± 6

[a]Mean and standard deviations for 4–6 separate determinations. [b]NBS SRM 1633a; no certified value for barium.

ON-LINE PRECONCENTRATION SYSTEMS WITH FLAME OR I.C.P. SPECTROMETRIC DETECTION

Liquid-liquid extraction and ion-exchange are the most often used techniques for the preconcentration or separation of trace constituents prior to a.a.s. or i.c.p. detection. The conventional operations are tedious and incompatible with the efficient determination by flame a.a.s. or i.c.p./a.e.s. Recently, large advances have been made in developing flow-injection systems for on-line extraction or ion-exchange preconcentration with spectrometric detection.

The flow-injection extraction system with flame a.a.s. detection proposed by Nord and Karlberg [23] was capable of achieving 15—20-fold enhancement in sensitivity at a sampling frequency of 40 h^{-1} in the determination of copper, nickel, lead and zinc; 4-methyl-2-pentanone (MIBK) was used with ammonium pyrrolidinedithiocarbamate (APDC) for the extraction. In order to attain high concentration rates by using low solvent/sample ratios while maintaining the optimal feed rate to the spectrometer, the extraction and feed systems were controlled separately with two injectors. The first injector was used to introduce the sample which was then merged with APDC and MIBK for the extraction. The organic extract was not fed directly to the nebulizer, but was first stored in the loop of a second injector and then introduced into an aqueous carrier which was pumped at optimum feed rate into the nebulizer. This technique should be useful in the analysis of agricultural and environmental samples, but applications have not been reported thus far. Recently, the method was extended to provide a sample work-up procedure compatible with graphite-furnace a.a.s. by extraction of heavy metals as dithiocarbamates into Freon-113 followed by back-extraction [24].

The first flow-injection system with on-line ion-exchange preconcentration and flame a.a.s. detection was introduced by Olsen et al. [25]. A small ion-exchange column (2 mm i.d., 50 mm long) containing Chelex-100 exchanger was used to preconcentrate copper, zinc, lead and cadmium from sea water on-line; the metals were later eluted directly into the nebulizer. The system was much more efficient than the manual method with a much lower sample consumption. This pioneering work was followed by a series of other papers dealing with important improvements in the design of the system. Most of the developments have been summarized in the paper by Fang et al. [2]. The concentration efficiencies for copper, zinc, lead and cadmium in a sea water matrix have been improved to 50—100-fold min^{-1} (Fig. 2), achieving a sensitivity comparable to that of graphite-furnace a.a.s. yet with a sample throughput 2—3-fold faster and with the additional advantage of separating most of the matrix elements. Although the sample volume (about 10 ml) is much larger than that required for a normal graphite-furnace a.a.s. determination, it is only 1—2% of the volume needed for a conventional ion-exchange preconcentration and is not a limiting

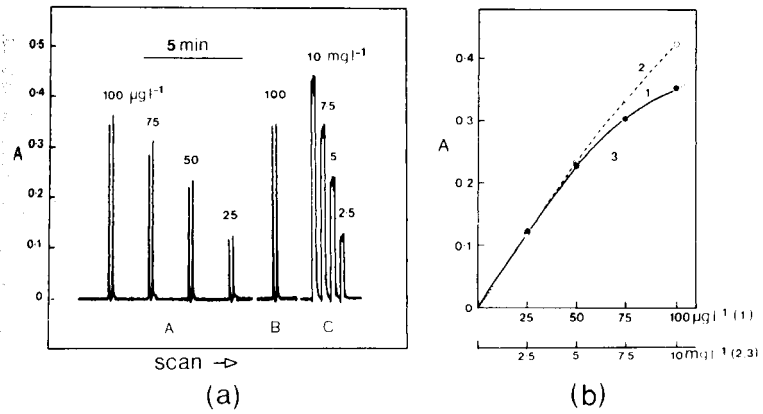

Fig. 2. (a) Recordings for standard lead solutions: A, with the on-line ion-exchange preconcentration system described earlier [2]; B, a 100 $\mu g\ l^{-1}$ lead solution in a matrix simulating sea water, under the same conditions as in A but with background correction; C, recordings by conventional flame a.a.s. for standard lead solutions with 100-fold higher concentrations than in A. (b) Calibration curves: (1, 2) based on the results from runs A and C, respectively; (3) constructed from data in the a.a.s. Varian-Techtron instrument handbook.

factor except in applications such as serum analysis. The different interferences encountered in the ion-exchange process when real samples are analyzed offer much more serious problems.

The Chelex-100 resin was used successfully in these preconcentration systems by Olsen et al. [25] and Fang et al. [2] for the determination of heavy metals in sea water. When other chelating ion-exchangers were tested, low recoveries were obtained for some of the metals studied, with cadmium being the worst, although one of the ion-exchangers (the 8-quinolinol chelating exchanger) was used successfully by Malamas et al. [26] in their application of a similar system to the determination of heavy metals in tap water. The differences in behaviour can be attributed to the different stabilities of the complexes formed on the exchangers and to competition in complex formation between the analytes and the matrix components.

As cadmium was shown to be the most liable to suffer from matrix effects because of its relatively low complexing ability with the functional groups of many chelating ion-exchangers, it was studied more closely by our group, as a model element in the determination of heavy metals in soil extracts. All the three ion-exchangers used in a previous study [2] were investigated; some results are listed in Table 2. Experiments were conducted with different column dimensions (3 mm i.d., 60 mm long and 2.8 mm i.d., 45 mm long), different preconcentration periods (45, 75 and 100 s), and with or without ammonium fluoride as a complexing agent to mask iron(III), aluminium and calcium in the extract matrix. Simulated matrices containing calcium, magnesium, iron(III) and aluminium at two concentration levels were tested for the recovery of cadmium under different conditions. These experiments

showed that preconcentration periods of 100 s (which was used in the determination of sea water samples) gave unacceptably low recoveries with only a marginal improvement in sensitivity compared to a 75-s preconcentration even in the presence of the masking agent. It was also observed that if the 0.1 M hydrochloric acid extracts were adjusted to pH 3 and merged with an ammonium acetate buffer (pH 10) before the column, the ion-exchange columns soon became blocked because of formation of hydrated iron(III) and aluminium oxides. As a high pH was preferable for improved sensitivities [25], no attempt was made to lower the pH but an ammonium fluoride complexing agent was added to the buffer; the final concentrations were 0.025 M ammonium acetate and 0.01 M fluoride in the sample when high concentrations of iron or aluminium were expected in the extracts. As the incorporation of fluoride produced better recoveries without affecting the sensitivity, it is wise to include it even when no precipitates are formed. It was found necessary to use a fairly large column (3 mm i.d., 60 mm long) in this study to ensure acceptable recoveries; when the smaller column was used, recoveries were about 10% lower than those in Table 2, suggesting a breakthrough of cadmium caused by competition from interferents in the ion-exchange process. When a shorter preconcentration period was used, the results were better than those in Table 2, but the concentration factor was smaller. The method compared well with the results obtained by a graphite-furnace a.a.s. procedure (Table 3) with a correlation coefficient of

TABLE 2

Recoveries (%) of cadmium (10 $\mu g\ l^{-1}$) from simulated soil extract matrices with different chelating ion-exchangers[a]

Matrix	Buffer/complexing agent[b]	Recovery (%)[c]		
		Chelex-100	8-Quinolinol	Resin 122 [27]
None	A	100 (52)	100 (75)	100 (60)
Ca (10)[d] Mg (10)	A	81 (42)	82 (62)	100 (60)
Al (5) Fe (2.5)	B	106 (55)	95 (71)	98 (58)
Ca (100) Mg (100)	A	—[e]	—[e]	—[e]
Al (50) Fe (25)	B	98 (51)	84 (63)	88 (53)

[a]Column dimensions: 3 mm i.d., 60 mm long, preconcentration period 75 s. [b]Buffer, complexing agent composition in sample solution: A, 0.025 M ammonium acetate pH 9.5; B, 0.025 M ammonium acetate/0.01 M ammonium fluoride pH 9.5. [c]Numbers in parentheses are the corresponding peak heights in mm. [d]Numbers in parentheses refer to mg l^{-1} in the matrix. [e]No results obtainable because of blocking of the column by precipitates formed.

TABLE 3

Comparison of on-line ion-exchange preconcentration with flame a.a.s. detection (method A) and graphite-furnace a.a.s. (method B) for the determination of cadmium in nine soil extracts[a]

Method	Cadmium content in soil ($\mu g\ g^{-1}$)								
A	0.39	0.41	0.20	0.26	0.12	0.35	0.87	0.57	0.84
B[b]	0.45	0.43	0.19	0.29	0.15	0.35	0.99	0.60	0.69

[a]Soil extractant 0.1 M HCl; soil/extractant = 1:5 (w/v). [b]Prior to graphite-furnace a.a.s., extraction with MIBK/iodide/ascorbic acid was used; 10 μl of this extract was injected into the furnace.

.962 and is capable of dealing with 70 samples per hour with a concentration factor of 30—40. The method was recently extended to the analysis of lant tissue digests. Preliminary results on the determination of lead in a IBS standard reference material (orchard leaves SRM 1571) showed fair greement with the certified value (45 ± 3 $\mu g\ g^{-1}$), the concentration found eing 40.5 $\mu g\ g^{-1}$.

Also working with a flow-injection preconcentration system including Chelex-100 column, Jørgensen and Petersen [28] made a detailed study of ne effects of sample dissolution procedures on the a.a.s. determination of eavy metals (cadmium, copper, lead and manganese) in grass, leek and ovine liver. A citrate complexing/buffer solution was added to the samples o prevent interference from calcium and magnesium phosphates at the igh pH required by the ion-exchange process. They found that the presence f sulphate in amounts corresponding to a sulphuric acid wet-ashing procedure caused a loss in sensitivity for all the four elements.

The combination of the on-line ion-exchange preconcentration system vith a multi-element detector such as the i.c.p. atomic emission spectrometer would be expected to produce fruitful results. This was proved by Hartenstein et al. [29] in an application of the preconcentration system lescribed earlier [2] to a multi-channel i.c.p. spectrometer. The detection imits obtained were at least 20 times better when the simultaneous integration mode was used for eight elements determined simultaneously at a ampling rate of 30 h^{-1}. The detection limits compared favourably with hose for a batch preconcentration method [30, 31].

GRADIENT-SCANNING FLOW-INJECTION SYSTEMS WITH FLAME EMISSION DETECTION

The gradient-scanning technique involves rapid scanning of two physical parameters (e.g., wavelength vs. absorbance or intensity) at a certain point

on the concentration gradient of a well-defined sample zone [32]. This technique was applied by Fang et al. [4] to a flow-injection system with flame spectrophotometric detection for the simultaneous determination of sodium, potassium, lithium and calcium in tap water and soil extracts using a fast scanning monochromator. The three-dimensional representation in Fig. 3 shows successive scans of a tap-water sample at 0.3-s intervals. The main advantages of the system are that multielement analysis is possible with a single injection and that optimal concentration ranges for all the analytes can be obtained by running fast scans on different sections of the dispersed sample zone; the possibilities of internal standardization and making standard additions at different levels of several analytes are also important. The flow system for making the standard additions was arranged so that when a sample was injected the carrier upstream was water or a blank solution and the carrier downstream was a standard solution of the analytes with the sample zone sandwiched in between; dispersion was controlled so that the two carriers did not overlap. This arrangement produced on the falling slope of the sample peak an almost infinite number of different sample/standard ratios which could be easily computed from dispersion measurements. The optimum ratio could be chosen for an element by selecting an appropriate time for running the wavelength/intensity scan; computer storage of data would enable appropriate times to be selected to provide optimum ratios for all the elements analyzed. Although the method was successfully applied to the determination of calcium in soil extracts with flame photometric detection it cannot be used to its full potential with a flame emission source exhibiting serious self-absorption effects. In order to extend the method, a computer will be needed to store and process the multi-scan data generated from a single injection. The new standard addition method might find its real value used in conjunction with an i.c.p. emission source equipped with a fast scanning monochromator and adequate computer facilities.

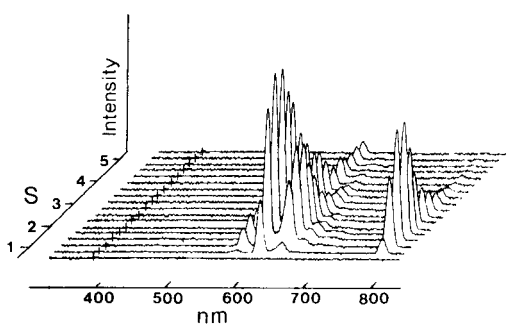

Fig. 3. Three-dimensional gradient-scanning recording of a 40-μl sample of tap water. Time between successive scannings 0.3 s. Wavelengths of peaks, left to right: CaOH 554 nm, Na 589 nm, CaOH 622 nm, K 767 nm.

FLOW-INJECTION SYSTEMS FOR HYDRIDE-GENERATION AND COLD-VAPOUR SPECTROMETRY

Hydride-generation atomic absorption spectrometry

The first flow-injection system for hydride-generation a.a.s. was introduced by Åström [33] who used the system to determine bismuth in 700-μl samples with a detection limit of 0.08 μg l^{-1}; a high sampling frequency of 180 h^{-1} was attained and the interference effects were substantially decreased.

A similar flow-injection system was constructed in this laboratory to determine trace amounts of selenium in soils, coal fly ash and plant tissues [3]. The flow system is shown in Fig. 4 and typical recordings for standard solutions are shown in Fig. 5. The detection limit was 0.06 μg l^{-1} which was somewhat better than that for a manual method used routinely in this laboratory, yet the sample consumption was only 400 μl, compared to 10 ml for the manual procedure. This gives the method a very low absolute detection limit of 2×10^{-11} g of selenium, which is equivalent to the detection limit of the graphite-furnace method, all with selenium hollow-cathode lamps. The sampling frequency was very high at 250—300 h^{-1} and the precision (r.s.d.) was 1.6% (n = 11) at the 4 μg l^{-1} level (Fig. 5b). The results from analyses of NBS standard reference materials of the environmental type show good agreement (Table 4). Results from recovery tests done on

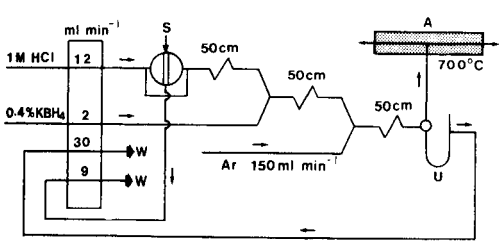

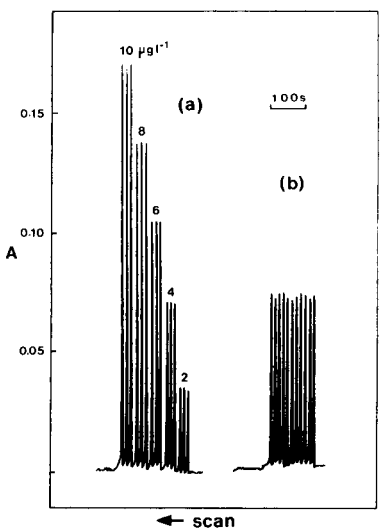

Fig. 4. Manifold for the hydride-generation a.a.s. system: U, gas-liquid separator; S, sample, 400 μl; W, waste; A, T-shaped quartz atomizer with electrical heating, 700° C.

Fig. 5. Recordings for standard selenium solutions obtained with the system in Fig. 4: (a) standard series in the range 2—10 μg l^{-1} selenium; (b) replicate injections of a 4 μg l^{-1} selenium standard.

TABLE 4

Determination of selenium in standard reference materials by the flow-injection hydride-generation method

NBS standard	Selenium content ($\mu g\ g^{-1}$)	
	Certified	Found[a]
Wheat flour (SRM 1567)	1.1 ± 0.2	0.97 ± 0.02
Orchard leaves (SRM 1571)	0.08 ± 0.01	0.073 ± 0.003
Coal fly ash (SRM 1633a)	10.3 ± 0.6	10.2 ± 0.3

[a] Average and standard deviation for 12 determinations from three separate digestions for each sample.

wheat, corn and soil digests spiked with 4 $\mu g\ l^{-1}$ selenium(IV) fall in the range 97—106%. Presently, the system is being used routinely for the analysis of thousands of soil and plant tissue samples. Besides increasing the efficiency of the determination almost four-fold, the decrease in sample volume also saves time in the sample preparation step. Reagent consumption has decreased to 10% of the amount consumed in the manual method and 5% of that consumed in an air-segmented continuous flow system [34]. The closed flow-injection system proved very advantageous for restricting the escape of acid fumes into the environment, which was very beneficial to the a.a.s. instrument. The flow-injection system was noteworthy for its greater tolerance of the interferences often reported in the literature on the determination of selenium by hydride-generation a.a.s. In Table 5, the tolerable concentrations of interferents for the flow-injection method are listed together with those for an air-segmented continuous flow hydride-generation a.a.s. method. Generally, the tolerable concentrations are 10—100-fold higher, except for antimony(II) which was the same. As has been suggested by Åström [33], this improvement is probably due to the fact that the residence time of the sample in the flow-injection system is very short and well controlled. This aspect is particularly favourable for the formation of hydrogen selenide which is fast, while the slower interfering reactions are suppressed.

With some minor modifications in the parameters, the system has been extended to the determination of arsenic and to mercury using the setup as a cold-vapour a.a.s. system. Preliminary results showed a detection limit for arsenic which was one order of magnitude higher than selenium. Mercury determinations gave better detection limits which were close to, or better than, those of conventional cold-vapour a.a.s. methods.

Cold-vapour a.a.s. determination of mercury

A flow-injection system incorporating a special vapour-diffusion flow cell, which acted both as a membrane separator and as an absorption cell for the

TABLE 5

Tolerable concentrations of interferences for determinations of selenium(IV) (10 $\mu g\ l^{-1}$) by hydride-generation a.a.s.

Method[a]	Tolerable concentration (mg l^{-1})[b]								
	Sb(III)	As(III)	Bi(III)	Sn^{2+}	Pb^{2+}	Hg^{2+}	Cu^{2+}	Co^{2+}	Ni^{2+}
A	0.1	1	1[c]	5	10	10	10	10	10
B	0.1	0.1	0.05	0.05	1	0.1	0.5	0.5	0.5

[a]Method A is the flow-injection system; method B is an air-segmented system [34]. [b]Highest concentration which produces a deviation of less than 10%. [c]Temperature of atomizer 800° C.

determination of mercury by a.a.s., was proposed by de Andrade et al. [35]. The device was based on the permeability of commercial teflon tape to mercury vapour which was formed in the carrier stream on one side of the teflon membrane and diffused directly into the absorption cell positioned in the light path. The detection limit was 1.4 $\mu g\ l^{-1}$ mercury with a sampling rate of 110 h^{-1}. The system was modified in this laboratory to improve the detection limit and sampling frequency and to increase the lifetime of the teflon membrane [5]. The modifications include: (a) the use of a thinner teflon tape (0.075 mm thick) to increase the diffusion efficiency of the mercury vapour; (b) a nylon gauze to reinforce the teflon membrane, thus increasing its lifetime by decreasing the pulsations caused by pressure differences on the two sides of the membrane; (c) a longer and narrower diffusion channel (1.5 × 110 mm) than the original design (3 × 50 mm) to limit sample dispersion in the channel; and (d) insertion of a 1-mm thick plexiglas plate between the membrane and the adsorption cell (the vapour could diffuse through the 1.5-mm slit on the plate, and this extra precaution prevented partial blocking of the absorption light path through fluctuations of the membrane, thus decreasing the baseline noise). The manifold and detailed structure of the flow cell are shown in Figs. 6 and 7.

With this modified system, the detection limit was 0.06 $\mu g\ l^{-1}$ mercury (3σ) and a characteristic concentration of 0.13 $\mu g\ l^{-1}$ with 400-μl samples at a sampling frequency of 200 h^{-1}. Precision (r.s.d.) was 1.0% at the 4 $\mu g\ l^{-1}$ level (n = 22) (Fig. 8). Although a substantial improvement was made in the performance of the earlier system [35], comparison of the method with a method based on the flow-injection system described above for hydride generation used as a cold-vapour system showed that the detection limit and sampling frequency were not superior. It seems that whilst the membrane phase-separator approach gains sensitivity by eliminating the gas-liquid separator which has a relatively large dead volume, it also loses sensitivity through incomplete transport of mercury through the membrane. At the present stage, there is really very little to choose between the two systems,

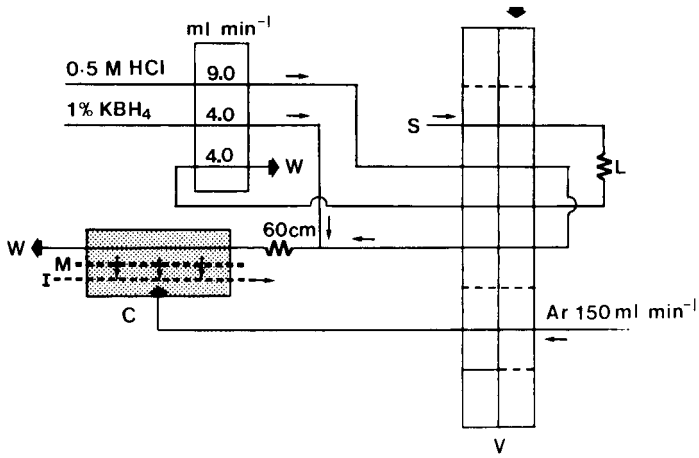

Fig. 6. Manifold for the flow-injection cold-vapour a.a.s. system with a membrane phase separator. C, phase separator and absorption cell; L, sample loop, 400 μl; V, 8-channel multi-functional valve [2] (dashed lines are blocked channels); M, teflon membrane with nylon gauze backing; S, sample; I, incident light from hollow-cathode lamp; W, waste.

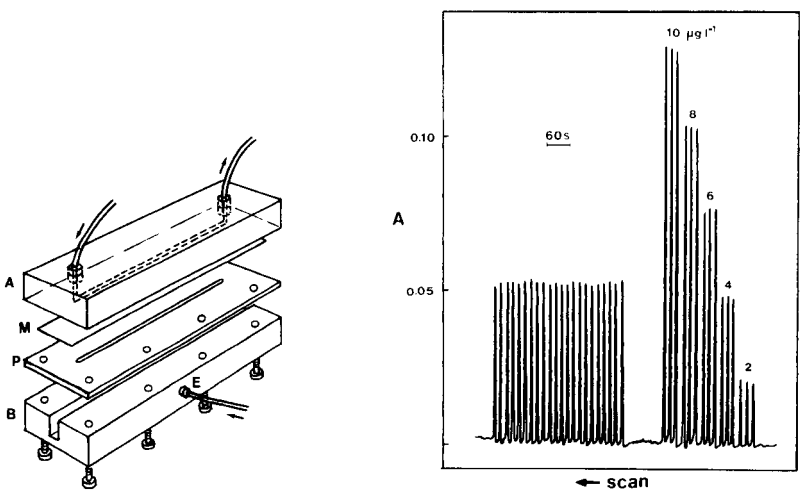

Fig. 7. Detailed structure of the combined phase separator/absorption flow cell. A, Plexiglas block with 1.5 × 110 mm channel at the bottom; B, plexiglas block with a 3 × 6 × 170 mm groove acting as absorption flow cell; M, teflon membrane backed with nylon gauze on the under side; P, 1-mm thick plexiglas plate with 1.5 × 110 mm slit in the centre; E, entrance for argon.

Fig. 8. Recordings for mercury standards obtained with the system in Fig. 6: (a) standard series in the range 2—10 μg l^{-1} mercury; (b) replicate injections of a 4 μg l^{-1} mercury standard.

except that the problem of membrane lifetime does not arise for the system shown in Fig. 4.

CONCLUSIONS

The combination of f.i.a. with atomic spectrometry has resulted in considerable extension of the capabilities of the conventional techniques in relation to sample throughput, sensitivity, precision, and saving of sample, reagent and time, which can be very advantageous in the routine analysis of agricultural and environmental samples. The development of new calibration methods via f.i.a. may almost completely obviate the need for volumetric manipulations and result in self-calibrating systems which could provide more accurate results in routine work.

Although the on-line ion-exchange preconcentration systems have already been used successfully in the determination of traces of heavy metals in some environmental samples, the potentials of the technique are far from being fully explored. The further combination of this technique to flow-injection systems for hydride generation and cold-vapour a.a.s. determinations could result in methods with ultra-high sensitivities. The method could also be used to advantage in the chemical speciation of trace constituents in environmental samples. However, more detailed studies on the interferences and kinetic aspects of the on-line ion-exchange processes on different ion-exchange materials will be necessary before it can be used routinely for samples with really complex matrices. One of the main drawbacks of the technique (i.e., the relatively large sample consumption) might be overcome by scaling down the systems through micro-conduit techniques [36]. Some attempts have already been made to produce nebulizers suitable for direct aspiration of samples at a low flow rate into a plasma which could be compatible with flow-injection systems [37].

Further development of the flow-injection systems for hydride-generation and cold-vapour a.a.s. determination will result in the production of much more efficient, compact yet cheaper equipment for routine use in the analysis of environmental samples.

The authors express their thanks to Lei Guo and Shihua Fan for their assistance in the i.c.p. spectrometric determinations and to Dr. Bo Karlberg of Tecator (Sweden) for supplying a bibliography.

REFERENCES

1 S. Zhang, L. Sun, H. Jiang and Z. Fang, Spectrosc. Spec. Anal. (in Chinese), 4(3) (1984) 42.
2 Z. Fang, J. Růžička and E. H. Hansen, Anal. Chim. Acta, 164 (1984) 23.
3 X. Wang and Z. Fang, Fenxi Huaxue, Kexue Tongbao, 30 (1985) 1598.
4 Z. Fang, J. M. Harris, J. Růžička and E. H. Hansen, Anal. Chem., 57 (1985) 1457.
5 S. Zhang and Z. Fang, Fenxi Huaxue, in press.

6 J. F. Tyson, Anal Proc. (London), 20 (1983) 488.
7 S. Greenfield, Spectrochim. Acta, Part B: 38 (1983) 93.
8 M. W. Brown and J. Růžička, Analyst (London), 109 (1984) 1091.
9 S. Greenfield, Ind. Res. Dev., 23 (1981) 140.
10 A. S. Attiyat and G. D. Christian, Anal Chem., 56 (1984) 439.
11 T. Ito, H. Kawaguchi and A. Mizuike, Bunseki Kagaku, 23 (1980) 332.
12 W. R. Wolf and K. K. Stewart, Anal. Chem., 51 (1979) 1201.
13 B. D. Mindel and B. Karlberg, Lab. Pract., 30 (1981) 719.
14 N. Zhou, W. Frech and E. Lundberg, Anal. Chim. Acta, 153 (1983) 23.
15 B. F. Reis, A. O. Jacintho, J. Mortatti, F. J. Krug, E. A. G. Zagatto, H. Bergamin F°. and L. C. R. Pessenda, Anal. Chim. Acta, 123 (1981) 221.
16 E. A. G. Zagatto, F. J. Krug, H. Bergamin F°, S. S. Jørgensen and B. F. Reis, Anal. Chim. Acta, 104 (1979) 279.
17 A. O. Jacintho, E. A. G. Zagatto, H. Bergamin F°, F. J. Krug, B. F. Reis, R. E. Bruns and B. R. Kowalski, Anal. Chim. Acta, 130 (1981) 243.
18 E. A. G. Zagatto, A. O. Jacintho, F. J. Krug, B. F. Reis, R. E. Bruns and M. C. U. Araújo, Anal. Chim. Acta, 145 (1983) 169.
19 J. F. Tyson, J. M. H. Appleton and A. B. Idris, Anal. Chim. Acta, 145 (1983) 159.
20 J. F. Tyson and A. B. Idris, Analyst (London), 109 (1984) 23.
21 J. F. Tyson, Analyst (London), 109 (1984) 319.
22 Y. Israel and R. M. Barnes, Anal. Chem., 56 (1984) 188.
23 L. Nord and B. Karlberg, Anal. Chim. Acta, 145 (1983) 151.
24 K. Backstrom, L.-G. Danielsson and L. Nord, Analyst (London), 109 (1984) 323.
25 S. Olsen, L. C. R. Pessenda, J. Růžička and E. H. Hansen, Analyst (London), 108 (1983) 905.
26 F. Malamas, M. Bengtsson and G. Johansson, Anal. Chim. Acta, 160 (1984) 1.
27 Z. Fang, S. Xu and S. Zhang, Anal. Chim. Acta, 164 (1984) 41.
28 S. S. Jørgensen and K. Petersen, Paper presented at 9th Nordic Atomic Spectroscopy and Trace Element Conference, Reykjavik, Iceland (1983); and personal communication.
29 S. D. Hartenstein, J. Růžička and G. D. Christian, Anal. Chem., 57 (1985) 21.
30 R. M. Barnes and J. S. Gena, Anal. Chem., 53 (1981) 299.
31 H. S. Mahanti and R. M. Barnes, Anal. Chim. Acta, 151 (1983) 409.
32 J. Růžička and E. H. Hansen, Anal. Chim. Acta, 145 (1983) 1.
33 O. Åström, Anal. Chem., 54 (1982) 190.
34 K. S. Subramanian, Z. Anal. Chem., 305 (1981) 382.
35 J. C. de Andrade, C. Pasquini, W. Baccan and J. C. Van Loon, Spectrochim. Acta, Part B: 38 (1983) 1329.
36 J. Růžička and E. H. Hansen, Anal. Chim. Acta, 161 (1984) 1.
37 K. E. Lawrence, G. W. Rice and V. A. Fassel, Anal. Chem., 56 (1984) 289.

Analytica Chimica Acta, 179 (1986) 341—349
Elsevier Science Publishers B.V., Amsterdam — Printed in The Netherlands

SEQUENTIAL ATOMIC ABSORPTION SPECTROMETRIC DETERMINATION OF NITRATE AND NITRITE IN MEATS BY LIQUID-LIQUID EXTRACTION IN A FLOW-INJECTION SYSTEM

M. SILVA, M. GALLEGO and M. VALCÁRCEL*

Department of Analytical Chemistry, Faculty of Sciences, University of Córdoba, Córdoba 14005 (Spain)

(Received 12th June 1985)

SUMMARY

Sequential determinations of nitrate and nitrite based on continuous liquid-liquid extraction, and suitable for their routine determinations in meats, are reported. Nitrate reacts with bis(2,9-dimethyl-1,10-phenanthrolinato)copper(I) to form an ion-pair which is extracted into 4-methyl-2-pentanone in a flow-injection manifold. In one aliquot of sample, nitrite is oxidized by cerium(IV), so that total nitrate is determined. In another, nitrite is converted to nitrogen with sulfamic acid, so that only the original nitrate is determined. By measuring the atomic absorption signal of copper in the organic phase, mixtures of these anions can be determined at $\mu g\ ml^{-1}$ levels for nitrate/nitrite ratios from 10:1 to 1:10, with a sampling frequency of ca. 20 h^{-1}.

Numerous methods for the determination of nitrate and nitrite in mixtures are based on reduction of nitrate to nitrite which is subsequently determined colorimetrically [1—4]. Many of these methods have been adapted to automatic air-segmented continuous flow systems. Currently, the problems associated with the use of an air-segmented stream can be circumvented by using flow injection analysis (f.i.a.) [5]. Several authors [6—9] have used this methodology to develop simultaneous spectrophotometric determinations for nitrate and nitrite based on prior reduction of nitrate to nitrite by means of a reducing column.

The flow-injection technique can be considered as a means of sample introduction when atomic absorption spectrometry (a.a.s.) is used as the detection system. Gallego et al. [10] have summarized the advantages of this association. Nord and Karlberg [11] described the first manifold incorporating liquid-liquid extraction for the direct determination of metal ions in aqueous samples, with ammonium pyrrolidinedithiocarbamate (APDC) dissolved in 4-methyl-2-pentanone (MIBK), using a.a.s. as the detection system.

The use of the a.a.s./f.i.a. in conjunction with liquid-liquid extraction has recently been developed in this laboratory for indirect determinations. Thus, a determination of perchlorate in human urine and serum samples has been based on the formation of an ion-pair with [Cu(6-methylpicolinealdehyde

0003-2670/86/$03.50

azine)$_2$]$^+$, which is extracted into MIBK [12], and a determination of nitrate or nitrite has involved extraction of the ion-pairs with bis(2,9-dimethyl-1,10-phenanthroline)copper(I) [13].

This paper describes a simple and accurate method for the sequential determination of nitrate and nitrite in mixtures which can be used for their routine determination in meats and meat products. The method is based on the formation of the ion-pair of nitrate with bis(2,9-dimethyl-1,10-phenanthroline)copper(I), its extraction into MIBK in the flow system, and monitoring the copper in the extract by a.a.s. The resolution of nitrate and nitrite involves the following steps: first, cerium(IV) sulfate is added to oxidize nitrite to nitrate, both anions thus being determined; then sulfamic acid is added to reduce nitrite to nitrogen, and nitrate is determined alone. The difference between these two measurements provides the nitrite content.

EXPERIMENTAL

Reagents

A 2.4×10^{-3} M 2,9-dimethyl-1,10-phenanthroline (neocuproine) solution in 4-methyl-2-pentanone was used. Nitrate and nitrite standard solutions (1.000 g l^{-1}) were prepared from their potassium salts (dried at 110°C) with distilled water. A 1.00 g l^{-1} copper solution was prepared by dissolving 3.929 g of copper(II) sulfate pentahydrate in a small volume of concentrated sulfuric acid and diluting to 1 l with distilled water. A 0.25 M phosphate buffer solution (pH 4.5) was prepared. All chemicals were of analytical-reagent grade.

The carrier solution was prepared daily by mixing 2.0 ml of the 1.00 g l^{-1} copper solution, 3 ml of 0.15 M hydroxylammonium sulfate and 5 ml of the phosphate buffer, and diluting to 100 ml with distilled water.

Equipment

The Perkin-Elmer 380 atomic absorption spectrometer used was equipped with a copper hollow-cathode lamp working at 324.7 nm and an air/acetylene flame, the spectral bandpass was 0.7 nm. The output was displayed on a Radiometer REC-80 Servograph chart recorder.

The flow system used consisted of two peristaltic pumps (Ismatec S-240 and Gilson Minipuls 2), an injection valve (Tecator 100-L), and an extraction unit (Bifok 5005-044) comprising a segmentor, an extraction coil and a glass/teflon T-separator, as well as displacement bottles for pumping the organic phase. Flexible teflon tubing (0.5 mm i.d.) was used for the coils.

Flow-injection manifold. A schematic diagram of the flow-injection system is shown in Fig. 1. Sample (in the presence of cerium(IV) or sulfamic acid) or the corresponding blank is pumped into the extraction system. It is noteworthy that the introduction of air into the extraction system does not affect the signal because there is a restrictor in the system. The carrier solution is mixed with the sample in the mixing coil and introduced into a segmentor

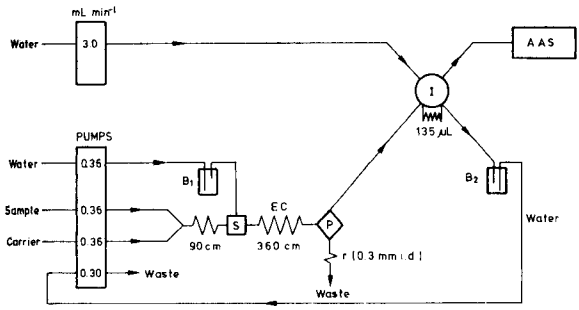

Fig. 1. Manifold for the determination of nitrate and nitrite in mixtures: (S) segmentor; (P) phase separator; (EC) extraction coil; (B_1, B_2) displacement bottles for producing organic streams; (r) restrictor; (I) injection valve. All tubes are teflon (0.5 mm i.d., except where specified).

where it merges with a stream of neocuproine solution in MIBK from displacement bottle B_1. Extraction takes place in the extraction coil and a fraction of the extract controlled by bottle B_2 is separated in the phase separator. The extracted portion fills the loop of the injector and the aqueous phase is led to waste together with the remaining organic phase via a short restrictor. The extract is injected into the water stream and transported with minimal dispersion to the nebulizer of the spectrometer.

Procedure

The manifold described above and the optimum instrumental conditions are used, and mixed solutions (pH 3.5—10) of nitrate and nitrite (each at 0.13—2.20 μg ml^{-1}) containing 50 μg ml^{-1} of cerium(IV) or 200 μg ml^{-1} of sulfamic acid are pumped continuously into the system and mixed with the carrier solution. Extraction takes place in the coil and 135 μl of the extract is injected into the water stream, subsequently being led to the spectrometer. A subsequent experiment demonstrated that neither back-extraction nor dispersion of the organic plug occurs; the same results were obtained by continuous aspiration of the organic phase. The peak height of the signal produced by the extracted copper is directly proportional to nitrate plus nitrite concentration in the presence of cerium(IV) and to the nitrate concentration alone in the presence of sulfamic acid. The difference between the height of the peaks obtained in both steps is directly proportional to the nitrite concentration.

RESULTS AND DISCUSSION

The classical indirect method for determination of nitrate by a.a.s. involves the reaction of nitrate with the neocuproine/copper(I) chelate in a weakly acidic medium and extraction of the ion-pair formed into MIBK [14]. This method was adapted to a continuous flow-injection system [13] which had

advantages of lower detection limit and greater selectivity over the conventional method. Nitrite was extracted under the same conditions as nitrate but with about a tenth of the sensitivity. The determination of nitrate and nitrite in foodstuffs requires an increased sensitivity for nitrite because its concentration is normally very low.

The sensitivity of the nitrite determination can be increased by oxidation to nitrate with cerium(IV) sulfate, so that a total nitrate/nitrite content is evaluated. The amount of cerium(IV) sulfate required to achieve complete oxidation of nitrite was studied on samples containing 2.2 μg ml^{-1} nitrite. The results showed that the cerium(IV) content in the sample must be >20 μg ml^{-1}; 50 μg ml^{-1} cerium(IV) was used to ensure complete oxidation of possible nitrite contents. Differentiation between nitrate and nitrite was achieved by adding sulfamic acid, which reduces nitrite to nitrogen, so that the final signal corresponds to the nitrate concentration only. The effect of sulfamic acid concentration was studied in the range 50—400 μg ml^{-1} for mixtures containing 2.2 μg ml^{-1} nitrite; any sulfamic acid concentration between 100 and 400 μg ml^{-1} ensured the complete reduction of nitrite. A concentration of 200 μg ml^{-1} was chosen for further studies.

The effects of other chemical variables as well as the flow-injection variables were the same as for the indirect determination of nitrate described previously [13]. The optimum concentration ranges for both anions were 0.13—2.20 μg ml^{-1} for the manifold outlined in Fig. 1.

Determination of nitrate/nitrite mixtures

A typical recorder output obtained for different standard nitrate solutions and for a nitrate/nitrite mixture are shown in Fig. 2. There is a linear relationship between the peak height and the nitrate concentration between 0.13 and 2.20 μg ml^{-1}. The nitrite and nitrate concentrations in several standard mix-

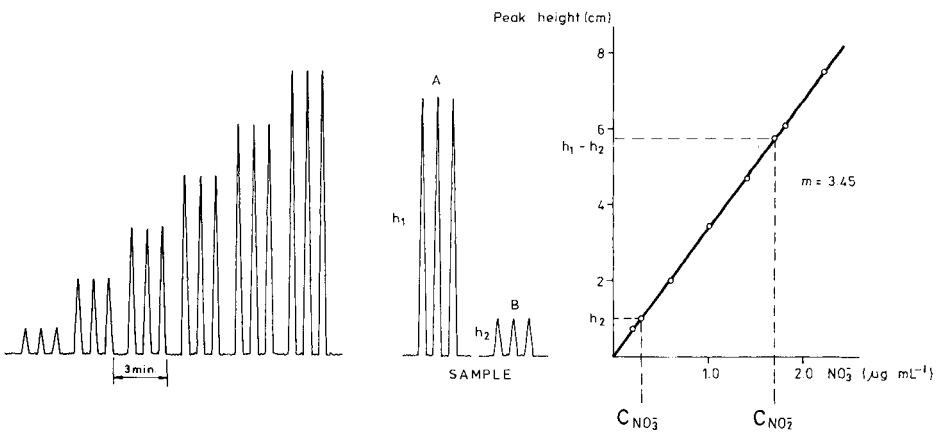

Fig. 2. Calibration peaks for triplicate injections of 0.2—2.2 μg ml^{-1} nitrate solutions, and peaks for nitrate/nitrite mixtures (0.3 μg NO_3^- ml^{-1}/1.7 μg NO_2^- ml^{-1}) after addition of: (A) 50 μg ml^{-1} cerium(IV); (B) 200 μg ml^{-1} sulfamic acid.

tures were assessed from the peak heights obtained for the two sets of experimental conditions and by using the calibration graph obtained with standards. Table 1 shows the data obtained; the determination of nitrate/nitrite mixtures is feasible in the ratio range 1:10 to 10:1 (relative error ±5%), which includes the ratio in which these species are likely to occur in foodstuffs.

Twenty consecutive analyses were made on a sample containing nitrate and nitrite concentrations of 0.7 μg ml^{-1} each. The detection and quantification limits (0.04 and 0.13 μg ml^{-1}, respectively) for both nitrate and nitrite were calculated as three and ten times, respectively, the standard deviation of the peak height for thirty injections of the same sample. When the recommended procedure was applied to a series of eleven samples with 0.7 μg ml^{-1} each of nitrate and nitrite, the relative standard deviation was ±3.7% for nitrate and ±4.1% for nitrite.

The influence of various amounts of other anions on the indirect determination of 0.7 μg ml^{-1} each of nitrate and nitrite was investigated. Other anions were added at a maximum level of 700 μg ml^{-1} (tolerance ratio to nitrate or nitrite, 1000:1), as sodium or potassium salts. The tolerance limits were taken as the largest amount yielding an error of less than ±5% in the peak height (Table 2). All interfering species increased the signal, probably because of additive interference, except for oxalate, which caused a decrease in the peak height. As can be seen from Table 2, anions such as phosphate and ascorbate, which are present together with nitrite and nitrate in cured meat, are tolerated at high ratios and therefore do not interfere with determinations in such samples. The most serious interference in the analysis of foodstuffs is posed by chloride, although as is shown below, it can readily be controlled.

Determination of nitrate and nitrite in foodstuffs

The procedure for nitrate and nitrite described above was examined for application to vegetable and meat products. There are many procedures in

TABLE 1

Analysis of synthetic mixtures of nitrate and nitrite

Amounts taken (μg ml^{-1})		Amounts found[a] (μg ml^{-1})		Amounts taken (μg ml^{-1})		Amounts found[a] (μg ml^{-1})	
Nitrate	Nitrite	Nitrate	Nitrite	Nitrate	Nitrite	Nitrate	Nitrite
0.20	0.20	0.21(5)	0.20(0)	0.20	0.60	0.21(5)	0.59(−2)
0.60	0.20	0.59(−2)	0.21(5)	0.20	1.20	0.19(−5)	1.24(3)
1.20	0.20	1.23(2.5)	0.19(−5)	0.20	1.60	0.20(0)	1.60(0)
1.60	0.20	1.56(−2.5)	0.20(0)	0.20	2.00	0.21(5)	1.94(−3)
2.00	0.20	2.04(2)	0.19(−5)				

[a]Absolute % errors are given in parentheses.

TABLE 2

Tolerance limits for other anions in the indirect determination of 0.7 μg ml^{-1} each of nitrate and nitrite

Tolerance limit (μg ml^{-1})	Anion
700	SO_3^{2-}, SO_4^{2-}, CO_3^{2-}, PO_4^{3-}, AsO_4^{3-}, AsO_2^-, $B_4O_7^{2-}$, tartrate
350	$P_3O_{10}^{5-}$, $P_2O_7^{4-}$, acetate
140	F^-
70	IO_3^-, citrate, ascorbic acid
35	$C_2O_4^{2-}$
7	$S_2O_8^{2-}$, Cl^-
3.5	Br^-, BrO_3^-
1.4	CrO_4^{2-}, I^-, ClO^-, IO_4^-, $S_2O_3^{2-}$
0.7	SCN^-, ClO_4^-, ClO_3^-

the literature for the treatment of such samples prior to the determination of residual nitrite and nitrate. Thus, food samples can be extracted with water and heated in a nitrogen atmosphere [15], with saturated sodium acetate and heated in a boiling water bath for 30 min [16], with water and potassium aluminium sulfate in order to precipitate organic matter [17], with zinc sulfate at 80°C for 20 min [18] as well as with water containing a small amount of sodium hydroxide [19], etc. In this paper, in order to avoid the introduction of substances that could interfere in the final determination, and taking into account the possible loss of labile nitrite during lengthy heating, the samples were treated as follows. The vegetable or meat products were chopped and 10 g of the slurry was transferred to a 250-ml beaker, with 50 ml of distilled water. After shaking for 15 min and filtering, 2.5 ml of saturated ammonium aluminium sulfate solution was added to the filtrate, and the solution was set aside for 30 min in order to allow precipitation of organic matter. After filtering through fluted paper into a 100-ml volumetric flask, the solution was made up to the mark with distilled water.

Chloride was the most serious interferent in the determination. It can be removed by precipitation with silver sulfate [20] or with an ion-exchange resin (Ag^+ form) [21]. However, it can be of interest to determine the content of chloride in these samples rather than to eliminate it. Thus, in this work, chloride ion was determined in the presence of nitrate and nitrite ions by using chromotropic acid. This substance can be nitrated with nitrogen-containing compounds in the presence of chloride and thus, a chloride/nitrate/nitrite mixture gives rise to a single a.a.s. signal (related to the chloride) [22]. It was found that any chromotropic acid concentration above 12 μg ml^{-1} was adequate for samples containing 2.2 μg ml^{-1} of nitrate plus nitrite, and a linear calibration graph for chloride was obtained. The detection limit was 4.6 μg ml^{-1} chloride in a flow-injection system.

The recoveries obtained for nitrate and nitrite in meat products are shown

in Table 3. All the aliquots taken were diluted to 50 ml with distilled water prior to injection, and each recovery was calculated by comparing the results obtained before and after adding the nitrate and nitrite standard solutions. The concentrations of nitrate plus nitrite added in all cases were 1.0 $\mu g\ ml^{-1}$, except to pork meat. Recoveries ranged from 95.6 to 102.8%, with an average of 99.7% for nitrate and 100.3% for nitrite. The relative standard deviations for the whole procedure were 1.97% and 1.91% for nitrate and nitrite, respectively, for 15 determinations. Table 4 shows the results obtained for

TABLE 3

Recovery of nitrate and nitrite added to meat products

Sample	Aliquot (ml)	Nitrate				Nitrite			
		Found ($\mu g\ ml^{-1}$)	Added ($\mu g\ ml^{-1}$)	Recovery		Found ($\mu g\ ml^{-1}$)	Added ($\mu g\ ml^{-1}$)	Recovery	
				($\mu g\ ml^{-1}$)	(%)			($\mu g\ ml^{-1}$)	(%)
Pork meat	10.0	<0.04				<0.04			
	10.0	—	0.50	0.51	102	—	1.50	1.51	101
	10.0	—	1.00	1.01	101	—	1.00	0.97	97
	10.0	—	1.50	1.48	99	—	0.50	0.52	104
Cooked ham	6.0	0.15				0.90			
	6.0	0.15	0.30	0.44	98	0.90	0.70	1.60	100
	6.0	0.15	0.50	0.64	98	0.90	0.50	1.42	101
	6.0	0.15	0.70	0.86	101	0.90	0.30	1.17	98
Chopped pork	6.0	0.16				0.42			
	6.0	0.16	0.30	0.44	96	0.42	0.70	1.12	100
	6.0	0.16	0.50	0.66	100	0.42	0.50	0.90	98
	6.0	0.16	0.70	0.84	98	0.42	0.30	0.74	103
Frankfurter	10.0	0.17				0.40			
	10.0	0.17	0.30	0.48	102	0.40	0.70	1.10	100
	10.0	0.17	0.50	0.66	99	0.40	0.50	0.92	102
	10.0	0.17	0.70	0.89	102	0.40	0.30	0.71	101
Mortadella	2.0	0.23				0.16			
	2.0	0.23	0.30	0.51	96	0.16	0.70	0.85	99
	2.0	0.23	0.50	0.74	101	0.16	0.50	0.67	102
	2.0	0.23	0.70	0.95	102	0.16	0.30	0.46	100

TABLE 4

Determination of nitrate, nitrite and chloride in meat products

Sample	Composition found[a]		
	Nitrate (mg kg^{-1})	Nitrite (mg kg^{-1})	Chloride (%)
Pork meat	<2.0	<2.0	<0.02
Cooked ham	12.3 ± 0.8	72 ± 2	0.43
Chopped pork	12.5 ± 0.9	35 ± 1	0.62
Frankfurter	8.7 ± 0.6	20.4 ± 0.5	0.58
Mortadella	57 ± 4	40 ± 2	0.86

[a]Average of four separate determinations ± standard deviation.

TABLE 5

Recovery of nitrate and nitrite added to various vegetable products[a]

Sample	Nitrate content (mg kg^{-1})			Nitrite content (mg kg^{-1})		
	Added	Found	Mean recovery (%)	Added	Found	Mean recovery (%)
Tomato	75.0	77.5, 75.0, 71.0	99	175.0	190.0, 172.5, 177.0	102.7
	125.0	127.5, 115.0, 122.5	97	125.0	125.0, 122.5, 128.0	100.1
	175.0	187.5, 177.5, 172.5	102	75.0	77.0, 73.7, 75.5	100.5
Potato	75.0	70.0, 80.0, 77.5	101	175.0	177.5, 180.0, 165.0	99.5
	125.0	125.0, 123.7, 122.5	99	125.0	125.0, 127.5, 121.2	99.6
	175.0	175.0, 172.3, 176.2	100	75.0	70.0, 75.0, 72.5	96.6
Carrot	75.0	77.5, 71.2, 72.5	98	175.0	180.0, 172.5, 173.7	100.2
	125.0	125.0, 123.7, 122.5	99	125.0	125.0, 126.2, 120.0	98.9
	175.0	177.5, 175.0, 173.7	100	75.0	80.0, 77.5, 72.5	102.2
Pepper	75.0	75.0, 72.5, 72.5	98	175.0	180.0, 177.5, 170.0	100.4
	125.0	135.0, 122.5, 122.5	101	125.0	125.0, 125.0, 122.5	99.3
	175.0	180.0, 172.5, 177.5	101	75.0	75.0, 77.5, 70.0	98.8
Cauliflower	75.0	70.0, 71.2, 80.0	98	175.0	175.0, 175.0, 177.5	100.4
	125.0	125.0, 127.5, 122.5	100	125.0	125.0, 127.5, 122.5	100.0
	175.0	177.5, 170.0, 170.0	99	75.0	75.0, 71.3, 72.5	97.2
		Mean	99.5		Mean	99.7
		Standard deviation	1.45		Standard deviation	1.58

[a]Nitrate and nitrite were added to 2 ml of the vegetable extract which was then diluted to 50 ml.

the determination of nitrate, nitrite and chloride in this type of sample. Such data are in agreement with the average content of these additives in meat products according to Spanish food legislation.

In order to check the validity of the proposed procedure for nitrate and nitrite in vegetable products, the recoveries of nitrate and nitrite added to various vegetables were determined. As can be observed in Table 5, these species were not detected in the samples analyzed, but the mean recoveries and standard deviations for 45 determinations of nitrate or nitrite added to vegetables were very good.

Conclusions

The results reported above show that combining a continuous liquid-liquid extractor to a flow-injection a.a.s. system is suitable for the routine determinations of nitrate and nitrite in meats. The method offers several advantages such as low reagent and sample consumption, wide pH range and good sensitivity and selectivity. The redox reactions involved in the experiments are done in a homogeneous medium and do not require the use of a reductor column as in other flow-injection methods, thus avoiding the problems associated with its activation.

The authors are grateful to the C.A.I.C.Y.T. (Project No. 2012/83) for financial support.

REFERENCES

1 J. B. Mullin and J. P. Riley, Anal. Chim. Acta, 12 (1955) 464.
2 T. J. Chow and M. S. Johnstone, Anal. Chim. Acta, 27 (1962) 441.
3 A. W. Morris and J. P. Riley, Anal. Chim. Acta, 29 (1963) 272.
4 A. Henriksen and A. R. Selmer-Olsen, Analyst (London), 95 (1970) 514.
5 J. Růžička and E. H. Hansen, Flow Injection Analysis, 1st edn., Wiley, New York, 1981.
6 L. Anderson, Anal. Chim. Acta, 110 (1979) 123.
7 M. F. Gine, F. Bergamin, E. A. G. Zagatto and B. Reis, Anal. Chim. Acta, 114 (1980) 191.
8 J. F. Van Staden, Anal. Chim. Acta, 138 (1982) 403.
9 S. Xu and Z. Fang, Feuxi Huaxue, 11 (1983) 93.
10 M. Gallego, M. D. Luque de Castro and M. Valcárcel, Atom. Spectrosc., 6 (1985) 16.
11 L. Nord and B. Karlberg, Anal. Chim. Acta, 145 (1983) 151.
12 M. Gallego and M. Valcárcel, Anal. Chim. Acta, 169 (1985) 161.
13 M. Gallego, M. Silva and M. Valcárcel, Fresenius Z. Anal. Chem., in press.
14 M. S. Cresser, The Role of Solvent Extraction in Flame Spectrometric Analysis, Butterworths, London, 1978, p. 9.
15 V. Kures and J. Lát, Prummysl Potravin, 10 (1959) 208.
16 J. H. Dhont, Analyst (London), 85 (1960) 114.
17 E. D. Coppola, A. F. Wickroski and J. G. Hanna, J. Assoc. Off. Anal. Chem., 58 (1975) 469.
18 A. Tanaka, N. Nose and A. Watanabe, Shokuhin Eiseigaku Zasshi, 22 (1981) 14.
19 A. Tanaka, N. Nose and H. Iwasaki, Analyst (London), 107 (1982) 190.
20 Y. Yamamoto, N. Okamoto and E. Tao, J. Chem. Soc. Jpn., 89 (1968) 399.
21 G. Hoshikawa and Y. Fudano, Kagawa Daigaku Nogakuba Gakujutsu Hokoku, 27 (1976) 111.
22 S. S. M. Hassan, Microchem. J., 18 (1973) 486.

Analytica Chimica Acta, 179 (1986) 351—357
Elsevier Science Publishers B.V., Amsterdam — Printed in The Netherlands

FLOW INJECTION AND MICROWAVE-OVEN SAMPLE DECOMPOSITION FOR DETERMINATION OF COPPER, ZINC AND IRON IN WHOLE BLOOD BY ATOMIC ABSORPTION SPECTROMETRY

M. BURGUERA* and J. L. BURGUERA

Departamento de Química, Facultad de Ciencias, Universidad de Los Andes, Apartado Postal 542, Mérida 5101 (Venezuela)

O. M. ALARCÓN

Departamento de Bioquímica, Facultad de Medicina, Universidad de Los Andes, Mérida 5101 (Venezuela)

(Received 2nd April 1985)

SUMMARY

A simple and rapid method is proposed for the determination of copper, zinc and iron in whole blood. The injected sample is mineralized in the flow system on passage through a microwave oven and the metals are determined by atomic absorption spectrometry. Prior sample destruction or removal of organic material prior to injection is not necessary. The required volumes for each analysis are 90, 60 and 100 μl for copper, zinc and iron, respectively. The relative standard deviations were less than 3% in all cases. There was good agreement between the results obtained with the flow-injection method and those attained by conventional spectrophotometric measurements.

The importance of zinc, copper and iron in human nutrition and health has been documented extensively [1—4]. Various methods can be used for the determination of these elements in serum, plasma or whole blood with satisfactory results [5]. Recently, methods based on continuous flow and flow injection analysis (f.i.a.) have been described for the determination of some metals in blood serum or plasma [6—14] with the aim of developing fast, reliable and simple methods for routine analysis. Microwave sample dissolution (m.s.d.) has been used in the determination of numerous elements (including Cu, Zn and Fe) in coal, fly ash, oil shales, rock sediments and biological materials by atomic absorption spectrometry (a.a.s.), neutron activation analysis and atomic emission spectrometry [15—17]. A combination of m.s.d. with f.i.a. has not been reported before. In this paper some experiments on this concept are described. Its potential for determining elements in biological samples is illustrated; copper, zinc and iron were determined in whole blood by using m.s.d./f.i.a./a.a.s.

0003-2670/86/$03.50

EXPERIMENTAL

Instruments, equipment and manifolds

The flow system used is shown schematically in Fig. 1. A commercial domestic microwave oven (Panasonic, model NE-7660/6660) was used. The oven has an available timing cycle from 15 s to 30 min and a variable heating cycle based on power setting from "warm" through "high" equivalent to 70—700 W output. The microwave frequency is 2.45 MHz. The capacity of the oven is 1.0 ft^3.

The Varian-Techtron model AA-1475 atomic absorption spectrometer used was connected to a Varian-Techtron model 9176 chart recorder. Conventional hollow-cathode lamps were used for the copper, zinc and iron measurements. A five-channel peristaltic pump (model 375, Sage, Orion Research, Cambridge, MA) was used, with Solvaflex pumping tubes, which were replaced weekly.

Sample and reagent were injected in parallel into the flow system by means of a home-made double-injection valve similar to that described previously by Mindegaard [18], in which the injected volumes could be altered by using interchangeable loops. The double injector permitted synchronous merging of sample and reagent in a symmetrical system [19]. After the sample and reagent had passed through equal lengths of tubing, they mixed at point A in Fig. 1, and continued downstream while being mixed and dispersed into the carrier stream. At point B in Fig. 1, the sample/reagent mixture went through a pyrex coiled decomposition tube (l_3) of the same diameter as the pumping tubes, which was located inside the microwave oven. The tube was fixed in two holes drilled in the rear wall of the microwave oven. While the sample/reagent mixture was flowing through the dissolution tube, the microwave heating encouraged mineralization of the blood. The mineralized sample was then pumped into the nebulizer of the atomic

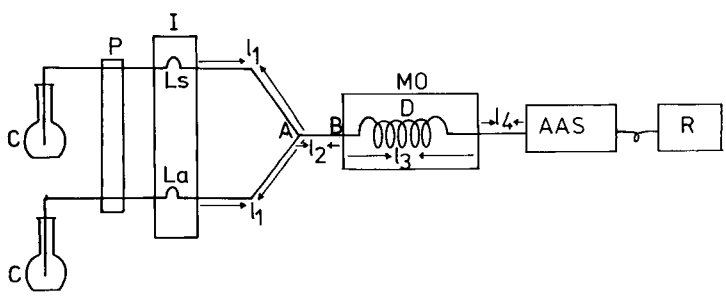

Fig. 1. Flow diagram of the system used for the determination of copper, zinc and iron in whole blood: (C) carrier solution; (P) peristaltic pump; (I) double injector; (D) decomposition tube; (MO) microwave oven; (AAS) atomic absorption spectrometer; (R) recorder. The sample and reagent solutions fill loops Ls and La, which are the volumes introduced into the carrier streams; l_1—l_4 denote the lengths of the various tubing.

absorption spectrometer, and the analytical signal was recorded as a transient peak on the chart recorder.

Reagents, samples and standards

All reagents were of analytical grade, unless otherwise stated, and all water was double-distilled and deionized. An acid reagent stock solution (6.0 M hydrochloric acid and 8.0 M nitric acid) was prepared in water. Working acid reagent solutions were prepared daily by appropriate dilution with water. A set of stock copper, zinc and iron (1000 μg ml^{-1}) solutions was prepared weekly by dissolving metal strip or granules (99.99%) in the minimum volume of (1 + 1) nitric acid (copper) or (1 + 1) hydrochloric acid (zinc and iron) and the solution was diluted to 1 l with water. More dilute standard solutions were prepared from the respective stock solutions daily by dilution with water. Blood samples were drawn by Vacutainer or syringe into 10-ml heparinized polyethylene tubes (with polyethylene stoppers) and stored at about -4°C. Before analysis, the samples were allowed to warm to room temperature.

A set of whole blood standards was prepared by adding to 0.25 ml of well-mixed whole blood, 0.75 ml of Triton X-100 solution (1 g l^{-1}), containing known amounts of the ions under study, and mixing by inversion. From this set, calibration graphs were prepared for each ion. The addition of Triton X-100 was necessary to avoid the clogging of the tubing by blood samples observed in preliminary work.

RESULTS AND DISCUSSION

In the procedure, a diluted whole blood sample and acid reagent solution are transferred to the corresponding loops of the injector resting in the sampling position. On switching the injector, the selected volumes of sample and reagent are introduced into the corresponding carrier streams of water containing 1 g l^{-1} Triton X-100.

The introduction of samples or blood standards gives rise to peak response, as illustrated in Fig. 2. The peak height and shape would be expected to vary according to the parameters governing f.i.a. (sample and reagent volumes, carrier stream flow rates, length and diameter of tubing), a.a.s. (flame composition, hollow-cathode lamp operating current, slit-width, burner height and wavelength), reagent concentration and microwave-oven power settings. The highest peaks with least tailing were obtained under the conditions listed in Table 1.

The microwave oven acts simply as a source of intense energy which rapidly heats the sample, and a suitable chemical reaction is necessary for mineralization to occur in the system. The use of a dilute mixture of hydrochloric (0.3 M) and nitric (0.4 M) acids proved to be satisfactory for this purpose, giving good recoveries as described below. A 100-μl portion of this acid reagent was adequate for the sample sizes used; acid concentrations and reagent

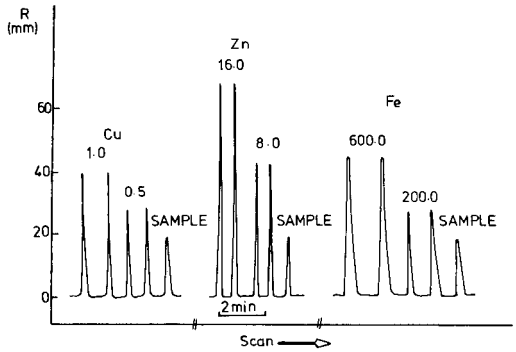

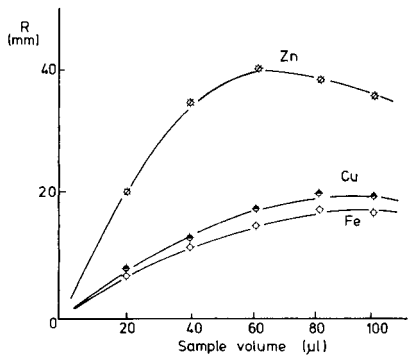

Fig. 2. Injection of two standards in duplicate and a sample containing copper, zinc and iron. The numbers above the peaks represent mg l^{-1}. Recorder sensitivity: 50, 100 and 5000 mV full scale for copper, zinc and iron, respectively.

Fig. 3. Effect of sample volume on peak height. Recorder sensitivity as in Fig. 2. To the sample, 1.0, 20.0 and 400 mg l^{-1} copper, zinc and iron were added, respectively. Other conditions as in Table 1.

TABLE 1

Experimental parameters used in the m.s.d./f.i.a./a.a.s. system for the determination of copper, zinc and iron in whole blood

Component	Parameter	Cu	Zn	Fe
F.i.a.[a]	Sample volume (µl)	90	60	100
	Reagent volume (µl)[b]	100	100	100
	Carrier flow rates (ml min^{-1})	1.8	1.8	1.8
A.a.s.	Lamp current (mA)	4.0	5.0	5.0
	Wavelength (nm)	324.7	213.9	248.4
	Slit-width (nm)	0.5	1.0	0.2
	Air/acetylene (l min^{-1})	3.4/1.5	3.0/1.6	2.8/1.5
M.s.d.	Microwave-oven power select control	High (ca. 700 W, full power) for 1 min.		

[a]Tubes l_1, l_2, l_3 and l_4 (Fig. 1) were 10, 40, 50 and 30 cm, respectively; the internal diameter of the tubing was 0.5 mm. [b]0.3 M HCl/0.4 M HNO_3.

volumes greater than 0.5 M HCl, 0.6 M HNO_3 and 150 µl, respectively, start to produce acid fumes within the coiled dissolution tube located inside the microwave-oven (l_3) which affect the flow pattern and degrade the reproducibility.

The lengths of tubing l_1 (10 cm), l_2 (40 cm) and l_4 (30 cm) were kept as short as the instrumental uses allowed, in order to minimize dispersion. Length l_3 was optimized to achieve satisfactory mineralization. The residence time in this tube also depended on the carrier stream flow rates. The results

are presented in Table 2. As the tubing length was increased, the carrier stream flow rates were also increased to keep the residence time of the sample/reagent mixture in the oven between 15 and 26 s. Below 15 s, poor results were obtained because of incomplete acid attack; when the residence time was higher than 25 s, the carrier solution flow pattern started to be affected by gas evolution, probably from fumes generated during the dissolution. Taking into account the reproducibility and a minimum overall residence time in the flow-injection system, a tubing length l_3 of 50 cm and a carrier flow rate of 1.8 ml min^{-1} were chosen for all subsequent work. Peak broadening and tailing were found when the overall tubing internal diameter was increased from 0.50 to 0.75 or 1.0 mm; this again was due to increased dispersion.

The effect of sample volume was investigated. The sensitivity increased with increasing volumes (Fig. 3) but the injection of volumes larger than 90, 60 and 100 μl for the determination of copper, zinc and iron, respectively, led to smaller peak heights. This could have been due to incomplete digestion [15].

Precision, recovery and accuracy

The recovery of each metal was determined in ten samples of whole blood by addition of known amounts of copper, zinc and iron to the Triton X-100 solution (1 g l^{-1}) as mentioned above. The recoveries were 103.0 ± 2.0% (mean ± standard deviation) and 103.2 ± 2.0% for additions of 0.5 and 1.0 mg l^{-1} copper, respectively; 101.5 ± 4.0% and 101.1 ± 3.2% for additions of 8.0 and 16.0 mg l^{-1} zinc, respectively; and 102.8 ± 2.0% and 101.8 ± 2.2% for addition of 200 and 600 mg l^{-1} iron, respectively. These results confirm that the calibration graphs prepared as previously described can be used for these analyses, but that the concentrations read from these graphs should be corrected by 3.2, 4.2 and 2.2% for copper, zinc and iron, respectively, to accommodate the slight decrease in recoveries from whole blood samples.

TABLE 2

Correlation between the length of coiled tubing (l_3) inside the oven, carrier stream flow rates, residence time of the acid reagent in the oven and the relative standard deviation

l_3 (cm)	Carrier stream flow rates (ml min^{-1})	Sample residence time in oven[a] (s)	R.s.d. (%)[b]
25	1.0—0.6	15—26	2.3
50	2.0—1.2	14—25	2.5
100	4.0—2.4	14—26	7.2
150	6.0—8.8	15—24	8.9

[a]A dye was used to establish the sample residence time. [b]For 0.98 mg copper l^{-1} in a whole blood sample.

Day-to-day precision was established by analysis of seven whole blood samples at intervals of 4 to 6 days over a period of a month. After addition of Triton X-100 the whole blood samples were stored in a refrigerator at −4° C. The results, summarized in Table 3, show satisfactory precision. Although the copper, zinc and iron concentrations do not change systematically during storage, the use of fresh samples of whole blood is to be preferred.

To check the accuracy of the method, eight whole blood samples were also analyzed spectrophotometrically [20—23]. The results given in Table 4 show good agreement, which is an indication of the satisfactory accuracy of the present method. The present results agree well with previous reliable reports on copper, zinc and iron determination in whole blood [1—3, 5, 21—25].

This method is simple and suitable for determining these ions in whole blood without prior ashing, digestion or precipitation of samples, at a

TABLE 3

Day-to-day precision of the determination of copper, zinc and iron in whole blood

Sample	Average content (mg l^{-1})[a]			R.s.d. (%)		
	Cu	Zn	Fe	Cu	Zn	Fe
1	0.96	5.86	389	2.3	1.4	1.2
2	0.80	6.76	450	2.0	2.0	1.1
3	0.96	4.75	455	2.0	1.5	1.3
4	0.88	5.38	470	2.1	1.9	1.4
5	0.98	5.38	463	1.2	1.9	1.3
6	0.85	7.00	402	1.5	1.7	1.5
7	1.10	6.50	410	1.9	2.0	1.3

[a] Four determinations were made on each sample each day.

TABLE 4

Accuracy of the determination of copper, zinc and iron

Sample	Copper (mg l^{-1})		Zinc (mg l^{-1})		Iron (mg l^{-1})	
	This method	Ref.[a]	This method	Ref.[a]	This method	Ref.[a]
1	0.98	0.94	5.89	5.83	386	392
2	0.81	0.82	6.80	6.84	458	463
3	0.95	0.91	4.73	4.70	451	456
4	0.90	0.86	5.35	5.27	465	460
5	0.98	0.91	5.40	5.36	460	458
6	0.88	0.92	6.89	6.90	401	410
7	1.00	1.04	6.45	6.40	414	413
8	1.01	1.05	6.00	6.20	458	455

[a] Reference spectrophotometric method (see text).

sampling rate of ca. 80 h^{-1}. In all cases, the signal is measured in the most useful part of the calibration range, with a typical relative standard deviation of better than 5%. The flow-injection system described minimized the problem of acid fumes which are generated during the digestion of biological samples in the teflon vessels usually used in microwave sample decomposition.

REFERENCES

1 A. S. Prassad (Ed.), Trace Elements in Human Health and Disease, Vol. 1. Zinc and Copper, Academic Press, New York, 1976.
2 E. J. Underwood (Ed.), Trace Elements in Human and Animal Nutrition, 4th edn., Academic Press, New York, 1977, pp. 196—242.
3 A. S. Prassad, Crit. Rev. Clin. Lab. Sci., 8 (1977) 1.
4 C. E. Casey and K. M. Hambidge, in J. O. Nriagn (Ed.), Epidemiological Aspects of Human Zinc Deficiency, in Zinc in the Environment, Part III: Health Effects, Wiley, New York, 1980.
5 J. Versieck and R. Cornelis, Anal. Chim. Acta, 116 (1980) 217, and references therein.
6 B. Sampson, J. Autom. Chem., 5 (1983) 207.
7 B. F. Rocks, R. A. Sherwood and C. Riley, Clin. Chem., 28 (1982) 440; Ind. Chem., 28 (1982) 440.
8 B. F. Rocks, R. A. Sherwood, L. M. Bayford and C. Riley, Ann. Clin. Biochem., 19 (1982) 338.
9 J. Růžička, E. H. Hansen and E. A. Zagatto, Anal. Chim. Acta, 88 (1977) 1.
10 T. Uchida, C. S. Wei, C. Iida and H. Wada, Nagoya Kogyo Daigaku Gakuho, 33 (1982) 97.
11 S. M. Ramasamy and H. A. Mottola, Anal. Chim. Acta, 127 (1981) 39.
12 J. L. Burguera, M. Burguera, M. Gallignani and O. M. Alarcón, Clin. Chem., 29 (1983) 569.
13 J. L. Burguera, M. Burguera and M. Gallignani, Ann. Acad. Brasil Cienc., 55 (1983) 209.
14 C. Riley, B. F. Rocks and A. Sherwood, Talanta, 31 (1984) 879.
15 R. A. Nadkarni, Anal. Chem., 56 (1984) 2233.
16 A. Abou-Samra, J. S. Morris and S. R. Koirtyohann, Anal. Chem., 47 (1975) 1475.
17 P. Barrett, L. J. Davidowski, K. W. Penaro and T. R. Copeland, Anal. Chem., 50 (1978) 1021.
18 J. Mindegaard, Anal. Chim. Acta, 104 (1974) 185.
19 J. Růžička and E. H. Hansen, Anal. Chim. Acta, 106 (1977) 207.
20 B. L. Vallee and J. G. Gibson, J. Biol. Chem., 170 (1948) 435.
21 R. C. Dickenman, B. Crafts and B. Zak. Arch. Biochem. Biophys., 53 (1954) 381.
22 C. J. Gubler, M. E. Lahey, H. Ashenbrucker, G. Cartwright and M. M. Wintrobe, J. Biol. Chem., 196 (1952) 209.
23 P. del Castilho and R. F. M. Herber, Anal. Chim. Acta, 94 (1977) 269.
24 J. R. Alonso-Fernández, J. A. Cocho, M. C. Castineiras, J. Pena and J. M. Fraga, J. Inherited Metab. Dis., 6 (1983) 91.
25 S. A. Matthes, R. F. Farrell and A. Mackie, J. Tech. Prog. Rep. U.S. Bur. Mines, 1983, No. 120.

Analytica Chimica Acta, 179 (1986) 359—370
Elsevier Science Publishers B.V., Amsterdam — Printed in The Netherlands

POTENTIOMETRIC DETECTION IN FLOW ANALYSIS

K. TÓTH, J. FUCSKÓ, E. LINDNER, ZS. FEHÉR and E. PUNGOR

Institute for General and Analytical Chemistry, Technical University, H-1521 Budapest (Hungary)

(Received 9th September 1985)

SUMMARY

Special aspects of ion-selective electrodes relevant to applications in flow-through systems are discussed. The predominant role of the dynamic response characteristics of the sensors, especially in flow-injection analysis, is emphasized. Indirectly, these characteristics can affect the linear response range, the detection limit and the selectivity properties of the sensors. As examples, flow-injection methods are described for the determination of fluoride in rain-water samples and of potassium ion activity in blood sera.

Assessment of the general position of electrochemical sensors in flow-through analytical devices indicates that voltammetric (including amperometric and coulometric) sensors are the most widely used because of their applications in high-performance liquid chromatography. Ion-selective electrodes are, however, reliable tools for high-precision monitoring of ion activities in biological samples in continuous flow or in situ applications. As far as flow injection analysis is concerned, ion-selective sensors have proved to be really satisfactory only for a few special analytical problems. Conductivity and the "electrodeless" high-frequency (oscillometric) cells for monitoring solution conductivity and permittivity are applied primarily as detectors in industrial monitors and in ion chromatographic and high-performance liquid chromatographic systems.

Among the electrochemical sensors, the performance of the voltammetric cells differs most greatly between stationary and hydrodynamically controlled conditions. This is the reason why the theory of voltammetric detection under hydrodynamically controlled conditions has been developed extensively [1]. Moreover, because of their value as chromatographic detectors, much work has been devoted to the optimization of detector parameters relevant to chromatographic application. The theory of voltammetry under hydrodynamically controlled conditions has shown unambiguously that the performance of voltammetric detectors depends primarily on the geometry of the detector cell and on the hydrodynamic conditions prevailing in the system. In contrast when flow-through potentiometric detection is used, the electrochemical properties of the sensors incorporated in the detector cell play the predominant role.

0003-2670/86/$03.50

In the present paper, special aspects of flow-through potentiometric detection are discussed. To illustrate these aspects, methods will be outlined for the determination of fluoride in rain water and potassium in blood serum.

PERFORMANCE CHARACTERISTICS OF ION-SELECTIVE ELECTRODES

For the optimization of conditions during the development of a flow-through analytical method based on detection with an ion-selective electrode, the most important characteristics of the potentiometric sensors (e.g., measuring range, response time, selectivity and stability) must be studied under both batch and flow-through conditions. But it should be noted that these parameters and their effects can be quite different in continuous flow analysis and in flow-injection analysis. In the former, a steady-state signal carries the analytical information while in the latter case, a transient signal is involved.

Measuring range and detection limit

In continuous flow analysis, the measuring range and detection limit are generally much the same as in batch operation, but in special cases the flow system can be more favourable. With precipitate-based electrodes, for example, the behaviour of the sensor in the lower range of detection can be affected by adsorption, desorption and dissolution processes [2, 3], thus the detection limit and the linear response range are expected to improve under continuous flow conditions. This can be ascribed to the short residence time available for the sample in the detector cell compared to batch operation.

In contrast, with the flow-injection technique, the linear response range (i.e., the E vs. log a_i plot) as well as the lower limit of detection of the sensors are generally worse than in continuous flow or in batch measurements based on the same measuring cell, instruments, etc. [4]. This finding can be attributed partly to the sample dilution (dispersion coefficient, $D > 1$), but more importantly to the dynamic response characteristics of the potentiometric sensors. As is well known, the dynamic properties of ion-selective electrodes depend on the activity level, and the response time in the lower activity range is always longer than that at higher activity levels. Besides, the dynamic characteristics of the sensors are worse when a decrease in activity is introduced at the electrode surface (Fig. 1) [5]. Thus, because of the finite value of the response time, a steady-state signal cannot be attained at a fixed measuring time in a fast flow-injection system and the magnitude of the transient signals recorded depends on several parameters such as measuring time, flow rate, type of sensor, etc. (Fig. 2).

The correlation between the logarithm of the activity of the analyte and the steady-state signal recorded with ion-selective electrodes in continuous flow or batch measurements is Nernstian over a wide range of activities. In flow-injection systems, however, the correlation between the transient signal (i.e., the potential measured) and the sample concentration injected can be logarithmic or linear. The type of function is governed by several

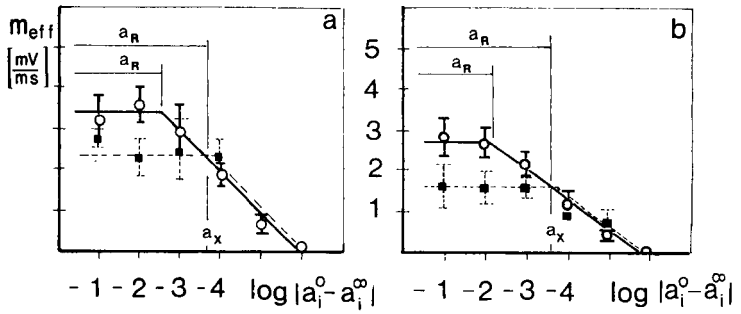

Fig. 1. The normalized values of the initial slope (m_{eff}) of response time curves as a function of decadic changes in activity: (a) with increase in activity; (b) with decrease in activity. Flow rates: (○) 140 ml min^{-1}; (■) 100 ml min^{-1}, a_R indicates ranges in which m_{eff} is independent of activity, and a_X the ranges of dependence on activity; $m_{eff} = m_{measured} S_{Nernstian}/S_{measured}$.

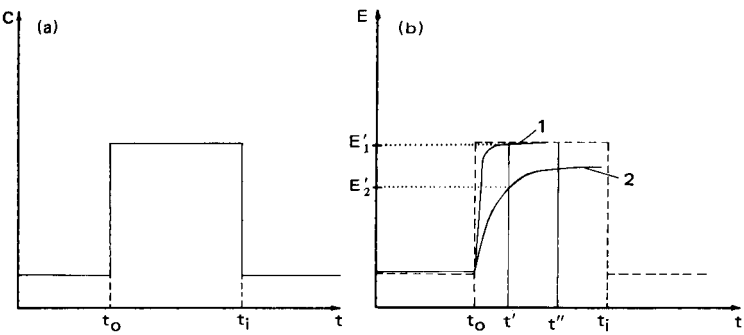

Fig. 2. Schematic illustration of the effect of the dynamic characteristics of the sensor on the potential recorded in flow analysis. (a) Input function, concentration (C) vs. time (t); (b) response function, E vs. t. (t', t'') measurement time. Flow rate: (1) fast; (2) slow.

factors such as the primary ion concentration in the carrier stream, the fluid velocity in the flow-through system, and the volume of sample injected. Consequently, the different (linear and logarithmic) signal vs. concentration functions reported by different authors [6—8] are not necessarily contradictory, but can be expected theoretically.

Dynamic properties and response time

The dynamic response characteristics of potentiometric sensors can affect drastically not only the attainable rate of sample processing but also the magnitude of the signal measured and thus the sensitivity of the measurements in batch, continuous flow and flow-injection analysis.

With respect to dynamic characteristics, ion-selective electrodes can be classified in two groups: (1) the signals arise from separation of charge at the membrane solution interface (solid-state, ion-exchanger electrodes); (2) the

signal results from a selective ion-exchange reaction which is also influenced by bulk membrane transport processes (neutral carrier type electrodes). The dynamic response characteristics of sensors belonging to the first group are determined primarily by the rate of material transport in the solution phase towards the electrode surface, because the rate of the ion-exchange reaction (at a given activity in solution) is relatively fast. Thus, an equation describing the primary ion activity at the electrode surface could be derived on the basis of Fick's second law [9]. Material transport, however, can be affected by the hydrodynamics of the flow system, and accordingly the response time of potentiometric detectors can be improved by optimizing the hydrodynamic conditions in the detector cell, e.g., by increasing the flow or stirring rate, or by appropriate selection of the geometry and size of the sensing electrodes. At low primary ion activities, i.e., in diluted solutions, the response time of precipitate-based ion-selective electrodes is governed mainly by slow surface reactions (e.g., ion-transport within the membrane surface layer, dissolution, recrystallisation, adsorption, etc.) [5, 10, 11].

In contrast to the ion-selective electrodes discussed above, a description of the dynamic response characteristics of ionophore-based liquid-membrane electrodes requires consideration of the bulk membrane processes. The response time of this type of electrode, measured under the same hydrodynamic conditions as were used with precipitate-based electrodes, were found to be appreciably higher because of bulk membrane diffusion processes. Consequently, the response time of ionophore-based liquid-membrane electrodes could be altered by changing the composition of the membrane bulk [12]. This offers a possibility for optimization of liquid membranes, especially for the purposes of flow analysis.

With the aim of increasing the rate and precision of measurements in continuous flow systems based on ion-selective electrodes, Morf and Simon [12] suggested a method for determining the steady-state potential from the rising part of a dynamic response curve by the use of an appropriate mathematical equation and extrapolation by non-linear regression analysis. This method is of importance if the final value of the steady-state electrode potential is approached only slowly.

In flow-injection systems based on sensors with a finite response time, the sensitivity of the measurements can be increased by increasing the residence time of the sample in the detector cell [6]. This can be achieved by decreasing the flow rate or increasing the sample volume. Residence time can also be increased, but at the cost of sample dilution, by using a mixing chamber of appropriate volume, or a larger reactor volume. In selecting the appropriate residence time in a flow-injection system, a judicious choice must be made between the disadvantages with respect to response time produced by decreasing flow rates and the problems related to both sensitivity and response time that may be faced with large sample dispersions.

Naturally, other possible means of decreasing response time must also be exploited, e.g., selection of the optimal cell geometry, flow rate and electrode

membrane composition [12], the use of the appropriate pH, buffer capacity and primary ion concentration [6, 13] in the carrier stream, and the possible application of a washing electrolyte to clean the electrode surface by enhancing ion-desorption processes [14].

Selectivity

Sufficient selectivity with respect to the analyte in the sample is a prerequisite for use of the sensors. The selectivity requirements, however, depend to a great extent on the precision needed for the determination, as has been demonstrated for blood serum analysis [15].

Under continuous flow conditions, a steady-state signal is usually recorded, thus the selectivity data evaluated from batch measurements can be adopted without problems in most cases. In flow-injection analysis, however, the selectivity data from batch measurements must be used cautiously. An example will explain this in more detail. The transient signal recorded with an iodide-selective electrode in the so-called two-ion range (i.e., the range of primary and interfering ion ratios over which the electrode potential is governed mainly by the primary ion activity, and the change in potential (ΔE) caused by the interfering ion is maximally 18 mV) during an increase and a decrease in the activity of the interfering ion is shown in Fig. 3. The nonmonotonic dynamic response curve has three well-defined sections; a steep rising part (0.1-s range), a decreasing relaxation section (seconds range), and a slow drifting signal range (minutes range). This is the result of the following processes taking place consecutively or simultaneously at the electrode/solution interface [16, 17]. When the level of the interfering ion-activity is increased, the processes include: (1) diffusion of interfering ions from the solution bulk to the electrode surface, (2) adsorption or chemisorption of the interfering ion, (3) desorption of the primary ion, (4) diffusion of excess of primary ions into the bulk solution, and (5) change of the chemical composition and morphology of the membrane surface and related diffusion processes. The first three of these processes can be assigned to the first section of the transient signal, while the fourth and fifth processes are mainly responsible for the second and third sections of the response curve. It must be mentioned that all the parameters (ΔE or $t_{1/2}$ values) used to characterize the dynamic response curve are flow-rate dependent. Because of the dependence of the ΔE_2 value on the flow rate and time, the system cannot be in equilibrium under these conditions. Thus, the reliability of selectivity data evaluated from ΔE_2 values [18] must be questionable. Moreover, when this problem is considered in terms of flow-injection analysis, selection of the measurement time is clearly important. The existence of the variable dynamic response curve may distort the flow-injection recordings, resulting in unexpected signal shapes [19].

When an analytical method based on flow-injection analysis and potentiometric detection is developed, the selectivity coefficients should be evaluated with the actual measuring device, in the appropriate concentration range.

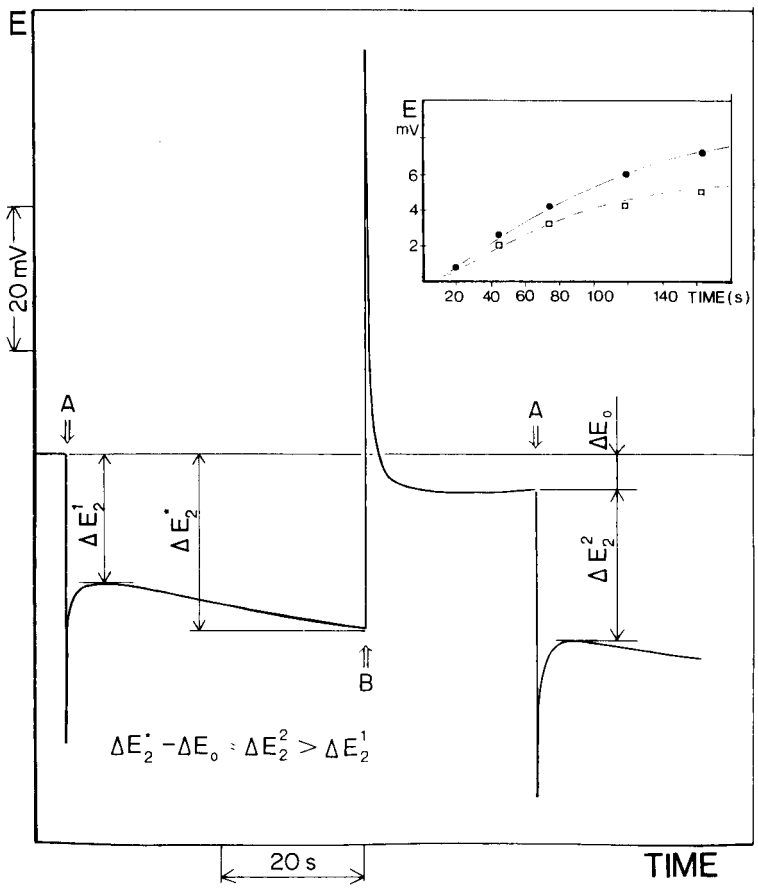

Fig. 3. Dynamic response curve recorded in the two-ion range with an iodide-selective precipitate-based electrode. The arrows indicate a change from a 10^{-5} M KI/10^{-1} M KNO_3 solution to a 10^{-5} M KI/10^{-1} M KNO_3/2 × 10^{-2} M KBr solution (A), followed by a return to the first solution (B). The inset shows changes of potential with time: (□) change in E_0 (ΔE_0); (•) change in ΔE_2 (ΔK_{ij}^{pot}).

Stability and lifetime

For the use of sensors in continuous flow devices, general stability and lifetime are obviously important requirements, and can limit applications (e.g., enzyme electrodes). However, the stability requirements for the sensors differ somewhat for different flow methods. Naturally, long-term stability of the sensors is most crucial for high-precision monitoring of ion activities, e.g., in blood analysis [20]. However, recalibration of the detector system does not pose many problems in continuous flow systems, and is especially simple in flow-injection analysis. The stability of the sensors can be improved by selecting a streaming solution of optimal composition, quite apart from the obvious point of membrane composition [6, 21].

DETERMINATION OF FLUORIDE IN THE LOW CONCENTRATION RANGE BY A FLOW-INJECTION METHOD

Among the anion-selective electrodes, the fluoride-selective electrode is the most frequently used because of its favourable selectivity properties and because of the scarcity of competitive methods for the determination of low concentrations of fluoride. Various efforts have been made to develop flow-injection methods incorporating a fluoride electrode as sensor for the determination of low concentrations of fluoride in samples such as rain water, surface water and urine. Quite apart from the sensitivity problem caused by the fluoride level in such samples being in the vicinity of the detection limit of the sensor, the dynamic response properties of the fluoride electrode are not good enough for fast sample throughput [10, 11].

Van den Winkel et al. [22] studied the behaviour of the fluoride electrode in a flow-injection system and found the dynamic response of the sensor rather poor. With a relatively high flow rate (5.5 ml min^{-1}) and large sample volumes, the sample throughput was 120 h^{-1} in the range 1.5×10^{-5}—5×10^{-4} M fluoride. The limit of the linear response range (E vs. log C_F) for the fluoride-selective sensor in flow-injection analysis was found to be $10^{-4.6}$ M by Trojanowicz and Matuszewski [4]. For the determination of fluoride in rain and surface waters, Slanina et al. [7] designed a computer-controlled flow-injection system based on a fluoride electrode. Appropriate selection of the carrier stream composition and the conditions allowed rain-water samples to be analyzed for fluoride in the $\mu g\ l^{-1}$ range (10^{-6} M) at a rate of 60 h^{-1}. For the measurements, they used an amplifier specially designed for the precise measurement of small potential changes.

The aim of the work described below was to develop a flow-injection system and a method for the determination of the fluoride content of rain water, which would be comparable in terms of sensitivity with ion-chromatographic methods [23]. As the dynamic response of the sensor is a crucial parameter, it was studied for the fluoride electrode. The time constant of the potential response curves was found to lie in the minute range at 10^{-6} M fluoride levels, but was heavily dependent on the surface condition of the lanthanum fluoride crystal. Consequently, the importance of proper selection of the composition of the carrier solution and the residence time of the sample in the measuring cell is indisputable.

Measurement system and calibration

In the flow-injection system, the carrier solution was transported by applying an appropriate nitrogen pressure to the carrier reservoir. The nitrogen pressure was generally 1 bar. The loop (250 μl) of the injector (Labor MIM OE-320) was filled by using a simple air suction pump. The dispersion section of the system consisted of a 1-m or 2-m teflon coil (0.6 mm i.d.). The detector was a tubular flow-through fluoride-selective electrode (Radelkis, OP-F-7443) used with a conventional double-junction

Ag/AgCl (0.1 M KCl, 0.1 M KNO_3) reference electrode (Radelkis OP-820). The potential measured with a Radelkis OP-211/1 digital pH/mV meter was amplified about twenty times before recording with a Radelkis OH-814/1 linear chart recorder.

The carrier solution was a conventional total-ionic-strength adjustment buffer (TISAB; 7.14 g l^{-1} EDTA, 9 g l^{-1} NaCl, 1.5 M acetic acid/sodium acetate buffer, pH 5.0—5.3) to which was added an appropriate amount of sodium fluoride before dilution (1 + 1) with distilled water.

For calibration, sodium fluoride solutions of appropriate concentration were diluted (1 + 1) with TISAB.

Results

From the calibration graph for the flow-through fluoride electrode in continuous-flow operation (Fig. 4), it can be seen that the electrode response is Nernstian down to 10^{-5} M fluoride. In selecting the experimental conditions for the flow-injection system, the problems discussed earlier had to be faced, namely the need for sensitive measurements at low levels of fluoride and the unfavourable dynamic response of the sensor at such low activities.

To improve the sensitivity of the flow-injection measurements, the concentration of fluoride in the carrier stream should be decreased but then different problems arise: the electrode stability decreases, the response time

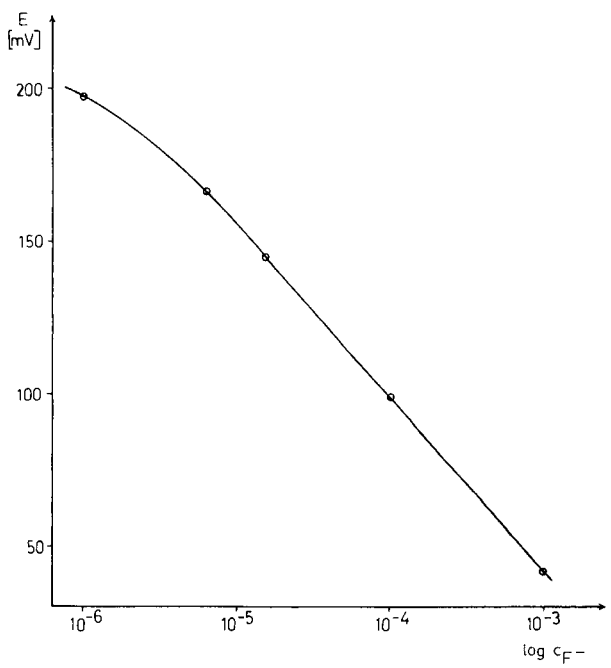

Fig. 4. Calibration graph for the flow-through fluoride electrode in a continuous flow system. Flow rate, 1 ml min^{-1}.

increases, and the potential vs. log C_F function is not Nernstian below 10^{-5} M fluoride. A study of the effects of the fluoride level in the carrier stream, the flow rate of the carrier and the volume of the sample injected showed that the best results were obtained with a TISAB carrier stream containing 10^{-6} M fluoride at a flow rate of 1 ml min^{-1}, a coil length of 1 m (0.6 mm i.d.) and 250 μl sample injection. The relevant recorder trace and calibration plot are shown in Fig. 5. As can be seen, the function between the potential measured and the sample concentration injected is linear over a decade concentration range.

The reproducibility of the results was good; e.g., the mean peak height (ΔE) for a 2.5×10^{-7} M fluoride solution was 12.02 mV with a deviation (2σ) of ± 0.05 ($n = 15$) and a similar deviation was obtained for 5×10^{-7} M fluoride. The injection rate depends to a great extent on the fluoride content of the carrier stream. When 10^{-6} M or 5×10^{-6} M fluoride was present in the carrier stream, 40—60 samples could be injected per hour. With the method developed, the fluoride contents of rain water samples were found to be in the range $1-5 \times 10^{-7}$ M.

DETERMINATION OF POTASSIUM IN BLOOD SERUM

Recently, a potassium ion-selective electrode based on a new bis(crown ether) derivative has been developed in this laboratory. The most important performance characteristics (measuring range, selectivity properties, etc.) of this sensor are comparable with those of the most widely used valinomycin-based sensor [24]. The favourable lipophilicity of the ionophore and other

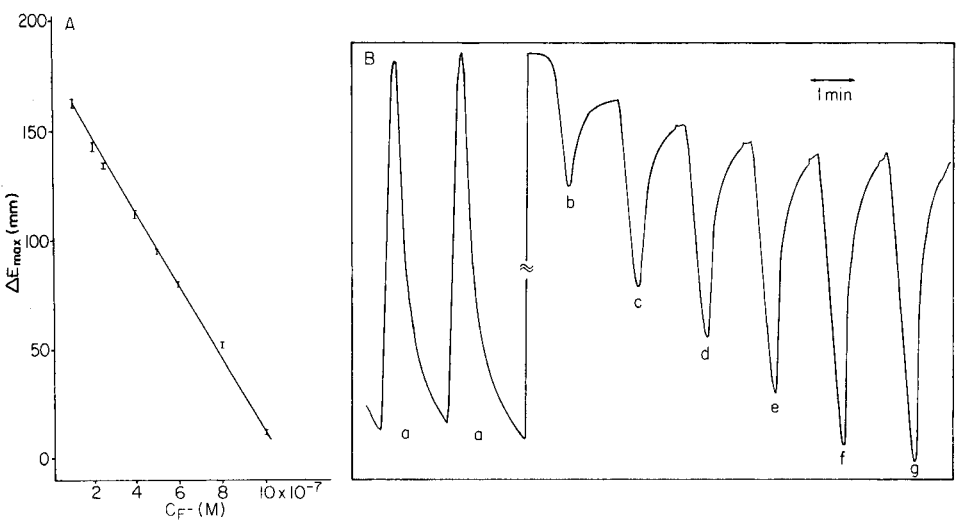

Fig. 5. Calibration graph (A) and recording (B) for flow-injection fluoride measurements. Conditions: 1.0 ml min^{-1} flow rate, 1-m coil length, 250-μl injections, 1×10^{-6} M fluoride in TISAB as carrier. Injected fluoride concentration: (a) 2.5×10^{-6} M; (b) 8.0×10^{-7} M; (c) 6.0×10^{-7} M; (d) 5.0×10^{-7} M; (e) 4.0×10^{-7} M; (f) 2.5×10^{-7} M; (g) 2.0×10^{-7} M.

membrane components ensures favourable long-term stability and lifetime. These properties make the sensor useful as a detector in continuous analyzers for precise monitoring of the potassium ion activity or concentration in blood serum and whole blood. Work on such determinations by continuous flow techniques has been reviewed by Meier et al. [25]. However, flow-injection techniques have rarely been used for this determination, possibly because of the difficulties connected with the required high precision [26].

The new bis(crown ether), 2,2-bis[3,4-(15-crown-5)-2-nitrophenylcarbamoxymethyl]tetradecane (BME-44) [24], was applied here in a flow-injection system for the determination of the potassium ion content of blood serum. The measuring set-up was similar to that used for the determination of fluoride. The indicator electrode was a Horiba 8411-A flow-through electrode incorporating the BME-44-based potassium sensor; the reference was a Horiba 2431-A flow-through Ag/AgCl electrode. A straight teflon tube (0.5 mm i.d., 10 cm long) served as the dispersion section. The sample volume injected was 20 μl.

The calibration properties relevant to batch and continuous flow measurements are shown in Fig. 6. The selectivity coefficient for potassium against

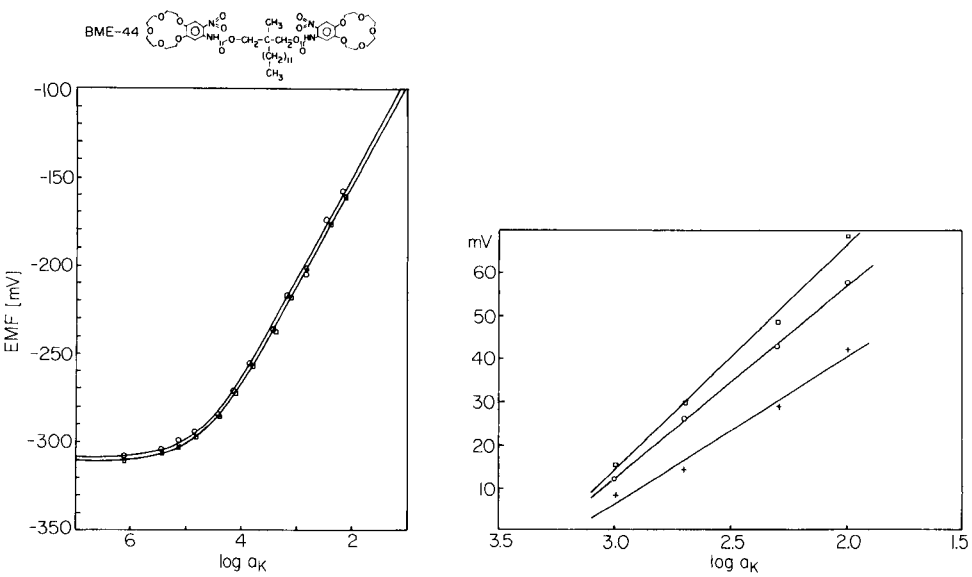

Fig. 6. Calibration properties of the BME-44-based potassium ion-selective electrode in an electrolyte corresponding to blood serum (140.0 mmol l^{-1} Na^+, 1.1 mmol l^{-1} Ca^{2+}, 0.6 mmol l^{-1} Mg^{2+}, 119.4 mmol l^{-1} Cl^-, and 24.0 mmol l^{-1} HCO_3^-). (○) Stationary solutions; (□) flowing solution (2 ml min^{-1}; 0.23 ml min^{-1} through the reference electrode).

Fig. 7. Flow-injection calibration graphs for potassium assay. Potassium concentration added to electrolyte: (□) 1×10^{-5} M; (○) 5×10^{-5} M; (+) 1×10^{-4} M. Conditions: volume injected, 20 μl; flow rate, 0.8 ml min^{-1}; length of tubing (0.5 mm i.d.) from injection point to detector, 100 mm.

sodium was log $K^{pot}_{K,Na} = -3.6$. In the application to the determination of potassium in blood serum in a flow-injection system, the selectivity of the sensor is important, as it will greatly affect the accuracy of the results. To mitigate selectivity problems and matrix effects, the electrolyte chosen contained the main components of blood serum with potassium ions added. Different concentrations of potassium ion (10^{-5} M, 5×10^{-5} M and 10^{-4} M) were tested; with respect to sensitivity, the addition of 1×10^{-5} M potassium ion to the electrolyte (see legend to Fig. 6) proved to be the most appropriate for the carrier solution (Fig. 7).

The potassium ion concentrations of blood sera determined with the new bis(crown ether) sensor showed good correlation with those measured with a valinomycin-based sensor and also with flame-photometric data. To indicate the precision of the measurements, 1×10^{-3}, 2×10^{-3} and 5×10^{-3} M potassium solutions were injected; the mean peak heights obtained ($\pm 2\sigma$, $n = 10$) were 18.66 ± 0.34, 30.62 ± 0.61 and 50.64 ± 0.71 mV, respectively. The results prove that the new potassium-selective sensor can be used successfully in a flow-injection system for the determination of the potassium ion concentration in blood serum.

The authors thank B. Ágai, I. Bitter and L. Töke for their collaboration in developing the new potassium ionophore, and H. Puxbaum for discussions on the problems of determining fluoride in rain water.

REFERENCES

1 E. Pungor, Zs. Fehér and M. Váradi, CRC Crit. Rev. Anal. Chem., 9 (1980) 97.
2 E. G. Harsányi, K. Tóth, L. Pólos and E. Pungor, Anal. Chem., 54 (1982) 1094.
3 A. Hulanicki, A. Lewenstam and M. Maj-Zurawska, Anal. Chim. Acta, 107 (1979) 121.
4 M. Trojanowicz and W. Matuszewski, Anal. Chim. Acta, 138 (1982) 71.
5 E. Lindner, K. Tóth and E. Pungor, Anal. Chem., 54 (1982) 72.
6 E. Pungor, Zs. Fehér, G. Nagy, K. Tóth, Gy. Horvai and M. Gratzl, Anal. Chim. Acta, 109 (1979) 1.
7 J. Slanina, W. A. Lingerak and F. Bakker, Anal. Chim. Acta, 117 (1980) 91.
8 D. Midgley, Anal. Chem., 49 (1977) 1211.
9 E. Lindner, K. Tóth and E. Pungor, Anal. Chem., 48 (1976) 1051.
10 R. C. Hawkings, L. P. V. Corriveau, S. A. Kushneriuk and P. Y. Wong, Anal. Chim. Acta, 102 (1978) 61.
11 J. Buffle and N. Parthasarathy, Anal. Chim. Acta, 93 (1977) 111.
12 W. E. Morf and W. Simon, in H. Freiser (Ed.), Ion-Selective Electrodes in Analytical Chemistry, Vol. 1, Plenum Press, New York, 1978, p. 211.
13 Zs. Fehér, G. Nagy, K. Tóth and E. Pungor, Anal. Chim. Acta, 98 (1978) 193.
14 J. Cl. Landry, F. Cupelin and C. Michal, Analyst (London), 106 (1981) 1275.
15 U. Oesch, P. Anker, D. Ammann and W. Simon, in E. Pungor and I. Buzás (Eds.), Ion-Selective Electrodes, Akadémiai Kiadó, Budapest, 1985, p. 81.
16 E. Lindner, K. Tóth and E. Pungor, Anal. Chem., 54 (1982) 202.

17 M. Gratzl, E. Lindner and E. Pungor, Anal. Chem., 57 (1985) 1506.
18 R. E. Reinsfelder and F. A. Schultz, Anal. Chim. Acta, 65 (1973) 425.
19 E. H. Hansen, A. K. Ghose and J. Růžička, Analyst (London), 102 (1977) 705.
20 P. C. Meier, D. Ammann, H. F. Osswald and W. Simon, Med. Progr. Technol., 5 (1977) 1.
21 U. Oesch and W. Simon, Anal. Chem., 52 (1980) 692.
22 P. van den Winkel, G. De Backer, M. Vandeputte, F. Mertens, L. Dryon and D. L. Massart, Anal. Chim. Acta, 145 (1983) 207.
23 J. Slanina, F. P. Bakker, P. A. C. Jongejan, L. Van Lamoen and J. J. Möls, Anal. Chim. Acta, 130 (1981) 1.
24 J. Tarcali, G. Nagy, G. Juhász, K. Tóth, T. Kukorelli and E. Pungor, Anal. Chim. Acta, 178 (1985) 231.
25 P. C. Meier, D. Ammann, W. E. Morf and W. Simon, in J. Koryta (Ed.), Medical and Biological Applications of Electrochemical Devices, Wiley, New York, 1980, p. 13.
26 J. Růžička, E. H. Hansen and E. A. Zagatto, Anal. Chim. Acta, 88 (1977) 1.

Analytica Chimica Acta, 179 (1986) 371—379
Elsevier Science Publishers B.V., Amsterdam — Printed in The Netherlands

A GLUCOSE SENSOR BASED ON GLUCOSE DEHYDROGENASE ADSORBED ON A MODIFIED CARBON ELECTRODE

GYÖRGY MARKO-VARGA, ROGER APPELQVIST and LO GORTON*
Department of Analytical Chemistry, University of Lund, P.O. Box 124, S-221 00 Lund (Sweden)

(Received 27th August 1985)

SUMMARY

A glucose sensor is prepared by adsorption of the mediator Meldola blue (*N,N*-dimethyl-7-amino-1,2-benzophenoxazinium ion) as well as glucose dehydrogenase, on the surface of a carbon electrode. The nicotinamide coenzyme, which is present in the solution, is reduced in the enzymatic reaction and is re-oxidized amperometrically at 0 mV vs. Ag/AgCl. The properties of such electrodes depend on whether the mediator or the enzyme is adsorbed first; possible models for the molecular arrangements at the surface are discussed. The modified electrode is mounted in a flow-through cell in a flow-injection system and tested with 50-μl injections of β-D-glucose. The calibration graphs were linear in the range 5×10^{-6}—2×10^{-3} M β-D-glucose with the highest sensitivity at pH 6.0. The membrane-free enzyme electrode has a fast response; peak widths are 12 s at half height (flow rate 0.7 ml min^{-1}), making it possible to process 100 samples h^{-1}.

Chemically modified electrodes [1] offer new possibilities of preparing electrochemical sensors, particularly for monitoring enzymatic reaction products which otherwise would require high overvoltages. Meldola blue adsorbs spontaneously on graphite or carbon electrodes and the modified electrode will oxidize the reduced nicotinamide coenzymes even around 0 V vs. SCE [2, 3]. An enzyme can be adsorbed on graphite materials with retained catalytic activity [4—6] and it should, therefore, be possible to prepare membrane-free enzyme electrodes. This paper reports on the properties of a sensor made by adsorption of mediator as well as glucose dehydrogenase on the same surface.

EXPERIMENTAL

Carbon rods (Ringsdorff-Werke; RW 203, 3.1-mm diameter) were polished on wet, fine emery paper and mounted in a flow-through cell so that only the circular end surface contacted the solution. The enzyme adsorbs better to carbon than to graphite and the former material was therefore preferred in this study. Electrodes made from carbon were noisier, however, and they had higher background currents than those made from graphite. Electrode modification was done [2, 3] by dipping the electrode into a solution of

0003-2670/86/$03.50

Meldola blue (*N,N*-dimethyl-7-amino-1,2-benzophenoxazinium ion, MB^+; Boehringer-Mannheim, cat. no. 258 504) until the surface coverage, as determined by cyclic voltammetry, became about 10 nmol cm^{-2}. About 10 μl of glucose dehydrogenase (EC. 1.1.1.47 from *Bacillus megaterium*, 500 IU ml^{-1}; United States Biochemical Corp., Cleveland) was applied on the surface of the Meldola blue-modified electrode. The electrode was washed after 5 min and it was then ready for use.

1,4-Dihydronicotinamide adenine dinucleotide (NADH) and NAD^+ (nicotinamide adenine dinucleotide) were obtained from Sigma (cat. nos. N-8129 and N-7004, respectively) and used as received. The concentrations of solutions were calculated from the known molar absorptivities.

The electrode was mounted in a flow-through cell of the confined wall jet type with a distance of 1.4 mm between the jet and the electrode surface. The properties of the flow-through cell have been described previously [3]. The dispersion coefficient [7] of the complete flow-injection system was 1.15 for glucose. The sample volume was 50 μl and the carrier solution was a 0.1 M phosphate buffer containing 2.5 mM NAD^+. The response of the glucose sensor increased with the coenzyme concentration to a plateau which was reached around 2 mM NAD^+. A potential of 0 mV vs. Ag/AgCl/0.1 M KCl was applied to the working electrode with a potentiostat. The background current reached a constant level of 50 nA after about 30 min and the noise was then 5—10 nA with the potentiostat time constant set to 0.3 s.

RESULTS AND DISCUSSION

Effect of differences in the preparation

The response factor (i.e., the sensitivity) increased with time of contact between the enzyme solution and a carbon rod saturated with Meldola blue (Table 1). The results can be explained by assuming that the response is approximately proportional to the amount of enzyme on the electrode and that a certain number of enzyme molecules can find sites on the surface. Saturation seems to be complete after about 1.5 min and no more enzyme could be adsorbed from a solution which was twice as concentrated.

Two procedures were used to prepare the enzyme electrodes. Either the mediator was adsorbed first and the enzyme afterwards (method I) or they were adsorbed in the reverse order (method II). The response factors varied with the amount of mediator as shown in Fig. 1 for electrodes prepared by the two methods. The electrodes had been saturated with enzyme (see above). Each point in Fig. 1 represents a different electrode and the smoothness of the curves also illustrates, therefore, that the preparation was fairly reproducible. Electrodes prepared by method I show a high level of activity even at low coverages for both NADH and glucose samples (curves b and c). The activity/coverage relation (curve c) is in fact fairly similar to that observed earlier for NADH alone at a Meldola blue-modified

TABLE 1

Electrode sensitivity as a function of the time allowed for adsorption of enzyme[a]

Time (min)	0.5	1.0	1.5	2.5	3.0	4.0
Current (μA)	1.60	1.63	1.89	1.89	1.88	1.87

[a]Conditions: pH 6.0, 2 mM NAD^+, 1 mM β-D-glucose, flow rate 1 ml min^{-1}, applied potential 0 mV, surface coverage 17 nmol cm^{-2}.

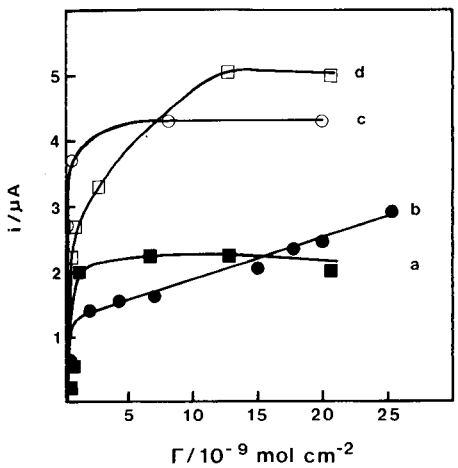

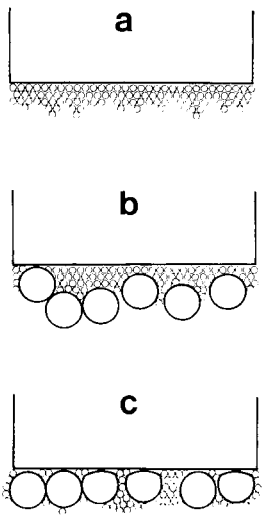

Fig. 1. Peak heights obtained with 50-μl samples containing 0.5 mM NADH or 1 mM β-D-glucose with electrodes prepared by different methods: (a) β-D-glucose, method II, (b) β-D-glucose, method I; (c) NADH, method I; (d) NADH, method II. Conditions: pH 6.0, 2.0 mM NAD^+, flow rate 0.7 ml min^{-1}, applied potential 0 mV.

Fig. 2. Models of the molecular arrangement on the surface of modified electrodes when much more mediator is applied than for a monolayer coverage: (a) mediator only; (b) mediator applied first, enzyme afterwards (method I); (c) enzyme applied first, mediator afterwards (method II). Large spheres represent the adsorbed glucose dehydrogenase and small spheres Meldola blue.

graphite electrode [3]. The currents were about 25% less, however, probably because the enzyme layer decreased the transport rate of NADH.

The response for NADH increased gradually for electrodes prepared with method II (curve d) and the explanation may be that the enzyme blocks a large number of adsorption sites if it is applied first (see Fig. 2c). Meldola blue is assumed to form a monolayer on graphite at a surface coverage of about 1×10^{-9} mol cm^{-2} [2] and the mediator molecules will stack on top of each other if the coverage is increased above this value. The contact between the carbon and the mediator will be restricted to fewer places with

electrodes prepared by method II, than with electrodes prepared by method I (Fig. 2b). The glucose response increased with coverage for electrodes prepared by method I, although the NADH response remained constant. The reason may be that the enzyme molecules can penetrate into the mediator layers so that a good diffusional contact can be established (Fig. 2b). The constancy of the response to glucose for electrodes made by method I (curve a), in spite of the increasing NADH response (curve d), may be due to a decrease in the diffusion of glucose by mediator stacked at the outer part of the enzyme molecules. The differences in the mediator saturation concentrations, as indicated by the last point on curves a and b in Fig. 1, may be due to blocking of the carbon surface by enzyme molecules when the electrode is made by method II.

The mediator molecules must contact each other so that intermolecular electron transfer can take place; otherwise, there will be no mediation, and no change of redox state during a voltammetric sweep; i.e., non-contacting molecules will be electrochemically inert. Any mediator molecules adsorbed on the enzyme (Fig. 2c) will also be unable to transfer charges to the electrode. The possibility of charge transfer through molecular diffusion of mediator molecules can be ruled out with reference to the stability of the electrode. Diffusing mediator molecules would quickly be lost to the surrounding, flowing, mediator-free solution.

The difference in curve shape for electrodes prepared by the two methods can be explained if it is assumed that more enzyme can be adsorbed on a naked than on a mediator-covered electrode. The thick enzyme layer will reduce the transport rate of NADH to the mediator very near the carbon surface; low currents were obtained at low coverages (Fig. 1, curve d). Stacked mediator molecules will be accessible from the sides, through the enzyme, so that high currents will be obtained at high coverages. With glucose samples, the amount of NADH which is produced will depend on the amount of enzyme and on the probability of catching the NADH molecules before they are lost to the bulk solution. The mediator will catch more NADH as the stacks become more extended.

The electrochemical reactions at constant pH have been described [2, 3]. First, the charge-transfer complex $NADH \cdot MB^+$, is formed in equilibrium with the two reactants, and decomposes in a rate-limiting step to produce NAD^+ and the reduced mediator MBH, which is oxidized electrochemically to MB^+ in a fast 2-electron step. Addition of large amounts of mediator will have little effect because of the rate limitation in the second step and possibly because of limited access of NADH to mediator molecules inside the stacks. A rate limitation will give an almost constant sensitivity, (i.e., an almost horizontal line in Fig. 1) at high mediator coverages.

Electrode properties

Only electrodes prepared by method I and saturated with enzyme were investigated. A main reason for preferring this type of electrode was that it

produced less electrical noise, probably because of lower surface resistance. The response factor for NADH remained essentially constant for a few hours, but decreased by 10—15% for glucose during the first 15 min. The sensitivity for glucose then stabilized and remained fairly constant for a few hours, depending on the number of glucose injections, and also depending on the particular electrode specimen. The initial decrease started only when glucose samples were introduced, even if this was done after carrier or NADH samples had been pumped for long time spans.

Dehydrogenases are known to change their conformation during catalysis and this could explain the observed stabilities. Some loosely bound enzyme is shed during the first 15 min of glucose sample introduction and the thickness of the enzyme layer will thus decrease. More NADH will therefore be able to reach the mediator and the response factor for NADH will increase slightly. Conformational changes of the enzyme is probably a major reason for loss of activity even later in the electrode life, because the response factor for glucose decreased more quickly when more frequent injections were made. The enzyme purity is also of importance; it was found that the reproducibility of electrodes prepared from an old enzyme solution was less satisfactory. The mediator was also deactivated but the effect on the response was small for high coverages (cf. Fig. 1). Cyclic voltammetry showed that the coverage decreased 20—30% during a day.

Table 2 indicates the peak heights obtained for injections of 1-mM samples of NADH and glucose. The peak height for a glucose sample is much smaller than that for NADH, because only a fraction of the glucose reacts to give NADH. As there is no NADH in the bulk solution in this case, NADH diffuses both towards the mediator molecules and into the surrounding medium. The overall apparent conversion of glucose was 24%.

The response of the electrode in the flow system depends on the flow rate (Fig. 3). The flow dependence of the wall-jet electrode itself was studied with a naked electrode and an electrochemically reversible compound. The current increased rapidly up to about 1 ml min^{-1} and then somewhat more slowly at higher flow rates (not shown). The steady-state response of the modified electrode for NADH increased less rapidly with the flow rate

TABLE 2

Sensitivity of a modified electrode prepared by method I[a]

Electrode	Current (μA)	
	1 mM NADH	1 mM β-D-Glucose
Mediator only	12	0
Mediator first, enzyme next	8.6	2.1

[a]Conditions: pH 6.0, 2.5 mM NAD^+, flow rate 0.7 ml min^{-1}, applied potential 0 mV, surface coverage 8.2 nmol cm^{-2}.

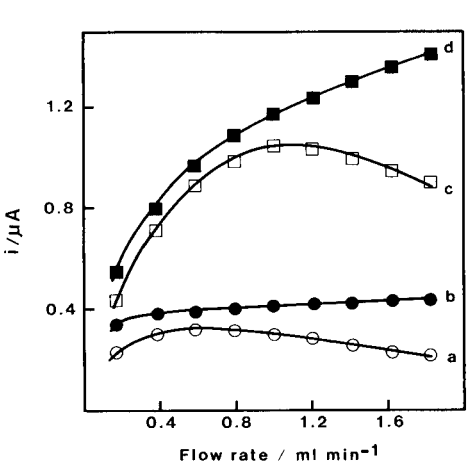

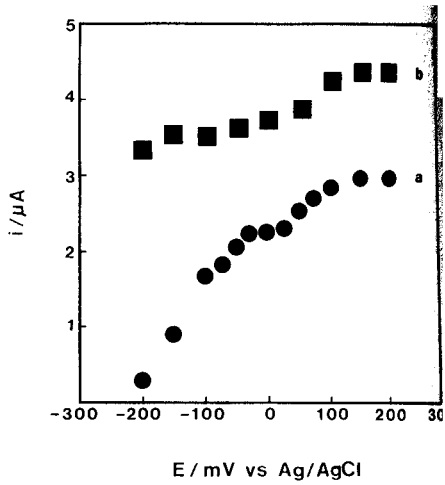

Fig. 3. The flow dependence of the modified electrode (method I) mounted in a confined wall-jet cell (pH 6.0, 2.5 mM NAD^+, applied potential 0 mV): (a) 0.1 mM β-D-glucose, peak height; (b) 0.1 mM β-D-glucose, steady-state; (c) 0.1 mM NADH, peak height; (d) 0.1 mM NADH, steady-state.

Fig. 4. Current vs. applied voltage for the modified electrode (method I). Conditions: pH 6.0, 2.5 mM NAD^+, flow rate 0.7 ml min^{-1}, applied potential 0 mV. Sample: (a) 1 mM β-D-glucose; (b) 1 mM NADH.

because of the slowness of the transport in the enzyme layer (curve d). Theory for membrane electrodes [8], and in particular for enzyme electrodes, predicts that the peak height should decrease with flow rate when the membrane diffusion time becomes long compared to the injection profile in time units. This is actually observed at high flow rates (Fig. 3, curve c). The steady-state response for glucose is governed by the rate of reaction of the enzyme and the collection efficiency of the formed NADH. The concentration polarization of glucose just outside the enzyme layer will decrease as the flow rate increases, which acts to increase the sensitivity. The increased flow will, however, also increase the loss of NADH, which tends to decrease the sensitivity. These two effects seem to balance out over much of the range (Fig. 3, curve b). The response for a transient input profile in glucose is shown by curve a. The peak height becomes a somewhat smaller fraction of the steady-state response because of the combined effects of membrane diffusion and enzyme kinetics.

The formal potential of the mediator is −195 mV vs. Ag/AgCl/0.1 M KC at pH 6.0 [2] and a modified electrode without enzyme reaches a voltammetric plateau at −150 mV which remains flat to large positive voltages The enzyme-covered electrode behaved differently in that a further increase in current was observed at +50 mV (Fig. 4, curve b). A corresponding increase can also be seen on the glucose response curve. The effect may be due to voltage-induced changes in the enzyme layer so that transport of NADH is facilitated. The production of glucose does not reach full speed

unless the applied voltage is at least 0 mV, which suggests that the enzyme is affected by the applied voltage.

Series of glucose samples (50 μl) were injected and the corresponding calibration graphs were drawn (Fig. 5, part of the range). The plots were linear from the detection limit, 4—5 μM, to 2 mM β-D-glucose. Highest sensitivity was reached at pH 6 where the NADH · MB^+ complex decomposes quickly and the enzymatic reaction is fairly close to its pH optimum (pH 7.5 for soluble glucose dehydrogenase). The NADH·MB^+ mediator reaction is so much slower at pH 7.0 that lower sensitivity is obtained despite the faster

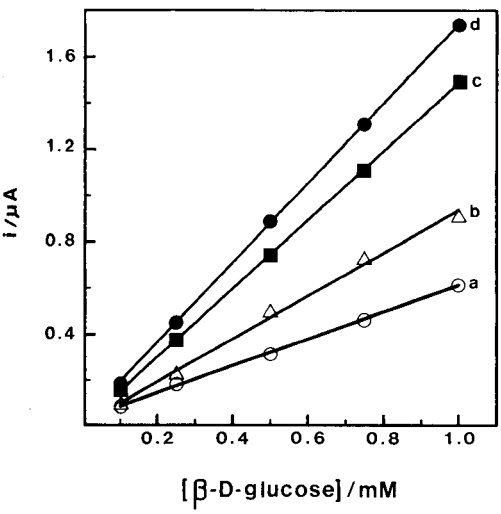

Fig. 5. Calibration graphs for glucose with the modified electrode (2.5 mM NAD^+, flow rate 0.7 ml min^{-1}, applied potential 0 mV): (a) pH 4.0; (b) pH 5.0; (c) pH 7.0; (d) pH 6.0.

TABLE 3

Relative responses of soluble glucose dehydrogenase [9] and of the glucose sensor with adsorbed enzyme[a]

Substrate	Soluble enzyme (%)	Glucose sensor (%)	Substrate	Soluble enzyme (%)	Glucose sensor (%)
β-D-Glucose	—	100	β-Lactose	—	<0.1
D-Glucose	100	64	β-D(—)-Fructose	0	<0.1
2-Deoxy-D-glucose	114	67	Sucrose, raffinose	—	<0.1
D(+)-Xylose	6	1	D(+)-Galactose	0	<0.1
D(+)-Mannose	0.8	0.7	Xylitol, sorbitol	—	<0.1
D(+)-Glucosamine	—	1.4	D-Arabinose	0	<0.1
D(+)-Cellubiose	—	0.2			

[a]Conditions: pH 6.0, 2.5 mM NAD^+, 1 mM substrate, flow rate 0.7 ml min^{-1}, applied potential 0 mV.

rate of the enzymatic reaction. The lower sensitivity at pH 5.0 and 4.0 is due to the slow enzymatic reaction.

The selectivity (Table 3) depends on the relative rate of substrate supply, enzyme catalysis, and coenzyme re-oxidation. The selectivity of this glucose sensor was better than that obtained with a packed bed reactor [3], which is expected from the theory for reactors with high conversion. It also exceeded the reported selectivity of the soluble enzyme [9], probably because of differences in the reaction conditions.

Conclusions

Several types of enzyme electrodes with short membrane-diffusion time constants have been described [10] and have been adapted to fast flow-injection systems with sampling frequencies of up to 300 samples h^{-1}, as will be described elsewhere. Direct immobilization of enzyme on the electrode surface represents another approach to making fast enzyme electrodes which should have some advantages. Sampling frequencies of about 100 samples h^{-1} could be reached with the present electrodes. The peak widths at half peak heights were of the order of 12 s at a flow rate of 0.7 ml min^{-1}.

Electrode modification by adsorption of a mediator makes it possible to oxidize the coenzyme around potentials at which the residual current is quite low and at which there are few electrochemical interferences from other oxidizing or reducing reactions.

The limited stability of the electrode is partly offset by the simple preparation, but future work will be directed towards improving both the mediator and the enzyme binding to the electrode surface. Covalent immobilization of another enzyme, glucose oxidase, to graphite electrode surfaces has proved to be extremely stable [11] (several months), although the mediator in this case was unstable. Another mediator for the nicotinamide coenzyme oxidation was found to desorb much less [12] and to be more stable in alkaline solution [13], although its reaction rate was almost an order of magnitude less than that of Meldola blue. The prospects of future progress in this area seems therefore to be good.

The authors thank Prof. Gillis Johansson for valuable discussions. This work was supported by grants from the Swedish Natural Research Council.

REFERENCES

1 R. W. Murray, in A. J. Bard (Ed.), Electroanalytical Chemistry, Vol. 13, Dekker, New York, 1984, p. 191.
2 L. Gorton, A. Torstensson, H. Jaegfeldt and G. Johansson, J. Electroanal. Chem., 161 (1984) 103.
3 R. Appelqvist, G. Marko-Varga, L. Gorton, A. Torstensson and G. Johansson, Anal. Chim. Acta, 169 (1985) 237.
4 V. J. Razumas, J. J. Jasaitis and J. J. Kulys, Bioelectrochem. Bioenerg., 12 (1984) 297.

5 T. Ikeda, I. Katasho, M. Kamei and M. Senda, Agric. Biol. Chem., 48 (1984) 1969.
6 J. F. Castner and L. B. Wingard, Jr., Biochemistry, 23 (1984) 2203.
7 J. Růžička and E. H. Hansen, Flow Injection Analysis, Wiley, New York, 1981.
8 L. O. Mell and J. T. Maloy, Anal. Chem., 47 (1979) 299.
9 H. E. Pauly and G. Pfleiderer, Hoppe-Seyler's Z. Physiol. Chem., 356 (1975) 1613.
10 G. G. Guilbault, Analytical Uses of Immobilized Enzymes, Dekker, New York, 1984.
11 G. Jönsson and L. Gorton, Biosensors, in press.
12 L. Gorton, G. Johansson and A. Torstensson, J. Electroanal. Chem., 196 (1985) 81.
13 M. Kotouček and J. Zavadilová, Collect. Czech. Chem. Commun., 37 (1972) 3212.

Analytica Chimica Acta, 179 (1986) 381—388
Elsevier Science Publishers B.V., Amsterdam — Printed in The Netherlands

CONSTANT-POTENTIAL PULSE POLAROGRAPHIC DETECTION IN FLOW-INJECTION ANALYSIS WITHOUT DEAERATION OF SOLVENT OR SAMPLE

GLEN G. NEUBURGER and DENNIS C. JOHNSON*
Department of Chemistry, Iowa State University, Ames, IA 50011 (U.S.A.)
(Received 7th August 1985)

SUMMARY

A constant-potential pulse waveform is applicable for the polarographic analysis of buffered solutions (pH $\leqslant$ 7) of cathodically active metal ions without voltammetric interference from dissolved oxygen. The technique is demonstrated at a dropping mercury electrode for detection of lead(II) and cadmium(II) in a conventional polarographic cell (ca. 75 ml) as well as for small samples (2 ml) in a flow-injection system. The flow-injection polarographic technique is recommended for higher sample throughput than conventional polarography and is demonstrated for an electroless copper plating solution containing about 1.5×10^{-2} M copper(II).

The necessity of thorough deaeration of solutions prior to polarographic analysis to eliminate faradaic interference from reduction of dissolved oxygen is well known [1, 2]. Oxygen is reduced to hydrogen peroxide (n = 2) with $E_{1/2}$ = ca. 0.0 V vs. SCE, and the peroxide is then reduced to water (n = 4 for $O_2 \rightarrow H_2O$) with $E_{1/2}$ = ca. −1.2 V. This electroactivity of oxygen over ca. 80% of the accessible potential range at mercury electrodes has been a major deterent to their application for cathodic detections in flow-injection and liquid chromatographic systems [3, 4]. Various approaches have been described for elimination of dissolved oxygen in flow systems [3, 5] including placement of the entire apparatus in a drybox purged with inert gas [6]. Here, the use of constant-potential pulse (c.p.p.) polarography is demonstrated for eliminating interference from dissolved oxygen in polarographic determinations of reducible metal ions. The significance of the c.p.p. waveform (E/t) is made apparent by comparison to the more familiar normal pulse (n.p.) and reverse-pulse (r.p.) polarographic methods.

Normal-pulse polarography is well known for increased sensitivity (μA M^{-1}) in comparison to linear-sweep (d.c.) polarography. The n.p. waveform, as depicted in Fig. 1A for a reducible analyte, utilizes a value of initial potential more positive than the half-wave potential of the analyte ($E_i \geqslant E_{1/2}$) with a negative scan of ΔE. The ratio of the limiting currents for n.p. and d.c. polarography at a dropping mercury electrode (DME) is given by

0003-2670/86/$03.50

$$i_{n.p.}/i_{d.c.} = (3\tau/7t_p)^{1/2} \quad (1)$$

where τ is the drop lifetime, t_p is the pulse period and $\tau = t_i + t_p$ [7]. The value of $i_{d.c.}$ is given by

$$i_{d.c.} = nFAC^b\ (7D/3\pi\tau)^{1/2} \quad (2)$$

where n, F, A and C^b have their usual electrochemical significance.

Oldham and Parry [8] described scan-reversal polarography in which the n.p.p. waveform is applied but with polarities reversed, i.e., $E_i \ll E_{1/2}$ and ΔE is scanned in a positive direction. Osteryoung and Kirowa-Eisner [9] reviewed the theory and assigned the preferred name of reverse-pulse polarography (r.p.p.). In r.p.p., applied for a reducible analyte, the product of the cathodic reaction at E_i can be detected anodically for $E_d \gg E_{1/2}$, where $E_d = E_i + \Delta E$, and the i/E response curve contains both the cathodic and anodic components characteristic of the redox couple. Oldham and Parry [8] recommended this technique for study of electrochemical reversibility and this application has been pursued by others [10, 11].

In r.p.p. at a DME, the limiting cathodic current detected at $E_d \ll E_{1/2}$ is equal to $i_{d.c.}$ (Eqn. 2). The limiting anodic current ($i_{r.p.}$) for $E_d \gg E_{1/2}$ is related to $i_{d.c.}$ by

$$-i_{r.p.}/i_{d.c.} = (n_{red}/n_{ox})\ \{(3\tau/7t_p)^{1/2} - [3\tau/(3\tau + 7t_p)]^{1/2}\} \quad (3)$$

where n_{red} and n_{ox} are the numbers of electrons for the reductive and oxidative processes, respectively [8, 9]. For $t_p \ll \tau$, Eqn. 3 simplifies to

$$-i_{r.p.}/i_{d.c.} = (n_{red}/n_{ox})[(3\tau/7t_p)^{1/2} - 1] \quad (4)$$

and in the limit for $\tau/t_p \to \infty$, Eqn. 4 becomes identical to Eqn. 1 for $n_{red} = n_{ox}$. If the product of the reaction at E_i undergoes an irreversible homogeneous conversion to an electro-inactive product, $i_{r.p.}$ is less than predicted by Eqn. 3 [9] and the deviation can be applied for kinetic studies of following chemical reactions coupled to the electron-transfer processes [12].

Maitoza and Johnson [13] recognized that when r.p.p. is used, dissolved oxygen is not detected for $E_d \gg$ ca. 0.0 V vs. SCE, because of the irreversibility of the reduction of oxygen at mercury. They demonstrated that the amperometric form of r.p.p. (i.e., constant ΔE) can be used for detection of reducible metal ions without interference from oxygen in flow-injection and liquid-chromatographic analyses using a flow-through detector based on a DME. Hsi and Johnson [14] recently applied this technique for the ion-chromatographic determination of Cu^{2+}, Zn^{2+}, Ni^{2+}, Pb^{2+}, Cd^{2+} and Fe^{2+}, using a low capacity cation-exchange column with a tartrate buffer (pH 3.5—4.5) containing magnesium ion as the mobile phase. Representative detection limits for 100-μl samples were 1.3 ng Zn^{2+} and 6.4 ng Cu^{2+}. The detection limits were lowered 100-fold by using a 10-ml sample with on-line preconcentration on a high-capacity precolumn.

Christie et al. [15] introduced constant-potential pulse polarography

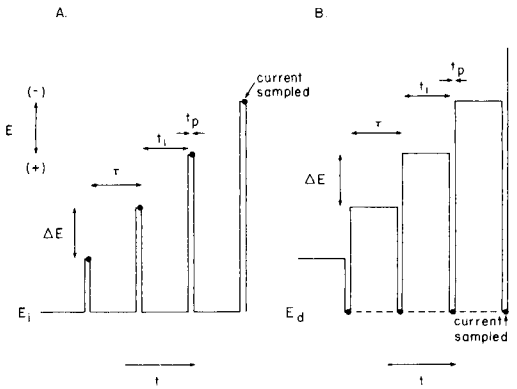

Fig. 1. Pulse waveforms for reducible analytes: (A) normal-pulse polarography (n.p.p.); (B) constant-potential pulse polarography (c.p.p.p.).

(c.p.p.p.) (see waveform B in Fig. 1). Their study emphasized the comparison of faradaic and capacitive responses of c.p.p.p. with n.p.p. and differential pulse polarography (d.p.p.). In c.p.p.p., E_i is scanned with current sampling at a constant detection potential, E_d, and the current measured at E_d is plotted vs. E_i. The i/E response curve obtained for a reducible analyte with $E_d \ll E_{1/2}$, in the absence of dissolved oxygen, will be similar to that for r.p.p. The i/E curve for $E_d \gg E_{1/2}$ will show only an anodic wave with a limiting current ($i_{c.p.p.}$) equal to $i_{r.p.}$ (see Eqns. 1—3). Hara and Nomura [16] applied c.p.p.p. for the determination of barium(II) and alkali metal cations in solutions of low pH. The reduction waves for these species are hidden by the large current for reduction of H^+ at the mercury electrode. The applicability of r.p.p. for the study of waves unresolved from solvent breakdown was recognized by Osteryoung and Kirowa-Eisner [9].

Hara and Nomura [16] noted for c.p.p.p., in agreement with Maitoza and Johnson [13] for r.p.p., that dissolved oxygen is not detected for $E_d \gg$ ca. 0.0 V. It should be noted that the waveforms for the amperometric versions of r.p.p. and c.p.p.p. are identical (ΔE is constant). Here c.p.p.p. is applied in the analysis of solutions of reducible metal ions in conventional polarographic cells and in a flow-injection system without interference from dissolved oxygen. The use of flow-injection c.p.p.p. without deaeration is recommended to increase significantly the sample throughput of polarography.

EXPERIMENTAL

All solutions were prepared from analytical reagent-grade chemicals (Fisher Scientific certified A.C.S. grade) and triply distilled water. Mercury was triply distilled. When applicable, solutions were deaerated by purging with reagent-grade argon (99.99%) for 10 min. The supporting electrolyte was 0.1 M KNO_3/0.01 M HNO_3 in all cases.

A modified Model 264A Polarographic Analyzer (EG&G Princeton Applied Research Corporation) was used. The analyzer was modified by EG&G PARC to conform to the technique of c.p.p.p. A mechanical drop-timer assembly (PARC Model 174/70) was used with the DME and a lifetime of 1.0 s was chosen for all work. A natural lifetime of ca. 10 s was selected to minimize noise caused by mechanical vibrations of the drop. Polarograms were recorded on an X—Y recorder (PARC Model RE0074) or a strip chart recorder (Model 250-1B, Curken Instrument Co., Hawleyville, CT). All potentials are reported versus the SCE.

The flow-injection system consisted of a Gilson Minipuls-2 peristaltic pump in line with two inverted T-shaped pulse dampeners, a 10-foot coil of 0.5-mm i.d. teflon tubing, a manual injection valve (Model CV-6-uHPa-N60; Valco Instrument Co.), and finally a perpendicular flow-cell detector mounted on the end of the DME capillary in the style of the PARC Model 310 detector. The 2-ml sample loop was constructed from 1.0-mm teflon tubing. The retention volume (V_r) of the system from injector to detector was ca. 0.25 ml.

RESULTS AND DISCUSSION

Comparison of the polarographic methods

Current/potential (i/E) curves obtained by r.p.p., n.p.p. and c.p.p.p. are compared in Fig. 2 for 0.5 mM lead(II) and cadmium(II) in 0.1 M KNO_3/0.01 M HNO_3 with and without oxygen present. The reductions of lead(II)

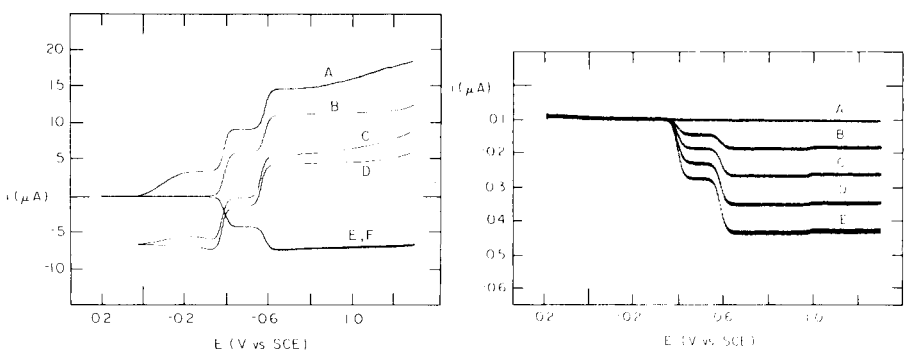

Fig. 2. Current/potential curves for 0.5 mM Pb(II) + 0.5 mM Cd(II) in 0.1 M KNO_3/0.01 M HNO_3. Conditions: ΔE = 5 mV, τ = 1.0 s. Curves: (A) n.p.p. air-saturated, E_i = 0.2 V; (B) n.p.p., argon-saturated, E_i = 0.2 V; (C) r.p.p., air-saturated, E_i = —1.3 V; (D) r.p.p., argon-saturated, E_i = —1.3 V; (E) c.p.p.p., air-saturated, E_d = 0.2 V; (F) c.p.p.p., argon-saturated, E_d = 0.2 V.

Fig. 3. Current/potential curves by c.p.p.p. for Pb(II) and Cd(II) in 0.1 M KNO_3/0.01 M HNO_3. Conditions: ΔE = 5 mV, τ = 1.0 s. Concentrations: (A) blank; (B) 5.0 μM Pb(II), 5.0 μM Cd(II); (C) 10.0 μM Pb(II), 10.0 μM Cd(II); (D) 15.0 μM Pb(II), 15.0 μM Cd(II); (E) 20.0 μM Pb(II), 20.0 μM Cd(II).

and cadmium(II) to their corresponding metal amalgams are reversible with $E_{1/2}$ values of ca. −0.4 V and −0.6 V, respectively. As observed by Maitoza and Johnson [13], the total anodic current in r.p.p. for $E_d \gg 0.0$ V is not a function of dissolved oxygen and r.p. amperometry is useful without deaeration; r.p.p. (with the sweep of E_d) is not particularly useful in the presence of oxygen. Only for c.p.p.p., with constant $E_d \gg 0.0$ V, is the i/E response identical over the entire potential range whether or not oxygen is present. The ratio of the total anodic current for c.p.p.p. to the cathodic current for n.p.p. (with oxygen absent) at −0.7 V is 0.67. This compares favorably with the predicted ratio of 0.65 for t_p = 50 ms and τ = 1 s, on the basis of Eqns. 1—3, using the equality $i_{c.p.p.} = i_{r.p.}$.

The major advantage of all pulse polarographic techniques is the increased signal-to-noise ratio and, therefore, better detection limits are obtained than for d.c. polarography. Because $i_{c.p.p.}$ is nearly 70% the value of $i_{n.p.}$, for this case (τ and t_p values), low detection limits are also expected for c.p.p.p. in addition to the advantage gained by elimination of oxygen interference. Polarographic curves are shown in Fig. 3 for lead(II) and cadmium(II) in the range 5—20 μM with and without deaeration. The thickness of the pen tracing results from instrumental noise originating within the potentiostat, apparently associated with switching in the sample-hold circuit.

Interference from dissolved oxygen is observed in c.p.p.p. in unbuffered solutions, as illustrated in Fig. 4 for 0.1 M KNO_3. This is caused by the increase in pH at the electrode surface resulting from reduction of oxygen with subsequent anodic detection of OH^-:

$$O_2 + 2H_2O + 2e^- \rightarrow H_2O_2 + 2OH^- \quad (0.0\ V > E_i > -1.2\ V) \tag{5}$$

$$O_2 + 2H_2O + 4e^- \rightarrow 4OH^- \quad (-1.2\ V > E_i) \tag{6}$$

$$2OH^- + Hg \rightarrow Hg(OH)_2 + 2e^- \quad (E_d > -0.1\ V) \tag{7}$$

The detection of hydroxide produced by the cathodic reaction at E_i is observed also in r.p.p. and was applied by Brestovisky et al. [17] in a study of the reduction of hydrogen peroxide. Because of the response to hydroxide, c.p.p.p. cannot be applied in alkaline solutions for $E_d > -0.1$ V. When $E_d < -0.1$ V, removal of dissolved oxygen is required.

Interesting results are obtained when the c.p.p.p. waveform depicted in Fig. 1B is applied for analytes which yield anodic waves by stabilizing the product of mercury oxidation (e.g., halides and chelate-forming anions). This application of the waveform should be known as reverse c.p.p.p. and is related to c.p.p.p. in the same manner as r.p.p. is related to n.p.p. Polarographic curves are shown for iodide by reverse c.p.p.p. in Fig. 5 (curves A—E). The electrode reaction for $E \gg$ ca. −0.1 V is

$$2I^- + Hg \rightarrow Hg_2I_2(s) + 2e^- \tag{8}$$

For $E_i \gg -0.1$ V, the anodic current corresponds to $i_{d.c.}$ for iodide. When $E_i \ll$ ca. −0.1 V, the anodic current equals that of $i_{n.p.}$ for iodide. The i/E

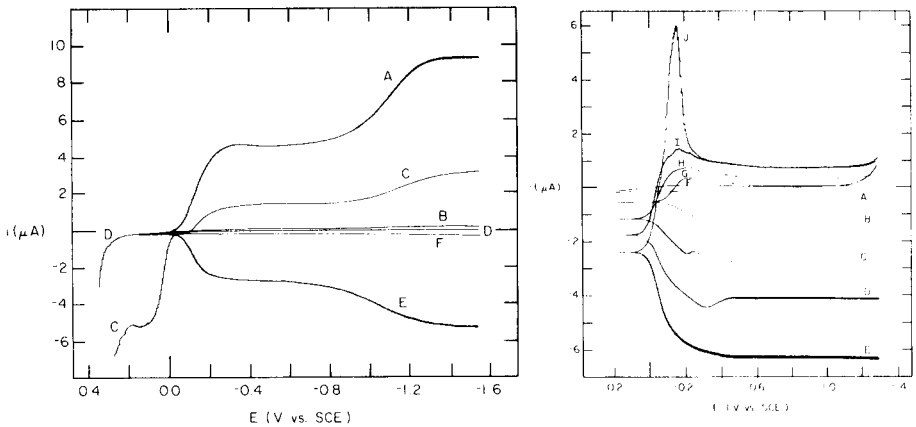

Fig. 4. Current/potential curves for unbuffered 0.1 M KNO_3. Conditions: ΔE = 5 mV, τ = 1.0 s, natural pH = 4.8. Curves: (A) n.p.p., air-saturated, E_i = 0.2 V; (B) n.p.p., argon-saturated, E_i = 0.2 V; (C) r.p.p., air-saturated, E_i = −1.5 V; (D) r.p.p., argon-saturated, E_i = −1.5 V; (E) c.p.p.p., air-saturated, E_d = 0.2 V; (F) c.p.p.p., argon-saturated, E_d = 0.2 V.

Fig. 5. Current/potential curves for iodide in 0.1 M KNO_3/0.01 M HNO_3. Conditions: ΔE = 5 mV, τ = 1.0 s; c.p.p.p. (A—E), E_d = 0.2 V; r.p.p. (F—J), E_i = 0.2 V. Concentration of iodide (mM): (A,F) blank; (B,G) 0.20; (C,H) 0.40; (D,I) 0.60; (E,J) 0.80.

response of reverse c.p.p.p. is more complicated than that for n.p.p. because of the two-step wave, although the advantage is retained regarding tolerance for dissolved oxygen. The slight incongruities in the otherwise smooth *i/E* curves for reverse c.p.p.p. are attributed to the diffusion barrier offered by the surface film of insoluble mercury(I) iodide. Shown for comparison in Fig. 5 (curves F—J) are polarographic curves for iodide obtained by r.p.p. (E_i = 0.2 V) taken in the absence of dissolved oxygen.

Application in flow-injection systems

Elimination of the need for oxygen removal in c.p.p.p. renders this technique suitable for polarographic analysis in automated flow-injection systems. Accordingly, in flow-injection/c.p.p.p., sample volumes (V_s) of 1—2 ml are injected into a flow system having a low retention volume (V_r) between the injection valve and detector. When $V_s \gg V_r$, the system is characterized as having a very low dispersion and there is a significant period of time during which the concentration profile (C vs. t) at the detector is in a steady-state condition ($dC/d_t = 0$) with a plateau concentration equal to the analytical concentration of the sample injected. The *i/t* response is shown in Fig. 6 for injection of 2.0 ml of 2.0 mM cadmium(II) and lead(II) into the flow-injection system with V_r = ca. 0.25 ml and a flow rate of 0.50 ml min^{-1}. For ΔE = 10 mV and τ = 1.0 s, completion of a 1.2-V potential sweep was achieved in 2 min. For this system, an injection interval of ca.

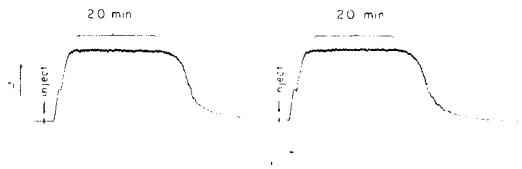

Fig. 6. Current/time profile for pulse amperometric detection in the flow-injection system. Carrier solution: air-saturated 0.1 M KNO_3/0.01 M HNO_3 at 0.50 ml min^{-1}. Sample: 2.0 mM Pb(II) + 2.0 mM Cd(II) in 0.1 M KNO_3/0.01 M HNO_3 ; V_s = 2.0 ml. Detection: E_i = −1.0 V, E_d = 0.2 V; τ = 1.0 s.

6 min allowed for complete washout of the system between samples and the sample throughput of the system was ca. 10 h^{-1}. This throughput could be easily doubled or tripled using smaller V_s and V_r with faster scan rates and shorter drop lifetimes. Application of flow-injection c.p.p.p. for analysis of solutions of cadmium(II) and lead(II) is shown in Fig. 7A. Application to a copper plating bath is shown in Fig. 7B; the equation of the line obtained for the standard additions plot was $-i = 1.40 + 1.04 \times 10^4$ Cu(II) and the concentration of copper(II) in the original plating bath was calculated as 1.34×10^{-2} M. In both cases, no attempt was made to remove dissolved oxygen in samples or the carrier solution.

Conclusions

It has been demonstrated that c.p.p.p. is suitable for the analysis of metal solutions buffered at moderate to low pH in conventional polarographic cells and in flow systems without adverse effects from dissolved oxygen. The application to flow injection analysis offers exciting possibilities for automated polarographic analysis with reasonably high sample throughput.

Future developments related to c.p.p.p. will include alternate-drop differential c.p.p.p. for higher resolving power in complex mixtures similar to

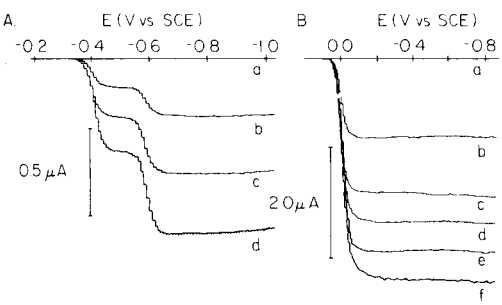

Fig. 7. Flow-injection polarographic analyses with c.p.p.p. detection (E_d = 0.2 V, ΔE = 10 mV, τ = 1.0 s, V_s = 2.0 ml, 0.50 ml min^{-1} flow rate). (A) Curves for Pb(II) + Cd(II) in 0.1 M KNO_3/0.01 M HNO_3: (a) blank; (b) 0.20; (c) 0.40; (d) 0.60 mM in each ion. (B) Curves for a copper plating bath diluted 100-fold in 0.035 M acetic acid/0.23 M formic acid/0.1 M KNO_3: (a) blank; (b) plating bath; (c—f) standard additions of Cu(II) to diluted plating bath. Cu(II) added: (c) 0.05, (d) 0.10, (e) 0.15, (f) 0.20 mM.

d.p.p. Development is expected also of rapid-scan c.p.p.p. and differential c.p.p.p. at a single mercury-drop electrode.

This work was initiated with support of a summer research fellowship to G.G.N. from Fiatron Systems, Inc. (Milwaukee, WI) and completed with support from National Science Foundation (Grant No. CHE-8312032).

REFERENCES

1 I. M. Kolthoff and J. J. Lingane, Polarography, 2nd edn., Interscience, New York, 1952; Vol. 2, pp. 552–5.
2 L. Meites, Polarographic Techniques, 2nd edn., Interscience, New York, 1965, p. 87.
3 K. Bratin and P. T. Kissinger, J. Liq. Chromatogr., 4(2) (1981) 321.
4 J. Debowski, K. Duszczyk, W. Kutner, D. Sybilska and W. Kemula, J. Chromatogr., 241 (1982) 141.
5 J. N. Brown, M. Nervins, J. H. M. Van der Linden and R. J. Lynch, J. Chromatogr., 204 (1981) 115.
6 W. A. MacCrehan and R. A. Durst, Anal. Chem., 50 (1978) 2108.
7 A. M. Bond, Modern Polarographic Methods in Analytical Chemistry, M. Dekker, New York, 1980, Chap. 6.
8 K. B. Oldham and E. P. Parry, Anal. Chem., 42 (1970) 229.
9 J. Osteryoung and E. Kirowa-Eisner, Anal. Chem., 52 (1980) 62.
10 A. Saito and S. Himeno, J. Electroanal. Chem., 101 (1979) 257.
11 J. Hermolin, S. Kashti-Kaplan and E. Kirowa-Eisner, J. Electroanal. Chem., 123 (1981) 307.
12 J. Osteryoung, D. Talmor, J. Hermolin and E. Kirowa-Eisner, J. Phys. Chem., 85 (1981) 285.
13 P. Maitoza and D. C. Johnson, Anal. Chim. Acta, 118 (1980) 233.
14 T. Hsi and D. C. Johnson, Anal. Chim. Acta, 175 (1985) 23.
15 J. H. Christie, L. L. Jackson and R. A. Osteryoung, Anal. Chem., 48 (1976) 561.
16 M. Hara and N. Nomura, Bunseki Kagaku, 32 (1983) E185; Talanta, 31 (1984) 105.
17 A. Brestovisky, E. Kirowa-Eisner and J. Osteryoung, Anal. Chem., 55 (1983) 2063.

Analytica Chimica Acta, 179 (1986) 389—398
Elsevier Science Publishers B.V., Amsterdam — Printed in The Netherlands

FLOW-INJECTION POTENTIOMETRIC STRIPPING ANALYSIS — A NEW CONCEPT FOR FAST TRACE DETERMINATIONS

WOLFGANG FRENZEL* and PETER BRÄTTER

Hahn-Meitner-Institut für Kernforschung, Glienicker Str. 100, D-1000 Berlin 39 (Federal Republic of Germany)

(Received 7th August 1985)

SUMMARY

Flow-injection potentiometric stripping analysis is introduced as a highly versatile technique for micro and trace determinations of heavy metals. The simple instrumentation used, with extremely short residence times (below 1 s), permits a sample throughput of 200 h^{-1}. Up to four elements can be determined simultaneously at lower $\mu g\ l^{-1}$ levels up to % levels. On-line sample manipulation (e.g., dilution and matrix modification) is possible with one- and two-channel flow systems. The utility of f.i.p.s.a. is evaluated by comparing response, sensitivity, and practical aspects of four different flow-through cells. The method is successfully applied to the fast sequential measurement of zinc, lead and copper in tap water and to the direct determination of lead and cadmium in acid digests of biological samples without further treatment.

Electrochemical stripping analysis has become recognized as a useful means for trace determinations of heavy metals. The capability of simultaneously determining very low concentrations in different kinds of samples has made stripping voltammetry one of the popular approaches to environmental, clinical and industrial analysis. Anodic stripping voltammetry (a.s.v.) is mainly used but during the last decade potentiometric stripping analysis (p.s.a.) [1—3] has attracted attention as an interesting alternative [4]. Both techniques compare well with respect to sensitivity and accuracy, but p.s.a. requires much simpler instrumentation and is less prone to interferences from oxygen [5] or organic substances [6, 7].

Environmental surveillance of heavy metal pollution demands fast and possibly continuous monitoring. Although concepts for the automation of electrochemical stripping techniques have been published for batch procedures [8], the development of flow-through detectors can be regarded as the most important step in continuous and automatic electrochemical stripping analysis [9, 10]. Many papers demonstrate the advantages of flow-through stripping analysis particularly with respect to cell design [11—13], matrix-exchange procedures [14, 15] and many applications in various fields of trace analysis have been discussed.

The advent of flow injection analysis (f.i.a.) [16, 17] has greatly extended the horizon of flow analysis. The general method is characterized by injec-

0003-2670/86/$03.50

tion of the sample into the delivery system, constant residence time of the sample (exact timing), and controllable dispersion of the sample plug. Even though there is neither complete mixing of the sample and reagents nor attainment of equilibrium of the chemical reaction, the transient detector signal at any time represents the concentration of the sample or reaction product. The application of electrochemical stripping techniques in f.i.a. is particularly unusual, in that, in principle, transient signals cannot be recorded. Moreover, there is usually no chemical reaction so that in this respect f.i.a. can be regarded simply as an uncomplicated means for well defined handling of microliter samples. However, recent developments in f.i.a. (e.g., gradient techniques, multidetector systems, on-line preconcentration, miniaturization) have demonstrated its immense potential for being much more than 'a new concept for fast continuous flow analysis' as pointed out in 1975 [18].

The aim of this paper is to introduce flow-injection potentiometric stripping analysis (f.i.p.s.a.), for heavy metal determinations whenever high sample throughput is required. The method is very versatile and is characterized by simple instrumentation, easy operation, short start-up time, and high flexibility in changing the flow scheme to fit different analytical procedures. The same basic set-up can be used not only for trace determinations below 1 $\mu g\ l^{-1}$ but also for determinations at the % level. On-line sample manipulation (e.g., dilution, buffering, matrix modification) is possible in one- or two-channel systems, which further increases the versatility of f.i.p.s.a.

EXPERIMENTAL

Apparatus and reagents

All the potentiometric stripping measurements were done with a PAR 174A polarographic analyzer in combination with a PAR 315A electroanalysis controller (EG&G, Princeton, NJ). The potential/time curves were recorded with a high-speed *x-t* recorder (Striptec System, Tecator AB, Höganäs, Sweden). The basic flow-injection system was described recently [19]. Solution flow was maintained by gravity flow or by means of nitrogen pressure. Flow rates were checked volumetrically in the waste. A manual injection valve allowed the introduction of variable sample volumes down to 14 μl. Teflon tubes of 0.5 mm i.d. were used for all interconnections. A two-channel system was used when on-line sample manipulation was needed (Fig. 2).

Four different flow-through cells were used: a Metrohm EA1096 wall-jet detector (Metrohm, Herisau, Switzerland), a laboratory-made wall-jet cell, a thin-layer cell and an open thin-layer cell. The specially made wall-jet cell (Fig. 1) is similar to one described by Wang and Dewald [20] and differs from the commercial detector in that the solution flow is directed parallel to the electrode surface after entering the cell. Moreover, the distance between inlet and working electrode surface can be adjusted precisely from 0 to

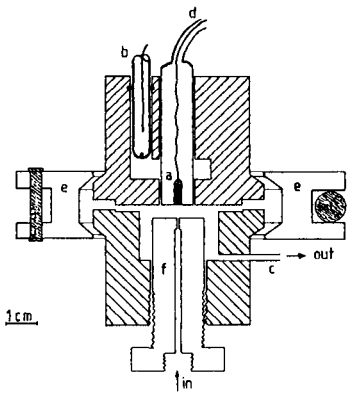

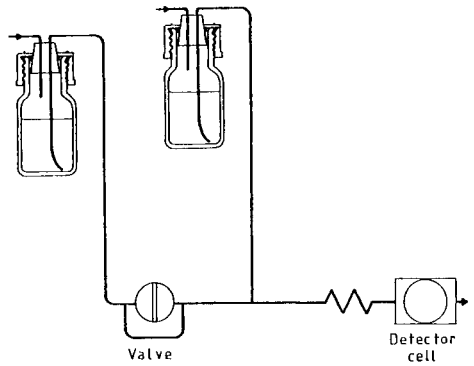

Fig. 1. Schematic diagram of the laboratory-built wall-jet cell: (a) 1 mm glassy-carbon electrode; (b) Ag/AgCl reference electrode; (c) stainless steel auxiliary electrode; (d) lead to working electrode; (e) clamp; (f) plexiglas inlet screw.

Fig. 2. Two-channel system for on-line sample manipulation.

6 mm. Unless otherwise stated, a 1-mm distance was used in this work. The Ag/AgCl reference electrode is connected to the cell via a ring-shaped salt bridge around the working electrode. The stainless steel needle which is used as solution outlet serves as the auxiliary electrode. The two teflon parts of the cell are held together by means of a clamp (see Fig. 1).

The thin-layer cell described earlier [21] was altered; now the reference electrode is positioned directly perpendicular to the surface of the 1-mm glassy-carbon working electrode. This minimizes the ohmic drop and so provides exact potential control. The open thin-layer cell will be described in detail elsewhere; it simply consists of the upper part of the thin-layer cell. The flow channel is replaced by a small strip of filter paper, which adheres to the plexiglas body, covering the inlet hole as well as the working and auxiliary electrodes. The lower end of the filter strip dips into the waste reservoir where the reference electrode is located. The filter paper (Schleicher & Schüll, No. 589[2]) exactly covers the surface of the working electrode.

Standard solutions were prepared daily by appropriate dilution of the metal ion stock solutions containing 1 g l^{-1} (Merck Titrisol) with twice-distilled water. All mineral acids and salts were high-purity chemicals; other reagents were of analytical grade.

Procedure

The carrier solution containing different amounts of mercury ion flowed continuously through the injection valve and detector cell to waste. When deaeration of the carrier was needed, the solution in the reservoir was purged with purified nitrogen overnight and throughout the experiment. Gravity flow was used for low flow rates (0.1—1 ml min^{-1}) by adjusting the height of the carrier reservoir. Higher flow rates (1—6 ml min^{-1}) were obtained by adjusting the nitrogen pressure to the carrier reservoir. To

maintain a constant flow rate, care must be taken that the hydrodynamic resistance of the sample loop corresponds to free flow.

At the beginning of an experiment, a mercury film was preplated at the glassy-carbon surface by applying a deposition potential of −1.0 V to the working electrode for at least 3 min. Then, simultaneously, the electrical circuit was disconnected and the strip-chart was started in order to record the resulting potential/time curve. To prevent calomel formation, a protection potential of −0.1 V was applied to the working electrode immediately after the recording and during working breaks. This possibility was obtained by a change of the electronics of the controller unit so that at the end of the analytical cycle, an appropriate potential was applied automatically to the working electrode. This procedure yielded a stable mercury film which could be used for several hours with reproducible responses. At the end of the experiment, the film was wiped away with a soft tissue and the surface was cleaned with acetone.

In f.i.p.s.a., the actual electrolysis time is given by the residence time of the sample and this depends on flow rate, injection volume and dispersion of the sample plug. In order to select an appropriate preset electrolysis time, it is necessary to determine the residence time. This was done by injecting 0.1 mol l^{-1} dichromate solution and then recording the potential change between the working and reference electrodes in open circuit. A positive potential change was observed immediately after the sample entered the cell, returning to the initial value after complete passage.

RESULTS AND DISCUSSION

Cell design

In order to compare the four flow-through cells used, the influence of the flow rate and the injection volume on the residence time of the sample was investigated. If, in the ideal case, no dispersion occurs, the residence time is given by $\tau = V_I/\dot{V}$ where V_I is the injection volume and $\dot{V}$ is the volume flow rate. Table 1 shows the theoretical and experimental data obtained under equivalent conditions. A certain degree of dispersion is observed in all cells, but is more pronounced in the case of the two thin-layer cells. This is probably due to the shape of the flow channel and to diffusion effects in the filter strip in these two cases, respectively.

The theory of f.i.p.s.a., which will be discussed in a later paper, predicts a linear signal dependence on the residence time of the sample. This was checked in the 0.5—600 s range for different injection volumes, flow rates and metal ion concentrations. The prediction was found to be true for all four cells. In contrast to theoretical predictions for flow-injection anodic stripping voltammetry [22], the stripping time in f.i.p.s.a. is inversely proportional to the flow rate as long as the flow rate is not altered between deposition and stripping. This is due to the fact that the increased plating efficiency at higher flow rates is compensated by the likewise faster trans-

TABLE 1

Influence of injection volume and flow rate on the residence time for the four detector cells used
(All data are the mean of three measurements. Experimental conditions are given in the text.)

$\dot{V}$ (ml min^{-1})	V_I (μl)	$\tau_{theor.}$ (s)	$\tau_{exp.}$ (s)			
			Metrohm wall-jet	Home-made wall-jet	Thin-layer cell	Open thin-layer cell
0.21	20	5.71	7.5	6.0	8.5	11.2
	100	28.62	37.8	29.8	42.7	56.7
	500	142.91	188.5	152.3	214.6	271.5
0.85	20	1.43	2.0	1.2	2.3	2.7
	100	7.14	10.4	6.3	11.9	13.5
	500	35.70	49.8	30.7	58.2	64.9
1.65	20	0.73	1.0	0.8	1.1	1.5
	100	3.64	5.3	3.8	5.9	7.4
	500	18.20	24.5	19.7	26.9	37.3
4.32	20	0.28	0.4[a]	0.3[a]	0.5[a]	—
	100	1.39	1.7	1.5	2.3	—
	500	6.94	8.9	7.2	11.8	—

[a]These values are close to the time resolution of the strip-chart recorder and lack precision.

port of oxidizing agent during stripping. In all cases, experimental verification was obtained for flow rates in the 0.2—6 ml min^{-1} range except for the open thin-layer cell where the maximum useful flow rate is 2 ml min^{-1} because the filter strip is flushed away at higher flow rates.

The question of which cell is best suited for f.i.p.s.a. cannot be answered unambiguously. The shape and length of the stripping curves were nearly identical under comparable experimental conditions. With respect to fast response and minimum carry-over, the laboratory-made wall-jet cell is favourable. Considering practical aspects, the open thin-layer cell described above is preferable because dismantling for cleaning and removing air or hydrogen bubbles is, of course, unnecessary. The remainder of the work was done with the laboratory-made wall-jet cell except as noted.

Carrier composition

In a one-channel f.i.p.s. system, the carrier solution fulfills several roles; it is used as preplating, stripping, and rinsing solution. The composition depends mainly on the analytical problem. The application of medium exchange, inherent in f.i.p.s.a., allows the stripping step to proceed in an optimized solution, irrespective of the sample composition. With respect to sensitivity, low mercury levels in deaerated carrier are reasonable, thus increasing the sensitivity up to two orders of magnitude [21]. Improved selectivity in the simultaneous determination of several elements can be obtained by addition of suitable complexing agents [15, 23].

Sample composition and pretreatment

In trace element analysis, sample manipulation should be minimized in order to avoid contamination, losses, or changes of the chemical form of the species to be determined. Conventional batch procedures for stripping analysis often require the addition of reagents, pH adjustment, and deaeration prior to the measurement step; such treatments are unnecessary or can be done on-line in f.i.p.s.a.

To investigate the influence of sample composition on the stripping signal, various solutions were prepared and spiked with 1 mg l^{-1} cadmium, lead or copper. It was found that deaeration of the sample and the choice of the mineral acid had no influence on signal shape and length. Highly acidic solutions (up to 5 mol l^{-1}) gave signals identical with those from neutral solutions. However, after several successive injections, small hydrogen bubbles were observed at the electrode surface which disturbed the response. To remove these bubbles, the cell had to be dismantled and usually the glassy-carbon electrode had to be plated again with mercury. When the open thin-layer cell was used, such effects did not appear, even after long-term exposure to concentrated acids.

Preliminary results with the two-channel system (Fig. 2) indicate that on-line buffering can be done before the sample enters the cell. This set-up was applied successfully for pH adjustment of neutral and alkaline samples and for the addition of base electrolyte to nearly electrolyte-free solutions (e.g., distilled water, methanol, acetone).

Sample dilution is often considered to be a simple step, but it is often very time-consuming with a high risk of human failure and contamination. The zone-sampling procedure [24] described for f.i.a. can be used in f.i.p.s.a. in a modified manner. After injection of the sample, the electrolysis potential is set with a specified time delay which allows part of the analyte to pass through the cell without being deposited. When low-dispersion systems are used, small variations in the time delay cause large deviations in the stripping time. This is particularly true if the manipulation of the valve and the potentiostat is done manually. However, there are many possibilities for increasing the dispersion in a flow-injection system [16]. The simplest are to increase the tube diameter or length between the injection valve and flow cell.

To demonstrate the application of zone sampling in f.i.p.s.a., a dispersion coil (20 cm long, 1.5 mm i.d.) was introduced between the valve and cell leading to a nearly 15-fold increase in residence time. A 50-μl injection volume and a flow rate of 1.6 ml min^{-1} were used, resulting in a 35-s residence time. Figure 3 shows the p.s.a. curves obtained for successive injections of 100 mg l^{-1} lead(II) solution into a nondeaerated carrier. The potential was applied at different delay times after the moment of injection. A 15-s delay (Fig. 3c) corresponds to an approximately 10-fold dilution and a 28-s delay (Fig. 3e) to an approximately 100-fold dilution. Injections of even higher concentrations (up to 1%) at decreased injection volumes were also

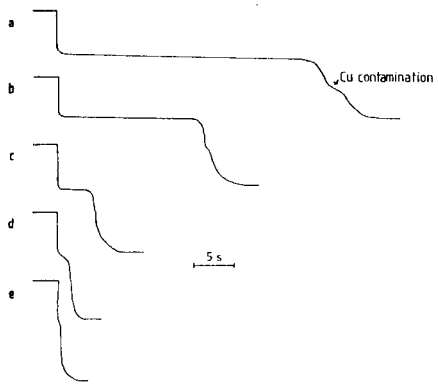

Fig. 3. Zone sampling in f.i.p.s.a. Signals obtained with different delay times: (a) 0 s; (b) 8 s; (c) 15 s; (d) 23 s; (e) 28 s. For explanation see text.

examined. However, this technique lacks adequate reproducibility because manual operation of the valve and potentiostat is unreliable. If computerized systems [25, 26] were used for automatic operation, a high degree of precision could be achieved in these steps.

Calibration

All calibration measurements were done with the laboratory-made wall-jet cell.

Low-level determinations require long residence times and low concentrations of oxidizing agent. Therefore a deaerated carrier was used containing 10 mg l^{-1} Hg^{2+} in 0.1 mol l^{-1} hydrochloric acid. The flow rate was adjusted to 0.2 ml min^{-1}. For a 1-ml injection volume, the residence time was shown to be 5 min and this was set at the controller unit. Calibration in the 5—100 μg l^{-1} range yielded rectilinear plots for lead and cadmium with slopes of 0.034 ± 0.0002 s l^{-1} and 0.060 ± 0.0005 s l^{-1} with correlation coefficients of 0.9998 and 0.9994, respectively. On the basis of these calibration plots, the system blank (signal obtained without injection of sample) can be estimated as 0.5 and <0.2 μg l^{-1} for lead and cadmium, respectively.

Calibration curves in the upper μg l^{-1} and lower mg l^{-1} ranges were obtained by decreasing the injection volume and/or increasing the flow rate. This is, of course, not strictly necessary because the dynamic range of p.s.a. covers at least three orders of magnitude. However, with respect to sample throughput, decreased residence times are desirable. Comparatively high concentrations were determined with a 14-μl injection volume at a flow rate of 5.8 ml min^{-1}. The corresponding residence time was well below 1 s. Successive injection of 10 samples containing 10 mg l^{-1} lead and cadmium into a deaerated carrier yielded stripping times of 0.63 ± 0.03 s and 0.81 ± 0.05 s, respectively. The complete analysis took about 2 s which, theoreti-

cally, would correspond to a sample throughput of 1800 h^{-1}. In practice, the frequency is primarily limited by the time required to fill the sample loop and to operate the controller unit. When these steps are done manually, about 20 s are necessary for one run, corresponding to an injection rate of 200 h^{-1}.

Applications

The f.i.p.s. method was successfully applied to the fast sequential monitoring of zinc, lead, and copper in tap water. A bypass was made and connected directly to the valve; 500-μl samples were successively injected into the deaerated carrier. The flow rate was adjusted to 1 ml min^{-1}, which corresponds to a residence time of about 40 s and allows determinations down to about 20 $\mu g\ l^{-1}$. This suffices to meet the requirements of the public health regulations in West Germany for the monitoring of lead and zinc content in drinking water.

Figure 4 shows four of 50 signals obtained in an uninterrupted run lasting for 3 h. Recalibration at the end of the experiment yielded identical signals for zinc and lead but slightly decreased signals for copper. However, the potential steps became less and less pronounced with successive injections which impeded the calculation of the stripping time. Sometimes bubbles of carbon dioxide occur and cause problems in work with the wall-jet cell. The use of the open thin-layer cell was also tested but it suffered from lower sensitivity caused by enhanced oxidation by gaseous oxygen and therefore was inadequate for the proposed purpose. Computerized p.s.a. [26] increases the detection limits by at least two orders of magnitude and should be useful for monitoring cadmium and thallium which are normally present at much lower levels as well.

In the life sciences, heavy metals are often determined in digested samples, which are usually highly acidic and have to be diluted or buffered prior to the measurement step. As it would be advantageous to minimize contamination problems and to maximize sensitivity achievement, direct injection of such samples was tested. Accurate results, which compared favourably with data obtained by neutron activation, electrothermal atomic absorption, inductively-coupled plasma atomic emission spectroscopy and anodic stripping

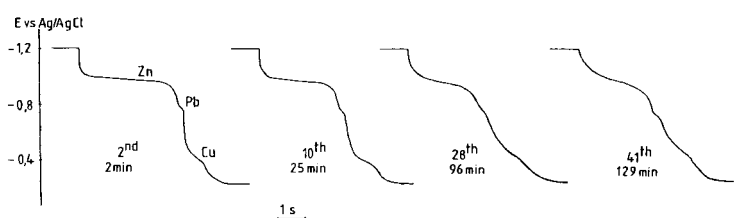

Fig. 4. Quasi-continuous monitoring of zinc, lead, and copper in tap water. Four characteristic potential/time curves taken during an uninterrupted 3-h period of analysis.

voltammetry, were obtained for the cadmium content in horse kidney, a new IAEA reference material [27]. However, as mentioned above, hydrogen evolution occurs at the electrode at longer residence times, leading to erroneous results. Thus, only small sample volumes (ca. 100 μl) can be injected, which limits the sensitivity to about 50 $\mu g\ l^{-1}$ for cadmium and lead. Future work will concentrate on the possibilities of on-line buffering, matrix modification, and the adoption of an automatic standard addition procedure.

In applications of speciation, it would be interesting to analyze body fluids (e.g., blood, serum, urine, or breast milk) directly without decomposition in order to obtain information on the contents of bound elements and free metal ions. Test runs with urine samples spiked with lead and cadmium were not successful. The cadmium signal in particular decreased very rapidly when successive injections of the same samples were made. This is evidently caused by adsorption phenomena at the electrode surface. Two recent papers concerning a membrane-covered electrode [28, 29] seem very promising to overcome such problems. Considering the open thin-layer cell, the filter strip could be replaced by a suitable dialysis membrane.

Conclusions

The ability to determine simultaneously up to four elements at the $mg\ l^{-1}$ level in a few seconds is an outstanding feature of f.i.p.s.a. Until now, stripping analysis has been used primarily in cases where high sensitivity is required. In the future it may be applied to new areas of analysis. The simple and low-cost instrumentation is distinctly suitable for the surveillance of heavy metal pollution in the field.

The fast response of f.i.p.s.a. combined with its multi-element capability may find interest in process control. Being a microanalytical technique, f.i.p.s.a. can also be applied whenever small or rare samples have to be analyzed (e.g., archaeological and clinical samples).

The authors are indebted to Frank Chisela for his interest in this work and for helpful discussions during the preparation of the paper.

REFERENCES

1 D. Jagner and A. Granéli, Anal. Chim. Acta, 83 (1976) 19.
2 D. Jagner, Analyst (London), 107 (1982) 593.
3 S. Jaya and T. Prassada Rao, Rev. Anal. Chem., 6 (1982) 343.
4 T. M. Florence, J. Electroanal. Chem., 168 (1984) 207.
5 D. Jagner, Anal. Chem., 51 (1979) 342.
6 L.-G. Danielsson, D. Jagner, M. Josefson and S. Westerlund, Anal. Chim. Acta, 127 (1981) 147.
7 F. Wahdat and R. Neeb, Fresenius Z. Anal. Chem., 316 (1983) 770.
8 See, e.g. P. Valenta, H. Rützel, P. Krumpen, K. H. Salgert and P. Klahre, Fresenius Z. Anal. Chem., 292 (1978) 120.
9 A. Zirino and S. H. Liebermann, In Analytical Methods in Oceanography, Am. Chem. Soc., Washington, D.C., 1975, p. 88.

10 K. Tóth, G. Nagy, Z. Fehér, G. Horvai and E. Pungor, Anal. Chim. Acta, 114 (1980) 45.
11 J. Wang and M. Ariel, J. Electroanal. Chem., 83 (1977) 217.
12 E. O. Martins and G. Johansson, Anal. Chim. Acta, 140 (1982) 29.
13 J. Wang and B. A. Freiha, Anal. Chem., 57 (1985) 1776.
14 E. B. Buchanan and D. D. Soleta, Talanta, 29 (1982) 207.
15 G. Schulze, W. Bönigk and W. Frenzel, Fresenius Z. Anal. Chem., 322 (1985) 255.
16 J. Růžička and E. H. Hansen, Flow Injection Analysis, Wiley, New York, 1981.
17 J. Růžička and E. H. Hansen, Anal. Chim. Acta, 114 (1980) 19.
18 J. Růžička and E. H. Hansen, Anal. Chim. Acta, 78 (1975) 145.
19 G. Schulze, M. Husch and W. Frenzel, Mikrochim. Acta, I (1984) 191.
20 J. Wang and H. D. Dewald, Anal. Chim. Acta, 136 (1982) 77.
21 G. Schulze and W. Frenzel, Fresenius Z. Anal. Chem., 316 (1983) 26.
22 J. Wang and H. D. Dewald, Anal. Chim. Acta, 162 (1984) 189.
23 L. Anderson, D. Jagner and M. Josefson, Anal. Chem., 54 (1982) 1371.
24 B. F. Reis, A. D. Jacintho, J. Mortatti, F. J. Krug, E. A. G. Zagatto, H. Bergamin and L. C. R. Pessenda, Anal. Chim. Acta, 123 (1981) 221.
25 D. Jagner, Trends Anal. Chem., 2 (1983) 53.
26 A. Granéli, D. Jagner and M. Josefson, Anal. Chem., 52 (1980) 220.
27 Progress Report No. 1, Intercomparison of Cadmium and other Elements in IAEA Horse Kidney (H-8), International Atomic Energy Agency, Vienna, Austria, 1985.
28 E. E. Stewart and R. B. Smart, Anal. Chem., 56 (1984) 1131.
29 R. B. Smart and E. E. Stewart, Environ. Sci. Technol., 19 (1985) 137.

Analytica Chimica Acta, 179 (1986) 399—405
Elsevier Science Publishers B.V., Amsterdam — Printed in The Netherlands

FLOW-INJECTION DETERMINATION OF SULPHITE AND ASSAY OF SULPHITE OXIDASE

M. MASOOM and ALAN TOWNSHEND*
Chemistry Department, University of Hull, Hull HU6 7RX (Great Britain)
(Received 28th June 1985)

SUMMARY

Sulphite ($1—80 \times 10^{-5}$ M) in formaldehyde-stabilized solutions is determined by injection into a flowing stream of pH 8.5 phosphate buffer, passing through a mini-column of sulphite oxidase immobilized on controlled-pore glass, with amperometric detection of the hydrogen peroxide produced. Sulphite oxidase ($5—100$ U l^{-1}) is determined by injection into a flowing stream of formaldehyde-stabilized 2×10^{-3} M sodium sulphite in pH 8.0 phosphate buffer; hydrogen peroxide is again monitored.

Sulphite is commonly used as a preservative in food and in the pharmaceutical industry. It is added to food products to prevent oxidation and bacterial growth. Sulphite is present in air as sulphur dioxide and is one of the commonest pollutants. Many methods have been applied to the determination of sulphite and sulphur dioxide in solution [1, 2], but most have drawbacks such as lack of reproducibility, sensitivity or reliability in routine use, or suffer from severe interferences [3, 4]. Sulphite is an important intermediate in the metabolism of sulphur amino acids to sulphate ion:

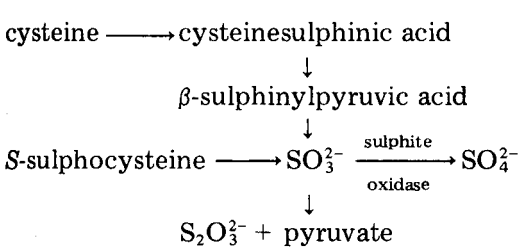

Sulphite oxidase (SOD), which catalyzes the oxidation of sulphite to sulphate in this metabolic process, has been purified from several animal sources. The enzyme has been shown to contain a cytochrome b5-type haem and molybdenum [5]. Its molecular weight ranges from 110 000 (chicken) to 122 000 (human). The catalyzed reaction is:

$$SO_3^{2-} + O_2 + H_2O \xrightarrow{SOD} SO_4^{2-} + H_2O_2$$

In this paper, sulphite is determined by use of the enzyme immobilized on

0003-2670/86/$03.50

controlled-pore glass (CPG) incorporated into a flow-injection manifold similar to that previously described for use with other immobilized oxidases such as glucose oxidase [6] and cholesterol oxidase [7].

The assay of sulphite oxidase is of clinical diagnostic value. Deficiency of human sulphite oxidase has been associated with an hereditary disorder of sulphur metabolism [8—10]. The clinical manifestations of this disorder have included dislocated lenses, severe brain damage, mental retardation and early death. Biochemical investigations of these cases revealed the presence of increased amounts of sulphite and thiosulphate and a massive urinary excretion of an unusual amino acid identified as *S*-sulphocysteine. At the same time the excretion of only very small amounts of inorganic sulphate suggested the lack of ability to oxidize sulphite to sulphate.

Screening tests for sulphite oxidase have been based on chromatographic separation of *S*-sulphocysteine [11] and on determination of thiosulphate by Sorbo's spectrophotometric method [5] or a modification thereof [12]. A report on the direct assay of sulphite oxidase in acetone extracts of powdered tissue is available [10]. In this paper, a direct, sensitive and rapid assay for sulphite oxidase is described.

EXPERIMENTAL

Reagents

Sulphite oxidase (sulphite:oxygen oxidoreductase, EC 1.8.3.1, ex. chicken liver) was obtained as a suspension (10 units of enzyme) in ammonium sulphate solution (Boehringer Mannheim). Sodium sulphite was AnalaR grade (BDH Chemicals). The formaldehyde solution was laboratory-reagent grade. All other reagents used were as reported previously [6].

Immobilization of sulphite oxidase. The provided sulphite oxidase (10 units) was immobilized on 0.2 g of controlled-pore glass (CPG) by cross-linking with glutaraldehyde, following the procedure described previously [6]. The resulting immobilized enzyme was packed in a glass column (2.5 × 25 mm).

The supernatant liquid from the immobilization procedure (2 ml) was carefully removed from the immobilization vessel and assayed for sulphite oxidase activity by the flow-injection procedure for sulphite oxidase determination described below. An activity of 1.0 U ml^{-1} was found, which means that 2 units of sulphite oxidase remained in the supernatant solution, and $\leqslant 8$ units were immobilized.

Recommended procedures

Apparatus and procedure for the determination of sulphite. The flow-injection manifold used for sulphite determination is shown in Fig. 1. The components, including the amperometric detector, were as reported previously [6]. Sulphite solutions (20 μl) were injected into the carrier stream (0.1 M phosphate buffer, pH 8.5). On passage through the sulphite oxidase

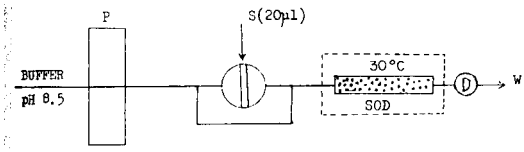

Fig. 1. Manifold for sulphite determination: P, pump; S, sample; D, detector; W, waste.

column, sulphite was oxidized to sulphate with the production of hydrogen peroxide, which was detected in the amperometric flow cell.

Assay of sulphite oxidase. The manifold for the assay of sulphite oxidase was the same as in Fig. 1, except that the enzyme reactor in the thermostat was replaced by a 30-cm reaction coil at room temperature. An aqueous 2×10^{-3} M solution of sulphite stabilized with 2×10^{-3} M formaldehyde in 0.1 M phosphate buffer (pH 8.0) was used as a carrier stream, into which the sample (20 μl) containing sulphite oxidase was injected. The reaction took place in the flow coil and the hydrogen peroxide formed was monitored as above. Enzyme samples of various activities were prepared by diluting with water the commercial enzyme preparation extracted from chicken liver.

RESULTS AND DISCUSSION

Optimization of conditions for sulphite determination

The effect of pH on the activity of immobilized sulphite oxidase was investigated by using phosphate buffers (0.1 M) of various pH values as the carrier stream. The results are shown in Fig. 2. Maximum activity is found between pH 8.5 and 9.0, compared to 8.5 for the soluble enzyme [13] extracted from chicken liver and 8.0 for the enzyme extracted from *Thiobacillus thioparous* [14]; pH 8.5 was used in the further investigation of conditions.

The effect of sample flow rate was also studied. The results are shown in Table 1. A slight decrease in peak height is observed with increasing flow rate. As the immobilized enzyme column holds only a small quantity ($\leqslant 8$ units) of sulphite oxidase, some decrease in peak height would be expected. A flow rate of 2.0 ml min^{-1} was used in subsequent investigations, which allowed a reasonable sample throughput of ca. 200 h^{-1}.

Soluble sulphite oxidase has very poor thermal stability. Lyric and Suzuki [14] observed a 20% loss in activity of the soluble enzyme after 6 h at room temperature and a 95% loss at 55° C for 9 min. The effect of temperature on the activity of the immobilized enzyme was investigated by flowing water at various temperatures around the immobilized enzyme column. The results are shown in Fig. 3. There is an increase in response with increase in temperature up to 50° C. After this experiment, the enzyme remained active for all subsequent studies, for which the column was maintained at 30° C.

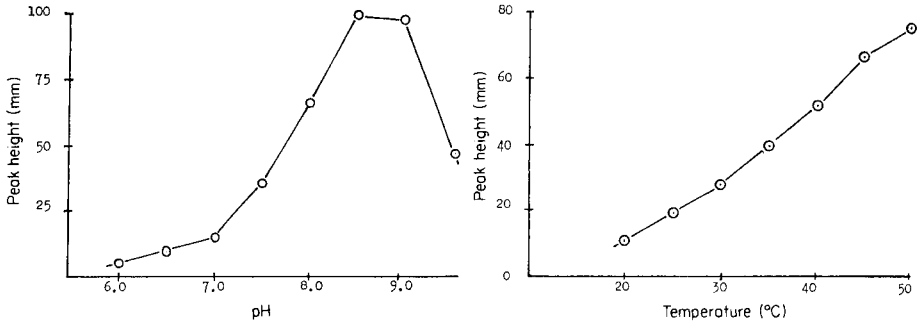

Fig. 2. Effect of pH on activity of the immobilized enzyme (8×10^{-4} M sodium sulphite).

Fig. 3. Effect of temperature on activity of immobilized sulphite oxidase (2×10^{-4} M Na_2SO_3).

TABLE 1

Effect of flow rate on peak height

Flow rate (ml min^{-1})	1.0	1.5	2.0	2.5	3.0
Peak height (mm)	48.5	46.0	44.0	41.5	40.0

Determination of sulphite

Aqueous solutions of sodium sulphite were prepared in deaerated water and immediately injected into the manifold shown in Fig. 1; a linear calibration graph was obtained for the range $0.5—8.0 \times 10^{-4}$ M sulphite. As expected, the sulphite solutions were unstable; when a second calibration graph was obtained by injecting the same standard solutions of sulphite, when they were 2 h old, the peak heights had decreased by 25—30%. Deaeration of water with nitrogen prior to sodium sulphite addition, therefore, had not prevented oxidation.

The oxidation of sulphite in solution has been a major problem in the determination of sulphite. Various stabilizers have been proposed, the most popular of which is sodium tetrachloromercurate(II) [1]. However, mercury-(II) is reported to be a strong inhibitor of sulphite oxidase [13], so that it could not be used in the present system. Formaldehyde is known to be an effective stabilizer for sulphite [15] with which it forms a hydroxysulphonate: $HCHO + HSO_3^- \rightarrow HCH(OH)SO_3^-$. Formaldehyde seemed to be a possible stabilizer for use in the present immobilized enzyme system. The soluble enzyme was not inhibited by 8.0×10^{-4} M formaldehyde (see below). Therefore, solutions of sulphite containing equimolar amounts of formaldehyde were prepared in deaerated water. The formaldehyde-stabilized solutions of sulphite were immediately injected into the system shown in Fig. 1. The calibration peaks for sulphite are shown in Fig. 4. The calibration graph was linear at least up to 8×10^{-4} M sulphite. The limit of detection (2 × noise)

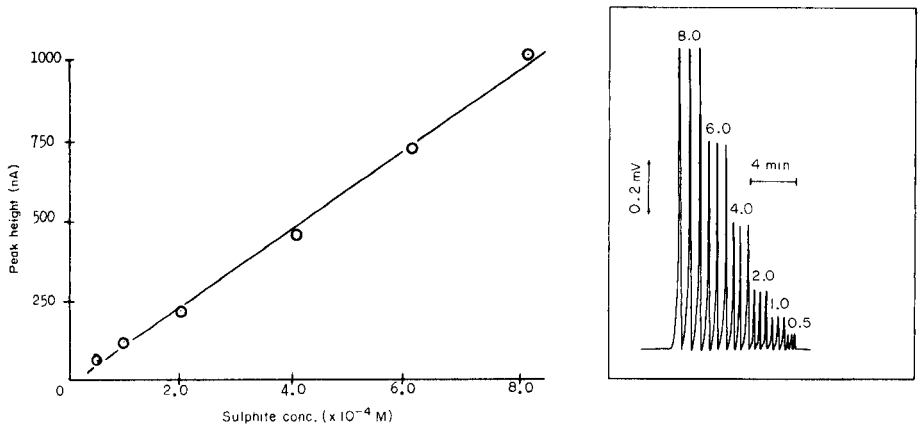

Fig. 4. Calibration graph and peaks for sulphite stabilized with formaldehyde. The numbers on the peaks relate to 0.5—8.0 × 10^{-4} M sodium sulphite.

was 1 × 10^{-5} M sulphite. The relative standard deviation for 3 injections of 4 × 10^{-4} M sulphite was 2.2%.

When 6 × 10^{-4} M formaldehyde solutions were injected alone into the system and passed directly to the detector, it was observed that formaldehyde itself was oxidized at the electrode to give a small response (43 nA from 8 × 10^{-4} M formaldehyde). These readings were subtracted from the calibration results. The sulphite solutions were stable at room temperature and showed no change in response after 24 h. The same column of immobilized enzyme was used at room temperature for 10 weeks with no loss in activity.

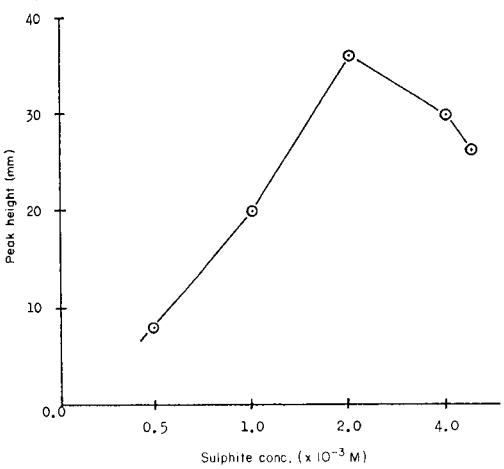

Fig. 5. Effect of sulphite concentration on response to sulphite oxidase (0.04 U ml^{-1}).

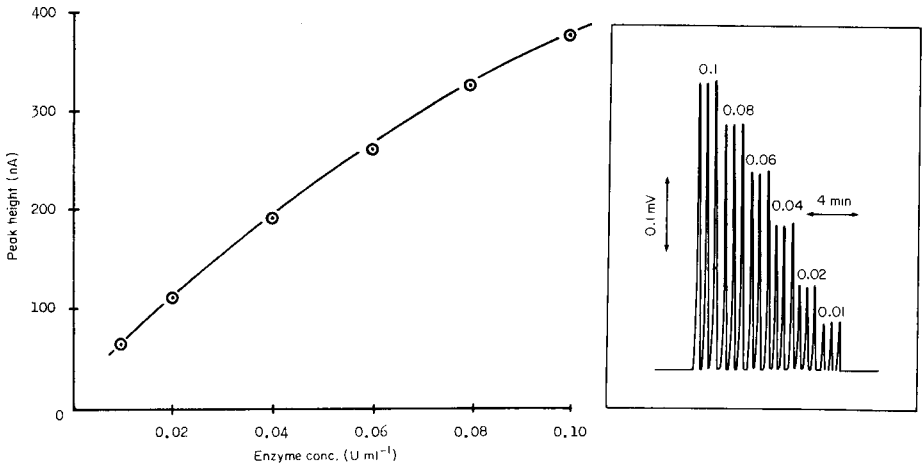

Fig. 6. Calibration graph and peaks for sulphite oxidase assay. The numbers on the peaks relate to 0.01—0.1 U ml^{-1}.

Flow-injection assay of sulphite oxidase

The effect of concentration of sulphite stabilized with formaldehyde used as a carrier stream on the activity of sulphite oxidase was studied. The solution was pH 10.9. The results are shown in Fig. 5. The highest activity was obtained at 2.0×10^{-3} M sulphite. This solution, stabilized by an equimolar concentration of formaldehyde, was used as the carrier stream for assay of the enzyme.

Standard solutions of sulphite oxidase (0.0—0.1 U ml^{-1}) were prepared in phosphate buffer (0.1 M, pH 8.0) and injected into the reagent stream. Figure 6 shows the calibration graph and the recorder responses for the standards. An activity of 5 U l^{-1} is the minimum level detectable by this assay procedure. The sensitivity of the assay can be increased by stopping the enzyme with the reagent in the reaction coil for 1—2 min. However, the present method is sensitive enough to be applied directly to sulphite oxidase assay in tissue extracts and biological fluids. The sample throughput was ca. 100 h^{-1}.

REFERENCES

1 P. W. West and G. C. Gaeke, Anal. Chem., 28 (1956) 1216.
2 S. M. Ramasamy and H. A. Mottola, Anal. Chem., 54 (1982) 283.
3 M. D. Thomas, J. Air Pollution Control Assoc., 14 (1964) 517.
4 P. K. Mueller, F. P. Terraglio and Y. Tokiva, Chemical Interferences in Continuous Air Analysis, 7th Conference on Methods in Air Pollution Studies, Union Oil Centre, Los Angeles, CA, January 1965.
5 S. Sorbo, Biochim. Biophys. Acta, 24 (1957) 324.
6 M. Masoom and A. Townshend, Anal. Chim. Acta, 166 (1984) 111.
7 M. Masoom and A. Townshend, Anal. Chim. Acta, 174 (1985) 293.

8 J. L. Johnson and K. V. Rajagopalan, J. Clin. Invest., 58 (1976) 551.
9 V. E. Shih, N. Eng. J. Med., 297 (1977) 1022.
10 S. H. Mudd, F. Irrevere and L. Laster, Science, 156 (1967) 1599.
11 I. H. Segal and M. J. Johnson, Anal. Biochem., 5 (1963) 330.
12 V. E. Shih, M. M. Carney and R. Mandell, Clin. Chim. Acta, 95 (1979) 143.
13 D. L. Kessler and K. V. Rajagopalan, J. Biol. Chem., 247 (1972) 6566.
14 R. M. Lyric and I. Suzuki, Can. J. Biochem., 48 (1970) 334.
15 M. Lindgren and A. Cedergren, Anal. Chim. Acta, 141 (1982) 279.

Analytica Chimica Acta, 179 (1986) 407—417
Elsevier Science Publishers B.V., Amsterdam — Printed in The Netherlands

A COATED TUBULAR SOLID-STATE CHLORIDE-SELECTIVE ELECTRODE IN FLOW-INJECTION ANALYSIS

J. F. VAN STADEN

Department of Chemistry, University of Pretoria, Pretoria 0002 (South Africa)

(Received 10th July 1985)

SUMMARY

The construction, suitability and behaviour of a coated tubular solid-state chloride ion-selective electrode in continuous flow analysis are discussed. The flow-through cell is constructed easily from Tygon tubing and silver foil, which is treated to give a silver/silver chloride electrode. The optimum contact area is obtained with a tube 5 mm long and of 2 mm internal diameter, for a total flow rate of 4.7 cm^3 min^{-1}; the carrier streams are 1.0 mol dm^3 potassium nitrate. Response times are fast (3—4 s for 95% response). With 30-μl samples, the working range covers 5—5000 mg dm^3 chloride with a reproducibility better than 1.7% (relative standard deviation); the stability of the system is excellent. Interferences are similar to those found in batch analysis with Ag/AgCl electrodes, but are less severe in the flow system; pH has no effect in the range 2—12. Results obtained for chloride in waters at a sample throughput rate of about 120 h^{-1} agree well with results by a standard spectrophotometric automated method.

The numerous publications to date suggest that spectrophotometric detection is still the most popular choice in flow-injection analysis (f.i.a.), but there has been an increase in the use of electrochemical detection in flowing streams [1—3]. The development of different types of detector for use with flow-injection systems forms part of the innovative expansion of the general method.

An ideal detector in flow-injection systems must have a fast response to cope with the high sampling rates that can be achieved, and it should respond linearly over a wide concentration range of the components transported to the detector as reaction products from the manifold systems used. Responses should be repeatable over extended periods of time so that frequent calibration runs necessitated by detector weaknesses are not required. The detector should have very low inherent electrical noise characteristics, and be sensitive enough to yield the highest possible reproducibility, as well as being compatible with data-processing systems. In order to achieve these requirements for flow-through electrodes and potentiometric cells in flow-injection systems, special attention must be given to cell design and construction, geometry of the flow-through cell and cell volume.

There are several considerations in the design of flow-through electrochemical detectors. Potentiometric and amperometric detectors have included

0003-2670/86/$03.50

wall- (or open) tubular, packed-bed (or porous) tubular, wire, cascade, wall-jet and thin-layer designs. The use of open-tubular electrodes as detectors for continuous flow measurements has also received considerable attention. Pioneered by the work of Blaedel and co-workers [4—6], as well as work done by Thompson and Rechnitz [7], the cylindrical geometrical detectors seem to be the ideal configuration to interface with flow-injection analysis, as the hydrodynamic flow conditions can be kept constant throughout the system. However, most of the open-tubular type of electrodes described to date have been used for amperometric (voltammetric) detection [4—8].

Recently some novel flow-through tubular arrangements for ion-selective electrodes have been reported. Meyerhoff and Kovach [9] described a simple tubular polymer membrane potassium-selective electrode which was prepared by replacing the wall of a narrow piece of Tygon tubing with a PVC/valinomycin membrane. Van der Linden and Oostervink [10] constructed a tubular solid-membrane copper(II)-selective electrode in which a pellet is embedded in the polymer Polypol PS230; the flow-through channel in the body and the pellet was made by careful drilling. Alegret et al. [11] reported a tubular flow-through nitrate-selective electrode based on a mobile carrier held in a PVC matrix without inner reference solution.

The desire to miniaturize, simplify and to produce cheaper ion-selective electrodes has motivated attempts to interface coated tubular solid-state ion-selective electrodes based on inorganic salts with flow-injection analysis. Although the well-known silver/silver halide electrodes were developed and used decades ago, the Ag/AgCl electrode usually serves as the reference, and the adoption of silver/silver halide indicator electrodes in routine analysis is still not widespread [12]. Harzdorf [12] investigated the response of halide ion-selective electrodes to redox systems in a comparison between silver/silver halide electrodes and silver sulphide-based halide ion-selective electrodes. Müller [13] developed a silver sulphide-based silver chloride detector which consists of a combination of two electrodes of identical membrane material, both with direct internal contact. This system was used particularly for the measurement of chloride in blood with a differential technique.

The main aim of the present work was first to construct a simple coated tubular chloride ion-selective electrode in which the active film would be continuous and would adhere well to the metal surface, and then to test the suitability and behaviour of the electrode in flow-injection analysis, with application to the determination of chloride in water over the very wide concentration range from zero to 5000 mg dm^{-3} chloride.

EXPERIMENTAL

Apparatus

The flow-injection system used is shown schematically in Fig. 1. A Carle microvolume two-position sampling valve (Carle. No. 2014) with two identical sample loops, each having a volume of 30 μl, was used. A series of

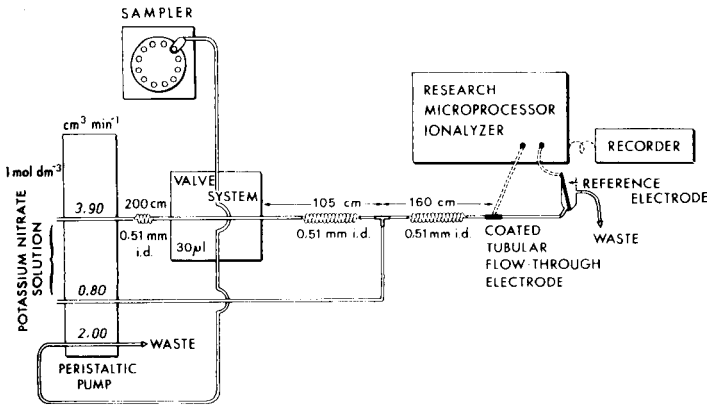

Fig. 1. Schematic diagram of the flow-injection system. Valve loop, 30 µl; tube length and i.d. are given in cm and mm, respectively.

samples from a Cenco sampler unit was supplied to the sampling valve system. The timing of the sampler unit was 30 s for sample introduction with zero wash time and valve actuation at 28 s.

The carrier and reagent streams were supplied with a Cenco peristaltic pump operating at 10 rpm, and the sampling valve system was synchronised with a Cenco sampler unit. Tygon tubing (0.51 mm i.d.) was used to construct the manifold; coils were wound round suitable lengths of glass tubing (15 mm o.d.).

The potentials were measured at room temperature with an Orion Research (model 901) microprocessor Ionalyzer. The detector output was recorded with a two-channel Cenco recorder (model 34195-041). The constructed flow-through tubular indicator electrodes were used in conjunction with an Orion 90-02 double-junction reference electrode with 10% (w/v) potassium nitrate as the outer chamber filling solution.

Reagents and solutions

All reagents were prepared from analytical reagent-grade chemicals unless otherwise specified. The stock solutions of chloride and ionic-strength adjustment solutions were prepared with double-distilled/deionized water. The water was tested beforehand for traces of chloride. Working standard chloride solutions were prepared by appropriate dilutions to cover the range 0—5000 mg dm^{-3} chloride. All solutions were degassed before measurements by use of a water vacuum pump.

Construction of the coated tubular electrode

The final configuration of the constructed tubular flow-through electrode unit is shown in Fig. 2. A 0.025-mm thick silver metal foil was wound around two pieces of Tygon tubing at both ends. Electrical contact between the

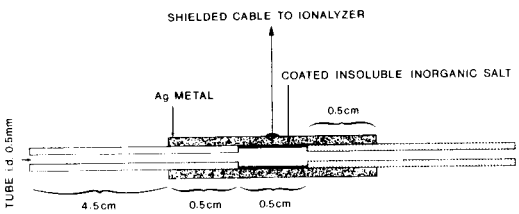

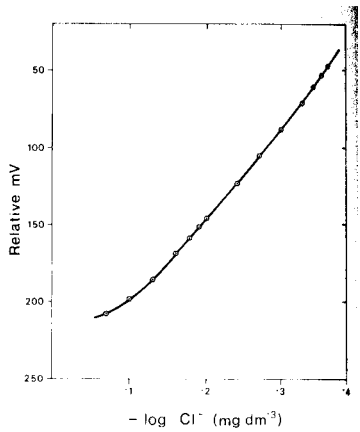

Fig. 2. Coated tubular solid-state chloride-selective electrode. The active electrode surface is ca. 2 mm i.d. and 5 mm long.

Fig. 3. Calibration curve for the electrode response under steady-state conditions.

Ionalyzer instrument and the tubular electrode was made by winding the inner wire of a shielded cable round the silver metal cylinder. The whole electrode system was isolated with Araldite epoxy resin. Then 20 cm^3 of household bleach (containing ca. 3.5% sodium hypochlorite) acidified with 5 drops of 0.1 mol dm^{-3} hydrochloric acid was circulated at a rate of 1.6 cm^3 min^{-1} for 120 min through the tubular cylinder. During this process, silver metal is oxidised to silver ions and simultaneously coated on the inner wall of the cylinder (shown by thick lines in Fig. 2), giving a fine membrane of silver chloride coated on the metal surface.

Procedure for the determination of chloride in water

The carrier stream (1 mol dm^{-3} potassium nitrate) is pumped at a constant flow rate of 3.90 cm^3 min^{-1} (Fig. 1). A pulse suppressor coil (200 cm × 0.51 mm i.d.) is incorporated between the peristaltic pump and the sampling valve. Samples from an automated sampler are injected automatically from a 30-μl sampling loop into the carrier stream by means of the two-position valve. While one loop serves the carrier stream, a sample is drawn through the other loop at a constant flow rate of 2.00 cm^3 min^{-1}. Injected samples are mixed with the carrier in a 105-cm mixing coil, and mixed again with 1 mol dm^{-3} potassium nitrate at a flow of 0.80 cm^3 min^{-1} in a second mixing coil (160 cm) before the potential is measured in the coated tubular electrode. A 30-s cycle sampling time is used, giving a capacity of 120 samples per hour. The valve system is actuated on a time basis which is correlated with the sampler unit; the sampling valve is actuated every 28 s.

RESULTS AND DISCUSSION

Behaviour of the coated tubular electrode

Preliminary experiments were conducted in order to optimize the flow-injection system parameters like line length, transmission tube inside diameter, flow rate and sample volume [14] as well as the performance of the electrode itself (design, contact area, volume). Initial results indicated a slight pulsation originating at the peristaltic pump as well as sample plug pulsation. Both were eliminated to a great extent, pump pulsation by the incorporation of a 200-cm coil as pulse suppressor between the pump and the sampling valve and plug pulsation by the incorporation of a 105-cm coil just after the sampling valve. The addition of 1 mol dm^{-3} potassium nitrate at 0.80 cm^3 min^{-1} further downstream improves the hydrodynamic flow conditions in terms of less pulsation observed (maybe because of some back-pressure), better resolution between peaks (return to baseline faster), better reproducibility and a more stable baseline. This flow arrangement gives better overall results than the use of a single carrier stream at a flow rate higher than 3.9 cm^3 min^{-1}. The effect of the ionic strength of the potassium nitrate carrier solutions on the behaviour of the coated tubular electrode was also studied. Results indicated that for concentrations lower than 1 mol dm^{-3}, the precision decreased mainly because the electrode system was less stable. This was particularly observed for chloride concentrations near the lower limit of the near-Nernstian response range.

Results obtained with ion-selective electrodes in flow-injection analysis can be greatly affected by the design, contact area and volume of the constructed units. Large dead cell volumes cause tailing of peaks, slower return to baseline and thus lower sample throughput. Therefore, cell volumes are kept small in order to minimize the hold-up volume and maximize the analyte velocity across the sensor membrane [15]. Maximum contact area is obtained by using a tubular electrode which is well coated. Coated tubular electrodes with different geometrical dimensions were constructed and evaluated. Results indicated that for tubular flow cells with an internal diameter of less than 0.5 mm, there was a tendency to pressure build-up in the manifold which led to lower precision, especially at higher flow rates. When the internal diameter exceeded 3 mm, the signal took longer to return to baseline; this became more prominent at low flow rates, and was also observed for increased electrode length. The electrode with an internal diameter of ca. 2 mm and a length of 5 mm gave the best results for the type of flow diagram in Fig. 1. The maximum sensitivity was obtained when the electrode was coated, tested, left in ca. 1000 mg dm^{-3} chloride solution, recoated, etc., until maximum response was obtained, and then left overnight in 1000 mg dm^{-3} chloride solution.

Linear response range

Trojanowicz and Matuszewski [16] reported a theoretical discussion of the limitations of the linear response for ion-selective electrodes in flow-injection

systems. They tried to explain why the dynamic measuring ranges for ion-selective electrodes are always much poorer than when the same electrodes are used in classical batch modes. They concluded that the lowest limit of determination on the linear part of the calibration curve is governed not only by the solubility of the electrode material but also by contamination or adsorption at the electrode surface.

The linear response range of the electrode was measured by pumping standard working chloride solutions in 1 mol dm^{-3} potassium nitrate at 3.9 cm^3 min^{-1} into a single-line manifold to the detector until a steady-state signal was obtained. The results (Fig. 3) showed a linear response up to 20 mg dm^{-3} which is a little better than the response of a flow-through cell based on a silver sulphide/silver chloride electrode [13]. The calculated Nernstian response of the tested electrode is 57.7 mV per decade with a correlation coefficient of 0.9998. However, the linear range also depends on the pretreatment of the electrode and care should be taken during the preparation of each new coated tubular electrode.

Of the various flow-injection parameters, experimental work showed that the injected volume influenced the results most strongly. The sample volume is not only crucial to the design of efficient flow-injection systems, but also plays a major part in the sensitivity and linearity of a calibration curve. The dynamic linear response range was less than that shown in Fig. 3, when a sample volume of 30 μl was injected into the flow system used in Fig. 1, which confirmed the results obtained by Trojanowicz and Matuszewski [16]. This volume, however, gave the best reproducibility as well as linearity and was chosen for further work. The dependence of the peak height on the concentration of a series of 30-μl injected standard chloride solutions is given in Fig. 4. It can be seen that the use of the simple coated tubular electrode enables the working chloride concentration range to be extended to 5000 mg dm^{-3} as needed and even more. This makes the method more versatile than the usual spectrophotometric procedure based on reaction with mercury(II) thiocyanate, which has a rather limited linear range [17—20] unless sample splitting or automatic sample dilution is used.

Practical response time

An important theoretical paper concerning the measurement of chemical response time of microelectrodes appeared recently [21]. Haemmerli et al. [21], as well as Pungor and Umezawa [22], gave guidelines for the determination of response times in electrochemical cells containing ion-selective electrodes in order to obtain a unified approach, which was used here. The dynamic response time of the coated tubular electrode was measured at 63% and 95% of the steady-state potential by injecting 30 μl of standard chloride solutions into the 1 mol dm^{-3} potassium nitrate carrier solution. The standard chloride solutions contained the same background electrolyte concentration as the carrier solution to obviate any mixing effects. It is clear from the results in Table 1 that the response times for the different chloride concentrations

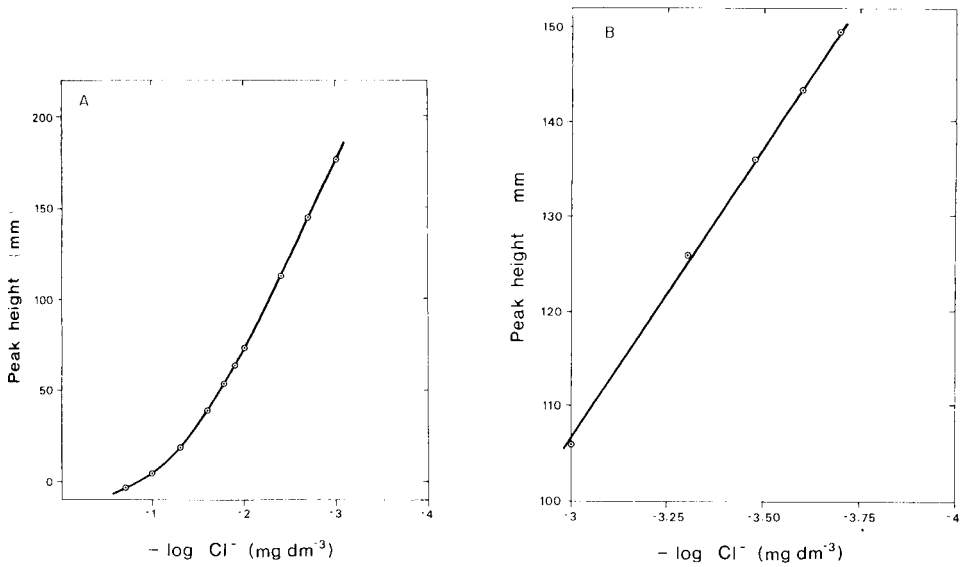

Fig. 4. Calibration curves for the determination of chloride in different concentration ranges with the manifold shown in Fig. 1: (A) 5—5000 mg dm^{-3} chloride; (B) 1000—5000 mg dm^{-3} chloride.

TABLE 1

Practical response time for the coated tubular solid-state chloride-selective electrode used with the flow-injection system[a]

Chloride concentration (mg dm^{-3})	Response time		Time recorded from baseline to baseline (s)[b]
	63%	95%	
5000	1.1(±0.2)	3.9(±0.3)	49.6(±1)
1000	1.4(±0.2)	3.3(±0.2)	43.1(±1)
500	1.5(±0.1)	3.2(±0.1)	38.4(±1)
100	1.6(±0.1)	3.1(±0.1)	29.4(±1)
40	1.9(±0.2)	3.0(±0.1)	24.2(±1)

[a]All data are the means and standard deviations for 5 measurements. [b]Measured with the flow diagram in Fig. 1.

were very fast. However, real sample throughput of chloride samples is dependent on the flow system (Fig. 1). Therefore the time required from baseline back to baseline was also measured (see Table 1). Although the time taken for a 5000 mg dm^{-3} chloride injection from baseline back to baseline was measured as 49.6(±1) s, the time taken for the same peak to go from baseline to 63% of the descending part of the peak was only 10.5 s, and the time from baseline to 2% of the descending part of the peak was 26 s. This gives the flow system used (Fig. 1) a sample throughput of about 138 h^{-1}.

Interferences

The electrode performance was not influenced when the pH in the samples was changed from 2 to 12. The presence of ammonia destroyed the electrode response rapidly, because of the formation of a soluble diammine silver complex.

As some water samples are preserved with a mercury(II) solution, the interference of mercury(II) ions on the electrode response was investigated. Although the interference was less and the destruction of the electrode was slower with the 30-μl sample injections than with a continuously aspirated sample, the effect was still disastrous. Therefore, the electrode is not suitable for use with water samples preserved with mercury(II).

The tubular coated chloride-selective electrode also suffers interference from ions forming insoluble salts, particularly those ions which form silver salts more insoluble than silver chloride. Thus bromide, iodide, cyanide, sulphide, arsenate and phosphate interfere. A baseline drift was found when the interference of each of these anions was investigated, an effect which became more pronounced with increasing concentration. But again the flow-injection system with only 30-μl injections was much less affected than the continuous sample-flow method. Investigation of the electrodes destroyed by bromide or iodide which was pumped continuously, showed yellow films of the silver halide covering the surface of the electrode in each case.

The inferferences of iodate, acetate and sulphate were also evaluated by using the flow-injection system. With sulphate, a slight interference became noticeable at about 80 mg dm^{-3} sulphate, and with acetate and iodate at about 200 mg dm^{-3}. However, the effect on results was only significant when the sulphate concentration was more than 500 mg dm^{-3} and when the acetate or iodate concentration was more than 1000 mg dm^{-3}.

Analysis of water samples

The system outlined in Fig. 1 is suitable for analysing water samples with chloride contents up to 5000 mg dm^{-3}. A representative output for the determination of chloride in surface, ground and domestic waters at a sampling rate of 120 h^{-1} is shown in Fig. 5. The potentiometric output is split and the two signals are recorded on a two-pen recorder at 20-mV and 50-mV settings. The 20-mV setting is used to cover the 0—1000 mg dm^{-3} chloride range and the 50-mV setting for the 1000—5000 mg dm^{-3} chloride range. The samples were injected in random order to test carry-over effects, which were found to be negligible. Little baseline drift was experienced and there was no consistent long-term bias in the baseline. Calibration curves for the two recorder settings are given in Fig. 4.

The performance and reproducibility of the proposed coated tubular solid-state chloride-selective method are shown in Table 2. In addition to a high sample throughput (120 h^{-1}) over a wide concentration range, the procedure is characterised by good reproducibility (<1.7%). The results obtained with the proposed procedure were evaluated against a standard automated

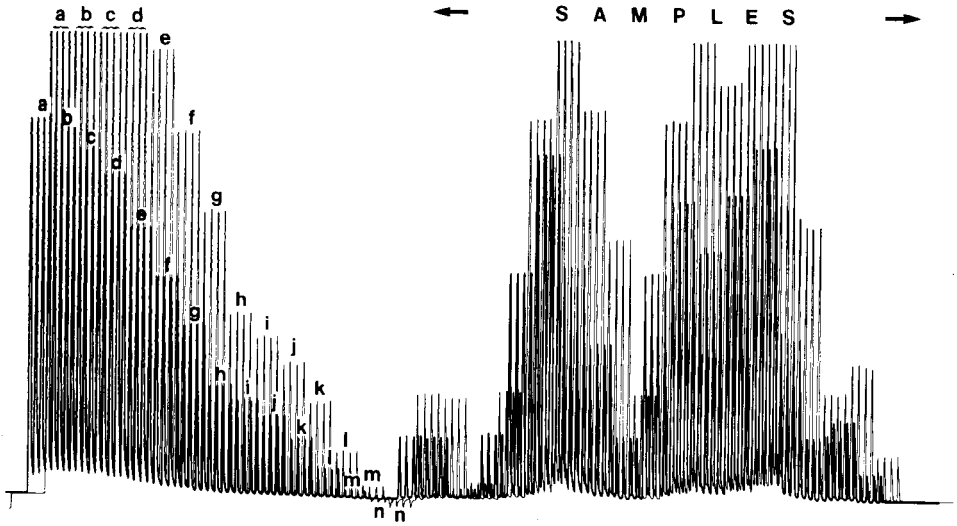

Fig. 5. Recorder tracings, with different recorder ranges, for the flow-injection determination of chloride in water. From left to right: 5—5000 mg dm^{-3} standard chloride solutions followed by routine water samples, each solution being injected four times. Recorder paper speed, 5 mm min^{-1}. Recorder ranges, 50 mV for 1000—5000 mg dm^{-3} chloride and 20 mV for 5—1000 mg dm^{-3} chloride. Chloride concentration (mg dm^{-3}): (a) 5000; (b) 4000; (c) 3000; (d) 2000; (e) 1000; (f) 500; (g) 250; (h) 100; (i) 80; (j) 60; (k) 40; (l) 20; (m) 10; (n) 5.

TABLE 2

Performance and reproducibility of the proposed method[a]

Sample	Chloride conc. (mg dm^{-3})		R.s.d. (%)	Sample	Chloride conc. (mg dm^{-3})		R.s.d. (%)
	Automated segmented method	F.i.a.			Automated segmented method	F.i.a.	
1	44	42	1.36	9	1709	1703	0.51
2	10	11	1.67	10	3708	3714	0.29
3	567	572	0.65	11	225	221	0.89
4	3236	3229	0.33	12	67	63	1.30
5	628	633	0.71	13	19	21	1.49
6	203	200	0.94	14	4649	4637	0.21
7	1512	1510	0.56	15	171	176	0.97
8	817	812	0.66	16	97	91	1.14

[a]Mean result of 15 tests in each case, with relative standard deviation for the flow-injection method.

segmented spectrophotometric method (Table 2). Good agreement is apparent. The accuracy of the proposed method was also tested by the standard additions method. Known amounts of chloride were added to water samples which were processed before and after addition. The mean recoveries for

TABLE 3

Performance and electrode response stability on a day-by-day basis
(All results are the mean of triplicate determinations.)

Period	Concentration of injected chloride solutions (mg dm^{-3})				
Day 1[a]	20	100	500	1000	5000
Day 2	19	97	495	991	4989
Day 7	18	94	489	984	4976

[a]Calibration standards started. Days 2 and 7 refer to the response obtained on day 1 as calibration.

water samples containing 67 and 114 mg dm^{-3} chloride were respectively 97.8% and 98.9%.

The performance and stability of the electrode response were tested on a daily basis (Table 3). Results indicated that the response was very stable, though it is necessary to do calibration on a daily basis. One electrode was stored for about seven months. The electrode maintained a slope of 58—55 mV. An electrode which was left in a dried-out beaker for the same period, gave a very good performance when the sensing film was renewed.

Conclusion

The coated tubular ion-selective electrode based on an inorganic salt offers certain advantages over conventional sensor end-caps and flow-through cells used in flow-injection analysis. The electrode is simple and easy to construct, inexpensive and has a very long lifetime. It is re-usable and, once the electrode has been prepared, it requires minimum maintenance which should be very attractive for routine laboratories. The tubular configuration can be used for the preparation and coating of any inorganic-based insoluble salt provided that good adhesion to the metal surface is obtained. A study of other inorganic-based salts is underway and preliminary results are promising.

The advantages of this concept can be further appreciated from the excellent characteristics of reproducibility and stability obtained from the proposed chloride ion-selective electrode interfaced with flow-injection analysis.

The author expresses his gratitude to the Council for Scientific and Industrial Research, Pretoria, and to the University of Pretoria for financial support, and also to the Hydrological Research Institute, Pretoria, for supplying the analysed samples.

REFERENCES

1 J. Růžička, E. H. Hansen and E. A. Zagatto, Anal. Chim. Acta, 88 (1977) 1.
2 E. Pungor, Zs. Fehér, G. Nagy, K. Tóth, G. Horvai and M. Gratzl, Anal. Chim. Acta, 109 (1979) 1.

3 K. Tóth, G. Nagy, Zs. Fehér, G. Horvai and E. Pungor, Anal. Chim. Acta, 114 (1980) 45.
4 W. J. Blaedel and L. N. Klatt, Anal. Chem., 38(7) (1966) 879.
5 W. J. Blaedel and D. E. Dinwiddie, Anal. Chem., 47(7) (1975) 1070.
6 W. J. Blaedel and D. G. Iverson, Anal. Chem., 49(11) (1977) 1563.
7 H. Thompson and G. A. Rechnitz, Chem. Instrum., 4(4) (1972) 239.
8 P. L. Meschi, Ph.D. Thesis, Iowa State University, Ames, IA, 1981.
9 M. E. Meyerhoff and P. M. Kovach, J. Chem. Educ., 60(9) (1983) 766.
10 W. E. van der Linden and R. Oostervink, Anal. Chim. Acta, 101 (1978) 419.
11 S. Alegret, J. Alonso, J. Bartroli, J. M. Paulis, J. L. F. C. Lima and A. A. S. C. Machado, Anal. Chim. Acta, 164 (1984) 147.
12 C. Harzdorf, Anal. Chim. Acta, 136 (1982) 61.
13 H. Müller, in E. Pungor (Ed.), Ion-selective electrodes 3. Proceedings of the Third Symposium, Matrafüred, Hungary, October 1980; Analytical Chemistry Symposia Series, Vol. 8, Elsevier, Amsterdam, 1981, p. 279.
14 J. Růžička and E. H. Hansen, Flow-Injection Analysis, Wiley, New York, 1981.
15 P. L. Bailey, Analysis with Ion-selective Electrodes, Heyden, London, 1980.
16 M. Trojanowicz and W. Matuszewski, Anal. Chim. Acta, 138 (1982) 71.
17 J. Růžička, J. W. B. Stewart and E. A. Zagatto, Anal. Chim. Acta, 81 (1976) 387.
18 J. Růžička, E. H. Hansen, H. Mosbaek and F. J. Krug, Anal. Chem., 49 (1977) 1858.
19 E. H. Hansen and J. Růžička, J. Chem. Educ., 56 (1979) 677.
20 W. D. Basson and J. F. van Staden, Water Res., 15 (1981) 333.
21 A. Haemmerli, J. Janata and H. M. Brown, Anal. Chim. Acta, 144 (1982) 115.
22 E. Pungor and Y. Umezawa, Anal. Chem., 55 (1983) 1432.

Analytica Chimica Acta, 179 (1986) 419—425
Elsevier Science Publishers B.V., Amsterdam — Printed in The Netherlands

ON-LINE APPLICATION OF ION CHROMATOGRAPHY IN A THERMAL POWER PLANT

L. BALCONI, R. PASCALI* and F. SIGON

ENEL (Central Electricity Generating Board), Research and Development Division, Thermal and Nuclear Research Centre, Via Rubattino 54, Milano (Italy)

(Received 3rd August 1985)

SUMMARY

Complete monitoring of the "condensate-feedwater" cycle in power plants requires reliable automatic methods suitable for very low concentrations of various chemical species. A complete on-line ion-chromatography monitoring system is under development. It comprises an automatic on-line sampling system, two Dionex Model QIC (process instrument) ion chromatographs, an on-line calibration system, and a data acquisition/processing system. The present model serves for the determination of sodium, chloride and sulfate ions. Detection limits are $<1\ \mu g\ l^{-1}$ ($P = 95\%$) with linear ranges up to $10\ \mu g\ l^{-1}$ or about $200\ \mu g\ l^{-1}$, depending on settings. The importance of statistical evaluation of data is emphasized. The instrumentation was tested for sequential samples from crucial points of a 320-MW thermal power station with satisfactory results. Problems of reliability are discussed.

Chemical monitoring in power stations has become increasingly important because of the better performance and reliability required from both thermal and nuclear power plants. In the present situation, the chemical characteristics of the cycle fluids pose considerable analytical problems because the concentrations of the species to be determined are very low, often in the $\mu g\ l^{-1}$ to ng l^{-1} range (10^{-8}—10^{-11} M). Few analytical techniques normally used for plant monitoring are adequate for such concentrations. In identifying the chemical causes of plant malfunctioning, the number of the chemical species that should be monitored also causes problems. The development of special analytical techniques suitable for on-line control is necessary, as well as complementary activities to allow further improvements in plant performance. In this context, the application of ion chromatography in both thermal and nuclear power plants has been examined.

Ion chromatography [1] makes it possible to determine ionic species in solution with low detection limits and good precision. Process chromatographic systems have been developed for on-line use in power plants; anions, cations and organic species can be determined [2, 3]. The choice of ion chromatography is justified by the very low concentration levels of the species to be determined, which means that contamination must be avoided in handling of samples. Automation also allows continuous operation, which

0003-2670/86/$03.50

results in an optimum use of the instrument. On-line automatic systems have been developed by General Electric/EPRI (Iontrac system for anions, cations, and organics), by Dionex and by a British combine [4]. In 1983, the Italian Electricity Generating Board initiated research on the development of a cheap on-line analytical system for anions and cations, with the aim of evaluating performance and costs for use both in conventional thermal power plants and in nuclear power plants. The system was developed particularly for the determination of sodium, chloride and sulphate ions, and is being tested in a conventional power plant, where it is used to monitor the most important points of the water-steam cycle.

EXPERIMENTAL

Instrumentation

The system developed consists of on-line sampling equipment, two ion chromatographs for quantifying cations and anions respectively, a calibration system and equipment for data acquisition and processing and automatic management of the instrument (Fig. 1). All these components are placed in a mobile double rack. A power supply unit which ensures a stable supply is also arranged in a mobile unit.

The sample is filtered through teflon filters (porosity 0.22 μm) to remove suspended or colloidal solids, and collected in a teflon container from which it is extracted by the sampling pump; excess of sample is diverted to waste. Containers with volumes of about 500 ml and 10 ml were tested so that average values for different integration volumes could be determined.

The system allows the analysis of five samples so that several points of interest in a power plant cycle can be monitored simultaneously. The samples are selected by a system of pneumatic valves (Fig. 2) which are suitably configured and controlled by the computer. The sampling pump is of the syringe type with a single sapphire piston and a teflon closing chamber. For washing

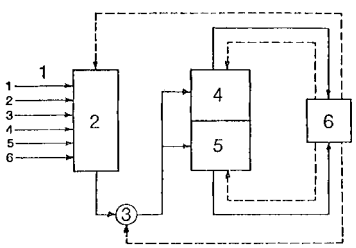

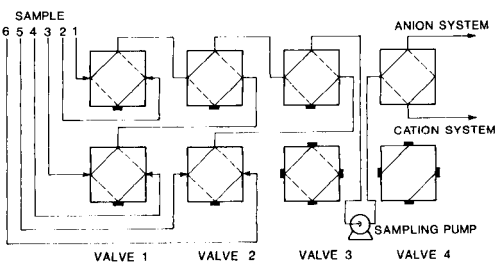

Fig. 1. Functional diagram of the on-line system. (1) Sampling lines, 1—6; (2) pneumatic valve system for sample selection; (3) sampling pump; (4) ion chromatograph for anions; (5) ion chromatograph for cations; (6) data acquisition and processing system.

Fig. 2. Configuration of the pneumatic valve system set for sample selection and delivery to the anion and cation systems.

the lines so as to minimize contamination of subsequent samples, the three-way pneumatic valve which allows loading and injection of the sample alternately was replaced by a suitable four-way valve (Fig. 3). The sample loading loop was also attached to a preconcentration column to reduce the detection limits.

The present calibration system consists of a multiple-head peristaltic pump which allows the production of standards with on-line dilution. This method was adopted to avoid the contamination phenomena which are difficult to eliminate in off-line preparation of standards. It was shown in preliminary work [5, 6] that difficulties in preparing standards have a decisive effect on the uncertainty associated with the calibration curves.

A Spectra Physics model 4270 computer deals with data acquisition and processing and management of the ion-chromatography system. It uses an 8-bit Z80A processor, is multitask and can be programmed in BASIC. The software for data acquisition and integration (written in machine language) and for chromatogram management (developed by Spectra Physics) occupies 48 kbyte of EPROM together with the operating system. The further 16 kbyte available in RAM can be used to develop the management program described below. Two interfaces including an A/D converter with 12-bit resolution allow the acquisition of chromatographic data; a further I/O interface with 12 TTL switches provides control of the valves and pumps. The RS232C outputs allow access to external peripherals or to networks with LABNET communication protocol.

The analytical system is made up of two Dionex model QIC ion chromatographs. The process model chosen is simple and reliable, but does not have the flexibility of the laboratory ion chromatographs. The operational conditions adopted are summarized in Table 1. With regard to the characteristics of the fluids considered, the sampling time used represents a compromise between the possibility of obtaining useful conductivity values at low concentrations and ensuring linearity of response at high concentrations. The flow rate of the sampling pump (2.5 ml min^{-1}) allows the quantitative preconcentration of the samples, as described by Dionex.

Calibration

Calibration graphs with two ranges, 0—10 and 0—200 $\mu g\ l^{-1}$ were constructed so that any concentration transients could be determined. The full-scale

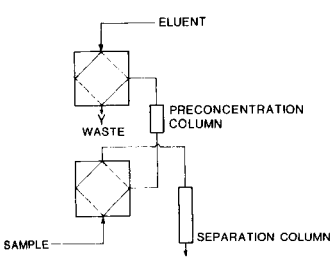

Fig. 3. Configuration of the pneumatic valve for sample loading and injection.

TABLE 1

Operating conditions adopted for cation and anion determinations

	Anion determination	Cation determination
Columns: preconcentration	HPIC-AG4	CG1
separation	HPIC-AS4	CS1
suppression	AFS[a]	CFS[a]
Eluent	2.8 mM $NaHCO_3$/2 mM Na_2CO_3	5 mM HCl
Regenerant	0.0125 M H_2SO_4	0.04 M TMAOH[b]
Eluent flow (ml min^{-1})	2	2.3
Regenerant flow (ml min^{-1})	2.5—3	2.5—3
Sampling time (min)	5	5
Sampling rate (ml min^{-1})	2.5	2.5
Conductimeter range (μS)	100	100

[a]Fibre suppressor. [b]Tetramethylammonium hydroxide.

values imposed allow measurements of conductivity relative to both the ranges indicated, because the characteristics of the A/D converter allow the acquisition of values with a resolution equal to 1×10^{-6} of the chosen full-scale value.

As a conventional power plant was to be monitored, the interference of ammonia and hydrazine in the determination of the three ions considered was evaluated. To do this, water from the condensate treatment was used; the conditioned fluid was simulated by the addition of 0.8 mg l^{-1} ammonia and 150 μg l^{-1} hydrazine, and the steam was simulated by the addition of 0.8 mg l^{-1} ammonia. No interferences were found for the sodium and sulphate ions with preconcentration times up to 8 min, whereas even with lower preconcentration times the presence of ammonia reduced the response for chloride. This can be ascribed to the eluotropic power of hydroxide towards the chloride ions which are eluted in the preconcentration phase. It was established that the rate of elution was a function of the concentration of ammonia in solution and of the volume of sample preconcentrated. Calibration graphs with and without ammonia were thus constructed for chloride, the ammonia concentration being equal to the average concentration present in the plant.

In the system designed, the calibration graphs were prepared manually in a preliminary step and the data obtained were processed by linear regression with the least-squares method directly on the SP4270. The processing, based on conventional techniques, gave the analysis of variance, slope, intercept and relative standard deviations, and correlation coefficient, as well as the detection limit C_d and its confidence interval. The parameters useful for evaluation of the standard error associated with each measurement on real samples were also calculated and printed. The standard error of the calibration graph is of particular importance, given the concentration levels investigated, for correct interpretation and safe use of the information contained in the analytical data.

When the system is operating automatically and the calibration has been done, it is checked with a standard to confirm the analytical response. This standard is prepared continuously by on-line dilution. One of the samples to be analysed is used as dilution water, preferably the sample immediately before the standard itself, and then its contribution to the concentration is subtracted. The uncertainty connected with the measurement of the standard is printed, taking into account the uncertainty associated with the measurement of the dilution water. As a plant fluid is used for the dilution, its analyte concentration constitutes the system blank and may vary with time. This makes it necessary to check if any trend in concentration is present and to repeat the measurement if a trend is found. If the system is not performing within present statistical limits, alarm messages are sent automatically to the operator.

Computer control

The management program includes data bases and special subprograms as well as interaction with the user. The data bases contain the default values of the parameters necessary for operation, which are accessible to the operator in interactive mode. This category includes the chromatographic integration parameters for the ion calibration lines and for the calculation of standard errors of measurements, as well as data on the chromatographic peaks which are needed for identification of the peaks.

The subprograms developed can be selected by the operator to provide greater control and management flexibility. It is possible to check the state of the system, before each new experiment, for (a) sampling and analysis sequence; (b) attribution of sampling lines, plant, group and data; (c) kind of ions chosen for the report; (d) parameters of the calibration graphs and measurement errors for each ion; and (e) concentration levels of the control standard and dilution water type. It is also possible to choose different options for the sampling sequence of the five sample lines with insertion of the standard at different points of the cycles. It is envisaged that two different calibration functions will be used in the analysis of real samples, depending on the concentration measured in the samples; the choice between the two functions will be made automatically by the system which will also consider the presence and effect of ammonia in the fluid. In the final step, values less than the lower limit of the confidence interval of the detection limit or higher than the upper limit of the calibration are rejected, the standard errors for the analytical data are calculated, and the data collected are printed out.

RESULTS AND DISCUSSION

The results obtained for all the calibrations are reported in Table 2. The detection limits and associated confidence intervals are calculated with a probability level of 95%. The standards for the low concentration levels were

TABLE 2

Detection limits, their confidence intervals and average standard errors connected with the calibration graphs constructed for sodium, chloride and sulfate ions

Ion	Detection limit C_d, P = 95% ($\mu g\ l^{-1}$)	Confidence interval on C_d, P = 95% ($\mu g\ l^{-1}$)	Average standard error ($\mu g\ l^{-1}$)
Concentration range: 0—200 $\mu g\ l^{-1}$ Na^+, SO_4^{2-}; 0—160 $\mu g\ l^{-1}$ Cl^-			
Na^+	3.0	±2.1	±1.8
Cl^-	3.3	±2.7	±2.1
Cl^-[a]	6.2	±3.1	±3.9
SO_4^{2-}	6.7	±3.9	±4.0
Concentration range: 0—10 $\mu g\ l^{-1}$			
Na^+	0.1[b]	±0.3	±0.1
	0.8[c]	±0.6	±0.5
Cl^-	0.4[b]	±0.8	±0.3
	0.7[c]	±0.4	±0.4
Cl^-[a]	0.9[b]	±2.0	±0.7
	1.7[c]	±1.5	±1.0
SO_4^{2-}	0.3[b]	±0.7	±0.2
	0.9[c]	±0.4	±0.5

[a]In presence of 0.8 mg l^{-1} ammonia. [b]Standards produced using a single pair of calibrated tubes and standards of different concentration. [c]Standards produced using several pairs of calibrated tubes and a standard of fixed concentration.

obtained in two different ways: varying the concentration of the standard to be diluted and using only one pair of calibrated tubes, or using one standard to be diluted and several pairs of calibrated tubes. The former procedure gave lower detection limits, probably because of variations in the flow rate of the calibration tubes, although they were calibrated at the beginning of the experiment. The confidence intervals were however larger, because fewer standards were used to construct the calibration graphs. The calibration graphs for chloride in the 0—200 $\mu g\ l^{-1}$ range deviated from linearity for concentrations greater than 160 $\mu g\ l^{-1}$, which was therefore considered as the upper measurement limit.

The ion-chromatography system has been used, in its present qualification stage, to monitor the following points of the water-steam cycle of a 320-MW thermal power plant: feed water, make-up water, superheated steam, blow-down, and condensate. Figure 4 gives typical examples of the results obtained.

The determination of chloride in the 0—10 $\mu g\ l^{-1}$ range in the presence of ammonia was found to be unreliable, because of the variability of the ammonia concentration with respect to the mean value considered. The present approach to this problem cannot be considered to be the best; it will be necessary to consider the uncertainty deriving from the variation of the ammonia concentration in the plant fluids and to associate this uncertainty with the standard error of the chloride measurement. The system has not so

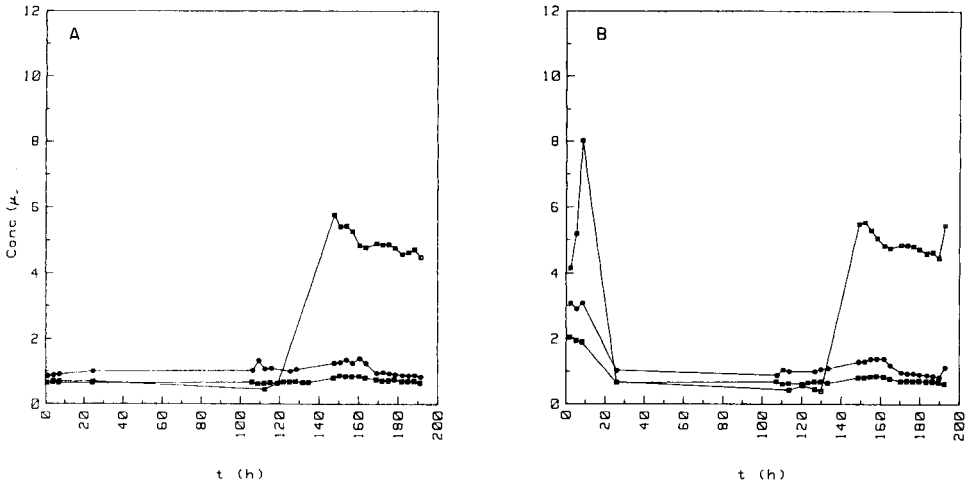

Fig. 4. Examples of data obtained at different points in the water-stream cycle: (A) make-up water; (B) blow down. Ions: (▪) sodium; (□) sulfate; (•) chloride.

far presented particular problems as far as the determinations of sodium and sulphate and the hydraulic and electronic reliability are concerned. The need for accurate checks of the sampling phase in relation to the pressure and flow values of the samplers was shown; a regulation system will be supplied in the later models. Further improvements in performance should be obtainable by improving the calibration methods.

REFERENCES

1 H. Small, T. Stevens, W. Bauman, Anal. Chem., 47 (1975) 1801.
2 ASTM Symposium on Plant Instrumentation for Measurement of High Purity Water Quality, Milwaukee, WI, June, 1980.
3 See, e.g., M. N. Robles and J. L. Simpson, G. Brobst, B. G. A. Alvi and T. O. Passell, On-line ion chromatographic measurement of impurities in the secondary water-steam system of two PWRs. Water Chemistry, 3, British Nuclear Energy Society, London, 1983.
4 M. D. H. Amey, G. R. Brown; Paper presented at International Conf. on Analytical Chemistry in Nuclear Technology, Karlsruhe, June, 1985.
5 M. L. Balconi, R. Brocchieri, F. Sigon; Internal report ENEL-N0-84-01, 1984.
6 M. L. Balconi, R. Pascali, F. Sigon; Paper presented at 15 Congresso Nazionale della Società Chimica Italiana. Grado, September, 1984.

Analytica Chimica Acta, 179 (1986) 427—432
Elsevier Science Publishers B.V., Amsterdam — Printed in The Netherlands

Short Communication

FLOW CELL AND DIFFUSION COEFFICIENT EFFECTS IN FLOW INJECTION ANALYSIS

D. C. STONE and J. F. TYSON*

Department of Chemistry, University of Technology, Loughborough, Leicestershire, LE11 3TU (Great Britain)

(Received 2nd August 1985)

Summary. The effects of flow cell geometry and nature of the solute on peak shape and dispersion/flow rate relationship are described. Flow cells produce significant effects caused by the finite volume sampled by the light beam and the disruption of laminar flow conditions. At low flow rates, the larger the molecules, the greater the dispersion.

Since the introduction of flow injection analysis (f.i.a.) by Růžička and Hansen in 1975 [1], several theoretical approaches have been used in attempts to provide a quantitative description of the dispersion processes that occur in flow-injection manifolds. These include the use of numerical techniques for solving the diffusion-convection equation [2], and the use of flow models borrowed from chemical engineering theory [3]. The reason for using such approaches is that it is not possible to obtain an exact solution to the diffusion-convection equation under the conditions employed in practical f.i.a.

Fundamental to the methods mentioned, is the concept of an ideal system or theoretical manifold. This concept arises from the assumptions commonly made, namely that (i) conditions of laminar flow exist, (ii) the flow is undisturbed by the injection process, (iii) flow occurs down a long, straight tube of circular cross-section, and (iv) the solute concentration is measured in a plane perpendicular to the direction of flow.

The problem in usefully applying such theoretical treatments to real flow-injection manifolds is that such assumptions are not valid. For example, although in principle laminar flow occurs in a manifold under the conditions of f.i.a., connections, valves and tight bends will all disrupt this primary flow pattern and introduce a variety of secondary flow patterns. Also, practical detectors have a finite volume, and may well give rise to major disruptions of the flow pattern as, for example, occurs in the nebulizer of a flame atomic absorption spectrometer, or in the path through a spectrophotometric flow-cell. Another problem in applying theory to practice is that manifolds for practical analyses are often more complicated than the simple, single-line case. A practical manifold may contain confluence points, segmentors, phase separators, dialysis units and so on.

0003-2670/86/$03.50

With these problems in mind, it seems unlikely that a rigorous theoretical treatment of flow-injection manifolds will be successful in producing accurate equations describing dispersion behaviour. A completely empirical approach, however, would be time-consuming, and would have no predictive power. Thus the use of flow models to describe the dispersion processes would seem to be an attractive proposition.

The single well-stirred tank model has been described for f.i.a./a.a.s [4], and this, together with other models, are currently being studied in this laboratory. As part of this study, an extensive investigation of the factors affecting dispersion is being conducted. In this communication, the results of studies of the effects of the type of flow cell and the solute used are presented.

Experimental

Apparatus. The same basic apparatus was used for all the experiments. This comprised of a peristaltic pump (Gilson Minipuls 2) fitted with an air-column depulser, an injection valve (Rheodyne 5020) fitted with a 113-μl sample loop, and one of four flow cells, connected via a 110-cm length of 0.58 mm i.d. PTFE tubing (RS Components). The flow cells used are shown in Fig. 1. Two of the cells were standard absorbance flow cells, having volumes of 8.0 and 60 μl (Pye-Unicam). The third cell was a combined absorption/fluorescence cell, having a volume of 25 μl (Hellma). The fourth cell was constructed from a piece of drawn glass capillary tubing (approximately 0.6 mm i.d.), mounted in a black perspex block at right angles to the light path of the instrument. The volume of this cell was estimated to be approximately 0.6 μl. The detector was a Pye-Unicam SP6-250 visible spectrophotometer, connected to a chart recorder (W + W Tarkan 600).

Materials. Materials used as tracers were potassium permanganate (1.33 g l^{-1}), cobalt(II) chloride (36.3 g l^{-1}), tartrazine (0.25 and 0.020 g l^{-1}; C.I.

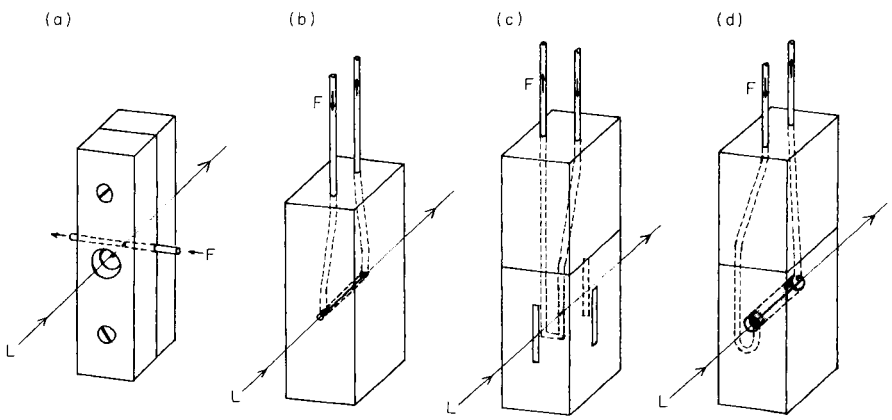

Fig. 1. The flow cells examined. F indicates flow path; L indicates light path; shading indicates optical volume. Cell volume: (a) 0.6 μl; (b) 8.0 μl; (c) 25 μl; (d) 60 μl.

19140, Pointing Ltd.), ponceau S (0.020 g l^{-1}; C.I. 27195, Fisons) and vitamin B_{12} (0.135 g l^{-1}; Sigma). Absorbances were monitored at wavelengths of 526, 513, 426, 532 and 550 nm, respectively. All the materials gave linear calibrations up to the concentrations given above.

Effect of flow cell. Solutions of tartrazine were used. The peak shapes obtained for flow rates of 0.84, 2.0 and 6.0 ml min^{-1} were recorded for each cell in turn at high chart speeds (10, 20 or 30 cm min^{-1}). Steady-state absorbance values were also measured, so that the peaks could be normalised for direct comparison, values being read directly from the chart recorder output.

Effect of solute. With the 8.0-μl cell in the spectrophotometer, the peak dispersion, D (defined as the ratio of injected to peak concentrations), was measured as a function of flow rate for each of the five solutes. Ten replicate injections were made for each sample at various flow rates in the range 0.3–10.0 ml min^{-1}. Each set of injections was followed by a measurement of the steady-state absorbance. The mean, standard deviation and 95% confidence interval about the mean were calculated for each measurement.

Results and discussion

Effect of flow cell. The peak shapes recorded for the different cells are shown in Fig. 2, plotted as normalised signal against time. For each flow rate, the curves for the 0.6-, 8.0- and 25-μl cells lie closely together. The slight differences in peak height and shape between these curves may indicate real differences between the cells, but could equally be attributed to the variation (evaluated in a separate experiment) produced by the breaking and making of connections required to change cells (see later). Although these

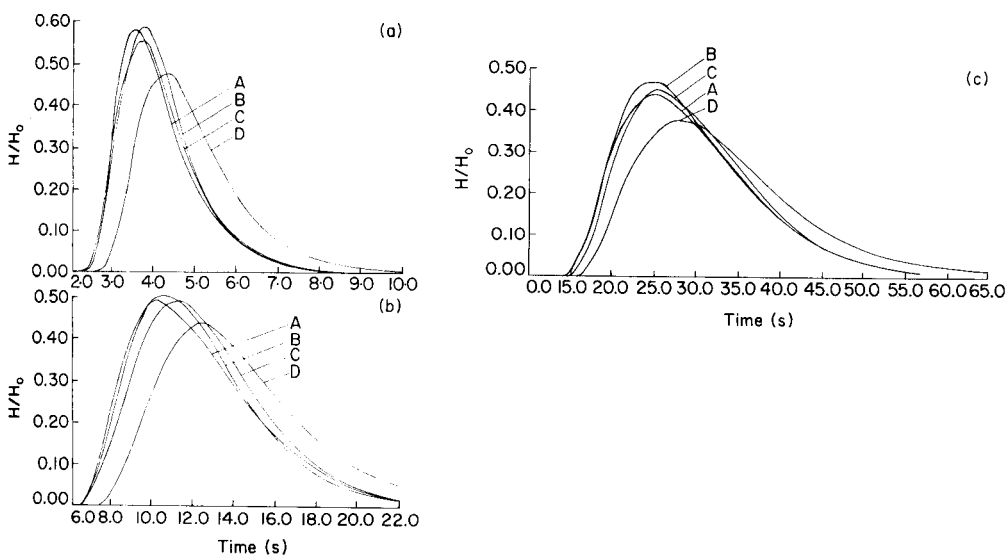

Fig. 2. Peak shapes obtained at different flow rates. Flow rate: (a) 6.00 ml min^{-1}; (b) 2.00 ml min^{-1}; (c) 0.84 ml min^{-1}. Cell volume: A, 0.6 μl; B, 8.0 μl; C, 25 μl; D, 60 μl.

three cells appear very different in size, the 0.6- and 25-μl cells represent similar measuring conditions because, for the 25-μl cell, detection also occurs across the flow, whilst only a small part of the cell coincided with the light path of the spectrophotometer, thus reducing the effective optical volume. The biggest difference in peak shape is observed between these three cells and the 60-μl cell. Peak height is significantly reduced, whilst peak width is correspondingly greater. The peak also appears significantly later in time, even though the connecting tubes were carefully cut to keep the distance between the injector and the optical volume constant. Similar results were obtained from calculations of the effect of different measuring volumes on peak shapes, in the absence of any additional mixing processes, computed from a well-stirred tank model. It was also found that the way in which the dispersion varies with flow rate can be strongly influenced by the flow cell used. These results suggest that the flow cell contributes to the observed dispersion coefficient for any manifold in two ways. One is the effect of measuring solute concentration within a finite volume; the other is the effect of bends, edges and changes in bore through the cell, giving rise to regions of turbulent mixing.

Effect of solute. The variation of the dispersion coefficient, *D*, with flow rate is shown for the five different solutes in Fig. 3. With the apparatus used, relative standard deviations for ten replicate injections were typically less than 1%. However, poorer precision was found for the value of *D* obtained under apparently identical conditions on a day-to-day basis. For a flow rate

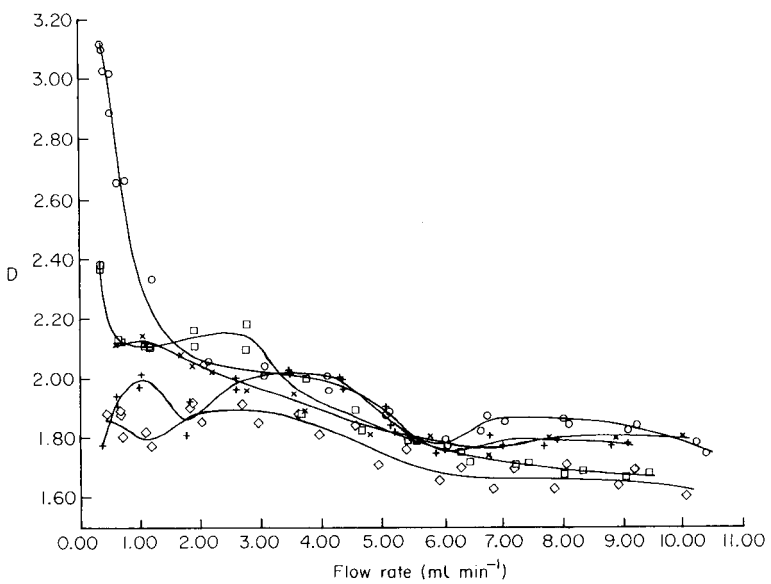

Fig. 3. Variation of the dispersion coefficient, *D*, with flow rate for different solutes: (○) vitamin B_{12}; (□) ponceau S; (×) tartrazine; (+) cobalt(II) chloride; (◇) potassium permanganate.

of 5.0 ml min^{-1}, the mean of ten individual measurements of D was found to be 1.95 with a 95% confidence interval of ±0.012. When these measurements were repeated over a period of several days, D was found to be 1.90 with 95% confidence interval ±0.089. These measurements involved the breaking and making of connections within the manifold.

Thus, some care needs to be exercised in interpreting the results obtained. Generally, the dispersion/flow rate curves for the same solute recorded on different days were in good agreement, some differences being observed at the lower flow rates. For all the solutes, the value of D tended to become constant above a flow rate of about 6 or 7 ml min^{-1}. This may indicate a limiting of the extent of dispersion by increased turbulent mixing at connections, valve and flow cell.

The biggest differences in behaviour occurred at low flow rates. Comparison of the confidence intervals for individual points for any given solute revealed that the observed changes in the value of D with flow rate represent a real effect, although the curves for each solute were not defined with great accuracy, given the poor reproducibility of the dispersion coefficient on a day-to-day basis. Differences in the value of D between the different solutes were tested by injecting each in turn at fixed flow rates, and were found to be real differences. That the diffusion coefficient of the solute should have an effect on the observed dispersion behaviour is to be expected from the diffusion-convection equation, a fact which has been exploited by Gerhardt and Adams [5] in the determination of the diffusion coefficients of molecules of biological interest.

It is proposed that the reason for the observed behaviour is that in regions of flow where the diffusion/convection equation is applicable, bigger molecules move only slowly between streamlines and are therefore subject to greater dispersion.

Conclusions

It has been shown that both the type of flow cell and the diffusion coefficient of the solute used have an influence on the observed dispersion for any given flow-injection manifold. Clearly, then, careful attention must be paid to the selection of the cell used, the cell volume and type being optimized for a particular analysis. Further, any solute used as a tracer for optimizing a flow manifold, especially for applications involving large molecules, should have similar physical properties to the analyte being determined. The results obtained also indicate that, with the injector, manifold and detector used here, the flow pattern is a function of flow rate; diffusion-convection mechanisms predominate at low flow rates but give way to a greater contribution from turbulent patterns at higher flow rates.

Financial support for D. C. S. from the SERC and Pye Unicam Ltd. is gratefully acknowledged.

REFERENCES

1. J. Růžička and E. H. Hansen, Anal. Chim. Acta, 78 (1975) 145.
2 J. T. Vanderslice, K. K. Stewart, A. G. Rosenfeld and D. Higgs, Talanta, 28 (1981) 11.
3 J. Růžička and E. H. Hansen, Anal. Chim. Acta, 99 (1978) 37.
4 J. F. Tyson and A. B. Idris, Analyst (London), 106 (1981) 1125.
5 G. Gerhardt and R. N. Adams, Anal. Chem., 54 (1982) 2618.

Analytica Chimica Acta, 179 (1986) 433–438
Elsevier Science Publishers B.V., Amsterdam — Printed in The Netherlands

Short Communication

A COMPUTER-CONTROLLED VOLTAMMETRIC FLOW-INJECTION SYSTEM

MIKAEL WASBERG and ARI IVASKA*
Laboratory of Analytical Chemistry, Åbo Akademi, SF-20500 Turku/Åbo (Finland)
(Received 30th September 1985)

Summary. Voltammetric measurements are done with a laboratory-made digital voltammeter; the detector is a thin-layer cell with a glassy carbon working electrode. Three 3-way and one 8-way magnetic valves are used to switch the flows to the detector. The 8-way valve can also be used as the injection valve. An ABC-80 computer controls the system, with a single-chip microcomputer as slave to control the voltammeter. The system was tested in continuous monitoring and in flow-injection determination of iodide. An automatic stripping voltammetric method for the determination of chloride is also described.

Spectrophotometric detection is still the most frequently used detection method in flow-injection applications, but various electrochemical techniques have been applied, including polarographic, voltammetric and amperometric detectors [1]. Reasons for the relatively few applications of voltammetric techniques are that they require more sophisticated instrumentation than most spectrophotometric methods and that the compounds to be determined should be electrochemically active unless some prior chemical reaction is utilized. A study on the application of a flow-through detector with different voltammetric techniques and using different working modes has been reported [2].

The purpose of the work presented here was to build a computer-controlled system which would allow rapid testing of voltammetric flow-through cells, and to develop detector systems for use in continuous monitoring of process flows or in environmental screening. Determinations of iodide and chloride are used to illustrate some of the possibilities of the system.

Experimental

Chemicals. All chemicals used were of analytical grade (p.a.; Merck). Double-distilled water was used to prepare the solutions.

Instrumentation. A schematic diagram of the instrumental system used is shown in Fig. 1. The complete system is monitored by a ABC-80 8-bit desktop computer with 32 kbyte of RAM. It is connected to a digital plotter and to two floppy disc drives, each 80 kbyte, which are used for program and data storage. The ABC-80 is used as the master computer and is programmed in both BASIC and assembly language. A laboratory-built interface unit is

0003-2670/86/$03.50

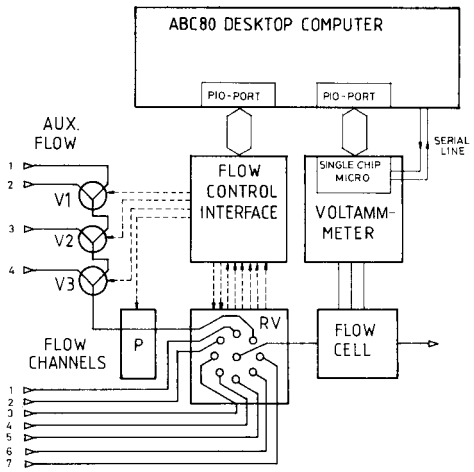

Fig. 1. The computer-controlled flow-through system.

used to control the revolving 8-way valve RV (MV-8, Pharmacia) and the three 3-way valves V1-V3 (Neptune Research). The interface unit handles the on/off power switching of the valves and the peristaltic pump (Desaga). Communication between the flow control interface unit and ABC-80 goes through a parallel in/out port (PIO). A laboratory-built digital voltammeter was used to conduct the electrochemical measurements. A single-chip microcomputer with 2 kbyte of ROM was used as slave computer to control the functions of the voltammeter as set by the master computer. The potential waveform generation and data acquisition were done by the slave, which communicated with the ABC-80 through serial and parallel lines.

The electrochemical flow-through cell was a thin-layer cell (Bioanalytical Systems) with glassy carbon as the working electrode. The Ag, AgCl/Cl (3 M NaCl) reference electrode was placed downstream from the working electrode; all potentials given are referred to this electrode. The counter electrode was a block of stainless steel.

Procedures. In the steady-state and flow-injection studies of oxidation of iodide, the standards were transferred to the flow-through cell or injected to the carrier stream by the 8-way revolving valve.

Plating of the mercury film on the glassy carbon electrode and its removal were studied as follows. Mercury(II) nitrate solution (1 mM) was passed through the detector for 2 min while the electrode potential was kept at −400 mV. The flow was then changed to 0.1 M KNO_3 and a staircase potential scan was applied from −400 mV to 1200 mV; the observed current (trace A) is shown in Fig. 2(a). A second potential sweep was applied immediately after the first scan, giving trace B in Fig. 2(a). As can be seen, some mercury remained on the glassy carbon after the first scan. Iodide solution is sometimes used to remove an old mercury film, but this approach

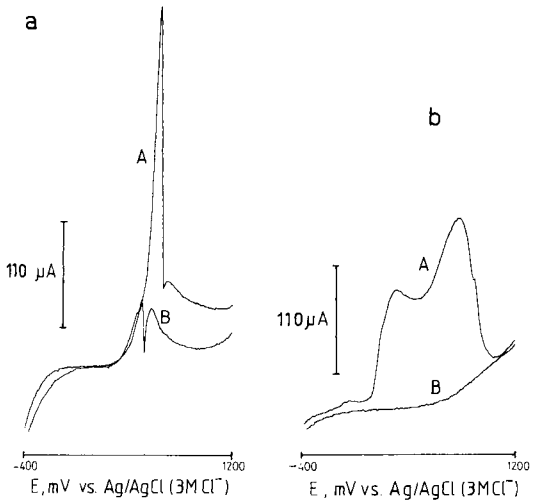

Fig. 2. Stripping of the mercury film from a glassy carbon electrode into a stream of (a) 0.1 M KNO_3 and (b) 0.1 M tetren. (A) first scan; (B) second scan, immediately after A. Scan rate 10 mV s^{-1}.

would not have been appropriate in the present study of the cathodic stripping of chloride because traces of iodide in the flow channels would have interfered seriously. Tetren (tetraethylenepentamine) forms a strong complex with mercury and was therefore chosen to aid in the removal of the old mercury film. Trace A (Fig. 2b) shows the stripping current for removal of mercury into a flow of 0.1 M tetren; trace B, obtained immediately after A, shows that the mercury had been effectively removed from the electrode surface. The double peak in Fig. 2(a, b) confirms that oxidation of mercury takes place in two steps. Complexation with tetren shifted the peak potentials and increased the peak resolution.

For the cathodic stripping determination of chloride, the mercury film was first plated on the glassy carbon electrode by applying a potential of −400 mV for 30 s while 1 mM mercury(II) nitrate solution from channel 6 of the 8-way valve passed through the detector. Then the valve was switched so that 0.1 M KNO_3 solution from channel 0 washed the detector and tubings for 1 min. With this potassium nitrate solution as the carrier stream, a standard chloride solution from channel 1 was injected for 40 s while the electrode potential was maintained at 350 mV. The flow rate was 0.18 ml min^{-1} (gravity flow was used), so that a 40-s injection means 120 µl. Then the precipitated calomel was stripped off in the carrier stream by scanning linearly at 2 mV s^{-1} from 350 to 200 mV while recording the current. Then the valve was revolved so that 0.1 M tetren solution from channel 6 flowed through the detector for 1.5 min while the potential was kept at 1000 mV, to remove the mercury film. Channel 0 was then used again to wash tetren from the system with the 0.1 M KNO_3. The whole procedure was repeated with

different chloride standards from channels 1—5. The different steps in the washing procedure are subroutines in the main control program.

The peristaltic pump (P) was by-passed in these experiments.

Results and discussion

Oxidation of iodide in 0.1 M acetate buffer pH 4.6 was chosen as the electrochemical process for testing the system described. A hydrodynamic voltammogram of iodide in the buffer was first recorded to find the working potential for the glassy carbon electrode. The current reached a plateau at 850 mV, which was chosen as the working potential. The steady-state signal was studied by passing iodide solutions of different concentrations through the detector. The revolving 8-way valve was used to switch the different flows after each other through the detector. A typical recording is shown in Fig. 3. The valve was in each position for ca. 50 s, which corresponds to 150 μl of each solution through the detector. A smooth and reproducible response was observed (Fig. 3). The change in current was linear with respect to iodide concentration; some noise can be seen on the highest peaks.

The revolving 8-way valve was also tested as the injection valve in a flow-injection experiment. The valve was switched between the buffer flow and the four different iodide solutions, remaining for 3.5 s in the position for injection of iodide solution and then returning for 26.5 s to the position for

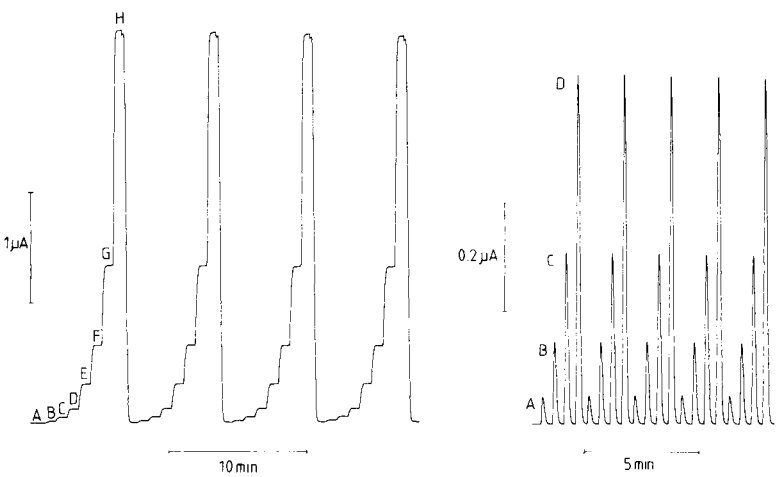

Fig. 3. Amperometric steady-state determination of iodide in 0.1 M acetate buffer pH 4.6. Steps: (A) buffer; (B) 0.01 mM; (C) 0.02 mM; (D) 0.04 mM; (E) 0.1 mM; (F) 0.2 mM; (G) 0.4 mM; (H) 1.0 mM. Applied potential, 850 mV vs. Ag/AgCl; flow rate, 0.18 ml min^{-1} (gravity). The trace corresponds to four revolutions of the 8-way valve.

Fig. 4. Flow-injection determination of iodide in 0.1 M acetate buffer pH 4.6 at 850 mV. Iodide concentration: (A) 0.04 mM; (B) 0.1 mM; (C) 0.2 mM; (D) 0.4 mM. The trace corresponds to five revolutions of the 8-way valve. Injection time was 3.5 s, corresponding to 10.5-μl injections.

buffer flow; this corresponds to an injection of 10.5 μl at the flow rate of 0.18 ml min^{-1}. The recording of this experiment (Fig. 4) shows that reproducibility was good and the signal was linearly dependent on the concentration of the sample with regression coefficient r = 0.9999 and rel. st. dev. ±3%(5) and ±0.6%(5) at the lower and higher end of the curve respectively.

The revolving valve can also be used to vary the injection volume by keeping the valve in the sampling position for different times at constant flow rate. This possibility was studied by switching the valve between two channels, 0 and 7 in Fig. 1; channel 0 passed the buffer flow through the detector whereas channel 7 passed different volumes of 1.0 mM iodide into the carrier stream. The results obtained for times of 2—10 s (6—30 μl) are shown in Fig. 5. The small peaks under A were observed when the valve was switched back to the buffer flow immediately after it had reached the sampling position, because there is always a short delay in the mechanical movement of the valve. The smallest injection volume, 6 μl, corresponds to 6 nmol of iodide. As can be seen in Fig. 5, reproducibility was good.

Computer control of the revolving 8-way valve and the additional 3-way valves allows the operator to use different sequences of the flows. This approach was tested in the determination of chloride by cathodic stripping with the flow-injection technique. The procedure is described in the experimental section. Standard chloride solutions were injected into the 0.1 M KNO_3 carrier stream. The observed stripping currents are shown in Fig. 6. Chloride from the reference electrode could not interfere because of its placement downstream. As can be seen, the stripping peak increases with the

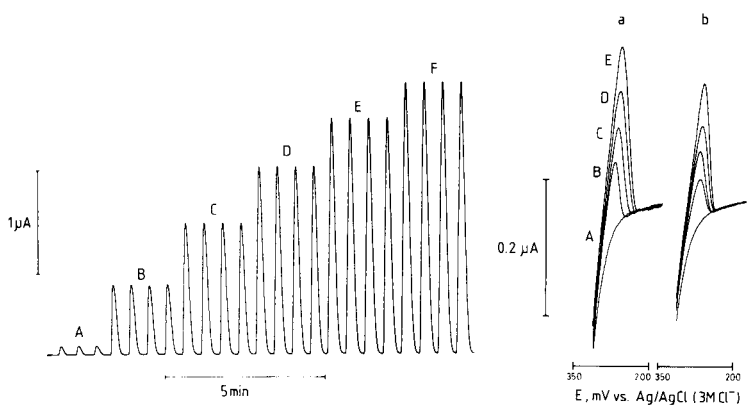

Fig. 5. Changing the injection volume by varying the time that the valve is in the sampling position. Carrier stream, 0.1 M acetate buffer pH 4.6; sample, 1.0 mM KI in the same buffer; detection and flow parameters as in Fig. 3. Injection times (volumes): (A) immediate return to the buffer flow; (B) 2 s (6 μl); (C) 4 s (12 μl); (D) 6 s (18 μl); (E) 8 s (24 μl); (F) 10 s (30 μl).

Fig. 6. Cathodic stripping voltammograms of chloride: (A) 0.1 M KNO_3 alone; (B) 0.08 mM; (C) 0.10 mM; (D) 0.12 mM; (E) 0.14 mM. (a) On a freshly polished glassy carbon electrode; (b) on the same electrode one day later after cleaning only with a wet tissue. Scan rate, 2 mV min^{-1}; flow conditions as in Fig. 3.

concentration of chloride. The peaks are slightly higher on the freshly polished electrode than on the electrode without pretreatment. In both cases, the calibration graph was linear over the concentration range studied. It should be noted that when the concentration of chloride was increased further, the stripping peak became smaller. Obviously, calomel is precipitated on the electrode surface and when this layer becomes too thick, the outer layers are only weakly attached to the electrode.

Conclusions

Computer control of flow-injection experiments combined with a revolving 8-way valve gives a flexible system. Sequential change of the sampling channel position allows injections from different flows to the carrier stream. The carrier stream can easily be changed to effect special plating and washing procedures. The 3-way valves allow three more flows to be introduced. These are of importance when studying, e.g., strongly adsorbing compounds. Voltammetric determinations of such compounds require efficient removal of the adsorbed layers from the electrode surface in order to obtain reproducible data. By switching between seven channels, samples, standards and different wash solutions can be selected as required.

REFERENCES

1 See, e.g., J. Růžička and E. H. Hansen, Anal. Chim. Acta, 179 (1986) 1.
2 A. Ivaska and W. F. Smyth, Anal. Chim. Acta, 114 (1980) 283.

Analytica Chimica Acta, 179 (1986) 439—444
Elsevier Science Publishers B.V., Amsterdam — Printed in The Netherlands

Short Communication

AMPEROMETRIC ACETYLCHOLINE AND CHOLINE SENSORS WITH IMMOBILIZED ENZYMES

MARCO MASCINI* and DANILA MOSCONE

Dipartimento di Scienze e Tecnologie Chimiche, II Universitá di Roma, Tor Vergata, 00172 Roma (Italy)

(Received 6th September 1985)

Summary. Acetylcholine and choline sensors are prepared by immobilizing enzymes on nylon net attached to a hydrogen peroxide sensor. Choline oxidase is used for the choline sensor; acetylcholinesterase and choline oxidase are used for acetylcholine. The platinum/silver electrode pair is polarized at +0.6 V. The assembly is protected with an acetate cellulose membrane to enhance selectivity. The ranges measured are 1—10 μmol l^{-1} in 0.1—1 ml of sample. The response times are 1—2 min.

Acetylcholine is the first documented neurotransmitter and choline is its metabolite. There is considerable interest in the in vivo measurement of such neurotransmitters [1, 2]. Voltammetric measurements of oxidizable compounds in extracellular fluid provide an active area of research [3, 4], but acetylcholine and choline are not oxidizable. Ion-selective microelectrodes have been described [5] but the sensitivity (around 0.1 mmol l^{-1}) and selectivity are inadequate for clinical purposes. The assembly of choline electrodes based on immobilized choline oxidase and an oxygen electrode [6, 7] and a chemically modified platinum electrode [8] have been reported. The coupling between the oxygen sensor and choline oxidase was exploited for the determination of phospholipids in several biological matrices [9]. Acetylcholine and choline in nerve tissue have been measured reliably by liquid chromatography with electrochemical detection, but a lengthy clean-up is needed before introduction of the sample [10, 11].

A simultaneous determination of both acetylcholine and choline in a single sample with two sensors, one selective for choline and the other for acetylcholine, is described below. Membranes with immobilized enzymes are coupled with amperometric hydrogen peroxide sensors. Both batch and flow procedures are possible. Micromolar concentrations and volumes as small as 0.1 ml can be handled. For the choline-selective sensor, choline oxidase is immobilized on nylon net; for the acetylcholine-selective sensor, choline oxidase and acetylcholine esterase are immobilized on opposite sides of the net. These sensors are very selective and can be used for determinations of these substances in nerve tissue extract.

0003-2670/86/$03.50

Experimental

Reagents. Choline oxidase (EC. 1.1.3.17, 10 IU mg^{-1}, from *Alcaligenes* sp.), acetylcholinesterase (EC. 3.1.1.7, 1000 IU mg^{-1}, from electric eel), choline chloride and acetylcholine chloride (all from Sigma) were used as received. Cellulose acetate and poly(vinyl acetate) were from Carlo Erba (Milan). Other reagents were of reagent grade. Nylon net (108 threads/cm^2, thickness 120 μm) was obtained from A. Bozzone (Appiano Gentile, Italy).

Apparatus. The hydrogen peroxide sensor was a platinum/silver couple. The platinum was sealed in glass and its area was 0.5 mm^2. The potential applied was +0.6 V and the current was recorded through a Metrohm 641-VA detector with an Omniscribe recorder (Houston Instruments). Alternatively, a YSI-25 oxidase meter (Yellow Springs Co.) was used with a suitable recorder.

Preparation of the sensor. The active area of the hydrogen peroxide sensor is covered first with a cellulose acetate membrane, to prevent other oxidizable compounds (especially ascorbic acid) from being oxidized at the electrode, as described by Tsuchida and Yoda [10]. This is then covered with the nylon net with immobilized enzyme(s) and finally a dialysis membrane.

To prepare the cellulose acetate membrane, a solution of 39.6 g of acetylcellulose and 0.4 g of poly(vinyl acetate) in 600 ml of acetone and 400 ml of cyclohexanone was cast on a glass plate, with the aid of a precision gauge tool (Precision Gauge and Tool Co., Dayton, OH), to give a layer 200 μm thick. The membrane was dried in air and then peeled off by immersion of the glass plate in water. The resulting membrane was 20 μm thick and strong enough for easy use. This method seems to be simpler than the procedure reported by Taylor et al. [11].

The method of immobilizing enzymes on nylon net was described previously [12]. In the case of the acetylcholine sensor, asymmetric coupling was done with the two enzymes on opposite sides of the nylon net. Alternatively, an easier procedure slightly different from the earlier one [12] can be used with similar results: the nylon net is functionalized through the steps with dimethylsulphate, lysine and glutaraldehyde as before; it is then spread out and the enzyme (choline oxidase), still lyophilized (2 mg cm^{-2}), is coated onto the surface with a few microlitres of buffer. It is finally left for about 2 h at room temperature in a humid atmosphere. Further, the membrane with immobilized choline oxidase was washed with water, and acetylcholinesterase (1 mg cm^{-2}) was coated onto the same side of the net without further bonding procedure or chemicals. The esterase was thus immobilized only by adsorption on nylon and on the protein chemically immobilized. Such adsorption is however very strong; extensive treatment with mild chemicals (buffers in the pH range 5—10) did not wash out the enzyme completely. The main reason for using a dialysis membrane to cover the net was to protect the enzymes from other adsorption effects and from proteolytic microbial attack. This dialysis membrane was renewed every 2—3 days of operation.

The activity of the choline oxidase on the nylon net was in the range 200—400 nmol min^{-1} cm^{-2} and the activity of acetylcholinesterase was in the range 50—100 nmol min^{-1} cm^{-2}. The determination of activity has been described [12].

Procedures. The sensors were immersed in 2 ml of glycine buffer (0.1 mol l^{-1}, pH 9.0) and the current was recorded. The current varied in the first 30 min and then reached a steady state; the noise was in the range 1—2 pA. Several aliquots of standard solutions of choline and acetylcholine were then added and the currents were recorded.

In the flow system, the two sensors were fixed in a single cell [13] and solutions were aspirated through a peristaltic pump. The results obtained were similar to those in the batch procedure but the noise was higher.

Results and discussion

Choline sensor. Figure 1 shows the calibration graphs obtained with a choline sensor, four months old, in the range 1—10 μmol l^{-1}, which is well below the practical range of the oxygen electrode-based choline sensor [9] and of the ion-selective electrode [5]. The response times were about 1 min in the batch method and about 30 s in the flow method. The high sensitivity of the peroxide sensor makes it useful for measurements in biological media. Figure 2 outlines the response of the choline sensor to different buffer solutions; glycine buffer (0.1 mol l^{-1}, pH 9.0) was chosen for most of the determinations.

Table 1 lists the percentage conversion for two assembled choline sensors during three months of operation, indicating the stability of these sensors.

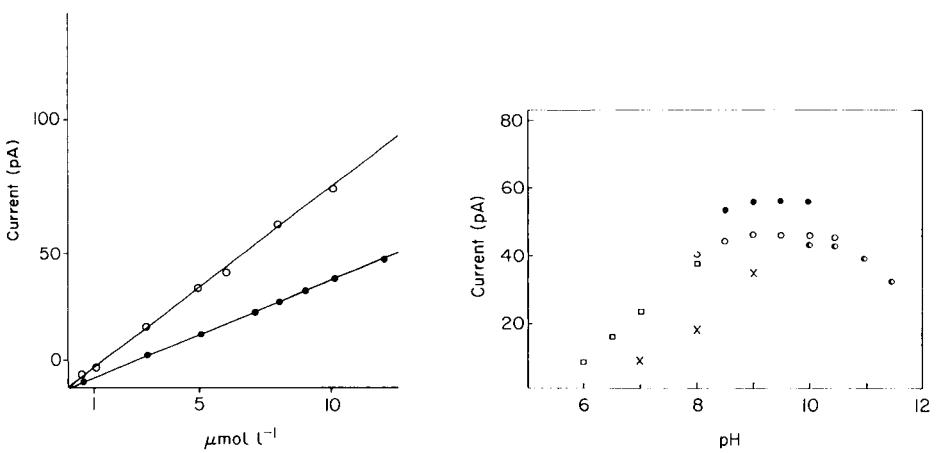

Fig. 1. Calibration of the choline sensor (4 months old) in glycine buffer (0.1 mol l^{-1}, pH 9.0) at 25°C: (○) choline standard solutions; (●) hydrogen peroxide standard solutions.

Fig. 2. Response of the choline sensor in different buffer solutions at several pH values to an addition of choline giving a final concentration of 10 μmol l^{-1}. Buffers: (●) glycine, 0.1 mol l^{-1}; (○) borax, 0.1 mol l^{-1}; (□) phosphate, 0.1 mol l^{-1}; (×) Tris, 0.1 mol l^{-1}; (◐) carbonate 0.1 mol l^{-1}.

TABLE 1

Responses of two assembled choline sensors during two months of operation

Day	H_2O_2 (pA/μmol l^{-1})	Choline (pA/μmol l^{-1})	Conversion (%)	H_2O_2 (pA/μmol l^{-1})	Choline (pA/μmol l^{-1})	Conversion (%)
	Sensor 1			*Sensor 2*		
1	24	34	142	—	—	—
10	24	37	154	23	45	197
20	24	36	150	24	37	154
30	26	36	138	29	37	128
40	16	21	131	25	36	144
50	16	22	138	25	43	172
60	4	6	150	28	57	203
70	3.5	7	200	28	56	200
80	2.5	4.5	180	16	28	175
90	3.0	5.6	187	24	34	121
100	—	—	—	26	30	115
110	—	—	—	22	32	145

The reaction is

$$\text{Choline} + 2O_2 + H_2O = \text{Betaine} + 2H_2O_2$$

The stoichiometry of this reaction explains why the response to choline is almost twice the response to hydrogen peroxide. From Table 1, some aging of the choline oxidase membrane is evident. The decrease in sensitivity to choline, however, is paralleled by a decrease in the sensitivity of the assembled sensor to hydrogen peroxide. This suggests that aging changes the permeability of the membrane to hydrogen peroxide, with some screening effect.

The response of the choline sensor to temperature in the range 15—40°C was evaluated. The response doubled as the temperature was increased from 15 to 20°C, but then increased only gradually above 25°C.

Table 2 reports the relative activity of possible interferents to the choline

TABLE 2

Substances with interference activity on the choline sensor[a]

Interferent (0.1 mol l^{-1})	Relative activity (%)	Interferent (0.1 mol l^{-1})	Relative activity (%)
Choline	100	Ethanolamine	3.5
Ascorbic acid	2.0	Diethanolamine	3.5
N-Methylamine	4.0	Triethanolamine	5.0
Dimethylamine	6.0	Betaine aldehyde	45.0

[a]There was no interference from acetylcholine, lecithin, methanol, ethanol, propanol, formaldehyde, acetaldehyde, propionaldehyde, cholesterol, taurocholic acid or glycocholic acid.

sensor. The selectivity with respect to ascorbic acid depends on the cellulose acetate membrane whereas the selectivity in relation to other compounds depends on the enzyme selectivity pattern of the enzyme [9].

Acetylcholine sensor. The calibration graphs for the acetylcholine sensor are shown in Fig. 3; the responses to choline and hydrogen peroxide are given for comparison. Table 3 lists the responses of four acetylcholine sensors on

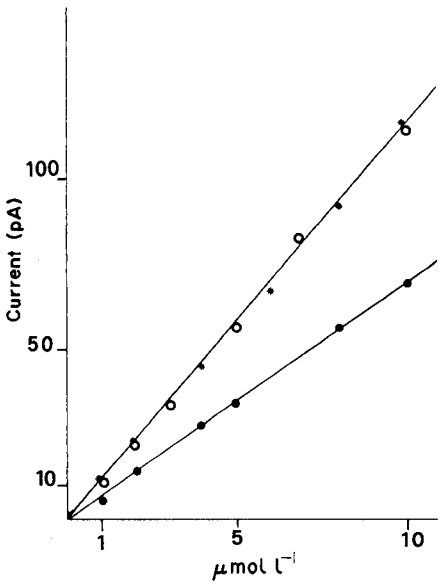

Fig. 3. Calibration of the acetylcholine sensor; (*) acetylcholine; (○) choline; (●) hydrogen peroxide. Glycine buffer, 0.1 mol l^{-1}, pH 9.0.

TABLE 3

Responses of acetylcholine sensors and average percentage conversions

Response (pA/μmol l^{-1})			Conversion (%)[a]	
Acetylcholine	Choline	H_2O_2	Choline	H_2O_2
11	13	6		
12	13	6	100	154
11.5	10	6.5		
12	10	6.5		
9.0	8.0	6.0	100	138
9.0	8.0	6.0		
9.0	9.0	6.0	100	144
9.0	9.0	6.5		
4.5	7.0	4.5	100	165
4.5	7.0	4.0		

[a]Average value for each electrode assembled.

different days and the percentage conversions. Both Fig. 3 and Table 3 show that the conversion of acetylcholine to choline is always complete. Thus the performance of the choline oxidase is the limiting factor. Acetylcholinesterase is in fact adsorbed very easily from biological media and seems very active. A choline sensor immersed in a solution containing acetylcholinesterase (e.g., a serum sample) becomes an acetylcholine sensor. However, the activity of the esterase commercially available is much higher than that of the choline oxidase available, which may account for the total conversion.

When the nylon net was prepared with the two immobilized enzymes by the asymmetric procedure [12], it was important to have the choline oxidase facing the electrode surface and the esterase facing the sample solution. The reverse situation gave only 10% of the response to acetylcholine.

The selectivity pattern for the acetylcholine sensor was similar to that given in Table 2 for the choline sensor. The lifetime of both membranes depends on their use and storage conditions but the lifetime of the acetylcholine sensor seems to be shorter.

REFERENCES

1 W. S. Lindsay, B. L. Kizzort, J. B. Justice, J. D. Salamone and D. B. Neill, Chem. Biomed. Environ. Instrum., 10 (1980) 311.
2 W. S. Lindsay, J. G. Herdon, R. D. Blakely, J. B. Justice and D. B. Neill, Brain Res., 220 (1981) 391.
3 R. M. Wightman, Anal. Chem., 53 (1981) 1125.
4 R. F. Lane, A. T. Hubbard and C. D. Blaha, J. Electroanal. Chem., 95 (1979) 117.
5 A. Jaramillo, S. Lopez, J. B. Justice, J. D. Salamone and D. B. Neill, Anal. Chim. Acta, 146 (1983) 149.
6 F. Mizutani and K. Tsuda, Anal. Chim. Acta, 139 (1982) 359.
7 I. Karube, K. Hara, I. Satoh and S. Suzuki, Anal. Chim. Acta, 106 (1979) 243.
8 T. Yao, Anal. Chim. Acta, 153 (1983) 169.
9 L. Campanella, M. Mascini, G. Palleschi and M. Tomassetti, Clin. Chim. Acta, 151 (1985) 71.
10 T. Tsuchida and K. Yoda, Clin. Chem., 29 (1983) 135.
11 P. J. Taylor, E. Kmetec and J. M. Johnson, Anal. Chem., 49 (1977) 789.
12 M. Mascini, M. Iannello and G. Palleschi, Anal. Chim. Acta, 146 (1983) 135.
13 M. Mascini and G. Palleschi, Anal. Chim. Acta, 145 (1983) 213.
14 P. W. Carr and L. D. Bowers, Immobilized Enzymes in Analytical and Clinical Chemistry, Wiley, New York, 1980.

Analytica Chimica Acta, 179 (1986) 445—451
Elsevier Science Publishers B.V., Amsterdam — Printed in The Netherlands

Short Communication

DETERMINATION OF SULPHUR DIOXIDE BY FLOW INJECTION ANALYSIS WITH AMPEROMETRIC DETECTION

M. GRANADOS[a], S. MASPOCH and M. BLANCO*

Department of Analytical Chemistry, Faculty of Sciences, Autonomous University of Barcelona, Bellaterra, Barcelona (Spain)

(Received 29th July 1985)

Summary. Sulphur dioxide can be determined at a sampling rate of 120 h^{-1}, with amperometric detection after separation in a diffusion cell with a teflon membrane. At 25°C, the calibration graph shows two linear ranges, between 0.06 and 6 mg l^{-1} and 12 and 110 ml l^{-1} sulphur dioxide, with a detection limit of 0.03 mg l^{-1}. At 50°C, the linear range is 0.04—5 mg l^{-1}, with a detection limit of 0.02 mg l^{-1}. The procedure has been applied to the determination of sulphur dioxide in wines.

Sulphur dioxide is widely used to prevent fermentation in wine. Its potential toxicity and the fact that the concentration necessary to stabilize wine is only slightly less than EEC limits makes its determination essential in control laboratories. The commonest procedures are spectrophotometric determination with pararosaniline, titration with iodine, and acid/base titration after oxidation. The first two methods can be applied directly only to white wines. Distillation of sulphur dioxide is necessary (usually through displacement with nitrogen) for its determination in red wine. This separation is always necessary in acid/base procedures and obviously prolongs the analysis. Yet, the direct titration with iodine tends to yield high results because of its reaction with other substances present (aldehydes, sugars, etc.).

Flow injection analysis (f.i.a.) can be valuable in quality control because of its simplicity and high sampling frequency. Several flow-injection determination procedures of sulphur dioxide/sulphite have been described [1—5] but only one of them has been applied for the determination of free sulphur dioxide in wines. The stopped-flow procedure is based on reaction with pararosaniline [1]. The method proposed here for sulphite/sulphur dioxide determination includes amperometric detection after direct injection or after separation in a diffusion cell. The latter procedure is applied to determine free sulphur dioxide in wines.

---

[a]Present address: Department of Analytical Chemistry, Faculty of Chemistry, University of Barcelona, Barcelona, Spain.

0003-2670/86/$03.50

Experimental

Reagents. All solutions were prepared from analytical reagent-grade chemicals and deionized, distilled water. Stock sodium sulphite solutions (1000 mg l^{-1}) were prepared with nitrogen-purged water, stabilized by adding 0.1% (v/v) glycerol [5] and standardized daily by iodimetric titration. Stock SO_2 solution and wine samples were diluted with degassed distilled water.

Apparatus. The flow systems are illustrated in Fig. 1. A Gilson Minipuls-2 peristaltic pump was used. Samples were injected by means of a Rheodyne 50 valve. The flow cell was of the wall-jet configuration (Metrohm model 656), fitted with carbon glassy electrodes as working and auxiliary electrodes and an Ag/AgCl (3 M KCl) reference electrode; it was used in conjunction with a Metrohm 641-VA potentiostat. The home-made diffusion cell comprised two equal blocks of acrylic resin, each with a groove (7 cm long, 3 mm wide, 0.2 mm deep) between which a membrane (see Table 1) was placed.

Stability of the working electrode. Problems related to the stability and activation of glassy carbon electrodes have been treated extensively [6, 7]. At the beginning of each work session, the surface of the electrode is activated by keeping it at about −1150 mV [7] for 2–3 min. After this treatment, baseline stability is obtained in ca. 30 min. The sensitivity of the response diminishes slowly with successive injections of SO_2, until it eventually becomes stable. This stabilization can be attained rapidly if a concentrated SO_2 solution (100–500 mg l^{-1}) is injected (Fig. 2A). When the detector is allowed to stand without exposure to SO_2 for a long time, its sensitivity increases.

Procedures for free sulphur dioxide in wine. A known volume of wine is diluted 25 times with degassed distilled water. This solution is injected into the manifold shown in Fig. 1B, with the following parameters: potential applied to the working electrode, +1150 mV; flow rate of both streams, 0.8 ml min^{-1}; C_1 = 1 M H_2SO_4, C_2 = 10^{-2} M H_2SO_4; length of mixing coil M, 50 cm; injection volume, 80 μl; temperature of water bath, 50°C. Peak heights are measured and concentrations are evaluated from a standard calibration graph (e.g., Fig. 2B).

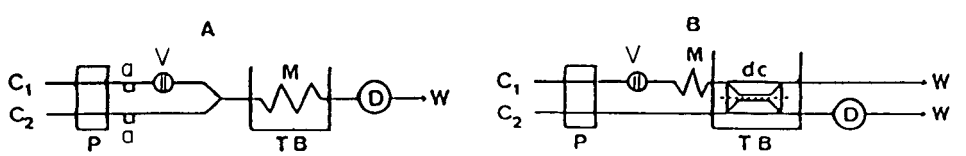

Fig. 1. Schematic diagrams of the manifolds used. P, peristaltic pump; V, injection valve; M, mixing coil; TB, thermostated bath; D, amperometric detector. (A) Simple system: a, pulse dampener; C_1, distilled water; C_2, sulphuric acid solution. (B) Diffusion system: dc, diffusion cell; C_1 and C_2, sulphuric acid solutions.

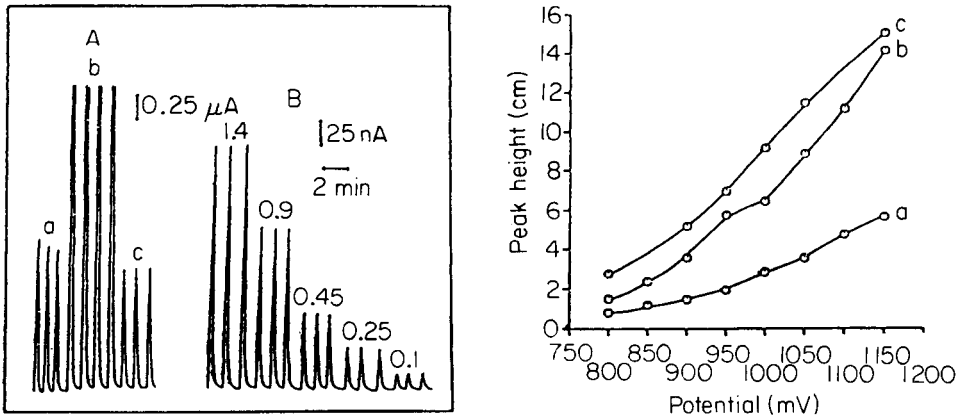

Fig. 2. Detector responses obtained with a diffusion cell fitted with a Fluoropore membrane. (A) Sulphur dioxide injected: (a) 6.7 mg l^{-1}; (b) 120 mg l^{-1}; (c) 6.7 mg l^{-1}. (B) Calibration graph for triplicate injections (80 μl) of standard solution at 25°C; numbers on the peaks represent mg l^{-1}.

Fig. 3. Variation of peak height with applied potential at various sulphuric acid concentrations: (a) 10^{-3} M; (b) 10^{-2} M; (c) 10^{-1} M.

Results and discussion

Sulphur dioxide can be oxidized or reduced, depending on conditions. Several procedures for its determination have been based on reduction at a dropping mercury electrode [8—11] and some of these have been applied to the determination of sulphur dioxide in wines [9, 11]. Oxidation of sulphur dioxide to sulphate constitutes the chemical basis of classical procedures (see above), but has been little used in electrochemical methods [12].

Simple flow-injection system. In this flow system, the response of electrochemical detector was found to be very sensitive to any variation of flow, whether momentary interruptions on injecting samples or pulsations from the pump. This forced the use of a double-channel system with pulse damping. The manifold used is outlined in Fig. 1A.

The variation of peak height as a function of the applied potential between 800 and 1150 mV (vs. Ag/AgCl) for various sulphuric acid (10^{-3}—10^{-1} M) concentrations is shown in Fig. 3. It can be seen that the best sensitivity is obtained with a 10^{-1} M acid. The effects of volume injected, flow rate and length of mixing coil on the responses to sulphur dioxide are shown in Fig. 4A. The peak height obtained diminishes with increased length of the mixing coil because of increased dispersion. The behaviour with increasing flow rate is more difficult to understand: the curve presents a maximum at 2.1 ml min^{-1}. It is generally accepted [13] that the ampero-

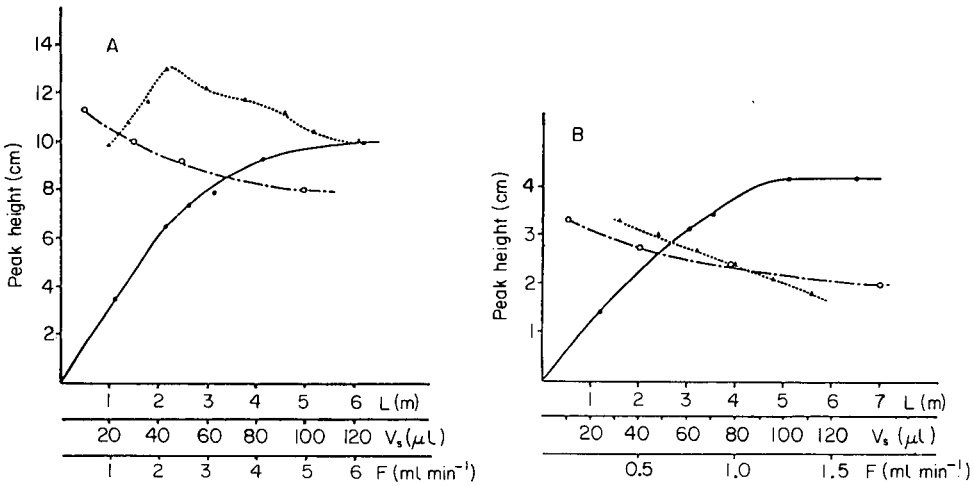

Fig. 4. Influence of manifold variables on peak height: (A) in the simple system; (B) in the system with diffusion cell. (——) Injection volume; (— · —) mixing coil M; (· · · ·) flow rate.

metric signal (I) is related to the flow rate (V) and concentration (C) according to the equation: $I = nFAkV^{\alpha}C$, where α is a function depending on the electrode geometry. For a Metrohm EA-1096 detector, an exponent of 0.44 has been obtained [14]. According to these considerations, the intensity and therefore the peak height should increase with flow rate. This equation, however, does not take into consideration the different phenomena, adsorption mechanisms and oxidation kinetics at the surface of the electrode. Seo and Sawyer [15] reported that the oxidation of sulphur dioxide on metal electrodes takes place with two mechanisms: electron transfer and chemical oxidation through a metal oxide film. On platinum, electron transfer predominates and for this process the rate-controlling step is a two-electron oxidation. The shape of the maximum in the plot of peak height vs. flow rate can be explained if it is assumed that oxidation of sulphur dioxide at a glassy carbon electrode is also an electron-transfer process with relatively slow kinetics. Thus, an increase of flow rate would be accompanied by diminution of the oxidation efficiency.

For the selected analytical conditions (applied potential 1150 mV, volume injected 50 μl, flow rate 1.1 ml min^{-1}, coil length 50 cm), the peak height is linear with concentration of sulphur dioxide between 1 and 50 mg l^{-1} with a detection limit (three times the peak-to-peak background noise) of 0.2 mg l^{-1}. The calibration equation is H(cm) = 0.33 + 1.21 [SO_2] (mg l^{-1}), with a regression coefficient of 0.99991. Unfortunately, the injection of a wine sample produced an enormous peak, because of the oxidation of other species in the wine.

System with diffusion cell. Figure 1B shows the manifold used for the determination of sulphur dioxide with separation prior to the amperometric

detector. It can be observed from Fig. 4B that the lower the flow rate and the shorter the mixing coil, the higher are the peak heights obtained. A 50-cm coil and a flow rate of 0.8 ml min^{-1} were chosen as a compromise between sensitivity and sampling frequency. Under these conditions the optimal injection volume is 80 μl.

The effect of the sulphuric acid concentrations in the channels of the diffusion cell is shown in Fig. 5. The plots show maxima for sulphuric acid concentrations of 0.3—1 M in the donor stream and 10^{-2}—5×10^{-2} M in the acceptor stream.

The permeabilities to sulphur dioxide of three commercial membranes were compared (Table 1). To quantify permeability while taking into account the dispersion caused by the volume of the diffusion cell, a calibration plot was prepared by injecting standard solutions of sulphur dioxide directly into the acceptor channel, after replacement of the porous membrane by an impermeable one. It was found that the permeability of teflon $\gg$ Celgar $>$ Millipore. There was a considerable increase in the peak heights when the diffusion cell was operated in a countercurrent which can be explained in part by reduced dispersion of the sample zone in the acceptor channel.

The peak heights increased with temperature over the range 25—60°C. At temperatures above 50°C the background noise also increased considerably, so that temperatures of 25°C or 50°C were chosen depending on the sensitivity needed.

Under the optimized operating conditions, at 25°C the calibration graph showed two linear intervals. For the range 0.06—5 mg l^{-1} SO_2, the calibration equation was H(cm) = $-(0.12 \pm 0.09) + (6.85 \pm 0.02)$ [SO_2] (r^2 = 0.9999), and for the range 12—110 mg l^{-1} SO_2, the calibration equation was H(cm) = $(0.57 \pm 0.13) + (0.065 \pm 0.001)$ [SO_2] (r^2 = 0.9991). At 50°C, the linear range was 0.06—5 mg l^{-1} SO_2, with the equation H(cm) = $(0.42 \pm 0.05) + (36.8 \pm 0.2)$ [SO_2] (r^2 = 0.9999).

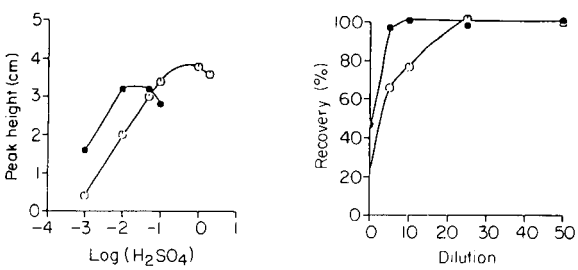

Fig. 5. Effect of sulphuric acid concentration in the two channels of the diffusion cell: (○) C_1; (●) C_2.

Fig. 6. Effect of wine dilution on recovery of sulphur dioxide: (○) at 25°C; (●) at 50°C.

TABLE 1

Membrane permeability[a]

Membrane	Permeability (%)	
	Normal flow	Countercurrent flow
PTFE[b]	30	65
Celgar 2500	12	16
Millipore GVHP-9050	10	12

[a]80 μl of 3.5 mg l^{-1} SO_2 solution injected; T = 25°C. [b]Teflon tape (plumber) with a thickness of 60 μm.

Relative standard deviations (7 replicates) for 3 mg l^{-1} SO_2 were 1.7% at 25°C and 2.3% at 50°C with detection limits of 0.03 and 0.02 mg l^{-1}, respectively.

The effects of some of the more frequently occurring anions and of substances producing volatile compounds in acidic medium were studied for determinations of 10 mg l^{-1} sulphur dioxide at 25°C. Ammonia was also considered. The maximum tolerable amounts, expressed as mg l^{-1} interferent/mg l^{-1} SO_2 were: 1000-fold nitrate, ammonium, acetate or cyanide, 500-fold chloride, and 100-fold carbonate. Sulphide and nitrite interfered at mg l^{-1} levels. The interference of sulphide can be eliminated by previous precipitation with cadmium ions.

Determination of sulphur dioxide in wines. When wine was injected under the above conditions, low results were found. The percentage of recovery increases considerably if the wine sample is diluted (Fig. 6). This is attributed to a matrix effect of the wine which limits the diffusion of sulphur dioxide. It was verified that the effect is not due to alcohol.

The proposed method was applied to several white and red wines with recoveries between 93 and 98%, as shown in Table 2.

TABLE 2

Determination of sulphur dioxide in wine

Wine	SO_2 found (mg l^{-1})	$\%R$[a]	Total SO_2 (mg l^{-1})
Red 1	0.53 ± 0.02	93	13.4 ± 0.5
Red 2	0.81 ± 0.03	95	20.3 ± 0.7
White 1	1.40 ± 0.02	98	34.9 ± 0.5
White 2	0.93 ± 0.02	97	23.3 ± 0.5

[a]Mean of recoveries for 1 and 3 mg l^{-1} SO_2 added.

Discussion

Several detection systems have been applied to determination of sulphur dioxide by f.i.a. Spectrophotometric detection is most popular and has been used in a direct method [2], in a stopped-flow procedure [1] and in a continuous-flow system with electrochemically regenerated reagent [3]. Chemiluminescence [4] and potentiometry [5] have also been used. Amperometric detection with a diffusion cell improves both sensitivity and instrumental simplicity.

Although direct injection of sulphur dioxide solution into a simple flow-injection system looks superficially very attractive, the background noise increases the detection limit considerably. Further, good sensitivity requires the application of a high potential, so that many substances interfere. The diffusion cell proved to be highly efficient for pulse damping, thus diminishing the background noise, as well as eliminating most of the interferences.

The main trouble is related to electrode stability, but the treatment applied allows continuous work during one day. The procedure is being extended to determinations of sulphur dioxide in other beverages and in the atmosphere.

Part of the apparatus was obtained through a CIRIT (Commissió Interdepartmental de Recerca i Innovació Tecnológica, Government of Catalonia) grant.

REFERENCES

1 J. Růžička and E. H. Hansen, Anal. Chim. Acta, 114 (1980) 19.
2 T. R. Williams, S. W. McElvany and E. C. Ighodalo, Anal. Chim. Acta, 123 (1981) 351.
3 S. M. Ramasamy and H. A. Mottola, Anal. Chem., 54 (1982) 283.
4 M. Yamada, Ts. Nakada and Sh. Suzuki, Anal. Chim. Acta, 147 (1983) 401.
5 G. B. Marshall and D. Midgley, Analyst (London), 108 (1983) 701.
6 E. Pungor and I. Buzas, Modern Trends in Analytical Chemistry. Part A. Electrochemical Detection in Flow Analysis, Elsevier, Amsterdam, 1984.
7 J. Wang and L. D. Hutchins, Anal. Chim. Acta, 167 (1985) 325.
8 I. M. Kolthoff and C. S. Miller, J. Am. Chem. Soc., 63 (1941) 2818.
9 W. Diemair, J. Koch and D. Hess, Z. Anal. Chem., 178 (1961) 321.
10 P. Bruno, M. Caselli, M. Della Monica and A. Di Fano, Talanta, 26 (1979) 1011.
11 P. Bruno, M. Caselli, A. Di Fano and A. Traini, Analyst (London), 104 (1979) 1083.
12 D. D. Nygaard, Anal. Chim. Acta, 127 (1981) 257.
13 D. MacKoul, D. C. Johnson and K. G. Schick, Anal. Chem., 56 (1984) 436.
14 H. B. Hanekamp and H. J. Van Nieuwkerk, Anal. Chim. Acta, 121 (1980) 13.
15 E. T. Seo and D. T. Sawyer, Electrochim. Acta, 10 (1965) 239.

Analytica Chimica Acta, 179 (1986) 453—457
Elsevier Science Publishers B.V., Amsterdam — Printed in The Netherlands

Short Communication

THE DETERMINATION OF BROMIDE IN NATURAL WATERS BY FLOW INJECTION ANALYSIS

TORBJÖRN ANFÄLT* and SIGRID TWENGSTRÖM
Bifok AB, Box 124, S-191 22 Sollentuna (Sweden)
(Received 31st July 1985)

Summary. Bromide can occur in well waters as a result of sea water intrusion. The phenol red method is adapted to a flow-injection system and interferences are studied by using a two-channel valve. Standards are injected from one loop of the valve while the possible interferent is injected from the other loop; this provides a fast means of evaluating interferences. Ammonia, cyanide and humic substances interfere. Bromide can be determined down to 2 μM at a rate of 80 samples per hour.

The contamination of well waters from sea-water intrusions can be a serious problem in coastal areas. A rapid and accurate method for following the bromide/chloride ratio is of interest not only for tracing sea water in fresh water but also for monitoring pollution, e.g., from the petroleum industry.

Bromide can be determined in various ways. Direct potentiometric determination lacks selectivity as well as sensitivity. Spectrophotometric methods are well suited for automation and normally possess adequate sensitivity. Various methods have been used to determine bromide [1, 2]. The phenol red method [3—6] is probably most widely accepted as the standard method for bromide; it is based on the bromination of phenol red to bromophenol blue after oxidation of bromide to bromine with chloramine-T in an acetate buffer. The method is sensitive and selective enough to meet most requirements. Basel et al. [6] presented a thorough study of interferences in an automated segmented flow system under fully equilibrated conditions. Ammonia and chloride were identified as the most important interferents.

Flow injection analysis is now a well established technique for automating procedures, one of its most appreciated properties being its simplicity. It also offers a simplified and time-saving way of studying possible interferences. The aim of the present communication is to show how the phenol red method can be adapted to a flow-injection system and to explain a simple, quite general, way of studying interferences when a new method is applied.

Experimental

Reagents. The stock solutions were 2% (w/v) phenol red (Merck) in ethanol,

0003-2670/86/$03.50

1% (w/v) chloramine-T trihydrate in water, and sodium acetate/acetic acid buffer to a total concentration of 0.8 M. Preliminary studies showed that the optimal pH to reach the highest sensitivity was 5.2. Both the chloramine-T and the indicator stock solutions had to be renewed weekly because of degradation. The reagent solutions used were prepared daily from the stock solutions. Reagent 1 was prepared by diluting 1 ml of the indicator stock solution to 100 ml with acetate buffer. Reagent 2 was prepared by diluting 10 ml of the chloramine-T stock solution to 100 ml with acetate buffer.

All bromide standards were prepared by diluting 0.1 M potassium bromide with deionized water. Freshly prepared solutions of possible interferents were used.

Apparatus. The Tecator 5020 Flow Injection Analyzer used was equipped with a V-200 double-channel, variable-volume valve. The manifold used was a Chemifold III. A Tecator 5023 spectrophotometer was used as detector at 590 nm.

For the study of possible interferences, mixing of interferent solutions with bromide standards was easily done by using a two-channel valve. Thus, in the manifold used (Fig. 1), two carrier streams were first merged and then reagents were added at lower flow rates to avoid unnecessary dilution in the system. The single reaction coil before the detector was varied in a preliminary study to decide the optimal length in terms of sensitivity and sampling rate. Lengths greater than 60 cm gave only slight increase in sensitivity at the expense of decreased sample throughput. The flow rates for the carrier streams (C in Fig. 1) were 1.5 ml min^{-1} each. The reagents (R in Fig. 1) were propelled at a flow rate of 0.6 ml min^{-1}.

Results and discussion

Bromide concentrations in natural waters can vary quite extensively. In order to establish the lower limit of detection, two matched 200-μl loops

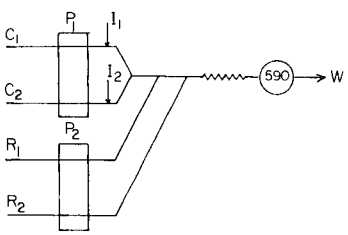

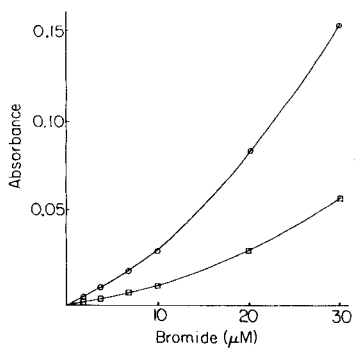

Fig. 1. Manifold for the determination of bromide. Loops I_1 and I_2 were normally 200 μl in volume. The teflon reaction coil was 600 mm long (0.7 mm i.d.). Flow rates of the carrier streams were 1.5 ml min^{-1} each and for the reagent 0.6 ml min^{-1} each.

Fig. 2. Calibration curves in the 0—3 × 10^{-5} M bromide range: (○) when both loops (200 μl each) are used to inject standards; (□) when only one loop is used to inject standards.

were installed in the injection valve. Further increase in the injected volume did not increase the peak height but only the peak width. Figure 2 shows calibration curves in the lower concentration region with standards in both channels or in only one channel. The curvature of the calibration in this region can probably be ascribed to the low reaction rate. In order to test this assumption, the pumps were stopped at the peak and the increase in absorbance was observed. A steady state was reached after 2 min, the peak height being increased about 2.5 times. The increase is greater for the lower concentrations of bromide. It would thus be possible to increase the sensitivity considerably by using a stopped-flow technique, but the loss in sample throughput could be a drawback for some purposes. When the sample is injected from only one of the loops, it is diluted about 1:2 by the other carrier stream. The dispersion of the sample in the rest of the system is low when high loop volumes are used. It can be seen from the calibration curves that the ratio of the responses is about 1:2 when one or two loops in the valve are used. The double-loop injection technique can be regarded as a way of premixing the samples before the reaction step. This feature of the system was conveniently used in studying the interferences from other substances and as a means of spiking the samples.

A large number of measurements with interferents could be studied within a reasonable time. Because natural waters always contain chloride, its possible interference was examined in detail, though initial experiments showed very little effect. Sodium chloride at two different concentrations was injected from one loop and a series of calibration solutions was injected from the other loop. The results are shown in Table 1. The chloride interference decreases slightly as the concentration of bromide increases, probably because of the faster rate of the main reaction at higher bromide concentrations. Also, any matrix effects in the detector will be greater at low bromide concentrations. The interference can be described as the ratio of Cl^-/Br^- concentrations at which the two ions contribute equally to the overall signal. For

TABLE 1

The interference of chloride on different concentrations of bromide

KBr conc.[a] (μM)	Absorbance with H_2O added[b]	Change in absorbance with NaCl added	
		0.1 M NaCl	0.7 M NaCl
2	0.0012	+0.0026	—
4	0.0028	+0.0024	+0.0256
7	0.0062	+0.0022	+0.0252
10	0.0092	+0.0026	+0.0260
20	0.0288	+0.0012	+0.0246
30	0.0582	+0.0012	+0.0192
50	0.1178	+0.0004	+0.0192

[a]Solution injected from loop 1. [b]Injection from loop 2.

chloride, this ratio is around 3.5×10^4, i.e., chloride at 3.5×10^4 times the concentration of bromide will produce a signal equal to that of bromide. The interference from chloride is thus usually negligible.

Other interferences which may have a greater influence are more easily studied by keeping the bromide concentration constant in one loop and varying the interferent concentration in the other loop. The results are shown in Table 2. Hydrogencarbonate, iodide and iron(III) all produced positive interferences. Hydrogencarbonate probably affects the pH and interferes only slightly except at concentrations well above the natural level. The reaction with iodide is, not surprisingly, more sensitive than that with bromide; however, the concentrations of iodide in natural waters are usually well below those of bromide. Iron(III) also interferes directly. The Fe^{3+}/Br^- interference ratio, calculated as described above, is approximately constant throughout the bromide concentration range at around 2.5×10^2. Both ammonium ion and cyanide produce negative interferences which are proportional to the concentration of the interfering ion. Cyanide would prove a considerable problem in the analysis of waste waters. Insertion of a cation-exchange column before the reagents are merged with the carrier stream avoids the interference from ammonium ion [6]; this was confirmed in tests for 0—30 μM bromide injections with 1 mM ammonium nitrate injected from loop 2. Apart from the interferences mentioned above, other substances can cause serious problems. Humic substances, normally present in natural waters, give negative interferences, but it is not easy to evaluate the extent of interference; the substances are partly removed by the cation-exchange column.

In order to study the applicability of the method, brackish water samples were taken from the Baltic Sea, two from the innermost archipelago of Stockholm (Edsviken and Värtan) and another at Öresund, at the west coast of Sweden, where the Baltic flows into the North Sea. The chloride contents of the samples were determined by flow injection analysis, using the standard method, after appropriate dilution. The results are shown in Table 3. The chloride/bromide ratio, expressed in molar units, for the water sample taken

TABLE 2

Effects of varying concentrations of interferents injected from one loop on the determination of 10 μM potassium bromide injected from the other loop. Interference is described by the change in peak absorbance, ΔA. The peak absorbance for 10 μM bromide alone is 0.0102

$NaHCO_3$		KI		$Fe(NO_3)_3$		KCN		NH_4NO_3	
mM	ΔA	μM	ΔA	mM	ΔA	μM	ΔA	μM	ΔA
1	+0.0008	0.5	+0.0012	0.1	+0.0004	5	−0.0014	10	−0.0004
10	+0.0012	1	+0.0040	0.5	+0.0018	10	−0.0038	50	−0.0040
100	+0.0068	5	+0.0154	1	+0.0040	50	−0.0182	100	−0.0068
		10	+0.0318	10	+0.0362	100	−0.0252	1000	−0.0196

TABLE 3

The concentration of bromide and chloride in sea-water samples

Sample	Br^- found (μM)	Cl^- found (mM)	[Cl]/[Br]
Edsviken	45	27	600
Värtan	42	26	619
Öresund	321	208	648

from the more saline Öresund is normal for North Atlantic waters whereas the ratios for the samples taken in the Stockholm archipelago are below normal for Baltic sea water.

The proposed method for bromide can be used down to 2 μM at a sample throughput of 80 h^{-1}. There are few interferences in natural waters, but care must be taken with ammonium ion, cyanide and humic substances. The method can, of course, be tailored to fit required concentration ranges above 2 μM.

REFERENCES

1 G. S. Pyen, M. J. Fishman and A. G. Hedley, Analyst (London), 105 (1980) 657.
2 R. E. D. Moxon and E. J. Dixon, J. Autom. Chem., 2 (1980) 139.
3 V. A. Stenger and I. M. Kolthoff, J. Am. Chem. Soc., 57 (1935) 831.
4 G. U. Houghton, J. Soc. Chem. Ind., 65 (1946) 277.
5 F. W. Sollo, T. E. Larson and F. F. McGurk, Environ. Sci. Technol., 5 (1971) 240.
6 C. L. Basel, J. D. Defreese and D. O. Whittemore, Anal. Chem., 54 (1982) 2090.

Analytica Chimica Acta, 179 (1986) 459—462
Elsevier Science Publishers B.V., Amsterdam — Printed in The Netherlands

Short Communication

SPECTROPHOTOMETRIC DETERMINATION OF NONIONIC SURFACTANTS BY FLOW INJECTION ANALYSIS UTILIZING ION-PAIR EXTRACTION AND AN IMPROVED PHASE SEPARATOR

M. J. WHITAKER

Conoco Inc., P.O. Box 1267, 346 RDE, Ponca City, OK 74603 (U.S.A.)

(Received 2nd July 1985)

Summary. The proposed flow-injection determination of nonionic surfactants of the general type $RO(CH_2CH_2O)_nH$ (where R is an alkyl or alkylphenyl group and n is the number of moles of oxyethylene group) is based on extraction of the colored ion-pair product formed between the nonionic surfactant and the reagent tetrabromophenolphthalein ethyl ester potassium salt (TBPE-K). The complex is extracted into 1,2-dichloroethane and measured at 609 nm. A new phase separator is described. Triton X-100 is used as a model compound, for which response is linear in the range 2—60 mg l^{-1}. Precision of the method is excellent with a relative standard deviation of <1.0%. The sensitivity of the method depends on the type of surfactant examined.

Several spectrophotometric methods for the determination of nonionic surfactants of the general type $RO(CH_2CH_2O)_nH$ have been developed [1—6] using a variety of reagents. The object of the present investigation was to automate a simple and sensitive method for the determination of nonionic surfactants in the 2—60 mg l^{-1} range. Tetrabromophenolphthalein ethyl ester potassium salt (TBPE-K) was the reagent selected for our study because of its sensitivity [6]. The reaction is based on the coordination of the polyoxyethylene chain and the potassium cation [4]. The cationic complex is extracted into 1,2-dichloroethane as its ion pair with TBPE, which is a sensitive anionic chromophore measured spectrophotometrically at 609 nm.

Predominantly two types of phase separators (tee and membrane) have been used in the automation of solution chemistry based on liquid-liquid extraction [7—12]. The tee separator was found to be very inefficient for phase separation and was abandoned early in this study. The membrane separator was also discarded because the matrix of some samples changed the permeability of the membrane, causing large changes in sensitivity between the first and last data in a run. Because of these deficiencies, an improved phase separator was developed which is more efficient than the tee separator in terms of quantity of reaction product being measured, and the permeability problem was eliminated.

0003-2670/86/$03.50

Experimental

Reagents. All chemicals used were of analytical-reagent grade. A borate buffer ion-pair reagent was prepared as follows: 4.7678 g (0.0125 M) of sodium tetraborate decahydrate and 7.4560 g (0.10 M) of potassium chloride were dissolved in 900 ml of deionized water and the pH was adjusted to 9.30 by adding 48 ml of 0.10 M potassium hydroxide; then 0.1500 g of TBPE-K was dissolved in 50 ml of ethanol and transferred to the borate buffer solution, which was finally diluted to 1 l with deionized water.

The extracting solvent was 1,2-dichloroethane. Both solutions, reagent and extracting solvent, were degassed before use.

Standards. A stock standard solution (1000 mg l^{-1}) of nonionic surfactant was prepared by weighing 1.0000 g of Triton X-100 (>99.9% pure) and diluting to 1 l with deionized water. The calibration standards (2—60 mg l^{-1}) were prepared from this stock by appropriate dilutions.

Apparatus and procedure. A diagram of the flow-injection system is shown in Fig. 1. The flow-injection analyzer used was a Tecator 5020 (Tecator, Herndon, VA) with a teflon injection valve having a 120-μl sample loop. The tubing used in the manifold was teflon (0.8 mm i.d.); the sample and reagent pumping tubes were Tygon, and all other pump tubes were Acidflex.

The 120-μl aqueous sample is injected into the TBPE-K carrier stream, and the reaction occurs in a 0.5-m mixing coil. The extracting solvent and carrier stream merge at the segmentor, and the reaction product is extracted into the organic phase in an extraction coil of 3-m length. The aqueous and organic phases are separated by the improved phase separator made of glass (Fig. 2) from which the heavier organic phase (1,2-dichloroethane with the extracted cation complex) passes to the detector and the aqueous phase passes to waste. The lower end of the improved phase separator resembles and functions like a separatory funnel. The 1,2-dichloroethane phase flows continuously to the detector. The phase separators that have been used here varied in volume from 250 to 350 μl (shaded area, Fig. 2); this difference in

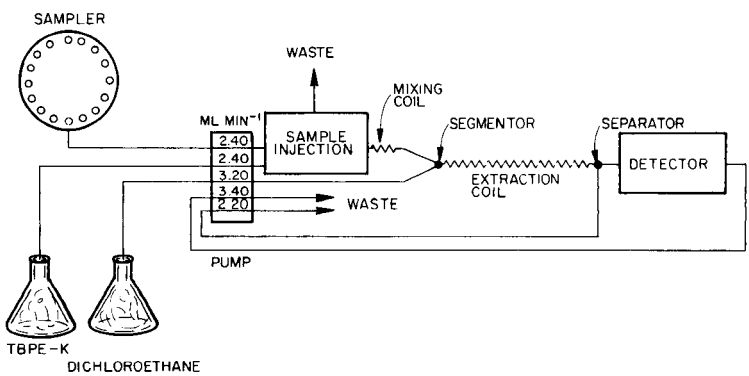

Fig. 1. Flow-injection manifold for the extraction-spectrophotometric determination of nonionic surfactants.

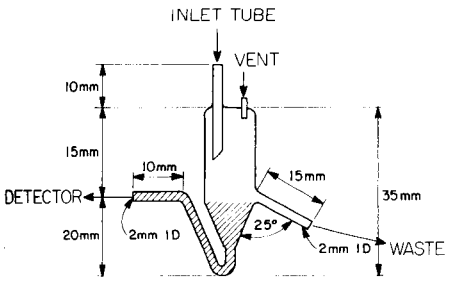

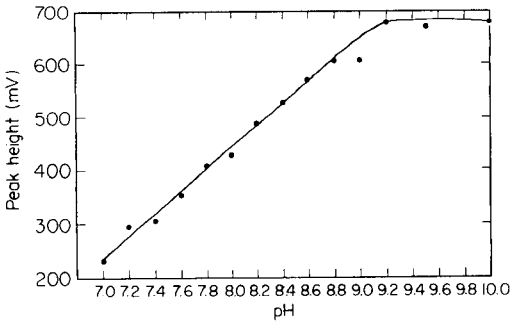

Fig. 2. Diagram of the improved glass-blown phase separator showing the directions of flow and the dimensions. The shaded area has a total volume of 250—350 μl.

Fig. 3. Effect of pH on the signal. A 40 mg l^{-1} Triton X-100 solution was injected while the pH of the TBPE-K reagent was varied from 7.0 to 10.0.

volume had no effect on the phase separation and little effect on dilution of the colored product.

The absorbance of the reaction product was measured at 609 nm with an Isco-V4 variable-wavelength detector (190—750 nm) (Isco, Lincoln, NE); the flow-through cell has a 5-mm path length and an illuminated volume of 10 μl. The reaction product was sometimes measured at 620 nm with a Glenco 57-V detector (Glenco Scientific, Houston, TX); the flow cell has a 10-mm path length and an illuminated volume of 50 μl.

Results and discussion

The pH of the TBPE-K reagent was varied from 7.0 to 10.0 to establish the optimum pH condition for the reaction to occur. Figure 3 shows the results obtained for a 40 mg l^{-1} Triton X-100 standard. The curve rises in linear fashion until the pH reaches 9.2 and then the signal remains almost constant to a pH of 10.0. For subsequent runs, the TBPE-K reagent was prepared at pH 9.3, because the reagent began to precipitate at higher pH values.

Table 1 shows the results of injecting a Triton X-100 standard (30 mg l^{-1}) and varying the extraction coil length from 3 to 9 m. Apparently, the ion-pair extraction takes place very rapidly because there is little difference in the peak response between a 3- and 9-m extraction coil. The 3-m coil was selected for the manifold shown in Fig. 1.

TABLE 1

Results of injecting a 30 mg l^{-1} standard with varying extraction-coil length

Coil length (m)	3	6	9
Average response (mV)[a]	453	461	460

[a] $n = 5$.

TABLE 2

Results of injecting 30 mg l^{-1} standards of four nonionic surfactants of the form $RO(CH_2CH_2O)_nH$

Surfactant	R	n	Response (mV)
Triton X-100	$CH_3C(CH_3)_2CH_2C(CH_3)_2$-	10	458
Antarox CO-430	n-C_9H_{19}-C_6H_4-	4	153
Antarox CO-630	n-C_9H_{19}-C_6H_4-	9	389
Antarox CO-710	n-C_9H_{19}-C_6H_4-	12	443

Under the recommended conditions, the calibration plot for the range 2—60 mg l^{-1} Triton X-100 had a slope of 0.01588 V l mg^{-1} (standard error 4.09×10^{-4}) with an intercept of -5.0×10^{-4} mg l^{-1} (correlation coefficient 0.9999).

Response of other nonionic surfactants. Table 2 shows the results obtained by injecting 30 mg l^{-1} standards of four different types of nonionic surfactants of the general formula $RO(CH_2CH_2O)_nH$. The Triton X-100 was the most responsive. The least responsive was Antarox CO-430, which also had the least amount of polymerization of the oxyethylene group. Generally, the response increases with the number of moles of oxyethylene, but of course the molecular weight and structure of the side-chains also influence the response.

Conclusion

The proposed method, because of the improved phase separator, increases the phase-separation efficiency and emphasizes the problem of the changing permeability of membranes caused by complex matrices. Nonionic surfactants of the general type $RO(CH_2CH_2O)_nH$ can be determined at low levels (2—60 mg l^{-1}) with the TBPE-K reagent. Each nonionic surfactant varies in its response to the TBPE-K reagent, because the reaction is primarily dependent on the number of oxyethylene groups in the compound. The flow-injection manifold is simple and will cope with 30 samples per hour. The precision of the method is excellent with a relative standard deviation (n = 10) of 0.87% for the 3 mg l^{-1} standard and 0.49% for the 50 mg l^{-1} standard.

REFERENCES

1 R. A. Greff, E. A. Setzkorn and W. D. Leslie, J. Am. Oil Chem. Soc., 42 (1965) 180.
2 N. T. Crabb and H. E. Persinger, J. Am. Oil Chem. Soc., 45 (1968) 611.
3 B. M. Milwidsky, Analyst (London), 94 (1969) 377.
4 L. Favretto and F. Tunis, Analyst (London), 101 (1976) 198.
5 L. Favretto, B. Stancher and F. Tunis, Analyst (London), 105 (1980) 833.
6 K. Toei, S. Motomizu and T. Umano, Talanta, 29 (1982) 103.
7 J. Kawase, A. Nakee and M. Yamanaka, Anal. Chem., 51 (1979) 1640.
8 B. Karlberg and S. Thelander, Anal. Chim. Acta, 98 (1978) 1.
9 B. Karlberg, Anal. Chim. Acta, 118 (1980) 285.
10 J. Kawase, Anal. Chem., 52 (1980) 2124.
11 D. C. Shelly, T. M. Rossi and I. M. Warner, Anal. Chem., 54 (1982) 87.
12 L. Fossey and F. F. Cantwell, Anal. Chem., 55 (1983) 1882.

Analytica Chimica Acta, 179 (1986) 463—468
Elsevier Science Publishers B.V., Amsterdam — Printed in The Netherlands

Short Communication

SIMULTANEOUS DETERMINATION BY ITERATIVE SPECTROPHOTOMETRIC DETECTION IN A CLOSED FLOW SYSTEM

A. RÍOS, M. D. LUQUE DE CASTRO and M. VALCÁRCEL*

Department of Analytical Chemistry, Faculty of Sciences, University of Córdoba, Córdoba (Spain)

(Received 7th July 1985)

Summary. A flow-injection configuration based on a closed flow system which includes a single spectrophotometric detector and allows iterative detection by passage of the reacting plug *n* times through the same detector is described. The information obtained can be used in the simultaneous determination of species by kinetic methods. The example given is the simultaneous determination of iron(III) and cobalt(II) via the EGTA/PAR ligand displacement reaction.

The simultaneous or sequential determination of different ions or compounds can be achieved in various ways in flow injection analysis (f.i.a.), with detectors of the same or different type located in series or in parallel [1], by using a single detector after different reaction times [2], and by applying fast-scan detectors [3, 4].

In the configuration used in this communication for the determination of two ions, a single detector is located in a closed flow system similar to the closed-loop procedures described by Mottola and coworkers [5, 6] and Roehrig et al. [7]. The difference from these is that no species is regenerated and that the circulating solution is not confined constantly within the system, but is rejected when equilibrium is attained. The basic configuration is very simple and provides a signal (peak) each time the reacting plug passes through the detector before physical equilibrium is attained. This iterative detection mode has been described in detail and applied to the determination of a single species from several kinetic parameters, using dilution, normal and amplification methods depending on the concentration of the analyte in the sample [8], and also for the calculation of reaction stoichiometries [9]. The iterative detection mode also allows application of kinetic methods such as the logarithmic extrapolation and single-point methods, for mixture resolution. The value of the analytical signal at equilibrium (S_∞) can be obtained, which is impossible by other flow-injection methods except for the stopped-flow mode. These methods are used here for the simultaneous determination of iron(III) and cobalt(II).

0003-2670/86/$03.50

Experimental

Reagents. The reagents used were aqueous solutions of ethyleneglycol bis-(β-aminoethyl ether)-*N,N,N',N'*-tetraacetic acid (EGTA; 1×10^{-3} M) and 4-(2-pyridylazo)resorcinol monosodium salt, monohydrate (PAR; 0.2% w/v). The buffer solution was boric acid/sodium hydroxide, pH 8.5. Standard stock solutions (1.00 g l^{-1}) of iron(III) and cobalt(II) were prepared.

Apparatus. A Pye-Unicam SP-500 single-beam spectrophotometer was used with a Hellma 178.12-QS flow cell (18 μl). A Gilson Minipuls-2 peristaltic pump, Tecator L100-1 and Rheodyne 5041 injection valves, and a Tecator TM-III Chemifold were also used. A Hewlett-Packard HP-85 microcomputer was used to collect the absorbance/time data at the maximum and minimum of the peaks from the spectrophotometer through an HP-IB 82937A interface.

Manifold. The configuration is shown in Fig. 1. The essential parts for the closed flow system are valve S and pump P'. Valve S is an ordinary switching valve which can be switched to select channel 1 or 2 while the other channel passes to waste. When channel 2 is selected, the flow is kept circulating by pump P'; although this pump increases the dispersion by 35%, the effect is reproducible. For the Fe(III), Co(II)/EGTA/PAR system, the sample is injected into the EGTA stream and then merges with the PAR stream. The resulting flow is introduced into the closed system. The PAR complexes are monitored at 510 nm.

The functioning is controlled and data acquisition and treatment are performed by the microcomputer, and the results are printed out. Typical recordings are series of peaks as shown in Fig. 2.

Results and discussion

Flow-injection methods based on differential kinetics normally make use of the proportional-equation method [1, 10]. The incorporation of several LEDs also allows the application of this method as well as the logarithmic-extrapolation method with slight modifications [11].

Recordings obtained with the recommended configuration (Fig. 1) consist of a series of peaks, the absorbance of which increases until equilibrium is attained (Fig. 2). The envelopes with the minima of these peaks define typical kinetic curves to which the classical differential-kinetic methods can be

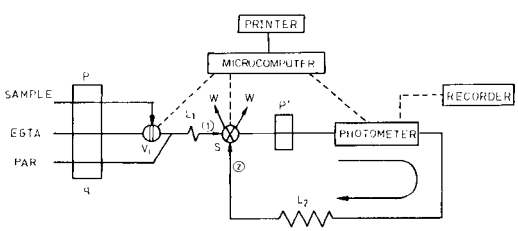

Fig. 1. Closed-flow configuration for simultaneous determination of Fe(III) and Co(II). For explanation, see text.

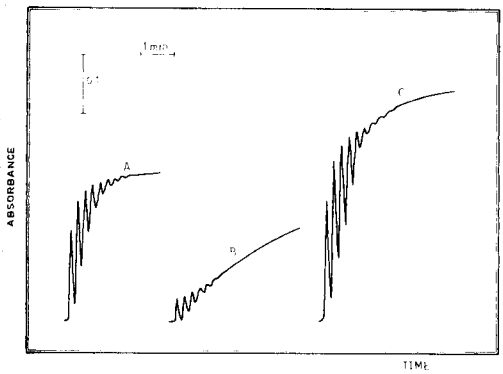

Fig. 2. Recordings obtained for the Fe(III)/Co(II) system: (A) Fe(III); (B) Co(II); (C) Fe(III)/Co(II) mixture. Concentration of each cation is 7.0 μg ml^{-1}.

applied; these allow the calculation of any kinetic (reaction rate, rate constant) or equilibrium parameter (final absorbance, molar absorptivity). The chemical system chosen was the ligand displacement reaction between EGTA and PAR with Fe(III) and Co(II), which have different rates (higher for iron) [12].

Determination of kinetic parameters. From the absorbance (A) of the minima and their times (t) of appearance, the usual procedures can be applied to calculate three features. First, the average reaction rate, $v = (A_2 - A_1)/(t_2 - t_1)$, corresponding to the initial reaction rate at the first two minima is considered. Then, rate constants, k, are calculated from the expression $\log (A_\infty - A_t) = \log (A_0 - A_\infty) - kt/2.303$, where A_0 is the initial absorbance, A_t the absorbance at time t and A_∞ the absorbance at equilibrium. The plot of $\log (A_\infty - A_t)$ vs. time is a straight line and its slope yields the value of k. Finally, partial reaction orders, defined as the slopes of the $\log v$ vs. $\log C$ plots, are calculated. It is important to note that in these flow-injection systems involving physical-kinetic processes together with the kinetics of the chemical reaction, the C variable also includes the flow-injection variables, i.e., flow rate (q), coil lengths (L) and injected volume (V_i) [1, 8].

Because differential-kinetic methods require the ratio between the rate constants of the reactions involved to be as high as possible for good mixture resolution, the chemical and flow-injection variables were optimized by maximizing the k'_{Fe}/k'_{Co} ratio. According to this criterion, the optimum reagent concentrations were 3×10^{-3} M EGTA (pH 9.7) and 0.035% (w/v) PAR with a 30% boric acid/sodium hydroxide buffer pH 8.5, the sample pH being 2.5. The values obtained for the flow-injection variables are: q = 3.6 ml min^{-1}, L_1 = 70 cm, L_2 = 80 cm and V_i = 68.3 μl (for tubing of 0.5 mm i.d.).

From the above-mentioned partial reaction orders, the following apparent reaction rates were evaluated for the Fe(III) and Co(II) systems:

$$v_{Fe} = k_{Fe}[Fe^{3+}][EGTA]^{-1/2}[PAR] + k'_{Fe}qL^{1/2}V_i^{2/3}$$

$$v_{Co} = k_{Co}[Co^{2+}][EGTA]^{-1/2}[PAR] + k'_{Co}q^{2/3}L^{1/10}V_i^{4/3}$$

The contribution of the flow-injection variables to the overall kinetics of the process is obviously as significant as, or even more significant than the contribution of the chemical variables, thus the systems can be manipulated over wide ranges.

Calibration graphs. The conditions established allowed the individual determination of cobalt and iron ions, depending on the parameter measured, from the following equations:

$A_1 = 0.018[Fe^{3+}] + 0.071$ [$r = 0.998$ for 2—18.0 μg ml^{-1} iron(III)]

$v_{1,2} = 0.028[Fe^{3+}] + 0.084$ [$r = 0.998$ for 1.5—22.0 μg ml^{-1} iron(III)]

$A_\infty = 0.022[Fe^{3+}] + 0.098$ [$r = 0.998$ for 0.7—24.0 μg ml^{-1} iron(III)]

$A_1 = 0.005[Co^{2+}] + 0.005$ [$r = 0.989$ for 5.0—20.0 μg ml^{-1} cobalt]

$v_{1,2} = 0.008[Co^{2+}] + 0.006$ [$r = 0.999$ for 5.0—25.0 μg ml^{-1} cobalt]

$A_\infty = 0.035[Co^{2+}] + 0.062$ [$r = 0.997$ for 2.0—14.0 μg ml^{-1} cobalt]

In these equations, A_1 is the absorbance of the first maximum, $v_{1,2}$ the average rate between the first two minima and A_∞ the absorbance at equilibrium. The higher sensitivity of the method for iron(III) is obvious.

Logarithmic extrapolation method for mixture resolution. By plotting log $(A_\infty - A_t)$ vs. t, a characteristic curve is obtained. If the faster reaction is almost complete, the plot is linear with intercept n. The Fe(III) and Co(II) concentrations in the mixture were obtained from the expressions: $[Co^{2+}] = 10^n/\epsilon_{Co}$ and $[Fe(III)] = (A_\infty - 10^n)/\epsilon_{Fe}$, where ϵ is the absorptivity of each complex, the values of which are obtained by averaging the results from experiments done with different concentrations of each component; it was found that the absorptivities obtained by conventional methods did not provide satisfactory results. The values obtained were $\epsilon_{Co} = 0.0595$ and $\epsilon_{Fe} = 0.0306$ expressed in l mg^{-1} cm^{-1} so that μg ml^{-1} data were easily calculated.

Table 1 lists the results obtained by using these expressions for resolution of several Fe(III)/Co(II) mixtures. In general, the errors found for Co(II) are larger than those for Fe(III), but they are acceptable and comparable to those obtained by the much slower conventional photometric method. The relative standard deviation, r.s.d., obtained for 11 mixtures containing 7.5 μg ml^{-1} Fe(III) and 5.5 μg ml^{-1} Co(II) were ±0.98% and ±1.52%, respectively.

Single-point method for mixture resolution. The concentration of each species is determined from A_∞ and the fraction of each species which has not reacted within a previously selected interval. The optimum measurement time is obtained from the Lee-Kolthoff equation: $t_{opt} = \ln (k_{Fe}/k_{Co})/(k_{Fe} - k_{Co})$. In this case it is similar to the appearance time of the fourth minimum, A_4 (about 68 s). A calibration graph was obtained previously for the molar fraction, Y, of Fe(III) in the sample; this was represented by the equation $(A_\infty - A_4)/A_\infty = -0.525\ Y_{Fe} + 0.834$. The value of Y_{Fe} was obtained from experi-

TABLE 1

Resolution of Fe(III)/Co(II) samples by the logarithmic-extrapolation and single-point methods

Added (μg ml^{-1})		Found (μg ml^{-1})		Errors (%)	
Fe(III)	Co(II)	Fe(III)	Co(II)	Fe(III)	Co(II)
Logarithmic-extrapolation method					
6.0	2.5	6.2	2.7	3.3	8.0
6.0	3.5	6.0	3.5	0.0	0.0
7.5	3.5	7.3	3.5	−2.6	0.0
5.0	5.0	5.1	4.7	2.0	−6.0
5.0	3.5	5.0	3.6	0.0	2.8
3.5	3.5	3.4	3.7	−2.8	5.7
6.0	6.0	5.8	5.7	−3.3	−5.0
5.0	2.5	5.0	2.7	0.0	8.0
Single-point method					
6.0	2.5	6.2	2.5	3.3	0.0
6.0	3.5	6.1	3.5	1.6	0.0
6.0	7.5	6.0	7.5	0.0	0.0
6.0	10.0	6.0	9.8	0.0	−2.0
3.5	7.5	3.4	7.3	−2.8	−2.6
5.0	7.5	5.0	7.8	0.0	4.0
5.0	10.0	5.1	10.1	2.0	1.0
3.5	3.5	3.4	3.6	−2.8	2.8

mental data for $(A_\infty - A_4)/A_\infty$, whilst the concentration of each metal ion in the mixtures was derived from $[Fe^{3+}] = Y_{Fe}A_\infty/\epsilon_{Fe}$ and $[Co^{2+}] = (1 - Y_{Fe})A_\infty/\epsilon_{Co}$. The following ϵ values were obtained empirically in this case: $\epsilon_{Fe} = 0.0401$ and $\epsilon_{Co} = 0.0408$ (l mg^{-1} cm^{-1}).

Table 1 shows the results for some Fe(III)/Co(II) synthetic mixtures resolved in this way. The errors encountered, similar for Fe(III) and Co(II), are smaller than those for the logarithmic extrapolation method. The r.s.d. corresponding to 11 samples containing 7.5 μg ml^{-1} Fe(III) and 5.0 μg ml^{-1} Co(II) were ±0.78% and ±0.77%, respectively.

Conclusions

The suggested methods reflect the potential of this type of configuration for simultaneous determinations. The large amount of data collected per sample provides much information about the system, thereby facilitating the application of different methods for mixture resolution.

The CAICyT is thanked for financial support (Grant No. 2012-83).

REFERENCES

1 See, e.g., M. D. Luque de Castro and M. Valcárcel, Analyst (London), 109 (1984) 413.
2 A. Fernández, M. A. Gómez-Nieto, M. D. Luque de Castro and M. Valcárcel, Anal. Chim. Acta, 165 (1984) 217.
3 J. Janata and J. Růžička, Anal. Chim. Acta, 139 (1982) 105.

4 F. Lázaro, A. Ríos, M. D. Luque de Castro and M. Valcárcel, Anal. Chim. Acta, 179 (1986) 279.
5 V. V. S. Eswara Dutt and H. A. Mottola, Anal. Chem., 47 (1975) 357.
6 S. M. Ramasamy and H. A. Mottola, Anal. Chim. Acta, 127 (1981) 39; Anal. Chem., 54 (1982) 283 (and references therein).
7 P. Roehrig, C. M. Wolff and J. P. Schwing, Anal. Chim. Acta, 153 (1983) 181.
8 A. Ríos, M. D. Luque de Castro and M. Valcárcel, Anal. Chem., 57 (1985) 1803.
9 A. Ríos, M. D. Luque de Castro and M. Valcárcel, J. Chem. Educ., Oct. (1986).
10 R. G. Garmon and C. N. Reilley, Anal. Chem., 34 (1962) 600.
11 D. J. Holley and R. E. Dessy, Anal. Chem., 55 (1983) 313.
12 M. Tanaka, S. Funashi and D. Shirai, Anal. Chim. Acta, 39 (1967) 437.

Analytica Chimica Acta, 179 (1986) 469—473
Elsevier Science Publishers B.V., Amsterdam — Printed in The Netherlands

Short Communication

SIMULTANEOUS SPECTROFLUORIMETRIC DETERMINATION OF CERIUM(III) AND CERIUM(IV) BY FLOW INJECTION ANALYSIS

KAMAIL H. AL-SOWDANI and ALAN TOWNSHEND*
Chemistry Department, University of Hull, Hull HU6 7RX (Great Britain)
(Received 20th June, 1985)

Summary. Cerium(III) (1—100 $\mu g\ l^{-1}$) is determined by injection into a carrier stream of hydrochloric, perchloric or sulphuric acid, and monitoring its native fluorescence. Cerium(IV) can be determined similarly by incorporating a zinc reductor minicolumn into the system. Splitting the injection sample so that only part passes through the reductor, and the remainder by-passes it, allows total cerium and cerium(III) to be detected from the two sequential fluorescence peaks obtained.

Spectrofluorimetry is a reliable technique for the quantitation of a wide range of lanthanides in solution [1—3]. Its inherent characteristics of high sensitivity and selectivity combined with the advantages of flow injection analysis (f.i.a.) provide an efficient and reproducible means of analysis [4—6]. Lanthanide ions, and those of uranium and thorium, are the only inorganic elements that can be detected in solution by the luminescence of their simple ions. Armstrong et al. [7] suggested the possibility of determining cerium(III) by fluorimetry, and later cerium(III) fluorescence was studied in inorganic acid solutions [8—11]. Cerium(III) has a characteristic fluorescence which has its excitation maximum at 260 nm and emission maximum at 350 nm. The detection limit in some cases is below 4 ng ml^{-1}, with no interferences from other lanthanides [10]. Cerium(IV) does not fluoresce, but can easily be reduced to cerium(III) which offers a method for the indirect spectrofluorimetric determination of cerium(IV), and of several other species which cannot be determined directly by spectrofluorimetry but which can reduce cerium(IV) to cerium(III), e.g., iron(II) and arsenic(III) [8]. Nitrite, thiosulphate and iodide can similarly be determined after chromatographic separation by their reaction with cerium(IV) in a postcolumn packed reactor [12].

Recently, Faizullah and Townshend [13] described a f.i.a. procedure for the simultaneous spectrophotometric determination of iron(II) and iron(III). The injected sample was split into two; part reacted directly with 1,10-phenanthroline to give a response for iron(II), and the remainder was directed through a zinc reductor minicolumn before rejoining the original stream for reaction with 1,10-phenanthroline, so as to give a second peak corresponding

0003-2670/86/$03.50

to total iron. In this communication the direct spectrofluorimetric determination of cerium(III) by f.i.a. is reported as well as a simultaneous spectrofluorimetric determination of cerium(III) and cerium(IV) based on an analogous procedure to that described above for iron, in which part of the sample is directed through a zinc reductor minicolumn to reduce cerium(IV) to cerium(III).

Experimental

Reagents. All chemicals were of analytical grade except for cerium(III) nitrate hexahydrate (99.9% pure; Koch-Light Laboratories) and ammonium cerium(IV) nitrate (99.9% pure; Sigma Chemical Co.). A 100 μg ml^{-1} cerium(III) solution was prepared by dissolving 0.2810 g of the cerium(III) salt in distilled water and diluting to 1 l with water. A 100 μg ml^{-1} cerium(IV) solution was prepared by dissolving 0.3912 g of the cerium(IV) salt in 600 ml of water containing 10 ml of concentrated sulphuric acid, 2 g of sodium peroxodisulphate and 2 ml of 0.1 M silver nitrate; the solution was boiled for 10 min and diluted to 1 l with water [14]. Calibration solutions were prepared by serial dilution of these stock solutions with distilled water.

Apparatus. The detector used for all the measurements was a Perkin-Elmer model 3000 fluorescence spectrometer with a flow cell comprising a silica tube (2 mm i.d., 35 mm long) held vertically in the sample compartment in a rigid mount.

The zinc reductor minicolumn (2 mm i.d., 25 mm long) was prepared as described previously [13].

The flow manifold used for the determination of cerium(III) is shown in Fig. 1(a). A peristaltic pump (Ismatec SA-8031, Zurich) was used with 1 ml min^{-1} pump tubing, and the sample was introduced via a Rheodyne 5020 injection valve (Anachem) with a sample loop of 180 μl. Teflon tubing (0.5 mm i.d.) was used for the rest of the manifold. The fluorescence was

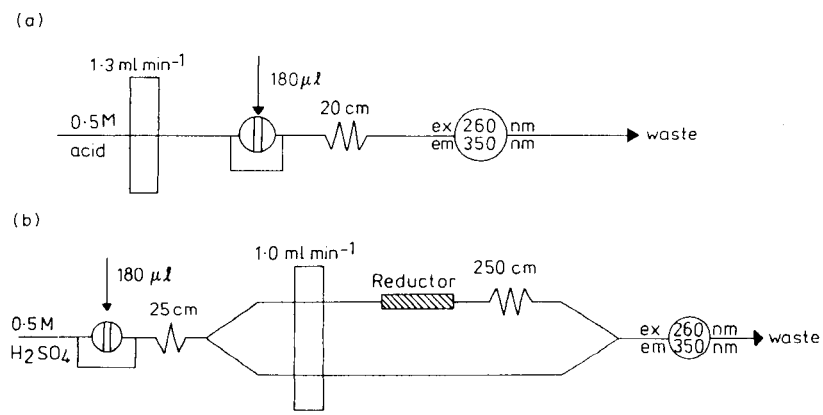

Fig. 1. Manifolds for the determination of: (a) cerium(III); (b) cerium(III) and total cerium.

measured at 260 nm (excitation) and 350 nm (emission) and the spectrofluorimeter was set with excitation and emission slits at 10. The spectrofluorimeter was connected to a Tekman Labwriter TE-200 recorder.

Results and discussion

The fluorescence spectra of cerium(III) were found to be the same in ca. 0.5 M solutions of hydrochloric, perchloric or sulphuric acid. Cerium(III) has an excitation maximum at 260 nm and fluorescence maximum at 350 nm. When the manifold in Fig. 1(a) was used, the signals (peak height) increased almost parabolically with increase in injected volume between 65 and 165 μl; the maximum peak height was obtained when 205—225 μl was injected, which is similar to the flow cell volume, but the peak shape was somewhat distorted, so 180 μl was injected in subsequent experiments. Greatest peak-height sensitivity was obtained at a flow rate of 1.3 ml min^{-1}. The concentration of inorganic acid was found not to affect the fluorescence of cerium(III) in the range 0.01—1 M, so 0.5 M was chosen.

A linear calibration graph was obtained for 0—100 ng ml^{-1} under the recommended conditions given in Fig. 1(a). The detection limit (2 × noise) was 1 ng. The dispersion coefficient was 3 and the residence time 23 s. The injection rate was 150 h^{-1}. The relative standard deviation for 10 injections of 40 ng of cerium(III) was 0.6%.

Interferences. Cukor and Weberling [8] studied the interferences of various ions including the lanthanides, copper, nitrate, nickel, lead and iron(II) and found that the most serious interferences were from iron(II) and nitrate when present at a concentration 50 times by weight that of cerium. Gazotti and Abrão [10] studied the quenching effect of thorium on cerium(III) fluorescence; a concentration of 200 g Th l^{-1} decreased the intensity to 20% of its value, but even so it was possible to determine 4 ng Ce ml^{-1} in a 200 g Th l^{-1} solution. Also they showed that iron(II) interfered seriously. In this work, only the effects of other lanthanide ions were studied (Fig. 2). Most lanthanides had no effect, but terbium and ytterbium depressed the fluorescence at higher concentrations. Cerium(IV) did not interfere at $\geqslant$100 times the cerium(III) concentration.

Determination of cerium(IV). Cerium(IV) can be determined by incorporating a zinc reductor minicolumn into the system between the pump and the 20-cm delay coil. A typical calibration graph obtained under these conditions for 180-μl injections of cerium(IV) is shown in Fig. 3. The mean r.s.d. was 1.8% for the peaks in this figure. Sodium peroxodisulphate was added when the cerium(IV) solutions were prepared in order to oxidize any cerium(III) present to cerium(IV), with silver nitrate to catalyse the oxidation [14]; the excess of peroxodisulphate was destroyed by boiling. Trace amounts of cerium(III) remaining in the cerium(IV) solution after this treatment gave fluorescence signals (1 mm peak height) which must be subtracted.

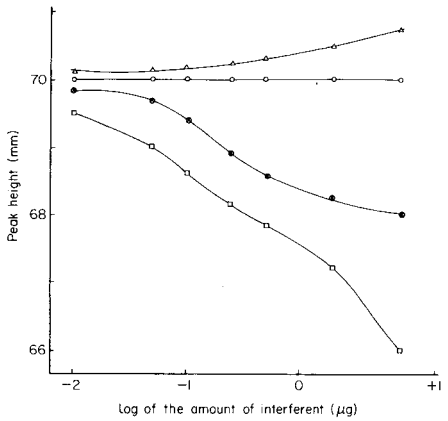

Fig. 2. Effect of other lanthanides on the determination of cerium(III) (40 ng ml^{-1} in 0.5 M $HClO_4$): (△) Sm; (×) Yb; (□) Tb; (○) La, Nd, Pr, Gd, Ce(IV). The amount of interferent refers to the aliquot injected.

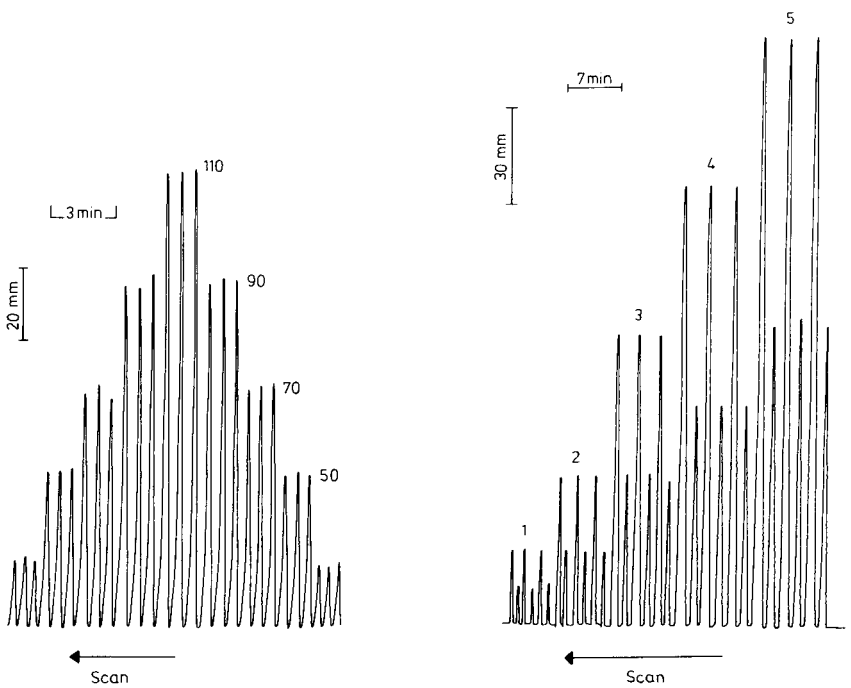

Fig. 3. Calibration peaks for injections of 30—110 ng ml^{-1} cerium(IV).

Fig. 4. Peaks obtained for cerium(III)/cerium(IV) mixtures at the following respective concentrations (ng ml^{-1}): (1) 500, 500; (2) 400, 400; (3) 300, 300; (4) 200, 200; (5) 100, 100. The larger peak in each pair represents total cerium.

Simultaneous determination of cerium(III) and cerium(IV). The simultaneous determination of cerium(III) and cerium(IV) can be achieved by incorporating a zinc reductor minicolumn into the system [13] as shown in Fig. 1(b). The injected sample is split into two streams, one of which bypasses the reductor, and therefore gives a response only to the original cerium(III) in the sample. The remainder passes through the reductor and a 250-cm delay coil, and then passes to the detector to give a second peak completely resolved from the first which represents the total cerium content of the sample. A perspex Y-piece (0.7 mm i.d.) with a 45° angle between the two outflow lines gave reproducible 1:1 stream splitting, with 0.5 mm i.d. pump tube connected to the reductor and 0.4 mm i.d. tube to other channel. The flow rate was very important, and should be less than 1.2 ml min^{-1} in order to reduce all cerium(IV) to cerium(III) in the reductor column. Typical calibration data for 180-μl injections of cerium(III)/cerium(IV) solutions are shown in Fig. 4. The injection rate was 30 h^{-1} with a mean r.s.d. of 2.5% over all the calibration peaks shown in Fig. 4.

K. H. Al-Sowdani thanks the Iraqi Government (Ministry of Higher Education and Scientific Research, University of Basrah) for the award of a scholarship.

REFERENCES

1 A. Zaidel and Ya. Larionov, Izv. An. SSSR, Ser. Fiz., 4 (1940) 25.
2 F. B. Huke, R. H. Heidel and V. A. Fassel, J. Opt. Soc. Am., 43 (1953) 400.
3 G. Alberti and M. Massucci, Anal. Chim. Acta, 35 (1966) 303.
4 T. A. Kelly and G. D. Christian, Anal. Chem., 53 (1981) 2110.
5 J. Burguera, M. Burguera and M. Gallignani, Acta Cient. Venez., 33 (1982) 99.
6 M. Morelos, M.Sc. Thesis, University of Hull, 1983.
7 W. A. Armstrong, D. W. Grant and W. G. Humphreys, Anal. Chem., 35 (1963) 1300.
8 P. Cukor and R. P. Weberling, Anal. Chim. Acta, 41 (1968) 404.
9 G. F. Kirkbright, T. S. West and C. Woodward, Anal. Chim. Acta, 36 (1966) 298.
10 P. I. Gazotti and A. Abrão, Publicaco TEA No. 294 (1973), Instituto de Energia Atômica, Brasil.
11 G. Albert and M. Massucci, Gazz. Quim. Ital., 95 (1965) 997.
12 Sun Haing Lee and L. R. Field, Anal. Chem., 56 (1984) 2647.
13 A. T. Faizullah and A. Townshend, Anal. Chim. Acta, 167 (1985) 225.
14 G. W. C. Milner and G. W. Sneddon, Atomic Energy Research Establishment C/R 1470 (1955), England.

Analytica Chimica Acta, 179 (1986) 475—479
Elsevier Science Publishers B.V., Amsterdam — Printed in The Netherlands

Short Communication

SPECTROPHOTOMETRIC DETERMINATION OF IODATE, IODIDE AND ACIDS BY FLOW INJECTION ANALYSIS

O. F. KAMSON
Chemistry Department, University of Lagos, Lagos (Nigeria)

(Received 15th April 1985)

Summary. The production of iodine by reaction of iodate and iodide in acidic solution is used for the spectrophotometric determination of 1—6 × 10^{-5} M iodate, 2—8 × 10^{-3} M iodide, and ca. 10^{-3} M acids. The sample is injected into a carrier stream containing the other two ions. The injection rate is ca. 100 h^{-1}.

In weakly acidic media (<0.1 M H^+) iodide reacts with iodate, and iodine is formed quantitatively [1]:

$$IO_3^- + 5I^- + 6H^+ \rightarrow 3I_2 + 3H_2O$$

This reaction is a convenient source for known amounts of iodine as six iodine atoms are liberated for each iodate ion present. The reaction has been used for determining small amounts of iodide after oxidation to iodate because of the inherent amplification factor, and also provides a very sensitive method for the determination of acids [1].

Flow injection analysis provides very fast methods which allow the exploitation of many chemical reactions [2]. The iodate/iodide reaction is fast in acidic solutions and so can readily be studied in a flow system. Its exploitation for the determination of iodate, iodide and acids is described in this communication.

Experimental

A single-line manifold was used. A peristaltic pump (Minipump, Schuco Scientific, London) comprising two 10-rpm motors operating in parallel was used to give the desired reagent flow rate (5 ml min^{-1}). Samples were injected with the aid of a multi-injection valve [3] which permits the injection of variable sample volumes by changing the lengths of the Tygon tubes (0.75 mm i.d.) used. Teflon tubing (1 mm i.d.) was used for the remainder of the flow system. After injection, the sample reacted in a 30-cm coil before it reached the flow-through cell (18-μl volume, 10-mm light path; Hellma type 178.12) placed in a Pye-Unicam SP6-550 spectrophotometer. The output was fed to a Perkin-Elmer model 56 chart recorder operated at 5-mV full-scale deflection.

0003-2670/86/$03.50

All reagents were analytical grade except where otherwise stated.

Results and discussion

Iodine in the presence of iodide forms triiodide, which has a high molar absorptivity at 350 nm [4] in an aqueous medium. This species was measured spectrophotometrically at 350 nm in all the procedures described.

Optimization of flow injection parameters. For these investigations, the experimental conditions recommended for the determination of iodate were used; a solution 0.1 M in iodide and 1×10^{-3} M in sulphuric acid was used as the carrier solution into which a 2×10^{-5} M iodate solution was injected.

The influence of flow rate (1.5—10 ml min^{-1}) on the detector response, measured as peak height, was investigated by injecting 30 μl of the iodate solution. The signals at 1.5 and 3.0 ml min^{-1} were 0.75 and 0.84 times, respectively, that at 5.0 ml min^{-1}, but remained constant at 5 ml min^{-1}, when the distance travelled between the injection point and the detector was 45 cm. A residence time of 8 s and a sampling rate of 120 h^{-1} were achieved at 5 ml min^{-1}, thus this flow rate was chosen in order to economise on reagents.

Tests with different tubing lengths between the injection point and the detector showed that 45 cm was satisfactory for 30-μl injections of the iodate solution into the carrier stream at 5 ml min^{-1}. The detector response decreased as the line length was increased, because of increased dispersion. The influence of the sample volume on the detector response was then investigated by injecting various volumes (12—70 μl) of the iodate solution into the carrier stream at the recommended flow rate and line length. The detector response increased as the sample volume was increased, the peak height for 70 μl being twice that for 30 μl. However, a sample volume of 30 μl was chosen for subsequent investigations because at a line length of 45 cm, a dispersion coefficient of 7 was obtained, thus implying medium dispersion. The use of larger sample volumes would be necessary if an increase in sensitivity were required.

Determination of iodate. Carrier streams consisting of various concentrations of iodide (5×10^{-4}—1×10^{-1} M) in various concentrations of sulphuric acid (10^{-6}—10^{-2} M) were investigated to establish the optimum carrier solution composition; 4×10^{-5} M iodate was used. The injection of 30 μl of the iodate solution into carrier solutions which were 1×10^{-3} M in iodide and 10^{-6}—10^{-4} M sulphuric acid gave no response. However, measurable signals were obtained when the acidity of the carrier was 1×10^{-3} M and the iodide ion concentration was 1×10^{-3} M. The signals obtained from a carrier stream containing 5×10^{-2} M iodide were 7.1 and 2.2 times that from carrier solutions of 5×10^{-3} M and 1×10^{-2} M iodide, respectively. Above 5×10^{-2} M, a constant signal was obtained. Consequently, in order to economise on reagent consumption, a carrier solution 5×10^{-2} M in iodide and 1×10^{-3} M in sulphuric acid is recommended for the determination of iodate.

For the injection of 30 μl of 1.0—6.0 $\times 10^{-5}$ M iodate, the peak heights

were linearly dependent on the concentration of iodate up to 6×10^{-5} M but remained constant for $>2 \times 10^{-4}$ M iodate. The detection limit was 1×10^{-6} M iodate, which was defined as the concentration that gave a peak height twice that produced on injection of deionised water. The r.s.d. for 4 determinations of 4×10^{-5} M iodate was 3.0%. When 2×10^{-5} M iodate was injected, the following ions did not interfere when present at up to 1000 times (mol mol^{-1}) that of iodate: Cl^-, Br^-, I^-, SCN^-, BrO_3^-, ClO_3^- and ClO_4^-. However, cyanide interfered when present at above 100 times the amount of iodate.

Determination of iodide. Preliminary investigation of the best composition of the carrier solution for this determination by oxidation with iodate showed that measurable signals were obtained on the injection of 30 μl of 4×10^{-3} M iodide into a carrier solution which was 1×10^{-3} M in iodate and 1×10^{-3} M in sulphuric acid. The responses for $2-8 \times 10^{-3}$ M iodide gave a linear calibration graph (Fig. 1, curve a). Injection of iodide 1.5×10^{-2} M produced constant peak heights. With a larger sample volume (70 μl), a shorter linear range and earlier saturation (at 1.0×10^{-2} M) of response were obtained (Fig. 1, curve b). The r.s.d. for 5 injections of 6×10^{-3} M iodide was 3.5% under the conditions of curve a. The use of stronger iodate solutions ($>1 \times 10^{-3}$ M) slightly increased the sensitivity at lower concentrations (Fig. 1, curves c, d) and displaced the linear range to lower concentrations (Table 1).

Determination of acids. Several iodide/iodate solutions were tested as carrier solutions for the determination of acids by injecting 30 μl of 5×10^{-4} M sulphuric acid under the above optimized flow injection conditions. Injection into a carrier solution which was 5×10^{-3} M in iodide and 1×10^{-3} M in iodate produced measurable signals. This carrier stream composi-

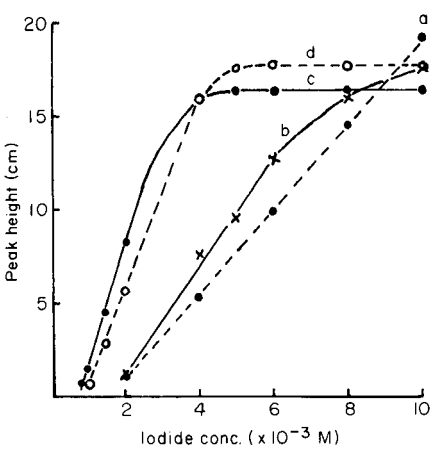

Fig. 1. Calibration graphs for iodide with different iodate concentrations in the flow stream: (a) 1×10^{-3} M; (b) 1×10^{-3} M; (c) 5×10^{-3} M; (d) 1×10^{-2} M. Volume of iodide solution injected: (a) 30 μl; (b—d) 70 μl.

TABLE 1

Linear range and limit of detection for iodide determinations

Iodate conc. ($\times 10^{-3}$ M)[a]	Iodide conc. ($\times 10^{-3}$ M)		
	Linear range	Limit of detection	Minimum giving max. response
1×10^{-3}	2.0—10.0[b]	1.0	15
1×10^{-3}	2.0—6.0[c]	1.0	10
5×10^{-3}	1.0—4.0[c]	0.5	5
1×10^{-2}	0.8—3.0[c]	0.3	4

[a]All carrier solutions were 1×10^{-3} M in sulphuric acid. [b]30-μl Sample. [c]70-μl Sample.

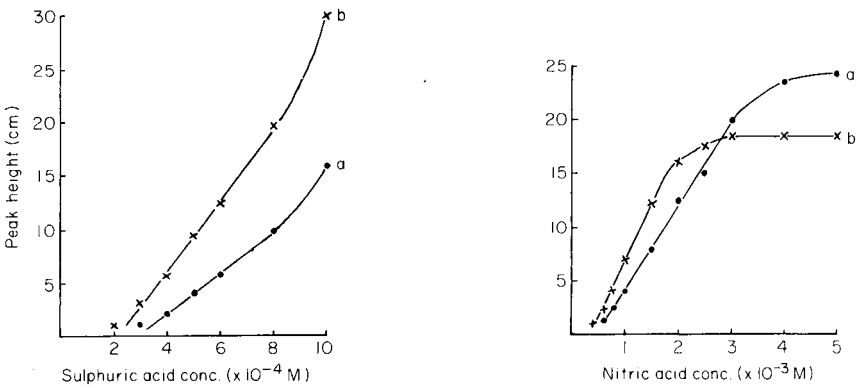

Fig. 2. Calibration graphs for sulphuric acid with different injected volumes: (a) 30 μl; (b) 70 μl.

Fig. 3. Calibration graphs for nitric acid with different injected volumes: (a) 30 μl; (b) 70 μl.

tion was used in further tests. Sulphuric acid between 4×10^{-4} and 8×10^{-4} M gave linear calibration for 30- and 70-μl injections (Fig. 2), the larger volume giving the greater sensitivity. Ten replicate injections of 5×10^{-4} M sulphuric acid gave signals with an r.s.d. of 1%. The calibration graph for nitric acid (expressed as molarity) was of lower slope and range (Fig. 3) but

TABLE 2

Determination of concentration ($\times 10^{-3}$ M) of hydrochloric acid

Conc. by flow injection	0.850	1.00	1.45	2.05	2.65
Conc. by acid/base titration	0.788	1.00	1.48	1.98	2.48

a single graph could be used for both nitric and hydrochloric acids over the range 0.3—5 × 10^{-3} M. Some results for the determination of hydrochloric acid (Table 2) showed good agreement with results from normal acid-base titrations. The use of a more concentrated carrier stream enhanced the sensitivity but reduced the linear range in the manifold used. Longer coil lengths would probably extend the ranges of application.

REFERENCES

1 R. Belcher and I. M. Kolthoff, Volumetric Analysis, Vol. III, Interscience, New York, 1957, p. 246.
2 J. Růžička and E. H. Hansen, Flow Injection Analysis, Wiley, New York, 1981.
3 J. Růžička and E. H. Hansen, Anal. Chim. Acta, 114 (1980) 19.
4 G. Nisli and A. Townshend, Talanta, 15 (1968) 1377.

Analytica Chimica Acta, 179 (1986) 481—486
Elsevier Science Publishers B.V., Amsterdam — Printed in The Netherlands

Short Communication

A MICROCOMPUTER-BASED PEAK-WIDTH METHOD OF EXTENDED CALIBRATION FOR FLOW-INJECTION ATOMIC ABSORPTION SPECTROMETRY

STEPHEN R. BYSOUTH and JULIAN F. TYSON*

Department of Chemistry, University of Technology, Loughborough, Leicestershire, LE11 3TU (Great Britain)

(Received 21st August 1985)

Summary. In the proposed method of extended calibration based on peak widths, all data collection and reduction are done by a microcomputer interfaced to the spectrometer. The method produces an estimate of concentration without dilution of the off-range samples. Calibrations covering the ranges 40—1000 mg l^{-1}, 1.0—50 mg l^{-1} and 20—1000 mg l^{-1} were obtained for chromium, magnesium and nickel, respectively.

The feasibility of using a peak-width calibration method to calculate off-range concentrations by injection of samples close to the nebulizer of a flow-injection system with an atomic absorption spectrometric detector has been demonstrated by Tyson [1], who derived an equation relating peak width to the concentration injected, according to the "single well-stirred mixing chamber" model [2]. Stewart and Rosenfeld [3] incorporated a real mixing chamber into a flow-injection system and used an equation derived by Pardue and Fields [4, 5] for flow-injection titrations, to provide an extended calibration. The derivation is complex, and in its application to calibration, some unnecessary simplifications were made. This produced an equation where peak width is proportional to the logarithm of the concentration injected, whereas if no approximations are made in deriving the equation [1], this is not the case. Both groups of workers measured the peak widths at one concentration level on the peak profile and produced linear calibration graphs, thus demonstrating the validity of the relationships. In this communication, results obtained by using a microcomputer for data acquisition and processing are presented. The calibrations were generated from the widths at several concentration levels on the peak profiles.

Experimental

Solutions. Standards containing chromium, nickel or magnesium were made by serial dilution of 1000 mg l^{-1} stock solutions (BDH Chemicals or Fisons).

Equipment. A Baird-Atomic A3400 spectrometer with an air/acetylene flame was optimized for maximum sensitivity for each element.

0003-2670/86/$03.50

The manifold (Fig. 1) consisted of a pneumatically operated injection valve (P.S. Analytical, T-series), a peristaltic pump (Ismatec 840) and a stream-switching valve (Pharmacia). The connection between the injection valve and nebulizer was 2 cm of teflon tubing (0.71 mm i.d.; Radio Spares, number 1). The flow rate used was 4.7 ml min^{-1} and the volume injected was 82.3 μl.

Interface and microcomputer. The chart recorder output of the spectrometer was connected to an Apple IIe microcomputer via an A/D converter (Micro-Control) and a signal-conditioning unit built in this laboratory. This unit allowed signal offset if required. Time values were read from a clock card (Mountain Hardware). The program was written in BASIC; copies are available from the authors on request.

Data acquisition. Thirty readings were made for all steady states (i.e., baseline and normally aspirated standards), the baseline being read before normal calibration and before injection of concentrated standards or samples. Three hundred time and absorbance data points were collected per injection at a rate of 14 s^{-1}.

Data processing. The rational function

$$A/C = a + bA + cA^2 \quad (1)$$

(where A is absorbance, C concentration and a, b and c are constants to be found during the curve-fitting process), was fitted to the normal calibration data points. This function [6] was found to give consistently good results in earlier work in this laboratory. Each data point consisted of the average of the thirty absorbance values collected and the corresponding concentration input from the keyboard. Curve-fitting was achieved by the method developed by Miller [7].

The 300 data points collected per injection were sorted into those containing peak information and those at the baseline level. Each absorbance on the rise portion of the peak was then matched to the closest absorbance value on the full curve. The associated times were subtracted to give the peak widths for each absorbance level. The absorbances were then converted to concentrations by using the rational function of the normal calibration. This process is summarized in Fig. 2. These values for peak width and concentration were then used, together with the concentration originally injected (entered via the keyboard), to obtain the peak width calibration function.

Initially the equation developed by Tyson [1]

$$t' = (V/u) \ln [(C_m/C') - 1] - (V/u) \ln (D - 1) \quad (2)$$

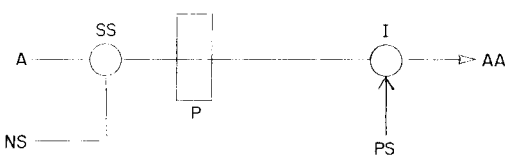

Fig. 1. Flow-injection manifold: SS, stream-switching valve; NS and PS, points where normal standards and peak-width standards are introduced, respectively; A, aqueous carrier; P, pump; I, injection valve; AA, spectrometer.

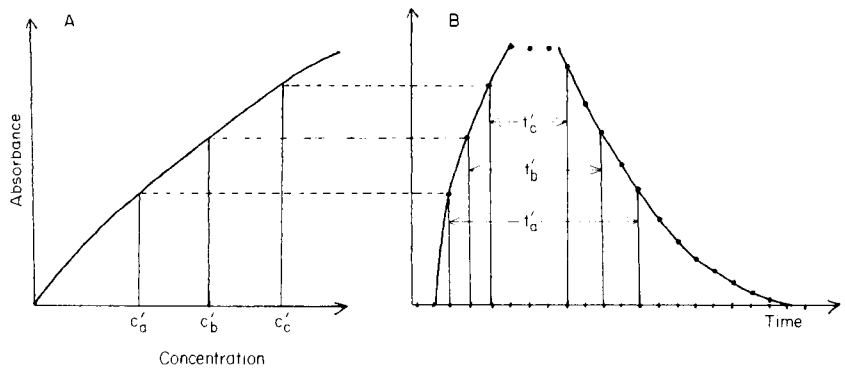

Fig. 2. Data conversion from time and absorbance to peak width and concentration: A, normal calibration; B, recorded peak. t'_a, t'_b and t'_c are the peak widths at concentrations C'_a, C'_b and C'_c respectively, calculated from absorbance (A), concentration (C) and time (t).

was fitted by using the least-squares procedure, as used for the normal calibration. (In Eqn. 2, t' is the width of the peak measured at a concentration C', V the theoretical volume of the mixing chamber, u the flow rate, C_m the concentration injected and D the dispersion of the system.)

Plotting the calibration data t' vs. ln $[(C_m/C') - 1]$ (Fig. 3) showed that the relationship was not linear as expected. A cubic function, suggested by the shape of the graph plotted, was used instead, fitted by least squares:

$$t' = d + eF + fF^2 + gF^3 \qquad (3)$$

where $F = \ln [(C_m/C') - 1]$ and d, e, f and g are constants to be found during the fitting procedure.

On injection of an unknown, the peak widths are transformed to F values by solving for the root of Eqn. 3 using Newton's approximation method [7]. The mean concentration injected is then calculated from the F values and the concentration levels (C') at which the corresponding widths were measured.

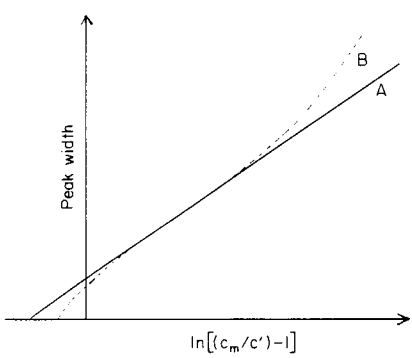

Fig. 3. Peak-width calibration curves: A, theoretical calibration line according to Eqn. 2; B, a typical calibration curve found in these experiments.

Procedure. The system was calibrated by aspiration of the standards for normal calibration. Valve SS (Fig. 1) was switched to the standard/sampling position, and the concentration of the standard was entered through the keyboard once steady state had been achieved. This initiated the reading cycle. The process was repeated for all the standards. Once a normal calibration had been generated, valve SS was turned again and three "peak-width" standards were injected in turn, the concentration of each being entered to initiate the read cycle. The concentrations of the five standards used for each of the normal calibrations covered the ranges 5—40 mg l^{-1} for chromium, 0.1—1.0 mg l^{-1} for magnesium and 5—20 mg l^{-1} for nickel. Fitting the rational function to these calibrations gave correlation coefficients of 0.9996, 0.9085 and 0.9984, respectively. The "peak-width" standards (Table 1) were then re-injected at least ten times as unknowns, in random order, to enable the calibration to be evaluated.

Evaluation of the calibration. The values obtained for each "unknown" were compared by using the Q test [8] and any outliers were rejected. The remaining values were used to calculate the standard deviation (s.d.), relative standard deviation (r.s.d.) and the mean value together with its 95% confidence interval, for each unknown.

Results and discussion

The peak-width calibration deviates from a straight line; peaks are broader than expected at higher concentrations. This could be due to the formation of large salt clotlets at high concentrations which would be slower to vaporize in the flame, giving larger peak widths and smaller C' values. Also, at high concentrations, the wash-out of an individual drop from the nebulizer spray chamber is readily detected as a small peak on the falling absorbance/concentration profile.

The results of the analyses are presented in Table 1. These results show about 8% r.s.d. and some bias at the 95% confidence level. Two main factors contribute to the errors in this method, namely, the goodness of fit of the calibration curve to the experimental points, and the random fluctuations in the absorbance/time profiles observed for replicate injections of the same concentration. Bias is most likely due to errors in the fit of the calibration curve. These will be increased if the instrument response drifts. The large r.s.d. values, compared with a conventional calibration procedure, are due to the logarithmic relationship between peak width and concentration. This will always be a limitation to any flow-injection peak-width method. To some extent the problem can be minimized by increasing the data acquisition rate. In the present method, the rate is 14 s^{-1} which is rather too slow for the rapid rise in absorbance obtained at higher concentrations, producing only a few points on the rise curve from which to calculate the average concentration.

The method has potential for use as a screening method for calculating dilution factors required to bring off-range samples within the range of the normal calibration. Dilution of such samples is usually done by time-consuming

TABLE 1

Peak-width calibration data and results

Metal	r^a	Concentrations of metal (mg l^{-1})			R.s.d. (%)	95% CI[d]
		Injected standards[b]	Calculated from peak-width calibration[c]	Mean calcd.		
Cr	0.9969	1000	1112, 1117, 1047, 1155, 1061, 1194, 1201, 1038, 943.1, 1110	1098	7.14	56.1
		100	105.9, 96.94, 95.95, 109.7, 111.8, 105.1, 105.1, 112.8, 107.4, 110.5	106.1	5.44	4.13
		40	41.66, 37.82, 34.89, 39.99, 38.96, 38.14, 41.44, 43.09, 37.17, 34.4, 38.10	38.70	7.03	1.95
Mg	0.9981	50	63.29, 47.06, 59.40, 55.09, 55.94, 60.22, 75.32, 48.49, 57.41, 61.68	56.5	11.2	4.31
		10	10.89, 10.66, 12.00, 14.75, 10.70, 11.00, 11.98, 10.49, 11.66, 11.03	11.16	5.16	0.443
		1.0	1.082, 1.146, 0.9426, 1.030, 1.077, 1.055, 1.050, 1.082, 1.028, 1.081	1.06	2.18	1.93×10^{-2}
Ni	0.9978	1000	1156, 909.0, 1118, 890.4, 1278, 938.4, 906.0, 1043, 1014, 955.9	1021	12.6	91.8
		100	142.8, 123.1, 103.4, 110.6, 127.0, 115.6, 130.2, 129.0, 88.93, 121.9	119.2	12.8	9.19
		20	19.18, 41.09, 24.67, 20.51, 20.49, 19.36, 21.02, 18.87, 20.91, 23.94	20.99	9.70	1.56

[a]Correlation coefficient. [b]Standards were injected for calibration and as samples. [c]Results which are underlined were rejected by the Q test and not used for subsequent calculation of mean values, RSD or confidence intervals. [d]Confidence interval.

trial and error. With the incorporation of a flow-injection dilution system, the sample could be diluted on-line for further measurements. Examples of dilution based on flow injection include zone sampling [9], variable volume injection [10], variable dispersion [11] and confluence dilution [12]. The concentration could then be calculated from the normal calibration curve already obtained and fitted by the computer, together with the relevant dispersion information.

Reducing the flow rate or introducing a mixing coil or chamber broadens the peaks which allows more data points to be collected on the rise portion of the peak. However, reducing the flow rate to the nebulizer can produce

noise. Placing a mixing coil or chamber before the nebulizer increases the peak widths and so the slope of the peak-width calibration [1].

Conclusion

The approximation that the nebulizer behaves as a single, well-stirred tank breaks down for high concentrations, giving rise to significant deviation from the linear relationship predicted on the basis of this model. A more accurate curve fit may be obtained by using a cubic function and the results so obtained can be used to calculate dilution factors to allow further measurements within the most accurate concentration range. The peak-width method is limited by both the reproducibility of the absorbance/time profiles and the data acquisition rate.

The authors thank the Trustees of the Analytical Chemistry Trust Fund of the Royal Society of Chemistry for the award of an SAC Research Studentship.

REFERENCES

1 J. F. Tyson, Analyst (London), 109 (1984) 319.
2 J. F. Tyson and A. B. Idris, Analyst (London), 106 (1981) 1125.
3 K. K. Stewart and A. G. Rosenfeld, Anal. Chem., 54 (1982) 2368.
4 H. L. Pardue and B. Fields, Anal. Chim. Acta, 124 (1981) 39.
5 H. L. Pardue and B. Fields, Anal. Chim. Acta, 124 (1981) 65.
6 J. R. Hall, Notes on Alphastar-2 Atomic Absorption Curve Correction, Baird-Atomic, 1982.
7 A. R. Miller, BASIC Programs for Scientists and Engineers, Sybex, Berkeley, 1981.
8 J. C. Miller and J. N. Miller, Statistics for Analytical Chemistry, Ellis Horwood, Chichester, 1984.
9 B. F. Reis, A. O. Jacintho, J. Mortatti, F. J. Krug, E. A. G. Zagatto, H. Bergamin F° and L. C. R. Pessenda, Anal. Chim. Acta, 123 (1981) 221.
10 J. F. Tyson, J. M. H. Appleton and A. B. Idris, Analyst (London), 108 (1983) 153.
11 J. F. Tyson, C. E. Adeeyinwo, J. M. H. Appleton, S. R. Bysouth, A. B. Idris and L. L. Sarkissian, Analyst (London), 110 (1985) 487.
12 E. A. G. Zagatto, F. J. Krug, H. Bergamin F°, S. S. Jørgensen and B. F. Reis, Anal. Chim. Acta, 104 (1979) 279.

Analytica Chimica Acta, 179 (1986) 487—490
Elsevier Science Publishers B.V., Amsterdam — Printed in The Netherlands

Short Communication

PRECONCENTRATION AND DETERMINATION OF TRACE CHROMIUM(III) BY FLOW INJECTION/INDUCTIVELY-COUPLED PLASMA/ATOMIC EMISSION SPECTROMETRY

ALAN G. COX and CAMERON W. McLEOD*
Department of Chemistry, Sheffield City Polytechnic, Sheffield S1 1WB (Great Britain)
(Received 19th September 1985)

Summary. A manifold incorporating an activated alumina (basic form) minicolumn is used to preconcentrate chromium(III), which is then eluted with 2 M nitric acid for detection. Calibration is linear up to 1000 $\mu g\ l^{-1}$ Cr, and the limit of detection for a 10-ml sample is 0.05 $\mu g\ l^{-1}$. The determination of chromium(III) in human urine is discussed.

There has been considerable activity in the development of methodology for the determination and speciation of chromium in biological and environmental samples. Such studies have been prompted by the knowledge that chromium(VI) compounds are relatively toxic whereas chromium(III) is an essential trace element [1]. Of the numerous speciation procedures reported for chromium, the combined use of high-performance liquid chromatography (h.p.l.c.) and d.c. plasma/atomic emission spectrometry (d.c.p./a.e.s.) as described by Krull et al. [2] is an attractive approach offering detection in the $\mu g\ l^{-1}$ range, relatively rapid sample throughput and minimal sample pretreatment. The last factor is particularly important because prolonged sample manipulation may affect the chromium species [3].

The use of flow injection analysis (f.i.a.) for rapid speciation of chromium has been demonstrated [4, 5]. Recently a novel flow-injection manifold incorporating a minicolumn of activated alumina (acid form) was combined with inductively-coupled plasma (i.c.p./a.e.s.) for rapid sequential determination of chromium(III) and chromium(VI) in synthetic solutions and reference waters [6]. The acid-form alumina has a high affinity for anionic chromium(VI) but not for chromium(III), and so, by selective preconcentration of the former species, chromium in the $ng\ l^{-1}$ range could be detected. Clearly, this procedure would be inappropriate for the preconcentration of chromium(III) unless it was first oxidized to chromium(VI). Oxidation was not attempted in the present work; instead the possibility of utilising a minicolumn of basic alumina for preconcentration of chromium(III) was investigated. It was established that chromium(III) could be quantitatively retained on basic alumina, and quantitatively eluted therefrom. The development of a method for the determination of chromium(III) in human urine, based on such a preconcentration step in conjunction with i.c.p./a.e.s. is described below.

0003-2670/86/$03.50

Experimental

Reagents and materials. Standard solutions of chromium(III) were prepared daily by appropriate dilution of a stock solution (1000 $\mu g\ ml^{-1}$) of chromium(III) as nitrate (AnalaR; BDH Chemicals). Nitric acid (2 M) and ammonia solution (0.02 M) were prepared from the concentrated reagents (Aristar; BDH Chemicals). Urine standard reference material (NBS SRM 2670) was reconstituted in the prescribed manner and fresh urine samples were collected as required. A synthetic urine which simulated the major element concentrations in human urine [7] (200 $\mu g\ ml^{-1}$ Ca, 2000 $\mu g\ ml^{-1}$ K, 50 $\mu g\ ml^{-1}$ Mg, 2000 $\mu g\ ml^{-1}$ Na, 1000 $\mu g\ ml^{-1}$ P) was prepared from high-purity chemicals. All solutions were stored in precleaned polypropylene (Nalgene) containers and high-purity water was used in solution preparation. Activated alumina (BDH Chemicals; Brockman Grade I, basic form, particle size 75–120 μm) was used for column packing.

Instrumentation and procedure. A complete description of the instrumentation and operating procedures is given elsewhere [6]. Chromium(III) was retained on the minicolumn of activated alumina by injection of the sample (0.2–10 ml) into the manifold. A solution of 2 M nitric acid (200 μl) was injected to elute chromium for introduction to the plasma. Residual chromium was removed from the column by a further 200-μl injection of the nitric acid before further samples were processed. A carrier stream of 0.02 M ammonia was used to maintain column alkalinity. Chromium(III) recovery was checked by calculating the ratio of peak areas for a 200-μl injection of standard solution with and without the minicolumn in the manifold.

Results and discussion

Adsorption/desorption of chromium(III). The emission/time response corresponding to the adsorption and desorption of chromium(III) is given in Fig. 1. The alkalinity of the carrier stream, acidity of eluant and sample pH were critical variables that were studied in order to maximize chromium(III) recovery. For sample solutions in the pH range 2–7, quantitative retention of chromium(III) (200 μl injections of 0.5 $\mu g\ Cr\ ml^{-1}$) was obtained for carrier streams of 0.01, 0.02, 0.05 and 0.1 M ammonia. However, the ammonia concentration affected the subsequent elution by nitric acid. Ammonia concentrations $\geqslant 0.05$ M decreased elution efficiency, while at 0.01 M a significant time (ca. 5 min) was required to re-establish column basicity. Satisfactory performance was achieved using 0.02 M ammonia as carrier. Relatively high acidities were required for efficient elution of chromium(III). For example, a recovery of $>93\%$ was achieved by a 200-μl injection of 2 M nitric acid compared to 30% for 0.1 M nitric acid.

As shown in Table 1, appreciable breakthrough of chromium(III) was noted for samples of pH $\leqslant 1.5$, but retention was quantitative at pH 2–7. Based on these findings, 0.02 M ammonia and 2.0 M nitric acid were used in further work.

Analytical performance. A calibration graph prepared from the results of

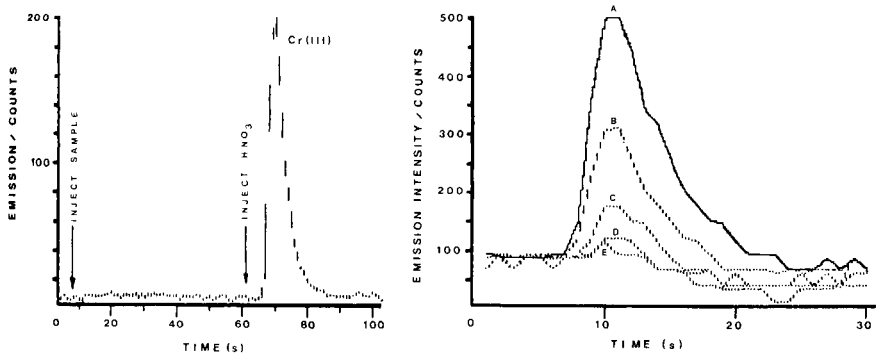

Fig. 1. Emission (267.72 nm)/time response for a 200-μl injection of chromium(III) solution (500 μg l^{-1}) and a 200-μl injection of 2 M nitric acid.

Fig. 2. Emission (267.72 nm)/time response for elution of chromium(III) (4 μg l^{-1}) with 200 μl of 2 M HNO_3. Injected sample volumes: (A) 10 ml; (B) 5 ml; (C) 2 ml; (D) 1 ml; (E) 0.2 ml.

triplicate 200-μl injections of chromium standard solutions (10, 20, 50, 100, 250, 500 and 1000 μg l^{-1}) had good linearity (correlation coefficient 0.99997). The limit of detection, calculated as twice the standard deviation of the background noise was 0.92 μg l^{-1} and the relative standard deviation (n = 10) at 10 μg l^{-1} was 12%. Figure 2 shows typical responses obtained for sample injections of 1, 2, 5 and 10 ml of chromium(III) solution (4 μg l^{-1}). The limit of detection for a 10-ml sample injection was 50 ng l^{-1}. The relative standard deviation (n = 10) at 10 μg l^{-1} for a 1-ml sample injection was 2.4%.

Determination of chromium(III) in human urine. Chromium(III) is present in human urine [8] and therefore the viability of the new procedure was tested on synthetic and human urine samples. Matrix effects associated with alkali and alkaline earth elements have been documented for the i.c.p./a.e.s. analysis of urine [9] and the possibility of similar interferences occurring in the present work was examined. Response curves generated for simple aqueous standard chromium(III) solutions and matrix-matched standard solutions (synthetic urine) revealed that chromium emission intensities were enhanced

TABLE 1

Effect of sample pH on retention of chromium(III)[a]

pH	6.9	6.3	4.0	2.1	1.5	1.0
Intensity[b]						
Unretained	0	0	0	0	2143	2158
Retained	2654	2514	2708	2501	170	80

[a]200 μl of a 500 μg l^{-1} Cr(III) solution was injected. Emission intensity measured at 267.72 nm with 18-s integration time. [b]Signal obtained after elution with 200 μl of 2 M HNO_3.

in the matrix-matched solutions. These results are in general agreement with the findings of Haas et al. [9] and are consistent with an increased background contribution as a result of stray light and ion/electron recombination emission. Emission intensity data obtained for the matrix elements during retention and elution showed that, for both synthetic and human urine, sodium and potassium were unretained on the minicolumn, while substantial retention occurred for calcium and magnesium. Subsequent injection of 200 μl of 2 M nitric acid ensured quantitative elution of the alkaline earth cations, as for chromium(III). These findings, although demonstrating the removal of sodium and potassium, indicated that stray light and ion/electron recombination emission arising from calcium and magnesium would not be eliminated. This conclusion was supported by wavelength scans done on samples (by continuous nebulisation) before and after passage through the alumina column. Acceptable analytical results were obtained for chromium(III) in the elevated urine standard reference material (certified value 0.085 ± 0.006; this work 0.079 ± 0.004 μg ml^{-1} for n = 10), but the present approach would be inappropriate for determinations at or below the μg l^{-1} level unless background correction was used.

REFERENCES

1 W. Mertz, Physiol. Rev., 49 (1969) 136.
2 I. S. Krull, K. W. Panaro and L. L. Gershman, J. Chromatogr. Sci., 21 (1983) 460.
3 T. M. Florence and G. E. Batley, CRC Crit. Rev. Anal. Chem., August (1980) 219.
4 T. P. Lynch, N. J. Kernoghan and J. N. Wilson, Analyst (London), 109 (1984) 839.
5 J. Carlos de Andrade, J. Cesar Rocha and N. Baccan, Analyst (London), 110 (1985) 197.
6 A. G. Cox, I. G. Cook and C. W. McLeod, Analyst (London), 110 (1985) 331.
7 D. L. Williams and V. Marks (Eds.), Scientific Foundations in Clinical Biochemistry, Heinemann Medical, New York, 2 (1983) 113.
8 Z. Mianzhi and R. M. Barnes, Spectrochim. Acta, 38B (1983) 259.
9 W. J. Haas, V. A. Fassel, F. Grabau IV, R. N. Kniseley and W. L. Sutherland, Adv. Chem. Ser., 172 (1979) 91.

Analytica Chimica Acta, 179 (1986) 491—496
Elsevier Science Publishers B.V., Amsterdam — Printed in The Netherlands

Short Communication

DETERMINATION OF LEAD IN GASOLINE BY A FLOW-INJECTION TECHNIQUE WITH ATOMIC ABSORPTION SPECTROMETRIC DETECTION

COLIN G. TAYLOR* and JOHN M. TREVASKIS[a]

Department of Chemistry and Biochemistry, The Polytechnic, Byrom Street, Liverpool L3 3AF (Great Britain)

(Received 31st July 1985)

Summary. The gasoline sample is treated with iodine and Aliquat-336 and diluted with 4-methylpentan-2-one; 100 μl is injected into a flowing acetone stream for aspiration into an atomic absorption spectrometer. Calibration is linear in the range 0—16 mg l^{-1} lead. Results for commercial gasoline samples agree well with those obtained by published titrimetric and atomic absorption methods. The precision for samples containing 300—400 mg l^{-1} lead is ± 1%; with increased recorder amplification, the limit of detection is 0.1 mg l^{-1} lead. The method is rapid and economic.

For sixty years, tetramethyllead (TML) and tetraethyllead (TEL) have been blended into gasoline for the purpose of suppressing uncontrolled ignition in the spark-ignited internal combustion engine. These additions have become recognised as possible sources of environmental pollution; in this country, the maximum permissible concentration of lead in gasoline is 0.4 g l^{-1}. In 1981, Government legislation was introduced fixing the maximum permissible concentration at 0.15 g l^{-1} by the end of 1985 [1]. In this communication, a rapid technique is described for the determination of lead in gasoline at present and possible future levels.

A wide variety of techniques has been used to quantify lead in gasoline. Among the classical procedures involving the use of iodine monochloride to convert the lead in TML and TEL to water-soluble dialkyllead halides, there is one in which lead is finally titrated with EDTA [2]; this procedure was used in the present work as a reference method. However, most of the rapid methods developed for determining lead in gasoline over the past twenty years are based on atomic absorption spectrometry (a.a.s.). In the first published a.a.s. method for lead in gasoline, samples were diluted with octane and aspirated into a total consumption burner with an oxyhydrogen flame [3]. The response obtained depends on the lead alkyl (the sensitivity for TML being greater than that for TEL by a factor of 2.5) [4], the composition of the gasoline [5], the diluent used [5, 6] and the position of the flame relative to the detector [6, 7].

[a]Present address: Dista Products Limited, Fleming Road, Liverpool, L24 9LN, Gt. Britain.

0003-2670/86/$03.50

Methods have been proposed for the determination of lead in gasoline by a.a.s. after reaction of the lead alkyls with aqueous iodine monochloride. In one such method, the aqueous extract is aspirated [8]; in another, the extracted lead is back-extracted into methyl isobutyl ketone (MIBK) which is then aspirated [9]. Both procedures are lengthy and the latter requires careful control of solution parameters. A faster measurement has been achieved by direct aspiration of the sample after dilution with MIBK and addition of excess of iodine [10]. In this procedure, the lead is converted to iodolead alkyls, which reduces, but does not eliminate, the effects of different alkyl groups in the gasoline. In a modification of the MIBK/iodine method, tricaprylmethylammonium chloride (Aliquat-336) is also added [11]. This method has been adopted, with minor changes, by the American Society for Testing and Materials [12]. All these a.a.s. methods require the use of organolead standards. This disadvantage can be overcome by using standard solutions containing lead chloride and Aliquat-336 in MIBK [13]. Such standards are stable over long periods of time and have been used for the evaluation of an a.a.s. method in an interlaboratory test programme [14].

Flow injection analysis (f.i.a.) in combination with a.a.s. was first used merely as a means to dilute the sample before introducing it into the flame [15]. It was quickly recognised that the flow-injection technique not only offered a convenient dilution step and reproducible transport of samples to the instrument, but also yielded rapid precise results [16]. Techniques of f.i.a./a.a.s. have been recently reviewed [17].

An f.i.a./a.a.s. method for the determination of lead in gasoline is described below; it is based on a previous reported a.a.s. method [13]. The organic lead is homogeneously oxidised with iodine, Aliquat-336 is added, the solution is diluted with MIBK and aliquots of the diluted solution are injected into a stream of acetone. Difficulties with the pumping of organic solvents in f.i.a. have been overcome by water-displacement of the solvent from a sealed bottle [18] or by using Solvaflex tubing [19]. In the present work, the water-miscible solvent is driven from a reservoir by nitrogen [20].

Experimental

Apparatus. A schematic diagram of the f.i.a./a.a.s. assembly is shown in Fig. 1. The cylinder was connected to the reservoir with polypropylene tubing (5 mm i.d.). The reservoir was connected with teflon tubing (0.6 mm i.d.) through the needle valve and the injection valve (Rheodyne Model 7125, 6-port with a 100-μl sample loop) to the spectrometer; the length of the tubing from injection valve to spectrometer was 18 cm. A Pye-Unicam SP6 spectrometer was used with a hollow-cathode lead lamp, a 10-cm slot burner, and a Philips PM 8521 pen recorder.

Reagents. Reagents were of analytical grade unless otherwise stated. The iodine solution in toluene was 3% (w/v). Tricaprylmethylammonium chloride (Aliquat-336; General Mills Chemicals, Minneapolis) was dissolved in MIBK to give 10% and 1% (w/v) solutions.

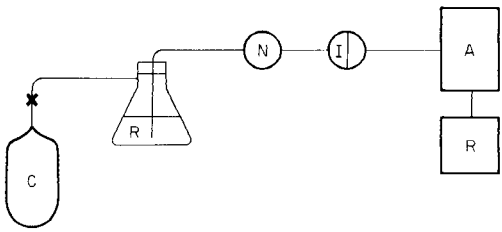

Fig. 1. The f.i.a./a.a.s. assembly for determination of lead in gasoline: C, nitrogen cylinder; R, acetone reservoir (500 ml Buchner flask); N, needle valve; I, injection valve; A, spectrometer; R, recorder.

Stock standard lead solution (1000 mg l^{-1}) was prepared by dissolving lead chloride (0.1342 g; dried at 105°C for 3 h) in Aliquat/MIBK (10%) and diluting with Aliquat/MIBK (10%) to 100.0 ml. This solution was stored in a tightly stoppered borosilicate glass bottle in the dark. Working lead standards (100 mg l^{-1}) were prepared daily by suitable dilution with Aliquat/MIBK (1%).

Procedure. Set the spectrometer parameters as follows: lamp current, 6 mA; wavelength, 283.3 nm; slit width, 0.5 nm; burner height, 8 cm; air/acetylene flow to give a fuel-lean oxidising flame. Adjust the aspiration rate into the spectrometer to about 3 ml min^{-1} by means of the bead control. Adjust the flow rate of acetone to about 4 ml min^{-1} by means of the reduction valve on the cylinder and the needle valve. Aspirate acetone into the spectrometer for at least 20 min before the first injection.

If necessary, allow the gasoline sample to attain ambient temperature (±2°C). Take a sample portion such that the final volume (50 ml) after treatment and dilution has a lead concentration between 4 and 16 mg l^{-1}. For a sample with an expected concentration of 200—400 mg l^{-1}, a 1.00-ml portion is appropriate. Add iodine/toluene reagent (0.2 ml) to the sample portion, swirl the mixture and allow it to stand for 2 min. Add Aliquat/MIBK (1%, 3 ml) to the mixture and dilute it with MIBK to 50.0 ml. Inject the solution into the acetone stream and measure the peak heights obtained. Evaluate the results from a calibration graph based on the following standards.

Preparation of standards. To portions of working standard lead solution (0.0, 2.0, 4.0, 6.0, 8.0 ml), add iodine/toluene reagent (0.2 ml) and a volume of iso-octane equal to the volume of the gasoline sample taken (in order to compensate for the matrix effect of hydrocarbons in the sample). Dilute the mixtures with MIBK to 50.0 ml to yield solutions containing 0—16 mg l^{-1} lead.

Results and discussion

The method was applied to the determination of the lead concentration in samples of four commercial brands of gasoline. Samples and standards were each injected in quadruplicate. Typical responses are displayed in Fig. 2. The

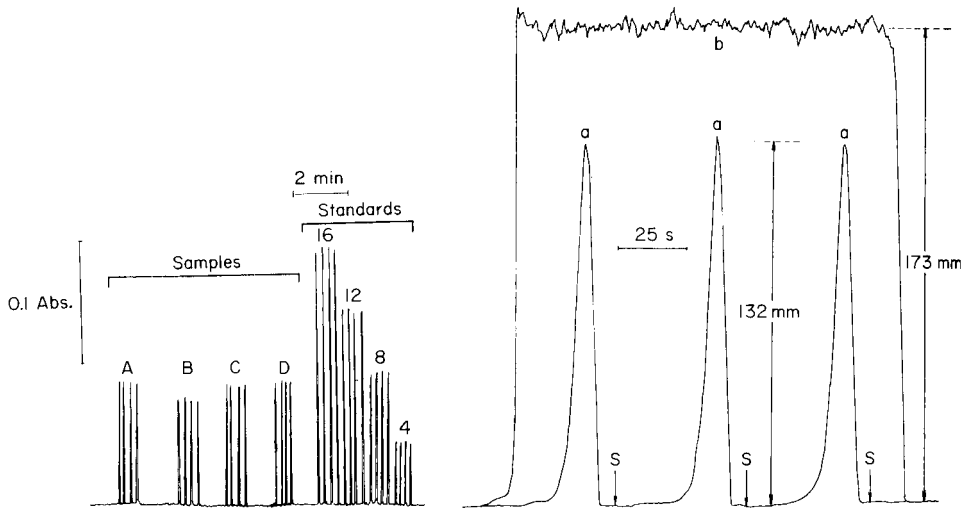

Fig. 2. Responses obtained from treated, diluted gasoline samples (A—D) and from standards, injected into an acetone stream. The numbers on the peaks are the concentrations (mg l^{-1}) of the lead standards.

Fig. 3. Recorder response for a 200 mg l^{-1} lead standard: (a) flow injection, 100 µl; (b) conventional aspiration.

calibration graph computed from the standard responses was linear (slope 5.73 ± 0.10 mm l mg^{-1}; intercept, 1.50 ± 1.05 mm; correlation coefficient 0.999; 100 mm = 0.22 absorbance). The values obtained for the concentrations of lead in the four samples are listed in Table 1; values obtained by an a.a.s. method [13] and a titrimetric method [2] are shown for comparison. Responses obtained in the f.i.a./a.a.s. procedure are highly reproducible, and the calibration is strictly linear. Values obtained by the three methods are not always in good agreement, but the agreement is similar to that obtained in interlaboratory analyses of gasolines [14]. In the interlaboratory study the results obtained for two of these samples were 384 ± 12 and 388 ± 13 mg l^{-1}. The precision of the results obtained from the classical titrimetric method is good. The results indicate overall that the concentration of lead in "two star" gasoline is not necessarily lower than that in "four star" gasoline.

In the proposed method, the carrier is propelled by gas pressure. The pressure system is cheaper, simpler and easier to maintain than a peristaltic pump; it is free from pulsing and therefore less prone to leaks at tube joints. Acetone was preferred to MIBK as the carrier for reasons of economy and convenience. In preliminary experiments, it was found necessary to aspirate MIBK into the flame for $\geqslant$1 h in order to achieve an acceptable baseline with acetone, this pre-aspiration period was only 20 min.

The usual rate of aspiration into the spectrometer (6.9 ml min^{-1}) was reduced to about 3 ml min^{-1} by moving the impinging bead in front of the

TABLE 1

The concentration of lead in samples of four brands of gasoline, determined by three different methods

Brand	Grade	Lead found (mg l^{-1})[a]		
		F.i.a./a.a.s.	A.a.s. [13]	Titrimetric [2]
A	Four star	379 ± 2	390 ± 4	379 ± 2
B	Two star	328 ± 4	350 ± 6	342 ± 1
C	Four star	366 ± 5	360 ± 5	333 ± 1
D	Two star	384 ± 2	370 ± 3	383 ± 1

[a]Mean and standard deviation (n = 4).

inlet jet of the atomisation chamber. This decreased the dispersion, which is directly proportional to flow rate. It is generally accepted that the flow rate of the carrier stream in f.i.a./a.a.s. should exceed the normal aspiration rate of the spectrometer [17]. Therefore in the present work the flow rate was adjusted to 4 ml min^{-1}. Dispersion was measured by injecting a lead standard under the conditions of the method and comparing the signal obtained with that from the same standard aspirated in the conventional mode. The responses, displayed in Fig. 3, indicate a dispersion (continuous signal/injection signal) of 1.3, i.e., the limited dispersion appropriate for samples which do not require reaction or dilution prior to detection [21]. It is evident from Fig. 3 that the precision of flow injection is superior to that of direct aspiration; also that the flow-injection response is more easily quantified than the continuous response, and that a sample throughput of at least 4 min^{-1} can be achieved.

By increasing the amplification of the chart recorder, clear responses can be obtained for 0.1 mg l^{-1} lead in the injected solution [22]. This concentration is the estimated limit of detection of the method. The limit of detection could be further improved by less dilution of samples or by injecting larger aliquots. The method should therefore be suitable for monitoring the lead content of the type of gasoline expected to be in general use by the end of the decade.

Modern flame spectrometric methods for the determination of lead in gasoline (TML or TEL or both) depend on the conversion of lead in the sample either to a single species, or to species which are indistinguishable in the analytical process. The conversion is said to proceed via the formation of dialkyllead iodides, which are stabilised by Aliquat-336, but the nature of the products resulting from the addition of Aliquat-336 does not appear to have been considered [14]. It is possible that an ion-association compound is formed, analogously to a reaction recently demonstrated for cadmium [23].

REFERENCES

1 Hawbury's Statutory Instruments, 17 (1984) 138. (The Motor Fuel (Lead Content of Petrol) Regulations, 1981, SI 1981/1523).
2 R. Moss and K. Campbell, J. Inst. Pet., London, 53 (1967) 89. Institute of Petroleum, IP 270/77, IP, London, 1977.
3 J. W. Robinson, Anal. Chim. Acta, 24 (1961) 451.
4 R. M. Dagnall and T. S. West, Talanta, 11 (1953) 64.
5 B. E. Buell, Special Problems in the Determination of Tetraethyllead in Gasoline by Flame Photometry, Symposium on Spectroscopy, Am. Soc. Testing Mater., (1959) 157.
6 B. E. Buell, Anal. Chem., 34 (1962) 635.
7 D. J. Trent, Perkin Elmer At. Absorpt. Newsl., 9 (1965) 348.
8 P. Johns, Spectrovision, 26 (1971) 16.
9 K. Campbell and J. M. Palmer, J. Inst. Pet., London, 58 (1972) 95.
10 M. Kashiki, S. Yamazoe and S. Oshima, Anal. Chim. Acta, 53 (1971) 95.
11 E. Lindemanis, Analytical Method No. M 113-71, E. I. du Pont, Wilmington.
12 American Society for Testing and Materials, D 3237/73, 1973.
13 T. J. Russell and K. Campbell, The Associated Octel Company Ltd., London, UK, 1977 (OP 77/1).
14 S. T. Holding and J. M. Palmer, Analyst (London), 109 (1984) 507.
15 E. A. G. Zagatto, F. J. Krug, F. H. Bergamin, S. S. Jorgensen and B. F. Reis, Anal Chim. Acta, 104 (1979) 279.
16 W. R. Wolf and K. K. Stewart, Anal. Chem., 51 (1979) 1201.
17 J. Tyson, Analyst (London), 110 (1985) 419.
18 L. Nord and B. Karlberg, Anal. Chim. Acta, 125 (1981) 199; 145 (1983) 151.
19 K. Backstrom, L.-G. Danielsson and L. Nord, Analyst (London), 109 (1984) 323.
20 S. Olsen, L. C. Pesseda, J. Růžička and E. H. Hansen, Analyst (London), 108 (1983) 905.
21 J. Růžička and E. H. Hansen, Flow Injection Analysis, Wiley-Interscience, New York U.S.A., 1981.
22 J. M. Trevaskis, M.Sc. Project Report, Liverpool Polytechnic, 1984.
23 K. Grudpan and C. G. Taylor, Analyst (London), 109 (1984) 585.

Analytica Chimica Acta, 179 (1986) 497—502
Elsevier Science Publishers B.V., Amsterdam — Printed in The Netherlands

Short Communication

DETERMINATION OF SOME ORGANOPHOSPHORUS INSECTICIDES BY FLOW INJECTION WITH A MOLECULAR EMISSION CAVITY DETECTOR

J. L. BURGUERA* and M. BURGUERA

Departamento de Química, Facultad de Ciencias, Universidad de Los Andes, Apartado 542, Mérida 5101-A (Venezuela)

(Received 18th April 1985)

Summary. The determination is based on the measurement of HPO emission at 528 nm in a H_2/N_2 flame. Organophosphorus insecticides are extracted with hexane/dichloromethane at pH < 7, the solvent is evaporated, and the residue is dissolved in ethanol. Up to 2 μl of the solution is injected into the flow system. Mixtures of dicrotophos, dimethoate, malathion and parathion were determined.

The insecticides dicrotophos (3-hydroxy-*N,N*-dimethyl-*cis*-crotonamide dimethyl phosphate), dimethoate (*O,O*-dimethyl-*S*-(*N*-methylcarbamoylmethylphosphorodithioate), malathion (*O,O*-dimethyl-*S*-(1,2-dicarboxyethylphosphorodithioate) and parathion (*O,O*-diethyl-*O*-nitrophenylphosphorothionate) are widely used. They are effective against many species of insects and mites [1]. Parathion and dicrotophos are highly toxic with acute oral LD_{50} to the rat of ca. 10 and 22—75 mg kg^{-1}, respectively; dimethoate and malathion are of moderate toxicity, with acute oral LD_{50} to the rat of ca. 500 and 2000 mg kg^{-1}, respectively [2, 3]. Relatively few methods have been proposed for the confirmation and determination of such compounds. Spectrophotometry, thin-layer chromatography, gas chromatography with a phosphorus-specific flame ionization detector and gas-liquid chromatography using hydrolysis or methylation techniques are preferred for determining dicrotophos [3, 4], dimethoate [4—6], malathion [7—9] and parathion [10—12] in waters, fruits, vegetables and other agricultural crops.

This communication describes a simple application of flow injection analysis (f.i.a.) combined with molecular emission cavity analysis (m.e.c.a.) to the determination of dicrotophos, dimethoate, malathion and parathion in water. Previously, this combination of techniques has been used for the determination of sulphur anions [13] and some organophosphorus compounds [14].

Experimental

Apparatus and reagents. The flow-injection m.e.c.a. system, tubing, connectors, injector, pump, spectrometer and recorder were the same as those

0003-2670/86/$03.50

used earlier [13]. The water-cooled cavity was constructed from a brass rod, and it had a side tube to connect the flow system to the centre of the rear wall of the cavity as previously described [13, 15]. However, the side tube also had a similar water-cooling system (Fig. 1), which was used in order to improve the resolution of the insecticide mixtures studied, as described below.

Solvents and other reagents were analytical grade (BDH). Deionized, double-distilled water was used throughout. Varian dimethoate (DMe), malathion (MAL) and parathion (PAR), and Supelco dicrotophos (DCT) standards were used.

All solutions were prepared in acid-washed glassware. Ethanol solutions of accurately known concentrations (1 mg P/10 ml) of each insecticide and of mixtures of them were prepared. Solutions containing lower concentrations of insecticides were prepared by appropriate dilution with ethanol. Preliminary tests and optimization of the experimental parameters were done with a MAL solution containing 20 ng P μl^{-1}.

Extraction and emission measurement procedures for organophosphorus insecticides. The extraction procedure was adapted from those described by Pressley and Longbottom [12] and Fabrini et al. [16]. A 10-ml portion of 15% dichloromethane in hexane was added to 100 ml of water containing organophosphorus insecticides at pH < 7. The mixture was shaken vigorously for 1 min in a 150-ml separatory funnel, and the organic phase was collected. The organic extract was dried over anhydrous sodium sulphate, and the solvent evaporated under reduced pressure. The residue was dissolved in 1 ml of ethanol and kept in a teflon-lined silicone rubber septum vial until it was used for injection.

The procedure for the measurement of the HPO emission in the proposed system was essentially the same as described previously [13, 14]. The intensity of the green HPO emission at 528 nm, contained within the cavity,

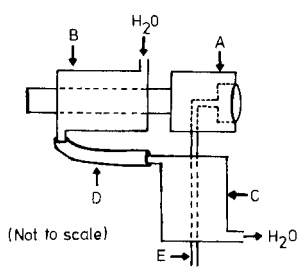

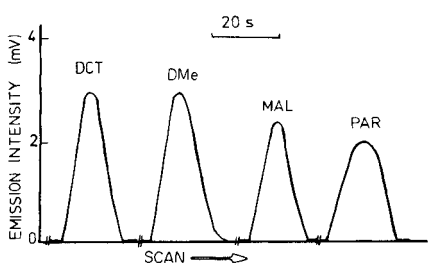

Fig. 1. Schematic diagram of the cavity system: (A) cavity; (B, C) water cooling systems for the back and the side arm of the cavity, respectively; (D) polyethylene tubing connecting the water cooling systems; (E) stainless steel tube connecting the cavity to the flow system.

Fig. 2. Recorded peaks for the insecticides (20 ng P for each compound; conditions as in the text).

was recorded as a function of time. All emission values were based on peak-height measurements.

Results and discussion

Optimization of analytical parameters. The parameters governing f.i.a. (sample volume, carrier flow rate, dispersion tube length and internal diameter) and m.e.c.a. (flame composition and cavity position) were optimized in order to obtain the highest peak with least tailing. The optimal parameters were all the same as found previously [14], except for the injected volume, which in this case was 2 μl, and the water cooling flow rate, which is described below. Typical peaks are shown in Fig. 2.

The effect of cooling the cavity. As the cavity was continuously situated within the flame, the water cooling flow rate was found to affect the time(s) of peak response (t_{app}) from insecticides as single compounds or as a mixture. When the cavity was used without water cooling, a similar single peak response was obtained regardless of the injected insecticide, whether present as a single compound or as a mixture (Fig. 3). The sensitivity for all the insecticides decreased when the cavity was cooled. However, when the temperature of the cavity and of the side tube (through which the carrier solution flowed, Fig. 1) was controlled by circulating water, it was possible to determine simultaneously ternary mixtures of the insecticides (Fig. 4), because resolved signals for each compound were obtained at different t_{app} values (Table 1). If the water flow rate was decreased the peaks were only partially resolved. Quaternary mixtures could not completely be resolved (Fig. 4), mainly because of the unresolved peaks of DCT and DMe. In order to achieve good resolution of nanogram amounts of organophosphorus insecticides, rigorous control of the cavity temperature is essential.

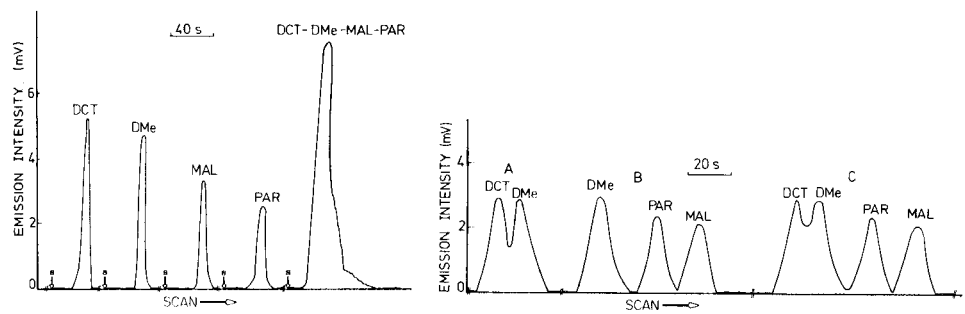

Fig. 3. Recorded peaks from the insecticides obtained without cooling the cavity: (S) sample injection. (Conditions as in Fig. 2.)

Fig. 4. Responses from different insecticide mixtures obtained with a cooled cavity: (A) mixture of DCT and DMe; (B) mixture of DMe, MAL and PAR; (C) mixture of all four insecticides. (Conditions as in Fig. 2.)

TABLE 1

Effect of cooling water flow rate on the time of appearance (t_{app}) of the peak response

Water flow rate (ml min^{-1})	Appearance time (s)			
	DCT	DMe	PAR	MAL
0	36	36	36	36
20	58	60	62	72
100	74	78	91	96
160	85	95	120	140

Solvent evaporation. Solvent effects have been observed in flame studies of phosphorus compounds when aspiration [17] and m.e.c.a. [18, 19] systems are used. Particularly, the addition of ethanol decreased the HPO emission in a nitrogen-diluted hydrogen diffusion flame [20]. In the present case, emission from ethanol was not detected at 528 nm, but was just detected at 431.5 nm; this CH emission occurs in the flame above the cavity and is thus largely out of view of the detector [19]. The t_{app} value for ethanol itself (at 431.5 nm) was ca. 20 s, regardless of the flow rate of the cooling water. This rapid evaporation of the solvent occurred well before the t_{app} values for the insecticides, so any removal of hydrogen atoms by the organic fragments originating from the solvent [19] is complete well before the formation of the HPO emitting species. Therefore, the ethanol used for preparation of the solutions did not affect the HPO intensity from the insecticides.

Calibration. Calibration graphs were prepared for all the compounds investigated. The results are summarized in Table 2, where the sensitivities given are the slopes of the linear calibration graphs. The procedure described can be used to determine the most sensitive compounds (DCT, DMe) in the range 5—100 ng of phosphorus and the less sensitive compounds (PAR, MAL) in the range 10—120 ng of phosphorus. These sensitivities can be directly linked with their appearance times (Table 1) and resistence to thermal breakdown. For ternary mixtures (DCT-PAR-MAL or DMe-PAR-MAL) where peaks are resolved, there is no effect of one component on the peak height of the other compound, and the calibration graphs coincide with those obtained for single substances.

Recovery and precision. Recoveries were studied by adding known quantities of each insecticide to water. The insecticide was extracted as described above, and the results were compared with those obtained from ethanolic standard solutions. The results (Table 3) indicate good recovery for the phosphorothioate (PAR) and phosphorodithioates (MAL, DMe), but a relatively low recovery for the organophosphate insecticide (DCT). In the procedure a correction of 26.6, 1.9, 3.5 and 3.6% for the determination of DCT, DMe, MAL and PAR, respectively, is required because of the incomplete recovery.

TABLE 2

Calibration characteristics for various organophosphorus insecticides

Compound	t_{app} (s)	Linear range (ng P)	Sensitivity (mV/ng P)[a]	Detection limit (ng P)[b]
DCT	85	5—100	1.75	0.8
DMe	95	5—100	1.65	1.2
MAL	140	10—120	1.50	2.0
PAR	120	10—130	1.40	2.5

[a]Slope of calibration graph. [b]2σ value. Sample volume, 2 μl; water-cooling flow rate, 160 ml min^{-1}; other conditions were as described in the text.

TABLE 3

Results of recovery study of insecticides (50 ng P) added to water

Insecticide	P found (ng)	Recovery (%)
Dicrotophos (DCT)	36.7 ± 0.4	73.4
Dimethoate (DMe)	49.0 ± 0.2	98.1
Malathion (MAL)	48.3 ± 0.2	96.5
Parathion (PAR)	48.2 ± 0.2	96.4

[a]Mean and standard error for four injections.

The method showed good reproducibility with relative standard deviations of 3.4, 2.8, 2.5 and 2.8% for 20 ng P in DCT, DMe, MAL and PAR, respectively (8 determinations).

The flow-injection m.e.c.a. system, therefore, was suitable for the determination of some mixtures of organophosphorus insecticides with a single injection, with modest reagent consumption and simple instrumentation. The method should be applicable to the confirmation and determination of such compounds at $\mu g\ l^{-1}$ levels in water.

REFERENCES

1 J. Sherma and G. Zweig, Anal. Chem., 55 (1983) 57R.
2 F. L. McEwen and G. R. Stephenson, The Use and Significance of Pesticides in the Environment, Chap. 10, Insecticides and their Use, Wiley, New York, 1979, pp. 155—216.
3 A. S. Y. Chan, B. K. Afghan and J. W. Robinson (Eds.), Analysis of Pesticides in Water, Vol. 1, Significance, Principles, Techniques and Chemistry of Pesticides, CRC Press, Boca Raton, 1982.
4 W. Horwitz (Ed.), Official Methods of Analysis of the Association of Official Analytical Chemists, 13th edn., 1979, pp. 466—496.
5 J. Askew, J. H. Růžička and B. B. Wheals, J. Chromatogr., 41 (1969) 180.
6 I. P. Nesterova, Zh. Anal. Khim., 32 (1977) 1790.

7 E. R. Clark and I. A. Qazi, Analyst (London), 104 (1979) 1129.
8 J. Singh and M. R. Lapointe, J. Assoc. Off. Anal. Chem., 57 (1974) 1285.
9 L. J. Carson, J. Assoc. Off. Anal. Chem., 64 (1981) 714.
10 H. Breuer, J. Chromatogr., 243 (1982) 183.
11 M. A. Forbes, B. F. Wilson, R. Greenhalgh and W. P. Cochrane, Bull. Environ. Cont. Toxicol., 13 (1974) 1272.
12 T. A. Pressley and J. E. Longbottom, Gov. Rep. Announce Index (U.S.), 82 (1982) 1544.
13 J. L. Burguera and M. Burguera, Anal. Chim. Acta, 157 (1984) 177.
14 J. L. Burguera, M. Burguera and D. Flores, Anal. Chim. Acta, 170 (1985) 331.
15 M. Burguera and J. L. Burguera, Anal. Chim. Acta, 153 (1983) 53.
16 R. Fabrini, T. La Noce, V. Leoni, A. Liberatori, M. Riva and C. Vannucchi, Metodi Anal. Acque, 1 (1982) 22.
17 A. Syty and J. A. Dean, Appl. Opt., 7 (1968) 1331.
18 R. Belcher, S. L. Bogdanski, O. Osibanjo and A. Townshend, Anal. Chim. Acta, 84 (1976) 1.
19 R. Belcher, S. L. Bogdanski, M. Burguera, E. Henden and A. Townshend, Anal. Chim. Acta, 100 (1978) 515.
20 R. M. Dagnall, K. C. Thompson and T. S. West, Analyst (London), 93 (1968) 72.

Analytica Chimica Acta, 179 (1986) 503—508
Elsevier Science Publishers B.V., Amsterdam — Printed in The Netherlands

Short Communication

SEQUENTIAL FLOW-INJECTION DETERMINATIONS OF CALCIUM AND MAGNESIUM IN WATERS

J. ALONSO and J. BARTROLI

Department de Química Analítica, Facultad de Ciencias, Universitat Autònoma de Barcelona, Bellaterra, Barcelona (Spain)

J. L. F. C. LIMA and A. A. S. C. MACHADO*

Departamento de Química, Faculdade de Ciências, Universidade do Porto, 4000 Porto (Portugal)

(Received 24th July 1985)

Summary. A tubular PVC membrane electrode for calcium without inner reference solution and a device for location of the reference electrode are described. In the flow-injection system, calcium is determined potentiometrically and then magnesium is determined by atomic absorption spectrometry. The electrode provides linear response to calcium in the range 5×10^{-5}—10^{-1} M. On-line dilution of the sample allows magnesium determination in the range 0—10 mg l^{-1}. Flow rates between 3 and 6 ml min^{-1} are possible. The sampling frequency is 60—90 h^{-1}.

Flow injection analysis (f.i.a.) has great versatility and most methods of detection can be used in it. There is increasing interest in the simultaneous or sequential determination of several species by f.i.a.; at least in principle, sequential use of detectors can provide simpler systems than other possibilities for determining several species together [1]. Various procedures involving simultaneous or sequential potentiometric detection have been reviewed [1]. In more recent work on sequential determinations by f.i.a., a spectrophotometric measurement is followed by atomic absorption spectrometry (a.a.s.) [2—4]. For obvious reasons, an a.a.s. detector must be placed last in any sequence of detectors. When potentiometric sensors are used in an intermediate position, a configuration is needed which does not alter the hydrodynamic flow characteristics.

Recently, a simple procedure was described for the construction of a solid-state tubular flow-through electrode with PVC membranes [5]. The use of this configuration in f.i.a. was tested with a nitrate sensor and it was found not to introduce any significant distortion in the flow [5]. This suggested its suitability for use in a sequential detector system. To test its behaviour, a calcium electrode was constructed and used, together with a.a.s., in a simple flow-injection procedure for routine determinations of calcium and magnesium in waters. Besides the tubular electrode, the potentiometric assembly used here includes a new support design for the reference electrode. Placing

0003-2670/86/$03.50

the reference electrode in a complete by-pass loop [6] was found to be a source of instability of the baseline, probably because of an irreproducible splitting ratio between the by-pass and the injection valve channel [7]. A device specially designed for locating the reference electrode in a closed branch of the main channel, connected obliquely near the active electrode, was found to give better reproducibility of the baseline.

Experimental

Apparatus. The flow systems presented in Fig. 1 were used in development of the method. The equipment included Gilson Minipuls-2 peristaltic pumps, a Rheodyne 5020 injection valve, teflon tubing (1 mm i.d.) for connections, stainless steel tubing (1 mm i.d.) for constructing the grounding electrode, a tubular flow-through calcium electrode constructed as previously described [5], a device for the location of the reference electrode (see detail in Fig. 2), and a double-junction reference electrode (Orion 90-02-00). Potentiometric measurements were made with a Radiometer PHM-64 millivoltmeter connected to a REA-100 interface and a Servograph REC-61 recorder. For a.a.s. measurements, an Instrumentation Laboratory 551 spectrometer was used with an air/acetylene flame and a conventional hollow-cathode lamp.

Reagents. All chemicals used were of analytical-reagent grade. Standard solutions of calcium and magnesium were prepared from stock standard solutions of calcium chloride (Radiometer) and magnesium chloride (prepared from the solid) by sequential dilution with redistilled water.

For the preparation of the electrode membrane, the chemicals used were dioctylphenylphosphonate (Ventron), tetrahydrofuran (Merck) and poly(vinyl chloride) (Fluka). Epoxy conductive resin was obtained from Epoxy Technology (P.O. Box 567, Billerica, MA 01821).

Construction of the tubular calcium electrode. The electrode was assembled as previously described [5]. Basically, the PVC membrane is formed by

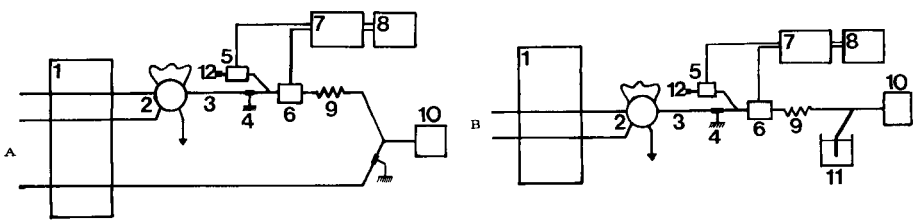

Fig. 1. Flow diagrams: (A) system with dilution channel; (B) system with compensation channel. (1) Pump (flow rates: A, main channel, 3.0 ml min^{-1}; dilution channel, 3.2 ml min^{-1}; B, 3.6 ml min^{-1}); (2) injection valve; (3) mixing coil (L = 30 cm, from injection valve to tubular electrode); (4) grounding electrode, placed as close as possible to the potentiometric cell; (5) reference electrode support device (see Fig. 2); (6) tubular calcium electrode; (7) potentiometer; (8) recorder; (9) dilution coil (L = 200 cm); (10) atomic absorption spectrometer; (11) water reservoir for compensation; (12) closed end of tube connected to one of the channels of (5).

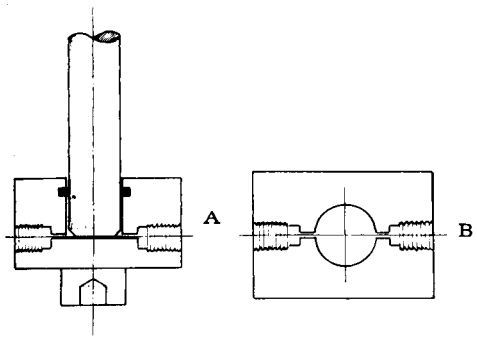

Fig. 2. Reference electrode support: (A) side view; (B) top view. For details, see text.

evaporating a mixture of calcium bis[di-(4-(1,1,3,3-tetramethylbutyl)phenyl)-phosphate (0.025 g), dioctylphenylphosphonate (0.36 g) and PVC (0.17 g) in 6 ml of tetrahydrofuran, on the inner surface of a hole drilled through a block of conductive epoxy. Electrical contact is established by connecting a shielded cable to the block.

Reference electrode support. The device for locating the reference electrode is outlined in Fig. 2. A cylindrical hole (about 1.5 cm deep) of suitable diameter for insertion of the electrode was machined in a block of perspex and an O-ring was fitted into it to hold the electrode tightly without leakage. Two channels were drilled perpendicularly to the axis of the cylinder to establish close contact of the liquid with the tip of the electrode, and screw threads for assembling the connectors of the flow systems were machined as shown in Fig. 2.

In the present assembly, one of the channels is connected by a Y-joint to the tubular electrode, the connecting tube being as short as possible. The tube connected to the second channel is closed after the device, with the electrode in place, has been filled with carrier solution. In Fig. 1, the device is shown placed in front of the tubular electrode but it may also be used after it.

Results and discussion

Potentiometric flow system. The calcium flow-through electrode with the sensor/mediator system comprising calcium bis[di(4-(1,1,3,3-tetramethylbutyl)phenyl)phosphate] and dioctylphenylphosphonate was chosen because of its superior selectivity towards calcium ions [8]. Moreover, it has been recently used in constructing a tubular flow-through electrode with internal reference solution [9] which is of more complex design than the present one. The calcium-selective and reference electrodes were inserted into the two flow-injection systems shown in Fig. 1. The systems included a grounding electrode placed as close as possible to the electrodes to eliminate parasitic currents generated by the peristaltic pump. The carrier solution was 0.15 M sodium chloride containing 10^{-6} M calcium chloride to stabilize the baseline.

The behaviour of the potentiometric flow cell was studied as before [5]. It was found that the use of an injection volume of 100 μl and a tube length of 30 cm allowed the flow rate to be varied over a wide range (3—6 ml min^{-1}) without affecting the quality of the electrode response. This is very convenient for versatility in the subsequent measurement of magnesium by a.a.s.

Under these conditions, the electrode gave Nernstian response between 5×10^{-5} and 10^{-1} M calcium ion with a slope of 29 ± 1 mV. Figure 3 shows a typical output and calibration plot. The precision of response of the electrode was tested by repeating the calibration of one of the units eight times during 5 h; the relative standard deviations from the mean peak heights for 10^{-2} and 10^{-3} M calcium ion were 1.5%, and 3.5% for 5×10^{-5} M.

Determination of magnesium by a.a.s. The configuration of the electrode used for calcium determination leaves the sample zone unaffected and allows direct determination of magnesium by a.a.s. As the range of linear response in this determination (in batch conditions) is narrow (0.1—0.4 mg l^{-1}), two configurations (Fig. 1, A and B) were used to allow for sample dilution within the system. System A included a dilution channel; system B included a compensation channel connected by a T-piece to the nebulizer, through which water was aspirated to make up the normal aspiration flow (about 6 ml min^{-1}) of the nebulizer. With both of these systems, a linear range of 0—10 mg l^{-1} magnesium was achieved.

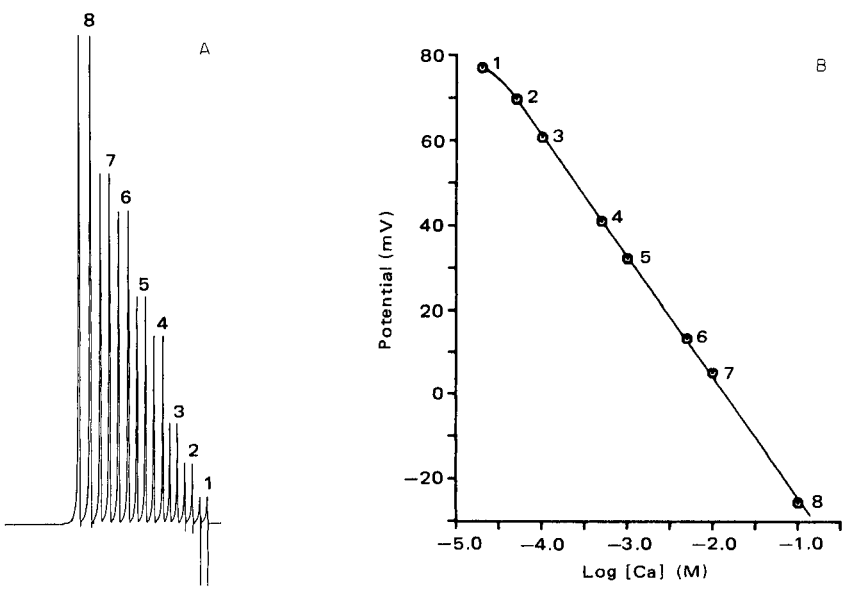

Fig. 3. Calibration of the flow-through tubular electrode: (A) recorder output; (B) calibration plot. Conditions: flow rate, 6 ml min^{-1}; other parameters as in the text. Ca^{2+} concentrations: (1) 2×10^{-5} M; (2) 5×10^{-5} M; (3) 1×10^{-4} M; (4) 5×10^{-4} M; (5) 1×10^{-3} M; (6) 5×10^{-3} M; (7) 1×10^{-2} M; (8) 1×10^{-1} M.

Determination of calcium and magnesium in waters. Both systems were tested for the measurement of calcium and magnesium in various water samples (from wells, rivers, waste waters). Results are presented in Table 1. The standard control procedures were potentiometric titration with EDTA for calcium and direct a.a.s. for magnesium. As is seen from Table 1, the results obtained by either of the flow-injection procedures compare well with those obtained by the control methods; deviations in most results are less than 5% and only a few samples show differences greater than 10%. The total composition of the samples was not monitored, so that effects of abnormal components may contribute to differences in some cases. Both the dilution and compensation procedures appear to be equally acceptable. Linear regression analyses of the data are presented in Table 2.

The potentiometric measurement limits the sampling rate; nevertheless, a rate of 60—90 h^{-1}, depending on the calcium concentration, was obtained.

Simultaneous determinations of calcium and magnesium by a different kinetic method based on dissociation of the (2,2,1)-cryptates has been proposed [10], but the present method appears to be more attractive for routine work, particularly as accurate determination of magnesium is possible even when the magnesium/calcium ratio is small.

In conclusion, the systems allow the determination of calcium and magnesium with results comparable to those of established methods, with a far superior sampling frequency. Work on the use of two potentiometric tubular electrodes in sequence together with other detectors is in progress.

TABLE 1

Results for water samples[a]

Sample	Metal ion content found ($\times 10^{-4}$ M)					
	Standard method[b]		Compensation configuration		Dilution configuration	
	Ca(II)	Mg(II)	Ca(II)	Mg(II)	Ca(II)	Mg(II)
1	1.38	0.543	1.43	0.49	1.34	0.60
2	6.23	1.42	6.20	1.51	6.30	1.53
3	3.60	2.40	3.71	2.39	3.66	2.47
4	21.5	0.159	21.5	0.23	22.1	0.164
5	8.97	2.95	8.94	2.95	8.32	2.80
6	0.66	0.122	0.664	0.107	0.675	0.118
7	2.57	2.07	2.77	2.18	2.97	2.18
8	5.37	1.90	—	—	5.34	2.12
9	1.28	0.115	—	—	1.04	0.115
10	3.50	1.59	—	—	3.66	1.69
11	7.88	3.48	—	—	8.46	3.54
12	7.80	1.54	—	—	8.11	1.54

[a]Averages of 2—4 determinations are given. [b]See text.

TABLE 2

Linear regression analysis of the results of the flow-injection method vs. standard methods

Ion	Slope	Intercept	Correlation coefficient
Dilution method (12 samples)			
Calcium(II)	1.024	4×10^{-6}	0.997
Magnesium(II)	1.003	4×10^{-6}	0.994
Compensation method (7 samples)			
Calcium(II)	0.995	7×10^{-6}	0.999
Magnesium(II)	1.006	2×10^{-6}	0.997

Financial support for the exchange of scientists received under a Portuguese-Spanish Integrated Action grant is gratefully acknowledged. We also thank Dr. J. D. R. Thomas and Dr. G. J. Moody (UWIST, Cardiff, Wales) for a sample of the calcium sensor and for discussions made possible by NATO grant no. 069/84.

REFERENCES

1 M. Valcárcel and M. D. Luque de Castro, Analyst (London), 109 (1984) 413 (and references therein).
2 T. P. Lynch, M. J. Kernoghan and J. M. Wilson, Analyst (London), 109 (1984) 839, 843.
3 A. Rios, M. D. Luque de Castro and M. Valcárcel, Analyst (London), 109 (1984) 1487.
4 J. L. Burguera and M. Burguera, Anal. Chim. Acta, 161 (1984) 375.
5 S. Alegret, J. Alonso, J. Bartroli, J. M. Paulis, J. L. F. C. Lima and A. A. S. C. Machado, Anal. Chim. Acta, 164 (1984) 147.
6 A. U. Ramsing, J. Janata, J. Růžička and M. Levy, Anal. Chim. Acta, 118 (1980) 45.
7 A. T. Faizullah and A. Townshend, Anal. Chim. Acta, 167 (1985) 225.
8 G. J. Moody and J. D. R. Thomas, Ion Selective Electrode Rev., 1 (1979) 3.
9 A. J. Frend, G. J. Moody and J. D. R. Thomas, Analyst (London), 108 (1983) 1357.
10 D. Espersen and A. Jensen, Anal. Chim. Acta, 108 (1979) 241.

Analytica Chimica Acta, 179 (1986) 509—514
Elsevier Science Publishers B.V., Amsterdam — Printed in The Netherlands

Short Communication

PRECONCENTRATION OF COPPER(II) ON IMMOBILIZED 8-QUINOLINOL IN A FLOW-INJECTION SYSTEM WITH AN ION-SELECTIVE ELECTRODE DETECTOR

LARS RISINGER

Department of Analytical Chemistry, University of Lund, P.O. Box 124, S-221 00 Lund (Sweden)

(Received 4th September 1985)

Summary. A column containing 8-quinolinol, immobilized on porous glass, is used for preconcentration and medium exchange in a flow-injection system with a copper ion-selective electrode detector. The metal ions are bound to the chelating ion exchanger while the anions and inert sample components pass to waste without contacting the electrode. Acid is then injected to elute the ions into a neutralizing buffer passing the electrode. Matrix effects are thus reduced because all measurements are made in the same buffer. The detection limits are 10^{-7} and 3×10^{-8} M copper(II) for sample volumes of 5 and 25 ml, respectively. The maximum throughput is 12 and 5 samples h^{-1} for the two stated injection volumes.

Ion-selective electrodes can seldom be used to monitor metal ion concentrations below 10^{-6} M and very long equilibrium times are required in the few cases where it is possible. Blaedel and Dinwiddie [1] were thus able to measure the Cu(II) ion concentration down to 10^{-9} M and with a Nernstian slope down to 10^{-8} M. The required equilibrium times were 48 and 6 h, respectively. It should be possible to extend the range downward by adding a preconcentration step, but little work has been done in this direction because most preconcentration methods are time-consuming themselves. The recently described methods for metal enrichment on chelating exchangers [2, 3] in a flow system seemed promising and work was therefore started to adapt the method to measurements with ion-selective electrodes. Potentiometric detection was used in early papers on flow injection analysis (f.i.a.) [4—6] and more recently for monitoring copper ion [7].

The performance of a flow-injection system is enhanced by a low dead volume and a fast response of the detector. It has been shown that the response time of a copper ion-selective electrode can be shortened by polishing the surface and treating it with silicone oil [8, 9]. The response time also depends on the concentrations and the ionic strength [10]. Several flow-through cells with low dead volumes have been described in the literature [4, 7, 11].

0003-2670/86/$03.50

Experimental

Flow-injection manifold. The manifold (Fig. 1) provides for sample introduction by a valve (3) which is activated for a certain time. The sample is pumped through channel B and out to waste with valve 3 in the stand-by position. Similarly, a carrier, which was water, is pumped through channel C and out into the system at D. Sample solution enters the system at D on activation of valve 3; this is equivalent to the introduction of a plug-formed sample at D. The sample volume is thus obtained by multiplying the flow rate by the time of valve activation. In some experiments, valve 3 was replaced by a loop injector with fixed volume. The output at D is mixed with a buffer pumped through channel E in order to obtain the pH suitable for metal ion preconcentration on the chelating ion exchanger (III). The output from the latter is diverted to waste through valve 5.

The metal ions are eluted by injection of 300 μl of 0.5 M nitric acid kept in a loop of valve 4. Valve 5 is switched on simultaneously with valve 4 so that the flow now is directed through the ion-selective electrode (ISE). The electrode response depends on both the pH and the ionic strength and it is therefore necessary to keep these parameters as constant as possible during the switching. A strong acetate buffer (1 M sodium acetate) of pH 5.0, was pumped through channel F to the ISE. It was mixed with 0.5 M acid when valve 5 was opened so that the pH decreased to 4.2 at the peak. The ionic strength of the acid, 0.5, was almost equal to that of the diluted buffer (0.1 M sodium acetate/1 M sodium nitrate) pumped through channel E.

A flow-through cell of the wall-jet type was made essentially as described by Thompson and Rechnitz [11]. The solution was directed from below towards the center of a copper ion-selective electrode (Orion Research, Model 94-29A). The outflow was through 8 holes, close to the circumference of the electrode, and passed into a chamber containing a calomel reference

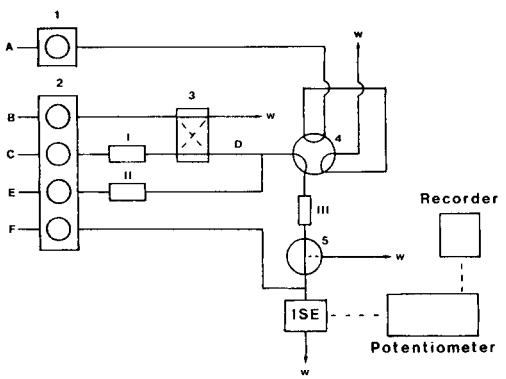

Fig. 1. Flow-injection system: 1, 2, peristaltic pumps; A, 0.5 M HNO_3; B, sample, 2.5 ml min^{-1}; C, water, 0.5 ml min^{-1}; E, 1 M $NaNO_3$/0.1 M sodium acetate, pH 5.4, 0.5 ml min^{-1}; F, 1 M sodium acetate/2 × 10^{-7} M Cu^{2+}, pH 5.0, 1.0 ml min^{-1}; 3, 4 and 5, valves; ISE, copper ion-selective electrode; w, waste; I and II, 2.3 ml chelating ion exchangers for purification; III, 100 μl chelating ion exchanger for metal ion preconcentration.

electrode (Radiometer, model K-401). The other components were a 4-channel (Gilson Minipuls 2) and a one-channel (Alitea, model 4) peristaltic pump, one 6-way rotary valve (Altex, series 202) and two pneumatically operated reciprocating valves (Cheminert LDC/Milton Roy). The connections were made of 0.5 or 0.3 mm i.d. teflon tubing.

Chelating ion-exchangers. The columns were made from three different preparations of 8-quinolinol immobilized on porous glass. Column A (250 μl) was filled with a commercial chelating ion exchanger (Pierce Chemical Co.; CPG 10, particle size 125—177 μm, pore size 50 nm; cat. no. 23750). Two columns (2.3 ml; I and II in Fig. 1) which were used for on-line removal of trace metals from the carrier and the buffer, were also filled with this material. Column B (100 μl) was made by azo-immobilization as described by Hill [12] on porous glass (CPG 10, particle size 80—125 μm, pore size 70 nm). Column C (53 μl) was made from a glass with larger surface area (CPG 10, particle size 90—110 μm, pore size 30 nm). The apparent dynamic ion-exchange capacities for copper ions were 0.25 μmol for column A and 0.5 μmol for columns B and C under the same experimental conditions as for the analytical determinations.

Results and discussion

Earlier work has shown [3] that 1 M nitric acid or 1 M HCl/0.1 M HNO_3 is required for total elution of all metal ions from a column containing immobilized 8-quinolinol. Chloride ions are known to induce surface effects on copper ion-selective electrodes [13] and nitric acid alone was therefore preferred here. An injection of strong acid into the column will temporarily lower the pH of the solution impinging on the electrode and this will produce an increase in the electrode potential because of corrosion potentials and liquid junction effects [8, 14]. The acid peak interferes at low copper concentrations and increases the detection limit.

The recording in f.i.a. will not have any well defined baseline because of the logarithmic response of the electrode. The potential will drift downward at a rate which decreases with decreasing copper concentrations and the actual level will depend on the time elapsed after the last copper peak. A copper ion-selective electrode can measure very low copper(II) concentrations if it is given sufficient time to reach equilibrium [1]. The size of the acid peak discussed above will also depend on when the elution is made. A background of 2×10^{-7} M Cu(II) was therefore added to the buffer to stabilize the background [15]; this gives a concentration of 1×10^{-7} M around the electrode after mixing with the eluent. A baseline which was stable within a few millivolts was then reached within 1—3 min, depending on the size of the preceding peak.

Figure 2 (curves 1—3) shows the peak shapes obtained when a 250-μl column of solid glass beads was inserted in place of the ion-exchanger; the peaks show the combined effects of dispersion and electrode response characteristics. A slight tendency to double peak formation can be seen for the

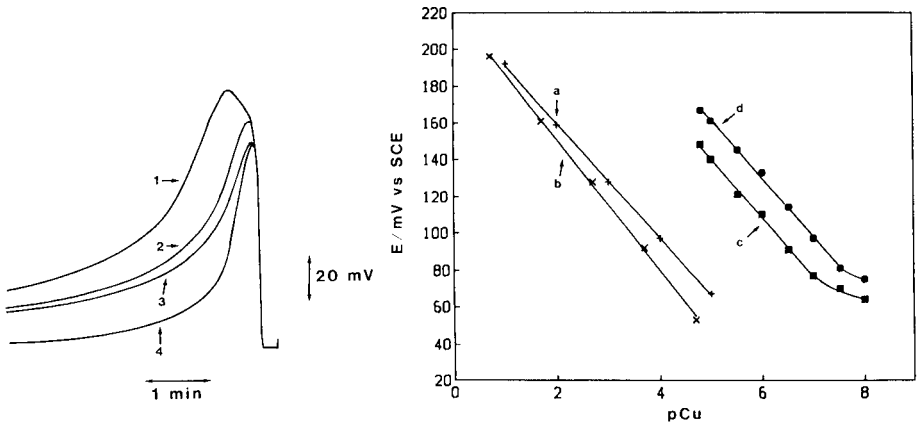

Fig. 2. Peak recordings of the response of the ion-selective electrode: (1—3) with solid glass beads in column III; (4) with chelating ion exchanger A in III. The volume of column III was 250 μl. Sample volumes: (1) 500 μl; (2) 100 μl; (3) 50 μl; (4) 50 μl. The sample concentration was 1 mM Cu(II) throughout.

Fig. 3. Calibration graphs for the copper ion-selective electrode in the flow system (a) with continuous pumping of the samples; (b) with 50-μl injections; (c) with 5-ml sample injections; (d) with 25-ml sample injections. The abscissa graduation refers to the sample concentrations. For (a) and (b), column III was removed; for (c) and (d), column B was in position III and conditions were as in Fig. 1.

largest injection volume. Curve 4 in Fig. 2 is the peak obtained with the chelating ion-exchanger in place. The metal ions were collected on the column and eluted with acid. It can be seen that the eluted peak is sharper than an unretained peak because of the dispersion-decreasing action of the ion exchanger. The logarithmic response gives an exaggerated visual impression of the tailing.

Different combinations of acid and buffer strengths were tried. The combination which was used in most of this work (0.5 M HNO_3/1 M acetate buffer) was capable of eluting more than 95% of the copper ions from the ion-exchanger with a slope of 31 mV/decade. Stronger acid (0.72 M HNO_3 2 M acetate buffer) gave more complete elution but with a higher slope (41—43 mV/decade). The slope does not change with ionic strength in a steady-state experiment in chloride-free solutions [16], but this does not hold for the transient response because of the changes in response time [10]. It should be noted that the transient slopes are obtained from the peak heights above the response towards the background and that an increased slope therefore corresponds to lower peaks at the lowest concentrations. The condition of the electrode surface and the silicone oil treatment [8] is of course also important for the slope of a dynamic calibration curve. A value of 37 mV/decade was obtained on one occasion with the 0.5 M acid/1 M buffer.

Three different columns with different volumes were prepared but no great differences in system behaviour was apparent. The peak shapes were almost the same but the elution was slightly more efficient with the smaller columns because there was less dispersion of the injected acid. Elution by backflushing the ion-exchanger (in a manifold with one additional valve) had negligible effects on the peak shapes [$<2\%$ in peak height at 10^{-5}—10^{-2} M Cu(II)].

Figure 3 (curve a) is a steady-state calibration curve of the electrode in the flow system. Columns I and III in Fig. 1 were removed and solutions with known copper content were pumped directly through the system to the electrode. The plotted concentration is that emerging from the open injection valve. Figure 3 (curve b) is a calibration curve obtained for 50-μl injections, again in a manifold without ion-exchange column. The difference in slope is due to the increased time constant of the electrode at low concentrations. Calibration curve (c) was obtained with 5-ml injections and pre-concentration on the chelating ion-exchanger; curve (d) is the corresponding plot for 25-ml injections. The bends in curves (c) and (d) are due to interference by the acid peak which hides small metal fractions. The peak shape was as shown in Fig.2 (curve 4) and was independent of the injection volume. The results shown in Fig. 3 demonstrate that pre-concentration on an ion-exchange column can extend the range of the ion-selective electrode downwards without requiring excessive equilibration times. The extension is less than the enrichment factor because of the pH changes during elution.

Measurements with copper ion-selective electrodes are normally affected by most anions and the medium exchange obtained by the ion-exchange should therefore be powerful in removing interferences. The flow-injection measurements are always made in a constant medium which favours accuracy. The reproducibility of the peak heights was ± 1.5 mV, which is worse than the reproducibility of a steady-state measurement. The selection of operating conditions involves several compromises, as discussed above, and the present system has a memory effect because of the incomplete elution. The errors will therefore be larger if the copper concentrations differ appreciably between samples, and double or triple injections may thus be necessary. The response was independent of the sample volume as shown in Table 1 and the enrichment factor can therefore be selected to give the most favourable conditions.

The nitrate, potassium, and sodium electrodes were reported to give reproducibilities as good as 0.2 mV in a flow-injection system run with more than 100 samples h^{-1} [4—6]. The poorer reproducibility reported here is due to the effects of the acid and possibly also to uneven mixing between eluant and buffer. A separate test of the copper ion-selective electrode with 0.1 M $NaNO_3$ carrier showed a reproducibility of 0.3 mV at the 2×10^{-4} M Cu(II) level when the time between the samples was kept constant. The reproducibility decreased to 0.8 mV if the spacing of the samples was varied. The copper ion-selective electrode seems therefore to be particularly sensitive to conditions at low levels because of its long time constant at low concentra-

TABLE 1

Peak heights for samples containing 5 nmol of copper(II) in different sample volumes

Volume (ml)	Concentration (μM)	E (mV)	Volume (ml)	Concentration (μM)	E (mV)
0.025	200	113	1.000	5	112
0.050	100	113	2.000	2.5	111
0.100	50	112	15.0	0.33	110
0.250	20	110	50.0	0.10	112
0.500	10	113			

tions. The reason is that copper ions are adsorbed on the electrode, which affects the response in the range below 10^{-4} M [14].

The author thanks Prof. Gillis Johansson and Dr. Lo Gorton for valuable discussions.

REFERENCES

1 W. J. Blaedel and D. E. Dinwiddie, Anal. Chem., 47 (1975) 1070.
2 S. Olsen, L. C. R. Pessenda, J. Růžička and E. H. Hansen, Analyst (London), 108 (1983) 905.
3 F. Malamas, M. Bengtsson and G. Johansson, Anal. Chim. Acta, 160 (1984) 1.
4 E. H. Hansen, F. J. Krug, A. K. Ghose and J. Růžička, Analyst (London), 102 (1977) 714.
5 J. Růžička, E. H. Hansen and E. A. Zagatto, Anal. Chim. Acta, 88 (1977) 1.
6 E. H. Hansen, J. Růžička and A. K. Ghose, Anal. Chim. Acta, 100 (1978) 151.
7 P. W. Alexander, M. Trojanowicz and P. R. Haddad, Anal. Lett., 17(A4) (1984) 309.
8 G. Johansson and K. Edström, Talanta, 19 (1972) 1623.
9 H. I. Thompson and G. A. Rechnitz, Chem. Instrum., 4(4) (1972) 239.
10 K. Tóth and E. Pungor, Anal. Chim. Acta, 64 (1973) 417.
11 H. I. Thompson and G. A. Rechnitz, Anal. Chem., 44 (1972) 300.
12 J. M. Hill, J. Chromatogr., 76 (1973) 455.
13 D. J. Crombie, G. J. Moody and J. D. R. Thomas, Talanta, 21 (1974) 1094.
14 E. G. Harsányi, K. Tóth and E. Pungor, Anal. Chim. Acta, 152 (1983) 163.
15 W. E. van der Linden and R. Oostervink, Anal. Chim. Acta, 101 (1978) 419.
16 G. B. Oglesby, W. C. Duer and F. J. Millero, Anal. Chem., 49 (1977) 877.

ANALYTICA CHIMICA ACTA, VOL. 179 (1986)

AUTHOR INDEX

(continued from inside back cover)

d from outside back cover)

(continued on p. 518)

CONTENTS

(Abstracted, Indexed in: Anal. Abstr.; Biol. Abstr.; Chem. Abstr.; Curr. Contents Phys. Chem. Earth Sci.; Life Sci.; Index Med.; Mass Spectrom. Bull.; Sci. Citation Index; Excerpta Med.)

International Conference on Flow Analysis III, September 5–8, 1985

(continued on inside ba